RENAL REGULATION OF WATER AND SODIUM IN HEALTH AND DISEASE

EDITED BY: Weidong Wang, Hyun Jun Jung and Soo Wan Kim
PUBLISHED IN: Frontiers in Physiology

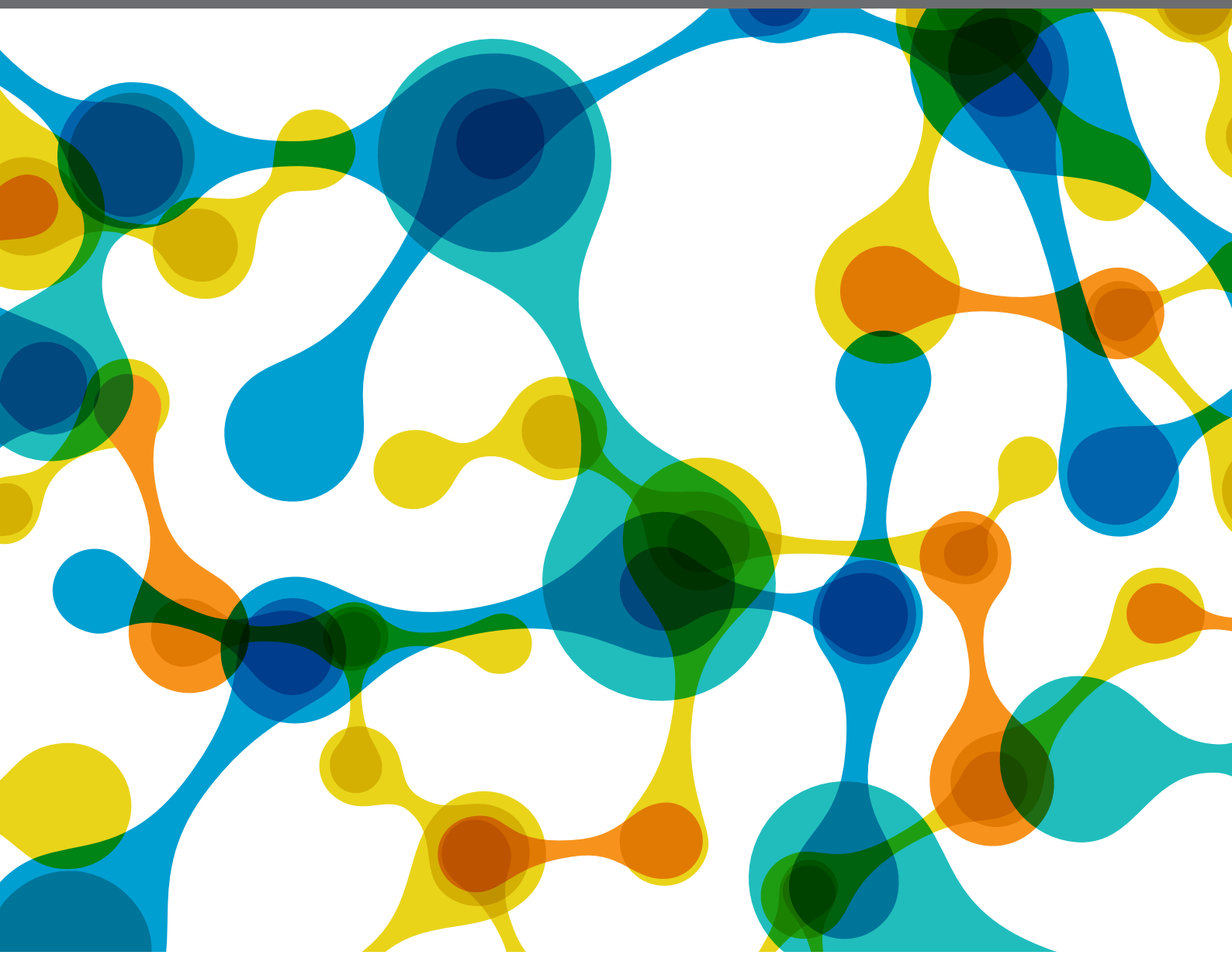

frontiers Research Topics

ISSN 1664-8714
ISBN 978-2-88976-479-2
DOI 10.3389/978-2-88976-479-2

About Frontiers

Frontiers is more than just an open-access publisher of scholarly articles: it is a pioneering approach to the world of academia, radically improving the way scholarly research is managed. The grand vision of Frontiers is a world where all people have an equal opportunity to seek, share and generate knowledge. Frontiers provides immediate and permanent online open access to all its publications, but this alone is not enough to realize our grand goals.

Frontiers Journal Series

The Frontiers Journal Series is a multi-tier and interdisciplinary set of open-access, online journals, promising a paradigm shift from the current review, selection and dissemination processes in academic publishing. All Frontiers journals are driven by researchers for researchers; therefore, they constitute a service to the scholarly community. At the same time, the Frontiers Journal Series operates on a revolutionary invention, the tiered publishing system, initially addressing specific communities of scholars, and gradually climbing up to broader public understanding, thus serving the interests of the lay society, too.

Dedication to Quality

Each Frontiers article is a landmark of the highest quality, thanks to genuinely collaborative interactions between authors and review editors, who include some of the world's best academicians. Research must be certified by peers before entering a stream of knowledge that may eventually reach the public - and shape society; therefore, Frontiers only applies the most rigorous and unbiased reviews.
Frontiers revolutionizes research publishing by freely delivering the most outstanding research, evaluated with no bias from both the academic and social point of view. By applying the most advanced information technologies, Frontiers is catapulting scholarly publishing into a new generation.

What are Frontiers Research Topics?

Frontiers Research Topics are very popular trademarks of the Frontiers Journals Series: they are collections of at least ten articles, all centered on a particular subject. With their unique mix of varied contributions from Original Research to Review Articles, Frontiers Research Topics unify the most influential researchers, the latest key findings and historical advances in a hot research area! Find out more on how to host your own Frontiers Research Topic or contribute to one as an author by contacting the Frontiers Editorial Office: frontiersin.org/about/contact

RENAL REGULATION OF WATER AND SODIUM IN HEALTH AND DISEASE

Topic Editors:
Weidong Wang, Sun Yat-sen University, China
Hyun Jun Jung, Johns Hopkins Medicine, United States
Soo Wan Kim, Chonnam National University Medical School, South Korea

Citation: Wang, W., Jung, H. J., Kim, S. W., eds. (2022). Renal Regulation of Water and Sodium in Health and Disease. Lausanne: Frontiers Media SA.
doi: 10.3389/978-2-88976-479-2

Table of Contents

04 ***Editorial: Renal Regulation of Water and Sodium in Health and Disease***
Sang Heon Suh, Hyun Jun Jung, Weidong Wang and Soo Wan Kim

06 ***Activation of the Thiazide-Sensitive Sodium-Chloride Cotransporter by Beta3-Adrenoreceptor in the Distal Convoluted Tubule***
Serena Milano, Monica Carmosino, Andrea Gerbino, Ilenia Saponara, Dominga Lapi, Massimo Dal Monte, Paola Bagnoli, Maria Svelto and Giuseppe Procino

18 ***Stimulation of the Epithelial Na^+ Channel in Renal Principal Cells by Gs-Coupled Designer Receptors Exclusively Activated by Designer Drugs***
Antonio G. Soares, Jorge Contreras, Crystal R. Archer, Elena Mironova, Rebecca Berdeaux, James D. Stockand and Tarek Mohamed Abd El-Aziz

28 ***α-Actinin 4 Links Vasopressin Short-Term and Long-Term Regulation of Aquaporin-2 in Kidney Collecting Duct Cells***
Cheng-Hsuan Ho, Hsiu-Hui Yang, Shih-Han Su, Ai-Hsin Yeh and Ming-Jiun Yu

42 ***The Role of Vasopressin V2 Receptor in Drug-Induced Hyponatremia***
Sua Kim, Chor Ho Jo and Gheun-Ho Kim

53 ***Selective Deletion of the Mechanistic Target of Rapamycin From the Renal Collecting Duct Principal Cell in Mice Down-Regulates the Epithelial Sodium Channel***
Bruce Chen, Maurice B. Fluitt, Aaron L. Brown, Samantha Scott, Anirudh Gadicherla and Carolyn M. Ecelbarger

68 ***Natriuresis During an Acute Intravenous Sodium Chloride Infusion in Conscious Sprague Dawley Rats Is Mediated by a Blood Pressure-Independent α_1-Adrenoceptor-Mediated Mechanism***
Alissa A. Frame, Kayla M. Nist, Kiyoung Kim, Jill T. Kuwabara and Richard D. Wainford

82 ***A Vasopressin-Induced Change in Prostaglandin Receptor Subtype Expression Explains the Differential Effect of PGE_2 on AQP2 Expression***
Peter M. T. Deen, Michelle Boone, Horst Schweer, Emma T. B. Olesen, Claudia Carmone, Jack F. M. Wetzels, Robert A. Fenton and Marleen L. A. Kortenoeven

95 ***Aldosterone-Regulated Sodium Transport and Blood Pressure***
Akaki Tsilosani, Chao Gao and Wenzheng Zhang

112 ***(Pro)renin Receptor Regulates Phosphate Homeostasis in Rats* via *Releasing Fibroblast Growth Factor-23***
Aihua Lu, Min Pu, Shiqi Mo, Jiahui Su, Jiajia Hu, Chunling Li, Weidong Wang and Tianxin Yang

124 ***Dissecting the Effects of Aldosterone and Hypokalemia on the Epithelial Na^+ Channel and the NaCl Cotransporter***
Mathias Kristensen, Robert A. Fenton and Søren B. Poulsen

frontiers | Frontiers in Physiology

EDITORIAL
published: 08 June 2022
doi: 10.3389/fphys.2022.925022

Editorial: Renal Regulation of Water and Sodium in Health and Disease

Sang Heon Suh[1], *Hyun Jun Jung*[2], *Weidong Wang*[3] *and Soo Wan Kim*[1]*

[1]Department of Internal Medicine, Chonnam National University Medical School and Chonnam National University Hospital, Gwangju, South Korea, [2]Division of Nephrology, Department of Medicine, Johns Hopkins University School of Medicine, Baltimore, MD, United States, [3]Institute of Hypertension, Zhongshan School of Medicine, Sun Yat-sen University, Guangzhou, China

Keywords: sodium, water, aquaporin, ENaC (epithelial sodium channel), sodium transporter

Editorial on the Research Topic

Renal Regulation of Water and Sodium in Health and Disease

A fine regulation of water and sodium balance is an integral part of body homeostasis. The kidney plays a pivotal role in the maintenance of water and sodium balance. Various water channels and sodium transporters, such as aquaporins, epithelial Na^+ channel (ENaC), and sodium-chloride cotransporter (NCC), are differentially expressed and regulated along the renal tubules and collecting ducts, contributing to body fluid homeostasis and blood pressure control (Noda et al., 2010; Warnock et al., 2014; Su et al., 2020; Meor Azlan et al., 2021; Prieto et al., 2021). A robust understanding of the physiology and pathophysiology of renal water and sodium regulation may facilitate the key solutions to unanswered clinical questions in various dysnatremic disorders and hypertension.

In this regard, the Frontier Research Topic, *Renal Regulation of Water and Sodium in Health and Disease*, has been contributed by a total of ten articles, shedding a light to the recent progress in the renal physiology of water and sodium regulation. Frame et al., taking advantage of pharmacologic interventions and physiological measurement in rodent surgical models, addressed the mechanism of natriuresis during acute intravenous sodium infusion, which is renal sympathetic nerves, but not circumventricular organs, and, more specifically, α 1-, but not β-adrenoreceptors. It is intriguing that the role of α 1-adrenoreceptors during acute sodium loading is opposite to the established roles of the renal sympathetic nerves on renal sodium handling *via* renal α 1-adrenoreceptor-evoked sodium reabsorption and renal β 1-adenoreceptors-mediated renin release. Milano et al. found that, in their loss-of-function studies, β 3-adenergic receptor activates NCC in the distal convoluted tubule by promoting phosphorylation *via* its upstream kinases, such as SPAK and WNKs, and that β 1/2-adenergic receptors regulate the expression of NCC, but not the phosphorylation state of NCC. Lu et al. discovered that high phosphate loading activates renin-angiotensin system, and that, by pharmacologic blockade of (pro)renin receptor, this in turn leads to activation of (pro)renin receptor to promotes phosphaturic response *via* stimulation of fibroblast growth factor 23 production and subsequent downregulation of renal Na/Pi-IIa expression. Kristensen et al., *via* various *in vivo* and *ex vivo* experiments, proved that increased expression and phosphorylation of NCC by excess aldosterone is likely an indirect effect of enhanced ENaC-mediated K^+ secretion and subsequent hypokalemia, concluding the debates on the association between hyperaldosteronism and upregulation of NCC in rodent models.

It is of note that four original articles are featured with collecting duct physiology. Chen et al. demonstrated that, using aquaporin-2 (AQP2) promoter-driven *Cre*-recombinase, mechanistic target of rapamycin (mTOR) from the renal collecting duct principal cell (PC) in mice down-regulates ENaC, and presented the evidence of the mechanisms by which ENaC activity is regulated by mTOR, such as regulation of type 1 serum glucocorticoid regulated kinase, ubiquitination, ENaC

OPEN ACCESS

Edited by:
Carolyn Mary Ecelbarger, Georgetown University, United States

Reviewed by:
Michel Burnier, Centre Hospitalier Universitaire Vaudois (CHUV), Switzerland

***Correspondence:**
Soo Wan Kim
skimw@chonnam.ac.kr

Specialty section:
This article was submitted to Renal and Epithelial Physiology, a section of the journal Frontiers in Physiology

Received: *21 April 2022*
Accepted: *19 May 2022*
Published: *08 June 2022*

Citation:
Suh SH, Jung HJ, Wang W and Kim SW (2022) Editorial: Renal Regulation of Water and Sodium in Health and Disease. Front. Physiol. 13:925022. doi: 10.3389/fphys.2022.925022

channel turnover and apical membrane residency. The selective deletion of mTOR in PC was ultimately sufficient to alter body sodium homeostasis. Soares et al. presented *in vivo* evidence that activation of Gs signaling exclusively in PCs is sufficient to increase ENaC activity and decrease urinary Na^+ excretion. The expression of Gs-DREADD (designer receptors exclusively activated by designer drugs) protein, which activates intracellular cAMP signal transduction pathway in response to synthetic, but not endogenous, ligand, such as clozapine N-oxide, was specifically induced kidney PCs in *Aqp2-cre* mice. Deen et al. dissected the underlying mechanism of the paradox that water absorption is increased in PCs by prostaglandin E2 (PGE2) in the absence of arginine vasopressin (AVP), but is decreased in the presence of AVP: In the absence of AVP, PGE2 binds to EP4 receptor that is coupled Gs protein, leading to cAMP generation, followed by AQP2 transcription and translocation. In contrast, AVP induces EP1 receptor, which leads to down-regulation of AQP2 expression, and reduces EP4 receptor. In the presence of AVP, PGE2 decreases AQP2 expression by stimulating EP1. Ho et al. defined a common mechanism of AQP2 regulation by α-actinin 4 that bridges short-term (trafficking of the water channel protein aquaporin-2 to the apical plasma membrane of PCs) and long-term (up-regulation of *AQP2* gene expression) response to AVP. This study unveiled that AVP reduces interaction of α-actinin 4 with F-actin, which facilitates F-actin depolymerization and, in turn, apical AQP2 insertion, while freed α-actinin 4 then enters the nuclei where it interacts with glucocorticoid receptor to enhance long-term vasopressin-induced *AQP2* gene expression.

The current Frontier Research Topic also includes two review articles. Tsilosani et al. summarized recent advances in the mechanisms of aldosterone-regulated sodium transport and its relevance with blood pressure, focusing on the signaling pathways involved in aldosterone synthesis and its effects on Na^+ reabsorption through ENaC. Kim et al. covered the central and nephrogenic mechanisms of drug-induced hyponatremia in drug-induced hyponatremia, emphasizing the importance of the canonical pathway of AQP2 regulation *via* vasopressin V2 receptor in "nephrogenic syndrome of inappropriate antidiuresis."

Taken together, this Frontier Research Topic expands our knowledge on physiologic function and pathologic adaptation of the renal nephron. The studies collected here are highlighting novel and sophisticated mechanisms of renal water and sodium handling, presenting robust evidence for further investigations.

AUTHOR CONTRIBUTIONS

SS drafted the Editorial while HJ, WW and SK contributed to editing. All authors conceived and designed the work and provided final approval of the version to be published.

REFERENCES

Meor Azlan, N. F., Koeners, M. P., and Zhang, J. (2021). Regulatory Control of the Na-Cl Co-transporter NCC and its Therapeutic Potential for Hypertension. *Acta Pharm. Sin. B* 11, 1117–1128. doi:10.1016/j.apsb.2020.09.009

Noda, Y., Sohara, E., Ohta, E., and Sasaki, S. (2010). Aquaporins in Kidney Pathophysiology. *Nat. Rev. Nephrol.* 6, 168–178. doi:10.1038/nrneph.2009.231

Prieto, M. C., Gonzalez, A. A., Visniauskas, B., and Navar, L. G. (2021). The Evolving Complexity of the Collecting Duct Renin-Angiotensin System in Hypertension. *Nat. Rev. Nephrol.* 17, 481–492. doi:10.1038/s41581-021-00414-6

Su, W., Cao, R., Zhang, X.-Y., and Guan, Y. (2020). Aquaporins in the Kidney: Physiology and Pathophysiology. *Am. J. Physiology-Renal Physiology* 318, F193–F203. doi:10.1152/ajprenal.00304.2019

Warnock, D. G., Kusche-Vihrog, K., Tarjus, A., Sheng, S., Oberleithner, H., Kleyman, T. R., et al. (2014). Blood Pressure and Amiloride-Sensitive Sodium Channels in Vascular and Renal Cells. *Nat. Rev. Nephrol.* 10, 146–157. doi:10.1038/nrneph.2013.275

Conflict of Interest: The authors declare that the research was conducted in the absence of any commercial or financial relationships that could be construed as a potential conflict of interest.

frontiers in Physiology

ORIGINAL RESEARCH
published: 13 August 2021
doi: 10.3389/fphys.2021.695824

Activation of the Thiazide-Sensitive Sodium-Chloride Cotransporter by Beta3-Adrenoreceptor in the Distal Convoluted Tubule

*Serena Milano[1], Monica Carmosino[2], Andrea Gerbino[1], Ilenia Saponara[1], Dominga Lapi[3], Massimo Dal Monte[3], Paola Bagnoli[3], Maria Svelto[1] and Giuseppe Procino[1]**

[1]Department of Biosciences, Biotechnologies and Biopharmaceutics, University of Bari, Bari, Italy, [2]Department of Sciences, University of Basilicata, Potenza, Italy, [3]Department of Biology, University of Pisa, Pisa, Italy

OPEN ACCESS

Edited by:
Weidong Wang,
Sun Yat-sen University, China

Reviewed by:
Tae-Hwan Kwon,
Kyungpook National University, South Korea
Arohan Subramanya,
University of Pittsburgh, United States
Hui Cai,
Emory University School of Medicine, United States

***Correspondence:**
Giuseppe Procino
giuseppe.procino@uniba.it

Specialty section:
This article was submitted to Renal and Epithelial Physiology, a section of the journal Frontiers in Physiology

Received: 15 April 2021
Accepted: 16 July 2021
Published: 13 August 2021

Citation:
Milano S, Carmosino M, Gerbino A, Saponara I, Lapi D, Dal Monte M, Bagnoli P, Svelto M and Procino G (2021) Activation of the Thiazide-Sensitive Sodium-Chloride Cotransporter by Beta3-Adrenoreceptor in the Distal Convoluted Tubule. Front. Physiol. 12:695824. doi: 10.3389/fphys.2021.695824

We previously showed that the beta-3 adrenergic receptor (BAR3) is expressed in most segments of the nephron where its agonism promotes a potent antidiuretic effect. We localized BAR3 in distal convoluted tubule (DCT) cells expressing the thiazide-sensitive sodium-chloride cotransporter (NCC). Aim of this study is to investigate the possible functional role of BAR3 on NCC modulation in DCT cells. Here, we found that, in mice, the knockout of BAR3 was paralleled by a significant attenuation of NCC phosphorylation, paralleled by reduced expression and activation of STE-20/SPS1-related proline-alanine-rich kinase (SPAK) and WNKs the main kinases involved in NCC activation. Conversely, in BAR1/2 knockout mice, we found reduced NCC abundance with no changes in the phosphorylation state of NCC. Moreover, selective BAR3 agonism promotes both SPAK and NCC activation in wild-type mouse kidney slices. In conclusion, our findings suggest a novel role for BAR3 in the regulation of NCC in DCT.

Keywords: beta3-adrenoreceptor, distal convoluted tubule, thiazide-sensitive Na-Cl cotransporter, sympathetic regulation, sodium-chloride cotransporter

INTRODUCTION

The beta-adrenergic system regulates numerous renal functions. Three subtypes of the beta-adrenoreceptors (BARs) are known as: BAR1, BAR2, and beta-3 adrenergic receptor (BAR3). While the expression and physiological roles of BAR1 and BAR2 in the kidney are widely documented, evidence regarding the renal expression of BAR3 was lacking until a few years ago. In particular, BAR1 is expressed in the mesangial cells, juxtaglomerular cells, macula densa epithelium, distal tubules, and collecting ducts. BAR2 is expressed mainly in the proximal, distal tubules, and collecting ducts (Boivin et al., 2001; Sata et al., 2018). Stimulation of both BAR1 and BAR2 participate in the regulation of glomerular filtration, sodium reabsorption, acid-base balance, and renin secretion.

We recently demonstrated that BAR3 is expressed in most of the nephron segments also expressing the type-2 vasopressin receptor (AVPR2), including the thick ascending limb (TAL) of Henle, the distal convoluted tubule (DCT), and the cortical and the outer medullary collecting duct (CD; Procino et al., 2016). In particular, we showed in mice that stimulation of BAR3

reduced urine excretion of water, Na^+, K^+, and Cl^-, as a result of increased plasma membrane expression of the water channel aquaporin 2 in the CD and increased the activation of the Na-K-2Cl symporter (NKCC2) in the TAL. Both proteins are key players in the urine concentrating process (Procino et al., 2016).

Here, we focused on the possible functional role of BAR3 in DCT where it localized at the basolateral membrane of epithelial cells expressing the thiazide-sensitive sodium-chloride cotransporter (NCC) at the apical side (Procino et al., 2016; Poulsen et al., 2021). NCC tightly tunes renal sodium reabsorption in DCT to fit blood pressure changes.

NCC activation is a consequence of its phosphorylation by a complex network of kinases including the with-no-lysine kinases WNK1 and WNK4, the STE-20/SPS1-related proline-alanine-rich kinase (SPAK), and Oxidative Stress Response 1 (Pacheco-Alvarez et al., 2006; Richardson et al., 2008; Huang and Cheng, 2015; Hadchouel et al., 2016).

Recent studies showed a direct influence of norepinephrine released by sympathetic nerves on NCC expression and activity (Rojas-Vega and Gamba, 2016). For instance, norepinephrine can increase NCC expression and phosphorylation by activating the BAR2-WNK4 pathway (Mu et al., 2011). Terker et al. (2014) reported that acute stimulation of DCT cells with norepinephrine increased NCC phosphorylation *via* BAR1 activation (Terker et al., 2014). Thus, the aim of the present study is to uncover the possible role of BAR3 stimulation in regulating NCC expression and activation in the DCT cells.

Interestingly, we found that in BAR3 knockout (ko) mice, the amount of phosphorylated NCC (pNCC) was significantly reduced, thus suggesting a regulatory role of BAR3 on NCC. The evidence was confirmed by the observation that BAR3 agonism promoted NCC phosphorylation in vital kidney slices from wt mice but not in those from BAR3 KO animals.

MATERIALS AND METHODS

Antibodies and Reagents

Selective BAR3 agonist BRL37344 (cat. no. sc-200154) and specific BAR3 antagonist L748337 (cat. no. sc-204044) were from Santa Cruz Biotechnology. The PKA inhibitor H-89 (cat. no. B1427) and (deamino-Cys1, D-Arg8)-vasopressin [1-deamino-8-D-argininevasopressin (dDAVP), cat. no. V-1005] were from Sigma (St. Louis, MO).

Antibodies anti-NCC (cat. no. SPC-402D) were from StressMarq Biosciences Inc. (Victoria, BC, Canada). Antibodies against the phosphorylated Thr 53 NCC (cat. no. p1311-53) were from Phosphosolutions. Anti-SPAK (cat. no. S669D) and anti-phospho Ser 373 SPAK (cat. no. S670B), anti-full-length WNK1 (cat. no. S062B), anti-phospho (Ser 382) WNK1 (cat. no. S099B), and anti-WNK4 (cat. no. S064B) antibodies were purchased from MRC-Protein Phosphorylation & Ubiquitylation Unit, University of Dundee, Scotland. Antibodies against PKC (isoform α; cat. no. 2056), phospho-PKC (pan; βII Ser660; cat. no. 9371), ERK1/2 (cat. no. 4695), and phospho-ERK1/2 (Thr202/Tyr204; cat. no. 4370) were from Cell Signaling Technology. Hydrochlorothiazide (HCTZ; cat. no. H4759) was from Sigma-Aldrich.

Animals

Procedures involving animals were carried out in compliance with the Italian guidelines for animal care (DL 26/14) and the European Communities Council Directive (2010/63/UE). Procedures were approved by the Ethical Committee in Animal Experiments of the University of Bari.

Mice were maintained on a 12-h light/12-h dark cycle, with free access to water and food (2018 Teklad rodent diet, Envigo), in accordance with the Italian Institute of Health Guide for the Care and Use of Laboratory Animals.

Knockout mice, BAR3, and BAR1/2 were derived from two distinct strains characterized by a different genetic background, for this reason, we used specific wild-type mice for each BARs ko model.

BAR3 ko and their wild-type mice (Boss et al., 1999) were purchased from the Jackson Laboratory (Bar Harbor, ME, United States). BAR1/2 ko and wild-type mice (Rohrer et al., 1999) were generated as previously described (Bernstein et al., 2005; Ecker et al., 2006). Experiments were conducted in male mice 4 months old.

Systolic blood pressure was measured in anesthetized mice by means of the "tail-cuff" sphygmomanometer method, as previously described (Martelli et al., 2013).

Metabolic cages were used to collect urine. Mice received a single i.p. injection (200 μl) of HCTZ (50 mg/kg) dissolved in DMSO and diluted 1:10 in sterile saline. Controls received the same volume of vehicle alone. Plasma and urine electrolytes were measured using the ion selective electrode method, aldosterone with R. I. A method.

Immunofluorescence

Mouse kidneys were fixed overnight with 4% paraformaldehyde at 4°C, cryopreserved in 30% sucrose for 24 h, and then embedded in optimal cutting temperature medium. Thin cryosections (7 μm) were subjected to immunofluorescence analysis as previously reported (Procino et al., 2016). Sections were incubated with the primary antibodies anti-NCC, anti-pNCC, anti-SPAK, anti-pSPAK, and the appropriate AlexaFluor-conjugated secondary Ab (Life Technologies) according to the manufacturer's instructions. Confocal images were obtained with a confocal laser-scanning fluorescence microscope (Leica TSC-SP2, Mannheim, Germany). For the quantification of the fluorescence intensity (FI expressed as arbitrary units), 18 confocal images (three for each mouse) were analyzed blindly for each genotype using ImageJ software. Images were then background subtracted and the appropriate threshold was automatically calculated for the two separate channels (green and red) obtained from each image. Then, the mean fluorescence intensity of each image was quantified using ImageJ.

Immunoblotting

Whole kidney isolated from wild type, BAR3 and BAR1/2 ko mice were homogenized in RIPA buffer as previously

described (Procino et al., 2014). 30 μg of each lysate was separated by SDS-PAGE using Mini-PROTEAN® TGX Stain-Free™ Precast Gels Bio-Rad and analyzed by Western blotting as previously described (Milano et al., 2018). Densitometry was performed using the Image Lab™ software (Bio-Rad) of ChemiDoc™ (Bio-Rad) imaging system, after normalization for the total protein content using the Stain-Free™ technology (Bio-Rad) according to manufacturer's instructions.

Kidney Slices

Sex-, age-, and weight-matched C57BL/6J (N = 6) or BAR3 ko (N = 6) male mice were used for the kidney slices experiments. Mice were anesthetized with tribromoethanol (250 mg/kg) and killed by cervical dislocation. Kidneys were collected and thin transversal slices (250 μm) were obtained using a Mcllwain Tissue Chopper (Ted Pella Inc.; Redding, CA, United States). Slices were left at 37°C in Dulbecco's Modified Eagle Medium/F12 medium (CTR) or stimulated for 40 min with dDAVP (10^{-7} M) or BRL37344 (10^{-5} M), the latter given alone or after 30 min of preincubation with either L748,337 (10^{-7} M) or H89 (10^{-5} M). Slices were processed for Western blotting experiments as described above or fixed in 4% paraformaldehyde and thin cryosections (7 μm) were subjected to immunofluorescence. For the quantification of fluorescence intensity, 30 confocal images (six for each condition) were analyzed.

Statistical Analysis

For statistical analysis, GraphPad Prism software (La Jolla, CA) was used. Unpaired Student's t-test was used to compare knockout and wild-type mice of each strain. For multiple comparison, one-way ANOVA was performed. All values are expressed as means ± SEMs. A difference of $p < 0.05$ was considered statistically significant. Details about statistical analyses are reported in figure legends.

RESULTS

Blood Chemistry of Animals Used in the Study

We previously characterized blood chemistry of BAR3 ko mice (Procino et al., 2016). Here, we compared blood chemistry between BAR3 ko, BAR1/2 ko mice, and their wt controls. As reported in **Table 1**, plasma Na^+, K^+, and Cl^- did not change significantly between genotypes. Plasma aldosterone concentrations were not significantly altered in BARs knockout, although they were higher in the genetic background in which BAR1/2 ko mice were generated (C56BL6), compared to FVB animals in which BAR3 ko mice were obtained. Systolic blood pressure was measured in all mouse genotypes and did not show significant differences in agreement with previously published data (Rohrer et al., 1999; Deschepper et al., 2004; Moens et al., 2009).

TABLE 1 | Plasma electrolytes, aldosteron and blood pressure in each genotype analyzed in the study.

Parameter (plasma)	BAR3 wt	BAR3 KO	BAR1/2 wt	BAR1/2 KO
Na^+ (mEq/L)	138 ± 3.05	141.3 ± 2.40	140 ± 1.15	139.3 ± 2.9
K^+ (mEq/L)	6.17 ± 1.6	5.77 ± 0.49	5.87 ± 0.39	6.63 ± 1.24
Cl^- (mEq/L)	102.7 ± 0.67	104 ± 2	101.3 ± 1.76	100 ± 1.15
Aldosterone (pg/ml)	204.7 ± 14.62	172.7 ± 16.18	318.7 ± 16.18	333.3 ± 24.04
Blood pressure (mmHg)	117 ± 1.8	120 ± 1.4	119 ± 2.1	119.6 ± 2

Values are means ± SEM of measurements in six mice/genotype. Statistical analysis was performed using an unpaired t-test.

BAR3 Ko Mice Show Reduced Urine Na^+ Excretion Upon HCTZ Administration

Although BAR3 ko mice did not show defects in plasma Na^+ handling, to test the hypothesis that gene deletion of the BAR3 receptor might affect the regulation of the NCC transporter in the DCT, we analyzed the urinary excretion of Na^+ after the administration of the diuretic HCTZ, a specific inhibitor of NCC. BAR3 ko mice and their wt controls (six for each genotype) were housed and acclimatized for 24 h in metabolic cages, i.p. injected with HCTZ (50 mg/Kg) or vehicle alone, and urine collected for the next 6 h post-injection. Increase of urine output confirmed the effect of the diuretic (not shown). Urine Na^+ excretion normalized for creatinine is reported in **Figure 1**. Among vehicle-injected animals, BAR3 ko mice had an increased Na^+ excretion compared to wt animals, as we previously reported (Procino et al., 2016). Interestingly, although HCTZ induced natriuresis in both genotypes, BAR3 ko mice showed a significantly reduced natriuresis compared to their wt controls, likely suggesting that BAR3 ko might have less active NCC to inhibit.

BAR3 Knockout Mice Show Reduced NCC Phosphorylation and Reduced Levels of SPAK and pSPAK

Based on the reduced effect of HCTZ in BAR3 ko mice, we investigated the abundance and activation of NCC in these animals. To this end, kidneys from wild type and BAR3 ko mice were subjected to Western blotting and immunofluorescence experiments to assess the abundance and localization of both total and pNCC. Western blotting analysis of total kidney lysates showed no difference in the abundance of total NCC between wt and BAR3 ko mice (**Figure 2A**). Conversely, pNCC was significantly reduced of about 60% in the kidney of BAR3 ko mice (**Figure 2A**) also after normalization to total NCC expression. It is known that SPAK activity is involved in NCC phosphorylation/activation. Therefore, we investigated whether the levels of total SPAK and its phosphorylated/activated form, pSPAK, were also changed in BAR3 ko animals. Western blotting analysis of kidneys lysates revealed that in BAR3 ko, compared to wt mice, both total and pSPAK were reduced by 30 and 60%, respectively (**Figure 2A**). After normalization to total SPAK, pSPAK was reduced by 40%. Immunofluorescence analysis

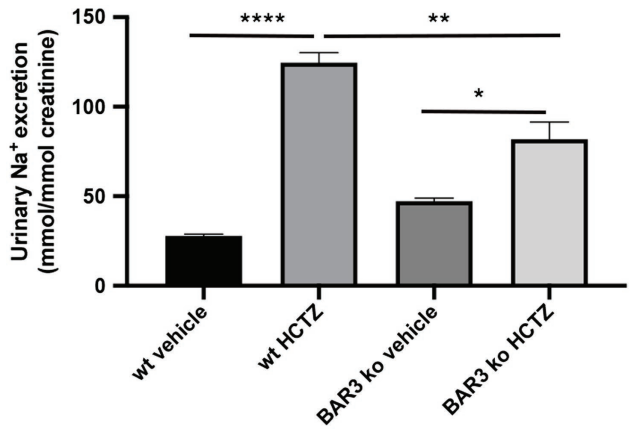

FIGURE 1 | Effect of hydrochlorothiazide diuretic on natriuresis in BAR2 ko mice. BAR3 ko mice and their age-matched wt controls ($N = 6$ for each group) were individually housed in metabolic cages for 24 h. Three animals for each group received an intraperitoneal injection of 50 mg/Kg HCTZ in sterile saline, while control animals received the vehicle alone. Urines were collected for 6 h after injection and Na^+ excretion analyzed and reported as mean values ± SEM. Both genotypes significantly increased natriuresis in response to HCTZ, although in BAR3 ko mice, this effect was significantly blunted compared to wt animals. Statistical analysis was performed by one-way ANOVA followed by Bonferroni multiple comparison test. $^*p < 0.05$; $^{**}p < 0.01$; and $^{****}p < 0.0001$.

of contralateral kidneys showed that NCC immunoreactivity in both genotypes was clearly concentrated at the apical plasma membrane of DCT cells (**Figure 2B** 6× magnification inset). The fluorescence intensity (FI) and subcellular distribution of NCC staining was comparable between BAR3 ko and wt mice (NCC FI: wt 5304 ± 95 vs. BAR3 ko 5597 ± 180). On the other hand, the intensity of pNCC staining in kidney sections from BAR3 ko mice was reduced compared to wt (pNCC FI: wt 10824 ± 350 vs. BAR3 ko 3894 ± 120, $p < 0.0001$) (**Figure 2B**).

As for total and pSPAK, confocal microscopy analysis supported the results obtained by Western blotting experiments. **Figure 2B** shows that both total and pSPAK were consistently less abundant in DCTs of BAR3 ko compared to wt mice (SPAK FI: wt 4067 ± 150 vs. BAR3 ko 2357 ± 130, $p < 0.0001$; pSPAK FI: wt 7105 ± 550 vs. BAR3 ko 3560 ± 370, $p = 0.0003$).

Together, the data suggest that BAR3 might be involved in the regulation of NCC phosphorylation/activation and the lack of BAR3 impaired the abundance and activation of SPAK.

Knockout of BAR1/2 Reduces NCC Expression Level but Does Not Affect Abundance and Activation of SPAK

To dissect the contribution of BAR subtypes in the sympathetic regulation of NCC, we analyzed the effects of the double knockout of BAR1 and BAR2 on NCC expression and activation, performing the same analysis reported above for BAR3 ko mice. As showed in **Figure 3A**, total NCC was reduced by 40% in BAR1/2 ko mice compared to their wt. In contrast, despite the high variability of pNCC levels between mice, the overall variation of pNCC between BAR1/2 ko and wt animals was not statistically significant (**Figure 3A**). After normalization to total NCC, pNCC showed an increase that was not statistically significant.

We also evaluated the levels of SPAK e pSPAK in BAR1/2 ko and their wild-type mice and we found no significant difference. After normalization to total SPAK, pSPAK was significantly increased in BAR1/2 ko mice.

These results were supported by immunofluorescence experiments showed in **Figure 3B**: The lack of BAR1/2 reduced the intensity of NCC staining in kidney sections (NCC FI: wt 4051 ± 210 vs. BAR 1/2 ko 1526 ± 186, $p < 0.0001$). Conversely, pNCC, although highly variable, did not change compared to wt mice (pNCC FI: wt 4869 ± 760 vs. BAR 1/2 ko 4580 ± 950, $p = 0.8168$; **Figure 3B**).

In addition, neither the abundance nor the phosphorylation state of SPAK changed in immunofluorescence experiments performed on BAR1/2 knockout mice (SPAK FI: wt 1325 ± 246 vs. BAR 1/2 ko 1238 ± 215, $p = 0.7961$; pSPAK FI: wt 1492 ± 118 vs. BAR 1/2 ko 1517 ± 236, $p = 0.9266$). These results support the hypothesis that BAR1 and BAR2 might participate in the control of NCC abundance rather than the phosphorylation/activation of the cotransporter.

Involvement of Upstream Regulators of NCC Activation

We further investigated the possible effect of BARs knockdown on upstream regulators of SPAK activity and/or on the activity of PKC and ERK1/2. As reported in **Figure 4**, in total kidney lysates from BAR3 ko animals, pWNK, but not the total levels of WNK1, was significantly reduced compared to the wt strain. Also, the expression of total WNK4 showed a significant reduction. On the other hand, when we analyzed the same kinases in kidneys from BAR1/2 ko mice, we found a significant increase of active WNK1.

As for ERK1/2, we found that total ERK1/2 was reduced in BAR3 ko mice, compared to their controls and this reflected on a parallel reduction of phosphorylated ERK1/2. Overall, after normalization of each form for the total protein load, the ratio between pERK/ERK was unchanged between BAR3 ko and their wt controls, likely suggesting that of ERK1/2 signaling is not affected by BAR3 ko. In kidneys from BAR1/2 ko animals, the upregulation of total ERK1/2 abundance was, as expected, paralleled by a significant increase of pERK1/2, but again, no changes in the ratio of pERK/ERK suggested that the also absence of functional BAR1/2 did not perturb ERK1/2 signaling. The effect of BARs ko on the PKC signaling pathway was investigated with an antibody against total PKC (α isoform) and a pan-antibody against phosphorylated PKC isoforms (pPKC). As shown in **Figure 4**, regardless of the genotype investigated, the total expression of PKC did not change, but a significant reduction of active pPKC was observed only in BAR3 ko mice, compared to their wt strain.

BAR3 Stimulation Promotes NCC Activation in Kidney Slices

Kidney slices from wt mice were incubated with the selective BAR3 agonist BRL37344, alone or after treatment with either

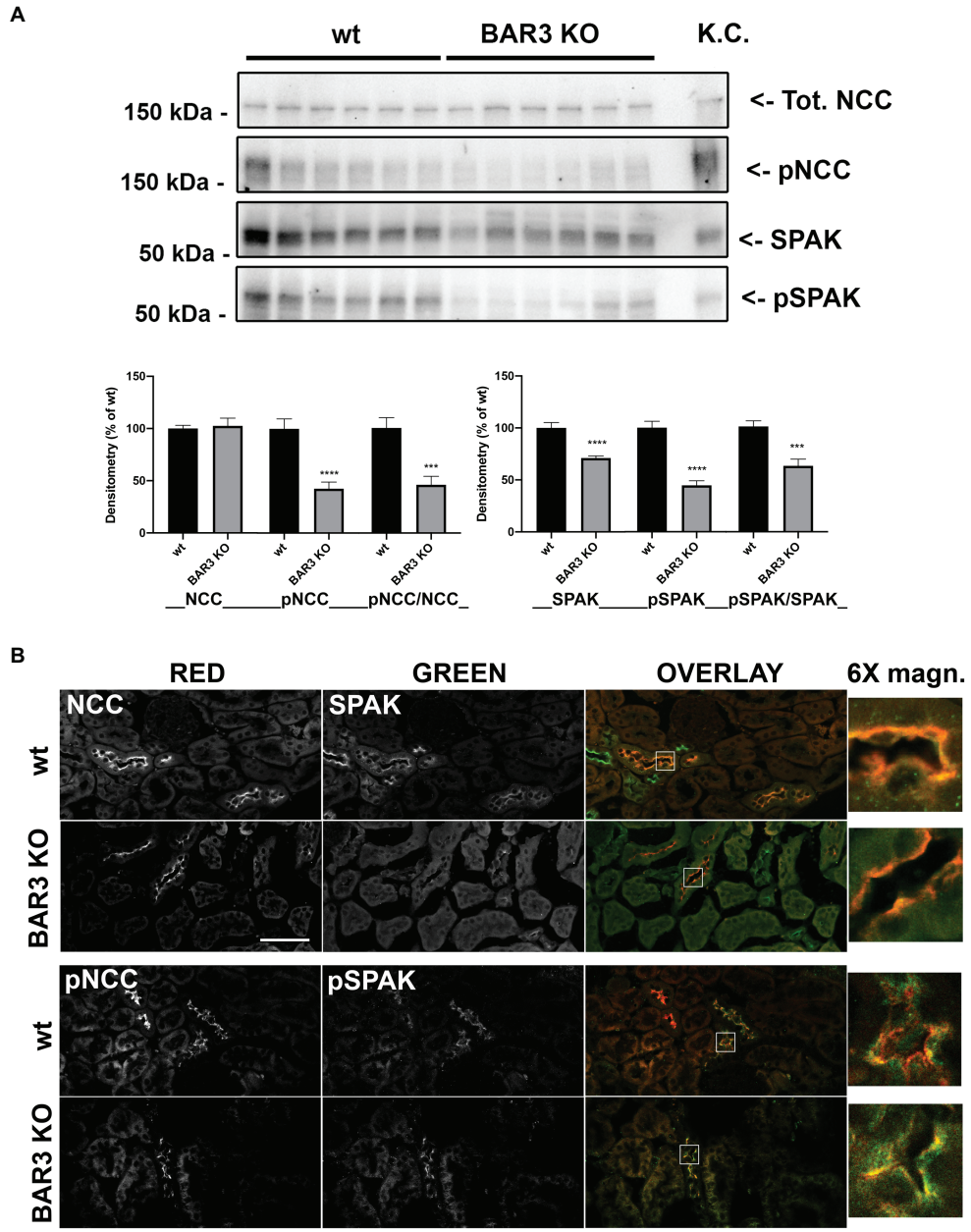

FIGURE 2 | Effect of BAR3 knockout on total and phosphorylated NCC (pNCC) and SPAK in the kidney. **(A)** Western blotting analysis of total and phosphorylated forms of both NCC and SPAK on total kidney homogenates from both wt and BAR3 ko mice. Protein extract from mouse kidney cortex (KC) was loaded as positive control. Densitometric analysis of NCC, pNCC, SPAK, and pSPAK bands, normalized to total lane protein content using the Stain-Free™ gels technology, from three independent experiments was reported as percentage of wt mice. Data are provided as mean ± SEM. ***$p < 0.001$; ****$p < 0.0001$ assessed by Student's *t*-test. $N = 6$ per group. **(B)** Kidney sections of wild type (wt) and BAR3 ko mice were subjected to immunofluorescence co-localization of NCC and SPAK or pNCC and pSPAK. Representative images are shown. $N = 6$ per group (bar = 25 μm).

L-748,337 (a specific BAR3 antagonist) or H89 (a PKA inhibitor). Stimulation with dDAVP was used as control for NCC and SPAK phosphorylation.

Figures 5A,B reported the Western blotting semi-quantitative analysis of the abundance of both pNCC and pSPAK, normalized for the total content of NCC and SPAK, respectively. Normalization of the phosphorylated form of both proteins to their total content was necessary considering that in kidney slices the number of DCT may be heterogeneous. Incubation with BRL37344 increased the phosphorylation of NCC and SPAK (of about 40 and 200%, respectively) and this effect was significantly prevented by both L748337 and H89. In kidney slices from BAR3 ko mice (**Figures 5C,D**), as expected, BRL 37344 did not increase the phosphorylation of NCC and SPAK,

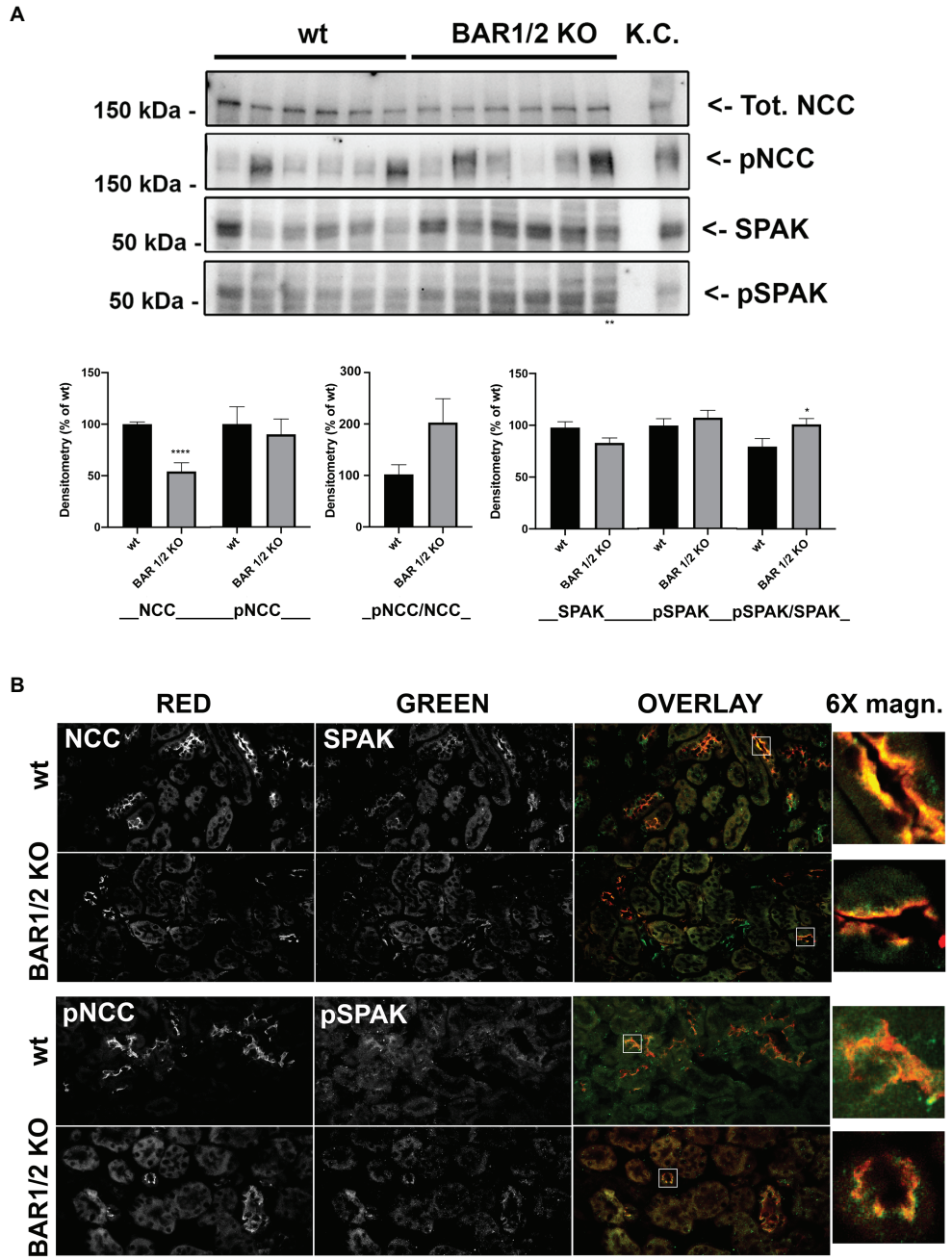

FIGURE 3 | Effect of BAR1/2 knockout on total and pNCC and SPAK in the kidney. **(A)** Western blotting analysis of total and phosphorylated forms of both NCC and SPAK on total kidney homogenates from both wt and BAR1/2 ko mice. Protein extract from mouse kidney cortex (KC) was loaded as positive control. Densitometric analysis of NCC, pNCC, SPAK, and pSPAK bands, normalized to total lane protein content using the Stain-Free™ gels technology, from three independent experiments was reported as percentage of wt mice. Data are provided as mean ± SEM. *$p < 0.05$; ****$p < 0.0001$ assessed by Student's *t*-test. $N = 6$ per group. **(B)** Kidney sections of wild type (wt) and BAR1/2 ko mice were subjected to immunofluorescence co-localization of NCC and SPAK or pNCC and pSPAK. Representative images are shown. $N = 6$ per group (bar = 25 μm).

thus confirming that the effect of BRL 37344 observed in wt animals was exclusively due to the BAR3 activation. A parallel set of kidney slices, treated as described above, was used for immunofluorescence analysis.

Confocal microscopy reported in **Figure 6A** showed that both BRL37344 and dDAVP increased the pNCC fluorescence signal, which was clearly brighter compared to that observed in resting slices (pNCC FI: CTR 3043 ± 180 vs. BRL 5560 ± 250, $p < 0.0001$; CTR vs. dDAVP 6485 ± 195, $p < 0.0001$). L748,337 prevented the effect of BRL37344 demonstrating that the increase in NCC phosphorylation was specifically attributable to BAR3 stimulation (pNCC FI: BRL + L748 2328 ± 210 vs. CTR ns – vs.

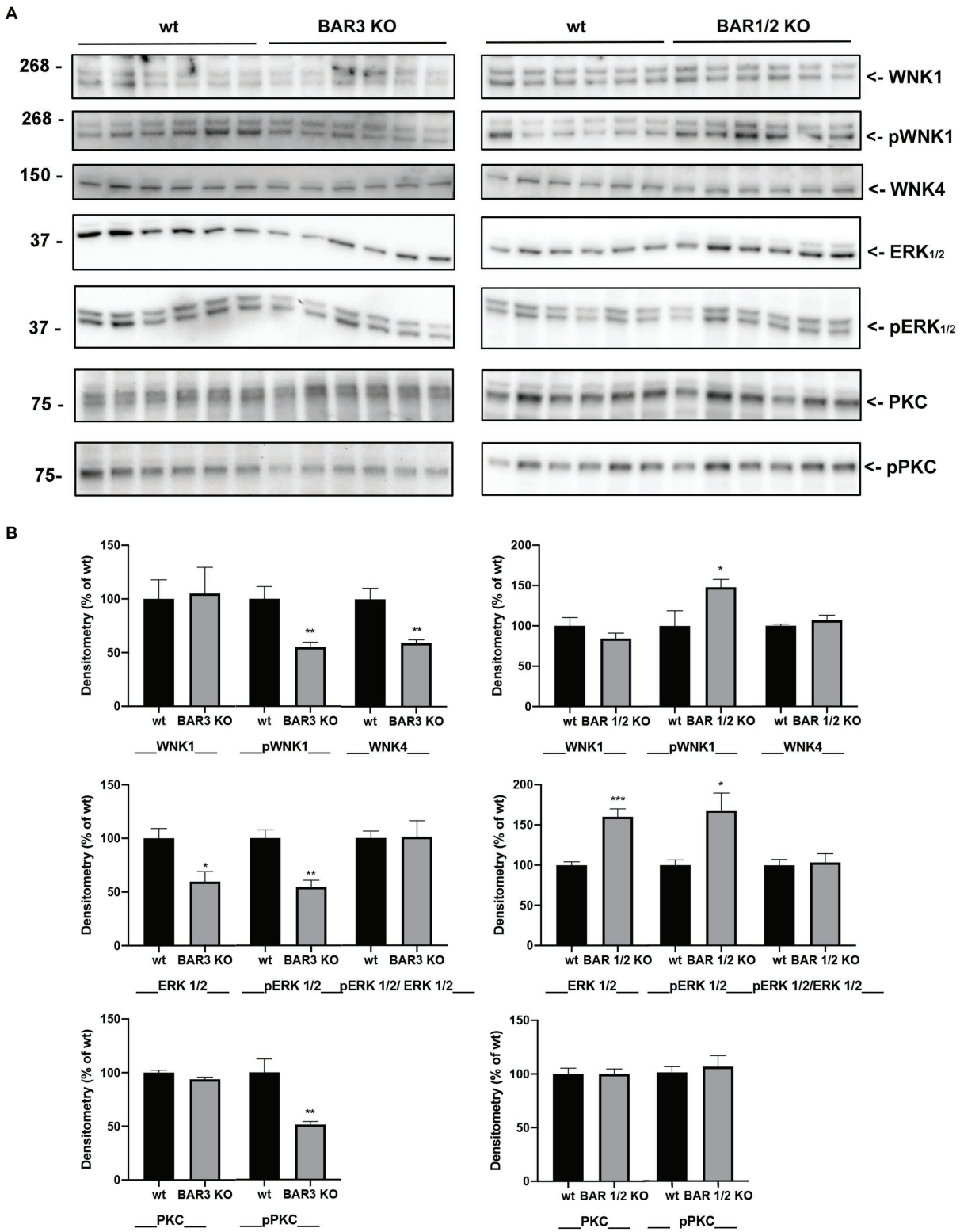

FIGURE 4 | (A) Western blotting analysis of total and phosphorylated (p) forms of WNK1, ERK1/2, and PKC and total WNK4, on total kidney homogenates from both BAR3 ko and BAR1/2 ko mice, compared to their respective wt mouse strains. Molecular weight in kDa is indicated on the left of each lane. **(B)** Densitometric analysis of each protein bands, normalized to total lane protein content using the Stain-Free™ gels technology, from three independent experiments was reported as percentage of wt mice. Data are provided as mean ± SEM. $^{*}p < 0.05$; $^{**}p < 0.01$; and $^{***}p < 0.001$ assessed by Student's *t*-test. $N = 6$ per group.

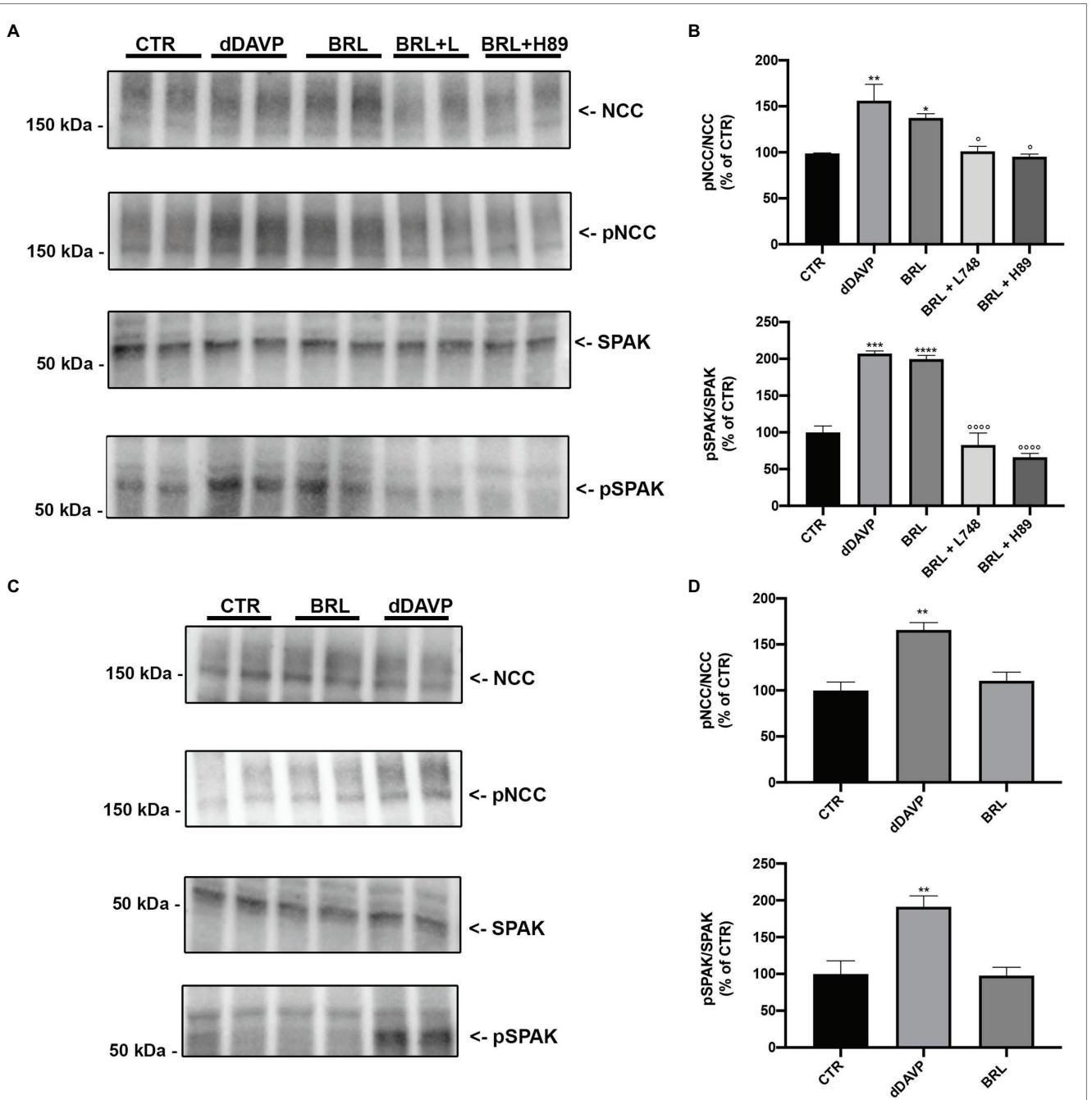

FIGURE 5 | Semi-quantitative analysis of the abundance of both pNCC and pSPAK after BAR3 stimulation in kidney slices. **(A,B)** Freshly isolated kidney slices from 6 wt mice were left untreated (CTR) or incubated for 40 min with dDAVP (10^{-7} M) or BRL37344 (BRL, 10^{-5} M), the latter given alone or after 30 min of preincubation with either the BAR3 antagonist L748337 (L748 10^{-7} M) or the protein kinase A inhibitor H89 (10^{-5} M). Representative immunoblots showed the effect of these treatments on the total and phosphorylated forms of NCC and SPAK. Each lane represents a lysate of kidney slices from three wt mice. The densitometric analysis, expressed as percentage of the CTR, from three independent experiments was reported. Error bars represent the SEM. *Indicates the comparison vs. CTR, °indicates the comparison vs. BRL; *, °$p < 0.05$; **$p < 0.01$; ***$p < 0.001$; ****, °°°°$p < 0.0001$ assessed by one-way ANOVA followed by Dunnett's multiple comparison test. **(C,D)** Freshly isolated kidney slices from 6 BAR3 ko mice were stimulated with BRL and dDAVP as described above. Each lane represents a lysate of kidney slices from three mice. The densitometric analysis, expressed as percentage of the CTR, from three independent experiments was reported. Error bars represent the SEM. **$p < 0.01$ vs. CTR assessed by one-way ANOVA followed by Dunnett's multiple comparison test.

BRL $p < 0.0001$). H89 prevented the effect of BRL37344 indicating the downstream involvement of PKA in the phosphorylation of NCC (pNCC FI: BRL + H89 2486 ± 168, vs. CTR ns – vs. BRL $p < 0.0001$).

Next, we also evaluated the levels of SPAK phosphorylation under the same experimental conditions. In **Figure 6B**, immunofluorescence analysis showed that the increase of pNCC induced by BRL37344 was paralleled by a concomitant

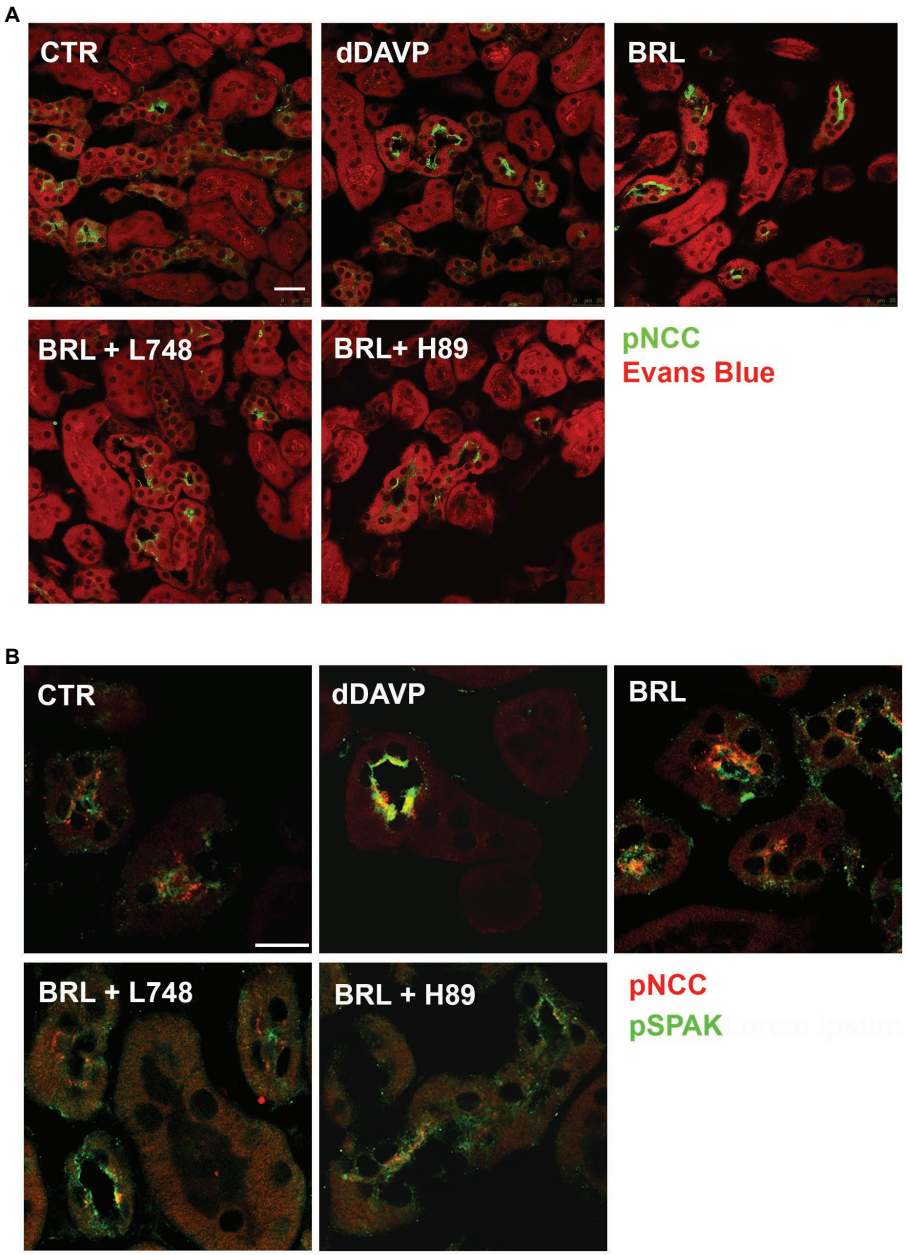

FIGURE 6 | In kidney slices, selective BAR3 stimulation promotes NCC phosphorylation by activating PKA and SPAK in DCT cells. Freshly isolated kidney slices from 6 wt mice were incubated for 40 min at 37°C in culture medium alone (CTR) or with dDAVP (10^{-7} M) or BRL37344 (BRL, 10^{-5} M), the latter given alone or after 30 min of preincubation with either the BAR3 antagonist L748,337 (L748 10^{-7} M) or the protein kinase A inhibitor H89 (10^{-5} M). **(A)** Immunofluorescence images of kidney sections showing pNCC (green) and counterstain with Evans blue (red; bar = 25 μm). **(B)** Confocal microscopy showed that the treatment with BRL increased the abundance of both pNCC and pSPAK at the apical plasma membrane of DCT cells. The BRL effect was prevented by either L748 or H89 (bar = 25 μm).

increase of pSPAK (pSPAK FI: CTR 2299 ± 250 vs. BRL 5863 ± 250, $p < 0.0001$; CTR vs. dDAVP 7024 ± 230, $p < 0.0001$). Pretreatment with either L748,337 or H89 prevented the effect of BRL37344 on the phosphorylation of both NCC and SPAK (pSPAK: BRL + L748 1929 ± 278 vs. CTR ns – vs. BRL $p < 0.0001$; BRL + H89 2997 ± 300, vs. CTR ns – vs. BRL $p < 0.0001$).

DISCUSSION

We previously showed the expression of BAR3 in the same nephron segments expressing AVPR2 and its role in promoting water and salt reabsorption (Procino et al., 2016). Interestingly, BAR3 ko mice exhibit an increased Na^+, K^+, and Cl^- urine excretion (Procino et al., 2016), a finding that could not

be explained only by the reduced activation of NKCC2 that we demonstrated in these animals. In fact, the main finding of the present study is that BAR3 regulates the activation of NCC in DCT cells.

Three evidence clearly support this conclusion: (1) HCTZ shows a reduced natriuretic effect *in vivo* in BAR3 ko mice; (2) BAR3 ko mice exhibit reduced pNCC levels compared to their controls; and (3) in vital mouse kidney slices, the pharmacologic agonism of BAR3 clearly promotes NCC phosphorylation which is prevented by specific BAR3 antagonism.

To date, the study of the relationship between sympathetic stimulation and increased NCC activity has been restricted to the contribution of BAR1 and BAR2. Using BAR1 ko and BAR2 ko mice, Mu et al. demonstrated that norepinephrine increased NCC expression and phosphorylation through the activation of BAR2 (Mu et al., 2011). On the other hand, Terker et al. showed that acute adrenergic stimulation increased the abundance of pNCC *via* BAR1 stimulation in mice (Terker et al., 2014). More recently, it has been shown that pharmacological stimulation of BAR2 with salbutamol increases both NCC phosphorylation and systolic blood pressure, the latter effect blunted by thiazide (Poulsen et al., 2021). In the present study, we demonstrated that also BAR3 plays an additional, crucial role in NCC modulation. Thus, all three subtypes of BARs are implicated in the control of sodium reabsorption by NCC in DCT.

Boivin et al. previously immunolocalized BAR1 and BAR2 at the apical membrane of DCT cells (Boivin et al., 2001), while we found BAR3 at the basolateral membrane of the same cells (Procino et al., 2016). Although the expression of all BARs in the same cell type could appear redundant, their polarized expression in different plasma membrane domains of the cell could suggest their sequential activation (in time and space) that might finely modulate the activation and expression of NCC. It is conceivable that, in chronological order, circulating catecholamines, upon release by sympathetic nerve terminals, might bind basolateral BAR3 and rapidly activate NCC. Upon prolonged release of catecholamines, they might be filtered by the glomerulus, activate apical BAR1 and BAR2 (Boivin et al., 2001), thus also increasing the expression of NCC. This hypothesis is supported by our findings in mice, that the absence of BAR3 decreased the phosphorylation of NCC and the absence of BAR1/2, preserved the levels of NCC phosphorylation likely because BAR3 might be tonically stimulated by catecholamines released by sympathetic nerves.

A key pathway that modulates NCC phosphorylation involves WNK kinases that interacting with SPAK and OSR1 can, in turn, directly phosphorylate the cotransporter (Richardson and Alessi, 2008). Here, we show that, in BAR3 ko, mice pSPAK was markedly reduced, even though total SPAK was also significantly downregulated, albeit to a lesser extent. Accordingly, we found that BAR3 ko mice have reduced levels of upstream SPAK modulators in the kidney, such as phosphorylated WNK1 and WNK4. This observation nicely fits with the current working model seeing WNKs phosphorylating SPAK (Vitari et al., 2005; Richardson and Alessi, 2008; Richardson et al., 2008), which in turn activates NCC by phosphorylation in DCT (Moriguchi et al., 2005; San-Cristobal et al., 2009). Our hypothesis is indeed that the reduction of WNK-SPAK signaling in the kidney upon BAR3 ko induces the reduction of NCC phosphorylation and activity in these mice. Although BAR2 is also involved in the activation of SPAK and WNK (Poulsen et al., 2021), in the kidney of BAR1/2 ko mice, the activity of SPAK and WNK resulted almost normal or slightly upregulated compared to their controls, thus suggesting that BAR3 alone is sufficient to preserve the WNK-SPAK pathway activation in the kidney under sympathetic stimulation.

Further studies are required to elucidate the mechanisms underlying SPAK downregulation in BAR3 ko mice.

We also explored in BAR3 ko mice, the activity of other pathways, either upstream or downstream the WNK-SPAK axis. It has been reported that WNK4 may affect the ERK1/2 pathway, which may in turn influence NCC activation (Zhou et al., 2012). However, we found that the ERK1/2-pERK1/2 ratio was unchanged in BAR3 ko animals compared to their wt controls, likely suggesting that the ERK signaling is not involved in the inactivation of NCC observed in these animals. PKC is also considered a modulator of WNK4 (Shibata et al., 2014), as its activation in physiological conditions phosphorylates Kelch-like 3 motifs of the ubiquitin ligases containing Cullin 3, preventing its binding to WNK4 and reducing its degradation. Interestingly, in our BAR3 ko mouse model, the levels of phosphorylated/active PKC were significantly reduced, in the absence of apparent PKC downregulation. This might explain the reduced expression of WNK4 in these mice. In this scenario, the absence of BAR3 expression at the basolateral membrane should reduce, at the same time, the activation of both PKA, through the Gαs subunit and PKC activation *via* the βγ dimer (Zhong et al., 2001).

The role of the cAMP/PKA pathway triggered by vasopressin in the DCT (Mutig et al., 2010; Pedersen et al., 2010; Saritas et al., 2013) has been recently further enriched by the observations that PKA might also phosphorylate WNK4 and, in turn, mediate the PPAK/OSR1-NCC activation (Castañeda-Bueno et al., 2017). As we demonstrated in renal cells (Milano et al., 2018), BAR3, like the vasopressin receptor AVPR2, is coupled to the cAMP pathway and this would explain the reduced NCC phosphorylation in BAR3 ko mice. Furthermore, the observation reported here, that H89 prevents the effect of BAR3 stimulation on NCC phosphorylation in kidney slices, supports a key role of PKA in the regulation of NCC activity by BAR3.

A limitation of our study could be that we only used male mice. Unfortunately, studies on NCC activation are not suitable in female since it has been reported that NCC expression and activity is higher in female than male due to ovarian hormones and prolactin (Rojas-Vega et al., 2015; Veiras et al., 2017). However, we think that this did not affect the impact of our findings in the scenario of kidney physiology.

This piece of information about the role of BAR3 in regulating NCC function in the DCT has a key importance in the context of the autonomic regulation of water and salt homeostasis in the kidney and, consequently, in the control of blood pressure (Crowley and Coffman, 2014).

It is known that the kidney is densely innervated by sympathetic nerves which activity is increased in hypertension (Sata et al., 2018), as demonstrated by catheter-based renal sympathetic denervation experiments (Krum et al., 2009; Schlaich et al., 2009). The critical role of NCC in the maintenance of blood pressure is also highlighted by genetic diseases as Gitelman (Riveira-Munoz et al., 2007) and Gordon's syndrome (Simonetti et al., 2012) and by its role in the development of salt-sensitive hypertension (Moes et al., 2014). Matayoshi e al. reported that a BAR3 gene polymorphism (T727C) was susceptible to the antihypertensive effect of thiazide in patients with essential hypertension (Matayoshi et al., 2004).

Our findings unveil a new BAR3-dependent regulatory mechanism of NCC activity in the DCT, which, in addition to the thick ascending limb, the connecting tubule and the collecting duct, play a pivotal role in the fine-tuning of sodium and water excretion. As the role of BAR3, as regulator of multiple segments of the kidney tubule becomes clearer, the emerging frame is that sympathetic activation might sustain stress responses by rapidly increasing blood pressure and blood perfusion in physiological conditions, independently of aldosteron and K^+ blood levels. The other side of the coin, which needs more in-depth studies, is that the pharmacological antagonism of BAR3 might represent a tool to take hypertension under control.

DATA AVAILABILITY STATEMENT

The raw data supporting the conclusions of this article will be made available by the authors, without undue reservation.

ETHICS STATEMENT

The animal study was reviewed and approved by the Procedures were approved by the Ethical Committee in Animal Experiments of the University of Bari.

AUTHOR CONTRIBUTIONS

SM and GP: conceptualization. SM: methodology and writing – original draft preparation. IS, AG, and MC: formal analysis. IS, SM, and DL: investigation. MD and PB: resources. GP, MD, PB, and MC: writing – review and editing. GP: visualization and supervision. MS: project administration. MS and GP: funding acquisition. All authors have read and agreed to the published version of the manuscript.

FUNDING

This work was funded by grants GGP15083 from the Fondazione Telethon to MS and Proof of Concept PoC01_00072 from MIUR to GP. SM is supported by "Attraction and International Mobility," PON "R&I" 2014–2020, Azione I.2″ (code AIM1893457).

ACKNOWLEDGMENTS

We are grateful to Gaetano De Vito for animal care.

REFERENCES

Bernstein, D., Fajardo, G., Zhao, M., Urashima, T., Powers, J., Berry, G., et al. (2005). Differential cardioprotective/cardiotoxic effects mediated by beta-adrenergic receptor subtypes. *Am. J. Physiol. Heart Circ. Physiol.* 289, H2441–H2449. doi: 10.1152/ajpheart.00005.2005

Boivin, V., Jahns, R., Gambaryan, S., Ness, W., Boege, F., and Lohse, M. J. (2001). Immunofluorescent imaging of β1- and β2-adrenergic receptors in rat kidney. *Kidney Int.* 59, 515–531. doi: 10.1046/j.1523-1755.2001.059002515.x

Boss, O., Bachman, E., Vidal-Puig, A., Zhang, C. Y., Peroni, O., and Lowell, B. B. (1999). Role of the β3-adrenergic receptor and/or a putative β4-adrenergic receptor on the expression of uncoupling proteins and peroxisome proliferator-activated receptor-γ coactivator-1. *Biochem. Biophys. Res. Commun.* 261, 870–876. doi: 10.1006/bbrc.1999.1145

Castañeda-Bueno, M., Arroyo, J. P., Zhang, J., Puthumana, J., Yarborough, O., Shibata, S., et al. (2017). Phosphorylation by PKC and PKA regulate the kinase activity and downstream signaling of WNK4. *Proc. Natl. Acad. Sci. U. S. A.* 114, E879–E886. doi: 10.1073/pnas.1620315114

Crowley, S. D., and Coffman, T. M. (2014). The inextricable role of the kidney in hypertension. *J. Clin. Invest.* 124, 2341–2347. doi: 10.1172/JCI72274

Deschepper, C. F., Olson, J. L., Otis, M., and Gallo-Payet, N. (2004). Characterization of blood pressure and morphological traits in cardiovascular-related organs in 13 different inbred mouse strains. *J. Appl. Physiol.* 97, 369–376. doi: 10.1152/japplphysiol.00073.2004

Ecker, P. M., Lin, C. C., Powers, J., Kobilka, B. K., Dubin, A. M., and Bernstein, D. (2006). Effect of targeted deletions of beta1- and beta2-adrenergic-receptor subtypes on heart rate variability. *Am. J. Physiol. Heart Circ. Physiol.* 290, H192–H199. doi: 10.1152/ajpheart.00032.2005

Hadchouel, J., Ellison, D. H., and Gamba, G. (2016). Regulation of renal electrolyte transport by WNK and SPAK-OSR1 kinases. *Annu. Rev. Physiol.* 78, 367–389. doi: 10.1146/annurev-physiol-021115-105431

Huang, C. L., and Cheng, C. J. (2015). A unifying mechanism for WNK kinase regulation of sodium-chloride cotransporter. *Pflugers Arch. Eur. J. Physiol.* 467, 2235–2241. doi: 10.1007/s00424-015-1708-2

Krum, H., Schlaich, M., Whitbourn, R., Sobotka, P. A., Sadowski, J., Bartus, K., et al. (2009). Catheter-based renal sympathetic denervation for resistant hypertension: a multicentre safety and proof-of-principle cohort study. *Lancet* 373, 1275–1281. doi: 10.1016/S0140-6736(09)60566-3

Martelli, A., Testai, L., Anzini, M., Cappelli, A., Di Capua, A., Biava, M., et al. (2013). The novel anti-inflammatory agent VA694, endowed with both NO-releasing and COX2-selective inhibiting properties, exhibits NO-mediated positive effects on blood pressure, coronary flow and endothelium in an experimental model of hypertension and endotheli. *Pharmacol. Res.* 78, 1–9. doi: 10.1016/j.phrs.2013.09.008

Matayoshi, T., Kamide, K., Takiuchi, S., Yoshii, M., Miwa, Y., Takami, Y., et al. (2004). The thiazide-sensitive Na^+-CI^- cotransporter gene, C1784T, and adrenergic receptor-β3 gene, T727C, may be gene polymorphisms susceptible to the antihypertensive effect of thiazide diuretics. *Hypertens. Res.* 27, 821–833. doi: 10.1291/hypres.27.821

Milano, S., Gerbino, A., Schena, G., Carmosino, M., Svelto, M., and Procino, G. (2018). Human β3-adrenoreceptor is resistant to agonist-induced desensitization in renal epithelial cells. *Cell. Physiol. Biochem.* 48, 847–862. doi: 10.1159/000491916

Moens, A. L., Leyton-Mange, J. S., Niu, X., Yang, R., Cingolani, O., Arkenbout, E. K., et al. (2009). Adverse ventricular remodeling and exacerbated NOS uncoupling from pressure-overload in mice lacking the β3-adrenoreceptor. *J. Mol. Cell. Cardiol.* 47, 576–585. doi: 10.1016/j.yjmcc.2009.06.005

Moes, A. D., van der Lubbe, N., Zietse, R., Loffing, J., and Hoorn, E. J. (2014). The sodium chloride cotransporter SLC12A3: new roles in sodium, potassium,

and blood pressure regulation. *Pflugers Arch. Eur. J. Physiol.* 466, 107–118. doi: 10.1007/s00424-013-1407-9

Moriguchi, T., Urushiyama, S., Hisamoto, N., Iemura, S., Uchida, S., Natsume, T., et al. (2005). WNK1 regulates phosphorylation of cation-chloride-coupled cotransporters via the STE20-related kinases, SPAK and OSR1. *J. Biol. Chem.* 280, 42685–42693. doi: 10.1074/jbc.M510042200

Mu, S. Y., Shimosawa, T., Ogura, S., Wang, H., Uetake, Y., Kawakami-Mori, F., et al. (2011). Epigenetic modulation of the renal β-adrenergicg-WNK4 pathway in salt-sensitive hypertension. *Nat. Med.* 17, 573–580. doi: 10.1038/nm.2337

Mutig, K., Saritas, T., Uchida, S., Kahl, T., Borowski, T., Paliege, A., et al. (2010). Short-term stimulation of the thiazide-sensitive Na^+-Cl^- cotransporter by vasopressin involves phosphorylation and membrane translocation. *Am. J. Physiol. Physiol.* 298, F502–F509. doi: 10.1152/ajprenal.00476.2009

Pacheco-Alvarez, D., San Cristóbal, P., Meade, P., Moreno, E., Vazquez, N., Muñoz, E., et al. (2006). The Na^+:Cl^- cotransporter is activated and phosphorylated at the amino-terminal domain upon intracellular chloride depletion. *J. Biol. Chem.* 281, 28755–28763. doi: 10.1074/jbc.M603773200

Pedersen, N. B., Hofmeister, M. V., Rosenbaek, L. L., Nielsen, J., and Fenton, R. A. (2010). Vasopressin induces phosphorylation of the thiazide-sensitive sodium chloride cotransporter in the distal convoluted tubule. *Kidney Int.* 78, 160–169. doi: 10.1038/ki.2010.130

Poulsen, S. B., Cheng, L., Penton, D., Kortenoeven, M. L. A., Matchkov, V. V., Loffing, J., et al. (2021). Activation of the kidney sodium chloride cotransporter by the β2-adrenergic receptor agonist salbutamol increases blood pressure. *Kidney Int.* doi: 10.1016/j.kint.2021.04.021 [Epub ahead of print]

Procino, G., Carmosino, M., Milano, S., Dal Monte, M., Schena, G., Mastrodonato, M., et al. (2016). β3 adrenergic receptor in the kidney may be a new player in sympathetic regulation of renal function. *Kidney Int.* 90, 555–567. doi: 10.1016/j.kint.2016.03.020

Procino, G., Milano, S., Carmosino, M., Barbieri, C., Nicoletti, M. C., Li, H. J., et al. (2014). Combination of secretin and fluvastatin ameliorates the polyuria associated with X-linked nephrogenic diabetes insipidus in mice. *Kidney Int.* 86, 127–138. doi: 10.1038/ki.2014.10

Richardson, C., and Alessi, D. R. (2008). The regulation of salt transport and blood pressure by the WNK-SPAK/OSR1 signalling pathway. *J. Cell Sci.* 121, 3293–3304. doi: 10.1242/jcs.029223

Richardson, C., Rafiqi, F. H., Karlsson, H. K. R., Moleleki, N., Vandewalle, A., Campbell, D. G., et al. (2008). Activation of the thiazide-sensitive Na^+-cl^- cotransporter by the WNK-regulated kinases SPAK and OSR1. *J. Cell Sci.* 121, 675–684. doi: 10.1242/jcs.025312

Riveira-Munoz, E., Chang, Q., Bindels, R. J., and Devuyst, O. (2007). Gitelman's syndrome: towards genotype-phenotype correlations? *Pediatr. Nephrol.* 22, 326–332. doi: 10.1007/s00467-006-0321-1

Rohrer, D. K., Chruscinski, A., Schauble, E. H., Bernstein, D., and Kobilka, B. K. (1999). Cardiovascular and metabolic alterations in mice lacking both β1- and β2-adrenergic receptors. *J. Biol. Chem.* 274, 16701–16708. doi: 10.1074/jbc.274.24.16701

Rojas-Vega, L., and Gamba, G. (2016). Mini-review: regulation of the renal NaCl cotransporter by hormones. *Am. J. Physiol. Ren. Physiol.* 310, F10–F14. doi: 10.1152/ajprenal.00354.2015

Rojas-Vega, L., Reyes-Castro, L. A., Ramírez, V., Bautista-Pérez, R., Rafael, C., Castañeda-Bueno, M., et al. (2015). Ovarian hormones and prolactin increase renal NaCl cotransporter phosphorylation. *Am. J. Physiol. Physiol.* 308, F799–F808. doi: 10.1152/ajprenal.00447.2014

San-Cristobal, P., Pacheco-Alvarez, D., Richardson, C., Ring, A. M., Vazquez, N., Rafiqi, F. H., et al. (2009). Angiotensin II signaling increases activity of the renal Na-Cl cotransporter through a WNK4-SPAK-dependent pathway. *Proc. Natl. Acad. Sci. U. S. A.* 106, 4384–4389. doi: 10.1073/pnas.0813238106

Saritas, T., Borschewski, A., McCormick, J. A., Paliege, A., Dathe, C., Uchida, S., et al. (2013). SPAK differentially mediates vasopressin effects on sodium cotransporters. *J. Am. Soc. Nephrol.* 24, 407–418. doi: 10.1681/ASN.2012040404

Sata, Y., Head, G. A., Denton, K., May, C. N., and Schlaich, M. P. (2018). Role of the sympathetic nervous system and its modulation in renal hypertension. *Front. Med.* 5:82. doi: 10.3389/fmed.2018.00082

Schlaich, M. P., Sobotka, P. A., Krum, H., Lambert, E., and Esler, M. D. (2009). Renal sympathetic-nerve ablation for uncontrolled hypertension. *N. Engl. J. Med.* 361, 932–934. doi: 10.1056/NEJMc0904179

Shibata, S., Arroyo, J. P., Castaneda-Bueno, M., Puthumana, J., Zhang, J., Uchida, S., et al. (2014). Angiotensin II signaling via protein kinase C phosphorylates kelch-like 3, preventing WNK4 degradation. *Proc. Natl. Acad. Sci. U. S. A.* 111, 15556–15561. doi: 10.1073/pnas.1418342111

Simonetti, G. D., Mohaupt, M. G., and Bianchetti, M. G. (2012). Monogenic forms of hypertension. *Eur. J. Pediatr.* 171, 1433–1439. doi: 10.1007/s00431-011-1440-7

Terker, A. S., Yang, C. L., McCormick, J. A., Meermeier, N. P., Rogers, S. L., Grossmann, S., et al. (2014). Sympathetic stimulation of thiazide-sensitive sodium chloride cotransport in the generation of salt-sensitive hypertension. *Hypertension* 64, 178–184. doi: 10.1161/HYPERTENSIONAHA.114.03335

Veiras, L. C., Girardi, A. C. C., Curry, J., Pei, L., Ralph, D. L., Tran, A., et al. (2017). Sexual dimorphic pattern of renal transporters and electrolyte homeostasis. *J. Am. Soc. Nephrol.* 28, 3504–3517. doi: 10.1681/ASN.2017030295

Vitari, A. C., Deak, M., Morrice, N. A., and Alessi, D. R. (2005). The WNK1 and WNK4 protein kinases that are mutated in Gordon's hypertension syndrome phosphorylate and activate SPAK and OSR1 protein kinases. *Biochem. J.* 391, 17–24. doi: 10.1042/BJ20051180

Zhong, J., Hume, J. R., and Keef, K. D. (2001). β-Adrenergic receptor stimulation of L-type Ca^{2+} channels in rabbit portal vein myocytes involves both αs and βγ G protein subunits. *J. Physiol.* 531, 105–115. doi: 10.1111/j.1469-7793.2001.0105j.x

Zhou, B., Wang, D., Feng, X., Zhang, Y., Wang, Y., Zhuang, J., et al. (2012). WNK4 inhibits NCC protein expression through MAPK ERK1/2 signaling pathway. *Am. J. Physiol. Physiol.* 302, F533–F539. doi: 10.1152/ajprenal.00032.2011

Conflict of Interest: The authors declare that the research was conducted in the absence of any commercial or financial relationships that could be construed as a potential conflict of interest.

Publisher's Note: All claims expressed in this article are solely those of the authors and do not necessarily represent those of their affiliated organizations, or those of the publisher, the editors and the reviewers. Any product that may be evaluated in this article, or claim that may be made by its manufacturer, is not guaranteed or endorsed by the publisher.

frontiers in Physiology

ORIGINAL RESEARCH
published: 25 August 2021
doi: 10.3389/fphys.2021.725782

Stimulation of the Epithelial Na^+ Channel in Renal Principal Cells by Gs-Coupled Designer Receptors Exclusively Activated by Designer Drugs

Antonio G. Soares[1], Jorge Contreras[1], Crystal R. Archer[1], Elena Mironova[1], Rebecca Berdeaux[2], James D. Stockand[1] and Tarek Mohamed Abd El-Aziz[1,3]*

[1] Department of Cellular and Integrative Physiology, University of Texas Health Science Center at San Antonio, San Antonio, TX, United States, [2] Department of Integrative Biology and Pharmacology, University of Texas Health Science Center at Houston, Houston, TX, United States, [3] Zoology Department, Faculty of Science, Minia University, Minya, Egypt

OPEN ACCESS

Edited by:
Soo Wan Kim, Chonnam National University Medical School, South Korea

Reviewed by:
Tingjun Chen, Mayo Clinic, United States
Ferruh Artunc, Tübingen University Hospital, Germany
Zhi-Ren Zhang, Harbin Medical University, China

***Correspondence:**
James D. Stockand
Stockand@uthscsa.edu

Specialty section:
This article was submitted to Renal and Epithelial Physiology, a section of the journal Frontiers in Physiology

Received: *15 June 2021*
Accepted: *28 July 2021*
Published: *25 August 2021*

Citation:
Soares AG, Contreras J, Archer CR, Mironova E, Berdeaux R, Stockand JD and Abd El-Aziz TM (2021) Stimulation of the Epithelial Na^+ Channel in Renal Principal Cells by Gs-Coupled Designer Receptors Exclusively Activated by Designer Drugs. Front. Physiol. 12:725782. doi: 10.3389/fphys.2021.725782

The activity of the Epithelial Na^+ Channel (ENaC) in renal principal cells (PC) fine-tunes sodium excretion and consequently, affects blood pressure. The Gs-adenylyl cyclase-cAMP signal transduction pathway is believed to play a central role in the normal control of ENaC activity in PCs. The current study quantifies the importance of this signaling pathway to the regulation of ENaC activity *in vivo* using a knock-in mouse that has conditional expression of Gs-DREADD (designer receptors exclusively activated by designer drugs; GsD) in renal PCs. The GsD mouse also contains a cAMP response element-luciferase reporter transgene for non-invasive bioluminescence monitoring of cAMP signaling. Clozapine N-oxide (CNO) was used to selectively and temporally stimulate GsD. Treatment with CNO significantly increased luciferase bioluminescence in the kidneys of PC-specific GsD but not control mice. CNO also significantly increased the activity of ENaC in principal cells in PC-specific GsD mice compared to untreated knock-in mice and CNO treated littermate controls. The cell permeable cAMP analog, 8-(4-chlorophenylthio)adenosine 3′,5′-cyclic monophosphate, significantly increased the activity and expression in the plasma membrane of recombinant ENaC expressed in CHO and COS-7 cells, respectively. Treatment of PC-specific GsD mice with CNO rapidly and significantly decreased urinary Na^+ excretion compared to untreated PC-specific GsD mice and treated littermate controls. This decrease in Na^+ excretion in response to CNO in PC-specific GsD mice was similar in magnitude and timing as that induced by the selective vasopressin receptor 2 agonist, desmopressin, in wild type mice. These findings demonstrate for the first time that targeted activation of Gs signaling exclusively in PCs is sufficient to increase ENaC activity and decrease dependent urinary Na^+ excretion in live animals.

Keywords: vasopressin, sodium excretion, sodium transport, hypertension, epithelial sodium channel

SUMMARY

This study shows that targeted stimulation of Gs signaling in renal principal cells is sufficient to increase ENaC activity and decrease dependent Na^+ excretion. Gs regulation of ENaC is critical to maximizing urine concentration and the normal control of blood pressure.

INTRODUCTION

The epithelial Na^+ channel (ENaC) is expressed in sodium (re)absorbing epithelial tissue to include that lining the aldosterone-sensitive distal nephron, which encompasses the late distal convoluted tubule, the connecting tubule and the collecting duct (Garty and Palmer, 1997; Rossier et al., 2002; Verouti et al., 2015; Hanukoglu and Hanukoglu, 2016). ENaC is restrictively expressed in the luminal plasma membranes of principal cells (PC) in the distal nephron. The activity of ENaC in the luminal plasma membrane of PCs is limiting for cell entry of Na^+ from the urine and consequently, transepithelial Na^+ reabsorption across the distal nephron (Kemendy et al., 1992; Canessa et al., 1993, 1994; Lingueglia et al., 1993). Ultimately, Na^+ reabsorbed via ENaC fine-tunes serum Na^+ levels, and contributes to the renal axial corticomedullary hypertonic gradient that concentrates urine (Reif et al., 1986; Perucca et al., 2008; Stockand, 2010). This makes the proper activity of ENaC critical to the normal control of blood pressure and for maximizing urinary water concentration (Bugaj et al., 2009). Because of this function, gain- and loss-of-function mutations in ENaC and its upstream regulatory pathways cause disordered blood pressure associated with abnormal renal salt excretion (Garty and Palmer, 1997; Rossier et al., 2002; Verouti et al., 2015; Hanukoglu and Hanukoglu, 2016). Consequently, this key renal ion channel is a druggable target for diuretics and antihypertensive agents to include triamterene and amiloride.

There is considerable evidence that G-protein coupled receptors (GPCRs) signaling through the Gs alpha subunit increase the activity of ENaC by stimulating adenylyl cyclase (AC) and dependent production of cAMP (Bugaj et al., 2009). The antidiuretic hormone, arginine vasopressin (AVP), is thought to increase ENaC activity in such a manner via the GPCR arginine vasopressin receptor 2 (AVPR2) to cause an anti-natriuresis along with its better understood antidiuretic ability (Perucca et al., 2008). Such activation of ENaC likely is key to AVP maximizing urine concentrating ability (Bugaj et al., 2009; Stockand, 2012; Mironova et al., 2012, 2015). While there is considerable evidence that Gs-coupled GPCR signaling is important to ENaC activity, the bulk of this evidence is correlative, derived from pharmacological intervention studies testing necessity, or from *in vitro* work. Moreover, the anti-natriuretic actions of AVP remain controversial (Stockand, 2010). Thus, it currently is obscure whether stimulating Gs signaling in isolation is sufficient to activate ENaC in living animals, and whether this alone is capable of inducing a quantifiable anti-natriuresis.

The current study tests the hypothesis that targeted stimulation of Gs in PCs is sufficient to increase ENaC activity in living animals and that such activation of ENaC is sufficient to drive decreases in urinary Na^+ excretion. Moreover, these studies determined the mechanism by which Gs-cAMP signaling increases ENaC activity. The current findings demonstrate that exclusive activation of Gs signaling in renal PCs is sufficient to rapidly increase ENaC activity to decrease Na^+ excretion. Gs signaling does this by promoting cAMP-mediated increases in ENaC expression in the plasma membrane, which increases channel activity.

MATERIALS AND METHODS

Animals

All animal use and welfare adhered to the National Institutes of Health *Guide for the Care and Use of Laboratory Animals*. Protocols were reviewed and approved by the Institutional Animal Care and Use Committee of the University of Texas Health Science Center at San Antonio. Mice were housed and cared for in the Laboratory Animal Resources Facility at the University of Texas Health Science Center at San Antonio, which is fully accredited by the Association for Assessment and Accreditation of Laboratory Animal Care, and licensed by the United States Department of Agriculture. Results involving animal studies were in compliance with Animal Research: Reporting of *in vivo* Experiments guidelines (Kilkenny et al., 2010).

Healthy young adult (2–3 months, 20.61 $\pm$ 0.18 g body weight) male and female mice were used in approximately equal proportions for these studies. Experimental mice had PC-specific expression of GsD and control mice were either wild type, Aqp2-cre negative, or GsD negative littermates (see below). All mice, during acclimation and experimental periods, were maintained on a normal 12:12 h light-dark cycle at room temperature and had free access to water and chow. All experimental perturbations, including injections with CNO and D-Luciferin were performed within a constant time window (midmorning) in the laboratory where mice were housed. The primary end points for experiments involving mice in these studies were whole body bioluminescence in live animals, 24 h urinary excretion studies, and humane euthanasia followed by collection of kidneys for microdissection of renal nephrons compatible with electrophysiological assessment of ENaC activity in the split-open connecting tubule/cortical collecting duct.

Creation of the Principal Cell-Specific Gs-DREADD Mouse

Target expression of Gs-DREADD (GsD) in renal PCs was achieved by crossing male *ROSA26-LSL-GsDREADD-CRE-luc* knock-in mice with female B6.Cg-Tg(Aqp2-cre)1Dek/J mice. With this knock-in allele, GsD is expressed in targeted cells following Cre-mediated recombination and deletion of the "lox-stop-lox" cassette (LSL), and cAMP-dependent signaling is reported by a cAMP-response element-sensitive luciferase (CRE-luc) independent of expression of Cre recombinase.

The *ROSA26-LSL-GsDREADD-CRE-luc* knock-in mouse was created by Dr. R. Berdeaux and has been described previously (Akhmedov et al., 2017). The B6.Cg-Tg(Aqp2-cre)1Dek/J mouse was from Dr. D. Kohan (University of Utah Health Science Center, Salt Lake City, Utah, United States) and has been described previously (Nelson et al., 1998; Stricklett et al., 1999). The PC-specific GsD knockin line was continued by backcrossing GsD:Aqp2-cre female to GsD male mice. GsD:Aqp2-cre-positive mice were used for experiments. Wild type and Aqp2-cre-negative littermates lacking or harboring GsD were used as control. No noticeable difference in behavior, body weight, pathology, or any other gross attribute was observed between GsD:Aqp2-cre and littermate controls.

For genotyping reactions, like those shown in **Figure 1**, the GsD transgene was identified with the forward 5′-CTCGAAGTACTCGGCGTAGG-3′ and reverse 5′-CTCGAAGTACTCGGCGTAGG-3′ PCR primers, producing an expected 206-bp product. The wild type allele, which lacked insertion of the GsD transgene, was identified with the forward 5′-AAGGGAGCTGCAGTGGAGTA-3′ (in the upstream homology arm) and reverse 5′-CCGAAAATCTGTGGGAAGTC-3′ (in the downstream homology arm) PCR primers, producing an expected 297-bp product. The Aqp2-cre transgene was identified with the forward 5′-CTCTGCAGGAACTGGTGCTGG-3′ and reverse 5′-GCGAACATCTTCAGGTTCTGCGG-3′ PCR primers, producing an expected 673-bp product.

cDNA Constructs and Cell Culture

African green monkey kidney fibroblast-like (COS-7) cells were purchased from ATCC (American Type Culture Collection, ATCC, Manassas, VA, United States). COS-7 cells were cultured in Dulbecco's modified Eagle's medium supplemented with 10% fetal bovine serum (FBS) and 1% penicillin-streptomycin (PS). CHO cells were cultured in Ham's F-12K Nutrient Mixture (Kaighn's Mod.) supplemented with 10% FBS and 1% PS. All cells were incubated at 37°C in a humidified incubator supplying 5% CO_2. For TIRF-FRAP experiments (see below), COS-7 cells were plated on glass bottom MatTek dishes (35 mm petri dish-14 mm microwell, MatTek Co., MA, United States) and transfected with plasmids encoding α-, β-, and γ-mouse ENaC subunits genetically linked to NH_2-terminal eYFP (Staruschenko et al., 2005) using Lipofectamine 3000 reagent (L3000015, Invitrogen, Carlsbad, CA, United States) according to the manufacturer's protocol. In brief, 60% confluent cells in a 35 mm dish were incubated with 2 μg of total plasmid cDNA for 4–5 h. Media was then removed and replaced with fresh media with cells used within 24–48 h after transfection. For patch-clamp recording of macroscopic ENaC currents (see below), CHO cells were plated on coverglass chips treated with 0.01% Poly-L-lysine (Sigma-Aldrich, St. Louis, MO, United States). Plated cells were transfected with plasmids encoding α-, β-, and γ-mouse ENaC subunits genetically linked to NH_2-terminal eCFP (Staruschenko et al., 2005) using Polyfect reagent (Qiagen, Valencia, CA, United States) according to the manufacturer's protocol. In brief, 60% confluent cells in a 35 mm dish were incubated with 2 μg of total plasmid cDNA for 4–5 h, media was then removed and replaced with fresh media, and transfected cells used within 24–48 h. Transfected cells were maintained in culture in the presence of 10 μM amiloride replenished daily.

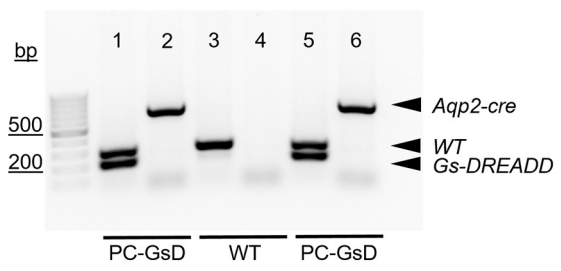

FIGURE 1 | PC-specific GsD mice. Micrograph of a representative gel containing products from genotyping reactions for two PC-specific GsD mice (lanes 1, 2, 5, and 6) and one wild type littermate control mouse (lanes 3 and 4). Products for the Aqp2-cre and GsD transgenes, and the wild type allele are indicated with arrowheads. For presentation purposes, contrast and brightness were adjusted, and the image was inverted (black to white) to maximize clarity without changing content. bp, base pairs.

Bioluminescence Reporter Imaging

Bioluminescence imaging was performed on mice before and 6 h after injection of CNO (10 mg/kg; s.c.) as previously described (Akhmedov et al., 2019). In brief, mice were anesthetized by isoflurane inhalation (2% v/v), injected (i.p.) with D-Luciferin (100 mg/kg), and transferred to the heated stage (37°C) of an Ivis Lumina XR Instrument (Capiler Life Science) for imaging (F-stop 1, binning 4). Image analysis was performed by selecting regions of interest to quantify luminescence signals using Caliper Living Image software. Pseudocolored images were overlaid onto photographs of the same animals and exported using matched visualization settings.

Single-Channel Patch-Clamp Electrophysiology

Split-open tubules amenable to patch clamp analysis were prepared as previously described (Mironova et al., 2013, 2019). In brief, freshly isolated mouse kidneys were sectioned transversely. Segments of the CNT and CCD were manually microdissected with watchmaker forceps under a stereomicroscope and adhered to a glass chip coated with 0.01% poly-lysine. These chips then were transferred to an inverted microscope, where tubules were split open with sharpened pipettes. Gap-free single-channel patch-clamp electrophysiology in the cell-attached configuration ($-V_p = -60$ mV) was then performed on the luminal plasma membranes of PCs in these split-opened tubules following standard protocols (Bugaj et al., 2012; Stockand et al., 2012; Berman et al., 2018; Mironova et al., 2019). Split-open tubules were used within 1–2 h of isolation. The bath solution contained (in mM): 150 NaCl, 5 KCl, 1 $CaCl_2$, 2 $MgCl_2$, 5 glucose and 10 HEPES (pH 7.4); and the pipette solution (in mM): 140 LiCl, 2 $MgCl_2$, and 10 HEPES (pH 7.4). Channel activity (NP_o; open

probability, P_o, multiplied by channel number, N) was calculated as previously described (Stockand et al., 2012; Berman et al., 2018; Mironova et al., 2019). ENaC activity was recorded in tubules pre-treated with vehicle or CNO (2 μg/ml) for 30 min prior to patch clamp analysis.

Total Internal Reflection Fluorescence Microscopy—Fluorescence Recovery After Photobleaching (TIRF-FRAP)

Total internal reflection fluorescence (TIRF) microscopy followed standard procedures (Staruschenko et al., 2005; Abd El-Aziz et al., 2021). In brief, fluorescence emissions from membrane eYFP-tagged ENaC were collected in COS-7 cells at room temperature using TIRF microscopy to selectively illuminate the plasma membrane. TIRF generates an evanescent field that declines exponentially with increasing distance from the interface between the cover glass and plasma membrane illuminating only a thin section (∼100 nm) of the cell in contact with the cover glass. All TIRF experiments were performed in the TIRF microscopy Core Facility housed within the Department of Cellular and Integrative Physiology at the University of Texas Health Science Center, San Antonio. Fluorescence emissions from fluorophore-tagged ENaC were collected using an inverted TE2000 microscope with through-the-lens (prismless) TIRF imaging (Nikon, Melville, NY, United States). This system is equipped with a vibration isolation system (Technical Manufacturing Co., Peabody, MA, United States) to minimize drift and noise. Samples were imaged through a plain Apo TIRF 60x oil immersion and high resolution (1.45 NA) objective. Fluorescence emissions from tagged subunits were collected with the Chroma Technology Co. (Bellows Falls, VT, United States) 514 nm laser filter set with band-pass emission (Z514BP) by exciting eYFP with an argon ion laser (80 mW) with an acoustic optic tunable filter (Prairie Technologies, Hutto, TX, United States) used to restrict excitation wavelength to 514 nm. In this system, a 514 nm dichroic mirror (Z514rdc) separates the 514/10 nm (Z514/10x) and 560/50 nm (HQ560/50m) excitation and emission filters. Fluorescence images were collected and processed with a 16-bit, cooled charge-coupled device camera (Cascade 512F; Roper Scientific, Sarasota, FL, United States) interfaced to a PC running Metamorph software (Molecular Devices, San Jose, CA, United States). This camera uses a front-illuminated EMCCD with on-chip multiplication gain. Images were collected with a 200 ms exposure time immediately before and after photobleaching and every subsequent minute for a total period of 10 min.

Fluorophore-tagged channels in the plasma membrane were photobleached with TIRF illumination using the argon ion laser (514 nm) at full power (100%) for 10 sec. Fluorescence emissions from membrane localized fluorophores were collected under TIRF illumination before and after photobleaching. Laser power, camera gain, and exposure times were constant throughout the course of these fluorescence recovery after photobleaching (FRAP) experiments except during photobleaching as noted above. All TIRF-FRAP experiments were performed 48 h after transfection.

Whole-Cell Patch Clamp Electrophysiology

Whole-cell macroscopic current recordings of mouse ENaC expressed in CHO cells were performed under voltage clamp condition using standard methods (Staruschenko et al., 2006). In brief, current through ENaC was the macroscopic, amiloride-sensitive Na^+ current with a bath solution of (in mM) 150 NaCl, 1 $CaCl_2$, 2 $MgCl_2$, and 10 HEPES (pH 7.4) and a pipette solution of (in mM) 120 CsCl, 5 NaCl, 2 $MgCl_2$, 5 EGTA, 10 HEPES, 2 ATP, and 0.1 GTP (pH 7.4). Current recordings were acquired with an Axopath 200B (Molecular Devices, San Jose, CA, United States) patch-clamp amplifier interfaced via a Digidata 1550B (Molecular Devices, San Jose, CA, United States) to a PC running pClamp 11 software (Molecular Devices, San Jose, CA, United States). All currents were filtered at 1 kHz. Cells were clamped to a 40 mV holding potential with voltage ramps (500 ms) from 60 to −100 mV. Whole-cell capacitance, on average 8–10 pF, was compensated. Series resistance, on average 3–6 MΩ, was also compensated. Current conducted by ENaC was the amiloride-sensitive Na^+ current.

Metabolic Cages Experiments

Metabolic cage experiments quantifying excretion over a 24 h period followed previously published protocols with minor modifications (Mironova et al., 2015, 2019; Berman et al., 2018). In brief, age and weight matched PC-specific GsD and littermate control mice were housed in metabolic cages (1 mouse/cage; Techniplast, Buguggiate, Italy) and allowed to acclimate for 2 days. On the third day, 24 h urines were collected before CNO injection. Urine (24 h) was collected again on the fourth day following injection with CNO (0.1 mg/kg; s.c.). In a second set of experiments, wild type littermate mice were treated with the AVPR2 selective agonist, deamino-Cys,D-Arginine-vasopressin (dDAVP; desmopressin; 1 μg/100 μl water, i.p.), prior to collection of 24 h urine on the fourth day. Collection surfaces in contact with urine where coated with Sigmacote (Sigma-Aldrich, St. Louis, MO, United States), and urine was collect under light mineral oil to increase the precision of these measurements by reducing resistance to flow to the final collecting reservoir and to minimize loss due to evaporation. Urinary Na^+ (U_{Na}) and K^+ (U_K) concentration were quantified with a flame photometer (Jenway, Staffordshire, United Kingdom). Urinary osmolality was quantified with a vapor pressure osmometer (Wescor, Logan, UT, United States). Urinary [Na^+] and [K^+] were multiplied by 24 h urine volume (V) to obtain excretion.

Statistical Analysis

Data were analyzed and plotted using GraphPad Prism 9 (GraphPad Software, Inc., San Diego, CA, United States). Values reported as mean ± standard error of the mean (SEM). Data were compared using a two-sample, two-tailed or paired *t*-test as appropriate, and a $P \leq 0.05$ was considered significance.

RESULTS

Targeted Stimulation of GsD Increases cAMP-Response Element Reporter Activity Selectively in the Kidneys of PC-Specific GsD Knockin Mice

We began these studies by testing whether targeted expression of GsD in PCs resulted in selective and temporal cAMP signaling in the kidney. *In vivo* bioluminescence responsive to signaling through the cAMP-response element (CRE) was evaluate in wild type littermate and PC-specific GsD mice before and 6 h after treatment with CNO. **Figure 2A** shows representative micrographs reporting CRE-sensitive bioluminescence in littermate controls (left) before (top) and after treatment with CNO (bottom), and in PC-specific GsD (right) mice before (top) and after (bottom) treatment with CNO. A summary graph of results from such experiments is shown in **Figure 2B**. As expected, no bioluminescence activity (above background) was observed in control mice in the absence (0.09 ± 0.05 photons/s $\times 10^7$) or presence (0.08 ± 0.04 photons/s $\times 10^7$) of CNO (not shown in summary figure; $n = 7$). In contrast, treatment with CNO significantly increased CRE-sensitive bioluminescence selectively in the kidneys of PC-specific GsD knockin mice from background levels of 0.12 ± 0.03 to 1.38 ± 0.29 photons/s $\times 10^7$ within 6 h of treatment.

Targeted Activation of Gs-DREADD in Principal Cells Increases ENaC Activity

We tested next whether selective stimulation of Gs signaling in PCs was sufficient to increase ENaC activity. ENaC activity (NP_o) in the apical plasma membranes of PCs in tubules isolated from littermate control and PC-specific GsD mice was quantified in cell-attached patches using patch clamp electrophysiology. **Figure 3** shows representative current traces for ENaC in tubules isolated from control (**Figure 3A**) and PC-specific GsD (**Figure 3B**) mice before (top) and after (bottom) treatment with CNO. **Figures 3C–F** summarize all such results. **Figure 3C** shows that ENaC activity (NP_o) in tubules from control mice was unaffected by treatment with CNO (0.42 ± 0.12 vs. 0.41 ± 0.14). In contrast, CNO significantly increased ENaC activity in PCs in tubules isolated from PC-specific GsD mice from 0.31 ± 0.13 to 0.90 ± 0.18 (**Figure 3D**). The activity of ENaC in tubules from PC-specific GsD mice in the absence of CNO was not different than that in littermate controls. Increases in both ENaC number (N; 1.73 ± 0.30 vs. 3.00 ± 0.36; **Figure 3E**) and open probability (P_o; 0.12 ± 0.03 vs. 0.27 ± 0.03; **Figure 3F**) drove activity increases in PC-specific GsD mice in response to CNO treatment.

cAMP Signaling Increases ENaC Expression in the Plasma Membrane, in Part, to Increase Channel Activity

Figure 4A shows representative fluorescence micrographs of the plasma membranes of COS-7 cells expressing eYFP-tagged ENaC in the absence (top) and presence (bottom) of treatment with CPT-cAMP (8-(4-chlorophenylthio)adenosine 3′,5′-cyclic monophosphate) before (left), 10 s after (middle) and 10 min after (right) photobleaching. **Figures 4B,C** show the time-course and magnitude, respectively, of the relative recovery (normalized to pre-bleach levels) of ENaC in the plasma membrane following photobleaching in the absence (white circles) and presence (black circles) of CPT-cAMP. Treatment with cAMP significantly increased relative FRAP of ENaC in the plasma membrane at 10 min from 0.46 ± 0.05 to 0.71 ± 0.05.

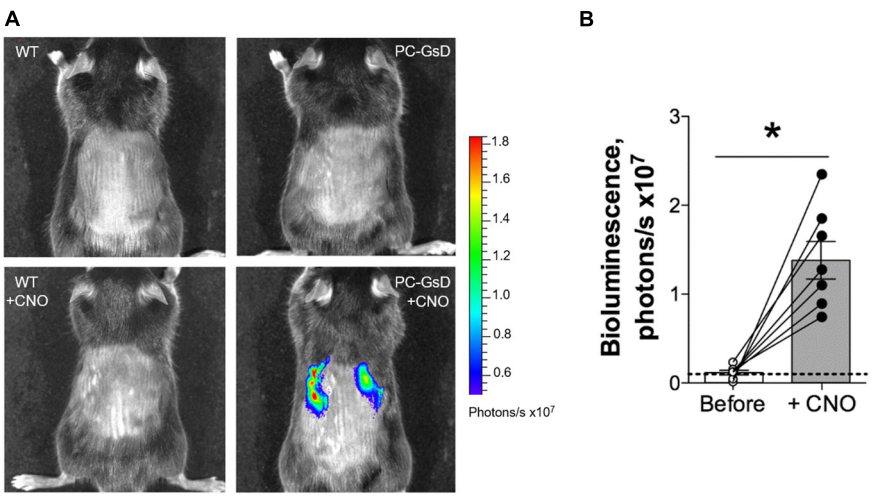

FIGURE 2 | CNO stimulates cAMP-signaling exclusively in the kidneys of PC-specific GsD mice. **(A)** Micrographs showing representative *in vivo* bioluminescence (pseudo-colored for intensity) in control (left) and PC-specific GsD (right) mice before (top) and after (bottom) treatment with CNO (10 mg/kg, 6 h). **(B)** Summary graph of paired data for bioluminescence (photons/s $\times 10^7$) in PC-specific GsD mice before (white circles) and after (black circles) treatment with CNO. Bioluminescence in WT mice in the absence and presence of CNO was never greater than background (not shown). Dashed line indicates background level. Data from experiments ($n = 7$ mice) identical to those shown in **(A)**. *$P < 0.05$ vs. before.

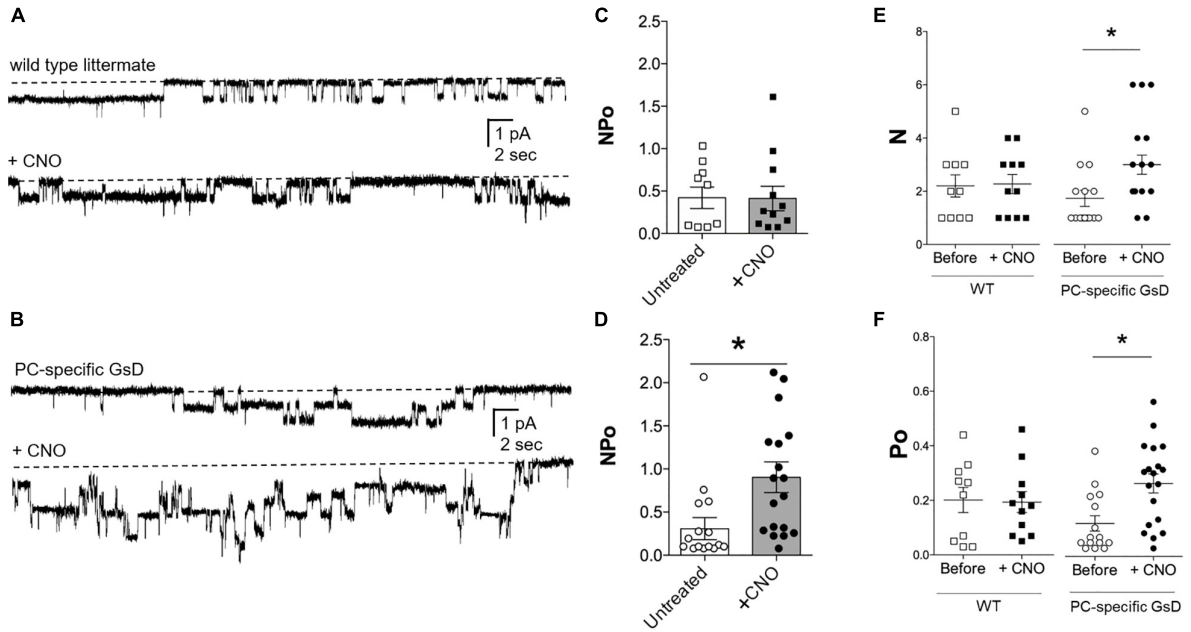

FIGURE 3 | CNO increases ENaC activity in PC-specific GsD mice. Representative gap-free current traces of ENaC in cell-attached patch clamp recordings of the apical membranes of PCs in isolated tubules from wild type littermates **(A)** and PC-specific GsD **(B)** mice in the absence (top) and presence (bottom) of pre-treating tubules with CNO (2 μg/ml, 30 min). Inward Na^+ current is downwards with dashed lines indicating the closed state. Summary graphs of ENaC activity (NP_o) in PCs in tubules isolated from wild type controls **(C)** without (white boxes, n = 9 patches from 3 distinct mice) and with CNO (black boxes; n = 11 patches from 3 distinct mice), and from PC-specific GsD mice **(D)** without (white circles, n = 15 patches from 3 distinct mice) and with CNO (black circles, n = 18 patches from 3 distinct mice). *$P < 0.05$ vs. no CNO treatment. Summary graphs of ENaC N **(E)** and P_o **(F)** in PCs in tubules isolated from wild type controls (white boxes, n = 10 from 3 distinct mice) and after CNO (black boxes, n = 10 from 3 distinct mice); and from PC-specific GsD mice before (white circles, n = 13 from 3 distinct mice) and after CNO (black circles, n = 10 from 3 distinct mice). Summary data from experiments identical to those shown in **(A,B)**. *$P < 0.05$ vs. Before.

Similarly, treatment with CPT-cAMP increased the activity (amiloride-sensitive current density at −100 mV) of recombinant ENaC expressed in CHO cells from 360.6 ± 33.1 in untreated cells to 660 ± 84.2 pA/pF in treated cells. **Figure 4D** shows overlays of representative macroscopic ENaC currents in CHO cells in the absence and presence of CPT-cAMP, and amiloride (dashed lines). Results from these experiments are summarized in **Figure 4E**.

Targeted Activation of Gs-DREADD in Principal Cells Decreases Na^+ Excretion

To understand the physiological consequences of Gs-stimulation of ENaC in PCs in the living animal, we quantified CNO-sensitive urinary Na^+ excretion ($U_{Na}V$) in control littermates and PC-specific GsD mice. **Figures 5A,B** show summary results from paired experiments quantifying $U_{Na}V$ before and after treatment with CNO in control (**Figure 5A**) and PC-specific GsD (**Figure 5B**) mice. Sodium excretion was not significantly affected by CNO in control mice (4.94 ± 0.28 vs. 6.06 ± 0.70 nmol/min/g BW). In contrast, CNO significantly decreased $U_{Na}V$ in PCs-specific GsD mice from 5.12 ± 0.48 to 2.67 ± 0.51 nmol/min/g BW. Sodium excretion in PCs-specific GsD mice before treatment with CNO was not different from that in untreated control mice. **Figure 5C** shows summary results for $U_{Na}V$ in PCs-specific GsD mice before and after treatment with CNO, and control littermates before and after treatment with the selective AVPR2 agonist, desmopressin. As expected, desmopressin significantly decreased sodium excretion from 6.72 ± 0.95 to 4.06 ± 0.23 nmol/min/g BW. Sodium excretion in PC-specific GsD with CNO, though, was not different from that in wild type mice with dDAVP at these doses and times. Similarly, $U_{Na}V$ in PC-GsD mice prior to treatment with CNO did not differ from that in untreated control mice. These summary results demonstrate that the effects on sodium excretion of CNO in PCs-specific GsD mice are similar to that of desmopressin in control mice with respect to timing and magnitude.

Table 1 shows summary results for U_KV and osmolality in WT and PC-specific GsD mice before and after treatment with CNO. Potassium excretion was not significantly affected by CNO in control mice (11.20 ± 1.3 vs. 10.37 ± 1.4 nmol/min/g BW). In contrast, CNO significantly increased U_KV in PCs-specific GsD mice from 14.27 ± 1.5 to 31.49 ± 4.7 nmol/min/g BW. Osmolality was not significantly affected by CNO in control mice (1,799 ± 105 vs. 1,836 ± 90.78 mmol/kg). CNO treatment significantly increased urine osmolality in PCs-specific GsD mice from 1,997 ± 119 vs. 2,438 ± 109 mmol/kg. These effects on potassium excretion and osmolality in the PCs-specific GsD mice are consistent with the actions of vasopressin and with effects on $U_{Na}V$, and consistent with targeted activation of ENaC in PCs of the distal nephron.

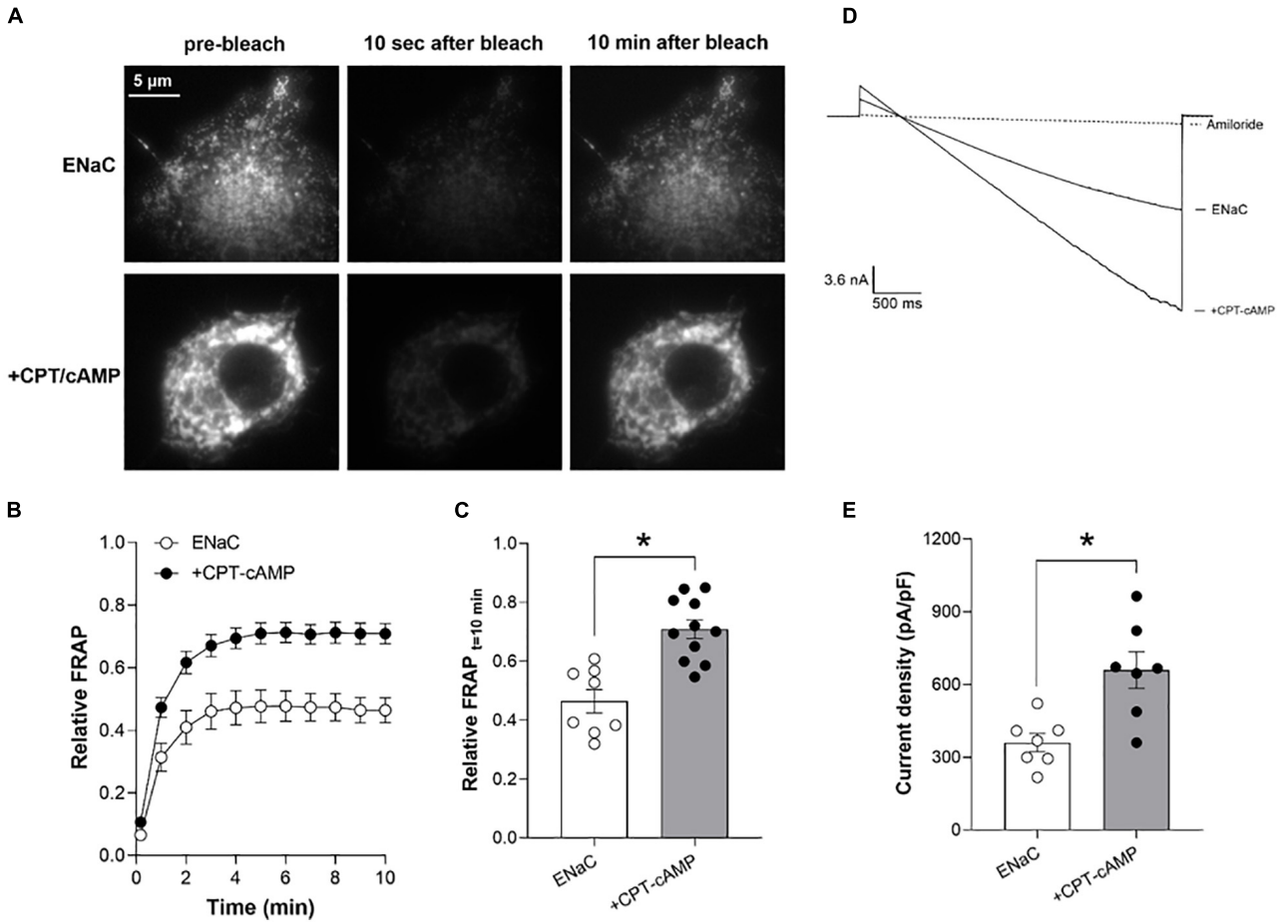

FIGURE 4 | cAMP signaling increases ENaC expression in the plasma membrane to increase channel activity. **(A)** Representative fluorescence micrographs of the plasma membranes of COS-7 cells expressing recombinant eYFP-ENaC in the absence (top) and presence of CPT-cAMP (bottom) prior to photobleaching (left) and 10 s (middle) and 10 min (right) after photobleaching. Images were collected with TIRF microscopy. **(B)** Time courses of relative FRAP at the plasma membrane for cells expressing eYFP-ENaC in the absence (white circles, $n = 8$) and presence of CPT-cAMP (200 mM; black circles; $n = 11$). Summary data from experiments identical to those shown in **(A)**. **(C)** Summary graph of relative FRAP 10 min after photobleaching in cells expressing eYFP-ENaC in the absence (white circles, white bar) and presence of CPT-cAMP (black circles, gray bar). Summary data from experiments identical to those shown in **(A)**. $^*P < 0.05$ vs. no CPT-cAMP. **(D)** Overlays of typical macroscopic current traces from representative CHO cells expressing recombinant mouse ENaC in the absence and presence of CPT-cAMP (200 mM) and after adding 10 mM amiloride (dotted lines). Currents elicited by voltage ramps stepped from a holding potential of 40–60 mV and ramped to –100 mV. **(E)** Summary graph of ENaC activity (amiloride-sensitive current density at –100 mV) quantified in whole-cell voltage clamped CHO cells transfected with mouse ENaC in the absence (white circles, white bar) and presence (black circles, gray bar) of CPT-cAMP treatment. Summary data from experiments ($n = 7$) identical to those shown in **(D)**. $^*P < 0.05$ vs. no CPT-cAMP.

DISCUSSION

These studies demonstrate that targeted stimulation of Gs signaling in renal PCs is sufficient to increase ENaC activity and decrease dependent urinary Na^+ excretion in live animals. This is important to understanding the role played by Na^+ reabsorption through ENaC in maximizing urine concentrating ability and control of blood pressure.

Arginine vasopressin has well understood antidiuretic action. In comparison, the consequences and underpinnings of potential anti-natriuretic effects of this hormone are more controversial (Stockand, 2010). AVP activates the Gs-coupled AVPR2 in renal PCs which stimulates AC to increase cellular cAMP levels. Nine AC isoforms have been identified but only three are expressed in renal PCs: AC3, AC4 and AC6 (Strait et al., 2010). Whereas AC3 and AC6, but not AC4, are necessary for some portion of AVP-dependent increases in cellular cAMP levels in inner medullary collecting duct cells, AC6, but not AC3, is necessary for AVP effects on ENaC in PCs in the intact mouse tubule (Strait et al., 2010; Roos et al., 2013; Kittikulsuth et al., 2014). Consequently, deletion of AC6 but not AC3 specifically in PCs results in a urine concentrating defect in mice that mimics global knockout of AC6 and nephrogenic diabetes insipidus (Rieg et al., 2010; Roos et al., 2012; Kittikulsuth et al., 2014). Gs-AC signaling ultimately increases ENaC activity by increasing cellular cAMP levels, and the Na^+ reabsorbed from the urine through cAMP-stimulated ENaC adds to the axial corticomedullary hyperosmotic gradient that allows maximal urinary concentration in the presence of

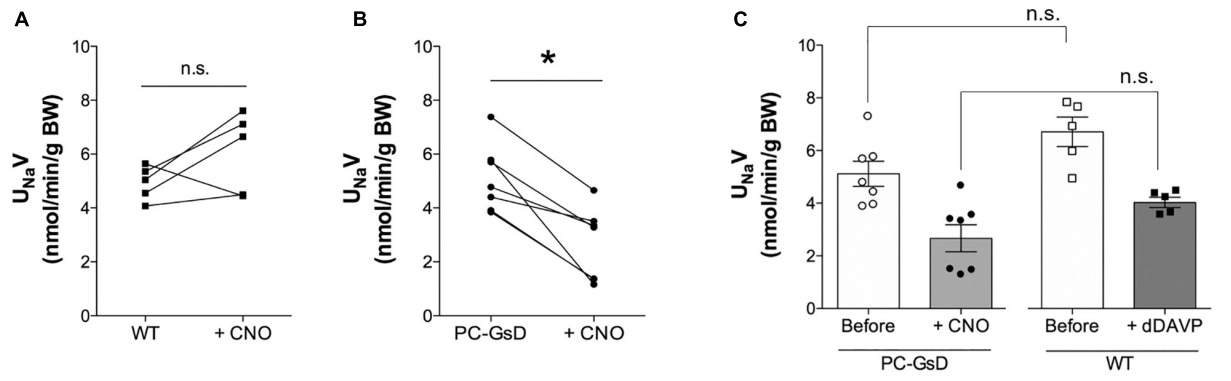

FIGURE 5 | CNO increases urinary Na^+ excretion in PC-specific GsD mice. Summary graphs from paired experiments showing 24 h urinary Na^+ excretion ($U_{Na}V$) before and after treatment with CNO (0.1 mg/kg) in wild type littermate controls (**A**, $n = 5$) and PC-specific GsD mice (**B**, $n = 7$). *$P < 0.05$ vs. before treatment. **(C)** Summary graph of 24 h urinary Na^+ excretion before (white circles, white bar) and after (black circles, gray bar) CNO treatment for PC-specific GsD mice, and control mice before (white boxes, white bar) and after (black boxes, dark gray bar) dDAVP treatment (1.0 mg/100 ml; $n = 5$).

AVP-stimulated AQP2 channels (Bugaj et al., 2009; Stockand, 2010; Mironova et al., 2012, 2015).

The products of genotyping reactions shown in **Figure 1** demonstrate that our PC-specific GsD mice are of the correct genotype. The *in vivo* bioluminescence results in **Figure 2** demonstrate the expected functional consequences of appropriate recombination upon crossing the GsD knock-in line with an Aqp2-cre driver line: restrictive and temporal expression of CNO-sensitive cAMP-signaling in the kidneys. This is consistent with cursory immunofluorescence studies showing GsD expression in ENaC expressing PCs in the distal nephron (see **Supplementary Figure 1**). Together this evidence demonstrates that the PC-specific GsD mouse used in these studies is as expected and expresses functional GsD in renal PCs.

Results in **Figure 3** demonstrate that targeted activation of Gs selectively in PCs in tubules from this PC-specific GsD mouse rapidly and robustly increases the activity of ENaC by increasing both the number of channels expressed in the apical plasma membrane and also the open probability these channels have. Such observations are in agreement with earlier work showing that AVP increases ENaC activity in PCs in native tubules in an AVPR2-dependent manner (Bugaj et al., 2009; Mironova et al., 2012). Such AVP-stimulation of ENaC contributes to maximizing urinary concentration and dilution of plasma (Bugaj et al., 2009). These findings in the current study provide novel independent evidence that direct stimulation of Gs in PCs is sufficient to increase ENaC activity. This complements the existing knowledge that AVPR2-Gs-AC6-cAMP signaling is necessary for AVP stimulation of ENaC in PCs. Thus, evidence in support of necessity and sufficiency now exists.

TABLE 1 | Urinary potassium excretion (U_KV) and osmolality in PC-specific GsD mice.

	U_KV (nmol/min/g BW)		Osmolality (mmol/kg)	
	Before	**After CNO**	**Before**	**After CNO**
WT	11.20 ± 1.3	10.37 ± 1.4	1,799 ± 105	1,836 ± 90.78
PC-specific GsD	14.27 ± 1.5	31.49 ± 4.7*,#	1,997 ± 119	2,438 ± 109*,#

*$P < 0.05$ vs. WT; #$P < 0.05$ vs. PC-specific before CNO.

The cellular mechanism by which Gs signaling increases ENaC activity is thought to be post-translational, culminating in changes in trafficking (and open probability) that result in increases in the levels of active channel in the plasma membrane (Snyder, 2000; Snyder et al., 2004; Fakitsas et al., 2007). Current findings as presented in **Figures 3**, **4** are consistent with this. We find that a cell permeable analog of cAMP that is resistant to hydrolysis, CPT-cAMP, markedly increases the levels of ENaC in the plasma membrane. While increasing cAMP levels with CPT-cAMP in the immortalized cells used in the current study to investigate mechanisms affecting activity of overexpressed ENaC is not a direct measurement of how stimulating Gs *in vivo* would affect ENaC, it is a reasonable surrogate for this that likely mimics with some fidelity how ENaC responds to stimulation of GsD in the living animal. Indeed, results from single channel patch clamp experiments on CNO-treated tubules from PC-specific GsD mice are in agreement that increases in channel number contributes to this mechanism.

Results in **Figure 5** demonstrate that targeted stimulation of GsD in PCs temporally decreases renal Na^+ excretion in live animals in a manner that is similar to the effects of desmopressin, an AVPR2 specific agonist. Such findings again demonstrate sufficiency, elaborating the physiological consequences of selective activation of Gs signaling and dependent stimulation of ENaC in PCs in the living animal. This novel finding is direct evidence that Gs signaling in PCs is anti-natriuretic. Elevated ENaC activity is the mechanistic underpinnings of this anti-natriuresis. Such findings add strong evidence to the argument that AVP has an anti-natriuretic effect in addition to its antidiuretic actions.

Together the anti-natriuretic and antidiuretic actions of AVP (via AVPR2-Gs-AC6-cAMP-ENaC/AQP2 signaling) contribute to maximal urine concentration and regulation of blood pressure (Stockand, 2010). The current findings provide the first direct evidence that stimulating Gs with subsequent activation of

ENaC is sufficient to contribute to this action of AVP in the living animal.

DATA AVAILABILITY STATEMENT

The original contributions presented in the study are included in the article/**Supplementary Material**, further inquiries can be directed to the corresponding author/s.

ETHICS STATEMENT

Protocols were reviewed and approved by the Institutional Animal Care and Use Committee of the University of Texas Health Science Center at San Antonio.

AUTHOR CONTRIBUTIONS

CA, EM, AS, JS, and TA conceived and designed the experiments. CA, RB, EM, JC, AS, and TA created the reagents and performed the experiments to collect the data. AS, TA, and JS created the manuscript figures and wrote the first draft of the manuscript, which was subsequently edited and approved by all authors.

FUNDING

This work was supported by the National Institutes of Health (NIH) grants R01 DK113816 and R01 DK117909 to JS. *In vivo* bioluminescence was quantified at the Core Optical Imaging Facility at UTHSCSA, which was funded by P30 CA54174 (https://lsom.uthscsa.edu/dcsa/research/cores-facilities/optical-imaging/).

SUPPLEMENTARY MATERIAL

The Supplementary Material for this article can be found online at: https://www.frontiersin.org/articles/10.3389/fphys.2021.725782/full#supplementary-material

REFERENCES

Abd El-Aziz, T. M., Soares, A. G., Mironova, E., Boiko, N., Kaur, A., Archer, C., et al., (2021). Mechanisms and consequences of casein kinase II and ankyrin-3 regulation of the epithelial Na^+ channel. *Sci. Rep.* 11:14600. doi: 10.1038/s41598-021-94118-3

Akhmedov, D., Kirkby, N. S., Mitchell, J. A., and Berdeaux, R. (2019). Imaging of tissue-specific and temporal activation of GPCR signaling using DREADD Knock-In Mice. *Methods Mol. Biol.* 1947, 361–376. doi: 10.1007/978-1-4939-9121-1_21

Akhmedov, D., Mendoza-Rodriguez, M. G., Rajendran, K., Rossi, M., Wess, J., Berdeaux, R., et al. (2017). Gs-DREADD knock-in mice for tissue-specific, temporal stimulation of cyclic AMP signaling. *Mol. Cell. Biol.* 37:e00584–16. doi: 10.1128/MCB.00584-16

Berman, J. M., Mironova, E., and Stockand, J. D. (2018). Physiological regulation of the epithelial Na(+) channel by casein kinase II. *Am. J. Physiol. Renal. Physiol.* 314, F367–F372. doi: 10.1152/ajprenal.00469.2017

Bugaj, V., Mironova, E., Kohan, D. E., and Stockand, J. D. (2012). Collecting duct-specific endothelin B receptor knockout increases ENaC activity. *Am. J. Physiol. Cell. Physiol.* 302, C188–C194. doi: 10.1152/ajpcell.00301.2011

Bugaj, V., Pochynyuk, O., and Stockand, J. D. (2009). Activation of the epithelial Na+ channel in the collecting duct by vasopressin contributes to water reabsorption. *Am. J. Physiol. Renal. Physiol.* 297, F1411–F1418. doi: 10.1152/ajprenal.00371.2009

Canessa, C. M., Horisberger, J. D., and Rossier, B. C. (1993). Epithelial sodium channel related to proteins involved in neurodegeneration. *Nature* 361, 467–470. doi: 10.1038/361467a0

Canessa, C. M., Schild, L., Buell, G., Thorens, B., Gautschi, I., Horisberger, J. D., et al. (1994). Amiloride-sensitive epithelial Na+ channel is made of three homologous subunits. *Nature* 367, 463–467. doi: 10.1038/367463a0

Fakitsas, P., Adam, G., Daidié, D., van Bemmelen, M. X., Fouladkou, F., Patrignani, A., et al. (2007). Early aldosterone-induced gene product regulates the epithelial sodium channel by deubiquitylation. *J. Am. Soc. Nephrol.* 18, 1084–1092. doi: 10.1681/ASN.2006080902

Garty, H., and Palmer, L. G. (1997). Epithelial sodium channels: function, structure, and regulation. *Physiol. Rev.* 77, 359–396.

Hanukoglu, I., and Hanukoglu, A. (2016). Epithelial sodium channel (ENaC) family: Phylogeny, structure-function, tissue distribution, and associated inherited diseases. *Gene* 579, 95–132. doi: 10.1016/j.gene.2015.12.061

Kemendy, A. E., Kleyman, T. R., and Eaton, D. C. (1992). Aldosterone alters the open probability of amiloride-blockable sodium channels in A6 epithelia. *Am. J. Physiol.* 263, C825–C837. doi: 10.1152/ajpcell.1992.263.4.C825

Kilkenny, C., Browne, W. J., Cuthill, I. C., Emerson, M., and Altman, D. G. (2010). Improving bioscience research reporting: the ARRIVE guidelines for reporting animal research. *PLoS Biol.* 8:e1000412. doi: 10.1371/journal.pbio.1000412

Kittikulsuth, W., Stuart, D., Van Hoek, A. N., Stockand, J. D., Bugaj, V., Mironova, E., et al. (2014). Lack of an effect of collecting duct-specific deletion of adenylyl cyclase 3 on renal Na+ and water excretion or arterial pressure. *Am. J. Physiol. Renal. Physiol.* 306, F597–F607. doi: 10.1152/ajprenal.00505.2013

Lingueglia, E., Voilley, N., Waldmann, R., Lazdunski, M., and Barbry, P. (1993). Expression cloning of an epithelial amiloride-sensitive Na+ channel. A new channel type with homologies to Caenorhabditis elegans degenerins. *FEBS Lett.* 318, 95–99.

Mironova, E., Bugaj, V., Roos, K. P., Kohan, D. E., and Stockand, J. D. (2012). Aldosterone-independent regulation of the epithelial Na+ channel (ENaC) by vasopressin in adrenalectomized mice. *Proc. Natl. Acad. Sci. U S A.* 109, 10095–10100. doi: 10.1073/pnas.1201978109

Mironova, E., Bugay, V., Pochynyuk, O., Staruschenko, A., and Stockand, J. D. (2013). Recording ion channels in isolated, split-opened tubules. *Methods Mol. Biol.* 998, 341–353. doi: 10.1007/978-1-62703-351-0_27

Mironova, E., Chen, Y., Pao, A. C., Roos, K. P., Kohan, D. E., Bugaj, V., et al. (2015). Activation of ENaC by AVP contributes to the urinary concentrating mechanism and dilution of plasma. *Am. J. Physiol. Renal. Physiol.* 308, F237–F243. doi: 10.1152/ajprenal.00246.2014

Mironova, E., Suliman, F., and Stockand, J. D. (2019). Renal Na(+) excretion consequent to pharmacogenetic activation of Gq-DREADD in principal cells. *Am. J. Physiol. Renal. Physiol.* 316, F758–F767. doi: 10.1152/ajprenal.00612.2018

Nelson, R. D., Stricklett, P., Gustafson, C., Stevens, A., Ausiello, D., Brown, D., et al. (1998). Expression of an AQP2 Cre recombinase transgene in kidney and male reproductive system of transgenic mice. *Am. J. Physiol.* 275, C216–C226.

Perucca, J., Bichet, D. G., Bardoux, P., Bouby, N., and Bankir, L. (2008). Sodium excretion in response to vasopressin and selective vasopressin receptor antagonists. *J. Am. Soc. Nephrol.* 19, 1721–1731. doi: 10.1681/ASN.2008010021

Reif, M. C., Troutman, S. L., and Schafer, J. A. (1986). Sodium transport by rat cortical collecting tubule. Effects of vasopressin and desoxycorticosterone. *J. Clin. Invest.* 77, 1291–1298. doi: 10.1172/JCI112433

Rieg, T., Tang, T., Murray, F., Schroth, J., Insel, P. A., Fenton, R. A., et al. (2010). Adenylate cyclase 6 determines cAMP formation and aquaporin-2

phosphorylation and trafficking in inner medulla. *J. Am. Soc. Nephrol.* 21, 2059–2068. doi: 10.1681/ASN.2010040409

Roos, K. P., Bugaj, V., Mironova, E., Stockand, J. D., Ramkumar, N., Rees, S., et al. (2013). Adenylyl cyclase VI mediates vasopressin-stimulated ENaC activity. *J. Am. Soc. Nephrol.* 24, 218–227. doi: 10.1681/ASN.2012050449

Roos, K. P., Strait, K. A., Raphael, K. L., Blount, M. A., and Kohan, D. E. (2012). Collecting duct-specific knockout of adenylyl cyclase type VI causes a urinary concentration defect in mice. *Am. J. Physiol. Renal. Physiol.* 302, F78–F84. doi: 10.1152/ajprenal.00397.2011

Rossier, B. C., Pradervand, S., Schild, L., and Hummler, E. (2002). Epithelial sodium channel and the control of sodium balance: interaction between genetic and environmental factors. *Annu. Rev. Physiol.* 64, 877–897. doi: 10.1146/annurev.physiol.64.082101.143243

Snyder, P. M. (2000). Liddle's syndrome mutations disrupt cAMP-mediated translocation of the epithelial Na(+) channel to the cell surface. *J. Clin. Invest.* 105, 45–53. doi: 10.1172/JCI7869

Snyder, P. M., Olson, D. R., Kabra, R., Zhou, R., and Steines, J. C. (2004). cAMP and serum and glucocorticoid-inducible kinase (SGK) regulate the epithelial Na(+) channel through convergent phosphorylation of Nedd4-2. *J. Biol. Chem.* 279, 45753–45758. doi: 10.1074/jbc.M407858200

Staruschenko, A., Adams, E., Booth, R. E., and Stockand, J. D. (2005). Epithelial Na+ channel subunit stoichiometry. *Biophys. J.* 88, 3966–3975. doi: 10.1529/biophysj.104.056804

Staruschenko, A., Booth, R. E., Pochynyuk, O., Stockand, J. D., and Tong, Q. (2006). Functional reconstitution of the human epithelial Na+ channel in a mammalian expression system. *Methods Mol. Biol.* 337, 3–13. doi: 10.1385/1-59745-095-2:3

Stockand, J. D. (2010). Vasopressin regulation of renal sodium excretion. *Kidney Int.* 78, 849–856. doi: 10.1038/ki.2010.276

Stockand, J. D. (2012). The role of the epithelial Na(+) channel (ENaC) in high AVP but low aldosterone states. *Front. Physiol.* 3:304. doi: 10.3389/fphys.2012.00304

Stockand, J. D., Vallon, V., and Ortiz, P. (2012). In vivo and ex vivo analysis of tubule function. *Compr. Physiol.* 2, 2495–2525. doi: 10.1002/cphy.c100051

Strait, K. A., Stricklett, P. K., Chapman, M., and Kohan, D. E. (2010). Characterization of vasopressin-responsive collecting duct adenylyl cyclases in the mouse. *Am. J. Physiol. Renal. Physiol.* 298, F859–F867. doi: 10.1152/ajprenal.00109.2009

Stricklett, P. K., Nelson, R. D., and Kohan, D. E. (1999). Targeting collecting tubules using the aquaporin-2 promoter. *Exp. Nephrol.* 7, 67–74. doi: 10.1159/000020587

Verouti, S. N., Boscardin, E., Hummler, E., and Frateschi, S. (2015). Regulation of blood pressure and renal function by NCC and ENaC: lessons from genetically engineered mice. *Curr. Opin. Pharmacol.* 21, 60–72. doi: 10.1016/j.coph.2014.12.012

Conflict of Interest: The authors declare that the research was conducted in the absence of any commercial or financial relationships that could be construed as a potential conflict of interest.

Publisher's Note: All claims expressed in this article are solely those of the authors and do not necessarily represent those of their affiliated organizations, or those of the publisher, the editors and the reviewers. Any product that may be evaluated in this article, or claim that may be made by its manufacturer, is not guaranteed or endorsed by the publisher.

frontiers in Physiology

ORIGINAL RESEARCH
published: 02 December 2021
doi: 10.3389/fphys.2021.725172

α-Actinin 4 Links Vasopressin Short-Term and Long-Term Regulation of Aquaporin-2 in Kidney Collecting Duct Cells

*Cheng-Hsuan Ho†, Hsiu-Hui Yang†, Shih-Han Su, Ai-Hsin Yeh and Ming-Jiun Yu**

College of Medicine, Institute of Biochemistry and Molecular Biology, National Taiwan University, Taipei, Taiwan

Water permeability of the kidney collecting ducts is regulated by the peptide hormone vasopressin. Between minutes and hours (short-term), vasopressin induces trafficking of the water channel protein aquaporin-2 to the apical plasma membrane of the collecting duct principal cells to increase water permeability. Between hours and days (long-term), vasopressin induces aquaporin-2 gene expression. Here, we investigated the mechanisms that bridge the short-term and long-term vasopressin-mediated aquaporin-2 regulation by α-actinin 4, an F-actin crosslinking protein and a transcription co-activator of the glucocorticoid receptor. Vasopressin induced F-actin depolymerization and α-actinin 4 nuclear translocation in the mpkCCD collecting duct cell model. Co-immunoprecipitation followed by immunoblotting showed increased interaction between α-actinin 4 and glucocorticoid receptor in response to vasopressin. ChIP-PCR showed results consistent with α-actinin 4 and glucocorticoid receptor binding to the aquaporin-2 promoter. α-actinin 4 knockdown reduced vasopressin-induced increases in aquaporin-2 mRNA and protein expression. α-actinin 4 knockdown did not affect vasopressin-induced glucocorticoid receptor nuclear translocation, suggesting independent mechanisms of vasopressin-induced nuclear translocation of α-actinin 4 and glucocorticoid receptor. Glucocorticoid receptor knockdown profoundly reduced vasopressin-induced increases in aquaporin-2 mRNA and protein expression. In the absence of glucocorticoid analog dexamethasone, vasopressin-induced increases in glucocorticoid receptor nuclear translocation and aquaporin-2 mRNA were greatly reduced. α-actinin 4 knockdown further reduced vasopressin-induced increase in aquaporin-2 mRNA in the absence of dexamethasone. We conclude that glucocorticoid receptor plays a major role in vasopressin-induced aquaporin-2 gene expression that can be enhanced by α-actinin 4. In the absence of vasopressin, α-actinin 4 crosslinks F-actin underneath the apical plasma membrane, impeding aquaporin-2 membrane insertion. Vasopressin-induced F-actin depolymerization in one hand facilitates aquaporin-2 apical membrane insertion and in the other hand frees α-actinin 4 to enter the nucleus where it binds glucocorticoid receptor to enhance aquaporin-2 gene expression.

Keywords: vasopressin, aquaporin-2, glucocorticoid receptor, collecting duct, α-actinin 4

OPEN ACCESS

Edited by:
Weidong Wang,
Sun Yat-sen University, China

Reviewed by:
Marleen L. A. Kortenoeven,
University of Southern Denmark, Denmark
Zhanjun Jia,
Nanjing Medical University, China

***Correspondence:**
Ming-Jiun Yu
mjyu@ntu.edu.tw

† These authors have contributed equally to this work

Specialty section:
This article was submitted to Renal and Epithelial Physiology, a section of the journal Frontiers in Physiology

Received: *15 June 2021*
Accepted: *31 October 2021*
Published: *02 December 2021*

Citation:
Ho C-H, Yang H-H, Su S-H, Yeh A-H and Yu M-J (2021) α-Actinin 4 Links Vasopressin Short-Term and Long-Term Regulation of Aquaporin-2 in Kidney Collecting Duct Cells. Front. Physiol. 12:725172. doi: 10.3389/fphys.2021.725172

INTRODUCTION

Vasopressin is a peptide hormone that regulates osmotic water reabsorption by the kidney collecting ducts (Knepper et al., 2015). It does so by elevating intracellular cAMP and Ca^{2+} concentrations that control the molecular water channel protein aquaporin-2 (AQP2) chiefly in two modes (Judith Radin et al., 2012; Pearce et al., 2015). Within minutes and hours (short-term), vasopressin induces AQP2 redistribution from the intracellular vesicles to the apical plasma membrane of the collecting duct principal cells to increase water permeability (Nielsen et al., 1995; Yamamoto et al., 1995). Within hours and days (long-term), vasopressin increases *AQP2* gene expression (DiGiovanni et al., 1994). Dysregulations in either regulatory mode cause a number of water balance disorders (Noda et al., 2010; Judith Radin et al., 2012; Moeller et al., 2013).

Long before the cloning of the *AQP2* gene (Fushimi et al., 1993), it has been known that the actions of vasopressin involve cytoskeleton and shuttling of intracellular membrane particles that contain transmembrane water channels (Taylor et al., 1973; Wade et al., 1981). It is now widely accepted that vasopressin depolymerizes F-actin to facilitate insertion of AQP2-containing intracellular vesicles to the apical plasma membrane of the kidney collecting duct principal cells (Simon et al., 1993; Nielsen et al., 1995; Noda et al., 2010; Fenton et al., 2020). Vasopressin-induced F-actin depolymerization was recorded in live mpkCCD cells (Loo et al., 2013), a collecting duct principal cell model that expresses all necessary molecular components required for the vasopressin actions (Yu et al., 2009). To add another layer of complexity, AQP2 constantly exocytoses to and endocytoses from the plasma membrane (Brown, 2003; Tajika et al., 2005; Wang et al., 2020). As actin is recruited to the sites of endocytosis to facilitate membrane invagination (Smythe and Ayscough, 2006), reagents that promote actin depolymerization increase AQP2 in the plasma membrane (Procino et al., 2010; Li et al., 2011). Thus, trafficking of AQP2 to and from the plasma membrane is tightly coupled with F-actin dynamics.

Efforts have been made to identify components that regulate F-actin dynamics with respect to vasopressin-induced AQP2 trafficking. An earlier proteomics study using AQP2 as a bait identified 13 AQP2-interacting proteins involved in F-actin dynamics: actin, α-actinin 4, α-II spectrin, α-tropomyosin 5b, annexin A2 and A6, gelsolin, ionized calcium binding adapter molecule 2, myosin heavy chain non-muscle type A, myosin regulatory light chain smooth muscle isoforms 2-A and 2-B, scinderin, and signal-induced proliferation-associated gene-1 (SPA-1) (Noda et al., 2005). SPA-1 is a GTPase-activating protein for Rap1, a GTPase that promotes F-actin depolymerization when bound with GTP (Richter et al., 2007). Loss-of-function mutation or deficiency in SPA-1 impairs apical AQP2 trafficking (Noda et al., 2004). The above observations led to the idea that AQP2 might, through interactions with F-actin regulatory proteins, catalyze F-actin depolymerization thereby facilitating AQP2 apical trafficking (Yui et al., 2012).

In addition to the above proteomics study, α-actinin 4 was repetitively identified in the transcriptomes and proteomes of rat kidney collecting ducts and mpkCCD cells (Uawithya et al., 2008; Yu et al., 2008, 2009; Yang et al., 2015b). Together with a network of actin regulatory proteins, α-actinin 4 protein was found in the apical plasma membrane as well as in the nuclear fraction of the mpkCCD cells (Schenk et al., 2012; Loo et al., 2013). In response to short-term vasopressin stimulation, α-actinin 4 undergoes a reciprocal abundance change in the 200,000 xg cytosolic fraction and the 17,000 xg membrane fraction (Yang et al., 2015a), suggesting dynamic shuttling of α-actinin 4 in these subcellular fractions. In response to long-term vasopressin stimulation, α-actinin 4 protein abundance increases by 30% (Khositseth et al., 2011). Apparently, α-actinin 4 is employed by vasopressin for both short- and long-term responses.

α-actinin 4 is among the four α-actinin isoforms with ∼86% amino acid homology to α-actinin 1 (Blanchard et al., 1989; Honda, 2015). α-actinin 2 and 3 belong to the muscle group whereas α-actinin 1 and 4 belong to the non-muscle group (Honda, 2015). In general, an α-actinin protein has two calponin homology domains that form an actin binding domain at the NH_2-terminus, follow by four spectrin repeats in the middle, and two EF-hand repeats that form a calmodulin-like domain at the COOH-terminus (Honda, 2015). α-actinin forms a dimer that bundles F-actin filaments (Honda, 2015). The muscle-type actinins mediate F-actin filament bundling and interactions with the Z-disk. The non-muscle type actinins also mediate F-actin filament bundling and interactions with the cell membranes associated with cell adhesion and migration (Honda, 2015). While the binding of the muscle α-actinins to F-actin is insensitive to Ca^{2+}, the binding of the non-muscle α-actinins such as α-actinin 4 to F-actin is abolished by Ca^{2+} (Blanchard et al., 1989). In addition to F-actin binding, α-actinin 4 has been shown to serve as a transcription co-activator for a number of nuclear receptors including glucocorticoid receptor (Khurana et al., 2012; Feng et al., 2015; Honda, 2015). We recently showed that the glucocorticoid receptor agonist dexamethasone potentiates vasopressin-induced *AQP2* gene expression in the mpkCCD cells (Kuo et al., 2018). Here, we provided evidence showing that vasopressin induces α-actinin 4 dissociation from F-actin and translocation into the nucleus where it interacts with glucocorticoid receptor to enhance *AQP2* gene expression.

MATERIALS AND METHODS

Cell Culture

The mpkCCD cells re-cloned from their original line (Duong Van Huyen et al., 1998) for the highest AQP2 expression level were maintained in DMEM/Ham's F-12 medium (DMEM/F-12, Cat. 11320033, Thermo-Fisher, United States) containing 2% fetal bovine serum (FBS) and supplements as described previously (Yu et al., 2009). Cells between 18 and 32 passages were grown on membrane supports (Transwell®, 0.4 μm pore size, Corning Costar, United States) prior to the experiments. FBS and supplements except dexamethasone (Kuo et al., 2018) were removed from the medium to facilitate cell polarization (transepithelial electrical resistance > 5,000 Ωxcm^2 measured with an EVOM2 Epithelial Volt/Ohm Meter, World Precision Instruments, United States) before the cells were exposed to

the vasopressin V2 receptor-specific agonist dDAVP (1-deamino-8-D-arginine vasopressin) in the basal medium to induce endogenous AQP2 expression. In some cases, dexamethasone was omitted from the experiments to examine the effects in the absence of the glucocorticoid receptor agonist. The HEK293T cells used for packaging small hairpin RNA (shRNA)-carrying lentivirus were maintained in the DMEM medium (Cat. 12491015, Thermo-Fisher, United States) containing 10% FBS.

Immunofluorescence Confocal Microscopy

The mpkCCD cells grown on Transwell® were washed with ice-cold PBS-CM [1 mM $MgCl_2$ and 0.1 mM $CaCl_2$ in 1X PBS (phosphate-buffered saline), pH6.4] three times prior to fixation with 4% paraformaldehyde (in PBS-CM) for 20 min at room temperature. The cells were then washed with PBS-CM three times before treated with membrane permeabilization buffer [0.3% Triton X-100, 0.1% BSA (bovine serum albumin), and 1 mM NaN_3 in 1X PBS] for 30 min at room temperature. To block non-specific binding, the cells were incubated with IF blocking buffer (1% BSA, 0.05% saponin, 0.2% gelatin, and 1 mM NaN_3 in 1X PBS) for 30 min at room temperature before incubated with primary antibody [α-actinin 4 (Actn4), Cat. GTX101669 or glucocorticoid receptor (GR), Cat. GTX101120, GeneTex, Taiwan] at 4°C overnight. After washes with IF washing buffer (0.1% BSA, 0.05% saponin, 0.2% gelatin, and 1 mM NaN_3 in 1X PBS) three times, the cells were incubated with Alexa488-conjugated secondary antibody (Cat. A21206, Invitrogen, United States) for 1 h at room temperature. Cell nuclei were stained with DAPI (4′,6-diamidino-2-phenylindole, 1 μg/mL in 1X PBS) at room temperature for 10 min. In some cases, F-actin was stained with rhodamine-conjugated phalloidin (Cat. R415, Invitrogen™, United States) at room temperature for 1 h. After two washes with PBS, the cells were mounted in fluorescent mounting medium (Cat. S3023, Agilent Technologies, United States) and covered with a cover glass. Confocal images were acquired with a Zeiss LSM880 microscope and processed with the ZEN blue software. Quantification of the images was done with the Imaris software (Bitplane AG, Switzerland). For colocalization measurements of two proteins, the fluorescence signals from each protein were determined with a set threshold value based on background noise, i.e., no primary antibody (or no phalloidin) staining control. Colocalization was calculated as percentage of the voxels that are doubly positive for two proteins divided by the voxels that was positive for one protein. Between 100 and 120 cells in one image were calculated, 3 images per experiment and repeated for 3 independent experiments.

Nucleus-Cytosol Fractionation

Cells were solubilized in 0.4 ml NC buffer (10 mM HEPES, 10 mM KCl, and 0.2 mM EDTA) containing protease inhibitor (Cat. 539134, Calbiochem, United States) and phosphatase inhibitor (Cat. 524625, Calbiochem, United States). The cell lysate was set on ice for 15 min before added with NP40 to a final concentration 0.6%. The mixture was vortexed for 20 s and spun at 1,500 ×g for 5 min at 4°C before the supernatant, i.e., the cytosolic fraction was collected. The pellet was washed with 1 ml NC buffer and centrifuged at 1,500 ×g for 5 min at 4°C. The pellet was re-suspended in 0.1 ml NC buffer and sonicated. After centrifugation at 16,000 ×g for 10 min at 4°C, the supernatant, i.e., the nuclear fraction, was collected for analysis.

Immunoblotting

Cell proteins were dissolved in SDS protein sample buffer [50 mM Tris, 150 mM NaCl, 5 mM EDTA, 1% NP40, 0.5% sodium deoxycholate, and 0.5% SDS (sodium dodecyl sulfate), pH7.4]. Protein concentrations were measured with bicinchoninic acid (Cat. 23225, Thermo-Fisher, United States). In general, 20 μg proteins were mixed with 5X loading buffer (7.5% SDS, 30% glycerol, 50 mM Tris, pH 6.8, 200 mM dithiothreitol, and bromophenol blue a few), and separated on a 10% SDS-PAGE gel at 15mA, 160V in 1X SDS-PAGE running buffer (25 mM Tris, 192 mM glycine, 0.1% SDS) for 100 min. Separated proteins in the gel were transferred to a nitrocellulose membrane (Cat. 10600004, GE Healthcare Life Science, United States) in 1X Fairbank buffer [25 mM Tris,192 mM glycine, and 20% (V/V) methanol] with 200 mA for 1 h. The membrane was incubated on a shaker at room temperature for 1 h with blocking buffer 0.1% BSA in 1X TBS-T (20 mM Tris, 150 mM NaCl, and 0.1% Tween-20). After removal of the blocking buffer, the membrane was incubated overnight with primary antibody diluted in the blocking buffer. The antibodies were Actn4 (Cat. GTX101669), glyceraldehyde-3-phosphate dehydrogenase (Gapdh, Cat. GTX100118), GR (Cat. GTX101120), histone 2A (H2A, Cat. GTX129418) from GeneTex, Taiwan, or AQP2 (sc-9880) from Santa Cruz, United States or β-actin (Cat. A5441) from Sigma-Aldrich, United States. The next day, the membrane was washed three times (10 min each) with TBS-T on a shaker, and incubated with secondary antibody (diluted in the blocking buffer) for 1 h on a shaker at room temperature. The secondary antibodies were: IRDye 800 goat anti-rabbit (Cat. 926-32211), IRDye 800 donkey anti-goat (Cat. 926-32214), or IRDye 680 goat anti-mouse (Cat. 926-68020) from Li-Cor, United States. Finally, the membrane was washed three times with TBS-T before visualization and quantification with a near-infrared fluorescence Odyssey scanner and software (Li-Cor, United States).

Co-immunoprecipitation

Cells were solubilized in 0.3 ml lysis buffer, i.e., 1% Triton® X-100 in 1X TBS (20 mM Tris and 150 mM NaCl), containing protease inhibitor and phosphatase inhibitor and left on ice for 30 min. The lysates were centrifuged (16,000 ×g, 10 min) before the protein concentrations were measured and adjusted to 2.5 mg/ml. Anti-GR antibody (Cat. sc-393232, Santa Cruz, United States) or IgG (Cat. 213111-01, GeneTex, Taiwan) was added to 1 mg lysates and incubated for 16 h at 4°C before protein G Mag Sepharose Xtra beads (Cat. GE28-9670-70, GE Healthcare, United States) were added for further incubation at 4°C for 5 h. The beads were washed with the lysis buffer before the bound proteins were eluted in the SDS protein sample buffer for SDS-PAGE and immunoblotting.

Chromatin Immunoprecipitation Coupled With Polymerase Chain Reaction

Chromatin immunoprecipitation (ChIP) assay was performed using the SimpleChIP Enzymatic Chromatin IP kit (Cat. 9003, Cell Signaling Technologies, United States). Briefly, mpkCCD cells were freed from the culture surface, counted, and diluted to 5×10^5 cells per ml in the cell culture medium. Formaldehyde (Cat. 252549, Sigma-Aldrich, United States) was added to a final concentration (1%) to crosslink proteins with chromatin at room temperature for 10 min. After the unreacted formaldehyde was quenched with glycine (125 mM) at room temperature for 5 min, chromatin was digested with 1,500 units micrococcal nuclease at 37°C for 20 min. The cells were then briefly sonicated to lyse nuclear membranes. After a brief spin at 9,400 ×g for 10 min, the supernatant was incubated with anti-GR antibody (Cat. GTX101120, GeneTex, Taiwan), anti-Actn4 antibody (Cat. M01975, Boster, United States), or control IgG antibody (provided in the kit) at 4°C with rotation overnight. The mixtures were then incubated with beads (Cat. 9006, Cell Signaling Technologies, United States) at 4°C with rotation for 2 h. After washes, the chromatin-protein complex was eluted in the ChIP Elution Buffer (Cat. 7009, Cell Signaling Technologies, United States) at 65°C for 30 min. The supernatant was then transferred to a new tube to reverse the crosslink with 200 mM NaCl and 2 μl proteinase K (Cat. 10012, Cell Signaling Technologies, United States) at 65°C for 2 h. The chromatin DNA was then purified with a spin column provided with the kit. The polymerase chain reaction (PCR) was done with 2X TOOL Taq MasterMix polymerase (Cat. KTT-BB, Tools, Taiwan) and a primer set specific to the AQP2 promoter region (forward GCAGCTCCATGGGGTAACTG and reverse CCACCCGAAGGCCTATCAC). The PCR steps were: (1) initial denaturation (94°C, 5 min); (2) denaturation (94°C, 30 s); (3) annealing (56°C, 30 s); (4) extension (72°C, 1 min); (5) repeat (steps 2–4 for 35 cycles); and (6) final extension (72°C, 5 min).

Small Hairpin RNA-Mediated Gene Knockdown

Small hairpin RNA (shRNA)-mediated gene knockdown was done via lentivirus-based transduction. Clones for shRNA were purchased from the National RNAi Core Facility, Academia Sinica, Taiwan: shCtrl (TRCN0000208001), shGR1 (TRCN0000238464), shGR2 (TRCN0000238463), shActn4-1 (TRCN0000090213), or shActn4-2 (TRCN0000090214). To make shRNA-carrying lentivirus, the HEK293T cells were seeded at 70% confluence in a 60-mm dish. On the day of transfection, the medium was replaced with fresh DMEM containing 1% BSA minus FBS and incubated for 30 min before transfection with a lentivirus-packaging plasmid mixture: 4 μg shRNA plasmid, 3.6 μg pCMV Δ8.91 plasmid, and 0.4 μg VSVG plasmid mixed in 250 μl Opti-MEM (Cat. 31985070, Thermo-Fisher, United States) plus 12 μl T-Pro NTR II (Cat. JT97-N002M, T-Pro Biotechnology, Taiwan). Two days after the transfection, the medium that contained lentiviral particles was collected and centrifuged at 1,200 ×g for 5 min. The supernatants that contained shRNA-carrying lentiviral particles were aliquoted and stored at −80°C until use. To knockdown genes, 6×10^5 mpkCCD cells were seeded in a 60-mm dish one day before infection with 1 ml lentivirus-containing medium plus 2 ml regular medium and 24 μl polybrene (hexadimethrine bromide, Cat. H9268, Sigma-Aldrich, United States, 1 mg/ml) for one day. The infected cells were selected for stable knockdown with puromycin (Watson Biotechnology, Taiwan, 2.5 μg/ml) for two passages.

RNA Extraction and Reverse Transcription

To each membrane support (12-mm Transwell®, Corning Costar, United States), 300 μl TriZOL® reagent (Cat. 15596081, Invitrogen, United States) were added to lyse the cells. Total RNA was then extracted with RNA extraction kit (Cat. E1011-A, ZYMO Research, United States). About 500 ng total RNA were reverse transcribed to cDNA with oligo$(dT)_{20}$ primer (Cat. 18418020, Invitrogen, United States) or random hexamers (Cat. N8080127, Invitrogen, United States) using SuperScript™ IV First-Strand Synthesis System (Cat. 18091050, Invitrogen, United States) following the manufacturer's instruction.

Quantitative Polymerase Chain Reaction

Quantitative polymerase chain reaction (qPCR) was carried out with SensiFAST SYBR® Hi-ROX (Cat. BIO-92005, Bioline, United States) with gene-specific primers in 8-strip qRT-PCR tubes. The primers for Actn4 were forward CCAGGAGGATGACTGGGAC and reverse GCCAGCCTTCC GAAGATGA. The primers for AQP2 were forward CCTCCTTGGGATCTATTTCA and reverse CAAACTTG CCAGTGACAACT. The primers for GR were forward GACTCCAAAGAATCCTTAGCTCC and reverse CTCCACCC CTCAGGGTTTTAT. The primers for Rplp0 (60S acidic ribosomal protein P0) were forward AGAT CGGGTACCCAACTGTT and reverse GGCCTTGACC TTTTCAGTAA. The primers span intron(s) to avoid amplification of PCR products from genomic DNA. The qPCR program was done in a thermal cycler (StepOnePlus Real-Time PCR Systems, Thermo-Fisher, United States) with the following steps: (1) polymerase activation (95°C, 3 min); (2) denaturation (95°C, 5 s); (3) annealing/extension (60°C, 30 s); (4) repeat (step 2–3, 40 cycles).

RESULTS

Vasopressin Freed α-Actinin 4 From F-Actin for Nuclear Translocation

Under the vehicle control conditions (**Figure 1A**), α-actinin 4 was detected in the cytoplasm and nuclei in the polarized mpkCCD cells with confocal immunofluorescence microscopy. On average, about 60.3% α-actinin 4 was found colocalized with F-actin, which had much pronounced staining at the cell periphery (**Figures 1A,B**). In response to 1 nM vasopressin analog dDAVP (**Figure 1A**), F-actin was more diffusive with

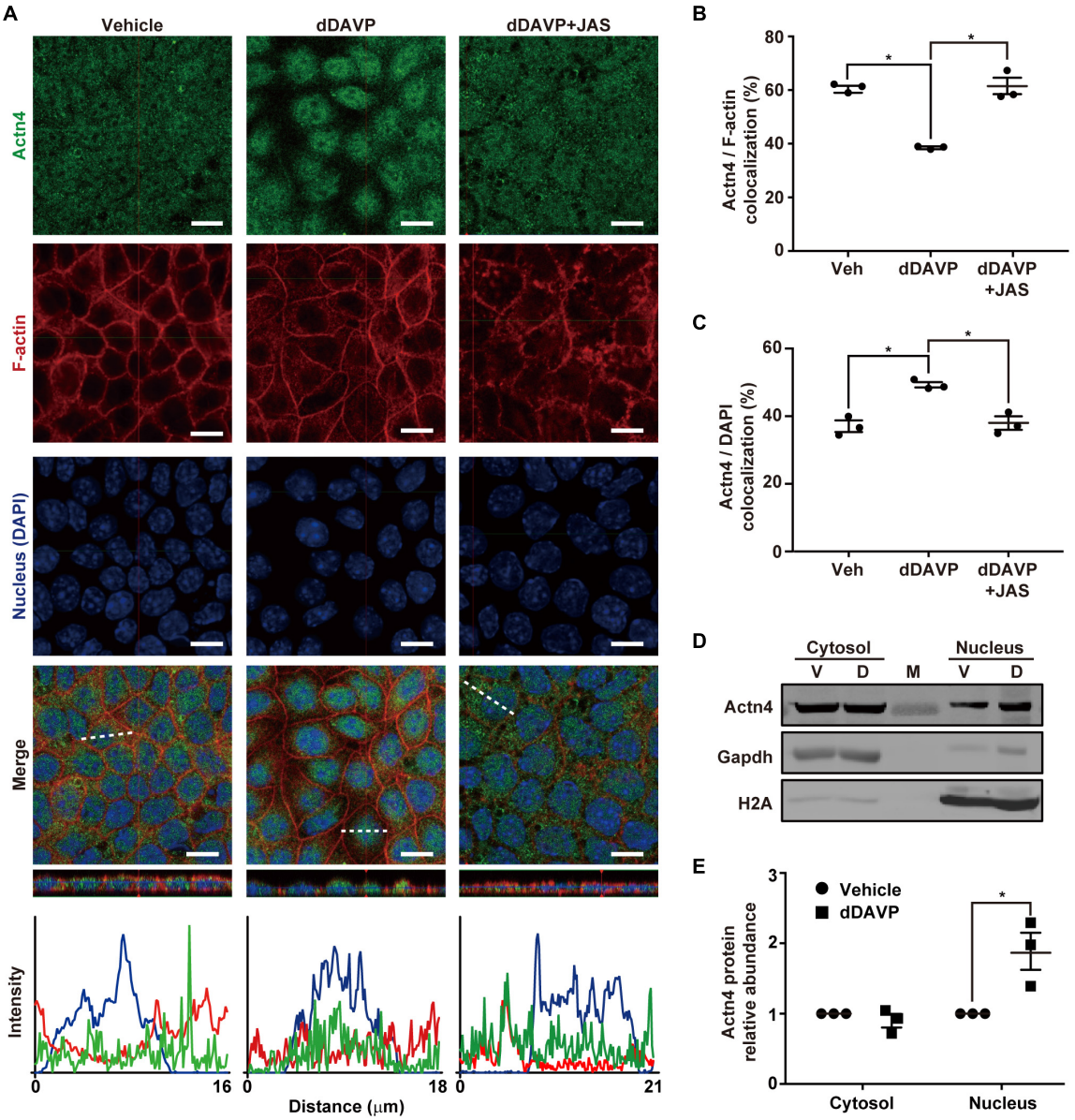

FIGURE 1 | Vasopressin freed α-actinin 4 from F-actin for nuclear translocation in the mpkCCD cells. **(A)** Confocal immunofluorescence micrographs of α-actinin 4 (Actn4, green) and F-actin (red). Polarized cells grown on Transwell® were exposed (24 h) to vehicle, 1 nM dDAVP, or 1 nM dDAVP plus 50 nM jasplakinolide (JAS) that binds and induces F-actin polymerization (Bubb et al., 2000). The nuclei were stained with DAPI (blue). Shown at the bottoms are signal profiles along the dotted lines. Bars indicate 10 μm. **(B,C)** Summaries of Actn4 colocalization with F-actin and DAPI, respectively. Numbers are means ± SEM, summarized from three independent experiments and about 330 cells per experiment. Asterisks indicate statistical significance, *t*-test $p < 0.05$. **(D,E)** Representative immunoblotting and summary of Actn4 in the cytosol vs. nuclei of the cells exposed to vehicle (V) vs. dDAVP (D). Numbers are means ± SEM, summarized from three independent experiments. Gapdh and H2A were markers for cytosol and nuclei, respectively. Protein intensities were corrected against those of Gapdh or H2A to avoid variations in the sample preparation. M, marker.

increased staining in the cytoplasm, suggestive of vasopressin-induced F-actin depolymerization. In the presence of dDAVP, less (38.5%) α-actinin 4 was found colocalized with F-actin (**Figures 1A,B**) and was detected primarily in the nuclei where it colocalized with DAPI that stains nucleic acids (**Figure 1A**). The increased nuclear α-actinin 4 staining (**Figure 1C**) is consistent with the idea that vasopressin frees α-actinin 4 from F-actin for nuclear translocation. In line with this, promoting F-actin polymerization with jasplakinolide significantly reduced dDAVP-induced α-actinin 4 nuclear translocation (**Figures 1A–C**, dDAVP + JAS). Nucleus-cytosol fractionation followed by immunoblotting showed results consistent with vasopressin-induced nuclear translocation of α-actinin 4 (**Figures 1D,E**).

Vasopressin Enhanced Interaction Between α-Actinin 4 and Glucocorticoid Receptor

Co-immunoprecipitation followed by immunoblotting showed that vasopressin enhanced interaction between α-actinin 4 and glucocorticoid receptor in the mpkCCD cells. Under the vehicle conditions, there was a basal amount of α-actinin 4 in the glucocorticoid receptor immunoprecipitate (**Figure 2A**). In response to dDAVP, the amount of α-actinin 4 in the immunoprecipitate increased to about 4.2 folds based on three independent experiments (**Figures 2A,B**). Specificity of the observations was reassured with the absence of α-actinin 4 in the control IgG immunoprecipitate. In line with α-actinin 4′s function as a transcription co-activator of the glucocorticoid receptor, chromatin immunoprecipitation coupled with polymerase chain reaction showed results consistent with binding of α-actinin 4 and glucocorticoid receptor with the AQP2 promoter (**Figures 2C,D**). No AQP2 PCR product was observed when a control IgG was used for chromatin immunoprecipitation.

α-Actinin 4 Knockdown Reduced Vasopressin-Induced *AQP2* Gene Expression

To test α-actinin 4′s transcription co-activator function, α-actinin 4 mRNA and protein were knocked down to about 16.1% and 32.0% of the control mpkCCD cells, with two small-hairpin RNA sequences (**Figures 3A–C**). Vehicle or dDAVP treatment did not affect the knockdown efficiency. α-actinin 4 knockdown did not affect cell polarization as the transepithelial resistance increased in a similar way regardless experimental conditions (**Figure 3D**). Under these conditions, dDAVP-induced increases in the AQP2 mRNA and protein levels were greatly reduced in the α-actinin 4 knockdown vs. the control cells (**Figures 3B,E,F**), in line with α-actinin 4′s transcription co-activator function in vasopressin-induced *AQP2* gene expression. Since dDAVP did not affect α-actinin 4 mRNA or protein levels (**Figures 3A–C**), the reduced *AQP2* gene expression levels reflect the effects of the reduced α-actinin 4 levels in the knockdown cells. Note that the α-actinin 4 knockdown cells still responded to dDAVP with *AQP2* gene expression (**Figures 3E,F**), albeit at much reduced levels.

Glucocorticoid Receptor Translocated Into the Nuclei in Response to Vasopressin

Under the vehicle control conditions, glucocorticoid receptor was detected in the cytoplasm and nuclei with confocal immunofluorescence microscopy (**Figure 4A**). On average, about 46.9% glucocorticoid receptor was found in the nuclei where it colocalized with DAPI (**Figure 4B**). In response to dDAVP, more (59.9%) glucocorticoid receptor was found in the nuclei (**Figures 4A,B**), in line with glucocorticoid receptor nuclear translocation in response to vasopressin. Nucleus-cytosol fractionation followed by immunoblotting showed results consistent with dDAVP-induced nuclear translocation of glucocorticoid receptor (**Figures 4C,D**).

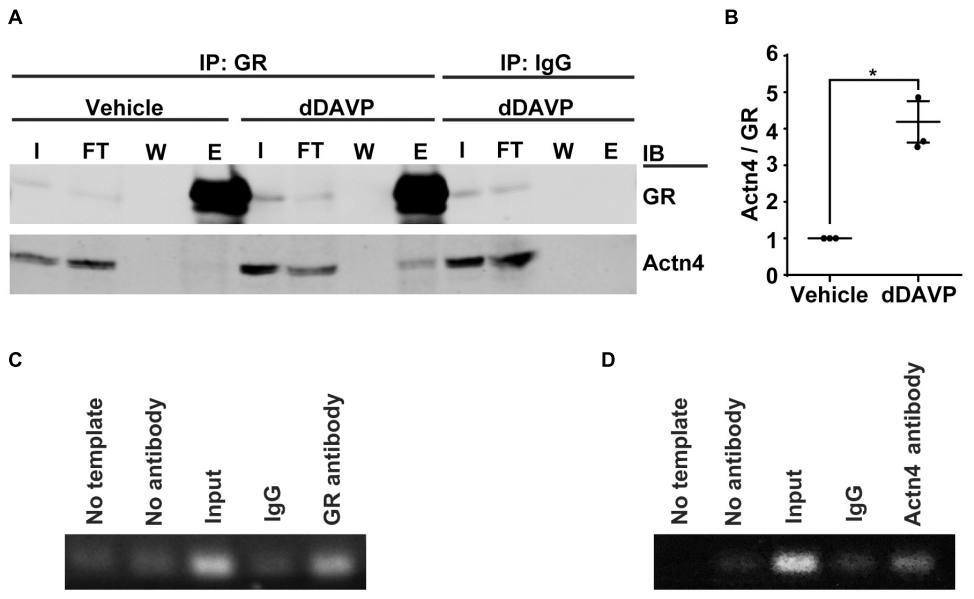

FIGURE 2 | Vasopressin enhanced interactions between α-actinin 4 and glucocorticoid receptor in the mpkCCD cells. **(A)** Co-immunoprecipitation (IP) of glucocorticoid receptor (GR) followed by immunoblotting (IB) for α-actinin 4 (Actn4) in the mpkCCD cells under vehicle vs. dDAVP (1nM, 24 h) conditions. **(B)** Summary from three independent experiments. Numbers are means ± SEM, summarized from three independent experiments. Asterisk indicates statistical significance, *t*-test $p < 0.05$. E, eluate; FT, flow through; I, input; W, wash. **(C,D)** Chromatin immunoprecipitation with antibody against GR, Actn4, or IgG followed by PCR amplification of AQP2 between –128 and –255 base pairs upstream to the AQP2 transcription start site.

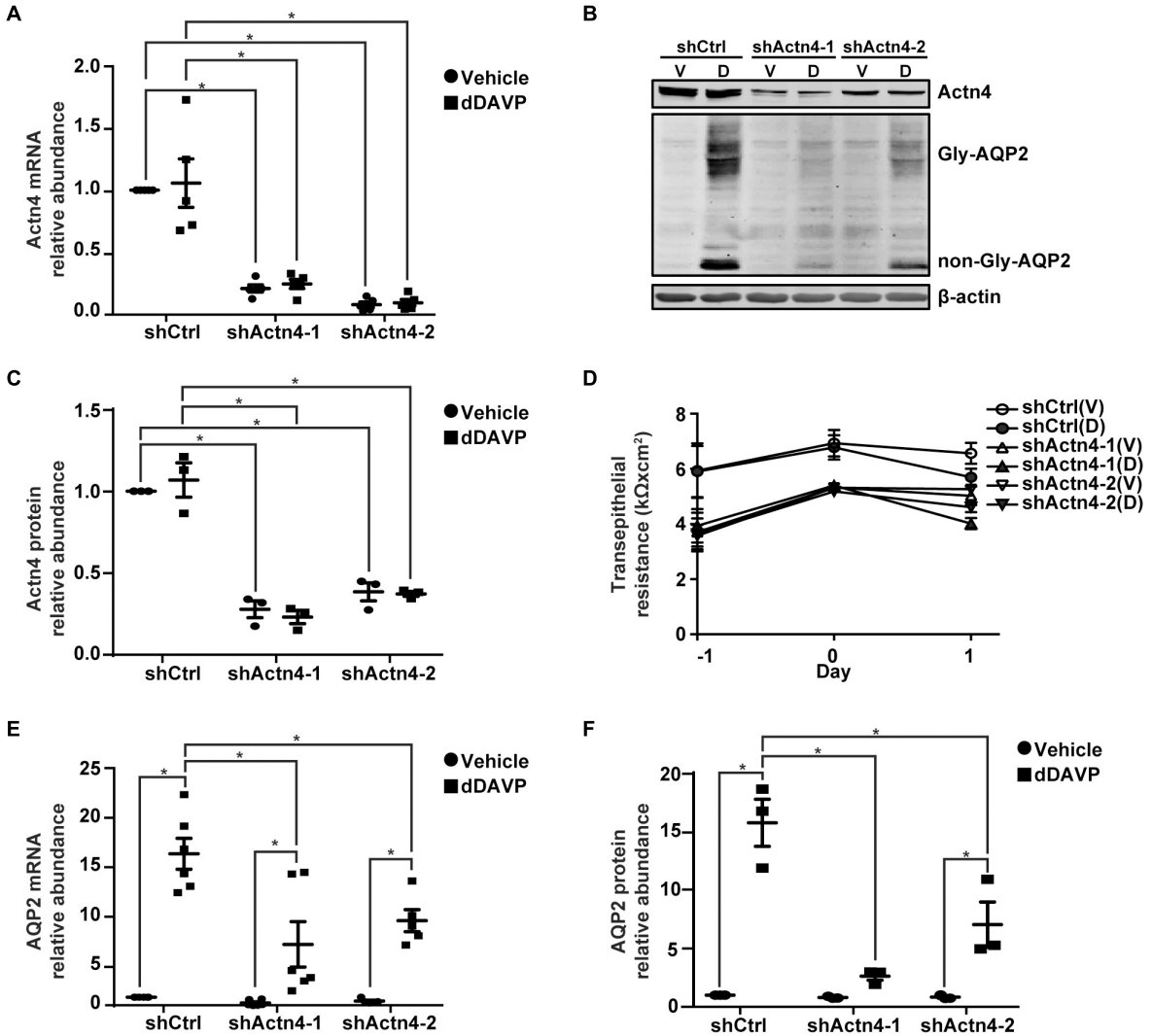

FIGURE 3 | α-actinin 4 knockdown reduced vasopressin-induced *AQP2* gene expression in the mpkCCD cells. **(A,E)** Quantitative RT-PCR measurements of α-actinin 4 (Actn4) and AQP2 mRNA in control (shCtrl) and Actn4 knockdown (shActn4) cells exposed to vehicle (V) vs. 1 nM dDAVP (D). Two shActn4 sequences were used (shActn4-1 and shActn4-2). Numbers are means ± SEM, summarized from five or six independent experiments. Two-way ANOVA was used for statistical test. Asterisks indicate statistical significance between samples ($p < 0.05$). **(B,C,F)** Representative immunoblots and summaries of Actn4 and AQP2 in shCtrl and shActn4 cells in response to vehicle vs. dDAVP. Gly-AQP2 and non-Gly-AQP2 are glycosylated and non-glycosylated AQP2, respectively. Numbers are means ± SEM, summarized from three independent experiments. **(D)** Transepithelial electrical resistance of the cells grown on Transwell® prior to vehicle vs. dDAVP stimulation. Day –1, cell polarization; day 0, dDAVP exposure; day 1, harvest for RNA/protein measurement.

Vasopressin-Induced Glucocorticoid Receptor Nuclear Translocation Was Independent of α-Actinin 4

To test whether vasopressin-induced glucocorticoid receptor nuclear translocation depends on α-actinin 4, α-actinin 4 was knocked down before confocal immunofluorescence microscopy. Glucocorticoid receptor was detected in the cytoplasm and nuclei in the control cells under the vehicle conditions (**Figure 5A**, shCtrl). In response to dDAVP, more glucocorticoid receptor was observed in the nuclei than in the cytoplasm in the control cells. Similar observations were made in the α-actinin 4 knockdown cells (**Figure 5A**, shActn4-1 and shActn4-2). Three independent experiments show similar results (**Figure 5C**). Thus, vasopressin-induced glucocorticoid receptor nuclear translocation did not depend on α-actinin 4. Specificity of the observation was reassured with no primary glucocorticoid receptor antibody control, which did not produce any signal (**Figure 5B**).

Glucocorticoid Receptor Knockdown Reduced Vasopressin-Induced *AQP2* Gene Expression

Glucocorticoid receptor mRNA and protein knockdown to about 40.9% or 63.1% (**Figures 6A–C**) did not affect mpkCCD cell

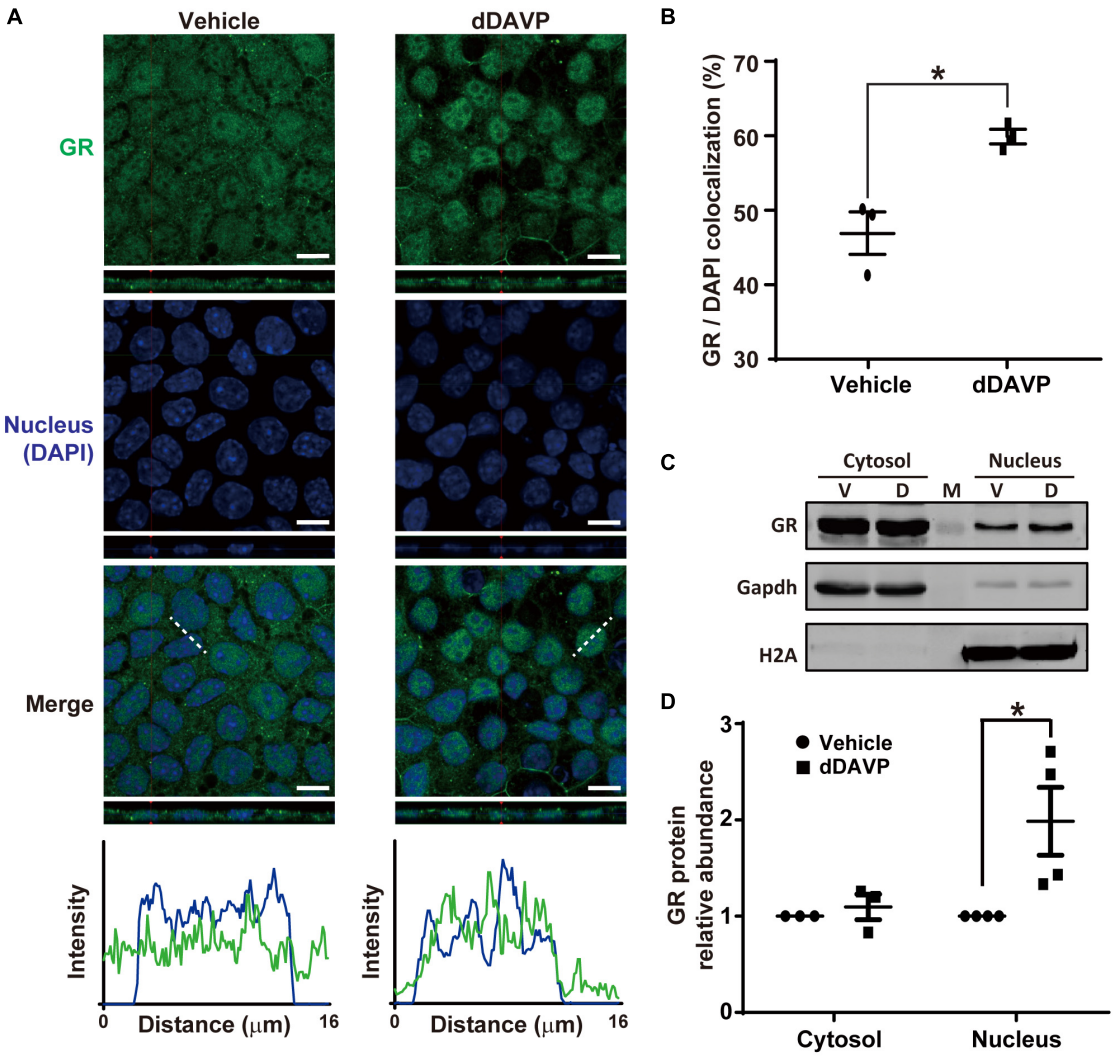

FIGURE 4 | Vasopressin induced glucocorticoid receptor nuclear translocation in the mpkCCD cells in the presence of dexamethasone. **(A)** Confocal immunofluorescence micrographs of glucocorticoid receptor (GR, green) and nuclei (DAPI, blue). Polarized cells grown on Transwell® were exposed (24 h) to vehicle, or 1 nM dDAVP. Shown at the bottoms are signal profiles along the dotted lines. Bars indicate 10 μm. **(B)** Summaries of GR colocalization with DAPI. Numbers are means ± SEM, summarized from three independent experiments and about 330 cells per experiment. Asterisk indicates statistical significance, *t*-test $p < 0.05$. **(C,D)** Representative immunoblots and summary of GR in the cytosol vs. nuclei of the cells exposed to vehicle (V) vs. dDAVP (D). Numbers are means ± SEM, summarized from three or four independent experiments. Gapdh and H2A were markers for cytosol and nucleus, respectively. Protein intensities were corrected against those of Gapdh or H2A to avoid variations in the sample preparation. M, marker.

polarization as the increases in the transepithelial resistance were similar for all experimental groups (**Figure 6D**). Under these conditions, the dDAVP-induced increases in the *AQP2* gene expression were profoundly reduced at both mRNA and protein levels in the glucocorticoid receptor knockdown cells (**Figures 6B,E,F**). dDAVP did not affect glucocorticoid receptor mRNA or protein levels in the control or knockdown cells exposed to vehicle or dDAVP (**Figures 6A–C**). Thus, the reduced *AQP2* gene expression were due to the effects of the reduced glucocorticoid receptor levels in the knockdown cells. Note that while the AQP2 mRNA and protein were detected in the α-actinin 4 knockdown cells (**Figures 3B,E,F**), they were barely detectable in the glucocorticoid receptor knockdown cells (**Figures 6B,E,F**), indicating a major role of glucocorticoid receptor in vasopressin-induced *AQP2* gene expression.

Vasopressin-Induced Glucocorticoid Receptor Nuclear Translocation and AQP2 mRNA Expression Were Reduced in the Absence of Dexamethasone

The above experiments were done in the presence of glucocorticoid receptor agonist dexamethasone that induces glucocorticoid receptor nuclear translocation (Gustafsson et al., 1987). To test whether vasopressin-induced glucocorticoid

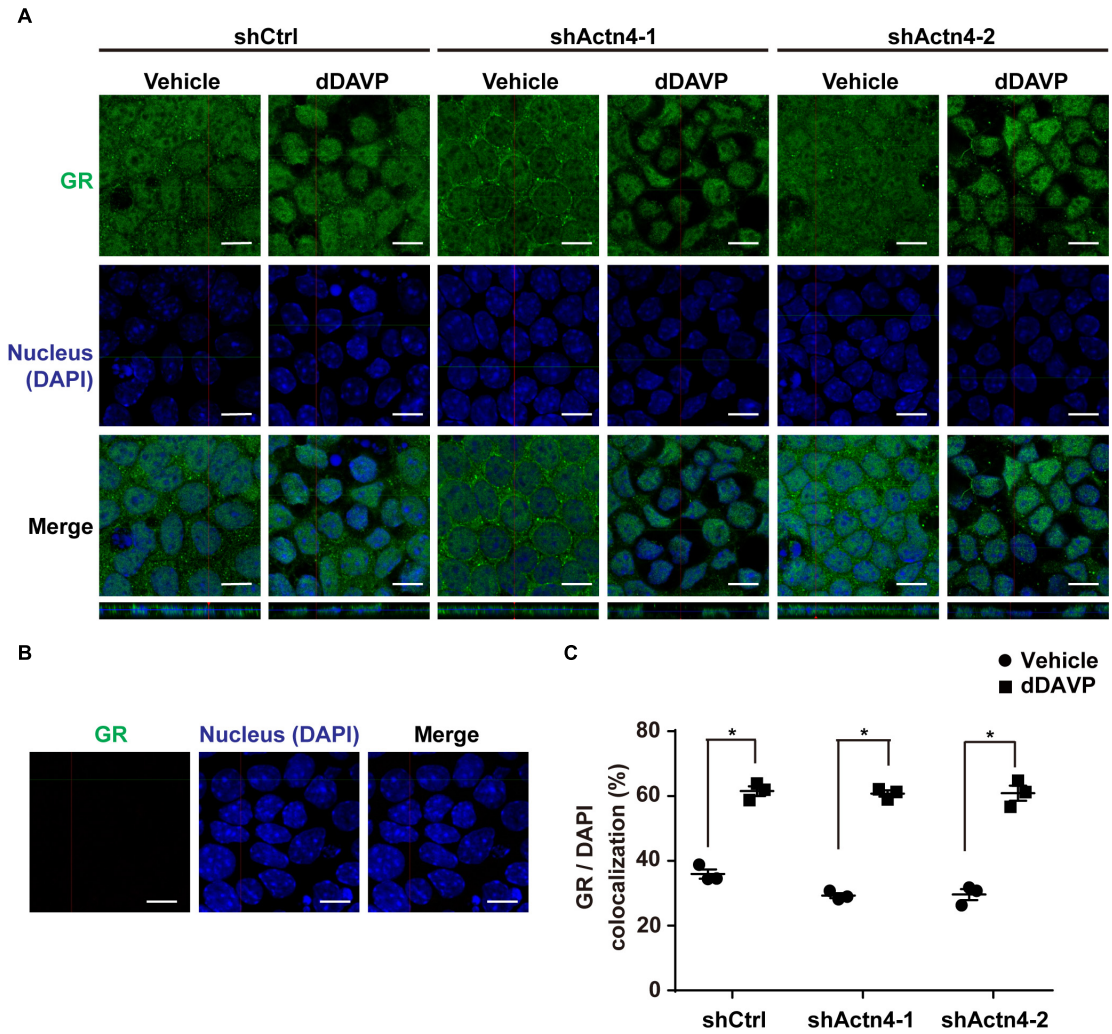

FIGURE 5 | Vasopressin-induced glucocorticoid receptor nuclear translocation was independent of α-actinin 4. **(A,B)** Confocal immunofluorescence micrographs of glucocorticoid receptor in control (shCtrl) and α-actinin 4 knockdown (shActn4-1 and shActn4-2) mpkCCD cells grown on Transwell® under vehicle vs. dDAVP (1 nM, 24 h) conditions. Bars indicate 10 μm. The primary antibody to glucocorticoid receptor was omitted in **(B)**. **(C)** Summary of the confocal imaging results. Numbers are means ± SEM from three independent experiments, about 330 cells in each experiment. Asterisks indicate statistical significance, *t*-test $p < 0.05$.

receptor nuclear translocation and *AQP2* gene expression depends on glucocorticoid, dexamethasone was omitted from the experiments. Confocal immunofluorescence microscopy showed cytoplasmic and nuclear staining of glucocorticoid receptor in the mpkCCD cells under the vehicle conditions in the absence of dexamethasone (**Figure 7A**). Stimulating the cells with dDAVP in the absence of dexamethasone slightly increased nuclear staining of glucocorticoid receptor. On average, the nuclear glucocorticoid receptor staining increased from 24.4% under the vehicle conditions to 37.2% under the dDAVP conditions in the absence of dexamethasone (**Figure 7B**). Thus, glucocorticoid binding plays a crucial role in vasopressin-induced glucocorticoid receptor nuclear translocation. Similarly, glucocorticoid binding also plays a crucial role in vasopressin-induced *AQP2* gene expression. In the presence of dexamethasone, dDAVP induced AQP2 mRNA to about 31.0 folds compared to that in the vehicle control (**Figure 7C**). In the absence of dexamethasone, the dDAVP-induced AQP2 mRNA level was reduced to about 1/3 of that in the presence of dexamethasone. In the absence of dexamethasone, the dDAVP-induced AQP2 mRNA level in the α-actinin 4 knockdown cells was further reduced to about 1/5 of that in the control cells (**Figure 7C**, shActn4 vs. shCtrl). Thus, dexamethasone plays a major role in vasopressin-induced glucocorticoid receptor nuclear translocation and *AQP2* gene expression, which can be enhanced by α-actinin 4.

DISCUSSION

In the present study, we showed for the first time that α-actinin 4 functions as a transcription co-activator for glucocorticoid receptor-mediated *AQP2* gene expression in the mpkCCD

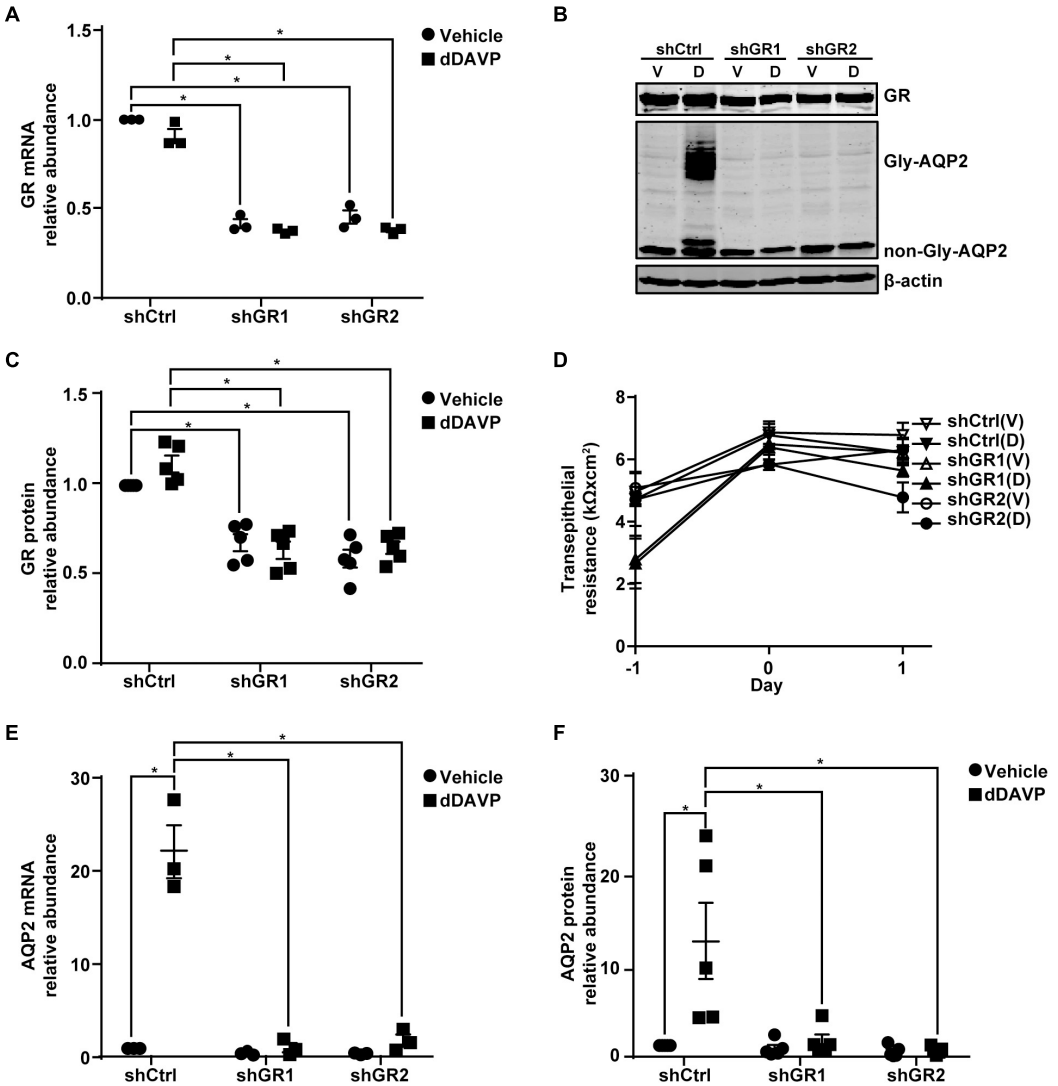

FIGURE 6 | Glucocorticoid receptor knockdown reduced vasopressin-induced *AQP2* gene expression in the mpkCCD cells. **(A,E)** Quantitative RT-PCR measurements of glucocorticoid receptor (GR) and AQP2 mRNA in control (shCtrl) and GR knockdown (shGR) cells in response to vehicle vs. 1 nM dDAVP. Two shGR sequences were used (shGR1 and shGR2). Numbers are means ± SEM, summarized from three independent experiments. Two-way ANOVA was used for statistical test. Asterisks indicate statistical significance between samples ($p < 0.05$, *t*-test). **(B,C,F)** Representative immunoblots and summaries of GR and AQP2 in shCtrl and shGR cells in response to vehicle (V) vs. dDAVP (D). Gly-AQP2 and non-Gly-AQP2 are glycosylated and non-glycosylated AQP2, respectively. Numbers are means ± SEM, summarized from five independent experiments. **(D)** Transepithelial electrical resistance of the cells grown on Transwell® prior to vehicle vs. dDAVP stimulation. Day −1, cell polarization; day 0, dDAVP exposure; day 1, harvest for RNA and protein measurements.

collecting duct cells in response to vasopressin (Kuo et al., 2018). Our findings suggest a role of α-actinin 4 that connects vasopressin-mediated short-term regulation of AQP2 trafficking to long-term regulation of *AQP2* gene expression (**Figure 8**). As an F-actin crosslinking protein, α-actinin 4 dimers bundle F-actin filaments and link them to the plasma membrane via direct or indirect interaction with integrin (Chen et al., 2012; Honda, 2015). This forms a cortical F-actin skeleton underneath the apical plasma membrane and impedes AQP2-containing vesicle from fusion with the membrane (Noda et al., 2010). Vasopressin-induced apical AQP2 insertion thus necessitates F-actin depolymerization at the apical plasma membrane (Noda et al., 2008; Yui et al., 2012; Loo et al., 2013). Via elevating intracellular Ca^{2+}, vasopressin reduces α-actinin 4 interaction with F-actin (Blanchard et al., 1989; Knepper et al., 2015). This should free up α-actinin 4 and promote F-actin depolymerization (Star et al., 1988; Blanchard et al., 1989), which is expected to facilitate short-term vasopressin-induced AQP2 insertion into the apical membrane. The so freed α-actinin 4 then enters the nuclei where it interacts with glucocorticoid receptor to enhance long-term vasopressin-induced *AQP2* gene expression.

Functions of F-actin in AQP2 trafficking are far more complex than those described above. As AQP2 constitutively recycles between the intracellular vesicles and the plasma

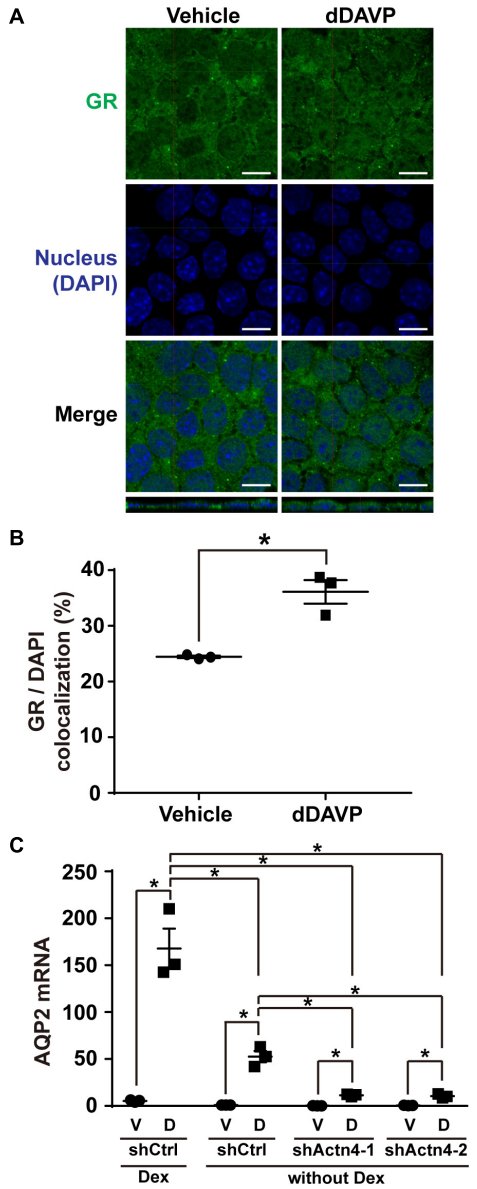

FIGURE 7 | Vasopressin-induced glucocorticoid receptor nuclear translocation and AQP2 mRNA expression were reduced in the absence of dexamethasone. **(A,B)** Representative and summary of confocal immunofluorescence micrographs of glucocorticoid receptor (GR) in the mpkCCD cells in response to vehicle or dDAVP in the absence of dexamethasone. The nuclei were stained with DAPI in blue. Numbers are means ± SEM, summarized from three independent experiments and about 330 cells per experiment. Asterisks indicate statistical significance, *t*-test $p < 0.05$. Bars indicate 10 μm. **(C)** Quantitative RT-PCR measurements of AQP2 mRNA in the control (shCtrl) and α-actinin 4 knockdown (shActn4-1 and shActn4-2) mpkCCD cells in response to dDAVP (D) vs. vehicle (V) in the presence or absence of dexamethasone (Dex). Numbers are means ± SEM, summarized from three independent experiments.

membrane (Brown, 2003; Tajika et al., 2005; Wang et al., 2020), the apical AQP2 abundance is a balanced result between AQP2 exocytosis to and endocytosis from the apical plasma membrane. While increased exocytosis increases the apical AQP2 abundance (Noda and Sasaki, 2005), decreased endocytosis also does so (Brown, 2003). The facts that AQP2 is endocytosed via clathrin-mediated processes (Sun et al., 2002) and that F-actin participates in near all aspects of clathrin-mediated endocytosis (Yarar et al., 2005) have alluded to functions of F-actin in AQP2 endocytosis. As F-actin is recruited to the sites of endocytosis to facilitate membrane invagination (Smythe and Ayscough, 2006), reagents that promote F-actin depolymerization reduce AQP2 endocytosis and increase AQP2 in the plasma membrane (Procino et al., 2010; Li et al., 2011). Conversely, F-actin polymerization promotes AQP2 endocytosis (Li et al., 2011, 2017). The above observations are compatible with the regulation of F-actin by α-actinin 4 in the collecting duct cells (**Figure 8**). In the absence of vasopressin, intracellular Ca^{2+} concentration is low, α-actinin 4 dimers bundle F-actin and connect them to the plasma membrane. This prevents AQP2 exocytosis in one hand and promotes AQP2 endocytosis in the other hand. In the presence of vasopressin, intracellular Ca^{2+} concentration elevates and reduces α-actinin 4 interaction with F-actin (Blanchard et al., 1989), promoting F-actin depolymerization. This is expected to reduce AQP2 endocytosis and to facilitate AQP2 exocytosis. Vasopressin-induced AQP2 phosphorylation further enhances apical AQP2 abundance via these two processes. S256 phosphorylation promotes F-actin depolymerization, which is expected to reduce AQP2 endocytosis and enhance exocytosis (Noda et al., 2008). S269 phosphorylation has been shown to reduce Sipa1l1-mediated AQP2 endocytosis (Wang et al., 2017).

Compared to α-actinin 4 knockdown, glucocorticoid receptor knockdown had much profound effects on vasopressin-induced *AQP2* gene expression. While AQP2 mRNA and protein were detected in the α-actinin 4 knockdown cells in the presence of vasopressin (**Figure 3**), they were barely detectable in the glucocorticoid receptor knockdown cells (**Figure 6**). This is consistent with the transcription co-activator role of α-actinin 4, which does not directly bind glucocorticoid response elements but complexes with glucocorticoid receptor to enhance transcriptional activity (Honda, 2015; Zhao et al., 2017). Note that the experiments in the present study were done in the presence of the glucocorticoid receptor agonist dexamethasone, which itself would bind glucocorticoid receptor and induce nuclear translocation. This may explain the nuclear staining of the glucocorticoid receptor in the absence of vasopressin (**Figure 4**). However, the nuclear dexamethasone-glucocorticoid receptor complex did not result in *AQP2* gene expression in the absence of vasopressin (**Figure 6**), consistent with our prior observation (Kuo et al., 2018). Thus, vasopressin must have elicited additional mechanisms to result in *AQP2* gene expression even in the presence of nuclear glucocorticoid receptor. Vasopressin-induced α-actinin 4 nuclear translocation and interaction with glucocorticoid receptor contribute a portion to the mechanism as α-actinin 4 knockdown reduces vasopressin-induced *AQP2* gene expression in the presence of dexamethasone (**Figures 1–3**).

How vasopressin leads to glucocorticoid receptor nuclear translocation requires further study. Vasopressin-enhanced

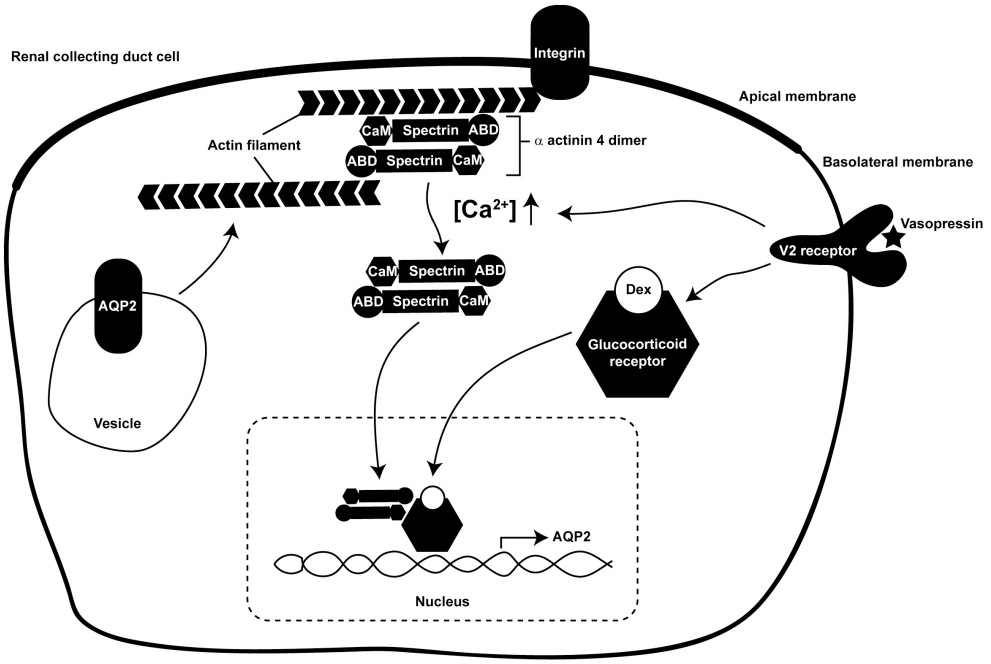

FIGURE 8 | A model illustrates dual functions of α-actinin 4 in vasopressin short-term and long-term actions in the kidney collecting duct cells. ABD, actin-binding domain; CaM, calmodulin-like domain; Dex, dexamethasone.

interaction between glucocorticoid receptor and α-actinin 4 (**Figure 2**) does not seem to provide such a mechanism because vasopressin still induces glucocorticoid receptor nuclear translocation in the α-actinin 4 knockdown cells (**Figure 5**) and still induces *AQP2* gene expression (**Figure 3**). Moreover, α-actinin 4 itself lacks nuclear localization signal (Honda et al., 1998). How α-actinin 4 translocates to the nucleus also requires further investigation. Our data suggest two independent pathways by which glucocorticoid receptor and α-actinin 4 enter the nucleus in response to vasopressin (**Figure 8**). Once in the nucleus, glucocorticoid receptor and α-actinin 4 interact to enhance *AQP2* gene expression. In fact, α-actinin 4 was found to interact with glucocorticoid receptor exclusively in the nuclei in human podocytes (Zhao et al., 2017).

The dual functional α-actinin 4 provides a molecular link that connects vasopressin short-term regulation in AQP2 trafficking to long-term regulation in *AQP2* gene transcription (**Figure 8**); however, the network of vasopressin-mediated *AQP2* gene transcription is far from complete. Based on promoter-reporter assays, several transcription factors have been implicated in AQP2 transcription including Creb1 (Hozawa et al., 1996; Yasui et al., 1997), Elf3 (Yu et al., 2009), Elf5 (Yu et al., 2009; Grassmeyer et al., 2017), Ehf (Yu et al., 2009), Gata-3 (Uchida et al., 1997), and Nfat5 (Hasler et al., 2006). Incorporation of these transcription factors into the AQP2 transcription network is challenging because the studies were done in various cell models that often do not express endogenous vasopressin V2 receptor or AQP2. For example, Creb1 has been the primary transcription factor for *AQP2* gene transcription in many review papers (Nielsen et al., 2002; Bockenhauer and Bichet, 2015; Pearce et al., 2015). However, recent ChIP-seq analysis of the re-cloned mpkCCD cells that express all necessary molecular components for vasopressin signaling, *AQP2* gene expression, and trafficking (Rinschen et al., 2010; Xie et al., 2010; Khositseth et al., 2011; Schenk et al., 2012; Loo et al., 2013) showed no clear evidence of Creb1's involvement in AQP2 transcription (Jung et al., 2018). Instead, a number of other transcription factor candidates were suggested for future investigation (Kikuchi et al., 2021), preferentially with CRISPR/Cas9-based gene knockout (Isobe et al., 2017, 2020; Datta et al., 2020) or small hairpin RNA-mediated gene knockdown when gene deletion is lethal (Wang et al., 2017, 2020; Kuo et al., 2018; Lin et al., 2019; Wong et al., 2020). Thus, a comprehensive AQP2 transcription network may be anticipated with the advent of the systems approaches that generate novel hypotheses addressable with modern molecular biological methods.

DATA AVAILABILITY STATEMENT

The raw data supporting the conclusions of this article will be made available by the authors, without undue reservation.

AUTHOR CONTRIBUTIONS

C-HH, H-HY, S-HS, and A-HY designed and performed experiments. C-HH, H-HY, S-HS, A-HY, and M-JY analyzed, presented, and interpreted the data. All authors wrote, edited, and approved the manuscript.

FUNDING

This work was supported by the Ministry of Science and Technology, Taiwan (MOST 107-2320-B-002-057-MY3 and MOST 110-2320-B-002-058 to M-JY).

ACKNOWLEDGMENTS

We thank the imaging core facility of the First Core Labs, National Taiwan University College of Medicine, for technical assistance.

REFERENCES

Blanchard, A., Ohanian, V., and Critchley, D. (1989). The structure and function of alpha-actinin. *J. Muscle Res. Cell Motil.* 10, 280–289.

Bockenhauer, D., and Bichet, D. G. (2015). Pathophysiology, diagnosis and management of nephrogenic diabetes insipidus. *Nat. Rev. Nephrol.* 11, 576–588. doi: 10.1038/nrneph.2015.89

Brown, D. (2003). The ins and outs of aquaporin-2 trafficking. *Am. J. Physiol. Renal Physiol.* 284, F893–F901. doi: 10.1152/ajprenal.00387.2002

Bubb, M. R., Spector, I., Beyer, B. B., and Fosen, K. M. (2000). Effects of jasplakinolide on the kinetics of actin polymerization. An explanation for certain *in vivo* observations. *J. Biol. Chem.* 275, 5163–5170. doi: 10.1074/jbc.275.7.5163

Chen, Y., Rice, W., Gu, Z., Li, J., Huang, J., Brenner, M. B., et al. (2012). Aquaporin 2 promotes cell migration and epithelial morphogenesis. *J. Am. Soc. Nephrol.* 23, 1506–1517. doi: 10.1681/asn.2012010079

Datta, A., Yang, C. R., Limbutara, K., Chou, C. L., Rinschen, M. M., Raghuram, V., et al. (2020). PKA-independent vasopressin signaling in renal collecting duct. *FASEB J.* 34, 6129–6146. doi: 10.1096/fj.201902982R

DiGiovanni, S. R., Nielsen, S., Christensen, E. I., and Knepper, M. A. (1994). Regulation of collecting duct water channel expression by vasopressin in Brattleboro rat. *Proc. Natl. Acad. Sci. U.S.A.* 91, 8984–8988.

Duong Van Huyen, J., Bens, M., and Vandewalle, A. (1998). Differential effects of aldosterone and vasopressin on chloride fluxes in transimmortalized mouse cortical collecting duct cells. *J. Membr. Biol.* 164, 79–90. doi: 10.1007/s002329900395

Feng, D., DuMontier, C., and Pollak, M. R. (2015). The role of alpha-actinin-4 in human kidney disease. *Cell Biosci.* 5:44.

Fenton, R. A., Murali, S. K., and Moeller, H. B. (2020). Advances in Aquaporin-2 trafficking mechanisms and their implications for treatment of water balance disorders. *Am. J. Physiol. Cell Physiol.* [Epub ahead of print]. doi: 10.1152/ajpcell.00150.2020

Fushimi, K., Uchida, S., Hara, Y., Hirata, Y., Marumo, F., and Sasaki, S. (1993). Cloning and expression of apical membrane water channel of rat kidney collecting tubule. *Nature* 361, 549–552.

Grassmeyer, J., Mukherjee, M., deRiso, J., Hettinger, C., Bailey, M., Sinha, S., et al. (2017). Elf5 is a principal cell lineage specific transcription factor in the kidney that contributes to Aqp2 and Avpr2 gene expression. *Dev. Biol.* 424, 77–89. doi: 10.1016/j.ydbio.2017.02.007

Gustafsson, J. A., Carlstedt-Duke, J., Poellinger, L., Okret, S., Wikstrom, A. C., Bronnegard, M., et al. (1987). Biochemistry, molecular biology, and physiology of the glucocorticoid receptor. *Endocr. Rev.* 8, 185–234.

Hasler, U., Jeon, U. S., Kim, J. A., Mordasini, D., Kwon, H. M., Feraille, E., et al. (2006). Tonicity-responsive enhancer binding protein is an essential regulator of aquaporin-2 expression in renal collecting duct principal cells. *J. Am. Soc. Nephrol.* 17, 1521–1531. doi: 10.1681/ASN.2005121317

Honda, K. (2015). The biological role of actinin-4 (ACTN4) in malignant phenotypes of cancer. *Cell Biosci.* 5:41.

Honda, K., Yamada, T., Endo, R., Ino, Y., Gotoh, M., Tsuda, H., et al. (1998). Actinin-4, a novel actin-bundling protein associated with cell motility and cancer invasion. *J. Cell Biol.* 140, 1383–1393. doi: 10.1083/jcb.140.6.1383

Hozawa, S., Holtzman, E. J., and Ausiello, D. A. (1996). cAMP motifs regulating transcription in the aquaporin 2 gene. *Am. J. Physiol.* 270, C1695–C1702.

Isobe, K., Jung, H. J., Yang, C. R., Claxton, J., Sandoval, P., Burg, M. B., et al. (2017). Systems-level identification of PKA-dependent signaling in epithelial cells. *Proc. Natl. Acad. Sci. U.S.A.* 114, E8875–E8884.

Isobe, K., Raghuram, V., Krishnan, L., Chou, C. L., Yang, C. R., and Knepper, M. A. (2020). CRISPR-Cas9/phosphoproteomics identifies multiple noncanonical targets of myosin light chain kinase. *Am. J. Physiol. Renal Physiol.* 318, F600–F616. doi: 10.1152/ajprenal.00431.2019

Judith Radin, M., Yu, M. J., Stoedkilde, L., Lance Miller, R., Hoffert, J. D., Frokiaer, J., et al. (2012). Aquaporin-2 regulation in health and disease. *Vet. Clin. Pathol.* 41, 455–470.

Jung, H. J., Raghuram, V., Lee, J. W., and Knepper, M. A. (2018). Genome-wide mapping of DNA accessibility and binding sites for CREB and C/EBPbeta in vasopressin-sensitive collecting duct cells. *J. Am. Soc. Nephrol.* 29, 1490–1500. doi: 10.1681/ASN.2017050545

Khositseth, S., Pisitkun, T., Slentz, D. H., Wang, G., Hoffert, J. D., Knepper, M. A., et al. (2011). Quantitative protein and mRNA profiling shows selective post-transcriptional control of protein expression by vasopressin in kidney cells. *Mol. Cell. Proteomics* 10:M110004036. doi: 10.1074/mcp.M110.004036

Khurana, S., Chakraborty, S., Lam, M., Liu, Y., Su, Y. T., Zhao, X., et al. (2012). Familial focal segmental glomerulosclerosis (FSGS)-linked alpha-actinin 4 (ACTN4) protein mutants lose ability to activate transcription by nuclear hormone receptors. *J. Biol. Chem.* 287, 12027–12035. doi: 10.1074/jbc.M112.345421

Kikuchi, H., Jung, H. J., Raghuram, V., Leo, K. T., Park, E., Yang, C. R., et al. (2021). Bayesian identification of candidate transcription factors for the regulation of Aqp2 gene expression. *Am. J. Physiol. Renal Physiol.* 321, F389–F401. doi: 10.1152/ajprenal.00204.2021

Knepper, M. A., Kwon, T. H., and Nielsen, S. (2015). Molecular physiology of water balance. *N. Engl. J. Med.* 372, 1349–1358.

Kuo, K. T., Yang, C. W., and Yu, M. J. (2018). Dexamethasone enhances vasopressin-induced aquaporin-2 gene expression in the mpkCCD cells. *Am. J. Physiol. Renal Physiol.* 314, F219–F229. doi: 10.1152/ajprenal.00218.2017

Li, W., Jin, W. W., Tsuji, K., Chen, Y., Nomura, N., Su, L., et al. (2017). Ezrin directly interacts with AQP2 and promotes its endocytosis. *J. Cell Sci.* 130, 2914–2925. doi: 10.1242/jcs.204842

Li, W., Zhang, Y., Bouley, R., Chen, Y., Matsuzaki, T., Nunes, P., et al. (2011). Simvastatin enhances aquaporin-2 surface expression and urinary concentration in vasopressin-deficient Brattleboro rats through modulation of Rho GTPase. *Am. J. Physiol. Renal Physiol.* 301, F309–F318. doi: 10.1152/ajprenal.00001.2011

Lin, S. T., Ma, C. C., Kuo, K. T., Su, Y. F., Wang, W. L., Chan, T. H., et al. (2019). Transcription Factor Elf3 Modulates Vasopressin-Induced Aquaporin-2 Gene Expression in Kidney Collecting Duct Cells. *Front Physiol* 10:1308. doi: 10.3389/fphys.2019.01308

Loo, C. S., Chen, C. W., Wang, P. J., Chen, P. Y., Lin, S. Y., Khoo, K. H., et al. (2013). Quantitative apical membrane proteomics reveals vasopressin-induced actin dynamics in collecting duct cells. *Proc. Natl. Acad. Sci. U.S.A.* 110, 17119–17124. doi: 10.1073/pnas.1309219110

Moeller, H. B., Rittig, S., and Fenton, R. A. (2013). Nephrogenic diabetes insipidus: essential insights into the molecular background and potential therapies for treatment. *Endocr. Rev.* 34, 278–301. doi: 10.1210/er.2012-1044

Nielsen, S., Chou, C. L., Marples, D., Christensen, E. I., Kishore, B. K., and Knepper, M. A. (1995). Vasopressin increases water permeability of kidney collecting duct by inducing translocation of aquaporin-CD water channels to plasma membrane. *Proc. Natl. Acad. Sci. U.S.A.* 92, 1013–1017. doi: 10.1073/pnas.92.4.1013

Nielsen, S., Frokiaer, J., Marples, D., Kwon, T. H., Agre, P., and Knepper, M. A. (2002). Aquaporins in the kidney: from molecules to medicine. *Physiol. Rev.* 82, 205–244. doi: 10.1152/physrev.00024.2001

Noda, Y., Horikawa, S., Furukawa, T., Hirai, K., Katayama, Y., Asai, T., et al. (2004). Aquaporin-2 trafficking is regulated by PDZ-domain containing protein SPA-1. *FEBS Lett.* 568, 139–145. doi: 10.1016/j.febslet.2004.05.021

Noda, Y., Horikawa, S., Kanda, E., Yamashita, M., Meng, H., Eto, K., et al. (2008). Reciprocal interaction with G-actin and tropomyosin is essential for aquaporin-2 trafficking. *J. Cell Biol.* 182, 587–601. doi: 10.1083/jcb.200709177

Noda, Y., Horikawa, S., Katayama, Y., and Sasaki, S. (2005). Identification of a multiprotein "motor" complex binding to water channel aquaporin-2.

Biochem. Biophys. Res. Commun. 330, 1041–1047. doi: 10.1016/j.bbrc.2005.03.079

Noda, Y., and Sasaki, S. (2005). Trafficking mechanism of water channel aquaporin-2. *Biol. Cell* 97, 885–892. doi: 10.1042/bc20040120

Noda, Y., Sohara, E., Ohta, E., and Sasaki, S. (2010). Aquaporins in kidney pathophysiology. *Nat. Rev. Nephrol.* 6, 168–178. doi: 10.1038/nrneph.2009.231

Pearce, D., Soundararajan, R., Trimpert, C., Kashlan, O. B., Deen, P. M., and Kohan, D. E. (2015). Collecting duct principal cell transport processes and their regulation. *Clin. J. Am. Soc. Nephrol.* 10, 135–146. doi: 10.2215/cjn.05760513

Procino, G., Barbieri, C., Carmosino, M., Rizzo, F., Valenti, G., and Svelto, M. (2010). Lovastatin-induced cholesterol depletion affects both apical sorting and endocytosis of aquaporin-2 in renal cells. *Am. J. Physiol. Renal Physiol.* 298, F266–F278. doi: 10.1152/ajprenal.00359.2009

Richter, M., Murai, K. K., Bourgin, C., Pak, D. T., and Pasquale, E. B. (2007). The EphA4 receptor regulates neuronal morphology through SPAR-mediated inactivation of Rap GTPases. *J. Neurosci.* 27, 14205–14215. doi: 10.1523/JNEUROSCI.2746-07.2007

Rinschen, M. M., Yu, M. J., Wang, G., Boja, E. S., Hoffert, J. D., Pisitkun, T., et al. (2010). Quantitative phosphoproteomic analysis reveals vasopressin V2-receptor-dependent signaling pathways in renal collecting duct cells. *Proc. Natl. Acad. Sci. U.S.A.* 107, 3882–3887. doi: 10.1073/pnas.0910646107

Schenk, L. K., Bolger, S. J., Luginbuhl, K., Gonzales, P. A., Rinschen, M. M., Yu, M. J., et al. (2012). Quantitative proteomics identifies vasopressin-responsive nuclear proteins in collecting duct cells. *J. Am. Soc. Nephrol.* 23, 1008–1018. doi: 10.1681/ASN.2011070738

Simon, H., Gao, Y., Franki, N., and Hays, R. M. (1993). Vasopressin depolymerizes apical F-actin in rat inner medullary collecting duct. *Am. J. Physiol.* 265, C757–C762. doi: 10.1152/ajpcell.1993.265.3.C757

Smythe, E., and Ayscough, K. R. (2006). Actin regulation in endocytosis. *J. Cell Sci.* 119, 4589–4598. doi: 10.1242/jcs.03247

Star, R. A., Nonoguchi, H., Balaban, R., and Knepper, M. A. (1988). Calcium and cyclic adenosine monophosphate as second messengers for vasopressin in the rat inner medullary collecting duct. *J. Clin. Invest.* 81, 1879–1888. doi: 10.1172/JCI113534

Sun, T. X., Van Hoek, A., Huang, Y., Bouley, R., McLaughlin, M., and Brown, D. (2002). Aquaporin-2 localization in clathrin-coated pits: inhibition of endocytosis by dominant-negative dynamin. *Am. J. Physiol. Renal Physiol.* 282, F998–F1011. doi: 10.1152/ajprenal.00257.2001

Tajika, Y., Matsuzaki, T., Suzuki, T., Ablimit, A., Aoki, T., Hagiwara, H., et al. (2005). Differential regulation of AQP2 trafficking in endosomes by microtubules and actin filaments. *Histochem. Cell Biol.* 124, 1–12. doi: 10.1007/s00418-005-0010-3

Taylor, A., Mamelak, M., Reaven, E., and Maffly, R. (1973). Vasopressin: possible role of microtubules and microfilaments in its action. *Science* 181, 347–350. doi: 10.1126/science.181.4097.347

Uawithya, P., Pisitkun, T., Ruttenberg, B. E., and Knepper, M. A. (2008). Transcriptional profiling of native inner medullary collecting duct cells from rat kidney. *Physiol. Genomics* 32, 229–253. doi: 10.1152/physiolgenomics.00201.2007

Uchida, S., Matsumura, Y., Rai, T., Sasaki, S., and Marumo, F. (1997). Regulation of aquaporin-2 gene transcription by GATA-3. *Biochem. Biophys. Res. Commun.* 232, 65–68. doi: 10.1006/bbrc.1997.6236

Wade, J. B., Stetson, D. L., and Lewis, S. A. (1981). ADH action: evidence for a membrane shuttle mechanism. *Ann. N. Y. Acad. Sci.* 372, 106–117. doi: 10.1111/j.1749-6632.1981.tb15464.x

Wang, P. J., Lin, S. T., Liu, S. H., Kuo, K. T., Hsu, C. H., Knepper, M. A., et al. (2017). Vasopressin-induced serine 269 phosphorylation reduces Sipa1l1 (signal-induced proliferation-associated 1 like 1)-mediated aquaporin-2 endocytosis. *J. Biol. Chem.* 292, 7984–7993. doi: 10.1074/jbc.M117.779611

Wang, W. L., Su, S. H., Wong, K. Y., Yang, C. W., Liu, C. F., and Yu, M. J. (2020). Rab7 involves Vps35 to mediate AQP2 sorting and apical trafficking in collecting duct cells. *Am. J. Physiol. Renal Physiol.* 318, F956–F970. doi: 10.1152/ajprenal.00297.2019

Wong, K. Y., Wang, W. L., Su, S. H., Liu, C. F., and Yu, M. J. (2020). Intracellular location of aquaporin-2 serine 269 phosphorylation and dephosphorylation in kidney collecting duct cells. *Am. J. Physiol. Renal Physiol.* 319, F592–F602. doi: 10.1152/ajprenal.00205.2020

Xie, L., Hoffert, J. D., Chou, C. L., Yu, M. J., Pisitkun, T., Knepper, M. A., et al. (2010). Quantitative analysis of aquaporin-2 phosphorylation. *Am. J. Physiol. Renal Physiol.* 298, F1018–F1023.

Yamamoto, T., Sasaki, S., Fushimi, K., Ishibashi, K., Yaoita, E., Kawasaki, K., et al. (1995). Vasopressin increases AQP-CD water channel in apical membrane of collecting duct cells in Brattleboro rats. *Am. J. Physiol.* 268, C1546–C1551.

Yang, C. R., Tongyoo, P., Emamian, M., Sandoval, P. C., Raghuram, V., and Knepper, M. A. (2015b). Deep proteomic profiling of vasopressin-sensitive collecting duct cells. I. Virtual Western blots and molecular weight distributions. *Am. J. Physiol. Cell Physiol.* 309, C785–C798. doi: 10.1152/ajpcell.00213.2015

Yang, C. R., Raghuram, V., Emamian, M., Sandoval, P. C., and Knepper, M. A. (2015a). Deep proteomic profiling of vasopressin-sensitive collecting duct cells. II. Bioinformatic analysis of vasopressin signaling. *Am. J. Physiol. Cell Physiol.* 309, C799–C812. doi: 10.1152/ajpcell.00214.2015

Yarar, D., Waterman-Storer, C. M., and Schmid, S. L. (2005). A dynamic actin cytoskeleton functions at multiple stages of clathrin-mediated endocytosis. *Mol. Biol. Cell* 16, 964–975. doi: 10.1091/mbc.e04-09-0774

Yasui, M., Zelenin, S. M., Celsi, G., and Aperia, A. (1997). Adenylate cyclase-coupled vasopressin receptor activates AQP2 promoter via a dual effect on CRE and AP1 elements. *Am. J. Physiol.* 272, F443–F450. doi: 10.1152/ajprenal.1997.272.4.F443

Yu, M. J., Miller, R. L., Uawithya, P., Rinschen, M. M., Khositseth, S., Braucht, D. W., et al. (2009). Systems-level analysis of cell-specific AQP2 gene expression in renal collecting duct. *Proc. Natl. Acad. Sci. U.S.A.* 106, 2441–2446. doi: 10.1073/pnas.0813002106

Yu, M. J., Pisitkun, T., Wang, G., Aranda, J. F., Gonzales, P. A., Tchapyjnikov, D., et al. (2008). Large-scale quantitative LC-MS/MS analysis of detergent-resistant membrane proteins from rat renal collecting duct. *Am. J. Physiol. Cell Physiol.* 295, C661–C678. doi: 10.1152/ajpcell.90650.2007

Yui, N., Lu, H. J., Bouley, R., and Brown, D. (2012). AQP2 is necessary for vasopressin- and forskolin-mediated filamentous actin depolymerization in renal epithelial cells. *Biol. Open* 1, 101–108. doi: 10.1242/bio.2011042

Zhao, X., Khurana, S., Charkraborty, S., Tian, Y., Sedor, J. R., Bruggman, L. A., et al. (2017). alpha Actinin 4 (ACTN4) regulates glucocorticoid receptor-mediated transactivation and transrepression in podocytes. *J. Biol. Chem.* 292, 1637–1647. doi: 10.1074/jbc.M116.755546

Conflict of Interest: The authors declare that the research was conducted in the absence of any commercial or financial relationships that could be construed as a potential conflict of interest.

Publisher's Note: All claims expressed in this article are solely those of the authors and do not necessarily represent those of their affiliated organizations, or those of the publisher, the editors and the reviewers. Any product that may be evaluated in this article, or claim that may be made by its manufacturer, is not guaranteed or endorsed by the publisher.

frontiers in Physiology

REVIEW
published: 10 December 2021
doi: 10.3389/fphys.2021.797039

The Role of Vasopressin V2 Receptor in Drug-Induced Hyponatremia

*Sua Kim[1], Chor Ho Jo[1] and Gheun-Ho Kim[1,2]**

[1]Institute of Biomedical Science, Hanyang University College of Medicine, Seoul, South Korea, [2]Department of Internal Medicine, Hanyang University College of Medicine, Seoul, South Korea

Hyponatremia is frequently encountered in clinical practice and usually induced by renal water retention. Many medications are considered to be among the various causes of hyponatremia, because they either stimulate the release of arginine vasopressin (AVP) or potentiate its action in the kidney. Antidepressants, anticonvulsants, antipsychotics, diuretics, and cytotoxic agents are the major causes of drug-induced hyponatremia. However, studies addressing the potential of these drugs to increase AVP release from the posterior pituitary gland or enhance urine concentration through intrarenal mechanisms are lacking. We previously showed that in the absence of AVP, sertraline, carbamazepine, haloperidol, and cyclophosphamide each increased vasopressin V2 receptor (V2R) mRNA and aquaporin-2 (AQP2) protein and mRNA expression in primary cultured inner medullary collecting duct cells. The upregulation of AQP2 was blocked by the V2R antagonist tolvaptan or protein kinase A (PKA) inhibitors. These findings led us to conclude that the nephrogenic syndrome of inappropriate antidiuresis (NSIAD) is the main mechanism of drug-induced hyponatremia. Previous studies have also shown that the V2R has a role in chlorpropamide-induced hyponatremia. Several other agents, including metformin and statins, have been found to induce antidiuresis and AQP2 upregulation through various V2R-independent pathways in animal experiments but are not associated with hyponatremia despite being frequently used clinically. In brief, drug-induced hyponatremia can be largely explained by AQP2 upregulation from V2R-cAMP-PKA signaling in the absence of AVP stimulation. This paper reviews the central and nephrogenic mechanisms of drug-induced hyponatremia and discusses the importance of the canonical pathway of AQP2 upregulation in drug-induced NSIAD.

Keywords: aquaporin-2, collecting duct, nephrogenic syndrome of inappropriate antidiuresis, syndrome of inappropriate ADH secretion, vasopressin, water

OPEN ACCESS

Edited by:
Soo Wan Kim, Chonnam National University Medical School, South Korea

Reviewed by:
Tae-Hwan Kwon, Kyungpook National University, South Korea
Chung-Lin Chou, National Institutes of Health (NIH), United States

****Correspondence:***
Gheun-Ho Kim
kimgh@hanyang.ac.kr
orcid.org/0000-0002-8445-9892

Specialty section:
This article was submitted to Renal and Epithelial Physiology, a section of the journal Frontiers in Physiology

Received: *18 October 2021*
Accepted: *19 November 2021*
Published: *10 December 2021*

Citation:
Kim S, Jo CH and Kim G-H (2021) The Role of Vasopressin V2 Receptor in Drug-Induced Hyponatremia. Front. Physiol. 12:797039. doi: 10.3389/fphys.2021.797039

PATHOGENESIS OF HYPONATREMIA AND RENAL ACTION OF VASOPRESSIN

Hyponatremia, defined as a serum sodium concentration <135 mmol/L, is caused by an excess of water relative to sodium in the extracellular fluid. Although sodium depletion may precede water retention, primary water excess can occur irrespective of sodium balance (**Figure 1**). Water is retained in the body as a result of excessive intake and/or reduced renal excretion. The former is called primary polydipsia, usually occurring in neuropsychiatric patients. The

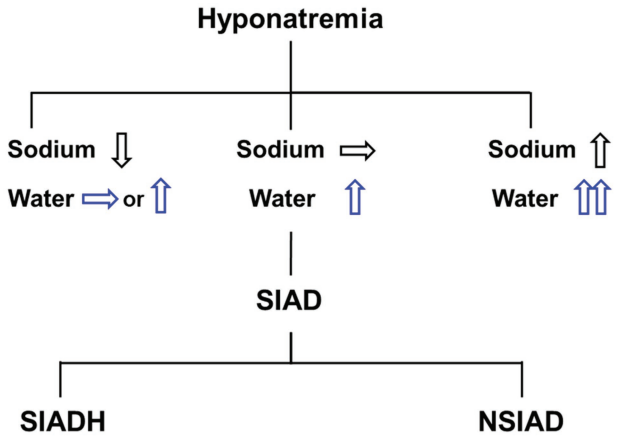

FIGURE 1 | Differential diagnosis of hyponatremia. Hyponatremia may include water and sodium balance disorder, and pure water excess presents clinically with euvolemic hyponatremia. The syndrome of inappropriate antidiuresis (SIAD) is the most common cause of euvolemic hyponatremia and can be classified into the syndrome of inappropriate antidiuretic hormone secretion (SIADH) and the nephrogenic syndrome of inappropriate antidiuresis (NSIAD).

latter can be induced by an absolute decrease in glomerular filtration rate (i.e., kidney failure) or abnormally increased water reabsorption along the renal tubule.

Renal water excretion is regulated by the action of arginine vasopressin (AVP), which is stored and released from the posterior pituitary gland. Synthesis of AVP in the hypothalamus is induced by both osmotic and non-osmotic stimuli, such as acute systemic hemodynamic changes, stress, and hypoxia (Schrier et al., 1979). In the kidney, the loop of Henle and collecting duct are the major sites of AVP action: AVP binds to the vasopressin V2 receptor (V2R) at the basolateral membrane of the collecting duct principal cells and induces osmotic water reabsorption through regulation of aquaporin-2 (AQP2) and aquaporin-3 (AQP3) water channel proteins (Jung and Kwon, 2016). The thick ascending limb of the loop of Henle plays an important role in countercurrent multiplication for urine concentration, and AVP strongly upregulates the expression of the Na-K-2Cl cotransporter 2 (NKCC2) of the thick ascending limb (Kim et al., 1999). The resultant outer medullary interstitial hypertonicity promotes osmotic water reabsorption along the collecting duct. On the other hand, inner medullary interstitial hypertonicity can be established by urea accumulation facilitated by urea transporters (UTs). By stimulating UT-A1 and UT-A3 in the inner medullary collecting duct and UT-A2 in the thin descending limb of Henle's loop (Wade et al., 2000), AVP promotes urea recycling.

THE SYNDROME OF INAPPROPRIATE ANTIDIURESIS AS A MAJOR CAUSE OF HYPONATREMIA

Hyponatremia is the most common electrolyte disorder in hospitalized patients and is potentially life-threatening because of the risk of cerebral edema (Adrogué and Madias, 2000). The "syndrome of inappropriate secretion of antidiuretic hormone (SIADH)" is the most frequent cause of hyponatremia, and a variety of drugs can stimulate the release of AVP or potentiate its action (Ellison and Berl, 2007). Thus, most cases of drug-induced hyponatremia are considered to be consistent with a diagnosis of the SIADH when hyponatremia is associated with the use of a particular agent in hypo-osmolar and euvolemic conditions (Smith et al., 2000; Janicic and Verbalis, 2003). Theoretically, the SIADH can be diagnosed when AVP release is inappropriately elevated despite low plasma osmolality. However, the diagnosis of the SIADH is usually made after identifying several clinical and laboratory features without measurement of AVP (Ellison and Berl, 2007). Measurement of AVP concentrations may not be feasible in clinical practice and the results may be unreliable, because AVP is highly unstable in isolated plasma and the pre-analytic procedures are complicated (Bolignano et al., 2014).

Alternately, Dr. Robertson proposed a diagnosis of the "syndrome of inappropriate antidiuresis (SIAD)," given plasma AVP is actually suppressed in a certain proportion of patients diagnosed as SIADH (Robertson, 1989). The term "nephrogenic syndrome of inappropriate antidiuresis (NSIAD)" was also coined by Feldman et al. when they described two infants whose clinical and laboratory evaluations were consistent with the presence of the SIADH but had undetectable AVP because of gain-of-function mutations in the V2R (Feldman et al., 2005). Thus, the SIAD caused by renal water retention can be grouped into SIADH (with an excess of antidiuretic hormone) and NSIAD (with appropriately suppressed AVP secretion) according to its pathogenesis (**Figure 1**).

DRUG-INDUCED HYPONATREMIA: THE SIADH VERSUS NSIAD

Table 1 presents the list of drugs that often cause hyponatremia in clinical practice. We classified them into AVP analogs, drugs that stimulate release of AVP, drugs that stimulate V2R in the kidney and induce the NSIAD, and others.

AVP ANALOGS

Desmopressin, a synthetic analog of AVP, has been prescribed for the treatment of diabetes insipidus and nocturnal polyuria. Although it is generally well tolerated, it can cause severe hyponatremia in susceptible patients because of its water-retaining effect (Kelleher and Henderson, 2006). Compared with AVP, desmopressin has a longer half-life and a greater antidiuretic effect caused by selective binding to the V2R (Kwon et al., 2013), but does not have unwanted vasopressor and uterotonic effects (Vilhardt, 1990). Together, V2R-mediated stimulation of adenylyl cyclases, elevation of cAMP, and activation of protein kinase A (PKA) are the canonical signaling pathways that trigger both increased AQP2 trafficking and AQP2 protein abundance (Jung and Kwon, 2016).

TABLE 1 | Drugs that can cause hyponatremia.

AVP analogs
Desmopressin (dDAVP)
Oxytocin
Drugs that stimulate release of arginine vasopressin
Vincristine
Ifosfamide
Drugs that stimulate the vasopressin V2 receptor in the kidney
Chlorpropamide
Antidepressants: selective serotonin-reuptake inhibitors
Anticonvulsants: carbamazepine
Antipsychotics: haloperidol
Cyclophosphamide
Diuretics
Thiazides
Prostaglandin synthesis inhibitors
Nonsteroidal anti-inflammatory drugs
Cyclooxygenase-2 inhibitors

A meta-analysis indicated the incidence of desmopressin-induced hyponatremia was 7.6% in adults with nocturia (Weatherall, 2004). The development of hyponatremia during desmopressin use is likely dependent on the dose of desmopressin. However, we found that even low doses of desmopressin could induce hyponatremia in predisposed patients and that advanced age and lower hemoglobin were the risk factors for hyponatremia in adults using desmopressin for nocturnal polyuria (Choi et al., 2015).

Oxytocin, used to induce labor or abortion, may be associated with hyponatremia because of its antidiuretic activity. As expected, the risk of hyponatremia is increased when oxytocin is diluted in intravenous hypotonic fluids (Ahmad et al., 1975). Oxytocin and AVP are closely related peptides secreted from the posterior pituitary, and both are nine-amino-acid peptide hormones, of which seven are identical (Baribeau and Anagnostou, 2015). Oxytocin was shown to act as an antidiuretic hormone because oxytocin increases osmotic water permeability in perfused inner medullary collecting ducts isolated from Sprague–Dawley rats (Chou et al., 1995b), and its hydrosmotic action was mediated by the V2R (Chou et al., 1995a). In Sprague–Dawley rats, oxytocin treatment induced apical and basolateral translocation of AQP2 protein along the collecting duct. This response was blocked by pretreatment with a V2R antagonist (Jeon et al., 2003). The antidiuretic action of oxytocin was also demonstrated in humans in association with AQP2 upregulation (Joo et al., 2004). Taken together, pharmacological doses of oxytocin can induce antidiuretic effects as a result of V2R stimulation and subsequent AQP2 upregulation (Cheng et al., 2009).

Drugs That Stimulate AVP Release

The anticancer chemotherapeutic agents, vincristine, vinblastine, cisplatin, and cyclophosphamide, were typically assumed to have stimulated release of AVP from the pituitary gland or to have increased production of AVP at the hypothalamus. However, evidence supporting these mechanisms is lacking (Berghmans, 1996).

Suskind et al. reported the case of a 3-year-old girl who was inadvertently administered an overdose of vincristine and developed clinical features compatible with the SIADH. Her blood vasopressin concentration was more than four times the normal value (Suskind et al., 1972). Stuart et al. showed that urinary vasopressin excretion was markedly elevated following administration of vincristine to a child with acute lymphatic leukemia (Stuart et al., 1975). Thus, the SIADH seems to be at the basis of vincristine-associated hyponatremia. Animal studies suggested that the SIADH may result from a direct toxic effect of vincristine on the neurohypophysis and the hypothalamic system (Uy et al., 1967; Robertson et al., 1973). In cases with increased plasma AVP concentration, however, dehydration due to vincristine toxicity or diarrhea needs to be differentiated from the SIADH (Jójárt et al., 1987).

Cyclophosphamide and ifosfamide are the representative alkylating agents that may be associated with hyponatremia. It is unclear whether plasma AVP concentrations are elevated following cyclophosphamide administration (Bressler and Huston, 1985; McCarron et al., 1995). On the other hand, elevated plasma AVP concentrations were found in a few cases of ifosfamide-induced hyponatremia (Cantwell et al., 1990; Kirch et al., 1997). Glezerman reported that ifosfamide-induced hyponatremia was corrected by the V2R antagonist conivaptan (Glezerman, 2009). This finding may support the possibility that the SIADH underlies ifosfamide-induced hyponatremia (Gross et al., 2011).

Drugs That Stimulate V2R in the Kidney

Renal water retention may result from the direct effects of some medications on the collecting duct epithelium in the absence of an AVP-mediated mechanism of action. Traditionally, such medications were classified as drugs that potentiate the renal action of AVP; however, they are now thought to act specifically as V2R agonists to induce the NSIAD.

Chlorpropamide

Chlorpropamide is a long-acting first-generation sulfonylurea, previously used to treat diabetes mellitus type 2. Chlorpropamide also has antidiuretic effects and has been used to treat diabetes insipidus (Kunstadter et al., 1969); although not currently used in clinical practice, the antidiuretic mechanisms of chlorpropamide are worthy of review.

High doses of chlorpropamide are associated with hyponatremia, and this effect was described as the SIADH since the first report in 1970 (Fine and Shedrovilzky, 1970). However, administration of chlorpropamide did not augment release of AVP in humans or rats (Pokracki et al., 1981). While the SIADH was seen in 4% of patients receiving

chlorpropamide in a clinic population, elevated plasma AVP concentrations were not demonstrated (Weissman et al., 1971).

Many studies have used the isolated toad urinary bladder to measure osmotic water permeability in response to chlorpropamide administration. Low concentrations of chlorpropamide enhanced the effect of AVP (Mendoza, 1969; Wales, 1971; Lozada et al., 1972; Hirji and Mucklow, 1991), whereas high concentrations increased water absorption across the membrane in the absence of AVP (Danisi et al., 1970; Urakabe et al., 1970; Ozer and Sharp, 1973; Mendoza and Brown, 1974).

Moses et al. investigated the mechanism by which chlorpropamide potentiates the action of AVP (Miller and Moses, 1970; Moses et al., 1982). They found that chlorpropamide enhanced the activity of renal medullary adenylate cyclase and increased renal medullary content of cAMP in response to desmopressin, supporting the concept that *in vivo* chlorpropamide acts at the V2R in the collecting duct to augment responsiveness to AVP (Moses et al., 1982). Other investigators have provided supporting evidence that chlorpropamide acts as a V2R agonist to exert its antidiuretic action. Chlorpropamide and AVP were first postulated to share a common site of action within the V2R in 1969 (Ingelfinger and Hays, 1969). Muta et al. (1989) showed that 1 mM chlorpropamide reduced AVP binding to the V2R within the rat renal tubular basolateral membrane in a competitive manner, indicating that chlorpropamide acts on the V2R (Muta et al., 1989). Using a radioiodinated derivative of AVP with high specific activity and high affinity for the V2R, Hensen et al. (1995) showed that low-dose oral chlorpropamide increased the V2R density without altering plasma AVP concentrations (Hensen et al., 1995); the V2R upregulation was therefore postulated to underlie chlorpropamide-induced hyponatremia.

Selective Serotonin Reuptake Inhibitors

A variety of antidepressants have been reported to be associated with hyponatremia: tricyclic antidepressants (TCAs), monoamine oxidase inhibitors, selective serotonin reuptake inhibitors (SSRIs), serotonin-norepinephrine reuptake inhibitors (SNRIs), and mirtazapine. These reports are supported by data from clinical and pre-clinical studies that indicate AVP plays an important role in the pathophysiology of major depression (Scott and Dinan, 2002). According to a cross-sectional study of elderly patients treated with antidepressants in the Netherlands, the prevalence of hyponatremia was 11.5% for the patients on TCAs, 10.2% for SSRI users, 8.6% for venlafaxine users, and 5.6% for patients using mirtazapine (Mannesse et al., 2013). Because non-suppressed plasma AVP levels were found in only a minority of these patients, the NSIAD was suggested as the underlying mechanism of SSRI-induced hyponatremia in most patients.

The mechanism of direct water retention from the kidney induced by SSRIs has been partly elucidated. Fluoxetine and sertraline are representative SSRIs that often associated with hyponatremia, causing significant morbidity and mortality (De Picker et al., 2014). An *in vitro* microperfused tubule study showed that in the absence of AVP, fluoxetine increased osmotic water permeability in the rat inner medullary collecting duct (IMCD). Furthermore, fluoxetine administration to rats for 10 days did not alter plasma AVP concentrations but increased AQP2 protein abundance in the kidney (Moyses et al., 2008).

We recently showed that in the rat IMCD, in the absence of vasopressin stimulation, sertraline upregulated AQP2 by inducing V2R-cAMP-PKA signaling (Kim et al., 2021). In IMCD suspensions, cAMP production was increased by sertraline and was attenuated by co-incubation with tolvaptan. In primary IMCD cell cultures, sertraline treatment increased total AQP2 and decreased phosphorylated AQP2 at S261. Notably, these responses were attenuated by co-incubation with tolvaptan or a PKA inhibitor. In addition, AQP2 membrane trafficking was induced by sertraline and blocked by co-incubation with tolvaptan or a PKA inhibitor. Furthermore, V2R and AQP2 mRNA expression and CREB-1 phosphorylation at S133 were induced by sertraline and blocked by co-incubation with tolvaptan. We concluded that sertraline acts as a V2R agonist in the kidney and leads to AQP upregulation by inducing AQP2 transcription and AQP2 dephosphorylation at S261 (Kim et al., 2021). Sertraline was reported to effectively reduce the number of wet episodes in adolescents with primary monosymptomatic enuresis who had experienced failure to desmopressin therapy (Mahdavi-Zafarghandi and Seyedi, 2014).

Carbamazepine

Carbamazepine and oxcarbazepine are the anticonvulsants most commonly reported to be associated with hyponatremia in epilepsy patients, although other anticonvulsants, such as eslicarbazepine, sodium valproate, lamotrigine, levetiracetam, and gabapentin, have also been reported to cause hyponatremia (Lu and Wang, 2017). The mechanism of anticonvulsant-associate hyponatremia has generally been considered to be inappropriate hypersecretion of AVP (Ashton et al., 1977; Smith et al., 1977), but an experimental study has indicated a direct effect of carbamazepine on the kidney through V2R stimulation without evidence of increased release of endogenous AVP (Meinders et al., 1975). Sekiya et al. also reported that 18-year-old male with carbamazepine-associated hyponatremia had features of the SIADH but had an undetectable level of plasma AVP and an elevated urine cyclic AMP excretion (Sekiya and Awazu, 2018). Thus, a human case of carbamazepine-induced NSIAD was demonstrated.

It has become clear that carbamazepine has a direct action on the collecting duct V2R, leading to AQP2 upregulation. *In vitro* microperfused tubule studies showed that in the absence of AVP, carbamazepine increased osmotic water absorption and AQP2 protein abundance in the rat IMCD by inducing the V2R-PKA pathway (de Bragança et al., 2010). We investigated the intracellular mechanisms of carbamazepine-induced AQP2 upregulation in the IMCD (Kim et al., 2021). In IMCD suspensions, cAMP production was increased by carbamazepine and was attenuated by co-incubation with tolvaptan. In primary IMCD cell cultures, incubation with carbamazepine increased the total AQP2 and decreased the phosphorylation of AQP2 at S261. Notably, these responses were reversed by co-incubation

with tolvaptan or a PKA inhibitor. In addition, AQP2 membrane trafficking was induced by carbamazepine and blocked by co-incubation with tolvaptan or a PKA inhibitor. Furthermore, V2R and AQP2 mRNA expression and CREB-1 phosphorylation at S133 were induced by carbamazepine and blocked by co-incubation with tolvaptan. We concluded that carbamazepine acts as a V2R agonist in the kidney and leads to AQP upregulation by inducing AQP2 transcription and AQP2 dephosphorylation at S261 (Kim et al., 2021). Compatible with our results, carbamazepine was shown to have antidiuretic activity in seven out of nine patients with central diabetes insipidus (Wales, 1975).

Oxcarbazepine is a keto-analog of carbamazepine and may be also associated with hyponatremia. Sachdeo et al. investigated the mechanisms by which oxcarbazepine can lead to hyponatremia in epilepsy and healthy subjects (Sachdeo et al., 2002). They found that, after the water load, solute-free water clearance was diminished in both groups without a concomitant increase in the blood AVP concentrations. Thus, oxcarbazepine-induced hyponatremia was not attributable to the SIADH. It seems that oxcarbazepine and carbamazepine share the common mechanisms of the NSIAD, namely direct action on the V2R.

Haloperidol

Antipsychotic drugs can be grouped into first-generation antipsychotics (e.g., chlorpromazine, chlorprotixene, dixyrazine, flupentixol, fluphenazine, haloperidol, levomepromazine, melperone, perphenazine, prochlorperazine, thioridazine, or zuclopenthixole) and second-generation antipsychotics (e.g., aripiprazole, clozapine, olanzapine, paliperidone, quetiapine, risperidone, or ziprasidone). A Swedish population-based case–control study found an association between antipsychotic therapy and hospitalization due to hyponatremia. The association was stronger for first-generation antipsychotics than second-generation antipsychotics (Falhammar et al., 2019). Several psychotropic drugs have been reported to be associated with the features of the SIADH, but without demonstration of unsuppressed plasma AVP (Peck and Shenkman, 1979; Whitten and Ruehter, 1997; Bachu et al., 2006).

On the other hand, plasma AVP concentrations did not change significantly when haloperidol was given to seven normal volunteers at a dose level (1.0 mg i.m.) known to have central nervous system effects (Kendler et al., 1978). Thus, we assessed whether haloperidol can induce renal water retention in the absence of AVP stimulation. In IMCD suspensions, cAMP production was increased by haloperidol and was attenuated by co-incubation with tolvaptan. In primary IMCD cell cultures, haloperidol increased the total AQP2 and decreased the AQP2 phosphorylation at S261. Notably, these responses were attenuated by co-incubation with tolvaptan or a PKA inhibitor. In addition, AQP2 membrane trafficking was induced by haloperidol and blocked by co-incubation with tolvaptan or a PKA inhibitor. Furthermore, V2R and AQP2 mRNA expression and CREB-1 phosphorylation at S133 were induced by haloperidol and were blocked by co-incubation with tolvaptan. We concluded that haloperidol acts as a V2R agonist in the kidney and leads to AQP2 upregulation by inducing AQP2 transcription and AQP2 dephosphorylation at S261 (Kim et al., 2021).

Cyclophosphamide

Hyponatremia can be induced by various doses of cyclophosphamide during the treatment of malignancy and rheumatological disease (Lee et al., 2010). As described above, plasma AVP concentrations are not elevated in patients following the administration of intravenous cyclophosphamide (Bode et al., 1980; Bressler and Huston, 1985; Larose et al., 1987). Furthermore, antidiuresis was reported to occur in response to intravenous cyclophosphamide in patients with central diabetes insipidus (Campbell et al., 2000; Steinman et al., 2015), excluding the possibility of the SIADH.

We showed that in the rat IMCD, the active metabolite of cyclophosphamide (4-hydroperoxycyclophosphamide) increased cAMP production, AQP2 protein and mRNA expression, and V2R mRNA expression in the absence of vasopressin stimulation (Kim et al., 2015). These changes were significantly ameliorated by co-administration of tolvaptan, suggestive of V2R-mediated NSIAD.

Thiazide Diuretics

Thiazide and loop diuretics are frequently used to treat edematous disorders. Although both classes of diuretic induce natriuresis, their effects on water balance may differ. Thiazides inhibit the Na-Cl cotransporter (NCC) in the distal convoluted tubule, the cortical diluting segment of the nephron. Thus, impairment of urine dilution and renal retention of water may be induced by thiazides (Hix et al., 2011). In contrast, loop diuretics, such as furosemide and torsemide, can inhibit the Na-K-2Cl cotransporter 2 (NKCC2) in the thick ascending limb, the outer medullary concentrating segment of the nephron. Thus, free-water clearance increases when urinary concentration is impaired by loop diuretics. Consequently, patients are prone to hyponatremia when using thiazides and hypernatremia when using loop diuretics.

Patients with thiazide-induced hyponatremia show features of the SIADH including low serum uric acid concentrations and increased fractional excretion of uric acid (Liamis et al., 2007). However, plasma AVP measurement in patients with thiazide-induced hyponatremia has produced conflicting results, with some studies reporting elevated AVP concentrations (Fichman et al., 1971; Luboshitzky et al., 1978), while others did not (Friedman et al., 1989; Frenkel et al., 2015; Ware et al., 2017). Ashraf et al. (1981) reported that plasma AVP was undetectable in metolazone-induced hyponatremia (Ashraf et al., 1981), suggestive of the NSIAD.

Thiazide-induced renal water retention may be independent of NCC inhibition in the distal convoluted tubule. No hyponatremia is found in Gitelman syndrome or Gitelman-mimic animals carrying a loss-of-function mutation in the NCC regulator Ste20 Proline-Alanine-rich Kinase (SPAK; Nadal et al., 2018). Hydrochlorothiazide administration resulted in reduced urine volume in lithium-treated NCC-knockout mice (Sinke et al., 2014). In particular, thiazides may act directly on the collecting duct, where water permeability is increased by vasopressin-independent mechanisms. Cesar and Magaldi performed *in vitro* microperfusion of IMCDs from AVP-deficient

Brattleboro rats and showed that addition of hydrochlorothiazide to the perfusate enhanced osmotic water permeability (César and Magaldi, 1999). This effect was attenuated by adding prostaglandin E2 to the perfusate, suggestive of the involvement of prostaglandin signaling.

We investigated the antidiuretic effect of hydrochlorothiazide in rats with lithium-induced nephrogenic diabetes insipidus (NDI) and explored the regulatory responses of AQP2 in the collecting duct (Kim et al., 2004). In association with antidiuresis, hydrochlorothiazide treatment caused a significant partial recovery of AQP2 abundance after lithium-induced downregulation. We believe thiazide diuretics have a direct action on the collecting duct principal cells and induce AQP2 upregulation by modulating prostaglandin E2 signaling pathways. This postulated mechanism was recently supported by the findings of a genetic and phenotyping analysis, suggestive of a role for genetically determined prostaglandin-E2-mediated increased water permeability of the collecting ducts in the development of thiazide-induced hyponatremia (Ware et al., 2017). A subgroup of patients with thiazide-induced hyponatremia may carry a variant allele of the prostaglandin transporter SLCO2A1 gene that leads to reduced ability to transport prostaglandin E2 across the apical cell membrane; this reduction of prostaglandin E2 transport leads to increased luminal prostaglandin E2 and activates luminal EP4 receptors, causing membrane trafficking of AQP2 in the absence of AVP, directly reducing urine dilution and free-water excretion (Filippone et al., 2020).

Prostaglandin Synthesis Inhibitors

Nonsteroidal anti-inflammatory drugs (NSAIDs), such as piroxicam, diclofenac, and indomethacin, are commonly used for pain control in daily clinical practice. They are rarely associated with hyponatremia, rather hyperkalemia and sodium retention with associated edema are much more frequently induced by NSAIDs (Raymond and Lifschitz, 1986); however, a few cases of severe NSAID-associated hyponatremia have been reported (Petersson et al., 1987). Prostaglandin E2 plays a critical physiologic and pathophysiologic role in inhibiting vasopressin action in the collecting duct (Breyer et al., 1990). Given NSAIDs inhibit prostaglandin synthesis, NSAIDs were thought to induce the SIADH (Demir et al., 2012); currently, potentiation of AVP action but not enhanced AVP release is considered as the most plausible explanation for NSAID-induced hyponatremia.

Prostaglandin E2 acts on the kidney through four different G-protein-coupled receptors, EP1-4 (Breyer and Breyer, 2001). In the presence of AVP, it can antagonize the renal AVP action *via* multiple EP receptors and signaling pathways (Breyer et al., 1990). However, prostaglandin E2 alone may increase collecting duct water permeability (Hébert et al., 1993). Olesen et al. showed that in the cortical collecting duct principal cells, EP2 and EP4 stimulation increased AQP2 apical membrane targeting, S256 phosphorylation, and S264 phosphorylation in the absence of AVP (Olesen et al., 2011). In addition, EP4 increases total kidney AQP2 protein abundance through an unknown mechanism (Li et al., 2009).

TABLE 2 | Experimental antidiuretic agents without causing hyponatremia.

Phosphodiesterase-5 inhibition
Sildenafil
AMP-activated protein kinase (AMPK) activation
Metformin
β-Hydroxy β-methylglutaryl-CoA (HMG-CoA) reductase inhibition
Simvastatin
Lovastatin
Rosuvastatin
Cerivastatin
Fluvastatin
$P2Y_{12}$ receptor antagonism
Clopidogrel
Epidermal growth factor receptor antagonism
Erlotinib
Azole antifungal agents
Fluconazole

On the other hand, EP3 has an important role in the diuretic effects of prostaglandin E2. EP3 inhibits NKCC2 through coupling to Gi and reduces countercurrent multiplication in the medullary thick ascending limb. In the collecting duct principal cells, EP3 decreases AQP2 apical membrane targeting as a result of cAMP suppression or RhoA stimulation (Olesen and Fenton, 2013).

NSAID-mediated cyclooxygenase (COX) inhibition results in the blockade of the EP3 action, which contributes to their antidiuretic action (Breyer and Breyer, 2001). We previously showed that in lithium-induced NDI rats, treatment with COX-2 inhibitors reduced polyuria by upregulating AQP2 and NKCC2 expression in the collecting duct and thick ascending limb, respectively (Kim et al., 2008). The antidiuretic effect of NSAIDs or COX-2 inhibitors has been useful in the treatment of human NDI. Indomethacin was effective in reducing polyuria in lithium-induced NDI (Allen et al., 1989); however, COX-2 inhibitors including rofecoxib and celecoxib may be preferable, because of their superior antidiuretic action without induction of upper gastrointestinal side effects (Soylu et al., 2005).

EXPERIMENTAL ANTIDIURETIC AGENTS WITHOUT CAUSING HYPONATREMIA

Other agents shown in **Table 2** can exert antidiuretic effects in animal models of NDI, but no cases of hyponatremia associated with their use have been reported (Liamis et al., 2008). Generally, these drugs upregulate AQP2 expression in the collecting duct without modulating V2R expression (**Figure 2**).

The phosphodiesterase-5 inhibitor sildenafil citrate reduced polyuria and increased AQP2 expression in rats with lithium-induced NDI (Sanches et al., 2012). Sildenafil citrate may increase nitric oxide and prevent degradation of cGMP,

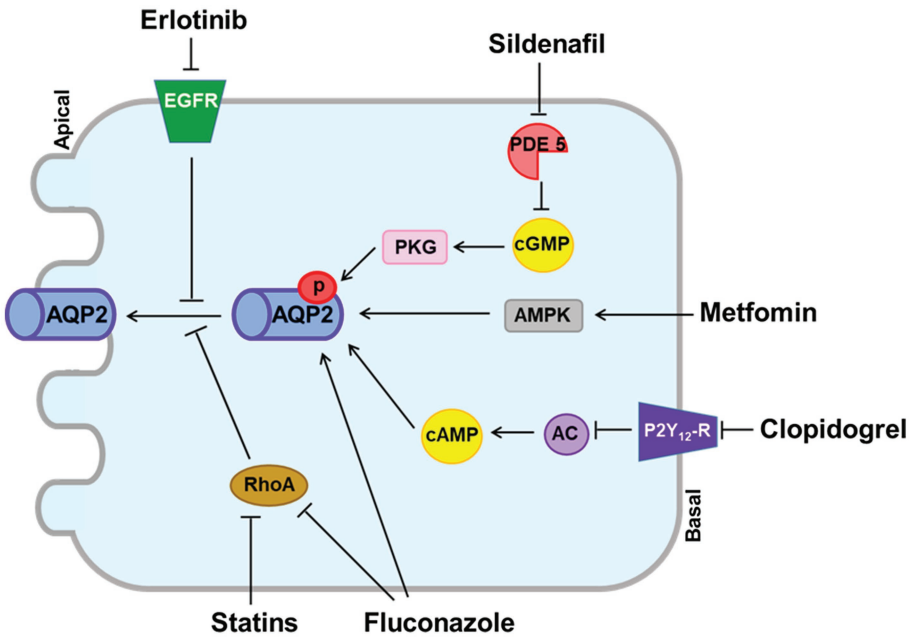

FIGURE 2 | Vasopressin V2 receptor (V2R)-independent pathways for aquaporin-2 (AQP2) upregulation induced by experimental antidiuretic agents. The phosphodiesterase-5 inhibitor sildenafil citrate prevents degradation of cGMP, resulting in increased AQP2 expression in the apical membrane. Erlotinib inhibits the tyrosine kinase activity of epidermal growth factor receptor (EGFR) and increases phosphorylation of AQP2 at Ser-256 and Ser-269. Metformin activates adenosine-monophosphate-activated protein kinase (AMPK) to phosphorylate AQP2. Clopidogrel inhibits the $P2Y_{12}$ receptor ($P2Y_{12}$-R) and increases adenylyl cyclase activity, resulting in AQP2 upregulation. Fluconazole upregulates AQP2 by increasing phosphorylation and abundance and by inhibiting RhoA. Statins inhibit RhoA, resulting in increased AQP2 expression in the apical membrane.

resulting in increased AQP2 abundance in the apical membrane (Bouley et al., 2005). However, no reduction of urine volume or increase in urine osmolality was observed in a small number of NDI patients participating in clinical trials with sildenafil citrate (Moeller et al., 2013).

Metformin is a first-line antidiabetic agent and activates adenosine-monophosphate-activated protein kinase (AMPK). Klein et al. found that AMPK was expressed in the rat inner medulla and that metformin increased osmotic water permeability in association with AQP2 phosphorylation and trafficking to the apical plasma membrane (Klein et al., 2016). They also reported that in tamoxifen-induced V2R-knockout mice, urine concentration was improved by metformin treatment (Efe et al., 2016). However, hyponatremia is not reported to be associated with metformin despite widespread use in clinical practice.

Statins are β-hydroxy β-methylglutaryl-CoA (HMG-CoA) reductase inhibitors that are commonly used to reduce serum cholesterol concentrations. Li et al. showed that in AVP-deficient Brattleboro rats, simvastatin reduced polyuria in association with enhanced AQP2 trafficking through downregulation of Rho GTPase activity (Li et al., 2011). AQP2 upregulation that bypassed the AVP-V2R signaling pathway was also induced by other statins including lovastatin, rosuvastatin, cerivastatin, and fluvastatin (Procino et al., 2011). However, a recent epidemiologic study disproved the association between statins and hyponatremia (Skov et al., 2021).

Like EP3, $P2Y_{12}$ receptor ($P2Y_{12}$-R) signaling is mediated through Gi in the collecting duct and can be inhibited by clopidogrel (Zhang et al., 2015b). Zhang et al. reported that in rats with lithium-induced NDI, clopidogrel attenuated polyuria as a result of increasing adenylyl cyclase activity and AQP2 protein expression (Zhang et al., 2015a). Although clopidogrel is frequently prescribed for atherosclerosis prevention, its use has not been associated with hyponatremia.

Erlotinib inhibits the tyrosine kinase activity of the epidermal growth factor receptor (EGFR) and is used for treatment of non-small-cell lung cancer and pancreatic cancer (Gridelli et al., 2010). Cheung et al. reported that in mice with lithium-induced NDI, erlotinib reduced polyuria and enhanced apical membrane expression of AQP2 by increasing phosphorylation of AQP2 at S256 and S269 and reducing phosphorylation of AQP2 at S261 (Cheung et al., 2016). However, erlotinib alone does not appear to induce hyponatremia in cancer patients.

Fluconazole, an azole antifungal agent, was shown to enhance urine concentration in mice. Its antidiuretic action was associated with AQP2 upregulation from increased AQP2 phosphorylation and abundance, as well as RhoA inhibition (Vukićević et al., 2019). However, fluconazole alone does not appear to induce hyponatremia in infectious patients.

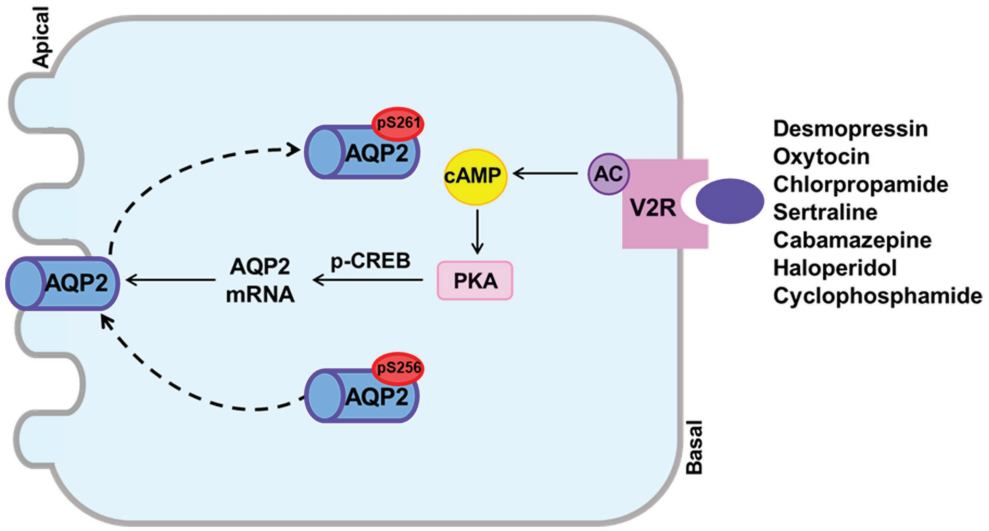

FIGURE 3 | The canonical pathway from the vasopressin V2 receptor (V2R) to aquaporin-2 (AQP2) upregulation to induce drug-induced hyponatremia. Drugs that can cause hyponatremia bind to the V2R at basolateral membranes of collecting ducts and stimulate adenylyl cyclase activity, resulting in increased cAMP production. The cAMP/PKA signaling also induces enhanced AQP2 targeting to the apical membrane and increased AQP2 transcription probably through CREB phosphorylation.

CONCLUSION

Drug-induced hyponatremia is caused by renal water retention and was previously explained as induction of the SIADH. However, the SIAD is now considered to be the correct expression for the mechanism of drug-induced hyponatremia because the SIADH and NSIAD share the same clinical features, but present with different plasma AVP levels. Our literature review showed that SIADH underlies the hyponatremia induced by desmopressin, oxytocin, vincristine and ifosfamide. On the other hand, direct action of the drug on the kidney for AQP2 upregulation or induction of the NSIAD may underlie most cases of drug-induced hyponatremia. Previous *in vitro* and *in vivo* studies have shown that chlorpropamide, once thought to cause the SIADH, can cause hyponatremia by inducing the V2R-mediated pathway in the absence of AVP. We have shown that haloperidol, sertraline, carbamazepine, and cyclophosphamide act directly on the V2R in the collecting duct and upregulate AQP2 by inducing cAMP production (**Figure 3**). This finding contrasts with the mechanism of other experimental antidiuretic agents, which upregulate AQP2 by inducing various V2R-independent signaling pathways, and are not associated with hyponatremia. We believe that the canonical pathway from V2R to AQP2 upregulation has a pivotal role in drug-induced hyponatremia.

AUTHOR CONTRIBUTIONS

G-HK and SK designed the study and drafted and revised the paper. SK and CJ carried out the experiments. G-HK, SK, and CJ collected and analyzed the data. SK made the figures. All authors contributed to the article and approved the submitted version.

FUNDING

This work was supported by a grant from the National Research Foundation of Korea (NRF-2020R1I1A1A01069274) to SK.

ACKNOWLEDGMENTS

The authors are indebted to Dr. Tae Hwan Kwon for the primary cultures of the IMCD cells.

REFERENCES

Adrogué, H. J., and Madias, N. E. (2000). Hyponatremia. *N. Engl. J. Med.* 342, 1581–1589. doi: 10.1056/nejm200005253422107

Ahmad, A. J., Clark, E. H., and Jacobs, H. S. (1975). Water intoxication associated with oxytocin infusion. *Postgrad. Med. J.* 51, 249–252. doi: 10.1136/bmj.1.6069.1134

Allen, H. M., Jackson, R. L., Winchester, M. D., Deck, L. V., and Allon, M. (1989). Indomethacin in the treatment of lithium-induced nephrogenic diabetes insipidus. *Arch. Intern. Med.* 149, 1123–1126. doi: 10.1001/archinte.1989.00390050095019

Ashraf, N., Locksley, R., and Arieff, A. I. (1981). Thiazide-induced hyponatremia associated with death or neurologic damage in outpatients. *Am. J. Med.* 70, 1163–1168. doi: 10.1016/0002-9343(81)90822-6

Ashton, M. G., Ball, S. G., Thomas, T. H., and Lee, M. R. (1977). Water intoxication associated with carbamazepine treatment. *Br. Med. J.* 1, 1134–1135. doi: 10.1136/bmj.1.6069.1134

Bachu, K., Godkar, D., Gasparyan, A., Sircar, P., Yakoby, M., and Niranjan, S. (2006). Aripiprazole-induced syndrome of inappropriate antidiuretic hormone secretion (SIADH). *Am. J. Ther.* 13, 370–372. doi: 10.1097/00045391-200607000-00014

Baribeau, D. A., and Anagnostou, E. (2015). Oxytocin and vasopressin: linking pituitary neuropeptides and their receptors to social neurocircuits. *Front. Neurosci.* 9:335. doi: 10.3389/fnins.2015.00335

Berghmans, T. (1996). Hyponatremia related to medical anticancer treatment. *Support Care Cancer* 4, 341–350. doi: 10.1007/bf01788840

Bode, U., Seif, S. M., and Levine, A. S. (1980). Studies on the antidiuretic effect of cyclophosphamide: vasopressin release and sodium excretion. *Med. Pediatr. Oncol.* 8, 295–303. doi: 10.1002/mpo.2950080312

Bolignano, D., Cabassi, A., Fiaccadori, E., Ghigo, E., Pasquali, R., Peracino, A., et al. (2014). Copeptin (CTproAVP), a new tool for understanding the role of vasopressin in pathophysiology. *Clin. Chem. Lab. Med.* 52, 1447–1456. doi: 10.1515/cclm-2014-0379

Bouley, R., Pastor-Soler, N., Cohen, O., Mclaughlin, M., Breton, S., and Brown, D. (2005). Stimulation of AQP2 membrane insertion in renal epithelial cells in vitro and in vivo by the cGMP phosphodiesterase inhibitor sildenafil citrate (Viagra). *Am. J. Physiol. Renal Physiol.* 288, F1103–F1112. doi: 10.1152/ajprenal.00337.2004

Bressler, R. B., and Huston, D. P. (1985). Water intoxication following moderate-dose intravenous cyclophosphamide. *Arch. Intern. Med.* 145, 548–549. doi: 10.1001/archinte.1985.00360030196034

Breyer, M. D., and Breyer, R. M. (2001). G protein-coupled prostanoid receptors and the kidney. *Annu. Rev. Physiol.* 63, 579–605. doi: 10.1146/annurev.physiol.63.1.579

Breyer, M. D., Jacobson, H. R., and Hebert, R. L. (1990). Cellular mechanisms of prostaglandin E2 and vasopressin interactions in the collecting duct. *Kidney Int.* 38, 618–624. doi: 10.1038/ki.1990.251

Campbell, D. M., Atkinson, A., Gillis, D., and Sochett, E. B. (2000). Cyclophosphamide and water retention: mechanism revisited. *J. Pediatr. Endocrinol. Metab.* 13, 673–675. doi: 10.1515/jpem.2000.13.6.673

Cantwell, B. M., Idle, M., Millward, M. J., Hall, G., and Lind, M. J. (1990). Encephalopathy with hyponatremia and inappropriate arginine vasopressin secretion following an intravenous ifosfamide infusion. *Ann. Oncol.* 1:232. doi: 10.1093/oxfordjournals.annonc.a057728

César, K. R., and Magaldi, A. J. (1999). Thiazide induces water absorption in the inner medullary collecting duct of normal and Brattleboro rats. *Am. J. Phys.* 277, F756–F760. doi: 10.1152/ajprenal.1999.277.5.F756

Cheng, C. Y., Chu, J. Y., and Chow, B. K. (2009). Vasopressin-independent mechanisms in controlling water homeostasis. *J. Mol. Endocrinol.* 43, 81–92. doi: 10.1677/jme-08-0123

Cheung, P. W., Nomura, N., Nair, A. V., Pathomthongtaweechai, N., Ueberdiek, L., Lu, H. A., et al. (2016). EGF receptor inhibition by Erlotinib increases aquaporin 2-mediated renal water reabsorption. *J. Am. Soc. Nephrol.* 27, 3105–3116. doi: 10.1681/asn.2015080903

Choi, E. Y., Park, J. S., Kim, Y. T., Park, S. Y., and Kim, G. H. (2015). The risk of hyponatremia with desmopressin use for nocturnal polyuria. *Am. J. Nephrol.* 41, 183–190. doi: 10.1159/000381562

Chou, C. L., Digiovanni, S. R., Luther, A., Lolait, S. J., and Knepper, M. A. (1995a). Oxytocin as an antidiuretic hormone. II. Role of V2 vasopressin receptor. *Am. J. Phys.* 269, F78–F85. doi: 10.1152/ajprenal.1995.269.1.F78

Chou, C. L., Digiovanni, S. R., Mejia, R., Nielsen, S., and Knepper, M. A. (1995b). Oxytocin as an antidiuretic hormone. I. Concentration dependence of action. *Am. J. Phys.* 269, F70–F77. doi: 10.1152/ajprenal.1995.269.1.F70

Danisi, G., Genta, E. N., Timoner, J., and Marcondes, M. (1970). Effect of chlorpropamide on urinary excretion of water and solute in patients with diabetes insipidus and on water flow across isolated toad bladder. *J. Clin. Endocrinol. Metab.* 30, 528–530. doi: 10.1210/jcem-30-4-528

De Bragança, A. C., Moyses, Z. P., and Magaldi, A. J. (2010). Carbamazepine can induce kidney water absorption by increasing aquaporin 2 expression. *Nephrol. Dial. Transplant.* 25, 3840–3845. doi: 10.1093/ndt/gfq317

De Picker, L., Van Den Eede, F., Dumont, G., Moorkens, G., and Sabbe, B. G. (2014). Antidepressants and the risk of hyponatremia: a class-by-class review of literature. *Psychosomatics* 55, 536–547. doi: 10.1016/j.psym.2014.01.010

Demir, M. E., Horoz, M., Ulas, T., Eren, M. A., and Ercan, Z. (2012). Nonsteroidal anti-inflammatory drug-induced severe hyponatremia. *Medicina* 48, 619–621. doi: 10.3390/medicina48120090

Efe, O., Klein, J. D., Larocque, L. M., Ren, H., and Sands, J. M. (2016). Metformin improves urine concentration in rodents with nephrogenic diabetes insipidus. *JCI Insight* 1. doi: 10.1172/jci.insight.88409

Ellison, D. H., and Berl, T. (2007). Clinical practice. The syndrome of inappropriate antidiuresis. *N. Engl. J. Med.* 356, 2064–2072. doi: 10.1056/NEJMcp066837

Falhammar, H., Lindh, J. D., Calissendorff, J., Skov, J., Nathanson, D., and Mannheimer, B. (2019). Antipsychotics and severe hyponatremia: A Swedish population-based case-control study. *Eur. J. Intern. Med.* 60, 71–77. doi: 10.1016/j.ejim.2018.11.011

Feldman, B. J., Rosenthal, S. M., Vargas, G. A., Fenwick, R. G., Huang, E. A., Matsuda-Abedini, M., et al. (2005). Nephrogenic syndrome of inappropriate antidiuresis. *N. Engl. J. Med.* 352, 1884–1890. doi: 10.1056/NEJMoa042743

Fichman, M. P., Vorherr, H., Kleeman, C. R., and Telfer, N. (1971). Diuretic-induced hyponatremia. *Ann. Intern. Med.* 75, 853–863. doi: 10.7326/0003-4819-75-6-853

Filippone, E. J., Ruzieh, M., and Foy, A. (2020). Thiazide-associated hyponatremia: clinical manifestations and pathophysiology. *Am. J. Kidney Dis.* 75, 256–264. doi: 10.1053/j.ajkd.2019.07.011

Fine, D., and Shedrovilzky, H. (1970). Hyponatremia due to chlorpropamide. A syndrome resembling inappropriate secretion of antidiuretic hormone. *Ann. Intern. Med.* 72, 83–87. doi: 10.7326/0003-4819-72-1-83

Frenkel, N. J., Vogt, L., De Rooij, S. E., Trimpert, C., Levi, M. M., Deen, P. M., et al. (2015). Thiazide-induced hyponatraemia is associated with increased water intake and impaired urea-mediated water excretion at low plasma antidiuretic hormone and urine aquaporin-2. *J. Hypertens.* 33, 627–633. doi: 10.1097/hjh.0000000000000423

Friedman, E., Shadel, M., Halkin, H., and Farfel, Z. (1989). Thiazide-induced hyponatremia. Reproducibility by single dose rechallenge and an analysis of pathogenesis. *Ann. Intern. Med.* 110, 24–30. doi: 10.7326/0003-4819-110-1-24

Glezerman, I. G. (2009). Successful treatment of ifosfamide-induced hyponatremia with AVP receptor antagonist without interruption of hydration for prevention of hemorrhagic cystitis. *Ann. Oncol.* 20, 1283–1285. doi: 10.1093/annonc/mdp312

Gridelli, C., Maione, P., Bareschino, M. A., Schettino, C., Sacco, P. C., Ambrosio, R., et al. (2010). Erlotinib in the treatment of non-small cell lung cancer: current status and future developments. *Anticancer Res.* 30, 1301–1310.

Gross, P. A., Wagner, A., and Decaux, G. (2011). Vaptans are not the mainstay of treatment in hyponatremia: perhaps not yet. *Kidney Int.* 80, 594–600. doi: 10.1038/ki.2011.78

Hébert, R. L., Jacobson, H. R., Fredin, D., and Breyer, M. D. (1993). Evidence that separate PGE2 receptors modulate water and sodium transport in rabbit cortical collecting duct. *Am. J. Phys.* 265, F643–F650. doi: 10.1152/ajprenal.1993.265.5.F643

Hensen, J., Haenelt, M., and Gross, P. (1995). Water retention after oral chlorpropamide is associated with an increase in renal papillary arginine vasopressin receptors. *Eur. J. Endocrinol.* 132, 459–464. doi: 10.1530/eje.0.1320459

Hirji, M. R., and Mucklow, J. C. (1991). Transepithelial water movement in response to carbamazepine, chlorpropamide and demeclocycline in toad urinary bladder. *Br. J. Pharmacol.* 104, 550–553. doi: 10.1111/j.1476-5381.1991.tb12466.x

Hix, J. K., Silver, S., and Sterns, R. H. (2011). Diuretic-associated hyponatremia. *Semin. Nephrol.* 31, 553–566. doi: 10.1016/j.semnephrol.2011.09.010

Ingelfinger, J. R., and Hays, R. M. (1969). Evidence that chlorpropamide and vasopressin share a common site of action. *J. Clin. Endocrinol. Metab.* 29, 738–740. doi: 10.1210/jcem-29-5-738

Janicic, N., and Verbalis, J. G. (2003). Evaluation and management of hypo-osmolality in hospitalized patients. *Endocrinol. Metab. Clin. N. Am.* 32, 459, vii–481. doi: 10.1016/s0889-8529(03)00004-5

Jeon, U. S., Joo, K. W., Na, K. Y., Kim, Y. S., Lee, J. S., Kim, J., et al. (2003). Oxytocin induces apical and basolateral redistribution of aquaporin-2 in rat kidney. *Nephron Exp. Nephrol.* 93, e36–e45. doi: 10.1159/000066651

Jójárt, I., Laczi, F., László, F. A., Boda, K., Csáti, S., and Janáky, T. (1987). Hyponatremia and increased secretion of vasopressin induced by vincristine administration in rat. *Exp. Clin. Endocrinol.* 90, 213–220. doi: 10.1055/s-0029-1210692

Joo, K. W., Jeon, U. S., Kim, G. H., Park, J., Oh, Y. K., Kim, Y. S., et al. (2004). Antidiuretic action of oxytocin is associated with increased urinary excretion of aquaporin-2. *Nephrol. Dial. Transplant.* 19, 2480–2486. doi: 10.1093/ndt/gfh413

Jung, H. J., and Kwon, T. H. (2016). Molecular mechanisms regulating aquaporin-2 in kidney collecting duct. *Am. J. Physiol. Renal Physiol.* 311, F1318–F1328. doi: 10.1152/ajprenal.00485.2016

Kelleher, H. B., and Henderson, S. O. (2006). Severe hyponatremia due to desmopressin. *J. Emerg. Med.* 30, 45–47. doi: 10.1016/j.jemermed.2005.02.020

Kendler, K. S., Weitzman, R. E., and Rubin, R. T. (1978). Lack of arginine vasopressin response to central dopamine blockade in normal adults. *J. Clin. Endocrinol. Metab.* 47, 204–207. doi: 10.1210/jcem-47-1-204

Kim, S., Choi, H. J., Jo, C. H., Park, J. S., Kwon, T. H., and Kim, G. H. (2015). Cyclophosphamide-induced vasopressin-independent activation of aquaporin-2 in the rat kidney. *Am. J. Physiol. Renal Physiol.* 309, F474–F483. doi: 10.1152/ajprenal.00477.2014

Kim, G. H., Choi, N. W., Jung, J. Y., Song, J. H., Lee, C. H., Kang, C. M., et al. (2008). Treating lithium-induced nephrogenic diabetes insipidus with a COX-2 inhibitor improves polyuria via upregulation of AQP2 and NKCC2. *Am. J. Physiol. Renal Physiol.* 294, F702–F709. doi: 10.1152/ajprenal.00366.2007

Kim, G. H., Ecelbarger, C. A., Mitchell, C., Packer, R. K., Wade, J. B., and Knepper, M. A. (1999). Vasopressin increases Na-K-2Cl cotransporter expression in thick ascending limb of Henle's loop. *Am. J. Phys.* 276, F96–f103. doi: 10.1152/ajprenal.1999.276.1.F96

Kim, S., Jo, C. H., and Kim, G. H. (2021). Psychotropic drugs upregulate aquaporin-2 via vasopressin-2 receptor/cAMP/protein kinase A signaling in inner medullary collecting duct cells. *Am. J. Physiol. Renal Physiol.* 320, F963–f971. doi: 10.1152/ajprenal.00576.2020

Kim, G. H., Lee, J. W., Oh, Y. K., Chang, H. R., Joo, K. W., Na, K. Y., et al. (2004). Antidiuretic effect of hydrochlorothiazide in lithium-induced nephrogenic diabetes insipidus is associated with upregulation of aquaporin-2, Na-cl co-transporter, and epithelial sodium channel. *J. Am. Soc. Nephrol.* 15, 2836–2843. doi: 10.1097/01.Asn.0000143476.93376.04

Kirch, C., Gachot, B., Germann, N., Blot, F., and Nitenberg, G. (1997). Recurrent ifosfamide-induced hyponatraemia. *Eur. J. Cancer* 33, 2438–2439. doi: 10.1016/s0959-8049(97)00329-8

Klein, J. D., Wang, Y., Blount, M. A., Molina, P. A., Larocque, L. M., Ruiz, J. A., et al. (2016). Metformin, an AMPK activator, stimulates the phosphorylation of aquaporin 2 and urea transporter A1 in inner medullary collecting ducts. *Am. J. Physiol. Renal Physiol.* 310, F1008–F1012. doi: 10.1152/ajprenal.00102.2016

Kunstadter, R. H., Cabana, E. C., and Oh, W. (1969). Treatment of vasopressin-sensitive diabetes insipidus with chlorpropamide. *Am. J. Dis. Child.* 117, 436–441. doi: 10.1001/archpedi.1969.02100030438009

Kwon, T. H., Frøkiær, J., and Nielsen, S. (2013). Regulation of aquaporin-2 in the kidney: A molecular mechanism of body-water homeostasis. *Kidney Res. Clin. Pract.* 32, 96–102. doi: 10.1016/j.krcp.2013.07.005

Larose, P., Ong, H., and Du Souich, P. (1987). The effect of cyclophosphamide on arginine vasopressin and the atrial natriuretic factor. *Biochem. Biophys. Res. Commun.* 143, 140–144. doi: 10.1016/0006-291x(87)90641-3

Lee, Y. C., Park, J. S., Lee, C. H., Bae, S. C., Kim, I. S., Kang, C. M., et al. (2010). Hyponatraemia induced by low-dose intravenous pulse cyclophosphamide. *Nephrol. Dial. Transplant.* 25, 1520–1524. doi: 10.1093/ndt/gfp657

Li, J. H., Chou, C. L., Li, B., Gavrilova, O., Eisner, C., Schnermann, J., et al. (2009). A selective EP4 PGE2 receptor agonist alleviates disease in a new mouse model of X-linked nephrogenic diabetes insipidus. *J. Clin. Invest.* 119, 3115–3126. doi: 10.1172/jci39680

Li, W., Zhang, Y., Bouley, R., Chen, Y., Matsuzaki, T., Nunes, P., et al. (2011). Simvastatin enhances aquaporin-2 surface expression and urinary concentration in vasopressin-deficient Brattleboro rats through modulation of rho GTPase. *Am. J. Physiol. Renal Physiol.* 301, F309–F318. doi: 10.1152/ajprenal.00001.2011

Liamis, G., Christidis, D., Alexandridis, G., Bairaktari, E., Madias, N. E., and Elisaf, M. (2007). Uric acid homeostasis in the evaluation of diuretic-induced hyponatremia. *J. Investig. Med.* 55, 36–44. doi: 10.2310/6650.2007.06027

Liamis, G., Milionis, H., and Elisaf, M. (2008). A review of drug-induced hyponatremia. *Am. J. Kidney Dis.* 52, 144–153. doi: 10.1053/j.ajkd.2008.03.004

Lozada, E. S., Gouaux, J., Franki, N., Appel, G. B., and Hays, R. M. (1972). Studies of the mode of action of the sulfonylureas and phenylacetamides in enhancing the effect of vasopressin. *J. Clin. Endocrinol. Metab.* 34, 704–712. doi: 10.1210/jcem-34-4-704

Lu, X., and Wang, X. (2017). Hyponatremia induced by antiepileptic drugs in patients with epilepsy. *Expert Opin. Drug Saf.* 16, 77–87. doi: 10.1080/14740338.2017.1248399

Luboshitzky, R., Tal-Or, Z., and Barzilai, D. (1978). Chlorthalidone-induced syndrome of inappropriate secretion of antidiuretic hormone. *J. Clin. Pharmacol.* 18, 336–339. doi: 10.1002/j.1552-4604.1978.tb01602.x

Mahdavi-Zafarghandi, R., and Seyedi, A. (2014). Treatment of monosymptomatic nocturnal enuresis: sertraline for non-responders to desmopressin. *Iran J. Med. Sci.* 39, 136–139.

Mannesse, C. K., Jansen, P. A., Van Marum, R. J., Sival, R. C., Kok, R. M., Haffmans, P. M., et al. (2013). Characteristics, prevalence, risk factors, and underlying mechanism of hyponatremia in elderly patients treated with antidepressants: a cross-sectional study. *Maturitas* 76, 357–363. doi: 10.1016/j.maturitas.2013.08.010

Mccarron, M., Wright, G. D., and Roberts, S. D. (1995). Water intoxication after low dose cyclophosphamide. *BMJ* 311:292. doi: 10.1136/bmj.311.7000.292

Meinders, A. E., Van Leeuwen, A. M., Borst, J. G., and Cejka, V. (1975). Paradoxical diuresis after vasopressin administration to patients with neurohypophyseal diabetes insipidus treated with chlorpropamide, carbamazepine or clofibrate. *Clin. Sci. Mol. Med.* 49, 283–290. doi: 10.1042/cs0490283

Mendoza, S. A. (1969). Effect of chlorpropamide on the permeability of the urinary bladder of the toad and the response to vasopressin, adenosine-3′,5′-monophosphate and theophylline. *Endocrinology* 84, 411–414. doi: 10.1210/endo-84-2-411

Mendoza, S. A., and Brown, C. F. Jr. (1974). Effect of chlorpropamide on osmotic water flow across toad bladder and the response to vasopressin, theophylline and cyclic AMP. *J. Clin. Endocrinol. Metab.* 38, 883–889. doi: 10.1210/jcem-38-5-883

Miller, M., and Moses, A. M. (1970). Potentiation of vasopressin action by chlorpropamide in vivo. *Endocrinology* 86, 1024–1027. doi: 10.1210/endo-86-5-1024

Moeller, H. B., Rittig, S., and Fenton, R. A. (2013). Nephrogenic diabetes insipidus: essential insights into the molecular background and potential therapies for treatment. *Endocr. Rev.* 34, 278–301. doi: 10.1210/er.2012-1044

Moses, A. M., Fenner, R., Schroeder, E. T., and Coulson, R. (1982). Further studies on the mechanism by which chlorpropamide alters the action of vasopressin. *Endocrinology* 111, 2025–2030. doi: 10.1210/endo-111-6-2025

Moyses, Z. P., Nakandakari, F. K., and Magaldi, A. J. (2008). Fluoxetine effect on kidney water reabsorption. *Nephrol. Dial. Transplant.* 23, 1173–1178. doi: 10.1093/ndt/gfm714

Muta, T., Takasugi, M., and Kuroiwa, A. (1989). Chlorpropamide alters AVP-receptor binding of rat renal tubular membranes. *Eur. J. Pharmacol.* 159, 191–194. doi: 10.1016/0014-2999(89)90705-x

Nadal, J., Channavajjhala, S. K., Jia, W., Clayton, J., Hall, I. P., and Glover, M. (2018). Clinical and molecular features of thiazide-induced hyponatremia. *Curr. Hypertens. Rep.* 20:31. doi: 10.1007/s11906-018-0826-6

Olesen, E. T., and Fenton, R. A. (2013). Is there a role for PGE2 in urinary concentration? *J. Am. Soc. Nephrol.* 24, 169–178. doi: 10.1681/asn.2012020217

Olesen, E. T., Rützler, M. R., Moeller, H. B., Praetorius, H. A., and Fenton, R. A. (2011). Vasopressin-independent targeting of aquaporin-2 by selective E-prostanoid receptor agonists alleviates nephrogenic diabetes insipidus. *Proc. Natl. Acad. Sci. U. S. A.* 108, 12949–12954. doi: 10.1073/pnas.1104691108

Ozer, A., and Sharp, G. W. (1973). Modulation of adenyl cyclase action in toad bladder by chlorpropamide: antagonism to prostaglandin E. *Eur. J. Pharmacol.* 22, 227–232. doi: 10.1016/0014-2999(73)90020-4

Peck, V., and Shenkman, L. (1979). Haloperidol-induced syndrome of inappropriate secretion of antidiuretic hormone. *Clin. Pharmacol. Ther.* 26, 442–444. doi: 10.1002/cpt1979264442

Petersson, I., Nilsson, G., Hansson, B. G., and Hedner, T. (1987). Water intoxication associated with non-steroidal anti-inflammatory drug therapy. *Acta Med. Scand.* 221, 221–223. doi: 10.1111/j.0954-6820.1987.tb01272.x

Pokracki, F. J., Robinson, A. G., and Seif, S. M. (1981). Chlorpropamide effect: measurement of neurophysin and vasopressin in humans and rats. *Metabolism* 30, 72–78. doi: 10.1016/0026-0495(81)90222-5

Procino, G., Barbieri, C., Carmosino, M., Tamma, G., Milano, S., De Benedictis, L., et al. (2011). Fluvastatin modulates renal water reabsorption in vivo through increased AQP2 availability at the apical plasma membrane of collecting duct cells. *Pflugers Arch.* 462, 753–766. doi: 10.1007/s00424-011-1007-5

Raymond, K. H., and Lifschitz, M. D. (1986). Effect of prostaglandins on renal salt and water excretion. *Am. J. Med.* 80, 22–33. doi: 10.1016/0002-9343(86)90929-0

Robertson, G. L. (1989). Syndrome of inappropriate antidiuresis. *N. Engl. J. Med.* 321, 538–539. doi: 10.1056/nejm198908243210810

Robertson, G. L., Bhoopalam, N., and Zelkowitz, L. J. (1973). Vincristine neurotoxicity and abnormal secretion of antidiuretic hormone. *Arch. Intern. Med.* 132, 717–720. doi: 10.1001/archinte.1973.03650110061013

Sachdeo, R. C., Wasserstein, A., Mesenbrink, P. J., and D'souza, J. (2002). Effects of oxcarbazepine on sodium concentration and water handling. *Ann. Neurol.* 51, 613–620. doi: 10.1002/ana.10190

Sanches, T. R., Volpini, R. A., Massola Shimizu, M. H., Bragança, A. C., Oshiro-Monreal, F., Seguro, A. C., et al. (2012). Sildenafil reduces polyuria in rats with lithium-induced NDI. *Am. J. Physiol. Renal Physiol.* 302, F216–F225. doi: 10.1152/ajprenal.00439.2010

Schrier, R. W., Berl, T., and Anderson, R. J. (1979). Osmotic and nonosmotic control of vasopressin release. *Am. J. Phys.* 236, F321–F332. doi: 10.1152/ajprenal.1979.236.4.F321

Scott, L. V., and Dinan, T. G. (2002). Vasopressin as a target for antidepressant development: an assessment of the available evidence. *J. Affect. Disord.* 72, 113–124. doi: 10.1016/s0165-0327(02)00026-5

Sekiya, N., and Awazu, M. (2018). A case of nephrogenic syndrome of inappropriate antidiuresis caused by carbamazepine. *CEN Case Rep.* 7, 66–68. doi: 10.1007/s13730-017-0295-9

Sinke, A. P., Kortenoeven, M. L., De Groot, T., Baumgarten, R., Devuyst, O., Wetzels, J. F., et al. (2014). Hydrochlorothiazide attenuates lithium-induced nephrogenic diabetes insipidus independently of the sodium-chloride cotransporter. *Am. J. Physiol. Renal Physiol.* 306, F525–F533. doi: 10.1152/ajprenal.00617.2013

Skov, J., Falhammar, H., Calissendorff, J., Lindh, J. D., and Mannheimer, B. (2021). Association between lipid-lowering agents and severe hyponatremia: a population-based case-control study. *Eur. J. Clin. Pharmacol.* 77, 747–755. doi: 10.1007/s00228-020-03006-8

Smith, N. J., Espir, M. L., and Baylis, P. H. (1977). Raised plasma arginine vasopressin concentration in carbamazepine-induced water intoxication. *Br. Med. J.* 2:804. doi: 10.1136/bmj.2.6090.804

Smith, D. M., Mckenna, K., and Thompson, C. J. (2000). Hyponatraemia. *Clin. Endocrinol.* 52, 667–678. doi: 10.1046/j.1365-2265.2000.01027.x

Soylu, A., Kasap, B., Oğün, N., Oztürk, Y., Türkmen, M., Hoefsloot, L., et al. (2005). Efficacy of COX-2 inhibitors in a case of congenital nephrogenic diabetes insipidus. *Pediatr. Nephrol.* 20, 1814–1817. doi: 10.1007/s00467-005-2057-8

Steinman, R. A., Schwab, S. E., and Munir, K. M. (2015). Cyclophosphamide-induced hyponatremia in a patient with diabetes insipidus. *J. Endocrinol. Metab.* 5(6), 337–339. doi: 10.14740/jem319w

Stuart, M. J., Cuaso, C., Miller, M., and Oski, F. A. (1975). Syndrome of recurrent increased secretion of antidiuretic hormone following multiple doses of vincristine. *Blood* 45, 315–320. doi: 10.1182/blood.V45.3.315.315

Suskind, R. M., Brusilow, S. W., and Zehr, J. (1972). Syndrome of inappropriate secretion of antidiuretic hormone produced by vincristine toxicity (with bioassay of ADH level). *J. Pediatr.* 81, 90–92. doi: 10.1016/s0022-3476(72)80381-0

Urakabe, S., Shirai, D., Ando, A., Takamitsu, Y., and Orita, Y. (1970). Effect of sulfonylureas on the permeability to water and electrical properties of the urinary bladder of the toad. *Jpn. Circ. J.* 34, 595–601. doi: 10.1253/jcj.34.595

Uy, Q. L., Moen, T. H., Johns, R. J., and Owens, A. H. Jr. (1967). Vincristine neurotoxicity in rodents. *Johns Hopkins Med. J.* 121, 349–360

Vilhardt, H. (1990). Basic pharmacology of desmopressin. *Drug Invest.* 2, 2–8. doi: 10.1007/BF03258235

Vukićević, T., Hinze, C., Baltzer, S., Himmerkus, N., Quintanova, C., Zühlke, K., et al. (2019). Fluconazole increases osmotic water transport in renal collecting duct through effects on aquaporin-2 trafficking. *J. Am. Soc. Nephrol.* 30, 795–810. doi: 10.1681/asn.2018060668

Wade, J. B., Lee, A. J., Liu, J., Ecelbarger, C. A., Mitchell, C., Bradford, A. D., et al. (2000). UT-A2: a 55-kDa urea transporter in thin descending limb whose abundance is regulated by vasopressin. *Am. J. Physiol. Renal Physiol.* 278, F52–F62. doi: 10.1152/ajprenal.2000.278.1.F52

Wales, J. K. (1971). The effect of chlorpropamide and related compounds on water transport across the toad bladder. *J. Endocrinol.* 49, 551–552. doi: 10.1677/joe.0.0490551

Wales, J. K. (1975). Treatment of diabetes insipidus with carbamazepine. *Lancet* 306, 948–951. doi: 10.1016/s0140-6736(75)90361-x

Ware, J. S., Wain, L. V., Channavajjhala, S. K., Jackson, V. E., Edwards, E., Lu, R., et al. (2017). Phenotypic and pharmacogenetic evaluation of patients with thiazide-induced hyponatremia. *J. Clin. Invest.* 127, 3367–3374. doi: 10.1172/jci89812

Weatherall, M. (2004). The risk of hyponatremia in older adults using desmopressin for nocturia: a systematic review and meta-analysis. *Neurourol. Urodyn.* 23, 302–305. doi: 10.1002/nau.20038

Weissman, P. N., Shenkman, L., and Gregerman, R. I. (1971). Chlorpropamide hyponatremia: drug-induced inappropriate antidiuretic-hormone activity. *N. Engl. J. Med.* 284, 65–71. doi: 10.1056/nejm197101142840202

Whitten, J. R., and Ruehter, V. L. (1997). Risperidone and hyponatremia: a case report. *Ann. Clin. Psychiatry* 9, 181–183. doi: 10.1023/a:1026286109635

Zhang, Y., Peti-Peterdi, J., Heiney, K. M., Riquier-Brison, A., Carlson, N. G., Müller, C. E., et al. (2015a). Clopidogrel attenuates lithium-induced alterations in renal water and sodium channels/transporters in mice. *Purinergic Signal* 11, 507–518. doi: 10.1007/s11302-015-9469-0

Zhang, Y., Peti-Peterdi, J., Müller, C. E., Carlson, N. G., Baqi, Y., Strasburg, D. L., et al. (2015b). P2Y12 receptor localizes in the renal collecting duct and its blockade augments arginine vasopressin action and alleviates nephrogenic diabetes insipidus. *J. Am. Soc. Nephrol.* 26, 2978–2987. doi: 10.1681/asn.2014010118

Conflict of Interest: The authors declare that the research was conducted in the absence of any commercial or financial relationships that could be construed as a potential conflict of interest.

Publisher's Note: All claims expressed in this article are solely those of the authors and do not necessarily represent those of their affiliated organizations, or those of the publisher, the editors and the reviewers. Any product that may be evaluated in this article, or claim that may be made by its manufacturer, is not guaranteed or endorsed by the publisher.

frontiers in Physiology

ORIGINAL RESEARCH
published: 04 January 2022
doi: 10.3389/fphys.2021.787521

Selective Deletion of the Mechanistic Target of Rapamycin From the Renal Collecting Duct Principal Cell in Mice Down-Regulates the Epithelial Sodium Channel

*Bruce Chen[1], Maurice B. Fluitt[1,2], Aaron L. Brown[1], Samantha Scott[1], Anirudh Gadicherla[1] and Carolyn M. Ecelbarger[1]**

[1] Division of Endocrinology and Metabolism, Department of Medicine, Georgetown University, Washington, DC, United States, [2] Department of Medicine, Howard University, Washington, DC, United States

The mechanistic target of rapamycin (mTOR), a serine-threonine-specific kinase, is a cellular energy sensor, integrating growth factor and nutrient signaling. In the collecting duct (CD) of the kidney, the epithelial sodium channel (ENaC) essential in the determination of final urine Na+ losses, has been demonstrated to be upregulated by mTOR, using cell culture and mTOR inhibition in *ex vivo* preparations. We tested whether CD-principal cell (PC) targeted deletion of mTOR using Cre-lox recombination would affect whole-body sodium homeostasis, blood pressure, and ENaC regulation in mice. Male and female CD-PC mTOR knockout (KO) mice and wild-type (WT) littermates (Cre-negative) were generated using aquaporin-2 (AQP2) promoter to drive Cre-recombinase. Under basal conditions, KO mice showed a reduced (∼30%) natriuretic response to benzamil (ENaC) antagonist, suggesting reduced *in vivo* ENaC activity. WT and KO mice were fed normal sodium (NS, 0.45% Na+) or a very low Na+ (LS, <0.02%) diet for 7-days. Switching from NS to LS resulted in significantly higher urine sodium losses (relative to WT) in the KO with adaptation occurring by day 2. Blood pressures were modestly (∼5–10 mm Hg) but significantly lower in KO mice under both diets. Western blotting showed KO mice had 20–40% reduced protein levels of all three subunits of ENaC under LS or NS diet. Immunohistochemistry (IHC) of kidney showed enhanced apical-vs.-cellular localization of all three subunits with LS, but a reduction in this ratio for γ-ENaC in the KO. Furthermore, the KO kidneys showed increased ubiquitination of α-ENaC and reduced phosphorylation of the serum and glucocorticoid regulated kinase, type 1 [serum glucocorticoid regulated kinase (SGK1)] on serine 422 (mTOR phosphorylation site). Taken together this suggests enhanced degradation as a consequence of reduced mTOR kinase activity and downstream upregulation of ubiquitination may have accounted for the reduction at least in α-ENaC. Overall, our data support a role for mTOR in ENaC activity likely *via* regulation of SGK1, ubiquitination, ENaC channel turnover and apical membrane residency. These data support a role for mTOR in the collecting duct in the maintenance of body sodium homeostasis.

Keywords: kidney, insulin, salt, ubiquitination, sex differences

OPEN ACCESS

Edited by:
Weidong Wang,
Sun Yat-sen University, China

Reviewed by:
Tae-Hwan Kwon,
Kyungpook National University, South Korea
Gilles Crambert,
ERL8228 Métabolisme et Physiologie Rénales, France

***Correspondence:**
Carolyn M. Ecelbarger
ecelbarc@georgetown.edu

Specialty section:
This article was submitted to Renal and Epithelial Physiology, a section of the journal Frontiers in Physiology

Received: *30 September 2021*
Accepted: *15 November 2021*
Published: *04 January 2022*

Citation:
Chen B, Fluitt MB, Brown AL, Scott S, Gadicherla A and Ecelbarger CM (2022) Selective Deletion of the Mechanistic Target of Rapamycin From the Renal Collecting Duct Principal Cell in Mice Down-Regulates the Epithelial Sodium Channel. Front. Physiol. 12:787521. doi: 10.3389/fphys.2021.787521

INTRODUCTION

The mechanistic target of rapamycin (mTOR) is a serine-threonine protein kinase involved in the regulation of cell growth, proliferation, metabolism, protein synthesis, and other mechanisms that promote tissue growth (Sarbassov et al., 2004; Betz et al., 2013; Weichhart, 2018). In the renal collecting duct, we and other laboratories have shown that it plays a role in the activation of the epithelial sodium channel (ENaC) (Lu et al., 2010; Pavlov et al., 2013; Lang and Pearce, 2016). Finely tuned regulation of ENaC is essential for electrolyte homeostasis and blood pressure control, as it represents the last regulated site of sodium-(and chloride and potassium) reabsorption along the renal tubule, from glomerulus to the ureter.

There are two distinct, multi-protein complexes that contain mTOR as a component, i.e., mTORC1 and mTORC2. The complexes have marginally different activators and effectors. MTORC1 (inhibitable by rapamycin) integrates input from growth factors, oxidative stress, and nutrients (amino acids). If cellular energy levels appear "high," mTORC1 activity increases leading to downstream protein transcription and translational events supporting cell and tissue growth (Laplante and Sabatini, 2012a,b). The mTORC1 complex includes mTOR, mammalian lethal with SEC13 protein 8 (MLST8), regulatory-associated protein of mTOR (RPTOR), proline-rich AKT1 substrate, type 40 (AKT1S1/PRAS40), and DEP domain-containing mTOR-interacting protein (DEPTOR), as ancillary proteins (Brown et al., 2018). The second complex, mTORC2 (primarily rapamycin insensitive) appears to be activated solely by growth factors, including insulin and insulin-like-growth factor type 1 (IGF1). MTORC2 contains mTOR, DEPTOR, rapamycin-insensitive companion of mTOR (RICTOR) stress-activated map kinase-interacting protein 1 (mSIN1), proline-rich protein 5 (PRR5), and proline-rich protein-5-like protein (PRR5-L) (Brown et al., 2018) and is involved in regulation of the cytoskeleton *via* stimulation of protein kinase C alpha (PKCα), promotion of cellular survival *via* Akt (protein kinase B) activation, as well as, ion transport and growth *via* serum-and-glucocorticoid-regulated kinase (SGK1) phosphorylation (Sarbassov et al., 2004; Betz et al., 2013; Heikamp et al., 2014).

Prior studies by our group and others revealed that insulin plays a role in sodium reabsorption in the renal collecting duct by activation of the ENaC (Blazer-Yost et al., 1998; Wang et al., 2001; Song et al., 2006; Tiwari et al., 2007; Pavlov et al., 2013). SGK1 is phosphorylated by mTORC2 on serine 422 (an activating phosphorylation in the hydrophobic motif), which partially explains the mechanistic link between insulin and ENaC. Insulin also activates PDPK1 (3-phosphoinositide dependent protein kinase 1), which phosphorylates SGK1 in the activation loop at threonine 256. Activated SGK1 phosphorylates and inhibits NEDD4-2 (an E3 ubiquitin ligase) reducing retrieval of mature channels from the apical membrane. Whether either complex of mTOR has a role in full-differentiation of the collecting duct with its assembly of transporters, channels, and exchangers is not clear.

The consequences of mTOR deletion has been studied in other tissues, including adipocytes and cardiomyocytes (Shan et al., 2016; Baba et al., 2018). Using a strategy similar to our own to delete floxed mTOR, investigators showed knockout (KO) from adipocytes led to a reduction in fat mass and insulin resistance of existing adipocytes (Shan et al., 2016). In another study, deletion of mTOR from cardiomyocytes in an iron-overload mouse model showed mTOR was protective against iron toxicity and apoptosis of the cardiac cells.

Because mTOR in the CD has been shown to regulate ENaC activity in response to insulin, our primary aim was to determine how deletion of mTOR affected ENaC subunit regulation, as well as whole-body electrolyte homeostasis and blood pressure. To accomplish this we bred collecting-duct-principal-cell-targeted mTOR knockout mice utilizing Cre-lox recombination and an aquaporin 2 (AQP2) promoter sequence to target the KO. AQP2 is the most highly expressed transcript in the cortical collecting duct (Lee et al., 2015), and its expression extends from the late distal convoluted tubule (DCT2) through the inner medullary collecting ducts (IMCD). We expected that mTOR deletion might affect activities of both mTORC1 and mTORC2, as it is contained in both complexes. Furthermore, increasing mTORC2 activity has been shown to reduce mTORC1 activity in a feedback loop. Thus, the overall impact on signaling and ENaC function would be difficult to predict without this animal model.

MATERIALS AND METHODS

Generation of Collecting-Duct-Principal-Cell Targeted Mechanistic Target of Rapamycin Knockout Mice

Mechanistic Target of Rapamycin knockout targeted to the kidney collecting duct principal cells ($Aqp2^{cre}$; $Insr^{flox/flox}$) were generated at Georgetown University on C57Bl6 background. $Aqp2^{cre}$ transgenic mice originating from the colony of Don Kohan (University of Utah) (Stricklett et al., 1999) and homozygously floxed *mTOR* mice (B6.129S4-$Mtor^{tm1.2Koz}$/J, JAX Laboratories) were crossed for two generations to produce $Aqp2^{cre}$ positive; $mTOR^{flox/flox}$ ("KO") and $Aqp2^{cre}$ negative, homozygously floxed littermates ("WT"). Mice were genotyped for the presence of $Aqp2^{cre}$ by standard PCR on tail snips. The mice were cared for under the guidelines and approved IACUC protocols of the U.S. National Institutes of Health (NIH) Guide for the Care and Use of Laboratory Animals.

Low- Na+ (LS) Diet Study Design, Blood Pressure, and Urine and Plasma Analyses

The ability of the mice to adapt to a 1-week feeding of a very-low Na^+ (LS, 0.01–0.02% Na+, Envigo TD.09228) was tested on adult (4–8 months of age) male and female KO mice. Mice were fed this diet or a normal salt (NS) diet (1% NaCl, Purina 5001), *ad libitum* with free-access to drinking water (n = 6/genotype/treatment/sex). In some sets of mice, urine was collected (24 h) in mouse metabolic cages (MMC100, Hatteras Instruments), while mice had free access to diet and water. In another set of mice, blood pressure was measured

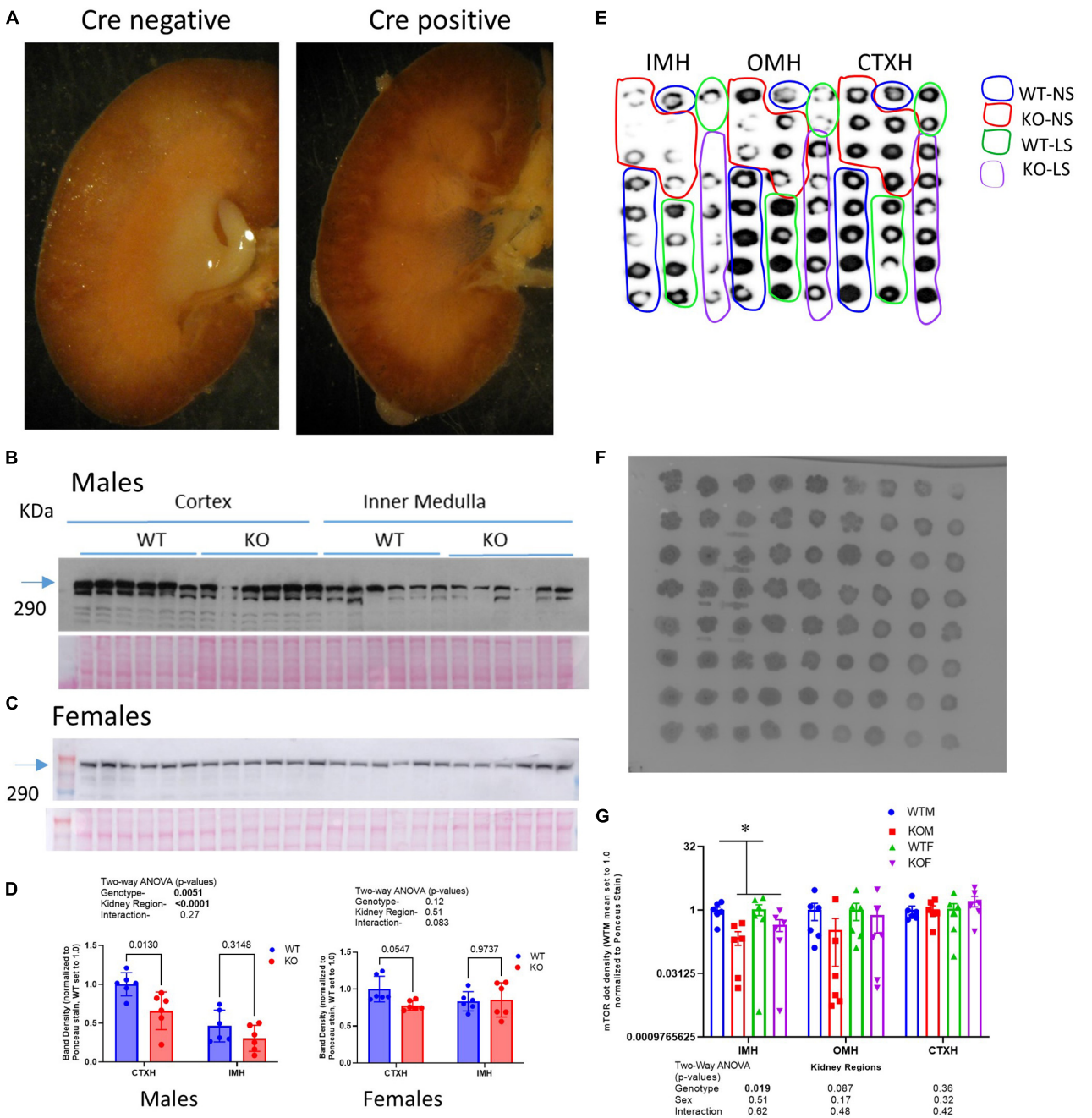

FIGURE 1 | Characterizing the CD-principal-cell targeted mTOR deletion. **(A)** To evaluate cellular location of Cre-recombinase activity, LacZ reporter mice were crossed with Aqp2^{cre} transgenic mice and the kidneys of offspring probed for β-galactosidase activity- blue stain; left (Cre-negative); right (Cre-positive) demonstrating staining specific to renal collecting duct in Cre positive mice. mTOR CD-KO mice were generating by crossing male Mtor$^{tm1.2Koz}$/J with female Aqp2^{cre} mice. Western blots of cortex and inner medulla homogenates (equal amounts of protein were loaded in each lane, 10 μg/lane) from wild-type (WT) and knockout (KO) **(B)** male and **(C)** female mice (n = 6/group) probed with anti-mTOR polyclonal antibody; **(D)** densitometric summaries of western blotting of mTOR in cortex (CTXH) and inner medullary homogenates (IMH, mean ± sem); **(E)** dot blot of inner medulla (IMH), outer medulla (OMH), and cortex (CTXH) homogenates (2 μl/dot) from WT and KO male and female mice (n = 6/group) probed with anti-mTOR antibody. **(F)** Ponceau S staining of proteins on dot blot for loading correction of mTOR dot blot; **(G)** density summary of dots normalized by Ponceau intensity. Two-way ANOVA (genotype × sex) is shown below bars; * indicates a significant ($p < 0.05$) difference between WT and KO.

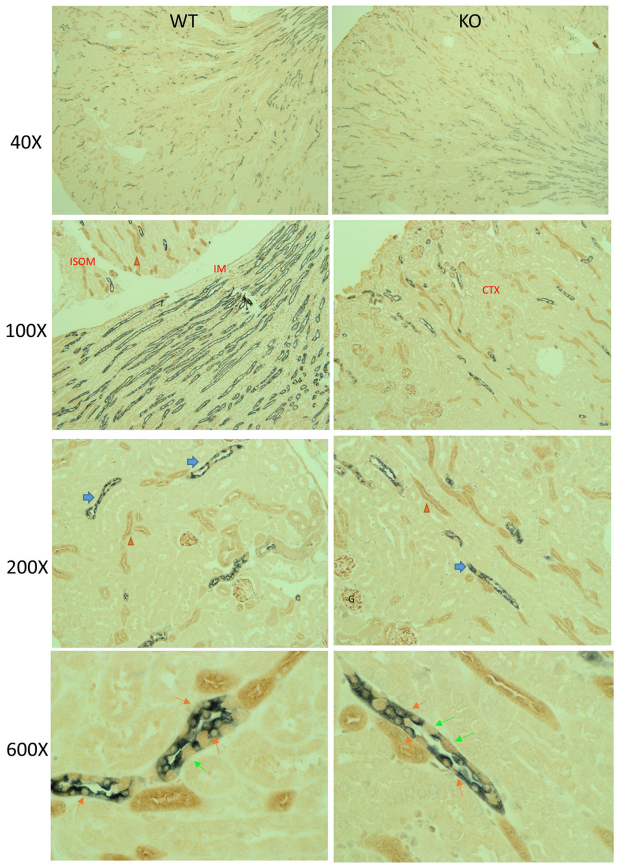

FIGURE 2 | Mechanistic Target of Rapamycin (mTOR) immunohistochemistry (IHC) in mouse kidney. Paraffin-embed kidney coronal sections were prepared for double-labeling IHC by standard chromogenic approaches; mTOR (brown) and AQP2 (gray) in male KO and WT mouse kidneys under control dietary conditions. Sections were imaged at 40×, 100×, 200×, and 600× total magnification, as indicated. At 200×, blue and orange arrows point to collecting duct and thick ascending limbs, respectively, which displayed relatively stronger mTOR labeling than other cells of the kidney (including proximal tubule). Glomerular (G) also displayed strong mTOR labeling. Under 600×, orange and lime-green arrows indicate principal and intercalated cells, respectively. Principal cells were identified by dual gray and brown label. KO mice had reduced brown labeling in cells co-staining with gray.

by tail-cuff plethysmography (Coda® High Throughput System, Kent Scientific Corporation). Mice were euthanized by Inactin (Thiobutabarbital, Sigma) overdose and blood was collected from the heart and analyzed with a VetScan® iSTAT1 chemical analyzer and EG6 cartridges (iSTAT, Abbott). After perfusion with phosphate-buffered saline (PBS), kidneys were rapidly removed and weighed. Plasma and urine aldosterone was measured by an ELISA (Cayman Chemical). Urine electrolytes were measured by a Medica EasyLyte Analyzer, and/or by flame photometry (BWB-XP flame photometer, BWB Technologies).

Benzamil-Sensitivity

The natriuretic response to benzamil (ENaC antagonist) was used to gauge ENaC activity in the mice. In an acute test, mice (on NS) were administered benzamil chloride (Sigma) intraperitoneally, dissolved in 0.45% NaCl in sterile water (0.2 ml/30 g·bw) at about 11:00 a.m. Urine was collected for 4 h in mouse metabolic cages with water and no food. Urine Na+ concentration (EasyLyte Electrolyte Analyzer, Medica) and volume were measured.

Cre-Reporter Staining

To test localization of Cre-recombinase activity, AQP2-Cre transgenic female mice were crossed with male reporter mice (The Jackson Laboratory, Bar Harbor, ME; catalog no. 002073 B6;129-Gtrosa26tm1Sor, Soriano Line) (Friedrich and Soriano, 1991). These mice were homozygous for a transgene with loxP sites flanking a DNA stop sequence proceeding a LacZ gene. Recombination without the stop sequence allowed for expression of β-galactosidase, which produced a blue precipitate with use of the β-Gal Staining Kit (Invitrogen, K146501).

Immunohistochemistry

The perfused left kidney was prepared for immunohistochemistry (IHC) by coronal bisection followed by immersion fixation in 4% paraformaldehyde overnight. This was followed by a buffer exchange to 30% sucrose in PBS for longer-term storage prior to embedding into paraffin (Histopathology & Tissue Shared Resource, Georgetown University). Sections (5 μm) were prepared for IHC. Immunoperoxidase-based staining for mTOR, AQP2, α-, β-, and γ-ENaC was performed as previously described (Tiwari et al., 2007). Double-staining for AQP2 (gray) and mTOR (brown) was accomplished by first localizing mTOR (mTOR polyclonal rabbit, PA5-34663 Invitrogen) followed by a 30-min incubation with biotinylated horse anti-rabbit IgG antibody (H + L) secondary (BP-100-50, Vector Laboratories) and DAB (3,3′-Diaminobenzidine)/hydrogen peroxide brown precipitation. The mTOR-primary/secondary antibody complex was stripped off @ 50°C for 1 h using glycine/20% SDS at pH 2.0. This was followed by washing and reprobing with AQP2 primary (our own polyclonal rabbit), secondary (as above) and alkaline phosphatase black staining with ImmPACT® (Vector Black, Vector Laboratories, Burlingame CA) which produced a gray precipitate. For ENaC subunits, the ratio of stain density near the apical membrane (∼0–10% of the distance from apical to basolateral membrane) to signal within the remaining 90% of this distance was determined These ratios were calculated for 10 selected cells from each mouse stained section and a median ratio determined for each mouse for each subunit (Image J, NIH). Stained sections were analyzed in a genotype- and treatment-blinded fashion.

Western Blotting

The right kidney was dissected into cortex, inner medulla, and inner stripe of the outer medulla and homogenates were prepared from each, as we have previously described (Ecelbarger et al., 2000). Western blotting was conducted as previously described (Tiwari et al., 2006). MTOR polyclonal antibody was obtained from Invitrogen (PA5-34663). We used our own rabbit polyclonal antibodies against aquaporin-2 (AQP2), aquaporin-3 (AQP3), β-ENaC (against AA 617-638), γ-ENaC (AA 629-650), and NaPi-2 (AA 614-637). These antibodies were made against sequences

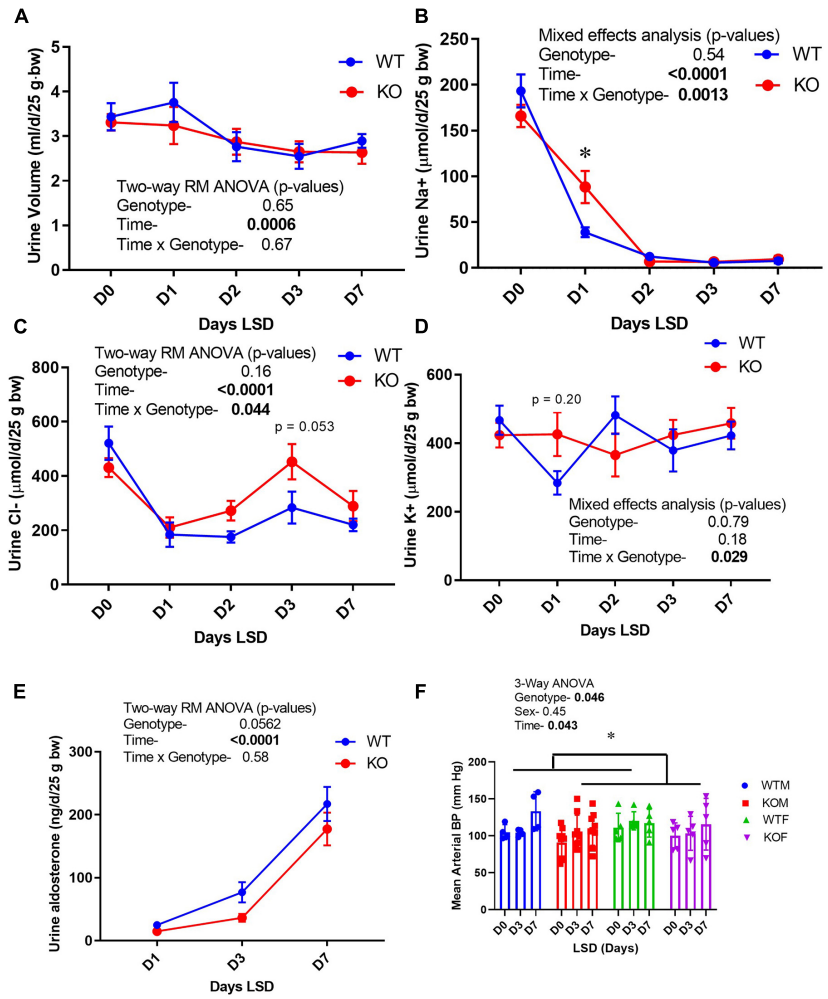

FIGURE 3 | Urine electrolyte excretion, blood pressure, and urine aldosterone under normal and low- Na+ diet. Urine (24 h) was collected on male mice in metabolic cages first under normal diet (D0) and then under 7 days of low- Na+ diet (LSD). Blood pressure (in both sexes) was recorded on a separate group of mice in the baseline and after 3 and 7 days of LSD. Mice were taken out of cages to reduce stress on days 5–6. Volume was recorded and electrolyte concentrations and aldosterone determined on urine and expressed as total excreted per day (d) normalized to 25 g body weight. **(A)** urine volume; **(B)** urine Na+ (volume × concentration); **(C)** Cl−; **(D)** K+, **(E)** aldosterone excretion patterns; **(F)** mean arterial blood pressure (tail cuff) in WT (blue) and KO (red) mice (n = 6 mice/genotype); results of two-way ANOVA provided in figure inset. KO mice showed attenuation in the reduction in urine Na+ on Day 1, and modestly but significantly reduced blood pressure. *indicates a significant difference due to genotype ($p < 0.05$) as determined by 2-way ANOVA.

previously described by Knepper and associates (Nielsen et al., 1993; Ecelbarger et al., 1995; Masilamani et al., 1999; Kim et al., 2000). Rabbit polyclonal antibodies against UT-A1 (403) and α-ENaC (AA 46-68, L909) were kind gifts from the laboratory of Mark A. Knepper (Epithelial Systems Biology Laboratory, NHLBI, NIH). The rabbit polyclonal Rhbg antibody was a kind gift from the laboratory of David Weiner (University of Florida). The rabbit polyclonal NHE3 antibody was from StressMarq Biosciences (catalog #SPC-400). The rabbit polyclonal NBCe1 antibody was from Proteintech (catalog #11885-I-AP). The rabbit oligoclonal SGK1 antibody was from Invitrogen (22 HCLC). The rabbit polyclonal p-^{S422}SGK1 antibody was from Santa Cruz (catalog #16745R). Membranes were exposed to chemiluminescence substrate (Pierce) for 1–5 min. The images were then obtained using film processed in a darkroom or by a digital imager (Amersham 600). Membranes were stained with 0.1% Ponceau-S stain (Thermo Fisher Scientific) directly after blotting to address loading, protein transfer, and allow for specific band normalization. Occasionally, the lower portion of the blot was probed with β-actin for normalization.

Ubiquitination of Epithelial Sodium Channel

To determine whether KO or LS diet affected ubiquitination of ENaC subunits, we used the UbiQuant S quantitative Ub-substrate ELISA (LifeSensors, Inc.) kit. All ubiquitinated proteins were immunoprecipitated into the plate wells containing anti-ubiquitin antibody. Then the wells were probed with either α-, β-, and γ-ENaC polyclonal antibodies. After washes, secondary

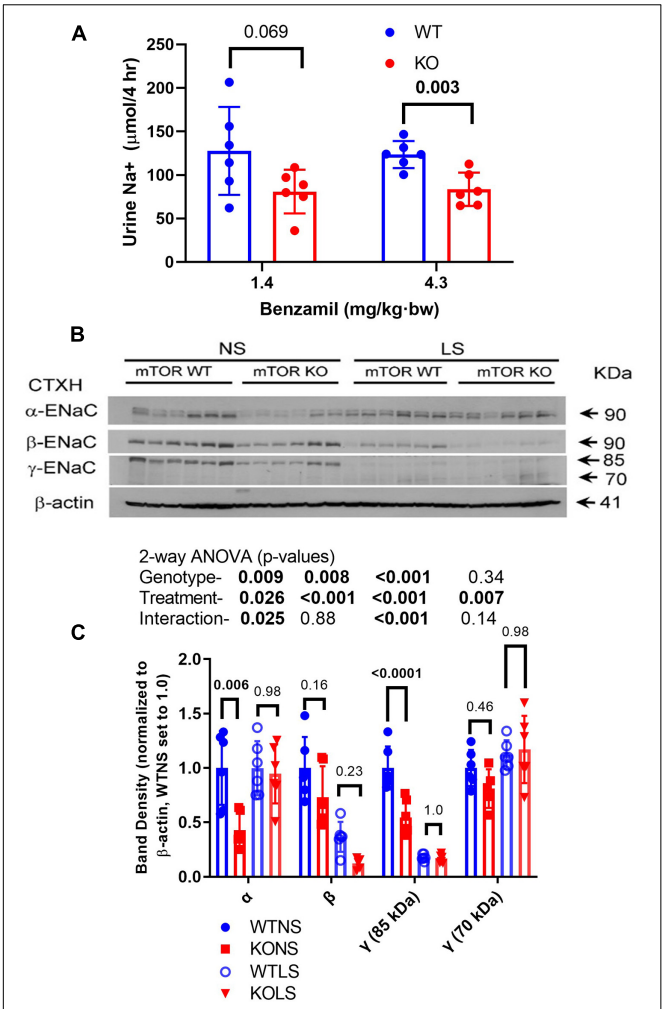

FIGURE 4 | Epithelial sodium channel (ENaC) activity and expression in kidney is reduced in KO mice. **(A)** Natriuretic sensitivity to the ENaC-select antagonist, benzamil was used as a surrogate for *in vivo* ENaC activity. Male mice (n = 6/genotype) were given a single intraperitoneal injection of benzamil @ 1.4 mg/kg·bw, urine collected in the subsequent 4-h period then measured for volume and Na+. The experiment was repeated the following week with 4.3 mg/kg·bw dose. **(B)** Male mice were fed NS or LS diet for 7-days (n = 6/genotype/diet) then euthanized and kidneys harvested. **(B)** Western blots of kidney cortex homogenates loaded with 30 µg/lane were probed with rabbit polyclonal antibodies against α-, β-, or γ-ENaC as indicated. A reprobe with β-actin (representative image) was used to normalize bands. **(C)** Band density summary (mean ± sem) and results of 2-way ANOVA (genotype × treatment). The major bands for all three subunits were significantly reduced ($p < 0.05$) in the KO, relative to WT. The LS diet also significantly affected abundance of all bands analyzed.

antibody was applied, followed by more washing then addition of chemiluminescence substrate. Chemiluminescent signal was recorded using an Amersham 600 Imager. Signal intensity of the well is related to the degree of ubiquitinated ENaC subunit.

Statistics

Data are presented using mean ± standard error means (SEM). Unpaired t-test was used when comparing two groups. With regard to urine data, mixed effected model (REML) or two-way (Time × Genotype) were used. Two-way ANOVA followed by Tukey's multiple comparisons testing was used to analyze western blotting data and membrane-to-cytosol density ratios for ENaC subunits. $P < 0.05$ was considered significant and corrected for multiple comparisons (GraphPad Prism 8.1.2).

RESULTS

Characterization of the Principal-Cell-Select Mechanistic Target of Rapamycin Knockout

Aquaporin-2-promoter-driven Cre recombinase localization was assessed by crossing AQP2-Cre transgenic mice with a LacZ reporter strain. In offspring that harbored the AQP2-Cre transgene, as predicted, β-galactosidase precipitate was localized to collecting duct principal cells, and highly concentrated in the inner medulla (**Figure 1A**). Demonstration of the mTOR protein deletion from principal cells was assessed by IHC, western and dot blotting. Using western blotting of whole-cell homogenates of cortex and inner medulla from males (**Figures 1B,D** left panel) and females (**Figures 1C,D** right panel), we found in general, reduced mTOR protein band densities in the KO cortex relative to WT. In contrast, band densities in the inner medullary homogenates were more variable and not significantly different between genotypes. Moreover, in males, mTOR showed greater density in cortex than in inner medulla, but in females, expression was similar between the regions. As the CD principal cell is a minority cell type in tissue homogenates, making the deletion difficult to observe by traditional western blotting, we also assessed the KO by dot blotting. We evaluated cortex, inner stripe of the outer medulla, and inner medulla homogenates from both sexes and genotypes on a single blot. Here we found (**Figures 1E–G**), a significant reduction (p = 0.019) in mTOR dot density in the inner medullary homogenates in the KO mice. Furthermore, there was a trend for a reduction in dot density in the KO in the outer medullary homogenates (OMH), although this did not reach significance (p = 0.087). No differences were observed using dot blotting in the cortex homogenates (CTXH). Finally, using the dot blotting approach for mTOR, we did not observe any sex differences.

Mechanistic Target of Rapamycin Immunohistochemistry in Renal Tubules

Immuno-based IHC for mTOR (brown) and AQP2 (gray) in male KO and WT mouse kidneys under control conditions is shown in **Figure 2**. In general, mTOR labeling was strongest in the thick ascending limb, distal tubule, and collecting duct (CD), relative to proximal tubule. Glomeruli also labeled with mTOR antibody. Dual labeling with AQP2 was used to identify CD principal cells. In the CD, qualitatively we observed less brown staining in cells co-stained with gray in the KO mice (orange arrows). We also observed strong labeling of mTOR in the intercalated cells in both genotypes (green arrows). The CD appeared, in general, of

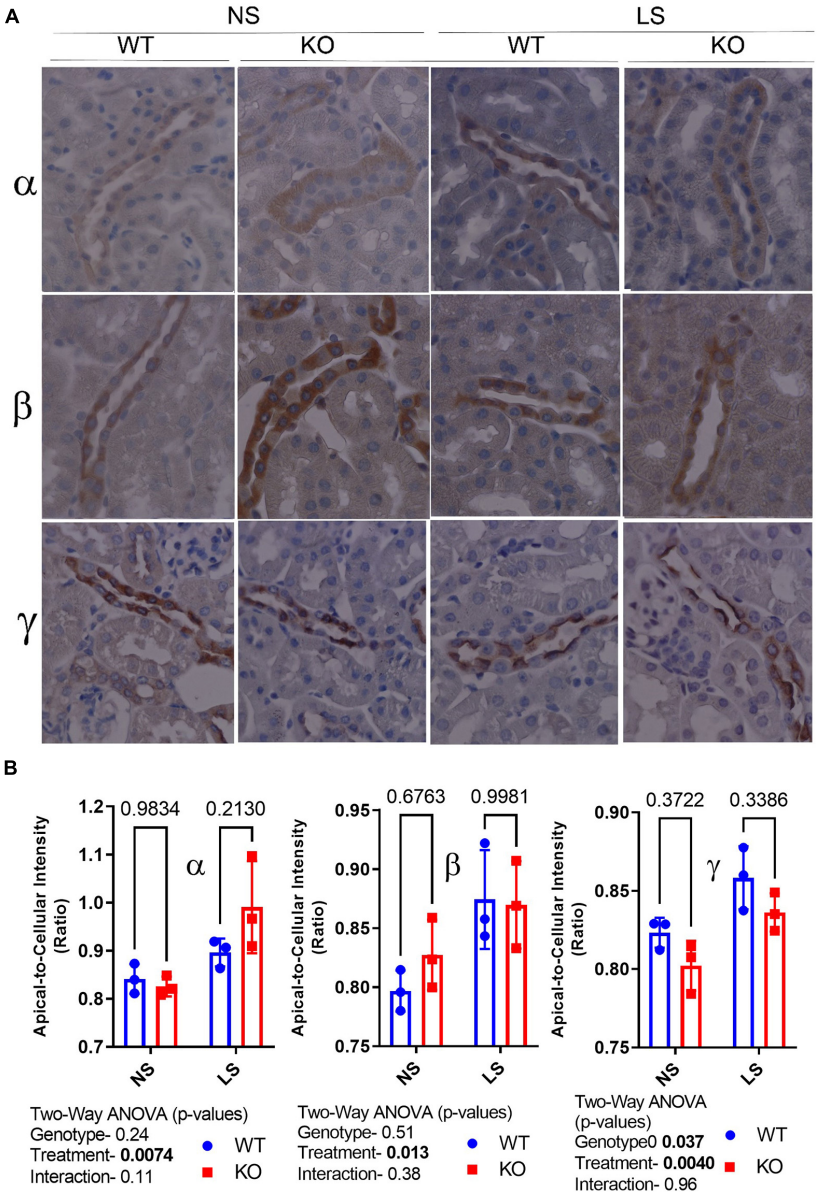

FIGURE 5 | Epithelial sodium channel (ENaC) subunit principal cell localization. **(A)** Immunoperoxidase-staining was used to assess intensity and sub-cellular localization of α- (top panel), β- (middle panel), and γ-(bottom panel) ENaC in 7-day NS or LS-treated male WT and KO mice. **(B)** Summary analysis of mean pixel intensity (Image J, NIH) in the apical-to-cellular regions of the principal cells (n = 10 replicate cells/stained section, n = 3 mice/group). LS diet increased relative apical localization of all ENaC subunits Moreover, γ-ENaC apical staining was lower in the KO (relative to WT).

normal diameter in the KO, with no obvious differences in the ratio of principal to intercalated cells.

Urinary Electrolyte Excretion With a Low-Na+ Diet

Because the CD is essential in the fine-tuning of Na+, Cl−, and K+ excretion, electrolyte excretion patterns upon switching from a normal (0.45%) to a low- (<0.02%) Na+ diet were evaluated (**Figure 3**). In the males, both genotypes experienced a slight decline in urine volume with increasing days on LS diet, with no differences between groups (**Figure 3A**). Daily excreted amounts of electrolytes, i.e., Na+ (**Figure 3B**), Cl− (**Figure 3C**), and K+ (**Figure 3D**) did not differ between genotypes on D0, indicating that WT and KO mice ate approximately the same amount of chow, and were in balance before initiating LS feeding. D1 Na+ losses were significantly higher in the KO, indicating retarded ability to rapidly reduce Na+ excretion. By day 2, however, Na+ losses were not different between genotypes. The significant (time × genotype) interaction, demonstrated that the WT and KO did not respond the same over time. Urine Cl− excretion also showed the time × genotype interaction, in that the

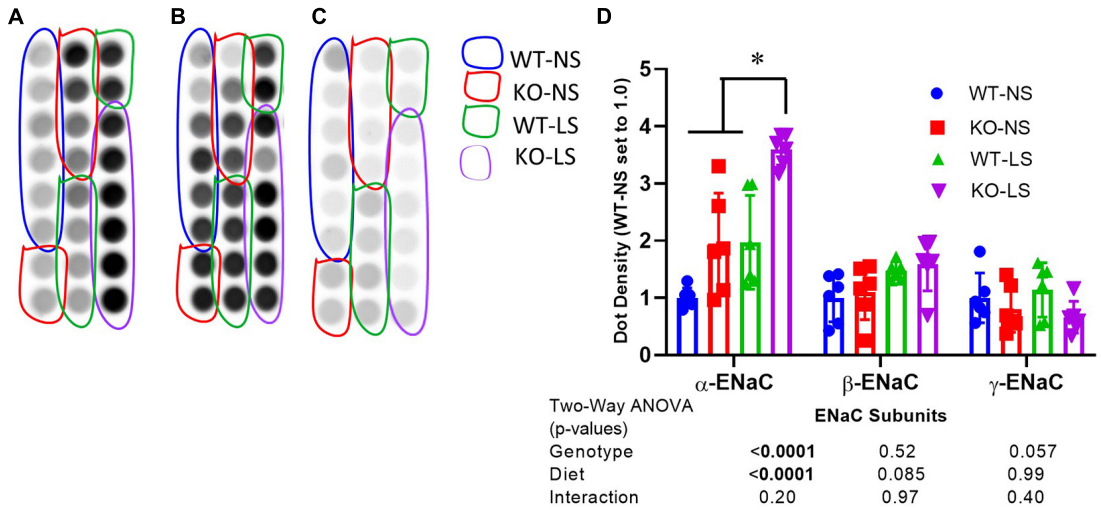

FIGURE 6 | Ubiquitination of α-ENaC increased in KO kidney. Ubiquitination of **(A)** α-, **(B)** β-, and **(C)** γ-ENaC in kidney cortex homogenates of LS and NS-treated male and female mice was assessed by an ELISA-based approach first immunoprecipitating all ubiquitinated proteins and then probing with anti-ENaC subunit antibodies. **(D)** Density summary of dots (mean ± sem) normalized to WT-NS (n = 6/genotype/sex/treatment). α-ENaC showed increased ubiquitination in the KO and reduced ubiquitination with LS diet. *indicates a significant difference ($p < 0.05$) by multiple comparisons testing following a significant 2-way ANOVA.

WT were able to reduce urine Cl− excretion to a greater extent on the LS diet, but this difference was delayed and sustained in the KO (relative to Na+ response, **Figure 3C**). Urine K+ also showed a time × genotype significant interaction in that there was a tendency for urine K+ to be higher on D1 and lower on D2 in the KO, in relation to WT (**Figure 3D**). Taken together these findings suggest a "sluggish," but eventually full capacity, adaptive response to the LS diet in the KO. Urine aldosterone was also measured (**Figure 3E**) and found to be increased as expected by LS diet in both genotypes. Surprisingly, the KO had a trend for suppressed urine aldosterone (p = 0.052). Blood pressures (**Figure 3F**) were measured in both male and female mice and found to be slightly, yet significantly, lower in the KO mice overall (p = 0.046). LS diet did not reduce blood pressure. Urine volume, Na+ and K+ measures are shown in **Supplementary Figure 1** in female mice. Female KO mice had an elevated basal excretion rate of urine Na+ with no genotype differences on subsequent daily collections. No differences in urine Cl− or K+ were observed in the female mice.

Reduced Epithelial Sodium Channel Activity and Protein Abundance in Knockout Mice

Because ENaC is a major regulator of sodium reabsorptive activity in the CD, we gauged *in vivo* activity of ENaC by benzamil (BNZ, ENaC antagonist) sensitivity (**Figure 4A**). WT and KO mice (male) were treated intraperitoneally with BNZ at two different doses and acute natriuretic response was measured. KO mice demonstrated relatively reduced (40–50%) urine Na+ excretion (in the 4-h post-injection collection) suggesting reduced ENaC activity. Kidneys were harvested from mice after 7-days of a normal or a low-NaCl diet. Western blotting of kidney cortex homogenates for the male mice are shown in **Figure 4B** with a summary of the density data provided in **Figure 4C** (females in **Supplementary Figure 2**). In the males, the major bands for all three subunits were significantly reduced in the KO relative to WT (two-way ANOVA). The LS diet attenuated differences between the genotypes and showed the expected increases in the 70-kDa band (cleavage band) for γ-ENaC in both genotypes. As has been reported previously (Masilamani et al., 2002), the major bands for β- and γ-ENaC were reduced by dietary Na+ restriction. In the female mice, a similar, but not identical pattern of ENaC-subunit-abundance regulation was observed. α-ENaC densities were significantly lower (∼40%) in the KO females under both diet conditions; however, no genotype difference was observed for β-ENaC, and γ-ENaC had a strong significant interaction in that it was reduced (relative to WT) with NS diet, but increased with LS diet. The LS diet produced similar responses in the females, as in the males, i.e., increased 70-kDa band for γ-ENaC and a reduction in the density of the β -ENaC band.

Reduced Apical Localization of the γ-Subunit of ENaC in Cortical Collecting Duct of Knockout Mice

Epithelial sodium channel activity is regulated by channel number, open probability, and subcellular localization. Thus, we evaluated subcellular distribution of the ENaC subunits by IHC (**Figure 5**). Representative labeling of a cortical CD in a male mouse in each of the treatments/genotypes is shown in **Figure 5A** as indicated. **Figure 5B** shows apical-to-cellular intensity of signal. Two-way ANOVA showed LS diet led to increased relative apical localization of α-, β-, and γ-ENaC staining. Moreover, γ-ENaC apical staining was lower in the KO (relative to WT).

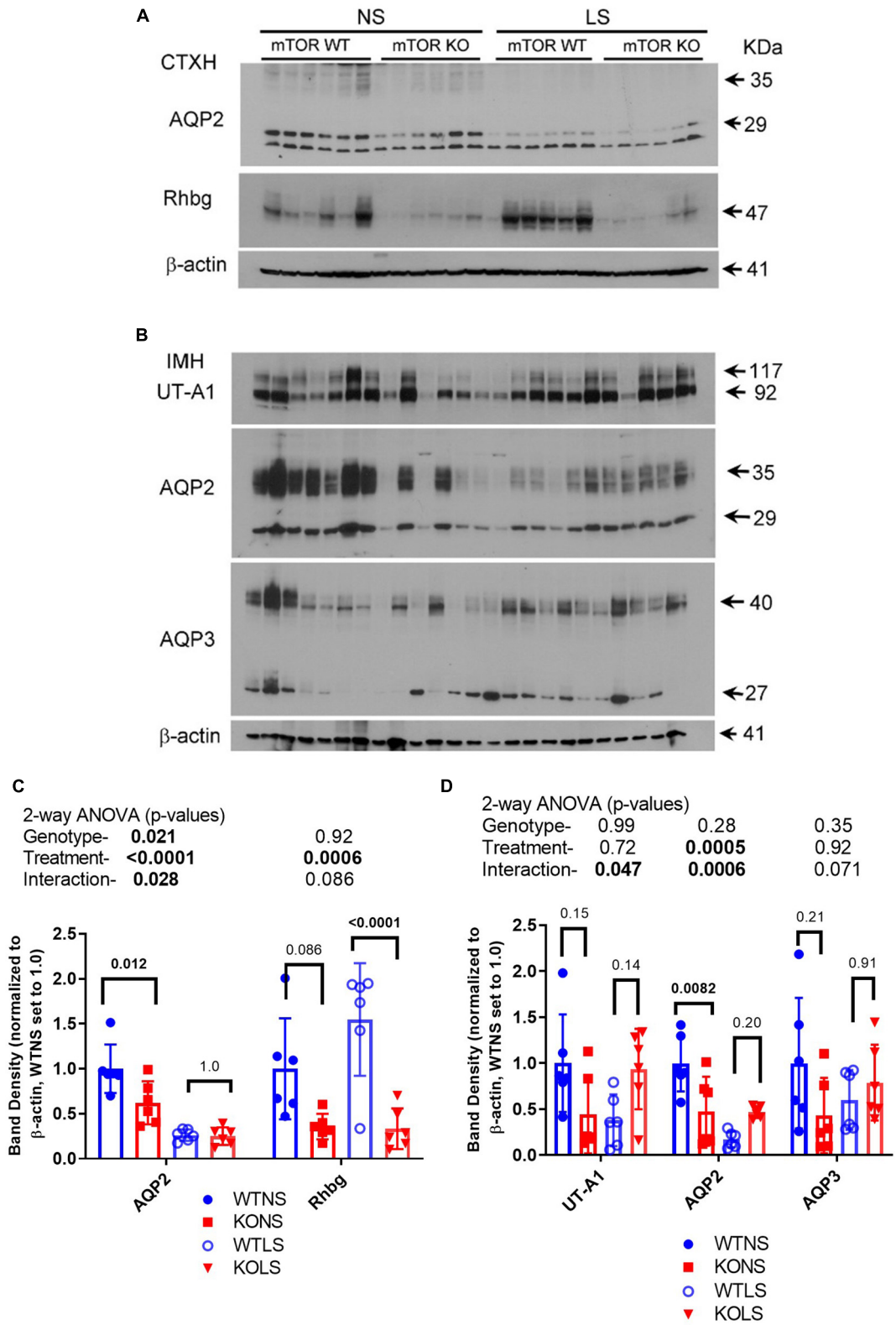

FIGURE 7 | Protein abundances of selected transport/channel proteins in collecting ducts. Western blots of kidney **(A)** cortex homogenates or **(B)** inner medullary homogenates from NS and LS diet fed male WT and KO mice were probed with antibodies against candidate proteins. **(C,D)** Band density (mean ± sem) summary (n = 6 mice/treatment/genotype) and two-way ANOVA p-values for major bands. AQP2, aquaporin-2; AQP3, aquaporin-3; Rhbg, ammonium transporter; UT-A1, urea transporter. KO mice had reduced protein levels for AQP2 and Rhbg in cortex. Inner medullary protein levels were less affected by the KO.

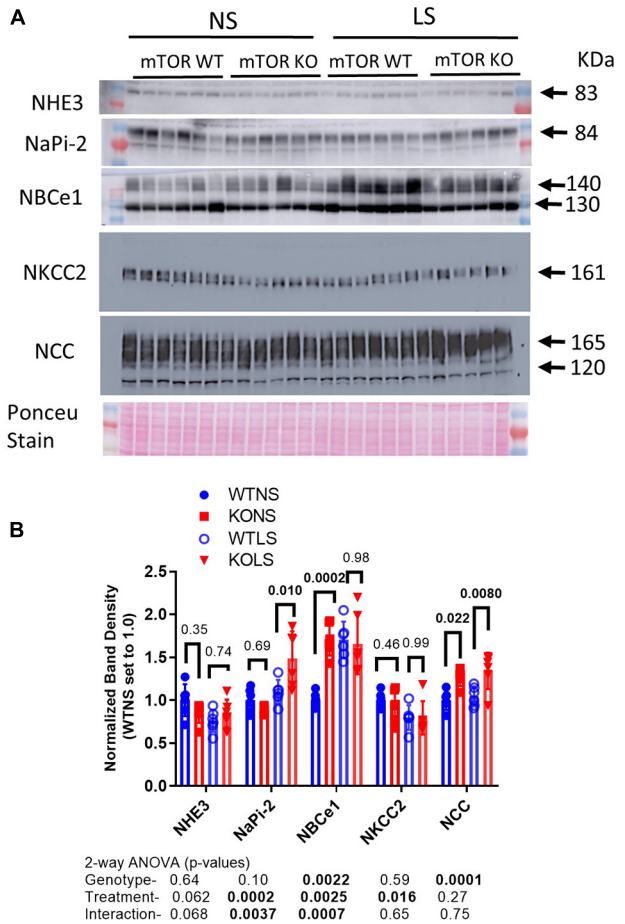

FIGURE 8 | Abundances of non-collecting-duct sodium reabsorptive proteins. Western blots of kidney **(A)** cortex homogenates from NS and LS diet fed male WT and KO mice were probed with antibodies against candidate proteins. **(B)** Band density (mean ± sem) summary (n = 6 mice/treatment/genotype) and two-way ANOVA p-values for major bands. NHE3, sodium hydrogen exchanger, type 3; NaPi-2, sodium phosphate cotransporter, type 2; NBCe1, electrogenic sodium bicarbonate cotransporter, type 1; NKCC2, bumetanide-sensitive sodium potassium 2 chloride cotransporter, type 2; NCC, thiazide-sensitive sodium chloride cotransporter. KO mice had increased protein levels of NaPi-2 under LS diet, NBCe1 under NS diet, and NCC under both diets relative to WT.

Evidence of Increased α-Epithelial Sodium Channel Ubiquitination in Knockout Mice Cortex Homogenates

To determine if the reduction in ENaC subunit protein in the KO may be due to enhanced protein degradation, we assessed ubiquitination of ENaC subunits in male mice fed normal or LSD (**Figure 6**). All ubiquitinated proteins (in cortex homogenate) were immunoprecipitated onto plates which were subsequently probed with ENaC antibodies. We found α-, but not β- or γ-ENaC had significantly increased ubiquitination (although γ- showed a strong trend, $p = 0.057$ in this direction). Furthermore, samples from the LS mice also showed higher levels of α-ENaC ubiquitination, which might represent elevated turnover (both production and degradation).

Reduced Aquaporin-2 and Rhbg in Kidney of Knockout Mice

We next assessed the protein abundance of other major transport/channel proteins in the CD in the male mice to determine whether they were similarly down-regulated in the KO (**Figure 7**). Aquaporin 2, another apical channel of the principal cells (DiGiovanni et al., 1994), was (like ENaC) significantly reduced in the KO, in cortex (**Figures 7A,C**) and medulla (**Figures 7B,D**), with NS, but not LS diet. LS diet also markedly reduced AQP2 abundance in both kidney regions. The urea transporter (UT-A1) of collecting duct principal cells showed a significant interactive term between treatment and genotype (**Figures 7B,D**) in that it was reduced in the KO under NS, but increased under LS diet. Rhbg, a collecting duct ammonium transporter found on the basolateral side of both intercalated and principal cells (Verlander et al., 2003) was down-regulated in the KO. AQP3, a basolateral water channel in principal cells (Ecelbarger et al., 1995), was not significantly different between genotypes or due to treatment.

Regulation of Non-collecting Duct Major Sodium Transporters and Exchangers

To determine if sodium transport might be upregulated at a different site along the renal tubule to compensate for reduced ENaC expression, we evaluated major sodium transporters in proximal tubule, thick ascending limb, and distal convoluted tubule (**Figure 8**). There was no effect of diet or genotype on the expression of the sodium hydrogen exchanger, type 3 (NHE3 or *slc9a3*). There was a significant effect of treatment (LS diet), as well as, a significant interaction between treatment and genotype for the sodium phosphate cotransporter, type 2 (NaPi-2, *slc34a2*). NaPi-2 was increased by LS diet in the KO but not the WT. Similarly, there was a significant interactive term for the sodium bicarbonate cotransporter (NBCe1, *slc4a4*) in that it was increased in the KO under normal, but not LS diet. The bumetanide-sensitive sodium potassium 2 chloride cotransporter, type 2 (NKCC2, *slc12a1*) was slightly, but significantly reduced by LS diet, but not different between genotypes, and the thiazide-sensitive sodium chloride cotransporter (NCC, *slc12a3*) was increased in the KO under both dietary conditions.

Blood Na+ Is Reduced in Knockout Mice

Mean Na^+ concentrations in the blood were significantly lower in the KO mice under NS diet (**Figure 9A**). LS diet reduced Na^+ concentrations in the blood of the WT, so they were no longer different from KO. Blood Cl− concentrations fell significantly in KO on LS diet, but not in WT (**Figure 9B**). No differences were observed for blood K+ (**Figure 9C**). Blood bicarbonate levels were significantly higher in the KO under both diets (**Figure 9D**). Additional whole blood measures (by iSTAT analysis) and plasma (ELISA) are provided in **Table 1**. LS diet increased blood glucose, hemoglobin, and aldosterone concentrations in both genotypes.

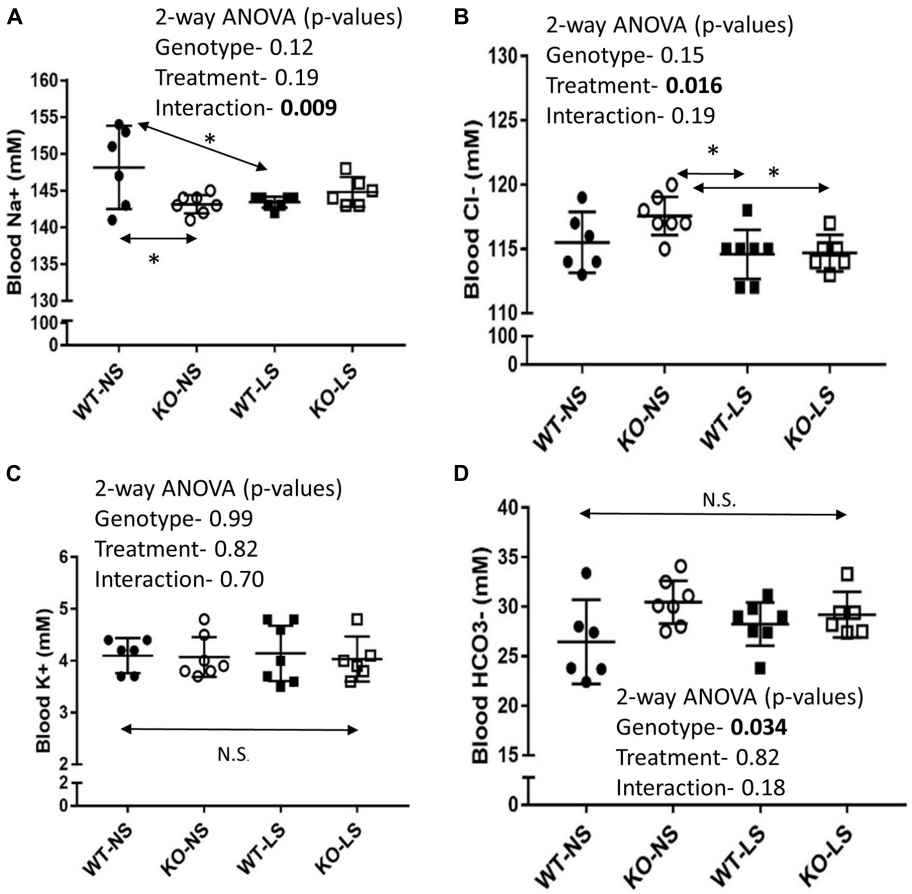

FIGURE 9 | Blood chemistry under normal and low-Na+ diet- Blood chemistry was performed by iSTAT after 7-days of NS or LS diet. **(A)** Na+, **(B)** Cl−, **(C)** K+, **(D)** HCO_3- (n = 6 mice/group). Two-way ANOVA p-values are shown within the panels. KO mice has reduced blood Na+ under NS, but not LS diet. LS reduced blood Cl− in both genotypes. No effects on blood K+ were noted. KO mice had significantly higher blood HCO_3- under both diets. * indicates a significant ($p < 0.05$) difference between groups.

TABLE 1 | Weight and Blood Parameters in male CD-PC mTOR KO mice under normal and low-NaCl diets.*

	WT-NS	KO-NS	WT-LS	KO-LS	Two-Way ANOVA (p-values)		
					Genotype	Diet	Interaction
Final body weight (g)	32.9 ± 2.0	27.1 ± 1.5	26.7 ± 1.7	28.2 ± 1.0	0.20	0.13	0.033
Kidney weight (g/25 g·bw)	0.125 ± 0.006	0.132 ± 0.002	0.138 ± 0.002	0.135 ± 0.002	0.46	0.026	0.18
BUN (mg/dL)	26.5 ± 0.8	25.6 ± 0.6	26.0 ± 0.8	24.7 ± 1.1	0.20	0.42	0.81
Glucose (mg/dL)†	194 ± 8^{AB}	185 ± 8^{B}	205 ± 5^{AB}	212 ± 2^{A}	0.94	0.005	0.24
Hct (%PCV)	33.7 ± 0.8	32.1 ± 0.8	33.7 ± 2.0	35 ± 0.7	0.93	0.26	0.28
Hb (g/dL)	11.4 ± 0.3	10.9 ± 0.3	11.9 ± 0.4	11.9 ± 0.2	0.38	0.026	0.43
pH (log H+)	7.18 ± 0.02^{B}	7.31 ± 0.03^{A}	7.23 ± 0.01^{AB}	7.26 ± 0.02^{AB}	0.001	0.94	0.053
Beecf (mM)	-1.83 ± 1.96^{B}	4.28 ± 0.99^{A}	0.71 ± 1.06^{AB}	2.33 ± 1.31^{AB}	0.009	0.83	0.107
AnGap (mM)	10.3 ± 4.4	−0.9 ± 1.3	4.8 ± 0.7	3.8 ± 1.8	0.016	0.87	0.04
Aldosterone (pM)	94 ± 17	60 ± 11	191 ± 70	317 ± 136	0.54	0.026	0.29

**Mean ± sem (n = 6, 7, 7, and 6 for WT-NS, KO-NS, WT-LS, KO-LS, respectively).*

†Non-fasted; Superscript letters indicate significant differences between groups as determined by Tukey's multiple comparisons test; "A" (assigned to highest mean) is significantly different from "B," but not "AB."

Blood chemistry conducted in the female mice are provided in **Supplementary Table 1**. No genotype differences in blood pH were found in the female mice; however, the KO females had significantly higher blood K+, hematocrit, and hemoglobin, and bicarbonate trended higher ($p = 0.11$), as compared to WT.

Reduced Phosphorylation of Serum Glucocorticoid Regulated Kinase on Serine 422 in Knockout Mouse Kidney

We predicted the reduction in sodium retentive-ability with LS diet in the KO mice and increased ubiquitination of ENaC might have been due to a reduction in phosphorylation of SGK1 on serine 422, this hydrophobic motif in SGK1 has been shown to be the target of mTORC2 (Garcia-Martinez and Alessi, 2008). In support of this, we found reduced band density for p-^{S422}SGK1 in cortex homogenates in the male mice. However, SGK1 and the ratio of p-^{S422}SGK1 to total SGK1 band densities were not significantly different. Furthermore, these band densities were not affected by the LS diet in either genotype (**Figure 10**).

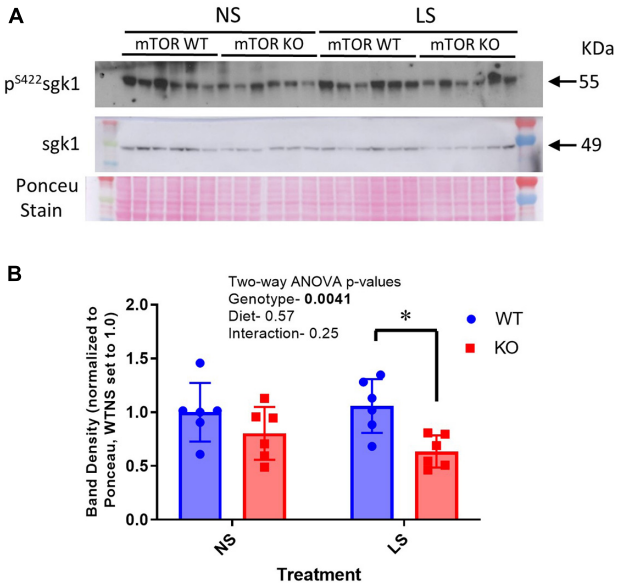

FIGURE 10 | Phosphorylation of SGK1 is reduced in KO kidney. **(A)** A western blot of cortex homogenates from NS and LS diet fed male mice probed with an antibody against phosphorylated SGK1 (pS422). **(B)** Mean band densities (mean ± sem) normalized to Ponceau stain. Two-way ANOVA *p*-values are shown within the panel; * indicates a significant ($p < 0.05$) difference between groups.

DISCUSSION

The mechanistic target of rapamycin (mTOR) is a central energy sensor expressed in nearly all cell types (Brown et al., 2018). Using Cre-recombinase-targeted knockout, we deleted mTOR in mice from all cell types expressing Aquaporin 2 (AQP2). This primarily focused the deletion to the principal cells of the distal tubule, including connecting tubule and collecting duct. In male mice, AQP2 is also expressed in several reproductive tissues (Uhlen et al., 2015), including ductus deferens, epididymis, and seminal vesicles, thus only female KO mice were used as breeders to maintain the line. In the principal cells, mTOR, which functions as a kinase, has been demonstrated to be upstream of the ENaC activation by insulin (Pavlov et al., 2013). Therefore, we focused on the regulation of ENaC and electrolyte homeostasis in this set of studies.

In the male KO mice, all three subunits of ENaC were significantly reduced at the protein level, when assessed in cortex homogenates. Furthermore, KO mice excreted significantly reduced amounts of sodium in urine in response to a single injection of benzamil (ENaC) antagonist, suggesting overall ENaC activity was reduced. To test this further, mice were placed on a very-low Na+ (LS) diet for 7-days. KO mice had a retarded ability to reduce sodium losses on the first day of sodium restriction; however, they eventually adapted. Furthermore, KO mice also had attenuated (and somewhat sustained) ability to reduce urinary chloride losses under LS diet. Chloride levels in the Na+ restricted diet were also low at 0.07% of dry weight (vs. 0.67% for the control diet). Thus, mTOR, most likely as a component of mTORC2, facilitates responses in the adaptation of ENaC activity under low-NaCl diet. The retarded ability to reabsorb chloride was likely secondary to reduced depolarization of the apical membrane, as chloride reabsorption is primarily through pendrin in the intercalated cells (which had intact mTOR).

The CD-mTOR KO mice were determined to have modestly lower blood pressure and reduced ENaC subunit expression under normal and low-NaCl diet conditions. The lower blood pressure, we surmise, may have been due to reduced ENaC activity with subsequently reduced plasma volume. We found hematocrit and hemoglobin levels to be higher in the female KO mice, an indication of mild volume contraction. We may speculate that male mice were somewhat more protected from this volume contraction.

In principal cells, mTOR, as a component of the mTORC2 complex, activates the serum and glucocorticoid regulated kinase 1 (SGK1) by phosphorylation in its hydrophobic motif on serine 422 (Lu et al., 2010; Lang and Pearce, 2016). SGK1 is further activated by phosphorylation in the activation loop by PI-3K. Activated SGK1 then phosphorylates NEDD4-2, an E3-ubiquitin ligase, which increases its association with 14-3-3 proteins and reduces its ability to ubiquitinate ENaC subunits. Thus, we hypothesized that KO of mTOR might lead to down-regulation of ENaC abundance by upregulating ubiquitination of ENaC subunits *via* reduced SGK1 activity. In agreement with our hypothesis, using an ELISA approach to pull-down all ubiquitinated proteins from the cortex homogenate, we found significantly increased representation of α-ENaC subunit in this pool in the CD-mTOR KO, vs. the WT, mice. This supports a greater proportion of cellular α-ENaC was ubiquitinated in the CD-mTOR KO mice. We also found reduced levels of phosphorylated SGK1 in cortex homogenates in the KO, further supporting the hypothetical pathway.

However, we did not observe any increase in β- or γ-ENaC ubiquitination, despite these subunits being reduced in total abundance. This might suggest that these two subunits are not as sensitive to this particular recycling regulatory pathway. In fact, γ-ENaC trended toward being reduced with regard to ubiquitination in the KO mice. Subunit differences in their relative ubiquitinated status might also have something to do with the binding of the polyclonal antibodies to their antigenic sites that may be modified by the ubiquitination process. It is important to note that band densities for the major bands for both γ- and β-ENaC show a reduction in density under conditions that have been shown to stimulate ENaC, e.g., low- Na+ diet. Thus, it is possible that these N-terminal region antibodies lose relative sensitivity with the activation of the channel itself. Further studies would be required to flesh this out.

We can compare and contrast our phenotype with those of α-ENaC knockout mice. In one model, the same AQP2-promoter targeting transgene was used to delete α-ENaC (Christensen et al., 2010). A second model knocked out α-ENaC using a doxycycline-inducible PAX8-promoter targeting transgene (Perrier et al., 2016). α-ENaC deletion in these mouse models caused significant sodium wasting, weight loss, and hyperkalemia. Because our model did not completely abolish α-ENaC expression, we can conclude mTOR activity is not essential, but rather is facilitatory of α-ENaC expression. These models did contrast, however, to deletion of α-ENaC using HOXB7 promoter targeting, in which mice showed no impairment in sodium or potassium homeostasis under various challenges (Rubera et al., 2003). While AQP2 and PAX8 are expressed in connecting tubule, as well as, collecting duct, HOXB7 is primarily collecting-duct associated. Taken together these findings highlight the importance of sodium reabsorption in the early distal tubule, i.e., the distal convoluted tubule and connecting tubule.

We also evaluated other major sodium transporters and exchangers of other sites along the renal tubule to evaluate potential compensation. We came up with a few possible compensatory changes that might have alleviated sodium losses in our mice. First NCC, a major aldosterone-regulated protein of the distal convoluted tubule (Wang et al., 2015) was increased about 20% in the KO under both dietary conditions. Surprisingly, we did not find this protein increased by LS diet in these mice, as has been shown in other studies at least with rats (Masilamani et al., 2002). Furthermore, NaPi-2 and NBCe1, sodium reabsorptive proteins of the proximal tubule were marginally increased in the KO, which may have enhanced proximal tubule sodium retention. Since aldosterone levels did not appear elevated in the KO mice (even trended lower), additional studies will be needed to understand these compensations.

Although this study did not set out to capture sex differences in the response to the KO, we did observe a similar abundance level of mTOR in the kidneys of male vs. female mice. However, male, but not female mice seemed to have relatively more mTOR in cortex homogenates, as compared to inner medulla, when equal amounts of protein were loaded, perhaps representing a greater reliance on this pathway in male proximal tubule. Both sexes also demonstrated a reduction in α-ENaC with KO. Female KO mice did show some increase in hematocrit, as well as an increase in urine sodium losses in the basal state, which may have reflected slight volume contraction, that was not as apparent in the male KO. Unfortunately, we did not have the opportunity to conduct all of the original analyses in the female sex that were conducted in the males.

One caveat to consider in interpretation of these data is that deletion of mTOR would result in a reduction in both mTORC1 and mTORC2 activity. In this particular set of studies, we focused primarily on an end-point downstream of mTORC2, i.e., at least as we currently understand it; however, it is possible that some of the changes we found in expression of renal proteins, blood chemistry, or whole-body adaptations to a low-sodium diet were due to changes in mTORC1 signaling and downstream effectors. Additional studies will be needed to fully characterize this aspect of our model system.

CONCLUSION

Collecting duct principal-cell-targeted mTOR deletion by Cre-recombinase mediated gene deletion results in a whole-body phenotype of modest salt wasting. At the cellular level, there is a delayed natriferic response to sodium restriction suggesting mTOR activity (along with the much more robust renin-angiotensin-system) facilitates sodium homeostasis under low-NaCl dietary conditions. Thus, dysregulation of this signaling cascade, e.g., during insulin resistance or type 2 diabetes, may hinder whole-body sodium homeostasis.

DATA AVAILABILITY STATEMENT

The original contributions presented in the study are included in the article/**Supplementary Material**, further inquiries can be directed to the corresponding author.

ETHICS STATEMENT

The animal study was reviewed and approved by the Georgetown University Institution Animal Care and Use Committee.

AUTHOR CONTRIBUTIONS

BC and MF conducted the experiments, performed the analysis, interpreted the data, drafted the manuscript, and proof-read the final manuscript version. SS and AB conducted the experiments, analyzed the data, and finalized the manuscript. AG conducted the experiments, performed the statistical analyses, and proof-read the final manuscript. CE designed the studies, wrote the animal protocols, interpreted the

data, graphed the figures, and finalized the manuscript. All authors contributed to the article and approved the submitted version.

FUNDING

The funding for this research was kindly provided from the Department of Medicine (CE) and the Biomedical Graduate Research Organization at the Georgetown University Medical Center (BGRO, CE).

ACKNOWLEDGMENTS

We thank Lijun Li for assistance with initial animal studies, genotyping, and ancillary data collection.

SUPPLEMENTARY MATERIAL

The Supplementary Material for this article can be found online at: https://www.frontiersin.org/articles/10.3389/fphys.2021.787521/full#supplementary-material

REFERENCES

Baba, Y., Higa, J. K., Shimada, B. K., Horiuchi, K. M., Suhara, T., Kobayashi, M., et al. (2018). Protective effects of the mechanistic target of rapamycin against excess iron and ferroptosis in cardiomyocytes. *Am. J. Physiol. Heart Circ. Physiol.* 314, H659–H668. doi: 10.1152/ajpheart.00452.2017

Betz, C., Stracka, D., Prescianotto-Baschong, C., Frieden, M., Demaurex, N., and Hall, M. N. (2013). Feature Article: mTOR complex 2-Akt signaling at mitochondria-associated endoplasmic reticulum membranes (MAM) regulates mitochondrial physiology. *Proc. Natl. Acad. Sci. U.S.A.* 110, 12526–12534. doi: 10.1073/pnas.1302455110

Blazer-Yost, B. L., Liu, X., and Helman, S. I. (1998). Hormonal regulation of ENaCs: insulin and aldosterone. *Am. J. Physiol.* 274(Pt 1), C1373–C1379.

Brown, A. L., Fluitt, M. B., and Ecelbarger, C. M. (2018). Mechanistic target of rapamycin: integrating growth factor and nutrient signaling in the collecting duct. *Am. J. Physiol. Renal Physiol.* 315, F413–F416. doi: 10.1152/ajprenal.00170.2018

Christensen, B. M., Perrier, R., Wang, Q., Zuber, A. M., Maillard, M., Mordasini, D., et al. (2010). Sodium and potassium balance depends on alphaENaC expression in connecting tubule. *J. Am. Soc. Nephrol.* 21, 1942–1951. doi: 10.1681/ASN.2009101077

DiGiovanni, S. R., Nielsen, S., Christensen, E. I., and Knepper, M. A. (1994). Regulation of collecting duct water channel expression by vasopressin in Brattleboro rat. *Proc. Natl. Acad. Sci. U.S.A.* 91, 8984–8988. doi: 10.1073/pnas.91.19.8984

Ecelbarger, C. A., Kim, G. H., Terris, J., Masilamani, S., Mitchell, C., Reyes, I., et al. (2000). Vasopressin-mediated regulation of epithelial sodium channel abundance in rat kidney. *Am. J. Physiol. Renal Physiol.* 279, F46–F53. doi: 10.1152/ajprenal.2000.279.1.F46

Ecelbarger, C. A., Terris, J., Frindt, G., Echevarria, M., Marples, D., Nielsen, S., et al. (1995). Aquaporin-3 water channel localization and regulation in rat kidney. *Am. J. Physiol.* 269(Pt 2), F663–F672.

Friedrich, G., and Soriano, P. (1991). Promoter traps in embryonic stem cells: a genetic screen to identify and mutate developmental genes in mice. *Genes Dev.* 5, 1513–1523. doi: 10.1101/gad.5.9.1513

Garcia-Martinez, J. M., and Alessi, D. R. (2008). mTOR complex 2 (mTORC2) controls hydrophobic motif phosphorylation and activation of serum- and glucocorticoid-induced protein kinase 1 (SGK1). *Biochem. J.* 416, 375–385. doi: 10.1042/BJ20081668

Heikamp, E. B., Patel, C. H., Collins, S., Waickman, A., Oh, M. H., Sun, I. H., et al. (2014). The AGC kinase SGK1 regulates TH1 and TH2 differentiation downstream of the mTORC2 complex. *Nat. Immunol.* 15, 457–464. doi: 10.1038/ni.2867

Kim, G. H., Martin, S. W., Fernandez-Llama, P., Masilamani, S., Packer, R. K., and Knepper, M. A. (2000). Long-term regulation of renal Na-dependent cotransporters and ENaC: response to altered acid-base intake. *Am. J. Physiol. Renal Physiol.* 279, F459–F467. doi: 10.1152/ajprenal.2000.279.3.F459

Lang, F., and Pearce, D. (2016). Regulation of the epithelial Na+ channel by the mTORC2/SGK1 pathway. *Nephrol. Dial Transplant.* 31, 200–205.

Laplante, M., and Sabatini, D. M. (2012a). mTOR signaling. *Cold Spring Harb. Perspect. Biol.* 4:a011593.

Laplante, M., and Sabatini, D. M. (2012b). mTOR signaling in growth control and disease. *Cell* 149, 274–293. doi: 10.1016/j.cell.2012.03.017

Lee, J. W., Chou, C. L., and Knepper, M. A. (2015). Deep sequencing in microdissected renal tubules identifies nephron segment-specific transcriptomes. *J. Am. Soc. Nephrol.* 26, 2669–2677. doi: 10.1681/ASN.2014111067

Lu, M., Wang, J., Jones, K. T., Ives, H. E., Feldman, M. E., Yao, L. J., et al. (2010). mTOR complex-2 activates ENaC by phosphorylating SGK1. *J. Am. Soc. Nephrol.* 21, 811–818.

Masilamani, S., Kim, G. H., Mitchell, C., Wade, J. B., and Knepper, M. A. (1999). Aldosterone-mediated regulation of ENaC alpha, beta, and gamma subunit proteins in rat kidney. *J. Clin. Invest.* 104, R19–R23.

Masilamani, S., Wang, X., Kim, G. H., Brooks, H., Nielsen, J., Nielsen, S., et al. (2002). Time course of renal Na-K-ATPase, NHE3, NKCC2, NCC, and ENaC abundance changes with dietary NaCl restriction. *Am. J. Physiol. Renal Physiol.* 283, F648–F657. doi: 10.1152/ajprenal.00016.2002

Nielsen, S., DiGiovanni, S. R., Christensen, E. I., Knepper, M. A., and Harris, H. W. (1993). Cellular and subcellular immunolocalization of vasopressin-regulated water channel in rat kidney. *Proc. Natl. Acad. Sci. U.S.A.* 90, 11663–11667. doi: 10.1073/pnas.90.24.11663

Pavlov, T. S., Ilatovskaya, D. V., Levchenko, V., Li, L., Ecelbarger, C. M., and Staruschenko, A. (2013). Regulation of ENaC in mice lacking renal insulin receptors in the collecting duct. *FASEB J.* 27, 2723–2732. doi: 10.1096/fj.12-223792

Perrier, R., Boscardin, E., Malsure, S., Sergi, C., Maillard, M. P., Loffing, J., et al. (2016). Severe salt-losing syndrome and hyperkalemia induced by adult nephron-specific knockout of the epithelial sodium channel alpha-subunit. *J. Am. Soc. Nephrol.* 27, 2309–2318. doi: 10.1681/asn.2015020154

Rubera, I., Loffing, J., Palmer, L. G., Frindt, G., Fowler-Jaeger, N., Sauter, D., et al. (2003). Collecting duct-specific gene inactivation of alphaENaC in the mouse kidney does not impair sodium and potassium balance. *J. Clin. Invest.* 112, 554–565. doi: 10.1172/JCI16956

Sarbassov, D. D., Ali, S. M., Kim, D. H., Guertin, D. A., Latek, R. R., Erdjument-Bromage, H., et al. (2004). Rictor, a novel binding partner of mTOR, defines a rapamycin-insensitive and raptor-independent pathway that regulates the cytoskeleton. *Curr. Biol.* 14, 1296–1302. doi: 10.1016/j.cub.2004.06.054

Shan, T., Zhang, P., Jiang, Q., Xiong, Y., Wang, Y., and Kuang, S. (2016). Adipocyte-specific deletion of mTOR inhibits adipose tissue development and causes insulin resistance in mice. *Diabetologia* 59, 1995–2004. doi: 10.1007/s00125-016-4006-4

Song, J., Hu, X., Riazi, S., Tiwari, S., Wade, J. B., and Ecelbarger, C. A. (2006). Regulation of blood pressure, the epithelial sodium channel (ENaC), and other key renal sodium transporters by chronic insulin infusion in rats. *Am. J. Physiol. Renal Physiol.* 290, F1055–F1064. doi: 10.1152/ajprenal.00108.2005

Stricklett, P. K., Nelson, R. D., and Kohan, D. E. (1999). Targeting collecting tubules using the aquaporin-2 promoter. *Exp. Nephrol.* 7, 67–74. doi: 10.1159/000020587

Tiwari, S., Nordquist, L., Halagappa, V. K., and Ecelbarger, C. A. (2007). Trafficking of ENaC subunits in response to acute insulin in mouse kidney. *Am. J. Physiol. Renal Physiol.* 293, F178–F185. doi: 10.1152/ajprenal.00447.2006

Tiwari, S., Packer, R. K., Hu, X., Sugimura, Y., Verbalis, J. G., and Ecelbarger, C. A. (2006). Increased renal alpha-ENaC and NCC abundance and elevated blood pressure are independent of hyperaldosteronism in vasopressin escape. *Am. J. Physiol. Renal Physiol.* 291, F49–F57. doi: 10.1152/ajprenal.00390.2005

Uhlen, M., Fagerberg, L., Hallstrom, B. M., Lindskog, C., Oksvold, P., Mardinoglu, A., et al. (2015). Proteomics. Tissue-based map of the human proteome. *Science* 347:1260419.

Verlander, J. W., Miller, R. T., Frank, A. E. I, Royaux, E., Kim, Y. H., and Weiner, I. D. (2003). Localization of the ammonium transporter proteins RhBG and RhCG in mouse kidney. *Am. J. Physiol. Renal Physiol.* 284, F323–F337.

Wang, J., Barbry, P., Maiyar, A. C., Rozansky, D. J., Bhargava, A., Leong, M., et al. (2001). SGK integrates insulin and mineralocorticoid regulation of epithelial sodium transport. *Am. J. Physiol. Renal Physiol.* 280, F303–F313. doi: 10.1152/ajprenal.2001.280.2.F303

Wang, L., Dong, C., Xi, Y. G., and Su, X. (2015). Thiazide-sensitive Na+-Cl− cotransporter: genetic polymorphisms and human diseases. *Acta Biochim. Biophys. Sin. (Shanghai)* 47, 325–334. doi: 10.1093/abbs/gmv020

Weichhart, T. (2018). mTOR as regulator of lifespan, aging, and cellular senescence: a mini-review. *Gerontology* 64, 127–134. doi: 10.1159/000484629

Conflict of Interest: The authors declare that the research was conducted in the absence of any commercial or financial relationships that could be construed as a potential conflict of interest.

frontiers in Physiology

ORIGINAL RESEARCH
published: 17 January 2022
doi: 10.3389/fphys.2021.784957

Natriuresis During an Acute Intravenous Sodium Chloride Infusion in Conscious Sprague Dawley Rats Is Mediated by a Blood Pressure-Independent α_1-Adrenoceptor-Mediated Mechanism

*Alissa A. Frame[1,2], Kayla M. Nist[2,3], Kiyoung Kim[1,2], Jill T. Kuwabara[1,2] and Richard D. Wainford[1,2]**

[1] Department of Pharmacology & Experimental Therapeutics, Boston University School of Medicine, Boston, MA, United States, [2] Whitaker Cardiovascular Institute, Boston University School of Medicine, Boston, MA, United States, [3] Department of Anatomy & Neurobiology, Boston University School of Medicine, Boston, MA, United States

OPEN ACCESS

Edited by:
Soo Wan Kim,
Chonnam National University Medical School, South Korea

Reviewed by:
Eduardo Colombari,
Universidade Estadual Paulista, Brazil
Andre Souza Mecawi,
Federal University of São Paulo, Brazil

***Correspondence:**
Richard D. Wainford
rwainf@bu.edu

Specialty section:
This article was submitted to Renal and Epithelial Physiology, a section of the journal Frontiers in Physiology

Received: 28 September 2021
Accepted: 15 December 2021
Published: 17 January 2022

Citation:
Frame AA, Nist KM, Kim K, Kuwabara JT and Wainford RD (2022) Natriuresis During an Acute Intravenous Sodium Chloride Infusion in Conscious Sprague Dawley Rats Is Mediated by a Blood Pressure-Independent α_1-Adrenoceptor-Mediated Mechanism. Front. Physiol. 12:784957. doi: 10.3389/fphys.2021.784957

The mechanisms that sense alterations in total body sodium content to facilitate sodium homeostasis in response to an acute sodium challenge that does not increase blood pressure have not been fully elucidated. We hypothesized that the renal sympathetic nerves are critical to mediate natriuresis via α_1- or β-adrenoceptors signal transduction pathways to maintain sodium balance in the face of acute increases in total body sodium content that do not activate the pressure-natriuresis mechanism. To address this hypothesis, we used acute bilateral renal denervation (RDNX), an anteroventral third ventricle (AV3V) lesion and α_1- or β-antagonism during an acute 1M NaCl sodium challenge in conscious male Sprague Dawley rats. An acute 1M NaCl infusion did not alter blood pressure and evoked profound natriuresis and sympathoinhibition. Acute bilateral RDNX attenuated the natriuretic and sympathoinhibitory responses evoked by a 1M NaCl infusion [peak natriuresis (μeq/min) sham 14.5 ± 1.3 vs. acute RDNX: 9.2 ± 1.4, $p < 0.05$; plasma NE (nmol/L) sham control: 44 ± 4 vs. sham 1M NaCl infusion 11 ± 2, $p < 0.05$; acute RDNX control: 42 ± 6 vs. acute RDNX 1M NaCl infusion 25 ± 3, $p < 0.05$]. In contrast, an AV3V lesion did not impact the cardiovascular, renal excretory or sympathoinhibitory responses to an acute 1M NaCl infusion. Acute i.v. α_1-adrenoceptor antagonism with terazosin evoked a significant drop in baseline blood pressure and significantly attenuated the natriuretic response to a 1M NaCl load [peak natriuresis (μeq/min) saline 17.2 ± 1.4 vs. i.v. terazosin 7.8 ± 2.5, $p < 0.05$]. In contrast, acute β-adrenoceptor antagonism with i.v. propranolol infusion did not impact the cardiovascular or renal excretory responses to an acute 1M NaCl infusion. Critically, the natriuretic response to an acute 1M NaCl infusion was significantly blunted in rats receiving a s.c. infusion of the α_1-adrenoceptor antagonist terazosin at a dose that did

not lower baseline blood pressure [peak natriuresis (μeq/min) sc saline: 18 ± 1 vs. sc terazosin 7 ± 2, $p < 0.05$]. Additionally, a s.c. infusion of the α_1-adrenoceptor antagonist terazosin further attenuated the natriuretic response to a 1M NaCl infusion in acutely RDNX animals. Collectively these data indicate a specific role of a blood pressure-independent renal sympathetic nerve-dependent α_1-adrenoceptor-mediated pathway in the natriuretic and sympathoinhibitory responses evoked by acute increases in total body sodium.

Keywords: natriuresis, renal sympathetic nerves, adrenoceptors, sodium homeostasis, pressure-natriuresis

INTRODUCTION

Maintenance of fluid and electrolyte homeostasis, which is essential for life, is dependent on neural, humoral, and hemodynamic mechanisms that alter renal sodium excretion in response to changes in total body sodium. Based on the classical model of "pressure-natriuresis," it has been hypothesized that increases in total body sodium always evoke elevations in fluid volume and arterial blood pressure that raise renal perfusion pressure, ultimately initiating natriuresis and a return to sodium homeostasis (Guyton, 1991). However, recent studies performed in human subjects and animal models, suggest that increased renal sodium excretion, natriuresis, can occur in the absence of detectable changes in arterial blood pressure in response to mild salt loading (Kompanowska-Jezierska et al., 2008; Bie, 2009; Wainford et al., 2013). Although the integrated mechanisms that facilitate sodium homeostasis independently of activation of the pressure-natriuresis mechanism are poorly understood it has been suggested that suppression of the renin-angiotensin system and renal sympathetic nerve activity are critical to facilitate the natriuretic responses activated to maintain sodium balance (DiBona and Kopp, 1997; Manunta et al., 2011; Wainford et al., 2013). The renal sympathetic nerves directly regulate renal sodium handling through several mechanisms, including activation of renal β_1-adrenergic receptors, resulting in renin release, and stimulation of renal α_1-adrenergic receptors, resulting in sodium reabsorption (Persson et al., 1989; DiBona and Kopp, 1997). However, the mechanisms by which the renal sympathetic nerves influence the acute natriuretic response to increases in total body sodium in the absence of detectable changes in arterial blood pressure have not been fully elucidated.

Our laboratory has delineated a sympathoinhibitory renal sympathetic nerve-dependent pathway that facilitates sodium homeostasis independently of the renin-angiotensin-aldosterone system in response to an acute isovolumetric NaCl challenge that does not increase arterial blood pressure in conscious male Sprague Dawley rats (Wainford et al., 2013). In our prior study using this approach, we did not assess the role of the anteroventral third ventricle (AV3V) region which contains osmo- and sodium-sensitive neurons and can modulate sympathetic outflow (Toney et al., 2003; Stocker et al., 2010, 2013b) or the direct role of α_1- or β-adrenoceptors in the observed acute natriuretic response. In the present study, we hypothesized that a renal sympathetic nerve-dependent α_1- or β-adrenoceptor-mediated pathway regulates the acute natriuretic response to increases in total body Nacl independently of the pressure-natriuresis mechanism. To address this hypothesis, we: (1) examined the role of the AV3V region and the renal sympathetic nerves in acute NaCl-evoked natriuresis that occurs independent of detectable increases in blood pressure and activation of the pressure-natriuresis mechanism and (2) administered an acute sodium challenge during pharmacological α_1- and β-adrenoceptor antagonism.

MATERIALS AND METHODS

Ethical Approval

All animal protocols were approved by the Institutional Animal Care and Use Committee (IACUC) in accordance with the guidelines of Boston University School of Medicine and the National Institutes of Health *Guide for the Care and Use of Laboratory Animals* under IACUC protocol number PROTO201800201. As detailed in our surgical procedures, all steps possible were taken to minimize pain and suffering. Additionally, all animal studies detailed in this manuscript fully comply with the ethical principles of Frontiers in Physiology.

Animals

Male Sprague Dawley rats aged 3-month-old, weighing 275–299 g, were purchased from Envigo (Indianapolis, Indiana, United States) for use in these studies. Prior to surgical intervention animals were pair-housed and were then housed individually post-surgery. Animals were housed in the Laboratory Animal Science Center at Boston University under a 12 h:12 h light:dark cycle under temperature (20–26°C) and humidity (30–70%) controlled conditions. Animals were provided tap water and standard irradiated rodent diet *ad libitum* [Envigo Teklad, WI, Teklad Global Diet #2918: 18% protein, 5% crude fat, 5% fiber, 0.6% K^+ content, with a total NaCl content of 0.6% (174 mEquiv Na^+ kg)]. All rats were randomly assigned to experimental groups.

Surgical Procedures

Acute Femoral Vein, Femoral Artery, and Bladder Cannulation

On the day of the acute study, rats were anesthetized with sodium methohexital (20 mg kg^{-1} I.P., supplemented with 10mg kg^{-1} I.V. as required during surgery) (Wainford et al., 2013; Carmichael et al., 2016; Walsh et al., 2016). Prior to a surgical

incision the area was injected with bupivacaine (2 mg/kg s.c.). Following the induction of anesthesia, the depth of anesthesia was confirmed by lack of response to a toe pinch. During all surgical procedures the depth of anesthesia was monitored continually by assessment of absence of a toe pinch response, observation of respiration, observation of mucous membranes and observation of any reaction to a surgical manipulation. Rats were instrumented with catheters in the left femoral vein, left femoral artery, and bladder to allow I.V. administration of isotonic saline, acute sodium challenges, and adrenoceptor antagonists, measurement of mean arterial pressure (MAP) and heart rate (HR), and assessment of renal function, respectively (Kapusta et al., 2012; Wainford et al., 2013; Carmichael et al., 2016; Walsh et al., 2016). Rats were placed in a Plexiglass rat holder and an I.V. infusion of isotonic saline (20 μL min^{-1}) was maintained during a 2-h surgical recovery period, allowing rats to return to full consciousness and stable renal and cardiovascular function prior to experimentation. Placement of the surgically instrumented rat in a Plexiglass holder that facilities the collection of stable cardiovascular parameters and urine and allows the rat forward and backward movement and does not restrain the rat. This experimental approach increases the rigor and reproducibility of our studies as it parallels that conducted in multiple studies conducted in our laboratory, including our prior study utilizing 1M NaCl infusion (Wainford et al., 2013). Mean arterial pressure and HR were recorded continuously via the surgically implanted femoral artery cannula using computer-driven BIOPAC data acquisition software (MP150 and AcqKnowledge 3.8.2, CA) connected to an external pressure transducer (P23XL; Viggo Spectramed Inc., CA) (Wainford et al., 2013; Carmichael et al., 2016; Walsh et al., 2016; Moreira et al., 2019). The arterial cannula was flushed with small volumes of 0.9% NaCl following collection of arterial blood samples as described in the experimental protocols. Following completion of acute experimental studies, as described below, all animals were euthanized by I.V. injection of sodium thiopental (20 mg/kg) in accordance with stated IAUCUC approval. Death was confirmed via (1) absence of heart rate as assessed by BIOPAC software, and (2) opening of the chest cavity.

Intracerebroventricular Cannulation

Seven to 10 days before the day of the acute study, a subset of rats, some of whom had previously undergone an AV3V lesion, were anesthetized with ketamine (30mg kg^{-1} I.P.) in combination with xylazine (3mg kg^{-1} IP). The depth of anesthesia was confirmed as described above. A stainless steel cannula was stereotaxically implanted into the right lateral cerebral ventricle (Wainford and Kapusta, 2009; Wainford et al., 2013; Carmichael et al., 2016; Walsh et al., 2016). Rats were placed in their home cages and monitored during surgical recovery.

AV3V Lesion

Twenty-five days before the day of acute study, a subset of rats were anesthetized with ketamine (30mg kg^{-1} I.P.) in combination with xylazine (3mg kg^{-1} I.P.). The depth of anesthesia was confirmed as described above. An anodal electrolytic lesion (2.5 mA for 25 s) was stereotaxically delivered to the AV3V [stereotaxic coordinates: 0.3 mm posterior to bregma, on midline, 7.5 mm ventral to the midsagittal sinus (Simmonds et al., 2014)] using an insulated 23-g nichrome wire exposed only at the tip. In a separate sham group, the nichrome wire was inserted 4 mm into the brain for 25s but no lesion was delivered. Rats were placed in their home cages and monitored during surgical recovery and received s.c. buprenorphine (0.03mg/kg) for 48-h post-surgery. AV3V lesion was verified by postlesion adipsia assessed as fluid intake less than 5 mL during the first 24 h post-lesion (Callahan et al., 1988) and the absence of a pressor response to i.c.v. Ang II (200 ng) (Moreira et al., 2009; Vieira et al., 2013) was assessed post-1M NaCl infusion study in a subset of rats instrumented with an i.c.v. cannula. Adipsic rats were given 5% sucrose water *ad libitum* to encourage drinking and gradually weaned to normal water over 5-days prior to assignment to an experimental study group.

Acute Bilateral Renal Denervation

In a subset of rats immediately following cannulation of the femoral vein, femoral artery, and bladder bilateral acute bilateral renal denervation (RDNX) was performed using standard techniques prior to the surgical recovery period. In brief, anesthesia was maintained with sodium methohexital (10mg kg^{-1} I.V. as required) and each kidney was exposed via a dorsal flank incision. The renal vein and artery were dissected from the surrounding fascia and stripped of visible nerve bundles. The renal artery and any visible nerve fibers were coated with a 10% phenol solution in ethanol to destroy any remaining nerve fibers. In a separate sham group, a similar surgical procedure was performed but nerves bundles were not disrupted or treated with phenol (Kapusta et al., 2013; Wainford et al., 2013, 2015; Carmichael et al., 2020). Rats were allowed to recover as described above prior to experimentation. The efficacy of acute RDNX was confirmed at the end of the study via ELISA analysis of norepinephrine (NE) content in kidney tissue as per the manufacturer's instructions (IB89537, IBL America, Minneapolis, MN, United States).

Subcutaneous Osmotic Minipump Implantation

Rats were anesthetized using sodium brevital (20 mg/kg IP) and were randomly assigned to be surgically implanted with an osmotic minipump (2ML4, Alzet) subcutaneously in the subscapular region (Walsh et al., 2016; Frame et al., 2019b) delivering a continuous 21-day s.c. infusion (2.5 μL/h) of 50/50 isotonic saline/DMSO or terazosin hydrochloride [10mg/kg/day (Maranon et al., 2015; Frame et al., 2019b) Sigma] dissolved in 50/50 saline/DMSO (Frame et al., 2019b; Puleo et al., 2020).

Acute Experimental Protocols

I.V. 1M NaCl Infusion

Following a 2h surgical recovery period, groups of intact, sham RDNX, bilateral RDNX, sham AV3V lesion and AV3V lesion rats (N = 6/group) underwent an acute 1M NaCl infusion protocol. The 5-h protocol consists of a 1-h control period (isotonic saline, 20 μL min^{-1}, I.V.) followed by a 2-h 1M NaCl infusion (1M NaCl, 20 μL min^{-1}, I.V.) and a subsequent 2-h recovery period

(isotonic saline, 20 μL min^{-1}, I.V.) (Kompanowska-Jezierska et al., 2008; Wainford et al., 2013). Mean arterial pressure and HR were monitored continuously and urine was collected in consecutive 15-min increments throughout the protocol. Arterial blood samples were collected at the start of the final 15-min increment of the control, 1M NaCl infusion and recovery periods for the measurement of hematocrit, EBV, EPV, plasma norepinephrine and plasma Na^+ (Wainford et al., 2013). To allow for the assessment of glomerular filtration rate (GFR) and renal blood flow (RBF) during the 1M NaCl infusion, a separate group of intact rats were infused with inulin (300 mg kg^{-1} h^{-1}) and para-aminohippurate (PAH; 40 mg kg^{-1} h^{-1}) for a 90-min equilibration period during the 2h surgical recovery period and continuing throughout the 5-h study protocol described above. Urine was collected in consecutive 15-min increments and blood was collected in the middle of each half hour period during the study protocol.

I.V. 1M NaCl Infusion During Acute α_1- or β-Adrenoceptor Antagonism

Following surgical recovery, groups of rats underwent a 1-h control period (isotonic saline, 20μL min^{-1}, I.V.) after which an I.V. infusion of an α_1-adrenoceptor antagonist (terazosin, 4.17 μg kg^{-1} min^{-1}; intact, ADNX and RDNX rats) or β-adrenoceptor antagonist (propranolol, 6.94 μg kg^{-1} min^{-1}; intact rats only) (N = 6/group) was initiated at the same 20 μL min^{-1} rate and was maintained throughout the protocol for an additional 1-h blockade baseline period immediately prior to a 2-h 1M NaCl co-infusion (1M NaCl, 20 μL min^{-1}, I.V.) and a 2-h recovery period. Mean arterial pressure and HR were recorded continuously and urine was collected in consecutive 15-min increments throughout the protocol. Arterial blood samples were collected at the start of the final 15-min increment of the control, blockade baseline, 1M NaCl infusion, and recovery periods for the measurement of hematocrit, EPV, EBV and plasma Na^+. After completion of the protocol, phenylephrine (4 μg bolus, I.V.) and isoproterenol (0.7 μg bolus, I.V.) were administered to confirm selective adrenoceptor blockade (Veitenheimer et al., 2012).

I.V. 1M NaCl Infusion During Chronic s.c.α_1-Adrenoceptor Antagonism

Following surgical recovery, groups of rats that have received a 21-day s.c. osmotic minipump infusion of vehicle or terazosin, and groups of rats that underwent acute RDNX on the morning of the acute study underwent an I.V. 1M NaCl infusion study as described above. After completion of the protocol, phenylephrine (4 μg bolus, I.V.) and isoproterenol (0.7 μg bolus, I.V.) were administered to confirm selective adrenoceptor blockade (Veitenheimer et al., 2012).

Analytical Techniques

Pulsatile Arterial Pressure (PAP) was assessed using the Hemodynamic Analysis parameter for peak systolic and diastolic pressure events using AcqKnowledge 3.8.2 software. This analysis was conducted on the continuous arterial blood pressure signal recorded in the 20-min control baseline period in all studies. Signals that exhibited a strong noise characteristic, as defined by the Hemodynamic Analysis Parameter were excluded from analysis. Urine volume was assessed gravimetrically assuming 1 g = 1 mL. Urine and plasma sodium content were determined by flame photometry (IL-943; Instrumentation Laboratory, Bedford, MA, United States). Hematocrit (Hct) was determined using a micro-hematocrit centrifuge (Adams Readacrit, Clay Adams, NJ). Estimated plasma volume (EPV) was calculated using the following equation: EPV = [0.065 × body weight (kg)] × (1 – Hct). Plasma NE content was determined via ELISA (Immuno-Biological Laboratories, Minneapolis, MN; IB89552) following the manufacturer's instructions. Hct was used to calculate estimated plasma volume (EPV) and estimated blood volume (EBV) using the following equations; EPV = [0.065 × body weight (kg)] × (100 – Hct), EBV = (EPV × 100)/(100-Hct).

Statistical Analysis

All data are expressed as mean ± SEM. The normal (Gaussian) distribution of the data was assessed by a Kolmogorov-Smirnow test. The magnitude of change in cardiovascular and renal excretory parameters at different time points after initiation of a 1M NaCl sodium infusion was compared with the average group control value by a one-way repeated-measures analysis of variance (ANOVA) with subsequent Dunnett's test. Differences between treatment groups (e.g., sham RDNX vs. acute RDNX) were assessed by a two-way repeated measure ANOVA with treatment group being one fixed effect and time the other, with the interaction included. The time (minutes) was used as the repeated factor. *Post hoc* analysis was performed using Bonferroni's test. In all studies, statistical significance was defined as $P < 0.05$. All statistical analyses were performed using Graphpad (GraphPad Prism v.8 for Mac OS X, GraphPad Software, San Diego, CA, United States).

RESULTS

Effect of an AV3V Lesion on the Cardiovascular, Renal, and Sympathoinhibitory Responses to a Non-pressor 1M NaCl Infusion

An acute 2-h 1M NaCl infusion did not alter MAP or HR at any time point in naïve rats (**Figure 1**). In naïve rats, and all other treatment groups, we observed a PAP of approximately 30 mmHg (**Table 1**). In terms of renal function, a 1M NaCl infusion evoked a profound natriuretic and diuretic response without altering GFR or RBF (**Figure 1**). Further, in these same animals a 1M NaCl infusion evoked suppression of plasma NE (**Figure 1D**) but did not alter plasma sodium levels [Plasma Na^+ (mEq/L); 0.9% Saline Infusion: Control 139.6 ± 0.4, 0.9% saline infusion 140.1 ± 0.5, Recovery 139.9 ± 0.5; 1M NaCl Infusion: Control 139.2 ± 0.6, 1M NaCl infusion140.4 ± 0.4, Recovery 139.8 ± 0.4], EBV or EPV (**Figures 1B,C**). An AV3V lesion had no impact on baseline cardiovascular and renal parameters or the physiological effects elicited by a 1M NaCl infusion compared to those observed in sham AV3V lesioned rats (**Figure 2**). In both groups, sham and AV3V lesioned, a 1M NaCl infusion had no impact on MAP, HR, plasma sodium, EPV or EBV, and resulted in significant

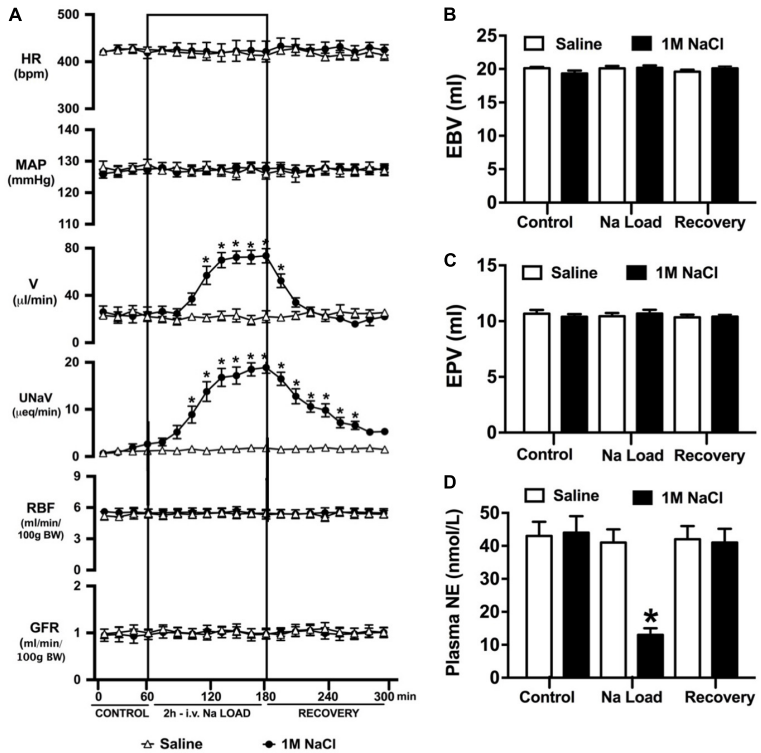

FIGURE 1 | Cardiovascular and renal responses to an acute 1M NaCl infusion **(A)** Cardiovascular and renal responses, **(B)** Estimated blood volume (ml), **(C)** Estimated plasma volume (ml), and **(D)** Plasma norepinephrine content (nmol/L) during a 1-h control isotonic saline infusion (20 μl/min), a 2-h 1M NaCl infusion (20 μl/min) and a 2-h recovery period of isotonic saline infusion (20 μl/min) in conscious male Sprague Dawley rats. HR = heart rate (bpm), MAP = mean arterial pressure (mmHg), V = urinary flow rate (μL/min), UNaV = urinary sodium excretion (μeq/min), GFR = glomerular filtration rate [ml/min/100g body weight (BW)], RPF = estimated renal plasma flow (ml/min/100 g BW). Data are presented as mean ± SEM, *N* = 6/group. *$p < 0.05$ vs. group baseline value in last 15-min of the control saline infusion.

diuresis, natriuresis and sympathoinhibition (**Figure 2**). AV3V lesions were confirmed by the observation of post-lesion adipsia in all animals [24h Fluid Intake post-lesion (ml); AV3V lesion 3.6 ± 0.7ml vs. Sham lesion 13.1 ± 0.6ml, $P < 0.05$, N = 8/group]. A subset of animals received an acute i.c.v. bolus injection of Ang II (200ng) following completion of the 1M NaCl infusion (*N* = 4/group). In sham animals we observed a significant pressor response to Ang II which was absent in all AV3V lesioned rats (**Figure 2E**).

Effect of Acute Renal Denervation on the Cardiovascular, Renal, and Sympathoinhibitory Responses to a Non-pressor 1M NaCl Infusion

An acute 2-h 1M NaCl infusion did not alter MAP or HR at any time point in sham RDNX rats (**Figure 3A**). In sham RDNX rats, in which the renal sympathetic nerves are intact, a 1M NaCl infusion evoked profound natriuresis and diuresis, reduced free water clearance and evoked suppression of plasma NE content (**Figures 3A,D**). Further, in these same sham RDNX animals a 1M NaCl infusion did not alter plasma sodium levels [Plasma Na^+ (mEq/L); 1M NaCl Infusion in Sham RDNX; Control 139.2 ± 0.6, 1M NaCl infusion 140.4 ± 0.4, Recovery 139.8 ± 0.4] or EBV and EPV (**Figures 3B,C**). In animals that underwent acute bilateral RDNX, similarly to naïve (**Figure 1**) and sham RDNX animals (**Figure 3**), a 1M NaCl infusion did not alter

TABLE 1 | Mean arterial pressure (MAP; mmHg), Systolic Blood Pressure (SBP; mmHg), Diastolic Blood Pressure (DBP, mmHg) and Pulsatile Arterial Pressure calculated as SBP – DBP (PAP; mmHg) assessed during the 20-min control baseline period in naïve, sham anteroventral third ventricle (AV3V) lesion, AV3V lesion, sham renal denervated (RDNX), acutely RDNX, i.v. terazosin, i.v. propranolol, s.c. saline, s.c. terazosin and s.c. terazosin + acutely RDNX male Sprague Dawley rats for which physiological data in presented in **Figures 1–7**.

	MAP (mmHg)	SBP (mmHg)	DBP (mmHg)	PAP (mmHg)
Naïve	127 ± 2	139 ± 4	109 ± 4	28 ± 3
Sham AV3V	128 ± 2	144 ± 4	111 ± 3	32 ± 3
AV3V lesion	126 ± 3	142 ± 4	116 ± 4	28 ± 3
Sham RDNX	129 ± 2	141 ± 3	110 ± 3	32 ± 2
RDNX	128 ± 2	141 ± 5	112 ± 4	29 ± 3
i.v. terazosin	126 ± 4	139 ± 6	112 ± 7	26 ± 4
i.v, propranolol	127 ± 6	139 ± 5	106 ± 7	28 ± 5
s.c. saline	124 ± 3	137 ± 5	107 ± 4	31 ± 4
s.c. terazosin	123 ± 4	134 ± 4	105 ± 3	28 ± 5
s.c terazosin + RDNX	124 ± 2	140 ± 3	113 ± 4	27 ± 3

Data are presented as mean ± SEM, N = 6/group with the exception of N = 8/group in sham AV3V and AV3V lesion groups.

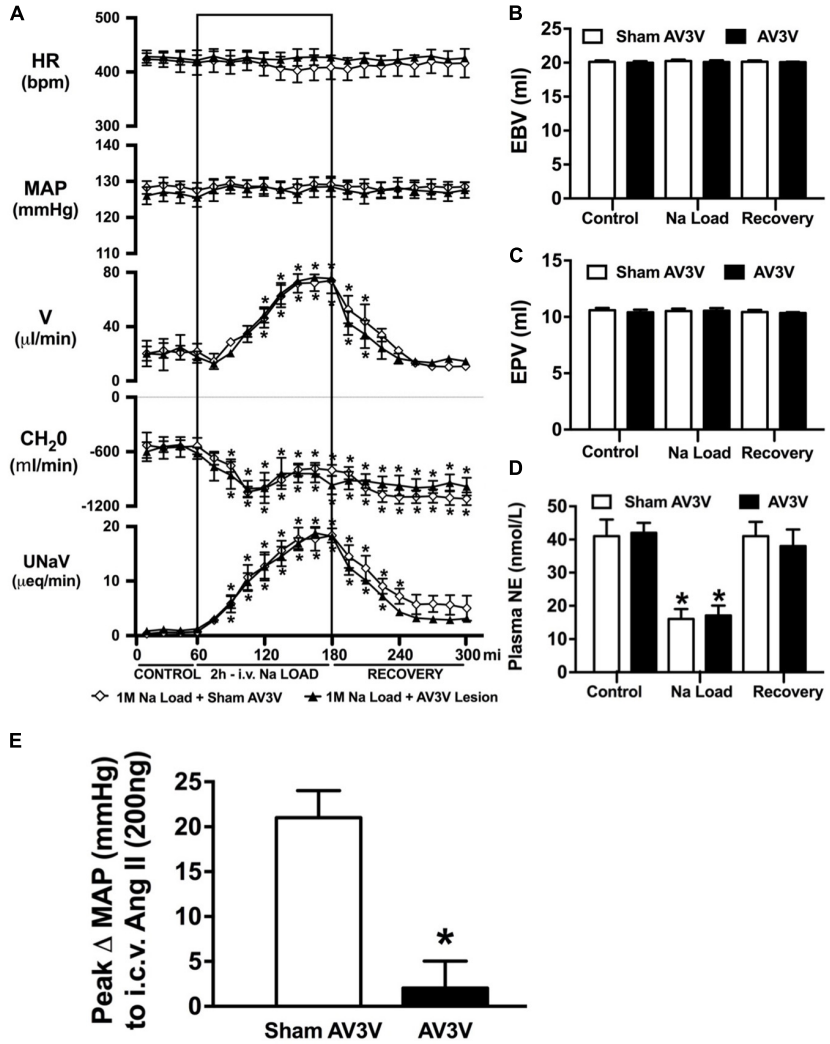

FIGURE 2 | Effect of an AV3V lesion on the cardiovascular and renal responses to an acute 1M NaCl infusion **(A)** Cardiovascular and renal responses, **(B)** Estimated blood volume (ml), **(C)** Estimated plasma volume (ml), and **(D)** Plasma norepinephrine content (nmol/L) during a 1-h control isotonic saline infusion (20 μl/min), a 2-h 1M NaCl infusion (20 μl/min) and a 2-h recovery period of isotonic saline infusion (20 μl/min) in sham or AV3V lesioned conscious male Sprague Dawley rats, and **(E)** peak Δ MAP following an i.c.v. bolus injection of Ang II (200 ng) *N* = 4/group for Ang II administration. HR = heart rate (bpm), MAP = mean arterial pressure (mmHg), V = urinary flow rate (μL/min), CH_2O = free water clearance, UNaV = urinary sodium excretion (μeq/min). Data are presented as mean ± SEM, *N* = 8/group except where indicated. *$p < 0.05$ vs. group baseline value in last 15-min of the control saline infusion.

cardiovascular parameters. Acute bilateral RDNX attenuated the natriuretic and diuretic responses to a 1M NaCl infusion [peak UNaV (μeq min^{-1}) sham 14.5 ± 1.3 versus. RDNX: 9.2 ± 1.4, $p < 0.05$; peak V (μL min^{-1}) sham: 62.6 ± 10.1 versus. RDNX: 38.8 ± 8.8, $p < 0.05$] and attenuated 1M NaCl-evoked suppression of plasma NE [plasma NE (nmol/L) Sham RDNX: control: 44 ± 4 versus. 1M NaCl infusion 11 ± 2, $p < 0.05$; RDNX: control: 42 ± 6 versus. 1M NaCl infusion 25 ± 3] (**Figure 3D**). Additionally, acute bilateral RDNX resulted in short term increases in EBV and EPV during the 1M NaCl infusion that returned to baseline during the recovery period (**Figures 3B,C**). However, acute RDNX did not impact plasma sodium levels [Plasma Na^+ (mEq/L); Control; Sham RDNX 139.6 ± 0.4 versus RDNX 140.1 ± 0.5, 1M NaCl infusion Sham RDNX 140.6 ± 0.5 versus RDNX 140.8 ± 0.5, Recovery Sham RDNX 139.9 ± 0.5 versus RDNX 140.3 ± 0.5]. The efficacy of acute bilateral RDNX was confirmed by assessment of renal norepinephrine content, in which renal NE content was reduced by approximately 90% in acutely denervated rats vs. sham RDNX animals (**Figure 3E**).

Effect of Acute α_1 vs. β-Adrenoceptor Antagonism on the Cardiovascular and Renal Responses to an Acute Non-pressor 1M NaCl Infusion

Acute α_1-adrenoceptor antagonism reduced baseline MAP by approximately 20 mmHg and increased HR by approximately 40 bpm (**Figure 4A**). In terms of renal parameters there was

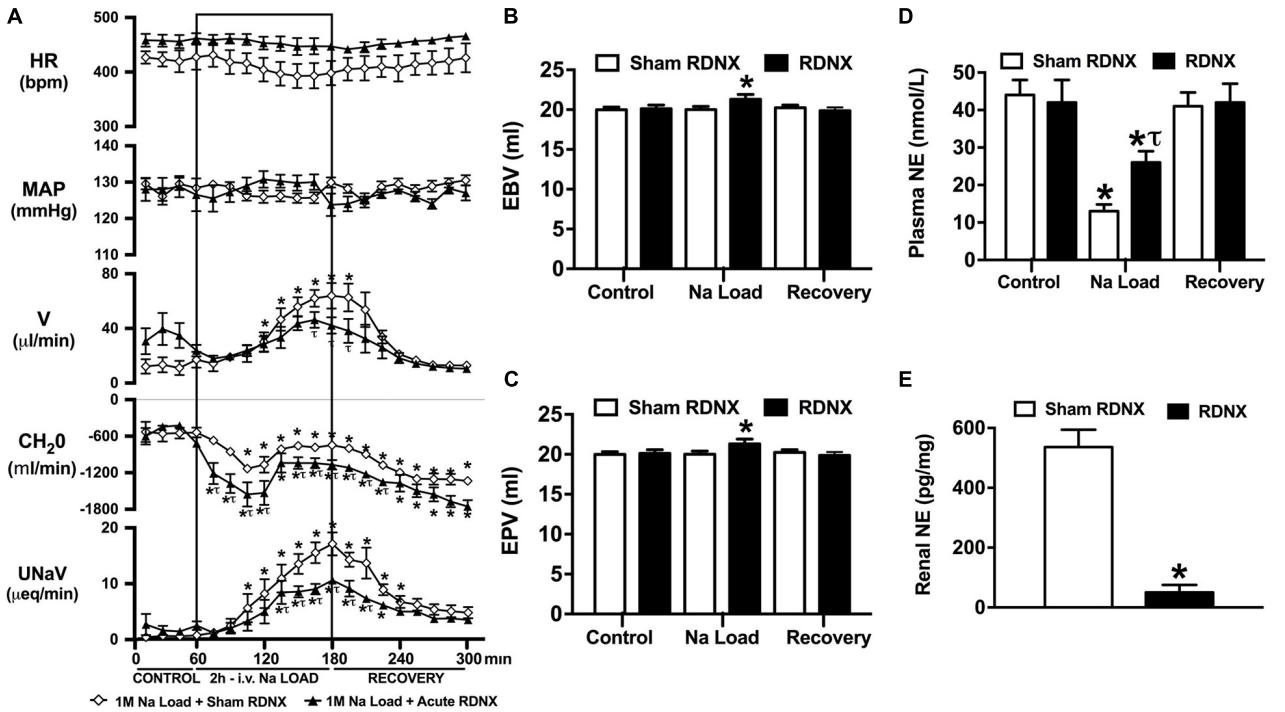

FIGURE 3 | Effect of acute renal denervation (RDNX) on the cardiovascular and renal responses to an acute 1M NaCl infusion **(A)** Cardiovascular and renal responses, **(B)** Estimated blood volume (ml), **(C)** Estimated plasma volume (ml), and **(D)** Plasma norepinephrine content (nmol/L) during a 1-h control isotonic saline infusion (20 µl/min), a 2-h 1M NaCl infusion (20 µl/min) and a 2-h recovery period of isotonic saline infusion (20 µl/min) in sham or acutely RDNX conscious male Sprague Dawley rats, **(E)** renal NE content (pg/mg). HR = heart rate (bpm), MAP = mean arterial pressure (mmHg), V = urinary flow rate (µL/min), CH_2O = free water clearance, UNaV = urinary sodium excretion (µeq/min). Data are presented as mean ± SEM, *N* = 6/group. **p* < 0.05 vs. group baseline value in last 15-min of the control saline infusion. τ*p* < 0.05 vs. respective sham RDNX group value.

a suppression of diuresis, free water clearance, with non-statistically significant reduction in natriuresis during acute α_1-adrenoceptor antagonism. In contrast, acute β-adrenoceptor antagonism had no effect on MAP or renal excretory parameters and reduced baseline HR approximately 100 bpm (**Figure 5A**). During α_1-adrenoceptor antagonism we observed no change in cardiovascular parameters but profound attenuation of the natriuretic and diuretic responses to a 1M NaCl infusion (**Figure 4A**). Further, α_1-adrenoceptor antagonism resulted in an increase in EBV and EPV during the 1M NaCl infusion and recovery periods (**Figures 4B,C**) – an increase not observed in naïve 1M NaCl treated animals. As observed following acute RDNX we did not see any alteration in plasma sodium content during 1M NaCl infusion [Plasma Na^+ (mEq/L); Control 140.2 ± 0.5, 1M NaCl infusion140.8 ± 0.6, Recovery 140.7 ± 0.6]. In contrast to profound renal effects observed of α_1 blockade during a 1M NaCl infusion acute β-adrenoceptor antagonism had no effect on the natriuretic and diuretic responses to 1M NaCl infusion, and did not alter EPV (**Figure 5**). Confirming the selectivity and efficacy adrenoceptor antagonism (1) the average MAP response to an IV bolus of the α_1-agonist phenylephrine was 22 ± 3 mmHg in propranolol treated rats vs. 2 ± 3 mmHg in terazosin treated rats, and (2) the average HR response to the β1-agonsit isoproterenol was 16 ± 7 bpm in propranolol treated rats vs. 95 ± 14 bpm in terazosin treated rats.

Effect of Chronic α_1-Adrenoceptor Antagonism on the Cardiovascular and Renal Responses to an Acute Non-pressor 1M NaCl Infusion

Chronic α_1-adrenoceptor antagonism, via s.c. osmotic minipump infusion, replicating our prior data in young normotensive Sprague Dawley rats, had no impact on baseline cardiovascular or renal parameters (**Figure 6A**). As observed during acute i.v. antagonism of α_1-adrenoceptors (**Figure 5**) during s.c. α_1-adrenoceptor antagonism we observed no change in cardiovascular parameters during a 1M NaCl infusion. Further, s.c. α_1-adrenoceptor antagonism resulted in significant attenuation of the natriuretic and diuretic responses to a 1M NaCl infusion (**Figure 6A**) and increased both EBV and EPV during the 1M NaCl infusion and recovery periods (**Figures 6B,C**). A 1M NaCl infusion did not alter plasma sodium in animals receiving a s.c. terazosin infusion [Plasma Na^+ (mEq/L); Control 140.1 ± 0.3, 1M NaCl infusion 140.3 ± 0.4, Recovery 140.3 ± 0.5]. Acute RDNX (confirmed by reduced renal NE content) immediately prior to the 1M NaCl load had no significant effect impact on the physiological responses observed during α_1-adrenoceptor antagonism (**Figure 7**). Confirming the selectivity and efficacy adrenoceptor antagonism in intact and RDNX rats (1) the average MAP response to an IV bolus of

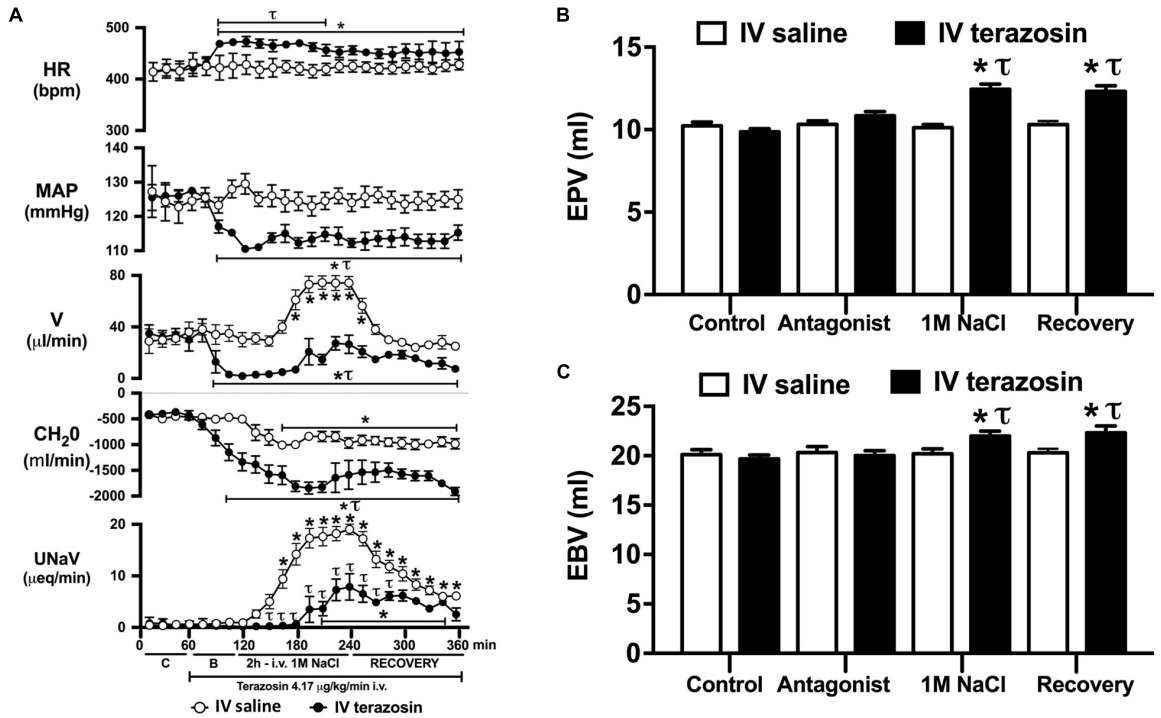

FIGURE 4 | Effect of acute i.v. terazosin-mediated α_1-drenoceptor antagonism on the cardiovascular and renal responses to an acute 1M NaCl infusion **(A)** Cardiovascular and renal responses, **(B)** Estimated blood volume (ml), and **(C)** Estimated plasma volume (ml) during a 1-h control isotonic saline infusion (20 μl/min), a 1-h baseline terazosin infusion (4.17 μg kg^{-1} min^{-1} in isotonic saline; 20 μl/min), a 2-h terazosin and 1M NaCl infusion (20 μl/min) and a 2-h recovery period of terazosin in isotonic saline infusion (20 μl/min) in intact conscious male Sprague Dawley rats, HR = heart rate (bpm), MAP = mean arterial pressure (mmHg), V = urinary flow rate (μL/min), CH_2O = free water clearance, UNaV = urinary sodium excretion (μeq/min), C = control saline infusion, B = Baseline during terazosin infusion. Data are presented as mean ± SEM, N = 6/group. *$p < 0.05$ vs. group baseline value in last 15-min of the control saline infusion. τ$p < 0.05$ vs. respective isotonic saline group infusion value.

the α_1-agonist phenylephrine was 24 ± 4 mmHg in s.c. vehicle infused rats (N = 6) vs. 1 ± 2 mmHg in s.c. terazosin infused rats (N = 12), and (2) the average HR response to the β1-agonsit isoproterenol was 98 ± 10 bpm in s.c. vehicle infused rats (N = 6) rats vs. 93 ± 12 bpm in s.c. terazosin infused rats.

DISCUSSION

The current studies were designed to delineate the role(s) of the renal sympathetic nerves and circumventricular organs, and α_1- and β-adrenoceptors in the natriuretic responses evoked by an acute change in total body sodium content. Extending our prior studies, we demonstrate a central role of the renal sympathetic nerves, but not circumventricular organs, in mediating the natriuretic response to an acute 1M NaCl infusion that does not increase blood pressure in conscious Sprague Dawley rats (Wainford et al., 2013). Further, in this experimental paradigm in which 1M NaCl does not increase blood pressure, we demonstrate via acute antagonism that α 1-, but not β-adrenoceptors, are essential to mediate the natriuretic response and to maintain fluid balance. To address the potential confounding effect of acute α_1-adrenoceptor antagonism evoking a drop in blood pressure we validated the role of α_1-adrenoceptors on the natriuretic response to a 1M NaCl infusion in animals in which α_1-adrenoceptors were chronically antagonized independent of a reduction in blood pressure. These data demonstrate a pivotal role of the renal sympathetic nerves and α_1-adrenoceptors in the acute natriuretic responses triggered by increased total body sodium.

It is well established that multiple sites within the body detect alterations in plasma sodium and osmolality via osmo/sodium receptors to trigger natriuretic responses – including the sensory afferent renal sympathetic nerves and the circumventricular organs (Stocker et al., 2013a; Johns, 2014; Kopp, 2015). To investigate the potential role(s) of the renal sympathetic nerves and the circumventricular organs in the acute natriuretic response to increased total body sodium content we utilized a 1M NaCl infusion (Wainford et al., 2013). A 2-h 1M NaCl infusion in conscious male Sprague Dawley rats evoked profound natriuresis, diuresis and sympathoinhibition without altering mean arterial blood pressure, plasma volume, renal blood flow, glomerular filtration rate or plasma sodium levels. These data are consistent with the effects of this acute sodium challenge paradigm in conscious and anesthetized rats as previously reported by several laboratories, including our own (Roson et al., 2006, 2010; Kompanowska-Jezierska et al., 2008; Wainford et al., 2013). Based on the absence of detectable alterations in renal hemodynamics or arterial blood pressure, we conclude that the

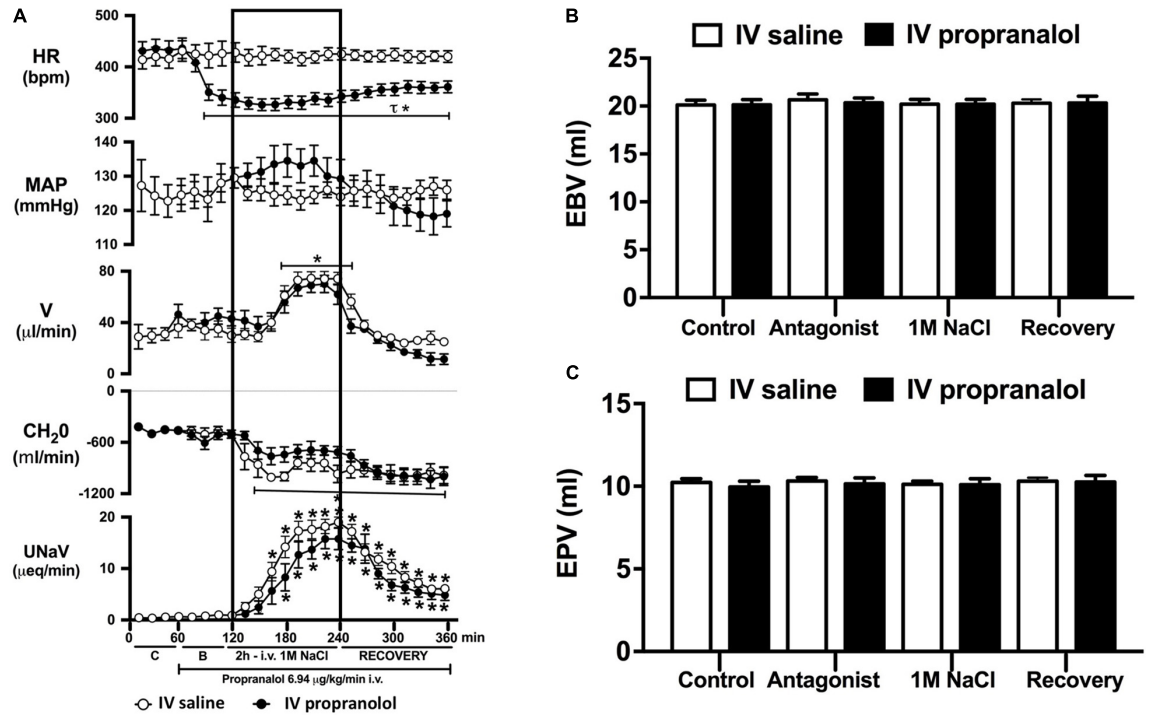

FIGURE 5 | Effect of acute i.v. propranolol-mediated β-adrenoceptor antagonism on the cardiovascular and renal responses to an acute 1M NaCl infusion **(A)** Cardiovascular and renal responses, **(B)** Estimated blood volume (ml), and **(C)** Estimated plasma volume (ml) during a 1-h control isotonic saline infusion (20 μl/min), a 1-h baseline propranolol infusion (6.94 μg kg^{-1} min^{-1} in isotonic saline; 20 μl/min), a 2-h propranolol and 1M NaCl infusion (20 μl/min) and a 2-h recovery period of propranolol in isotonic saline infusion (20 μl/min) in intact conscious male Sprague Dawley rats. HR = heart rate (bpm), MAP = mean arterial pressure (mmHg), V = urinary flow rate (μL/min), CH_2O = free water clearance, UNaV = urinary sodium excretion (μeq/min). Data are presented as mean ± SEM, N = 6/group. *$p < 0.05$ vs. group baseline value in last 15-min of the control saline infusion. τ$p < 0.05$ vs. respective isotonic saline group infusion value. Please note the same isotonic saline group data is presented in **Figures 4**, **5** for clarity.

observed sympathoinhibitory and natriuretic responses evoked by a 1M NaCl infusion occur independent of activation of the pressure-natriuresis mechanism. As such, this experimental paradigm enables the study of the control of renal excretion in response to a 1M NaCl infusion in a conscious rat independent of changes in arterial blood pressure – as occurs physiologically except in the setting of excessive intake of salt. We acknowledge that a limitation of this experimental paradigm, utilized in all studies in this manuscript, is that basal blood pressure is elevated due to surgical stress and placement in a plexiglass holder to permit the simultaneous collection of cardiovascular and renal excretory parameters. There is the potential that this mildly elevated basal blood pressure may have prevented the detection of a 1M NaCl infusion evoked alteration in blood pressure. However, it should be noted that is experimental paradigm has been widely used by our laboratory and in several prior studies, in animals with similar baseline blood pressures, we have observed alterations in blood pressure in response to physiological and pharmacological stimuli, including an IV 3M NaCl bolus administration (Carmichael et al., 2016) – which strongly suggests that our observation of no change in blood pressure during a 1M NaCl infusion is valid and not dependent on the mild elevation in baseline blood pressure. Further, our observation of a PAP of approximately 30 mmHg in all experimental groups is in accordance with the PAP reported in normotensive rat strains and is not indicative of hypertensive level of PAP such as is observed hypertensive rats, e.g., the spontaneously hypertensive rat (Safar and Laurent, 2003; Letson et al., 2019).

In our prior study utilizing this experimental paradigm we reported that chronic bilateral RDNX, in which the renal sympathetic nerves were removed 10–14 days prior to study, had no impact on the natriuretic or sympathoinhibitory responses evoked by a 1M NaCl infusion (Wainford et al., 2013). However, multiple renal sympathetic nerve-independent mechanisms become activated to facilitate the restoration of fluid and electrolyte balance following RDNX (DiBona and Sawin, 1983), potentially masking a direct role of the renal sympathetic nerves in our prior study. To directly assess the impact of the renal sympathetic nerves on the physiological responses to a 1M NaCl load in the absence of compensatory mechanisms, we conducted acute bilateral RDNX immediately prior to the acute experimental protocol. Given the short time frame between removal of the renal nerves and the administration of the 1M NaCl sodium infusion, approximately 3 h, we believe this approach avoids the confounding effects of non-renal nerve-mediated compensatory homeostatic mechanisms that take several days to restore sodium

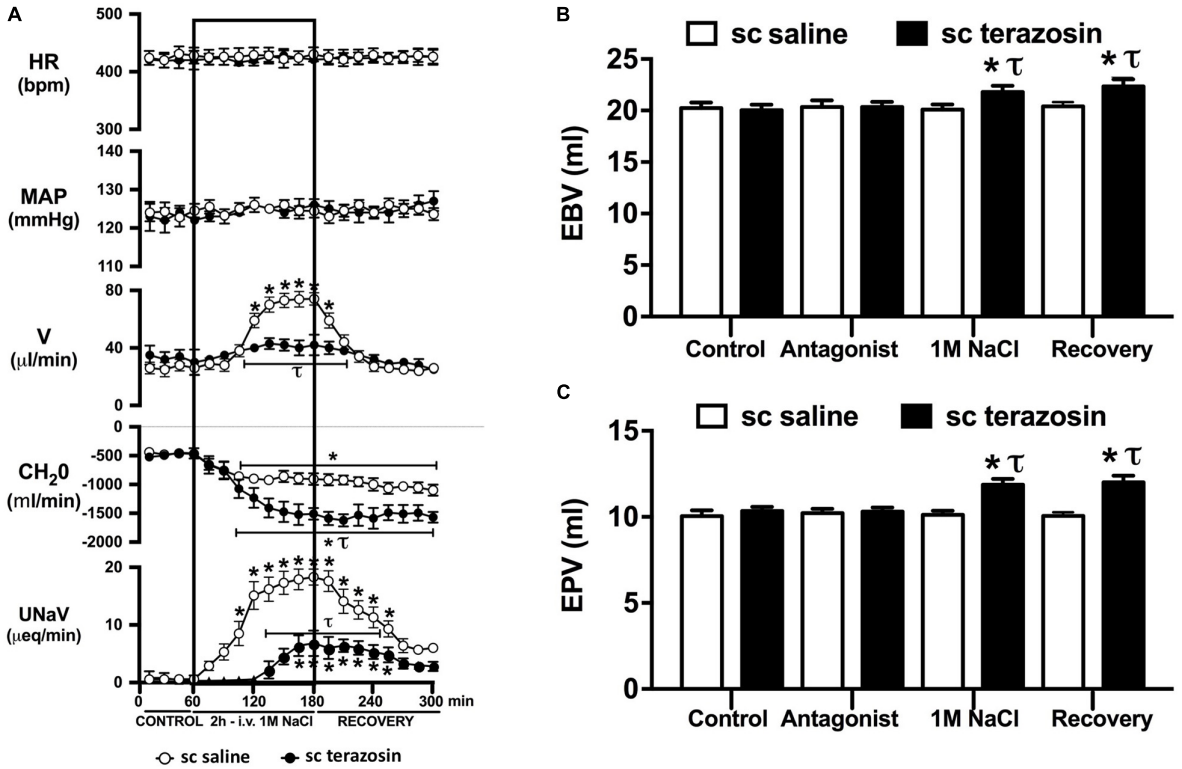

FIGURE 6 | Effect of chronic s.c. terazosin-mediated α_1-adrenoceptor antagonism on the cardiovascular and renal responses to an acute 1M NaCl infusion **(A)** Cardiovascular and renal responses, **(B)** Estimated blood volume (ml), and **(C)** Estimated plasma volume (ml) during a 1-h control isotonic saline infusion (20 μl/min), a 2-h 1M NaCl infusion (20 μl/min) and a 2-h recovery period of isotonic saline infusion (20 μl/min) in intact conscious male Sprague Dawley rats receiving a s.c. saline/DMSO vehicle or s.c. terazosin (10 mg/kg/day) infusion. HR = heart rate (bpm), MAP = mean arterial pressure (mmHg), V = urinary flow rate (μL/min), CH_2O = free water clearance, UNaV = urinary sodium excretion (μeq/min). Data are presented as mean ± SEM, *N* = 6/group. $^*p < 0.05$ vs. group baseline value in last 15-min of the control saline infusion. $\tau p < 0.05$ vs. respective sc saline/DMOS group infusion value.

and water balance (DiBona and Sawin, 1983). The efficacy of acute RNDX was confirmed by a significant reduction in renal norepinephrine content.

In accordance with our prior observations in Sprague Dawley rats that had intact renal sympathetic nerves or underwent chronic RDNX (Wainford et al., 2013), acute RDNX had no impact on baseline cardiovascular and renal parameters or baseline levels of circulating plasma NE. Further, we observed that following acute RDNX a 1M NaCl infusion did not alter blood pressure, heart rate or plasma sodium content. In these animals acute RDNX moderately blunted the diuresis, profoundly attenuated the natriuresis (peak natriuresis reduced approximately 50%) and attenuated the sympathoinhibitory response elicited by a 1M NaCl infusion. The absence of changes in heart rate or blood pressure during 1M NaCl infusion in intact or RDNX rats suggest that the observed alterations in circulating plasma NE do not reflect functional changes in sympathetic outflow to the heart or vasculature. Our observation of an attenuated natriuretic response, accompanied by increased estimated blood and plasma volume during an 1M NaCl infusion in acute RDNX rats, supports our hypothesis that the renal sympathetic nerves mediate a sympathoinhibitory pathway that modulates renal sodium excretion independently of the pressure-natriuresis mechanism. Based on our prior finding that selective ablation of the afferent renal nerves does not impact the physiological responses to a 1M NaCl infusion (Frame et al., 2019a) we speculate the observed sympathoinhibitory pathway is not mediated by the sympathoinhibitory afferent renal nerve mediated reno-renal reflex. Further, our finding that verified AV3V lesions, in which the osmo/sodium sensitive neurons of the circumventricular organs are ablated, have no impact on the natriuretic or sympathoinhibitory responses to a 2-h 1M NaCl infusion suggests afferent projections from osmosenstive forebrain structures (e.g., subfornical organ) do not mediate the observed responses during acute increases in total body NaCl. We acknowledge that the potential impact of the AV3V on ANP release (Antunes-Rodrigues et al., 1992) during a 1M NaCl infusion was not examined in these studies. However, given that an AV3V lesion did not impact the observed physiological responses to a 1M NaCl infusion we speculate that AV3V mediated release of ANP does not play a major role in this setting. It is possible that paraventricular nucleus (PVN)-specific sodium sensitive pathways (Frithiof et al., 2009) including the intrinsic osmosensitive magnocellular neurons that are present in the PVN and supraoptic nucleus (Prager-Khoutorsky and Bourque, 2015) or peripheral sodium sensitive mechanisms

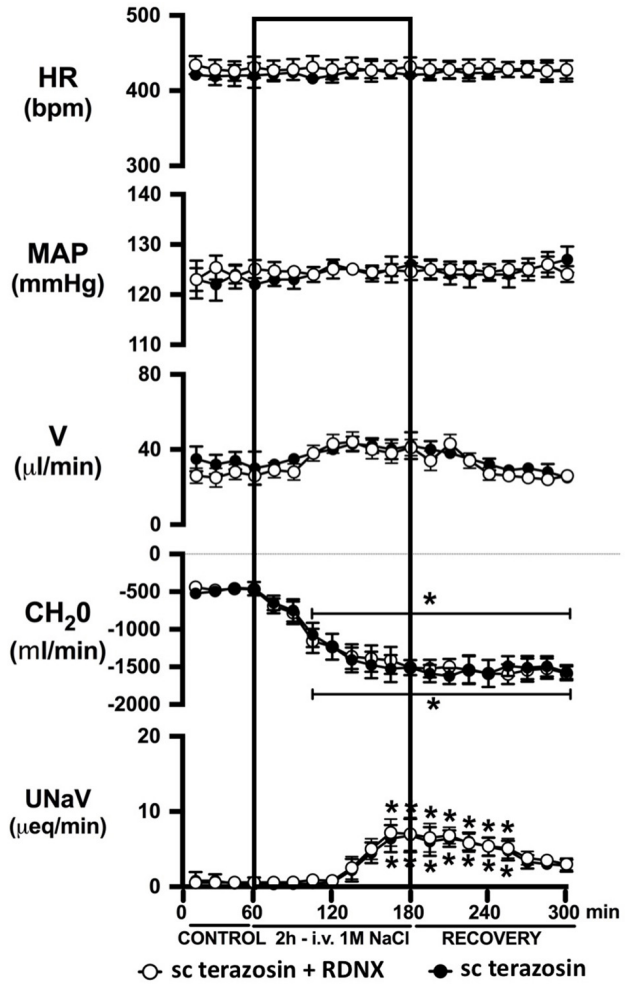

FIGURE 7 | Effect of acute RDNX in combination with chronic s.c. terazosin-mediated 1-adrenoceptor antagonism on the cardiovascular and renal responses to an acute 1M NaCl infusion Cardiovascular and renal responses during a 1-h control isotonic saline infusion (20 µl/min), a 2-h 1M NaCl infusion (20 µl/min) and a 2-h recovery period of isotonic saline infusion (20 µl/min) in intact or acutely RDNX conscious male Sprague Dawley rats receiving a sc terazosin (10 mg/kg/day) infusion. HR = heart rate (bpm), MAP = mean arterial pressure (mmHg), V = urinary flow rate (µL/min), CH_2O = free water clearance, UNaV = urinary sodium excretion (µeq/min). Data are presented as mean ± SEM, N = 6/group. *$p < 0.05$ vs. group baseline value in last 15-min of the control saline infusion. Please note the sc terazosin data in intact animals is transposed from **Figure 6** for clarity.

[e.g., hepato-portal sodium response (Morita et al., 1997)] may contribute to the observed sympathoinhibitory responses to the 1M NaCl infusion. Additionally, we acknowledge that the neurohypophysial secretion of oxytocin and vasopressin plays a central role in fluid and electrolyte homeostasis (Mecawi Ade et al., 2015), and was not addressed in the current studies due to the confounding impact of collecting sufficient repeated blood volumes to assess circulating levels of oxytocin and vasopressin during a 1M NaCl infusion and may be investigated in future studies.

Given that our data demonstrate a central role of the renal sympathetic nerves in the natriuretic response to an acute 1M NaCl infusion we next investigated the potential signaling pathways through which this may be occurring. It is well established that the renal sympathetic nerves influence renal sodium excretion via two predominant mechanisms: norepinephrine-mediated stimulation of renal α_1-adrenoceptors, evoking sodium reabsorption, or renal β1-adenoceptors, stimulating renin release (DiBona and Kopp, 1997). As such, we elected to investigate the impact of acute systemic α_1- and β-adrenoceptor antagonism during an acute 1M NaCl load. A 1-h infusion of the α_1-adrenoceptor antagonist terazosin, prior to administration of a 1M NaCl load, resulted in a reduction in arterial blood pressure (likely mediated by antagonism of vascular α_1-adrenoceptors) and an increase in heart rate. Further, α_1-adrenoceptor antagonism suppressed baseline diuresis and free water. Similar to our observations in in naïve and RDNX rats, a 1M NaCl did not impact cardiovascular parameters in rats receiving an α_1-adrenoceptor antagonist infusion. Significantly, α_1-adrenoceptor antagonism dramatically attenuated the natriuretic and diuretic responses to a 2-h 1M NaCl infusion – suppressing peak natriuresis to a similar magnitude as observed following acute RDNX. Also consistent with the impact of acute bilateral RDNX, α_1-adrenoceptor antagonism resulted in an increase in estimated plasma volume without altering plasma sodium content during the 1M NaCl infusion. In contrast to our findings in RDNX rats, plasma volume remained elevated throughout the recovery period in rats receiving an α_1-adrenoceptor antagonist infusion. This difference may reflect the continuous administration of an exogenous α_1-adrenoceptor antagonist during the recovery period versus a temporary endogenous response evoked by the 2 h 1M NaCl infusion that was reversed during the recovery period in acutely RDNX animals. Despite the profoundly attenuated natriuretic response observed in animals receiving the α_1-adrenoceptor antagonist infusion, we observed no increase in plasma sodium content. A possible explanation for this is the significantly greater decrease in free water clearance and increase in estimated plasma volume observed during sodium infusion compared with naïve rats, as these observations are consistent with enhanced renal water retention to maintain stable plasma sodium levels.

As noted, in our conscious rat model, acute α_1-adrenoceptor antagonism evokes a reduction in baseline blood pressure prior to administration of a 1M NaCl infusion. We acknowledge it is possible that this alteration in blood pressure influenced the observed attenuated natriuretic response. This may have occurred by alterations in renal medullary blood flow, which was not assessed in these studies, and may occur despite no detectable changes in renal blood flow in response to the 1M NaCl load. To address the potential confounding impact of the observed significant drop in blood pressure during acute α_1-adrenoceptor antagonism experimentally, we investigated the effects of α_1-adrenoceptor antagonism via s.c. terazosin infusion at a dose we have previously published does not impact blood pressure (Frame et al., 2019b; Puleo et al., 2020). Matching our data prior data (Frame et al., 2019b; Puleo et al., 2020), s.c. infusion of terazosin had no impact on baseline blood pressure

and fully and selectively antagonized the response to an α_1 agonist. Consistent with our data in rats that underwent an acute terazosin infusion we observed was no change in cardiovascular parameters but a profound attention of the natriuretic response to a 1M NaCl load that was accompanied by increased blood and plasma volume. Notably renal denervation did alter the impact of α_1-adrenoceptor antagonism on attenuating the natriuresis to a 1M NaCl load. Collectively, these data suggest a blood pressure-independent role for α_1-adrenoceptors in the natriuretic response to an acute increase in total body NaCl.

To assess the potential role of β-adrenoceptors in the natriuretic pathways activated during acute increases in total body sodium, conscious rats were administered an infusion of the β-adrenoceptor antagonist propranolol. Reflecting the established effect of β1-adrenoceptors in the heart, β-adrenoceptor antagonism resulted in a reduction in baseline heart rate, but had no effect on blood pressure or renal excretory parameters. In rats receiving a β-adrenoceptor antagonist infusion a 1M NaCl-infusion which did not alter cardiovascular parameters, we observed preservation of the profound natriuretic and diuretic responses observed in naïve rats and estimated blood and plasma volumes remained constant during the experimental protocol. Our current findings of a lack of role of β-adrenoceptors in the acute natriuretic responses to non-pressor 1M NaCl infusion are supported by studies in conscious dogs and humans indicating that the natriuretic response to a NaCl load that does not alter blood pressure remains intact during β1-adrenoceptor antagonism (Bie et al., 2009; Molstrom et al., 2009). Together, these data strengthen our hypothesis that there is a pivotal role for renal sympathetic nerve activated α_1-adrenoceptors in mediating the natriuresis during an acute challenge to total body NaCl homeostasis.

In light of the established mechanism whereby suppression of renal sympathetic outflow increases renal sodium excretion via reduced norepinephrine-α_1-adrenoceptor-driven sodium reabsorption at the level of the kidney, our findings appear paradoxical. Studies to elucidate the mechanisms underlying the observed attenuation in natriuresis remain beyond the scope of the current manuscript. However, there are alternative extra-renal and renal actions of α_1-adrenoceptors that could drive the observed clear attenuated natriuretic responses following α_1-adrenoceptor antagonism. A potential extra-renal pathway through which α_1-adrenoceptor antagonism, or a sympathoinhibitory reno-renal reflex, may reduce natriuresis is via a decrease in α_1-adrenoceptor mediated release of atrial natriuretic peptide (Luchner and Schunkert, 2004). Despite the current and prior studies by our group illustrating that a 1M NaCl infusion reduces sympathetic outflow, there remains the possibility that NaCl, when first sensed by the body, trigger rapid, short term sympathoexcitation to the heart, resulting in α_1-adrenoceptor-mediated release of atrial natriuretic peptide and natriuresis. An alternative hypothesis involves the renal nerves, as acute bilateral renal denervation attenuated natriuresis to approximately the same magnitude as that seen following acute pharmacological blockade of α_1-adrenoceptors during a 1M NaCl infusion and RDNX in combination with pharmacological blockade of α_1-adrenoceptors did not further impact the attenuation in natriuresis. These data support a role of the renal nerves in driving the natriuretic response to the infused 1M NaCl load. Additionally, it has been reported that renal pelvic α_1-adrenoceptors present on the renal sensory afferent fibers respond to pharmacological and physiological stimuli that include norepinephrine and increased efferent renal sympathetic nerve activity (Kopp et al., 2007). To directly test the role of renal sensory afferent α_1-adrenoceptors on the natriuretic responses to acute sodium, additional studies beyond the scope of this investigation in anesthetized rats in which α_1-adrenoceptor antagonists are administered by a renal pelvic infusion are required.

CONCLUSION

In conclusion, the present studies extend our knowledge of the renal sympathetic nerve mediated adrenoceptor-dependent signal transduction pathways that regulate natriuretic responses to acute increases in total body sodium in the absence of activation of the pressure-natriuresis mechanism. A key finding is that the α_1-adrenoceptor is the major receptor system involved in facilitating natriuresis to maintain fluid and electrolyte homeostasis in response to acute sodium challenges in which blood pressure remains stable. In contrast to the established roles of the renal sympathetic nerves on renal sodium handling via renal α_1-adrenoceptor-evoked sodium reabsorption and renal β1-adenoceptors-mediated renin release, our studies indicate that α_1-adrenoceptor activation is required for the acute renal sympathetic nerve-dependent natriuretic response to increases in total body NaCl. Given the proposed roles of α- and β-adrenoceptors on the chronic regulation of the sodium chloride cotransporter and long term sodium homeostasis (Mu et al., 2011; Terker et al., 2014; Frame et al., 2019b; Puleo et al., 2020) our findings suggest differential roles of the actions of the renal sympathetic nerves via α_1- and β-adrenoceptors during acute versus chronic challenges to sodium homeostasis, potentially via a sympathoinhibitory reno-renal reflex in the acute setting. These findings are physiologically relevant as increased understanding of the roles of the renal sympathetic nerve mediated mechanisms impacting the acute natriuretic responses to elevations in total body sodium has implications for the mechanisms underlying multiple pathophysiological states featuring sodium retention, e.g., heart failure, salt-sensitive hypertension.

DATA AVAILABILITY STATEMENT

The original contributions presented in the study are included in the article/supplementary material, further inquiries can be directed to the corresponding author.

ETHICS STATEMENT

The animal study was reviewed and approved by Boston University IACUC Committee.

AUTHOR CONTRIBUTIONS

AF, JK, and RW performed experiments. RW prepared figures. AF, KN, KK, and RW drafted manuscript. All authors approved final version of manuscript.

FUNDING

These studies were supported by National Heart, Lung, and Blood Institute (NHLBI) R01HL141406, R01HL139867, and National Institute on Aging (NIA) R01AG062515 to RW.

REFERENCES

Antunes-Rodrigues, J., Machado, B. H., Andrade, H. A., Mauad, H., Ramalho, M. J., Reis, L. C., et al. (1992). Carotid-aortic and renal baroreceptors mediate the atrial natriuretic peptide release induced by blood volume expansion. *Proc. Natl. Acad. Sci. U.S.A.* 89, 6828–6831. doi: 10.1073/pnas.89.15.6828

Bie, P. (2009). Blood volume, blood pressure and total body sodium: internal signalling and output control. *Acta Physiol.* 195, 187–196. doi: 10.1111/j.1748-1716.2008.01932.x

Bie, P., Molstrom, S., and Wamberg, S. (2009). Normotensive sodium loading in conscious dogs: regulation of renin secretion during beta-receptor blockade. *Am. J. Physiol. Regul. Integr. Comp. Physiol.* 296, R428–R435. doi: 10.1152/ajpregu.90753.2008

Callahan, M. F., Cunningham, J. T., Kirby, R. F., Johnson, A. K., and Gruber, K. A. (1988). Role of the anteroventral third ventricle (AV3V) region of the rat brain in the pressor response to gamma 2-melanocyte-stimulating hormone (gamma 2-MSH). *Brain Res.* 444, 177–180. doi: 10.1016/0006-8993(88)90925-0

Carmichael, C. Y., Carmichael, A. C., Kuwabara, J. T., Cunningham, J. T., and Wainford, R. D. (2016). Impaired sodium-evoked paraventricular nucleus neuronal activation and blood pressure regulation in conscious Sprague-Dawley rats lacking central Galphai2 proteins. *Acta Physiol.* 216, 314–329. doi: 10.1111/apha.12610

Carmichael, C. Y., Kuwabara, J. T., Pascale, C. L., Moreira, J. D., Mahne, S. E., Kapusta, D. R., et al. (2020). Hypothalamic Paraventricular Nucleus Galphai2 (Guanine Nucleotide-Binding Protein Alpha Inhibiting Activity Polypeptide 2) Protein-Mediated Neural Control of the Kidney and the Salt Sensitivity of Blood Pressure. *Hypertension* 75, 1002–1011. doi: 10.1161/HYPERTENSIONAHA.119.13777

DiBona, G. F., and Kopp, U. C. (1997). Neural control of renal function. *Physiol. Rev.* 77, 75–197. doi: 10.4199/C00034ED1V01Y201106ISP022

DiBona, G. F., and Sawin, L. L. (1983). Renal nerves in renal adaptation to dietary sodium restriction. *Am. J. Physiol.* 245, F322–F328. doi: 10.1152/ajprenal.1983.245.3.F322

Frame, A. A., Puleo, F., Kim, K., Walsh, K. R., Faudoa, E., Hoover, R. S., et al. (2019b). Sympathetic regulation of the NCC in norepinephrine-evoked salt-sensitive hypertension in Sprague-Dawley rats. *Am. J. Physiol. Renal Physiol.* 317, F1623–F1636.

Frame, A. A., Carmichael, C. Y., Kuwabara, J. T., Cunningham, J. T., and Wainford, R. D. (2019a). Role of the afferent renal nerves in sodium homeostasis and blood pressure regulation in rats. *Exp. Physiol.* 104, 1306–1323. doi: 10.1113/EP087700

Frithiof, R., Ramchandra, R., Hood, S., May, C., and Rundgren, M. (2009). Hypothalamic paraventricular nucleus mediates sodium-induced changes in cardiovascular and renal function in conscious sheep. *Am. J. Physiol. Regul. Integr. Comp. Physiol.* 297, R185–R193. doi: 10.1152/ajpregu.00058.2008

Guyton, A. C. (1991). Blood pressure control–special role of the kidneys and body fluids. *Science* 252, 1813–1816. doi: 10.1126/science.2063193

Johns, E. J. (2014). The neural regulation of the kidney in hypertension and renal failure. *Exp. Physiol.* 99, 289–294. doi: 10.1113/expphysiol.2013.072686

Kapusta, D. R., Pascale, C. L., Kuwabara, J. T., and Wainford, R. D. (2013). Central nervous system Galphai2-subunit proteins maintain salt resistance via a renal nerve-dependent sympathoinhibitory pathway. *Hypertension* 61, 368–375. doi: 10.1161/HYPERTENSIONAHA.111.00014

Kapusta, D. R., Pascale, C. L., and Wainford, R. D. (2012). Brain heterotrimeric Galphai(2)-subunit protein-gated pathways mediate central sympathoinhibition to maintain fluid and electrolyte homeostasis during stress. *FASEB J.* 26, 2776–2787. doi: 10.1096/fj.11-196550

Kompanowska-Jezierska, E., Wolff, H., Kuczeriszka, M., Gramsbergen, J. B., Walkowska, A., Johns, E. J., et al. (2008). Renal nerves and nNOS: roles in natriuresis of acute isovolumetric sodium loading in conscious rats. *Am. J. Physiol. Regul. Integr. Comp. Physiol.* 294, R1130–R1139. doi: 10.1152/ajpregu.00908.2007

Kopp, U. C. (2015). Role of renal sensory nerves in physiological and pathophysiological conditions. *Am. J. Physiol. Regul. Integr. Comp. Physiol.* 308, R79–R95. doi: 10.1152/ajpregu.00351.2014

Kopp, U. C., Cicha, M. Z., Smith, L. A., Mulder, J., and Hokfelt, T. (2007). Renal sympathetic nerve activity modulates afferent renal nerve activity by PGE2-dependent activation of alpha1- and alpha2-adrenoceptors on renal sensory nerve fibers. *Am. J. Physiol. Regul. Integr. Comp. Physiol.* 293, R1561–R1572. doi: 10.1152/ajpregu.00485.2007

Letson, H. L., Morris, J., Biros, E., and Dobson, G. P. (2019). Conventional and specific-pathogen free rats respond differently to anesthesia and surgical trauma. *Sci. Rep.* 9:9399. doi: 10.1038/s41598-019-45871-z

Luchner, A., and Schunkert, H. (2004). Interactions between the sympathetic nervous system and the cardiac natriuretic peptide system. *Cardiovasc. Res.* 63, 443–449. doi: 10.1016/j.cardiores.2004.05.004

Manunta, P., Hamlyn, J. M., Simonini, M., Messaggio, E., Lanzani, C., Bracale, M., et al. (2011). Endogenous ouabain and the renin-angiotensin-aldosterone system: distinct effects on Na handling and blood pressure in human hypertension. *J. Hypertens.* 29, 349–356. doi: 10.1097/HJH.0b013e32833ea821

Maranon, R., Lima, R., Spradley, F. T., do Carmo, J. M., Zhang, H., Smith, A. D., et al. (2015). Roles for the sympathetic nervous system, renal nerves, and CNS melanocortin-4 receptor in the elevated blood pressure in hyperandrogenemic female rats. *Am. J. Physiol. Regul. Integr. Comp. Physiol.* 308, R708–R713. doi: 10.1152/ajpregu.00411.2014

Mecawi Ade, S., Ruginsk, S. G., Elias, L. L., Varanda, W.A., and Antunes-Rodrigues, J. (2015). Neuroendocrine regulation of hydromineral homeostasis. *Compr. Physiol.* 5, 1465–1516. doi: 10.1002/cphy.c140031

Molstrom, S., Larsen, N. H., Simonsen, J. A., Washington, R., and Bie, P. (2009). Normotensive sodium loading in normal man: regulation of renin secretion during beta-receptor blockade. *Am. J. Physiol. Regul. Integr. Comp. Physiol.* 296, R436–R445. doi: 10.1152/ajpregu.90754.2008

Moreira, J. D., Chaudhary, P., Frame, A. A., Puleo, F., Nist, K. M., Abkin, E. A., et al. (2019). Inhibition of microglial activation in rats attenuates paraventricular nucleus inflammation in Galphai2 protein-dependent, salt-sensitive hypertension. *Exp. Physiol.* 104, 1892–1910. doi: 10.1113/EP087924

Moreira, T. S., Takaura, A. C., Colombari, E., and Menani, J. V. (2009). Antihypertensive effects of central ablations in spontaneously hypertensive rats. *Am. J. Physiol. Regul. Integr. Comp. Physiol.* 296, R1797–R1806. doi: 10.1152/ajpregu.90730.2008

Morita, H., Yamashita, Y., Nishida, Y., Tokuda, M., Hatase, O., and Hosomi, H. (1997). Fos induction in rat brain neurons after stimulation of the hepatoportal Na-sensitive mechanism. *Am. J. Physiol.* 272(3 Pt 2), R913–R923. doi: 10.1152/ajpregu.1997.272.3.R913

Mu, S., Shimosawa, T., Ogura, S., Wang, H., Uetake, Y., Kawakami-Mori, F., et al. (2011). Epigenetic modulation of the renal beta-adrenergic-WNK4 pathway in salt-sensitive hypertension. *Nat. Med.* 17, 573–580. doi: 10.1038/nm.2337

Persson, P. B., Ehmke, H., Kogler, U., and Kirchheim, H. (1989). Modulation of natriuresis by sympathetic nerves and angiotensin II in conscious dogs. *Am. J. Physiol.* 256(3 Pt 2), F485–F489. doi: 10.1152/ajprenal.1989.256.3.F485

Prager-Khoutorsky, M., and Bourque, C. W. (2015). Mechanical basis of osmosensory transduction in magnocellular neurosecretory neurones of the rat supraoptic nucleus. *J. Neuroendocrinol.* 27, 507–515. doi: 10.1111/jne.12270

Puleo, F., Kim, K., Frame, A. A., Walsh, K. R., Ferdaus, M. Z., Moreira, J. D., et al. (2020). Sympathetic regulation of the NCC (Sodium Chloride Cotransporter) in Dahl Salt-Sensitive Hypertension. *Hypertension* 76, 1461–1469. doi: 10.1161/HYPERTENSIONAHA.120.15928

Roson, M. I., Cavallero, S., Della Penna, S., Cao, G., Gorzalczany, S., and Pandolfo, M. (2006). Acute sodium overload produces renal tubulointerstitial inflammation in normal rats. *Kidney Int.* 70, 1439–1446. doi: 10.1038/sj.ki.5001831

Roson, M. I., Della Penna, S. L., Cao, G., Gorzalczany, S., Pandolfo, M., Toblli, J. E., et al. (2010). Different protective actions of losartan and tempol on the renal inflammatory response to acute sodium overload. *J. Cell. Physiol.* 224, 41–48. doi: 10.1002/jcp.22087

Safar, M. E., and Laurent, P. (2003). Pulse pressure and arterial stiffness in rats: comparison with humans. *Am. J. Physiol. Heart Circ. Physiol.* 285, H1363–H1369. doi: 10.1152/ajpheart.00513.2003

Simmonds, S. S., Lay, J., and Stocker, S. D. (2014). Dietary salt intake exaggerates sympathetic reflexes and increases blood pressure variability in normotensive rats. *Hypertension* 64, 583–589. doi: 10.1161/HYPERTENSIONAHA.114.03250

Stocker, S. D., Madden, C. J., and Sved, A. F. (2010). Excess dietary salt intake alters the excitability of central sympathetic networks. *Physiol. Behav.* 100, 519–524. doi: 10.1016/j.physbeh.2010.04.024

Stocker, S. D., Monahan, K. D., and Sinoway, L. I. (2013b). The hypothalamic paraventricular nucleus may not be at the heart of sympathetic outflow. *J. Physiol.* 591:1. doi: 10.1113/jphysiol.2012.237065

Stocker, S. D., Monahan, K. D., and Browning, K. N. (2013a). Neurogenic and sympathoexcitatory actions of NaCl in hypertension. *Curr. Hypertens. Rep.* 15, 538–546. doi: 10.1007/s11906-013-0385-9

Terker, A. S., Yang, C. L., McCormick, J. A., Meermeier, N. P., Rogers, S. L., Grossmann, S., et al. (2014). Sympathetic stimulation of thiazide-sensitive sodium chloride cotransport in the generation of salt-sensitive hypertension. *Hypertension* 64, 178–184. doi: 10.1161/HYPERTENSIONAHA.114.03335

Toney, G. M., Chen, Q. H., Cato, M. J., and Stocker, S. D. (2003). Central osmotic regulation of sympathetic nerve activity. *Acta Physiol. Scand.* 177, 43–55. doi: 10.1046/j.1365-201X.2003.01046.x

Veitenheimer, B. J., Engeland, W. C., Guzman, P. A., Fink, G. D., and Osborn, J. W. (2012). Effect of global and regional sympathetic blockade on arterial pressure during water deprivation in conscious rats. *Am. J. Physiol. Heart Circ. Physiol.* 303, H1022–H1034. doi: 10.1152/ajpheart.00413.2012

Vieira, A. A., Colombari, E., De Luca, L. A. Jr., Colombari, D. S., De PAula, P. M., and Menani, J. V. (2013). Cardiovascular responses to injections of angiotensin II or carbachol into the rostral ventrolateral medulla in rats with AV3V lesions. *Neurosci. Lett.* 556, 32–36. doi: 10.1016/j.neulet.2013.09.045

Wainford, R. D., Carmichael, C. Y., Pascale, C. L., and Kuwabara, J. T. (2015). Galphai2-protein-mediated signal transduction: central nervous system molecular mechanism countering the development of sodium-dependent hypertension. *Hypertension* 65, 178–186. doi: 10.1161/HYPERTENSIONAHA.114.04463

Wainford, R. D., and Kapusta, D. R. (2009). Chronic high-NaCl intake prolongs the cardiorenal responses to central N/OFQ and produces regional changes in the endogenous brain NOP receptor system. *Am. J. Physiol. Regul. Integr. Comp. Physiol.* 296, R280–R288. doi: 10.1152/ajpregu.00096.2008

Wainford, R. D., Pascale, C. L., and Kuwabara, J. T. (2013). Brain Galphai2-subunit protein-gated pathways are required to mediate the centrally evoked sympathoinhibitory mechanisms activated to maintain sodium homeostasis. *J. Hypertens.* 31, 747–757. doi: 10.1097/HJH.0b013e32835ebd54

Walsh, K. R., Kuwabara, J. T., Shim, J. W., and Wainford, R. D. (2016). Norepinephrine-evoked salt-sensitive hypertension requires impaired renal sodium chloride cotransporter activity in Sprague-Dawley rats. *Am. J. Physiol. Regul. Integr. Comp. Physiol.* 310, R115–R124. doi: 10.1152/ajpregu.00514.2014

Conflict of Interest: The authors declare that the research was conducted in the absence of any commercial or financial relationships that could be construed as a potential conflict of interest.

Publisher's Note: All claims expressed in this article are solely those of the authors and do not necessarily represent those of their affiliated organizations, or those of the publisher, the editors and the reviewers. Any product that may be evaluated in this article, or claim that may be made by its manufacturer, is not guaranteed or endorsed by the publisher.

frontiers in Physiology

ORIGINAL RESEARCH
published: 21 January 2022
doi: 10.3389/fphys.2021.787598

A Vasopressin-Induced Change in Prostaglandin Receptor Subtype Expression Explains the Differential Effect of PGE_2 on AQP2 Expression

*Peter M. T. Deen[1], Michelle Boone[1], Horst Schweer[2], Emma T. B. Olesen[3,4,5], Claudia Carmone[1], Jack F. M. Wetzels[6], Robert A. Fenton[3] and Marleen L. A. Kortenoeven[1,3,7]**

[1] Department of Physiology, Radboud University Nijmegen Medical Center, Nijmegen, Netherlands, [2] Department of Pediatrics, Philipps-University Marburg, Marburg, Germany, [3] Department of Biomedicine, Aarhus University, Aarhus, Denmark, [4] Department of Biomedical Sciences, University of Copenhagen, Copenhagen, Denmark, [5] Department of Endocrinology and Nephrology, North Zealand Hospital, Hillerød, Denmark, [6] Department of Nephrology, Radboud University Nijmegen Medical Center, Nijmegen, Netherlands, [7] Department of Cardiovascular and Renal Research, Institute of Molecular Medicine, University of Southern Denmark, Odense, Denmark

OPEN ACCESS

Edited by:
Hyun Jun Jung,
Johns Hopkins Medicine,
United States

Reviewed by:
Tae-Hwan Kwon,
Kyungpook National University,
South Korea
Vladimir T. Todorov,
Technical University Dresden,
Germany

***Correspondence:**
Marleen L. A. Kortenoeven
kortenoeven@health.sdu.dk

Specialty section:
This article was submitted to Renal and Epithelial Physiology, a section of the journal Frontiers in Physiology

Received: 30 September 2021
Accepted: 07 December 2021
Published: 21 January 2022

Citation:
Deen PMT, Boone M, Schweer H, Olesen ETB, Carmone C, Wetzels JFM, Fenton RA and Kortenoeven MLA (2022) A Vasopressin-Induced Change in Prostaglandin Receptor Subtype Expression Explains the Differential Effect of PGE_2 on AQP2 Expression. Front. Physiol. 12:787598. doi: 10.3389/fphys.2021.787598

Arginine vasopressin (AVP) stimulates the concentration of renal urine by increasing the principal cell expression of aquaporin-2 (AQP2) water channels. Prostaglandin E_2 (PGE_2) and prostaglandin$_{2\alpha}$ ($PGF_{2\alpha}$) increase the water absorption of the principal cell without AVP, but PGE_2 decreases it in the presence of AVP. The underlying mechanism of this paradoxical response was investigated here. Mouse cortical collecting duct ($mkpCCD_{c14}$) cells mimic principal cells as they endogenously express AQP2 in response to AVP. PGE_2 increased AQP2 abundance without desmopressin (dDAVP), while in the presence of dDAVP, PGE_2, and $PGF_{2\alpha}$ reduced AQP2 abundance. dDAVP increased the cellular PGD_2 and PGE_2 release and decreased the $PGF_{2\alpha}$ release. MpkCCD cells expressed mRNAs for the receptors of PGE_2 (EP1/EP4), PGF_2 (FP), and TxB_2 (TP). Incubation with dDAVP increased the expression of EP1 and FP but decreased the expression of EP4. In the absence of dDAVP, incubation of mpkCCD cells with an EP4, but not EP1/3, agonist increased AQP2 abundance, and the PGE_2-induced increase in AQP2 was blocked with an EP4 antagonist. Moreover, in the presence of dDAVP, an EP1/3, but not EP4, agonist decreased the AQP2 abundance, and the addition of EP1 antagonists prevented the PGE_2-mediated downregulation of AQP2. Our study shows that in $mpkCCD_{c14}$ cells, reduced EP4 receptor and increased EP1/FP receptor expression by dDAVP explains the differential effects of PGE_2 and $PGF_{2\alpha}$ on AQP2 abundance with or without dDAVP. As the V2R and EP4 receptor, but not the EP1 and FP receptor, can couple to Gs and stimulate the cyclic adenosine monophosphate (cAMP) pathway, our data support a view that cells can desensitize themselves for receptors activating the same pathway and sensitize themselves for receptors of alternative pathways.

Keywords: water transport, AQP2, vasopressin, prostaglandin, mpkCCD, PGE2, EP1, EP4

INTRODUCTION

To prevent dehydration, an adequate maintenance of water homeostasis is essential. In this process, the kidney plays a critical role. In response to hypernatremia or hypovolemia, arginine vasopressin (AVP) is released from the posterior pituitary gland. Subsequently, binding of AVP to the basolateral vasopressin type-2 receptor (V2R) in the connecting tubule and collecting duct principal cells in the kidney results in the redistribution of aquaporin-2 (AQP2) water channels from intracellular vesicles to the apical membrane, greatly increasing the osmotic water permeability, a prerequisite for forming concentrated urine (Knepper, 1997). In addition, AVP also increases the expression of AQP2 *via* phosphorylation of the cyclic adenosine monophosphate (cAMP)-responsive element binding protein, which activates transcription from the AQP2 promoter (Terris et al., 1996; Matsumura et al., 1997; Yasui et al., 1997).

Besides AVP, several other signaling molecules regulate the water balance by antagonizing the AVP-induced water transport (Boone and Deen, 2008). One such group of molecules is the prostaglandins (**Figure 1**). Prostaglandins can bind to their unique G-protein-coupled receptors (i.e., DP, FP, IP, and TP) or to one or more of four different PGE_2 receptors (i.e., EP1, EP2, EP3, and EP4). Some of these receptors (i.e., DP, EP2, EP4, and IP) are Gs-coupled and thus increase intracellular cAMP levels when activated, whereas others are coupled to Gi (i.e., EP3 and FP), reducing the cAMP synthesis, and/or Gq (i.e., EP1, FP, and TP), inducing calcium mobilization (Breyer et al., 1998; Hebert et al., 2005; Hao and Breyer, 2008).

Of the different prostaglandins, PGE_2 in particular has been shown to decrease AVP-stimulated water reabsorption in perfused collecting ducts (Hebert et al., 1990; Nadler et al., 1992; Sakairi et al., 1995). In addition, PGE_2 is also involved in the pathological regulation of water reabsorption. PGE_2 has been suggested to play an important role in the development of lithium-induced nephrogenic diabetes insipidus (NDI). This is based on the observation that the renal expression of the enzyme cyclooxygenase 2 (COX-2), involved in prostaglandin production, is markedly increased in lithium-treated mice, resulting in an increased excretion of urinary PGE_2 (Rao et al., 2005). Also, treatment with a COX-2 inhibitor alleviated lithium-induced polyuria (Kim et al., 2008). Similarly, in the bilateral ureteral obstruction, associated with AQP2 downregulation, COX-2 protein abundance as well as the concentrations of PGE_2 and other prostanoids are increased in the kidney inner medulla (Norregaard et al., 2010). Administration of COX-2 inhibitor prevents the increase of urinary PGE_2 and the downregulation of AQP2 in inner medullary collecting ducts seen after the bilateral ureteral obstruction (Norregaard et al., 2005). In addition, PGE_2 has recently been suggested to be instrumental in the increased free water reabsorption and volume expansion, leading to thiazide-induced hyponatremia (Ware et al., 2017). Besides PGE_2, $PGF_{2\alpha}$ can also inhibit AVP-stimulated water permeability in the collecting duct (Zook and Strandhoy, 1981; Hebert et al., 2005).

Paradoxically, PGE_2 increases the osmotic water permeability in the absence of AVP (Hebert et al., 1990; Sakairi et al., 1995). The underlying mechanism of this switch in function, however, is still unclear. Therefore, in the present study, we utilized the cortical collecting duct ($mpkCCD_{c14}$) cells of a mouse as a model system for the renal principal cell to delineate how prostaglandins can exert their diverse effects on the principal cell water reabsorption in the presence or absence of AVP.

MATERIALS AND METHODS

Cell Culture

Mouse $mpkCCD_{c14}$ cells were maintained essentially as described (Hasler et al., 2002). Cells were seeded at a density of 1.5×10^5 cells/cm^2 on semipermeable filters (Transwell®, 0.4 μm pore size, Corning Costar, Cambridge, MA) and cultured for 8 days. Unless stated otherwise, the cells were exposed to 1 nM of the V2R agonist desmopressin (dDAVP) at the basolateral side during the last 96 h, to maximally induce the AQP2 expression (Li et al., 2006). Cells were incubated with 10 μM indomethacin, 1 μM PGE_2 (both Sigma, St. Louis, MO, USA), 1 μM $PGF_{2\alpha}$ (Calbiochem, San Diego, CA), 300 nM of EP1/EP3 agonists sulprostone (Sigma, St. Louis, MO, USA), 1 μM of EP4 agonists CAY10580, 0.5 μM of EP4 antagonist Gw627368, 2.5 nM of the EP4 antagonist L161982, 20 μM of EP1 antagonist Sc-51089, or 100 nM of EP1 antagonist Ono-8711 (all Cayman Chemical, Ann Arbor, Michigan, USA) during the last 48 h. The medium was replaced after 24 h, or in experiments using the EP agonists or antagonists, the medium was replaced every 12 h.

Immunoblotting

$MpkCCD_{c14}$ cells grown on 1.13 cm^2 filters were lysed using 200 μl Laemmli. Sodium dodecyl sulfate-polyacrylamide gel electrophoresis, blotting, and blocking of the polyvinylidene fluoride membranes were carried out as described previously (Kamsteeg et al., 1999). Membranes were incubated for 16 h with 1:3,000-diluted affinity-purified rabbit anti-AQP2 antibodies [R7 (Deen et al., 1994) or Novus Biologicals, Littleton, CO] in Tris-buffered saline Tween-20 (TBS-T) supplemented with 1% w/v nonfat dried milk. Blots were incubated for 1 h with 1:5,000-diluted goat anti-rabbit IgGs (Sigma, St. Louis, MO) as secondary antibodies coupled to horseradish peroxidase. Proteins were visualized using enhanced chemiluminescence (ECL, Pierce, Rockford, IL).

(Quantitative) Reverse-Transcriptase Polymerase Chain Reaction

$MpkCCD_{c14}$ cells were grown as described above, and total RNA was isolated using the TriZol extraction reagent (Gibco, Life Technologies, Rockville, MD), according to the instructions of the manufacturer. To remove genomic DNA, total RNA was treated with DNase (Promega, Madison, WI) for 1 h at 37°C, extracted with phenol/chloroform, and precipitated. RNA was reverse-transcribed into cDNA using Moloney Murine Leukemia Virus reverse-transcriptase and random primers

(Promega, Madison, WI). During cDNA production, a control reaction without the reverse-transcriptase enzyme was conducted to exclude genomic DNA amplification. Exon overlapping primers were designed for prostaglandin receptors (see **Table 1**). Amplification was performed using the cDNA equivalent of 5 ng RNA for 40 cycles (i.e., 95°C 45 s, 50°C 1 min, and 72°C 1.5 min). β-actin was used as a positive control for cDNA amplification. cDNA from the tissue reported to express the particular receptor was taken along as a positive control. The proper identity of products was confirmed using the restriction analysis.

SYBR Green real-time quantitative reverse-transcriptase polymerase chain reaction (RT-PCR) was performed on an iQ5 Real-Time PCR Detection System from Bio-Rad by utilizing the SYBR Green PCR Master Mix (Applied Biosystems Foster City, CA). Signals for the ribosomal 18S were used to normalize for differences in the amount of starting cDNA.

Prostanoid Analysis

Samples were prepared as described previously (Schweer et al., 1994) with minor modifications. In brief, cell culture supernatants were spiked with ∼1 ng of deuterated internal standards, and the methoximes were obtained through the reaction with an O-methylhydroxylamine hydrochloride-acetate buffer. After acidification to pH 3.5, prostanoid derivatives were extracted, and the pentafluorobenzylesters were formed. Samples were purified by thin layer chromatography, and a broad zone with R_F 0.03–0.4 was eluted. After withdrawal of the organic layer, trimethylsilyl ethers were prepared by the reaction with bis(trimethylsilyl)-trifluoroacetamide and thereafter, subjected to the gas chromatography-tandem mass spectrometry (GC/MS/MS) analysis on a Finnigan MAT TSQ700 GC/MS/MS (Thermo Electron Corp., Dreieich, Germany) equipped with a Varian 3400 gas chromatograph (Palo Alto, CA) and a CTC A200S autosampler (CTC Analytics, Zwingen, Switzerland).

Statistical Analysis

Student's *t*-test was applied to compare two groups with Gaussian distribution. Comparisons of more than two groups were performed using a one-way ANOVA followed by a Dunnett multiple comparison test. Levene's test was used to compare variances. *P*-values <0.05 were considered significant. Immunoblotting signals were analyzed using the Bio-Rad software. Data are presented as mean ± standard error of the mean (SEM).

RESULTS

In MpkCCD Cells, Regulation of AQP2 Expression by Prostanoids Is Modulated by AVP

To analyze the effect of PGE_2 on the AQP2 expression, $mpkCCD_{c14}$ cells were grown to confluence for 8 days, either with or without 1 nM of the V2R agonist dDAVP for the last 4 days and with or without 1 μM PGE_2 during the last 48 h. PGE_2 increased the AQP2 abundance in the absence of dDAVP but decreased it in the presence of dDAVP (**Figure 2**). In the presence of dDAVP, 1 μM $PGF_{2\alpha}$ also decreased the AQP2 abundance.

To test whether COX inhibition affects the dDAVP-induced AQP2 expression, cells were grown as described above, i.e., the last 4 days in the presence of dDAVP and the last 48 h in the presence of 10 μM indomethacin. Subsequent immunoblotting showed an increased AQP2 abundance with indomethacin (**Figure 2**), suggesting that dDAVP-treated $mpkCCD_{c14}$ cells produce prostanoids, which decrease the AQP2 abundance.

dDAVP Changes Prostanoid Production in MpkCCD Cells

To determine whether $mpkCCD_{c14}$ cells produce PGE_2 or other prostanoids, and whether the presence of dDAVP affects the release of these prostanoids, cells were grown as above, i.e., with or without dDAVP for the last 4 days, after which the medium was collected and analyzed for the presence of prostanoids. Prostaglandin concentrations from the fresh medium were subtracted. The major prostanoids released from control cells were PGE_2 and $PGF_{2\alpha}$, while levels of PGD_2, 6-keto-$PGF_{1\alpha}$ (i.e., a stable metabolite of PGI_2), and TxB_2 (i.e., a stable metabolite of TxA_2) were lower and bordering on their detection limit (**Figure 3**). The dDAVP treatment significantly increased

TABLE 1 | Primer sequences.

Protein	Forward primer (5'-3')	Reverse primer (5'-3')	Product size (bp)
DP	AGGAGCTGGACCACTTTGTG	TCACAGACAGGAAACGCAAG	159
EP1	GCACGGAGCCGAGGAGC	GCAGGGGCTCATATCAGTGG	107
EP2	TCGCCATATGCTCCTTGC	TCCTCTGACACTTTCCACAAA	449
EP3	GCAGAATCACCACGGAGACG	GCGAAGCCAGGCGAACTG	190
EP4	TACGCCGCCTTCTCTTACAT	TTCACCACGTTTGGCTGATA	380
FP	CGTCACGGGAGTCACACTCT	TTCACAGGTCACTGGGGAAT	190
IP	CATGACCGTCATCATGGCCGTG	GTTGAAGGCGTTGAAGCGGAAGG	120
TP	GTGGGCATCATGGTGGTGG	CACACGCAGGTAGATGAGCAGC	168
β actin	GTATGCCTCTGGTCGTACCAC	ACGATTTCCCTCTCAGCTGTG	201
18S	GTAACCCGTTGAACCCCATT	CCATCCAATCGGTAGTAGCG	151

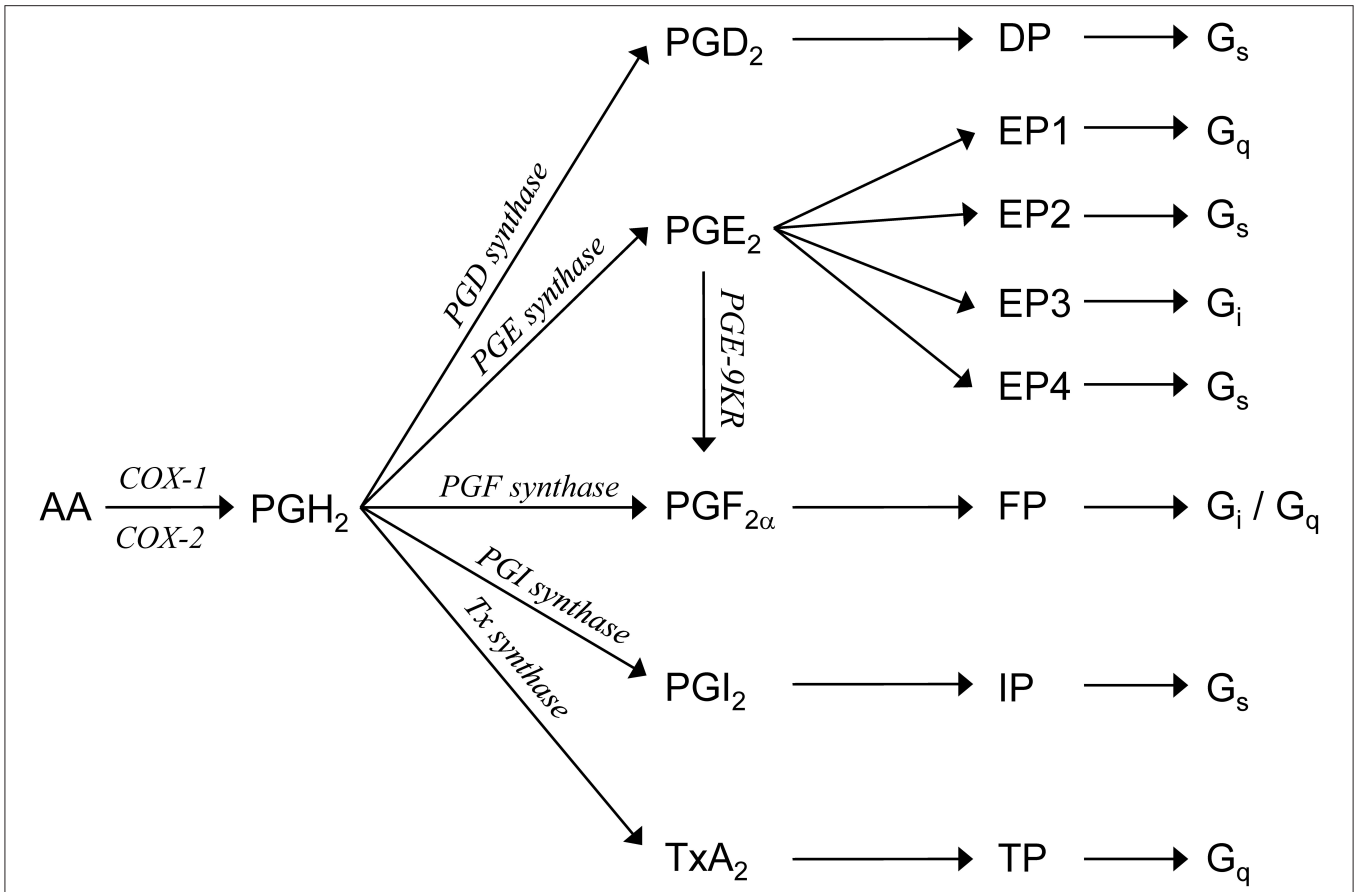

FIGURE 1 | Prostaglandin synthesis. Arachidonic acid (AA) is metabolized by COX1 or COX2 to PGH_2. PGH_2 is enzymatically converted, by specific synthases [prostaglandin D (PGD) synthase, prostaglandin E (PGE) synthase, prostaglandin F (PGF) synthase, prostaglandin I (PGI) synthase, and thromboxane synthase] or prostaglandin E 9-ketoreductase (PGE-9KR), to one of five primary prostanoids, namely, PGI_2, PGD_2, PGE_2, $PGF_{2\alpha}$, or TxA_2. Each prostanoid interacts with distinct members of a subfamily of the G-protein-coupled receptors. PGI_2 activates the IP receptor, PGD_2 activates the DP receptor, $PGF_{2\alpha}$ activates the FP receptor, and TxA_2 activates the TP receptor. PGE_2 interacts with one of four distinct EP receptors.

the production of PGD_2 and PGE_2, while $PGF_2\alpha$ levels were decreased. No effect of dDAVP was observed on the release of 6-keto-$PGF_{1\alpha}$ or TxB_2.

dDAVP Differentially Affects Prostanoid Receptor mRNA Expression in MpkCCD Cells

The effects of prostaglandins on the AQP2 expression are conferred by effects on their respective receptors. Immunoblotting was unsuitable to examine the expression of the individual prostaglandin receptors (not shown). Therefore, we determined the mRNA expression of the prostaglandin receptors in mpkCCD cells using the RT-PCR.

From unstimulated cells, cDNA products of the expected size were obtained for EP1, EP4, FP, and TP receptors (**Figure 4A**). While PCR products for EP2, EP3, or DP receptors were found in control tissues, no products were obtained in $mpkCCD_{c14}$ cells, indicating that these receptors are not expressed. A detectable expression of the IP receptor was inconsistent. The same receptors were expressed in mpkCCD cells treated with dDAVP (not shown).

To test if the levels of the expressed prostanoid receptors were influenced by dDAVP, we determined their relative expression by using the qRT-PCR. dDAVP increased the expression of the EP1 and FP receptor, while the expression of the EP4 receptor was significantly decreased (**Figure 4B**). No difference was detected in the expression of the TP receptor.

Modulation of PGE_2 Receptor Subtype Expression by dDAVP Explains the Differential Effect of Prostanoids on AQP2 Abundance

As the EP1/FP receptors and EP4 receptors are coupled to Gi/Gq and Gs (**Figure 1**), respectively, an altered activation of these receptors due to their changes in the expression with dDAVP could explain the differential effect of prostanoids on the AQP2 abundance. To further explore the roles of the different PGE_2 receptor subtypes in mediating the effects of

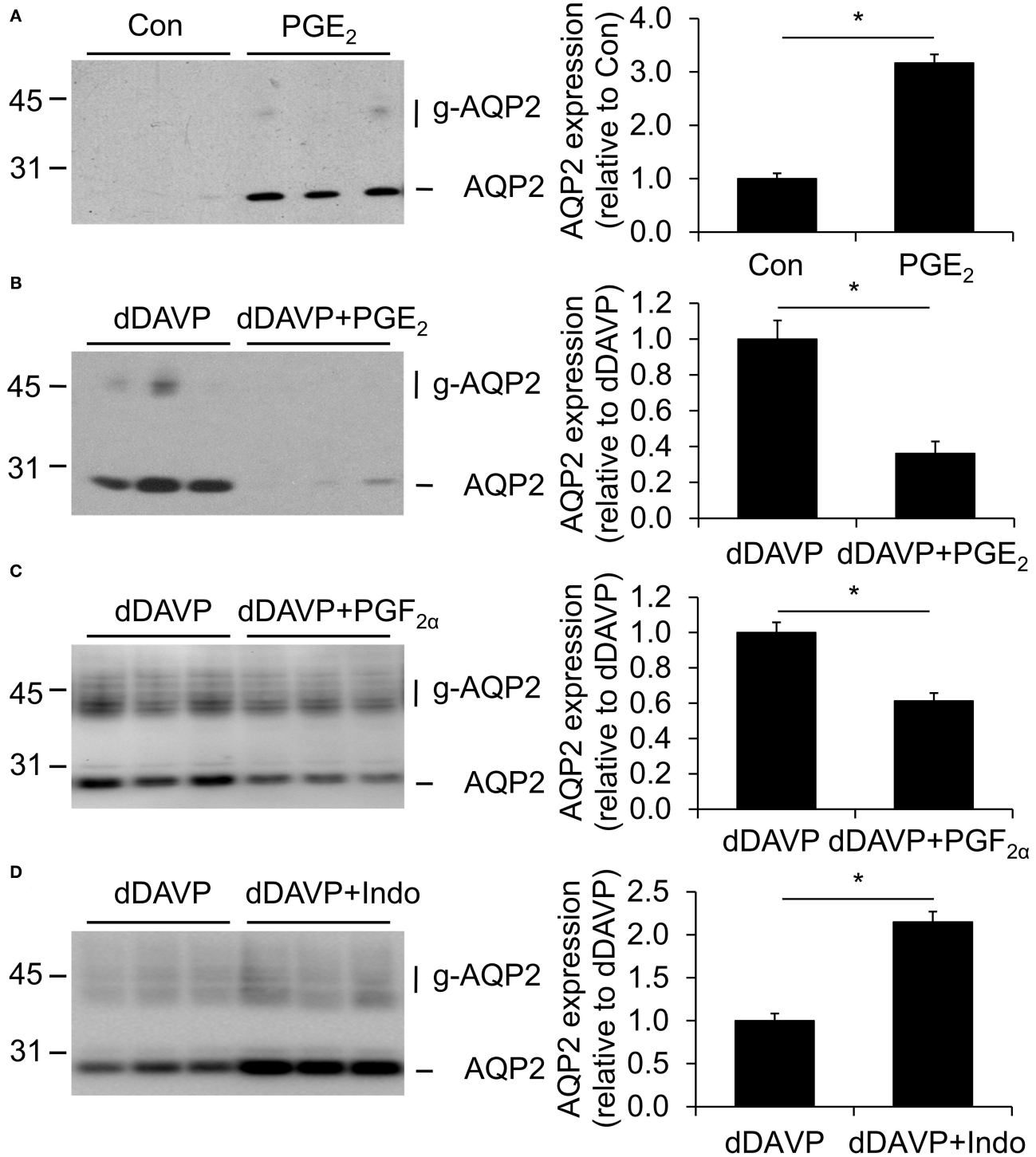

FIGURE 2 | Effect of prostaglandins on aquaporin-2 (AQP2) expression. MpkCCD$_{c14}$ cells were grown for 8 days, either with or without 1 nM desmopressin (dDAVP) stimulation for the last 4 days and with or without 1 μM PGE_2 **(A,B)**, 1 μM $PGF_{2\alpha}$ **(C)**, or 10 μM indomethacin **(D)** during the last 48 h. Cells were lysed and subjected to immunoblotting for AQP2. Molecular masses (in kDa) are indicated on the left. Nonglycosylated (AQP2) and complex-glycosylated (g-AQP2) forms of AQP2 are detected and densitometrically quantified. Significant differences from control or dDAVP alone ($p < 0.05$) are indicated by an asterisk. Bars are mean values of nine filters per condition (±SEM).

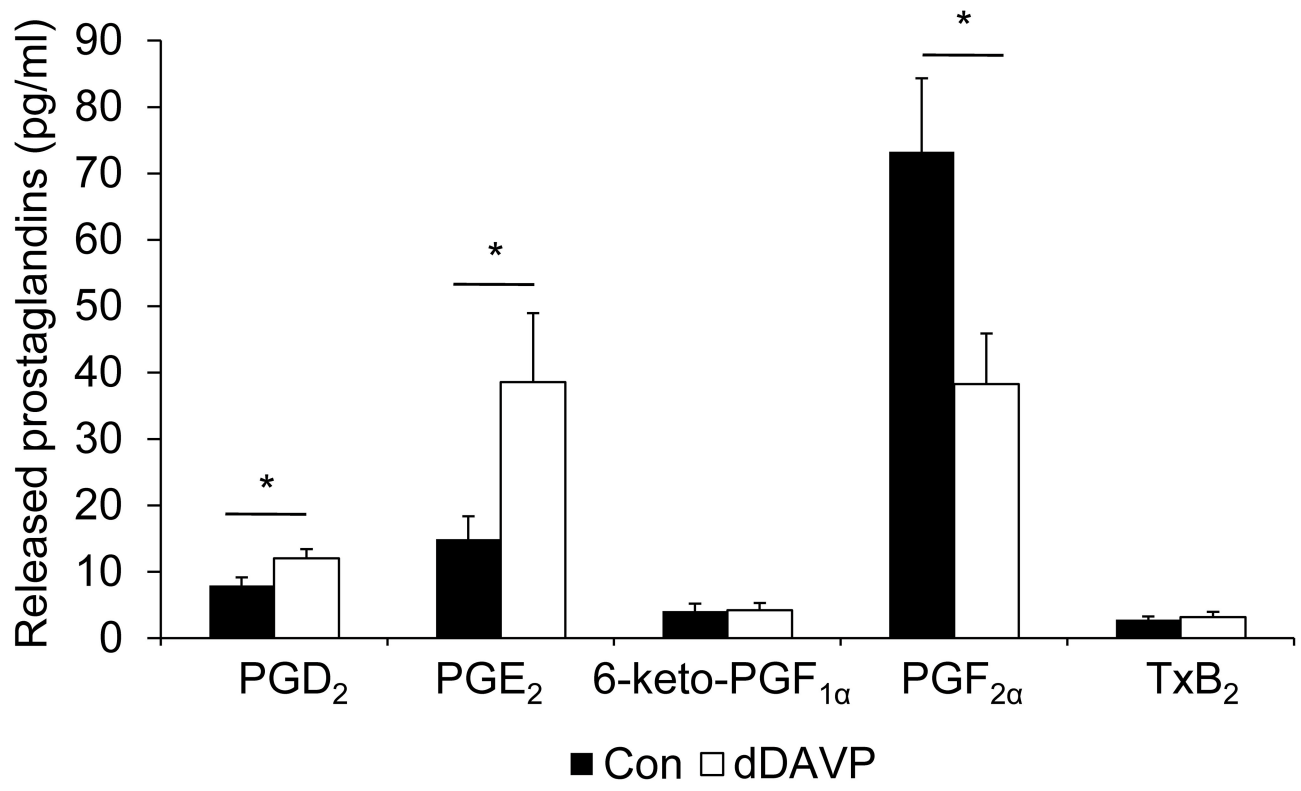

FIGURE 3 | Effect of dDAVP on prostaglandin production. MpkCCD$_{c14}$ cells were grown for 8 days and treated with or without (con) 1 nM dDAVP for the last 4 days. The medium from both sides, incubated with the cells for 24 h, was collected, and prostaglandin concentrations were determined. Bars are mean values of eight filters per condition (±SEM). Significant differences from control ($p < 0.05$) are indicated by an asterisk.

PGE_2 on AQP2 levels, we used EP receptor-specific agonists and antagonists.

MpkCCD cells were grown as described above, i.e., stimulated with or without dDAVP, and incubated with the EP4 agonist CAY10580 or the EP1/EP3 agonist sulprostone (Kiriyama et al., 1997; Billot et al., 2003) during the last 48 h. As the EP3 receptor is not expressed in mpkCCD cells (**Figure 4A**), sulprostone will act as a specific EP1 agonist in these cells. Consistent with a contribution of EP4 to the prostanoid-stimulated AQP2 abundance in unstimulated cells, CAY10580 and PGE_2 increased the AQP2 abundance as compared with unstimulated cells or cells incubated with sulprostone (**Figure 5A**). In cells stimulated with dDAVP, however, CAY10580 did not affect the AQP2 abundance, while both sulprostone and PGE_2 decreased the AQP2 abundance, therewith, illustrating an important contribution of the EP1 receptor in reducing the AQP2 abundance in dDAVP-stimulated mpkCCD, cells (**Figure 5B**).

To further investigate the role of the EP4 receptor in the prostanoid-induced AQP2 abundance, mpkCCD cells were treated with PGE_2 with or without the EP4 antagonists L161982 and Gw627368. While PGE_2 alone again increased the AQP2 abundance significantly, Gw627368 completely blocked the PGE_2-mediated AQP2 increase, whereas L161982 had a tendency to decrease the AQP2 expression relative to cells treated with PGE_2 alone (**Figure 5C**).

To investigate the role of EP1 in the PGE_2-mediated AQP2 decrease in dDAVP-treated cells, mpkCCD cells were stimulated with dDAVP and incubated with or without PGE_2 and the specific EP1 antagonists Sc-51089 or Ono-8711. Both antagonists fully prevented the PGE_2-mediated downregulation of AQP2 (**Figure 5D**), illustrating an important contribution of the EP1 receptor in the regulation of AQP2.

DISCUSSION

Prostanoids Affect AQP2 Expression in MpkCCD Cells

Prostaglandin E_2 reduce the AVP-stimulated water reabsorption in the collecting duct (Hebert et al., 1990; Nadler et al., 1992), while in the absence of AVP, *ex vivo* water permeability is increased by PGE_2 (Sakairi et al., 1995). A short-term action of PGE_2 is to alter the localization of AQP2 at the plasma membrane (Zelenina et al., 2000; Nejsum et al., 2005; Olesen et al., 2011). Here, we showed that long-term PGE_2 affects the abundance of the AQP2 protein. PGE_2 attenuated the dDAVP-induced AQP2 expression, while PGE_2 stimulated the AQP2

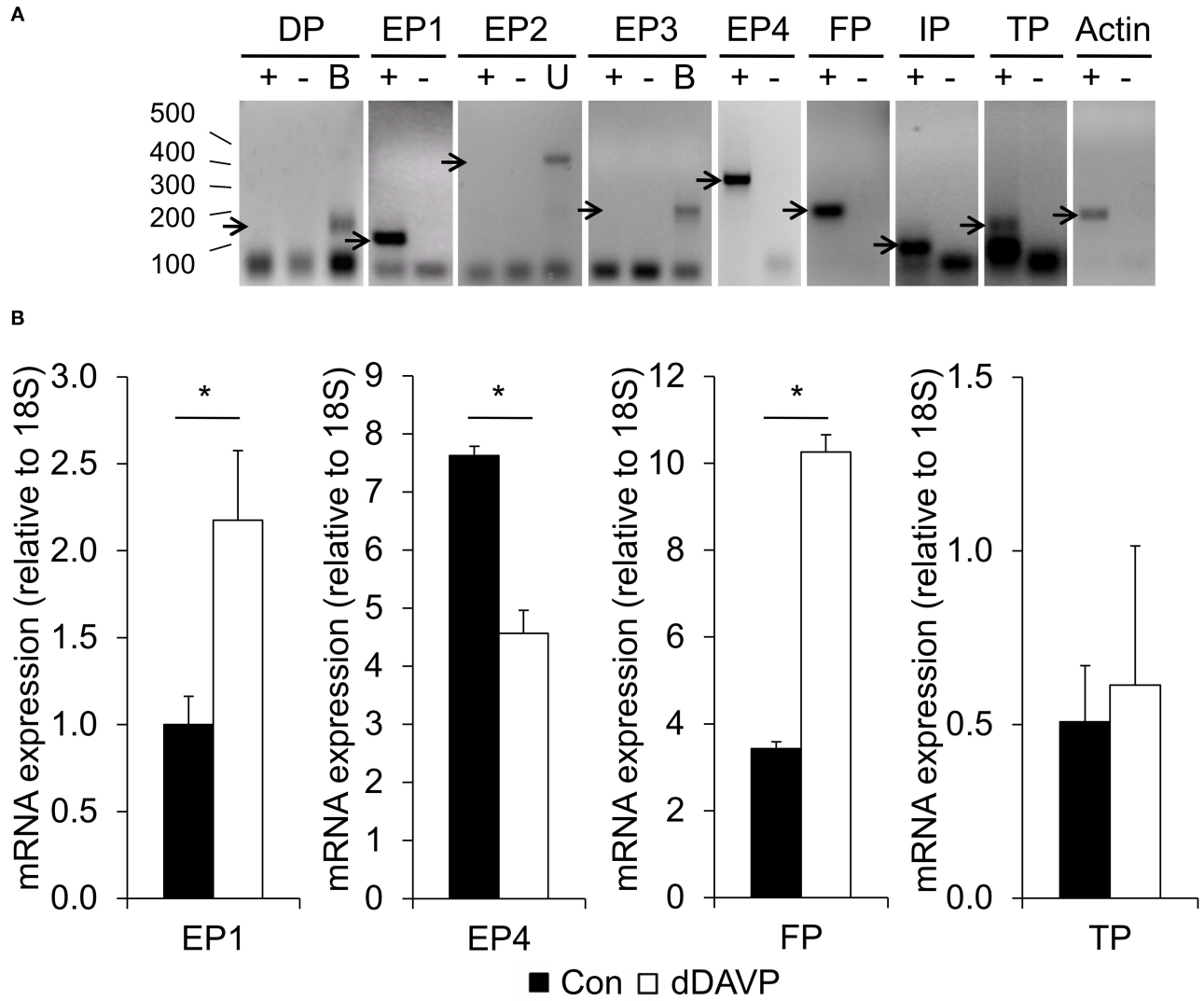

FIGURE 4 | Prostaglandin receptor expression. **(A)** MpkCCD$_{c14}$ cells were grown for 8 days. Cells were lysed, total RNA was isolated, and RNA was reverse-transcribed into cDNA. By using the reverse-transcriptase polymerase chain reaction (RT-PCR), the expression of the prostaglandin receptors was analyzed. β-actin was used as a positive control for cDNA amplification. ± = with or without reverse transcriptase during the cDNA production. B, brain, U, uterus. Sizes in bp are indicated on the left. Arrows point at product of expected size. **(B)** MpkCCD$_{c14}$ cells were grown for 8 days and incubated with or without (con) 1 nM dDAVP for the last 4 days. Total RNA was isolated, RNA was reverse-transcribed into cDNA, and the relative expression of the prostaglandin receptors was analyzed by performing the quantitative (q)RT-PCR. The signals obtained from the house-keeping 18S were used to normalize for difference in the amount of starting cDNA. Bars are mean values of eight filters per condition (±SEM). Significant differences ($p < 0.05$) from control are indicated by an asterisk.

abundance in the absence of dDAVP. In addition, dDAVP-stimulated AQP2 levels were decreased after the application of $PGF_{2\alpha}$, explaining the inhibition of water reabsorption in the collecting duct observed after the $PGF_{2\alpha}$ treatment (Zook and Strandhoy, 1981; Hebert et al., 2005). Furthermore, blocking the prostaglandin production by indomethacin increased the AQP2 abundance, showing that the dDAVP-stimulated AQP2 abundance is likely reduced due to the effects of endogenously produced prostaglandins. The major prostaglandins produced in mpkCCD cells are PGE_2 and $PGF_{2\alpha}$. The dDAVP stimulation significantly increased both the production of PGE_2 and PGD_2, while levels of $PGF_{2\alpha}$ were decreased. In agreement with these findings, it has been shown that AVP stimulates the PGE_2 synthesis in isolated collecting ducts (Schlondorff et al., 1985; Bonvalet et al., 1987).

In MpkCCD Cells, dDAVP-Induced Changes in PGE_2 Receptor Expression and Activation Explain the Different Effects of PGE_2 on AQP2 Abundance in the Presence or Absence of AVP

Consistent with previous studies, the PGE_2 receptors expressed in mpkCCD$_{c14}$ cells are EP1 and EP4 (Olesen et al., 2016). Our experiments using receptor antagonists and agonists show that it is the EP4 receptor that is involved in the stimulatory effect

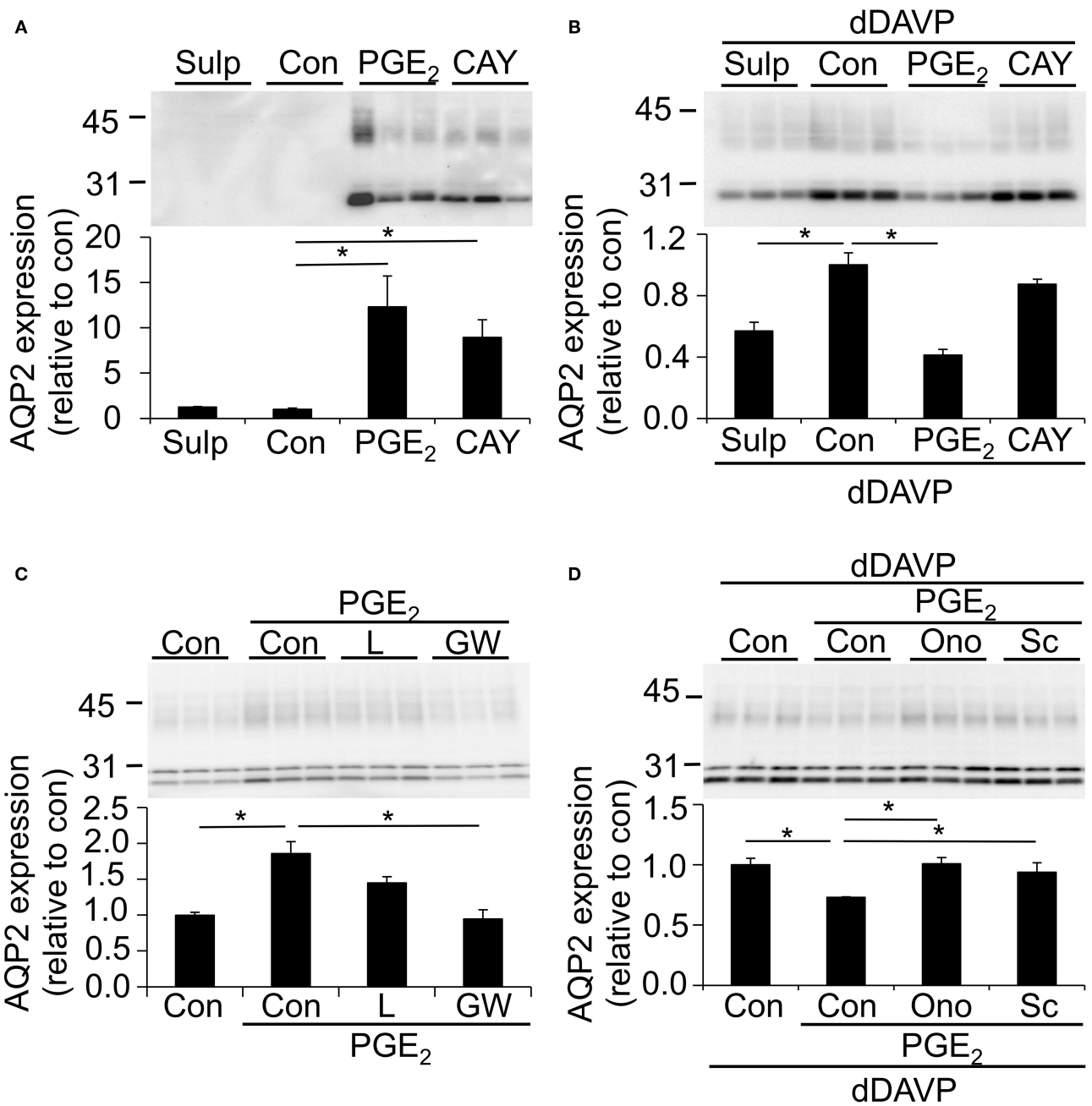

FIGURE 5 | Effect of different PGE_2 receptor agonists and antagonists on the AQP2 expression. $MpkCCD_{c14}$ cells were grown for 8 days, either with our without 1 nM dDAVP stimulation for the last 4 days and with or without 1 μM PGE_2 during the last 48 h. **(A,B)** Cells were incubated with1 μM sulprostone (Sulp) or 300 nM Cayman10580 (Cay) during the last 48 h. **(C)** Cells were incubated with 0.5 μM of EP4 antagonist Gw627368 (GW) or 2.5 nM of the EP4 antagonist L161982 (L) during the last 48 h. **(D)** Cells were incubated with 20 μM of EP1 antagonist Sc-51089 (Sc) or 100 nM of EP1 antagonist Ono-8711 (Ono) during the last 48 h. Cells were lysed and subjected to immunoblotting for AQP2. Molecular masses (in kDa) are indicated on the left. Nonglycosylated AQP2 (29 kDa) and complex-glycosylated (40–45 kDa) forms of AQP2 are detected and densitometrically quantified. Significant differences from control (con, $p < 0.05$) are indicated by an asterisk. Bars are mean values of 9 **(A,B)** or 6 **(C,D)** filters per condition (±SEM).

of PGE_2 on the AQP2 expression in mpkCCD cells. The EP4 receptor can couple to Gs-stimulated cAMP generation, thereby activating the same pathway as AVP. Incubation with dDAVP increased the expression of the EP1 receptor in mpkCCD cells but decreased the expression of the EP4 receptor. Additionally, our experiments showed that the activation of EP1 is the pathway

by which PGE_2 inhibits the dDAVP-induced AQP2 expression in mpkCCD cells (**Figure 6**). The EP1 receptors can couple to Gq and increase cytosolic Ca^{2+} and activate protein kinase C (PKC; Funk et al., 1993; Watabe et al., 1993). In microperfused collecting ducts, the inhibitory effect of PGE_2 on AVP-stimulated water permeability was dependent on the activity of PKC (Hebert et al., 1990; Nadler et al., 1992). PKC activation also promotes AQP2 endocytosis, similar to PGE_2 (Zelenina et al., 2000; Van Balkom et al., 2002; Nejsum et al., 2005), and increases AQP2 ubiquitination, leading to lysosomal degradation (Kamsteeg et al., 2006). This suggests that the EP1 activation will decrease the AQP2 abundance by lysosomal degradation (**Figure 6**).

The expression of the FP receptor was increased by dDAVP incubation in mpkCCD cells. As the activation of the FP receptor inhibits water reabsorption, the increase in the FP expression might be a compensatory mechanism to counteract AVP stimulation, similar to the increase in the EP1 expression.

As no DP receptor was detected in $mpkCCD_{c14}$ cells, the role of the dDAVP-stimulated increase in the PGD_2 production after dDAVP incubation is unclear. However, PGD_2 has been shown to bind to the FP receptor with an affinity close to that for the DP receptor, indicating that PGD_2 may act on the FP receptor (Kiriyama et al., 1997). The increase in PGD_2 might counteract the dDAVP-induced increase in the AQP2 expression, although levels are low compared with the PGE_2 and $PGF_{2\alpha}$ production.

While the TP receptor is expressed in $mpkCCD_{c14}$ cells, the expression of the IP receptor is inconclusive. Both thromboxane and PGI_2 were produced in very low amounts in $mpkCCD_{c14}$ cells, and the production was not affected by dDAVP. Whether these prostanoids have any role in water reabsorption remains unclear.

Relation of the MpkCCD Cell System to the *in vivo* Situation

A limitation of our study is that all experiments are performed in mpkCCD cells. However, a problem with *in vivo* studies investigating the effect of prostaglandins on the collecting duct is

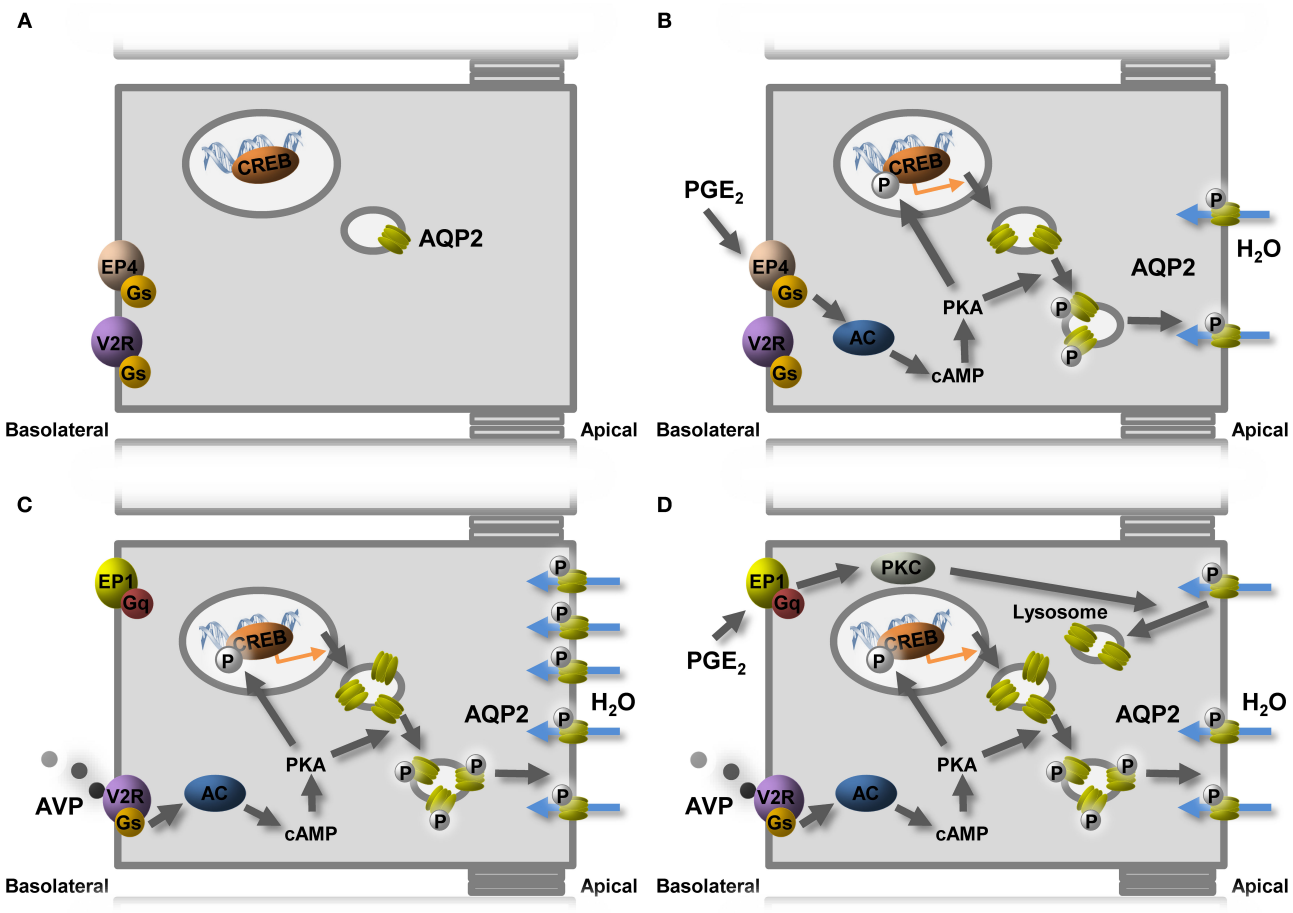

FIGURE 6 | Model of PGE_2-mediated regulation of AQP2-mediated water reabsorption. **(A)** In the absence of AVP, the AQP2 expression is low and present in intracellular vesicles. **(B)** PGE_2 stimulates water reabsorption by binding to the EP4 receptor, coupling to the Gs protein, leading to cAMP generation, followed by AQP2 transcription and translocation. **(C)** AVP increases the expression of AQP2 but also induces the expression of the AVP-counteracting EP1 receptor and reduces EP4. **(D)** In the presence of AVP, PGE_2 decreases the AQP2 expression by stimulating EP1. Indicated are AC, adenylate cyclase; AQP2, aquaporin-2; AVP, vasopressin; cAMP, cyclic adenosine monophosphate; PKA, protein kinase A; PKC, protein kinase C; V2R, vasopressin V2 receptor.

that these studies are complicated by the effect of prostaglandins on AVP release and on medullary osmolality, both of which will influence the AQP2 expression (Yamamoto et al., 1976; Stoff et al., 1981; Hasler et al., 2005). To study the effect of prostaglandins directly on principal cells, experiments were performed in mpkCCD cells, shown to display the essential functionalities characteristic of principal cells like the AVP-regulated AQP2 expression and aldosterone-mediated sodium transport *via* the epithelial sodium channel (Bens et al., 1999; Hasler et al., 2002).

The major prostaglandins produced in our cell system were PGE_2 and $PGF_{2\alpha}$, which is in agreement with *in vivo* findings, showing that PGE_2 is the most abundant prostanoid in both the renal cortex and medulla, followed by PGI_2 and $PGF_{2\alpha}$ (Qi et al., 2006). The synthases involved in the production of PGD_2, PGE_2, and $PGF_{2\alpha}$ are detected in the nephron (Vitzthum et al., 2002; Sakurai et al., 2005), where the production of PGE_2 and $PGF_{2\alpha}$ has been shown to occur mainly in the collecting ducts (Farman et al., 1987). Neither PGI synthase nor thromboxane synthase mRNA is detected in any tubular structure (Vitzthum et al., 2002).

The effects of prostaglandins on the AQP2 expression are conferred by PG receptors. In $mpkCCD_{c14}$ cells, EP1, EP4, and FP receptors are found, in agreement with expression in the collecting duct (Breyer et al., 1998; Saito et al., 2003).

In line with our data showing the role of EP4 in the stimulatory effect of PGE_2 on AQP2, a study by Gao et al. demonstrates that disruption of EP4 in the collecting duct impaired the urinary concentration by decreasing the AQP2 abundance and apical membrane targeting, providing evidence that EP4 can regulate the urine concentration *in vivo* (Gao et al., 2015). In addition, a selective EP4 agonist has been shown to increase the urine osmolality, decrease the urine volume, and increase the AQP2 expression in a mouse model for congenital NDI (Li et al., 2009).

In agreement with our findings that the activation of the EP1 receptor decreases the AVP-induced AQP2 expression, the stimulation of the EP1 receptor has been shown to decrease the vasotocin-induced osmotic water permeability of the frog urinary bladder, a model system of the collecting duct (Bachteeva et al., 2007). In addition, EP1-knockout mice have a urinary concentrating defect (Kennedy et al., 2007), and recent studies show that PGE_2 does not decrease AVP-mediated water transport in isolated collecting ducts of these mice (Nasrallah et al., 2018). Taken together with the present data, this suggests that EP1 conveys both acute and long-term modulation of the V2R activity.

Furthermore, TP and IP receptors are mainly localized in the glomerulus and vasculature, respectively, but have also been located in the collecting duct (Takahashi et al., 1996; Komhoff et al., 1998), in agreement with the expression seen in $mpkCCD_{c14}$ cells. Based on our mpkCCD data, however, we anticipated that the IP receptor does not have a major impact on the principal cell AQP2 expression in the presence or absence of AVP.

None of the receptors DP, EP2, and EP3 seems to be expressed in $mpkCCD_{c14}$ cells. While DP is also not expressed in the kidney, the presence of EP2 along the nephron is a matter of considerable debate (Breyer and Breyer, 2000; Olesen and Fenton, 2013). However, a previous study has shown that functionally, the collecting duct can respond to the stimulation of the EP2 receptor (Olesen et al., 2011).

The inhibitory effects of PGE_2 on AVP-induced water reabsorption have, besides *via* the activation of EP1, also been suggested to occur through the activation of EP3 (Hebert et al., 1993; Fleming et al., 1998). Our cell model does not express the EP3 receptor, which was found *in vivo* by the *in situ* hybridization and RT-PCR on microdissected tubules to be expressed in the collecting duct (Breyer et al., 1998). However, a study using single-cell RNA-Seq of intercalated and principal cells from the mouse kidney demonstrated that EP3 was selectively expressed in collecting duct-intercalated cells, while EP1 and EP4 were expressed in the principal cells (Chen et al., 2017). In addition, EP3-knockout mice exhibit a similar urine-concentrating ability during basal conditions as well as in response to AVP compared with wild-type mice, arguing against a role of EP3 in the AQP2 regulation (Fleming et al., 1998). The exact role of the EP3 receptor in the AQP2 regulation needs further investigation.

Central Mechanism for the Differential Effect of PGE_2 on AQP2 Expression

It is interesting to note that, while dDAVP increases the PGE_2 production and release, the mRNA expression of the EP4 receptor is reduced, whereas that of the EP1 receptor is increased. As both receptors are bound and activated by PGE_2, these data suggest that it is not the agonist *per se* that determines the expression level of the receptors. Instead, our data indicate that the signaling cascade that is mainly activated exerts a negative feedback regulation on receptors stimulating the same pathway and a positive feedback on receptors activating an opposite pathway: dDAVP increases the cAMP-AQP2 pathway, which can be stimulated by EP4, whereas EPl activates a pathway that leads to a decreased AQP2 expression and water permeability.

The same antagonizing mechanism can be seen in response to endothelin, which counteracts the AVP-mediated water permeability (Edwards et al., 1993), and at the same time, leads to an increased expression of the vasopressin V2 receptor in the inner medullary collecting duct of the rat (Sonntag et al., 2004). Similar to this antagonizing mechanism, dDAVP increases the mRNA levels of the purinergic receptor subunit $P2Y_2$ in mpkCCD cells and targets the subunits $P2Y_2$ and $P2X_2$ to the plasma membrane, where the activation of these receptors leads to the AQP2 internalization and a decrease in the water permeability (Wildman et al., 2009). A similar mechanism can be seen with the hormone angiotensin II, which increases renal proximal sodium reabsorption but at the same time increases expression of the D4 dopamine receptor in renal proximal tubule cells, which activation will decrease sodium reabsorption, thereby counteracting the direct effect of angiotensin II (Tang et al., 2017).

In conclusion, our study shows that in $mpkCCD_{c14}$ cells, both PGE_2 and $PGF_{2\alpha}$ decrease the dDAVP-stimulated AQP2

abundance, while in the absence of dDAVP, PGE_2 increases AQP2 levels. Furthermore, our study suggests that EP4 mediates the PGE_2-induced increase in the AQP2 abundance in the absence of dDAVP, while the PGE_2-mediated decrease in the AQP2 abundance in the presence of dDAVP is likely mediated *via* EP1. This paradoxical difference in response to PGE_2 is likely explained by the different receptor subtype expression induced by the dDAVP treatment, leading to an increase in EP1 and a decrease in EP4.

Based on our data above that a negative feedback is mediated by the signaling pathways activated instead of the agonist, we hypothesized that *in vivo* AVP increases, besides AQP2, the expression of EP1 and decreases the expression of EP4 receptors. Consequently, in conditions with the increased PGE_2 release, such as with lithium-NDI or bilateral uteral obstruction, the AVP-induced AQP2 expression would be reduced *via* the activation of these EP1 receptors.

DATA AVAILABILITY STATEMENT

The raw data supporting the conclusions of this article will be made available by the authors, without undue reservation.

AUTHOR CONTRIBUTIONS

MK, JW, RF, and PD designed experiments. MK, MB, HS, EO, and CC performed experiments. MK and PD wrote manuscript. All authors approved the final manuscript.

FUNDING

PD is a recipient of VICI grant 865.07.0h02 of the Netherlands Organization for Scientific research (NWO). This work was supported by grants from NWO (VICI grant 865.07.002) and RUNMC (2004.55) to PD and grants from the Independent Research Fund Denmark (Project No. 1333-00279 and 1331-00738B) and the Aarhus University Research Foundation to MK. RF was funded by the Independent Research Fund Denmark (Project No. 1026-00063B) and the Novo Nordisk Foundation.

ACKNOWLEDGMENTS

We thank Johan van Burgsteden and Michiel van den Brand, Nijmegen, and Christian Westberg, Aarhus, for their excellent technical assistance.

REFERENCES

Bachteeva, V., Fock, E., Lavrova, E., Nikolaeva, S., Gambaryan, S., and Parnova, R. (2007). Prostaglandin E2 inhibits vasotocin-induced osmotic water permeability in the frog urinary bladder by EP1-receptor-mediated activation of NO/cGMP pathway. *Am. J. Physiol Regul. Integr. Comp. Physiol.* 293, R528–R537. doi: 10.1152/ajpregu.00811.2006

Bens, M., Vallet, V., Cluzeaud, F., Pascual-Letallec, L., Kahn, A., Rafestin-Oblin, M. E., et al. (1999). Corticosteroid-dependent sodium transport in a novel immortalized mouse collecting duct principal cell line. *J. Am. Soc. Nephrol.* 10, 923–934. doi: 10.1681/ASN.V105923

Billot, X., Chateauneuf, A., Chauret, N., Denis, D., Greig, G., Mathieu, M. C., et al. (2003). Discovery of a potent and selective agonist of the prostaglandin EP4 receptor. *Bioorg. Med. Chem. Lett* 13, 1129–1132. doi: 10.1016/S0960-894X(03)00042-8

Bonvalet, J. P., Pradelles, P., and Farman, N. (1987). Segmental synthesis and actions of prostaglandins along the nephron. *Am. J. Physiol.* 253, F377–387. doi: 10.1152/ajprenal.1987.253.3.F377

Boone, M., and Deen, P. M. (2008). Physiology and pathophysiology of the vasopressin-regulated renal water reabsorption. *Pflugers Arch.* 456, 1005–1024. doi: 10.1007/s00424-008-0498-1

Breyer, M. D., and Breyer, R. M. (2000). Prostaglandin E receptors and the kidney. *Am. J. Physiol. Renal. Physiol.* 279, F12–F23. doi: 10.1152/ajprenal.2000.279.1.F12

Breyer, M. D., Zhang, Y., Guan, Y. F., Hao, C. M., Hebert, R. L., and Breyer, R. M. (1998). Regulation of renal function by prostaglandin E receptors. *Kidney Int. Suppl.* 67, S88–S94. doi: 10.1046/j.1523-1755.1998.06718.x

Chen, L., Lee, J. W., Chou, C. L., Nair, A. V., Battistone, M. A., Paunescu, T. G., et al. (2017). Transcriptomes of major renal collecting duct cell types in mouse identified by single-cell RNA-seq. *Proc. Natl. Acad. Sci. U. S. A.* 114, E9989–E9998. doi: 10.1073/pnas.1710964114

Deen, P. M. T., Verdijk, M. a. J., Knoers, N. V. a. M., Wieringa, B., Monnens, L. a. H., Van Os, C. H., et al. (1994). Requirement of human renal water channel aquaporin-2 for vasopressin-dependent concentration of urine. *Science* 264, 92–95. doi: 10.1126/science.8140421

Edwards, R. M., Stack, E. J., Pullen, M., and Nambi, P. (1993). Endothelin inhibits vasopressin action in rat inner medullary collecting duct *via* the ETB receptor. *J. Pharmacol. Exp. Ther.* 267, 1028–1033.

Farman, N., Pradelles, P., and Bonvalet, J. P. (1987). PGE2, PGF2 alpha, 6-keto-PGF1 alpha, and TxB2 synthesis along the rabbit nephron. *Am. J. Physiol.* 252, F53–F59. doi: 10.1152/ajprenal.1987.252.1.F53

Fleming, E. F., Athirakul, K., Oliverio, M. I., Key, M., Goulet, J., Koller, B. H., et al. (1998). Urinary concentrating function in mice lacking EP3 receptors for prostaglandin E2. *Am. J. Physiol* 275, F955–F961. doi: 10.1152/ajprenal.1998.275.6.F955

Funk, C. D., Furci, L., Fitzgerald, G. A., Grygorczyk, R., Rochette, C., Bayne, M. A., et al. (1993). Cloning and expression of a cDNA for the human prostaglandin E receptor EP1 subtype. *J. Biol. Chem.* 268, 26767–26772. doi: 10.1016/S0021-9258(19)74379-8

Gao, M., Cao, R., Du, S., Jia, X., Zheng, S., Huang, S., et al. (2015). Disruption of prostaglandin E2 receptor EP4 impairs urinary concentration *via* decreasing aquaporin 2 in renal collecting ducts. *Proc. Natl. Acad. Sci. U. S. A.* 112, 8397–8402. doi: 10.1073/pnas.1509565112

Hao, C. M., and Breyer, M. D. (2008). Physiological regulation of prostaglandins in the kidney. *Annu. Rev. Physiol.* 70, 357–377. doi: 10.1146/annurev.physiol.70.113006.100614

Hasler, U., Mordasini, D., Bens, M., Bianchi, M., Cluzeaud, F., Rousselot, M., et al. (2002). Long-term regulation of aquaporin-2 expression in vasopressin-responsive renal collecting duct principal cells. *J. Biol. Chem.* 277, 10379–10386. doi: 10.1074/jbc.M111880200

Hasler, U., Vinciguerra, M., Vandewalle, A., Martin, P. Y., and Feraille, E. (2005). Dual effects of hypertonicity on aquaporin-2 expression in cultured renal collecting duct principal cells. *J. Am. Soc. Nephrol.* 16, 1571–1582. doi: 10.1681/ASN.2004110930

Hebert, R. L., Carmosino, M., Saito, O., Yang, G., Jackson, C. A., Qi, Z., et al. (2005). Characterization of a rabbit kidney prostaglandin F(2{alpha}) receptor exhibiting G(i)-restricted signaling that inhibits water absorption in the collecting duct. *J. Biol. Chem.* 280, 35028–35037. doi: 10.1074/jbc.M505852200

Hebert, R. L., Jacobson, H. R., and Breyer, M. D. (1990). PGE2 inhibits AVP-induced water flow in cortical collecting ducts by protein kinase C activation. *Am. J. Physiol.* 259, F318–F325. doi: 10.1152/ajprenal.1990.259.2.F318

Hebert, R. L., Jacobson, H. R., Fredin, D., and Breyer, M. D. (1993). Evidence that separate PGE2 receptors modulate water and sodium

transport in rabbit cortical collecting duct. *Am. J. Physiol.* 265, F643–F650. doi: 10.1152/ajprenal.1993.265.5.F643

Kamsteeg, E. J., Hendriks, G., Boone, M., Konings, I. B., Oorschot, V., Van Der, S. P., et al. (2006). Short-chain ubiquitination mediates the regulated endocytosis of the aquaporin-2 water channel. *Proc. Natl. Acad. Sci. U. S. A.* 103, 18344–18349. doi: 10.1073/pnas.0604073103

Kamsteeg, E. J., Wormhoudt, T. A., Rijss, J. P. L., Van Os, C. H., and Deen, P. M. T. (1999). An impaired routing of wild-type aquaporin-2 after tetramerization with an aquaporin-2 mutant explains dominant nephrogenic diabetes insipidus. *EMBO J.* 18, 2394–2400. doi: 10.1093/emboj/18.9.2394

Kennedy, C. R., Xiong, H., Rahal, S., Vanderluit, J., Slack, R. S., Zhang, Y., et al. (2007). Urine concentrating defect in prostaglandin EP1-deficient mice. *Am. J. Physiol. Renal Physiol.* 292, F868–F875. doi: 10.1152/ajprenal.00183.2005

Kim, G. H., Choi, N. W., Jung, J. Y., Song, J. H., Lee, C. H., Kang, C. M., et al. (2008). Treating lithium-induced nephrogenic diabetes insipidus with a COX-2 inhibitor improves polyuria *via* upregulation of AQP2 and NKCC2. *Am. J. Physiol. Renal Physiol.* 294, F702–F709. doi: 10.1152/ajprenal.00366.2007

Kiriyama, M., Ushikubi, F., Kobayashi, T., Hirata, M., Sugimoto, Y., and Narumiya, S. (1997). Ligand binding specificities of the eight types and subtypes of the mouse prostanoid receptors expressed in Chinese hamster ovary cells. *Br. J. Pharmacol.* 122, 217–224. doi: 10.1038/sj.bjp.0701367

Knepper, M. A. (1997). Molecular physiology of urinary concentrating mechanism: regulation of aquaporin water channels by vasopressin. *Am. J. Physiol.* 41, F3–F12. doi: 10.1152/ajprenal.1997.272.1.F3

Komhoff, M., Lesener, B., Nakao, K., Seyberth, H. W., and Nusing, R. M. (1998). Localization of the prostacyclin receptor in human kidney. *Kidney Int.* 54, 1899–1908. doi: 10.1046/j.1523-1755.1998.00213.x

Li, J. H., Chou, C. L., Li, B., Gavrilova, O., Eisner, C., Schnermann, J., et al. (2009). A selective EP4 PGE2 receptor agonist alleviates disease in a new mouse model of X-linked nephrogenic diabetes insipidus. *J. Clin. Invest.* 119, 3115–3126. doi: 10.1172/JCI39680

Li, Y., Shaw, S., Kamsteeg, E. J., Vandewalle, A., and Deen, P. M. (2006). Development of lithium-induced nephrogenic diabetes insipidus is dissociated from adenylyl cyclase activity. *J. Am. Soc. Nephrol.* 17, 1063–1072. doi: 10.1681/ASN.2005080884

Matsumura, Y., Uchida, S., Rai, T., Sasaki, S., and Marumo, F. (1997). Transcriptional regulation of aquaporin-2 water channel gene by cAMP. *J. Am. Soc. Nephrol.* 8, 861–867. doi: 10.1681/ASN.V86861

Nadler, S. P., Zimpelmann, J. A., and Hebert, R. L. (1992). PGE2 inhibits water permeability at a post-cAMP site in rat terminal inner medullary collecting duct. *Am. J. Physiol.* 262, F229–F235. doi: 10.1152/ajprenal.1992.262.2.F229

Nasrallah, R., Zimpelmann, J., Eckert, D., Ghossein, J., Geddes, S., Beique, J. C., et al. (2018). PGE2 EP1 receptor inhibits vasopressin-dependent water reabsorption and sodium transport in mouse collecting duct. *Lab. Invest.* 98, 360–370. doi: 10.1038/labinvest.2017.133

Nejsum, L. N., Zelenina, M., Aperia, A., Frokiaer, J., and Nielsen, S. (2005). Bidirectional regulation of AQP2 trafficking and recycling: involvement of AQP2-S256 phosphorylation. *Am. J. Physiol. Renal. Physiol.* 288, F930–F938. doi: 10.1152/ajprenal.00291.2004

Norregaard, R., Jensen, B. L., Li, C., Wang, W., Knepper, M. A., Nielsen, S., et al. (2005). COX-2 inhibition prevents downregulation of key renal water and sodium transport proteins in response to bilateral ureteral obstruction. *Am. J. Physiol. Renal. Physiol.* 289, F322–F333. doi: 10.1152/ajprenal.00061.2005

Norregaard, R., Jensen, B. L., Topcu, S. O., Wang, G., Schweer, H., Nielsen, S., et al. (2010). Urinary tract obstruction induces transient accumulation of COX-2-derived prostanoids in kidney tissue. *Am. J. Physiol Regul. Integr. Comp Physiol* 298, R1017–R1025. doi: 10.1152/ajpregu.00336.2009

Olesen, E. T., and Fenton, R. A. (2013). Is there a role for PGE2 in urinary concentration? *J. Am. Soc. Nephrol.* 24, 169–178. doi: 10.1681/ASN.2012020217

Olesen, E. T., Moeller, H. B., Assentoft, M., Macaulay, N., and Fenton, R. A. (2016). The vasopressin type 2 receptor and prostaglandin receptors EP2 and EP4 can increase aquaporin-2 plasma membrane targeting through a cAMP-independent pathway. *Am. J. Physiol. Renal. Physiol.* 311, F935–F944. doi: 10.1152/ajprenal.00559.2015

Olesen, E. T., Rutzler, M. R., Moeller, H. B., Praetorius, H. A., and Fenton, R. A. (2011). Vasopressin-independent targeting of aquaporin-2 by selective E-prostanoid receptor agonists alleviates nephrogenic diabetes insipidus. *Proc. Natl. Acad. Sci. U. S. A.* 108, 12949–12954. doi: 10.1073/pnas.1104691108

Qi, Z., Cai, H., Morrow, J. D., and Breyer, M. D. (2006). Differentiation of cyclooxygenase 1- and 2-derived prostanoids in mouse kidney and aorta. *Hypertension* 48, 323–328. doi: 10.1161/01.HYP.0000231934.67549.b7

Rao, R., Zhang, M. Z., Zhao, M., Cai, H., Harris, R. C., Breyer, M. D., et al. (2005). Lithium treatment inhibits renal GSK-3 activity and promotes cyclooxygenase 2-dependent polyuria. *Am. J. Physiol. Renal. Physiol.* 288, F642–F649. doi: 10.1152/ajprenal.00287.2004

Saito, O., Guan, Y., Qi, Z., Davis, L. S., Komhoff, M., Sugimoto, Y., et al. (2003). Expression of the prostaglandin F receptor (FP) gene along the mouse genitourinary tract. *Am. J. Physiol Renal Physiol* 284, F1164–F1170. doi: 10.1152/ajprenal.00441.2002

Sakairi, Y., Jacobson, H. R., Noland, T. D., and Breyer, M. D. (1995). Luminal prostaglandin E receptors regulate salt and water transport in rabbit cortical collecting duct. *Am. J. Physiol.* 269, F257–F265. doi: 10.1152/ajprenal.1995.269.2.F257

Sakurai, M., Oishi, K., and Watanabe, K. (2005). Localization of cyclooxygenases-1 and−2, and prostaglandin F synthase in human kidney and renal cell carcinoma. *Biochem. Biophys. Res. Commun.* 338, 82–86. doi: 10.1016/j.bbrc.2005.08.194

Schlondorff, D., Satriano, J. A., and Schwartz, G. J. (1985). Synthesis of prostaglandin E2 in different segments of isolated collecting tubules from adult and neonatal rabbits. *Am. J. Physiol.* 248, F134–F144. doi: 10.1152/ajprenal.1985.248.1.F134

Schweer, H., Watzer, B., and Seyberth, H. W. (1994). Determination of seven prostanoids in 1 ml of urine by gas chromatography-negative ion chemical ionization triple stage quadrupole mass spectrometry. *J. Chromatogr.* 652, 221–227. doi: 10.1016/0378-4347(93)E0408-I

Sonntag, M., Wang, M. H., Huang, M. H., and Wong, N. L. (2004). Endothelin upregulates the expression of vasopressin V2 mRNA in the inner medullary collecting duct of the rat. *Metabolism* 53, 1177–1183. doi: 10.1016/j.metabol.2004.02.022

Stoff, J. S., Rosa, R. M., Silva, P., and Epstein, F. H. (1981). Indomethacin impairs water diuresis in the DI rat: role of prostaglandins independent of ADH. *Am. J. Physiol.* 241, F231–F237. doi: 10.1152/ajprenal.1981.241.3.F231

Takahashi, N., Takeuchi, K., Abe, T., Sugawara, A., and Abe, K. (1996). Immunolocalization of rat thromboxane receptor in the kidney. *Endocrinology* 137, 5170–5173. doi: 10.1210/endo.137.11.8895394

Tang, L., Zheng, S., Ren, H., He, D., Zeng, C., and Wang, W. E. (2017). Activation of angiotensin II type 1 receptors increases D4 dopamine receptor expression in rat renal proximal tubule cells. *Hypertens. Res.* 40, 652–657. doi: 10.1038/hr.2017.13

Terris, J., Ecelbarger, C. A., Nielsen, S., and Knepper, M. A. (1996). Long-term regulation of four renal aquaporins in rats. *Am. J. Physiol.* 40, F414–F422. doi: 10.1152/ajprenal.1996.271.2.F414

Van Balkom, B. W. M., Savelkoul, P. J., Markovich, D., Hofman, E., Nielsen, S., Van Der Sluijs, P., et al. (2002). The role of putative phosphorylation sites in the targeting and shuttling of the aquaporin-2 water channel. *J. Biol. Chem.* 277, 41473–41479. doi: 10.1074/jbc.M207525200

Vitzthum, H., Abt, I., Einhellig, S., and Kurtz, A. (2002). Gene expression of prostanoid forming enzymes along the rat nephron. *Kidney Int.* 62, 1570–1581. doi: 10.1046/j.1523-1755.2002.00615.x

Ware, J. S., Wain, L. V., Channavajjhala, S. K., Jackson, V. E., Edwards, E., Lu, R., et al. (2017). Phenotypic and pharmacogenetic evaluation of patients with thiazide-induced hyponatremia. *J. Clin. Invest.* 127, 3367–3374. doi: 10.1172/JCI89812

Watabe, A., Sugimoto, Y., Honda, A., Irie, A., Namba, T., Negishi, M., et al. (1993). Cloning and expression of cDNA for a mouse EP1 subtype of prostaglandin E receptor. *J. Biol. Chem.* 268, 20175–20178. doi: 10.1016/S0021-9258(20)80710-8

Wildman, S. S., Boone, M., Peppiatt-Wildman, C. M., Contreras-Sanz, A., King, B. F., Shirley, D. G., et al. (2009). Nucleotides downregulate aquaporin 2 *via* activation of apical P2 receptors. *J. Am. Soc. Nephrol.* 20, 1480–1490. doi: 10.1681/ASN.2008070686

Yamamoto, M., Share, L., and Shade, R. E. (1976). Vasopressin release during ventriculo-cisternal perfusion with prostaglandin E2 in the dog. *J. Endocrinol.* 71, 325–331. doi: 10.1677/joe.0.0710325

Yasui, M., Zelenin, S. M., Celsi, G., and Aperia, A. (1997). Adenylate cyclase-coupled vasopressin receptor activates AQP2 promoter *via* a dual effect on CRE and AP1 elements. *Am. J. Physiol.* 41, F443–F450. doi: 10.1152/ajprenal.1997.272.4.F443

Zelenina, M., Christensen, B. M., Palmer, J., Nairn, A. C., Nielsen, S., and Aperia, A. (2000). Prostaglandin E(2) interaction with AVP: effects on AQP2 phosphorylation and distribution. *Am. J. Physiol. Renal. Physiol.* 278, F388–F394. doi: 10.1152/ajprenal.2000.278.3.F388

Zook, T. E., and Strandhoy, J. W. (1981). Mechanisms of the natriuretic and diuretic effects of prostaglandin F2 alpha. *J. Pharmacol. Exp. Ther.* 217, 674–680.

Conflict of Interest: The authors declare that the research was conducted in the absence of any commercial or financial relationships that could be construed as a potential conflict of interest.

Publisher's Note: All claims expressed in this article are solely those of the authors and do not necessarily represent those of their affiliated organizations, or those of the publisher, the editors and the reviewers. Any product that may be evaluated in this article, or claim that may be made by its manufacturer, is not guaranteed or endorsed by the publisher.

frontiers in Physiology

REVIEW
published: 07 February 2022
doi: 10.3389/fphys.2022.770375

Aldosterone-Regulated Sodium Transport and Blood Pressure

*Akaki Tsilosani, Chao Gao and Wenzheng Zhang**

Department of Regenerative & Cancer Cell Biology, Albany Medical College, Albany, NY, United States

Aldosterone is a major mineralocorticoid steroid hormone secreted by glomerulosa cells in the adrenal cortex. It regulates a variety of physiological responses including those to oxidative stress, inflammation, fluid disruption, and abnormal blood pressure through its actions on various tissues including the kidney, heart, and the central nervous system. Aldosterone synthesis is primarily regulated by angiotensin II, K^+ concentration, and adrenocorticotrophic hormone. Elevated serum aldosterone levels increase blood pressure largely by increasing Na^+ re-absorption in the kidney through regulating transcription and activity of the epithelial sodium channel (ENaC). This review focuses on the signaling pathways involved in aldosterone synthesis and its effects on Na^+ reabsorption through ENaC.

Keywords: aldosterone, angiotensin II, ACTH, potassium, CYP11B2, ENaC, SGK1, Dot1

OPEN ACCESS

Edited by:
Weidong Wang,
Sun Yat-sen University, China

Reviewed by:
Ute Ingrid Scholl,
Charité Medical University of Berlin, Germany
Charles S. Wingo,
University of Florida, United States

***Correspondence:**
Wenzheng Zhang
zhangw1@mail.amc.edu

Specialty section:
This article was submitted to Renal and Epithelial Physiology, a section of the journal Frontiers in Physiology

Received: *03 September 2021*
Accepted: *06 January 2022*
Published: *07 February 2022*

Citation:
Tsilosani A, Gao C and Zhang W (2022) Aldosterone-Regulated Sodium Transport and Blood Pressure. Front. Physiol. 13:770375. doi: 10.3389/fphys.2022.770375

INTRODUCTION

Aldosterone is a mineralocorticoid steroid hormone first isolated and characterized in 1954 which functions mainly to raise blood pressure (Simpson et al., 1954). Aldosterone has been a topic of extensive research due to its crucial role in the regulation of fluid homeostasis. The secretion of aldosterone from glomerulosa cells (GC) located in the cortex of the adrenal glands is regulated by numerous factors, but the most prominent are extracellular K^+ concentration and the renin–angiotensin system (RAS; Bravo, 1977; Tremblay and LeHoux, 1993). Kidneys play a vital role in the initiation of RAS (**Figure 1**). Lowered blood pressure triggers the release of renin into the circulation from juxtaglomerular cells (JGC) in the afferent arteriole of the nephron (Friis et al., 2013). Renin release can also be triggered by the sympathetic nervous system and by decreased NaCl delivered to the distal tubule. Macula densa cells located in the juxtaglomerular apparatus sense low NaCl concentration of the filtrate and release paracrine signals that stimulate JGC (Peti-Peterdi and Harris, 2010). Renin is an aspartic protease that hydrolyzes liver-released proenzyme angiotensinogen creating angiotensin I, which undergoes further cleavage by carboxypeptidase angiotensin-converting enzyme (ACE) to create active angiotensin II (ANG II; Crisan and Carr, 2000). ANG II directly stimulates GC to secrete aldosterone. Multiple other factors are also able to regulate aldosterone synthesis, such as Klotho protein (KL), ACTH, natriuretic peptides (NPs), and circadian clock.

The nephron, the functional unit of the kidney, is the main target of aldosterone (**Figure 1**). Aldosterone exerts its action on the aldosterone-sensitive distal nephron (ASDN) comprising the late distal convoluted tubule (DCT2), the connecting tubule (CNT), and the collecting duct distal segments of the nephron (Bachmann et al., 1999; Reilly and Ellison, 2000). ASDN governs unidirectional Na^+ transport from the filtrate into the circulation and bi-directional

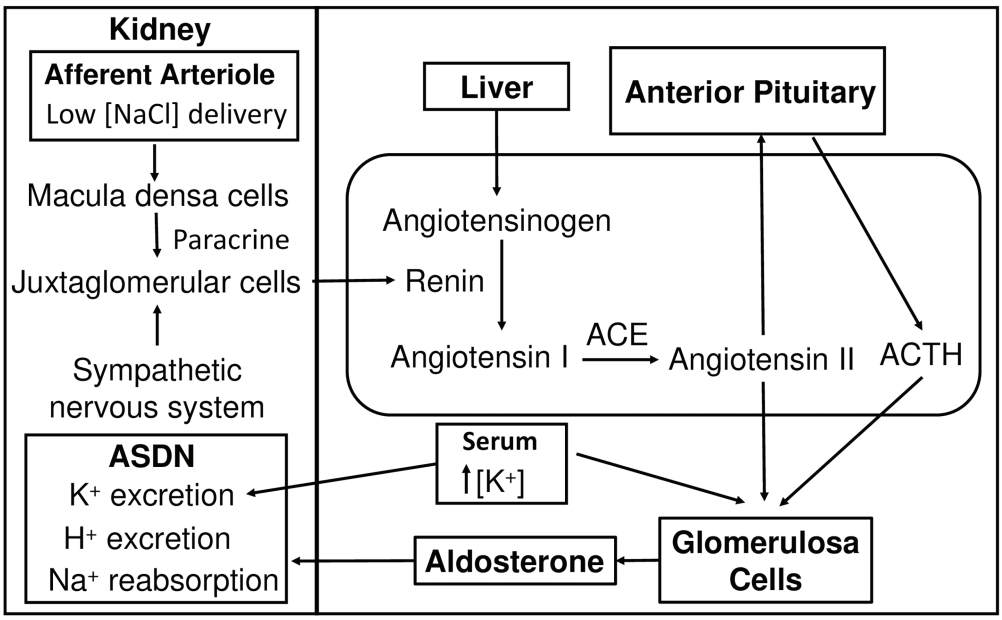

FIGURE 1 | Hypotension-induced activation of the renin-angiotensin-aldosterone system. As blood pressure drops, juxtaglomerular cells receive signals from macula densa cells and the sympathetic nervous system and secrete renin into the circulation. Renin hydrolyzes liver-synthesized angiotensinogen into inactive ANG I. ANG I is converted to active ANG II by ACE. ANG II stimulates glomerulosa cells in the adrenal cortex to secrete aldosterone and the anterior pituitary gland in the brain to secrete the ACTH, which also results in aldosterone production. High K^+ concentration stimulates aldosterone secretion from glomerulosa cells. Aldosterone increases Na^+ reabsorption, K^+ and H^+ secretion in ASDN leading to an increase in blood pressure. ANG I, angiotensin I; ANG II, angiotensin II; ACE, angiotensin-converting enzyme; ASDN, aldosterone-sensitive distal nephron.

K^+ transport (Gumz et al., 2015; Roy et al., 2015). There are two cell types in these segments: principal cells (PC) and intercalated cells (IC). PC are involved in Na^+ and K^+ transport while IC predominantly regulate acid–base homeostasis (Loffing and Kaissling, 2003; Roy et al., 2015). Aldosterone binds its mineralocorticoid receptor (MR; Shibata and Fujita, 2011). Almost all cells express MR, but whether they are affected by aldosterone depends on the presence of 11-β-hydroxysteroid dehydrogenase type-2 (11β-OHSD2), an enzyme that catalyzes 11-hydroxy-glucocorticoids to glucocorticoid metabolites (Funder et al., 1988). Mineralocorticoids and glucocorticoids have a common chemical structure and have equal binding affinity for MR (Arriza et al., 1987). To maintain the binding specificity in aldosterone-sensitive cells, 11β-OHSD2 catabolizes glucocorticoids rendering MR free to bind aldosterone. Both PC and IC express MR and 11β-OHSD2; however, PC has significantly higher levels of both proteins (Naray-Fejes-Toth et al., 1994; Kyossev et al., 1996). Ligand-bound MR translocates to the nucleus, where it regulates expression of its target genes (Naray-Fejes-Toth et al., 1994). Nevertheless, aldosterone also affects its target tissue through rapid non-genomic pathways (Arima et al., 2003; Funder, 2005; Funder, 2006).

Chronic elevation of aldosterone *via* intravenous injection has been demonstrated to increase arterial and mean circulatory filling pressure and resulted in significant water and sodium retention in dogs (Pan and Young, 1982). Aldosterone produces these effects by affecting electrolyte transport in both PC and IC. In PC, aldosterone regulates the expression and activity of epithelial sodium channel (ENaC) leading to increased Na^+ reabsorption from the filtrate into the circulation. Aldosterone also has significant

Abbreviations: ACE, Angiotensin-converting enzyme; ACTH, Adrenocorticotropic hormone; ACTHR, Adrenocorticotrophic hormone receptor; ADH, Antidiuretic hormone; ADS, Aldosterone synthase; ANG II, Angiotensin II; APA, Aldosterone-producing adenomas; ASDN, Aldosterone-sensitive distal nephron; AT1, Angiotensin receptor type I; CaMK, Ca^{2+}/Calmodulin-dependent protein kinase; CEH, Cholesterol ester hydrolase; CKD, Chronic kidney disease; CREB, cAMP-response binding element-binding protein; Cul3, Cullin 3; CYP21-21, Hydroxylase; DAG, Diacylglycerol; DOCP, Desoxycorticosterone pivalate; Dot1, Disruptor of telomeric silencing 1; EGFR, Epidermal growth factor receptor; EKODE, 2,13-epoxy-9-keto-10(trans)-octadecenoic acid; ENaC, Epithelial sodium channel; ERAD, Endoplasmic reticulum-associated degradation; ET-1, Endothelin 1; GC, Glomerulosa cell; GPCR, G protein-coupled receptor; HSB3D-3β, Hydroxysteroid dehydrogenase; ICL, Intercalated cells; IHC, Immunohistochemistry; IP3, Inositol 1,4,5 triphosphate; JGC, Juxtaglomerular cells; KCNJ5, Inward rectifier potassium channel; KCNSK3/9, Potassium channel subfamily K members 3 and 9; KL, Klotho protein; Kelch3, Kelch-like 3; MAPK, Mitogen activating protein kinase; MR, Mineralocorticoid receptor; Nedd4-2, Neural precursor cell expressed developmentally downregulated gene 4; PC, Principal cells; PDK1, Pyruvate dehydrogenase kinase 1; PH, Primary hyperaldosteronism; PHA, Pseudohypoaldosteronism type 1; PIP2, Phosphatidylinositol 4,5-bisphosphate; PKA, Protein kinase A; PKC, Protein kinase C; PKD, Protein kinase D; PM, Plasma membrane; PMA, Phorbol 12-myrstate 13-acetate; PLC, Phospholipase C; P450scc, Cholesterol side-chain cleavage enzyme; RAS, Renin angiotensin system; RT-PCR, Reverse transcription-polymerase chain reaction; SER, Smooth endoplasmic reticulum; SF1, Steroidogenic factor 1; StaR, Steroid acute regulatory protein; Tom22, Mitochondrial translocase receptor; WNK, With no lysine kinase; 11DCS-11, Deoxycorticosterone; 11β-OHSD2-11, β-hydroxysteroid dehydrogenase type-2.

effects on IC. There are two main types of IC: A-type and B-type; however, non-A type and non-B type have also been described (Teng-umnuay et al., 1996). Secretion of H^+ occurs in all types of IC through H+ ATPase and H^+/K^+-ATPase. H^+/K^+-ATPase exchanges H^+ for K^+ and consists of two catalytic subunits $HK\alpha_1$ and $HK\alpha_2$ (Gumz et al., 2010b). H^+/K^+-ATPase is located on the apical side of A-type IC and non-A and non-B IC and on basolateral side of B-type IC (Verlander et al., 1994; Roy et al., 2015). The expression of pendrin, a Na^+ independent Cl^-/HCO_3^- exchanger is also observed in non-A and non-B IC as well as in B-type IC (Tsuruoka and Schwartz, 1999). Mineralocorticoids influence both H^+ K^+-ATPase and pendrin. Mineralocorticoid excess increases the expression of $HK\alpha_2$ mRNA levels, blood K^+, and Cl^- and decreases blood Na^+ and HCO_3^+ levels (Greenlee et al., 2011). Aldosterone upregulates pendrin expression partially through regulated IC-specific MR phosphorylation (Shibata et al., 2013a; Hirohama et al., 2018). MR has an IC-specific phosphorylation site at S843. S843 phosphorylation prevents activation of MR. ANG II stimulates MR S843 dephosphorylation to increase its binding with aldosterone (Shibata et al., 2013a).

Due to its crucial function in the regulation of blood pressure, aldosterone imbalance is implicated in many diseases. Hyperaldosteronism (Crohn's disease) is a disease in which adrenal glands produce an excess of aldosterone leading to hypokalemia, hypertension, and chronic kidney disease (CKD; Papadopoulou-Marketou et al., 2000). In contrast, hypoaldosteronism is characterized by significantly low levels of aldosterone in the blood (DeFronzo, 1980). These two conditions represent both ends of the spectrum of diseases caused by aldosterone imbalance. Old age and obesity are part of this spectrum as they are risk factors of hypertension. Even though the principal targets of aldosterone are the epithelial cells of the kidney, it also exerts its action on non-epithelial cells of the heart, brain, and vasculature. Thus, imbalance in aldosterone levels result in cardiovascular diseases (Rocha and Funder, 2002; Yoshimoto and Hirata, 2007; Funder and Reincke, 2010; He and Anderson, 2013).

The goal of this article is to describe the recent understanding of aldosterone synthesis and its effect on electrolyte balance. Although aldosterone produces a variety of effects in multiple tissues, we focus on mechanisms by which aldosterone regulates sodium transport through ENaC in ASDN.

MECHANISMS OF ALDOSTERONE SECRETION

As mentioned above, ANG II, ACTH, and K^+ are the main signaling molecules that regulate the production of aldosterone. These inputs can have two modes of action: acute and chronic. The acute response happens within minutes and results in the rise of aldosterone due to activation of enzymes involved in the biosynthetic pathway and mobilization of cholesterol, while chronic effect takes place hours after the signal and involves alterations in gene expression.

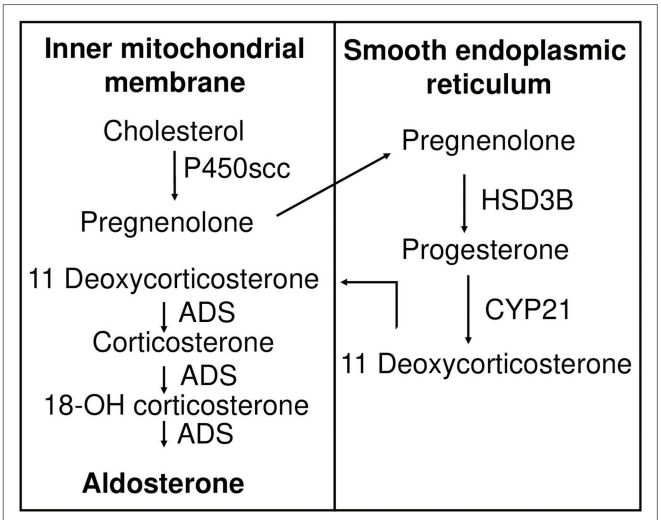

FIGURE 2 | Aldosterone biosynthesis pathway. Cholesterol is transported to the inner mitochondrial membrane, where it is hydroxylated and cleaved by cytochrome P450scc to produce pregnenolone. Pregnenolone is relocated to the membrane of smooth endoplasmic reticulum, where it is oxidized by HSB3D to produce progesterone. Eleven deoxycorticosterone is generated by CYP21-mediated hydroxylation of progesterone and moves back to the inner mitochondrial membrane, where it is subject to ADS-catalyzed sequential 11-hydroxylation, 18-hydroxylation, and 18-oxidation, producing corticosterone, 18-OH corticosterone, and finally aldosterone, respectively. P450scc, cytochrome P450 side chain cleavage enzyme; HSD3B, 3β-hydroxysteroid dehydrogenase; CYP 21, 21 hydroxylase; ADS, aldosterone synthase.

Aldosterone Biosynthesis Pathway

The adrenal cortex is divided into three functionally distinct regions: zona glomerulosa (production of mineralocorticoids), zona fasciculata (production of glucocorticoids), and zona reticularis (production of androgenic hormones; Vinson, 2016). Aldosterone biosynthesis occurs solely in the mitochondria of zona glomerulosa cells, which was demonstrated in the late 1980s where only isolated mitochondria of zona glomerulosa synthesized aldosterone (Ohnishi et al., 1988). This division of the adrenal cortex is crucial as adrenal steroid hormones are derived from cholesterol, thus functional zonation is one way to control the production of steroid hormones.

Like all other steroid hormones, aldosterone is derived from cholesterol (**Figure 2**). The first step in aldosterone biosynthesis is the transport of cholesterol to the inner mitochondrial membrane, where the cytochrome P450scc (cholesterol side-chain cleavage enzyme, encoded by *CYP11A1*), is located (Farkash et al., 1986). Through series of hydroxylation and cleavage, P450scc converts cholesterol into pregnenolone (Hume et al., 1984). 3β-hydroxysteroid dehydrogenase (HSD3B) and 21-hydroxylase (encoded by *CYP21* gene) convert pregnenolone to 11-deoxycorticosterone (11DCS). Electron microscopy and immunohistochemistry (IHC) demonstrated that these two enzymes reside on the membrane of the smooth endoplasmic reticulum (SER; Ishimura and Fujita, 1997). The last steps of the synthesis occur in mitochondria where aldosterone synthase (ADS), encoded by the *CYP11B2* gene, accomplishes

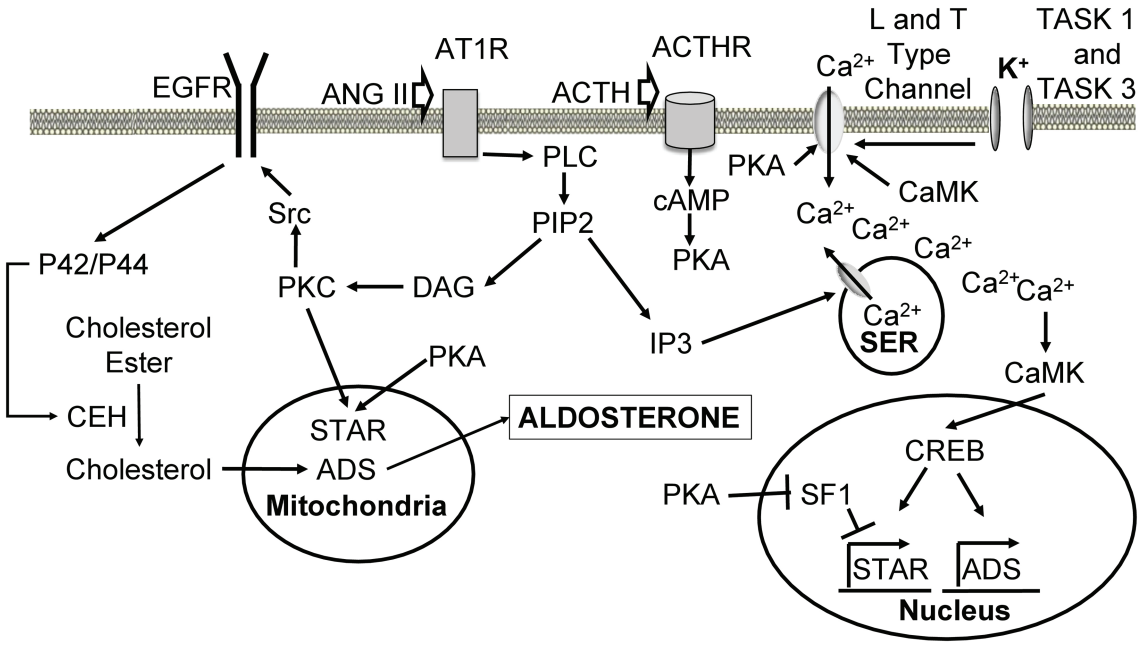

FIGURE 3 | Cellular mechanisms leading to increased aldosterone production upon angiotensin II, ACTH, and K^+ stimulation. Ang II binds to AT1R, leading to dissociation of the alpha subunit and activation of PLC. PLC hydrolyses PIP2 into DAG and IP3. IP3 binds to its receptor on the SER leading to the release of Ca^{2+} stores. Ca^{2+} activates CaMK, which causes an increase in ADS expression through CREB. DAG activates PKC to phosphorylate Src, which phosphorylates EGFR leading to activation of p42/p44 mitogen-activating protein kinase pathway. P42/p44 phosphorylates CEH to hydrolyze cholesterol esters located in the lipid droplets, making them available for transport to the inner mitochondrial membrane by STAR. PKC also phosphorylates and activates STAR. Cholesterol is used for aldosterone synthesis. ACTH binds its ACTHR leading to the activation of adenylate cyclase, which produces cAMP from ATP. cAMP triggers PKA-mediated phosphorylation and activation of STAR. PKA also phosphorylates L and T type Ca^{2+} channels causing Ca^{2+} influx. PKA increases the expression of ADS through relieving SF1-mediated inhibition of STAR. High extracellular K^+ concentration depolarizes cells and leads to activation of L and T type Ca^{2+} channels, which allow calcium inflow from the extracellular space. ANG II, angiotensin II; AT1R, angiotensin II receptor type 1; GPCR, G protein-coupled receptor; PLC, phospholipase C; PIP2, phosphatidylinositol 4,5-bisphosphate; DAG, diacylglycerol; IP3, inositol 1,4,5 triphosphate; SER, smooth endoplasmic reticulum; CaMK, Ca^{2+}/calmodulin-dependent protein kinase; ADS, aldosterone synthase; CREB, cAMP-response element binding protein; PKC, protein kinase C; EGFR, epidermal growth factor receptor; CEH, cholesterol ester hydrolase; STAR, steroid acute regulatory protein; ACTH, adrenocorticotropic hormone; ACTHR, adrenocorticotropic hormone receptor; SF1, steroidogenic factor 1.

11-hydroxylation, 18-hydroxylation, and 18-oxidation of 11DCS to produce aldosterone (Ishimura and Fujita, 1997). Thus, precursors of aldosterone are shuttled back and forth between mitochondria and SER. The actin cytoskeleton is thought to be involved in this transport (Sewer and Li, 2008). Steroid acute regulatory protein (STAR) regulates the rate-limiting step, conversion of cholesterol into pregnenolone. STAR is a 30 kDa protein that exists on the outer membrane of mitochondria and is responsible for transporting cholesterol to P450scc (Artemenko et al., 2001). STAR requires two phosphorylation events to reach its full activity (Fleury et al., 2004; Castillo et al., 2015). STAR plays a key role in aldosterone synthesis as mutations in *STAR* lead to deficiency in adrenal and gonadal aldosterone synthesis and are associated with lipoid congenital adrenal hyperplasia (Bose et al., 2000; Hasegawa et al., 2000).

Although the accepted notion is that aldosterone is produced solely by adrenal glands, some studies have shown that the heart can synthesize aldosterone in response to stress. RT-PCR analyses showed expression of *CYP11A1* and *CYP21*, the genes encoding steroidogenic enzymes involved in aldosterone synthesis, in adult human tissues (atria, ventricles, aorta apex, and intraventricular septum), and expression of *CYP11B2* in the aorta and fetal heart (Kayes-Wandover and White, 2000). Genetically hypertensive adrenalectomized and angiotensin II-treated rats had increased activity of ADS and produced aldosterone (Takeda et al., 2000). Interestingly, expression of *CYP11B2* was detectable by RT-PCR in failing human hearts, but not in normal hearts (Young et al., 2001). Bose et al. (2021) most recently reported a novel mitochondrial complex consisting of ADS, mitochondrial translocase receptor (Tom22), and STAR. This complex is responsible for the production of aldosterone in rat hearts upon stress. However, the ability of the heart to produce aldosterone is still controversial. More studies are needed to elucidate the mechanisms responsible for cardiac aldosterone synthesis.

Angiotensin II

ANG II triggers multiple signaling pathways (**Figure 3**) upon binding to its receptor angiotensin receptor type I (AT1), a G protein-coupled receptor (GPCR; Steckelings et al., 2010). The response of activated AT1 is similar to other GPCRs. ANG II binding leads to dissociation of GPCR subunits and

activation of phospholipase C beta (PLC), which hydrolyses phosphatidylinositol-4,5-bisphosphate (PIP2) to diacylglycerol (DAG) and inositol 1,4,5-trisphosphate (IP3). IP3 interacts with IP3 receptor on SER, opening Ca^{2+} channels and resulting in a transient increase in intracellular Ca^{2+} concentration (Taylor and Thorn, 2001). ANG II also causes the influx of calcium from the extracellular space (Spat et al., 1991). Ca^{2+} is thought to increase aldosterone production through Ca^{2+}/calmodulin-dependent protein kinase (CaMK).

To date, multiple CaMK have been identified (Takemoto-Kimura et al., 2017). CaMK I and II have been shown to play a role in aldosterone signaling in the adrenal gland. The role of CaMK in aldosterone production is crucial, as its inhibition abrogates the expression of ADS and aldosterone synthesis (Condon et al., 2002). IHC analysis shows that CaMK I is expressed in the adrenal cortex and transfection of adrenal cells with CaMK I coding sequence leads to increased expression of ADS (Condon et al., 2002). Compared to normal adrenal glands, aldosterone-producing adenomas (APA) have significantly higher mRNA and protein levels of CaMK I and ADS expression (Sackmann et al., 2011). KN62, a potent CaMK II inhibitor, decreased production of aldosterone in an adrenocortical tumor cell line (Clyne et al., 1995). CaMK II activation almost doubled in the presence of elevated ANG II or K^+ levels and diminished drastically upon KN62 treatment (Fern et al., 1995). CaMK II increases Ca^{2+} entry into the cell by phosphorylating Ser1198 in the II-III loop of a α1H T-type Ca^{2+} channel (Yao et al., 2006). CaMK can be phosphorylated by CaMK kinases (CaMKK). CaMKK are also crucial regulators of ADS expression (Nanba et al., 2015). Treatment with STO-609, a specific inhibitor of CaMKK, results in decreased expression of ADS and STAR in HAC15 human adrenal cell line. To determine whether CaMKK I or II are responsible for this effect, shRNA-mediated knockdown was performed. Knockdown of CaMKK II resulted in decreased ADS expression and aldosterone production, but silencing CaMKK I had no effect. Furthermore, IHC revealed expression of CaMKK II in GC (Nanba et al., 2015). One way by which ANG II increases aldosterone synthesis is through regulating transcription of ADS. cAMP-response element binding protein (CREB), a downstream target of CaMK I and II, appears to play an important role in this process (Tokumitsu et al., 1995; Nogueira and Rainey, 2010). ANG II stimulation leads to CaMK I nuclear localization, phosphorylation of CREB, and its association with ADS promoter, while mutations of CREB diminishes the effect of ANG II on ADS mRNA levels (Bassett et al., 2000; Sackmann et al., 2011).

Diacylglycerol seems to be a key second messenger of ANG II signaling as its inhibition dampens ANG II response in normal human adrenal GC (Natarajan et al., 1988a,b, 1990). DAG appears to control aldosterone synthesis through its downstream target protein kinase C (PKC), inhibition of which reduces aldosterone production upon ANG II stimulation (Kapas et al., 1995; Wang, 2006). PKC likely promotes steroidogenesis by increasing the expression and/or activity of STAR. Phorbol 12-myristate 13-acetate (PMA) activates PKC pathway, leading to increased STAR phosphorylation and expression, and progesterone synthesis (Manna et al., 2009). Protein kinase D (PKD) also promotes STAR expression since overexpression of constitutively active PKD mutant results in upregulated STAR mRNA expression (Olala et al., 2014). Both PKC and PKD effects on STAR expression are dependent on CREB (Manna et al., 2009; Olala et al., 2014).

ANG II has also been shown to increase the local concentration of cholesterol by promoting the uptake of lipoprotein cholesterol ester, increasing local mitochondrial cholesterol concentration, and activating cholesterol ester hydrolase (CEH; Cherradi et al., 2001, 2003). PKC is considered as an important factor in these effects because PMA-activated PKC pathway mimics ANG II-induced production of aldosterone, high-density lipoprotein receptor scavenger receptor class B type I, and the low-density lipoprotein receptor in the human NCI-H295R adrenocortical cell line (Pilon et al., 2003). PKC and Ca^{2+} activate nonreceptor Src kinase resulting in transactivation of epidermal growth factor receptor (EGFR) and activation of p42/p44 mitogen-activating protein kinase (MAPK) pathway (Hodges et al., 2007). ANG II stimulation activates p42/p44 MAPK in GC (Cherradi et al., 2003). P42/p44 likely phosphorylates CEH thereby increasing the concentration of cholesterol available for aldosterone synthesis. This process may be crucial, as the phosphorylation of CEH and production of pregnenolone are reduced upon p42/p44 inhibition (Cherradi et al., 2003).

Alteration in various aspects of ANG II signaling pathways has been implicated in APA. Patients with APA and idiopathic adrenal hyperplasia (IAH) have elevated serum AT1 autoantibodies, levels of which correlate with mean arterial pressure of the patients (Rossitto et al., 2013; Li et al., 2015). High levels of aldosterone production in APA seem to be the consequence of elevated serum autoantibodies. Human adrenocortical carcinoma cells incubated with IgG isolated from APA patient's serum-stimulated aldosterone production and *CYP11B2* expression (Piazza et al., 2019). Somatic mutations in G protein are also associated with APA. The gain of function mutation in *GNA11*, a gene coding the *α* subunit of the G protein, and its close homologue *GNAQ* have been identified in patients with APA. However, these mutations seem to be clinically silent without a codriver mutation in *CTNNB1*, a gene encoding catenin β1 (Zhou et al., 2021). The importance of aberrant activation of Wnt/β-catenin signaling pathways in APA is well characterized (Wang et al., 2017). An Increase in Ca^{2+} signaling also seems to play an important role in APA. Compared to the normal adrenal glands, APAs express higher levels of CaMKI and show increased CREB phosphorylation (Sackmann et al., 2011). Somatic mutations in *CACNA1D*, a gene encoding voltage-dependent, L type alpha 1D subunit, have been identified in APA (Azizan et al., 2013; Scholl et al., 2013). One of T-type Ca^{2+} channels, CaV3.2, is upregulated in APA and correlated with plasma aldosterone levels and *CYP11B2* expression (Felizola et al., 2014). Additionally, mutations in *CACNA1H*, a gene encoding the *α* subunit of CaV3.2 have been identified in APA and could be the cause of early-onset hypertension with primary aldosteronism (Scholl et al., 2015; Nanba et al., 2020). These mutations are thought to cause elevated Ca^{2+} influx, resulting in increased aldosterone synthesis (Reimer et al., 2016).

K^+

It is well known that extracellular K^+ concentration regulates ADS expression and aldosterone synthesis (Tremblay and LeHoux, 1993). Adrenal cortex and GC express potassium channel subfamily K members 3 and 9 (KCNSK3/9, also called TASK 1/3), which play a pivotal role in this process. These "leak" channels maintain a negative resting membrane potential by producing a background K^+ conductance (Quinn et al., 1987). However, increase in extracellular K^+ concentration or activation of GPCR inhibits these channels causing depolarization of the membrane leading to an influx of extracellular Ca^{2+} through L and T type Ca^{2+} channels (Lymangrover et al., 1982; Kanazirska et al., 1992; Varnai et al., 1995, 1998; Horvath et al., 1998; Bandulik et al., 2010). Consistently, inhibition of calcium in GC abolishes not only the effect of potassium but also the effect of ANG II (Rossier et al., 1998; Uebele et al., 2004). Interestingly, knockout of TASK 1 disrupted the functional zonation in the adrenal cortex suggesting that K^+ is a crucial factor in this process (Heitzmann et al., 2008). Effects of K^+ are independent of ANG II as high K^+ concentration was able to increase expression of ADS and the production of aldosterone in angiotensinogen knockout mice (Okubo et al., 1997). Thus, similar to ANG II, K^+ increases aldosterone synthesis through Ca^{2+} mediated pathways described above.

Disruption in K^+ transport in GC is implicated in multiple aldosterone-related diseases. The deletion of TASK 1 and 3 causes primary hyperaldosteronism (PH) and low-renin essential hypertension, respectively, due to constant depolarization of GC membrane in mice (Davies et al., 2008; Guagliardo et al., 2012). Mutations in another K^+ channel, a homotetrameric inward rectifier potassium channel (KCNJ5), are associated with (APA) and PH (Ishihara et al., 2009; Choi et al., 2011; Monticone et al., 2012; Mulatero et al., 2012; Williams et al., 2015). These mutations increase aldosterone production due to altered channel selectivity leading to depolarization of the membrane (Scholl et al., 2012; Oki et al., 2012b). In fact, ANG II-mediated regulation of aldosterone synthesis can occur by downregulating the expression of KCNJ5 (Kanazirska et al., 1992). Overexpression of KCNJ5 blunts ANG II stimulatory effects on membrane potential, intracellular Ca^{2+}, and expression of STAR and ADS (Oki et al., 2012a).

Adrenocorticotropic Hormone

ACTH is released by the anterior pituitary gland and binds ACTH receptor (ACTHR), a G protein-coupled receptor, on GC. Upon ligand binding ACTHR activates adenylate cyclase and cAMP, leading to activation of protein kinase A (PKA; Fridmanis et al., 2017). ACTH induces both acute and chronic stimulatory effects on aldosterone production. *In vitro* studies show that the acute effect occurs by the action of PKA, which phosphorylates STAR and increases its expression (Jo et al., 2005). Similarly to K^+ and ANG II, ACTH also elevates intracellular Ca^{2+} levels through PKA-mediated phosphorylation of L-type Ca^{2+} channels (Sculptoreanu et al., 1993).

The chronic response is mediated through steroidogenic factor-1 (SF1), which negatively regulates the transcription of *CYP11B2* and STAR in H295R and mouse Y1 cells (Gyles et al., 2001; Bassett et al., 2002). siRNA and shRNA-mediated silencing of SF1 drastically increased ADS expression and aldosterone production, while its overexpression elicited an opposite effect. Interestingly, these effects were observed in ANG II stimulated cells as well, suggesting that ANG II acts partially through regulating SF1 (Bassett et al., 2002; Ouyang et al., 2011). Moreover, SF1 deficient mice died shortly after birth and exhibited incomplete or absent development of adrenal glands and gonads, but showed normal expression of ADS in the placenta, which expressed both SF1 and ADS (Sadovsky et al., 1995) is phosphorylated on serine 203 by Erk1/2, resulting in its full activation (Hammer et al., 1999). The mechanism by which ACTH inhibits SF1 is not well understood. ACTH seems to have a biphasic effect on the activation of Erk1/2 and phosphorylation of SF1. Some reports show that ACTH induces Erk1/2 phosphorylation, which in turn phosphorylates SF1 abrogating its inhibitory effect on steroidogenesis (Hammer et al., 1999; Gyles et al., 2001; Le and Schimmer, 2001; Winnay and Hammer, 2006). On the other hand, ACTH-induced PKA activation led to *de novo* synthesis and activation of mitogen-activated protein kinase phosphatase 1 (MKP1), which dephosphorylated both SF1 and Erk1/2 (Bey et al., 2003; Sewer and Waterman, 2003; Winnay and Hammer, 2006). Both of these pathways seem to be important for aldosterone synthesis, as silencing of either Erk1/2 or MKP1 reduces steroidogenesis (Gyles et al., 2001; Sewer and Waterman, 2003).

While it is clear that ACTH induces aldosterone synthesis, this effect seems to be transient. At first ACTH increases aldosterone synthesis of GC cells; however, after continuous induction by ACTH, GC phenotype changes to that of zona fasciculata leading to a decrease in aldosterone synthesis (Crivello and Gill, 1983). *In vivo* findings are consistent with these results. Since ACTH is released in a pulsatile fashion in humans, Seely et al. (1989) investigated the effect of pulsatile and prolonged infusion of ACTH on aldosterone levels (Seely et al., 1989). Pulsatile infusion resulted in an increase and maintenance of aldosterone, while prolonged infusion led to sharp increase followed by a continuous decrease in aldosterone levels (Seely et al., 1989). These effects cannot be explained by sodium, potassium, angiotensin-II, or cortisol as their levels were the same in both groups, thus the mechanisms that govern these effects remain unknown. GC ADS mRNA levels were significantly increased and then dramatically decreased at 3 and 24 h after ACTH treatment in rats, respectively (Holland and Carr, 1993). Chronic infusion of ACTH for 2–3 weeks resulted in disappearance of GC and consequently a decrease in aldosterone production (Mitani et al., 1996). Similar transient effects of ACTH on aldosterone levels are seen in human male subjects (Fuchs-Hammoser et al., 1980).

Plasma renin and aldosterone follow a circadian rhythm because their levels fluctuated throughout the day, with their levels being highest in the mornings and lowest in the evenings in normal men (Cugini et al., 1981; Thosar et al., 2019). Similar results have been found in PA and essentially hypertensive

patients (Kem et al., 1973; Lamarre-Cliche et al., 2005). Interestingly, plasma aldosterone circadian rhythm (PACR) may be under androgenic rather than renin control, as aldosterone acrophase precedes renin and is associated with cortisol (Stern et al., 1986). Early studies in rats and human males found that dexamethasone treatment, a drug that suppresses ACTH, abolishes normal PACR, suggesting that it is under ACTH control (Hilfenhaus, 1976; Takeda et al., 1984). Multiple regression analysis of aldosterone-stimulating factors at 3 hourly intervals confirmed PACR dependence on ACTH rather than renin or ANG II (Takeda et al., 1984). The role of ACTH in PACR has also been implicated in PA (Sonoyama et al., 2014).

Klotho, Leptin, Natriuretic Peptides, and Circadian Rhythm

Although ANG II, K^+, and ACTH are thought to be the main stimulators of aldosterone production, there are other factors that can regulate this process, some of which are prominent in hypertensive conditions. Klotho protein (KL) is a single-pass transmembrane type 1 glycoprotein which has been regarded as an anti-aging molecule because as age increases serum KL levels decrease (Zhou et al., 2016). Low serum KL levels are associated with age-related disorders, such as coronary artery disease, atherosclerosis, myocardial infarction, and hypertension (Olejnik et al., 2018). Fischer et al. (2010) demonstrated the negative correlation between serum KL and aldosterone levels in mice. Hypomorphic KL ($KL^{+/-}$) mice showed increased ACTH, antidiuretic hormone (ADH), and aldosterone levels compared to WT. Interestingly, Ca^{2+} deficient diet alleviated the symptoms of hyperaldosteronism in $KL^{+/-}$ (Fischer et al., 2010). Overexpression of KL reduces aldosterone production while impaired expression of KL increases aldosterone production (Zhou et al., 2016). KL half deficiency seems to produce these effects by increasing the expression of ADS (Zhou et al., 2016). Similarly, there was a positive correlation between serum aldosterone level and CKD stage and a negative correlation between serum KL and aldosterone levels in human CKD patients, suggesting that the effect of KL on aldosterone in humans is similar to mice (Qian et al., 2018). Nevertheless, it remains unclear how a decrease in KL abundance results in an increase in aldosterone synthesis. One possibility is that KL acts as a negative regulator of aldosterone biosynthesis. This hypothesis can be tested *in vitro*. Reduced expression of key genes involved in aldosterone synthesis (such as ADS and STAR) as well as aldosterone levels in GC lines treated with KL would support this hypothesis.

Obesity is a well-known cause of hypertension and is characterized by high aldosterone levels (Goodfriend et al., 1998; Kurukulasuriya et al., 2011). One possibility is that adipocytes affect aldosterone production since they are active endocrine tissues (Ronti et al., 2006). Indeed, Ehrhart-Bornstein et al. (2003) showed that isolated adipocyte secretory products could dramatically increase aldosterone production independent of ANG II in adrenocortical cells (NCI-H295R; Ehrhart-Bornstein et al., 2003). 2,13-epoxy-9-keto-10 (trans)-octadecenoic acid (EKODE) has also been shown to increase aldosterone production in a GC line. EKODE is produced by the oxidation of linoleic acid by hepatocytes. Incubation of adrenal cells with EKODE increased aldosterone production independently of ANG II. Interestingly, adult humans have a positive correlation with blood EKODE and aldosterone levels (Goodfriend et al., 2004). However, EKODE is unlikely the molecule responsible for the effect seen by Ehrhart-Bornstein et al. (2003), as adipocyte secretory products were not oxidized by hepatocytes. A subsequent study showed that adipocyte-derived factors from SHR/cp rats (model of metabolic syndrome with hypertension) stimulate aldosterone production by increasing ADS expression and STAR activation despite ANG II receptor inhibition. Adipocyte-derived factors from normal rats failed to replicate these results (Nagase et al., 2006). These effects might be mediated by leptin, which is a protein hormone secreted by adipocytes and is abnormally high in obese individuals (Martinez-Rumayor et al., 2008; Huby et al., 2015). These *in vitro* studies have been validated and extended by *in vivo* investigations. For example, leptin infusion increased expression of ADS and serum aldosterone in a dose-dependent manner in mice with no effect on ANG II, K^+, and corticosterone levels (Belin de Chantemele et al., 2011; Huby et al., 2015). Huby et al. (2015) concluded that "leptin is a new regulatory factor of aldosterone secretion that acts directly in the adrenal cortex to promote ADS expression and aldosterone production" (Huby et al., 2015). The leptin stimulatory effect on ADS and aldosterone was not abolished upon administration of ANG II or β adrenergic receptor inhibitors in mice, further supporting the notion of leptin as a novel effector of aldosterone production (Huby et al., 2015). Leptin achieves these effects possibly through CaMK II, as leptin increased intracellular Ca^{2+} concentration and elevated expression calmodulin and CaMK II (Huby et al., 2015). Agreeably administration of leptin receptor antagonism abrogated leptin-mediated aldosterone secretion and lowered blood pressure in mice (Huby et al., 2016). These studies carry crucial importance as hypertension in the obese population is a devastating health issue (Kurukulasuriya et al., 2011).

Natriuretic peptides (NPs), cardiovascular peptides mostly secreted by the heart, play a role in vasodilation and fluid homeostasis. NPs have autocrine and paracrine signaling abilities and can function as endocrine components (Martinez-Rumayor et al., 2008). Due to their role in blood pressure, they have been hypothesized to regulate aldosterone secretion. Indeed, peptides in heart's crude extracts were able to inhibit aldosterone production by GC even upon ANG II and ACTH stimulation (Atarashi et al., 1984). Consequent studies confirmed these results *in vivo* and showed that atrial NPs dampen aldosterone response to ANG II in rats (Chartier et al., 1984; Atarashi et al., 1985). Similar effects were seen in human males. Administration of ANG II or ACTH alone raised blood pressure and plasma aldosterone levels. Simultaneous infusion of low levels of atrial NPs along with either ACTH or ANG II produced no significant change in blood pressure or aldosterone levels (Anderson et al., 1986; Weidmann et al., 1986; Cuneo et al., 1987). Another way by which NPs regulate blood pressure is by affecting renal filtration and renin release. Isolated rabbit afferent arterioles and suspended JGC exposed to NPs showed

drastic decrease in renin secretion (Itoh et al., 1987; Takagi et al., 1988). *In vivo* studies in dogs are consistent with these results as atrial NP infusion increased renal flow, glomerular filtration rate, sodium and potassium excretion and reduced blood pressure and renin production (Burnett et al., 1984; Maack et al., 1984). These results suggest that RAS and NPs may act as endogenous antagonists.

Circadian clock controls many physiological functions, such as blood pressure, immune response, and metabolism, potentially through four "circadian clock" proteins: period 1–3 (Per 1–3), Bmal1, Clock cryptochrome 1–2, and Clock (Eckel-Mahan and Sassone-Corsi, 2009; Agarwal, 2010; Bollinger et al., 2010; Dibner et al., 2010). Per1 regulates expression of αENaC in both aldosterone-dependent and-independent manners (Gumz et al., 2009, 2010a; Richards et al., 2013). It also coordinately regulates the expression of other genes involved in renal Na^+ reabsorption. These include Per1-mediated upregulation of Na^+-K^+-ATPase through Fxyd5 and downregulation of endothelin 1, which is a potential inhibitor of ENaC (Lubarski et al., 2005; Bugaj et al., 2008). Per-1 not only controls downstream targets of aldosterone, but also the plasma levels of aldosterone itself. This is supported by the findings in Per-1 knockout mice. Ablation of Per1 in mice led to decreased aldosterone and 3β-dehydrogenase isomerase levels (Richards et al., 2013). Interestingly, male mice appear to be more susceptible to adverse phenotypes of Per-1 KO than female mice. Treatment of Per-1 KO mice maintained on high salt diet with desoxycorticosterone pivalate (DOCP), an aldosterone analog, lead to increased mean arterial pressure and loss of normal circadian blood pressure (Solocinski et al., 2017). These effects are not observed in female Per-1 KO mice with similar treatments (Douma et al., 2019). This difference can be explained by endothelin 1. Male mice under high salt diet and DOCP treatment had decreased night/day ratio of urinary ET-1 and different ET-1 and ET-1 receptor gene expression compared to female mice (Douma et al., 2020).

MECHANISMS OF ALDOSTERONE ACTION

Upon binding to aldosterone, MR undergoes conformational changes, leading to dissociation from chaperone proteins, dimerization, and translocation to the nucleus, where it binds to the responsive elements in the promoter regions of target genes to regulate transcription. These changes in gene expression play a major role in the regulation of blood pressure, which is accomplished through the control of sodium reabsorption by regulating either transcription or the activity of the ENaC.

Epithelial Sodium Channel

Epithelial sodium channel is a highly selective Na^+ channel that is expressed on the apical membrane of various epithelial tissues, such as ASDN, colon, lungs, and sweat glands. ENaC is specific to Na^+ over other ions, such as K^+ and highly sensitive to diuretic amiloride. In the kidney, ENaC is exclusively expressed by principal cells where it reabsorbs Na^+ from the filtrate. Na^+ is then transported into the bloodstream by Na^+/K^+ ATPase located on the basolateral side leading to an increase in extracellular fluid volume and subsequently an increase in blood pressure (Pan and Young, 1982; Garty and Palmer, 1997).

Epithelial sodium channel is comprised of three subunits: *α*, *β*, and ϒ (Canessa et al., 1994). Although all three subunits are required for full functionality, the stoichiometric ratio of the subunits is still unclear. Originally it was thought that ENaC forms a tetramer with 2α, 1β, and 1ϒ subunits (Firsov et al., 1998; Dijkink et al., 2002; Anantharam and Palmer, 2007), but recent evidence suggests a 1:1:1 stoichiometric ratio (Staruschenko et al., 2005; Kashlan and Kleyman, 2011; Noreng et al., 2018). Each subunit spans the PM twice with both the COOH and NH_2 termini oriented toward the cytoplasm (Noreng et al., 2018). The COOH terminus of each subunit contains a PY domain that plays a crucial role in ENaC regulation. Deletions or mutations of this domain causes Liddle syndrome, a hereditary disease characterized by abnormally high ENaC activity and expression to the PM leading to hypertension (Firsov et al., 1996; Staub et al., 1996). For example, truncation or frameshift mutations in the COOH terminus of the βENaC were identified in subjects with Liddle syndrome (Shimkets et al., 1994) In contrast, mutations of the conserved glycine residues in the NH_2 terminus result in pseudohypoaldosteronism type 1 (PHA I), a life-threatening disease characterized by salt wasting, hyperkalemia, and metabolic acidosis (Chang et al., 1996).

Since ENaC dysfunction can be fatal, ENaC activity is tightly regulated. ENaC is primarily regulated by controlling its presence in the PM. ENaC is delivered to the PM through clathrin-mediated exocytosis and is removed from the PM through ubiquitylation. However, Na^+ transport is also regulated through proteolytic cleavage of ENaC (Rossier and Stutts, 2009). Multiple proteases have been shown to increase activity of ENaC including serine, cysteine, furin, and alkaline proteases (Chraibi et al., 1998; Hughey et al., 2004; Butterworth et al., 2012; Haerteis et al., 2012). Increase in activity of ENaC by proteolytic cleavage is achieved by releasing a 43-amino acid inhibitory domain of γ-subunit (Zachar et al., 2015). For a more comprehensive review please refer to (Kleyman and Eaton, 2020).

Serum Glucocorticoid-Induced Kinase 1

One of the keyways by which aldosterone regulates ENaC is through a serine/threonine serum glucocorticoid-induced kinase 1 (SGK1). SGK1 expression was increased 60 min post-injection of physiological dose of aldosterone (Chen et al., 1999; Bhargava et al., 2001). Although the levels of SGK1 rise in the presence of aldosterone, it must be phosphorylated at Thr256 and Ser422 by pyruvate dehydrogenase kinase 1 (PDK1) to be fully active (Park et al., 1999). Phosphorylation of a third highly conserved residue (Ser397) also increased SGK1 activity (Chen et al., 2009). mTORC2 was also identified as a kinase for SGK1 and is required for ENaC activation (Lu et al., 2010).

Neural precursor cell expressed developmentally downregulated gene 4 (Nedd4-2) is a ubiquitin ligase that plays

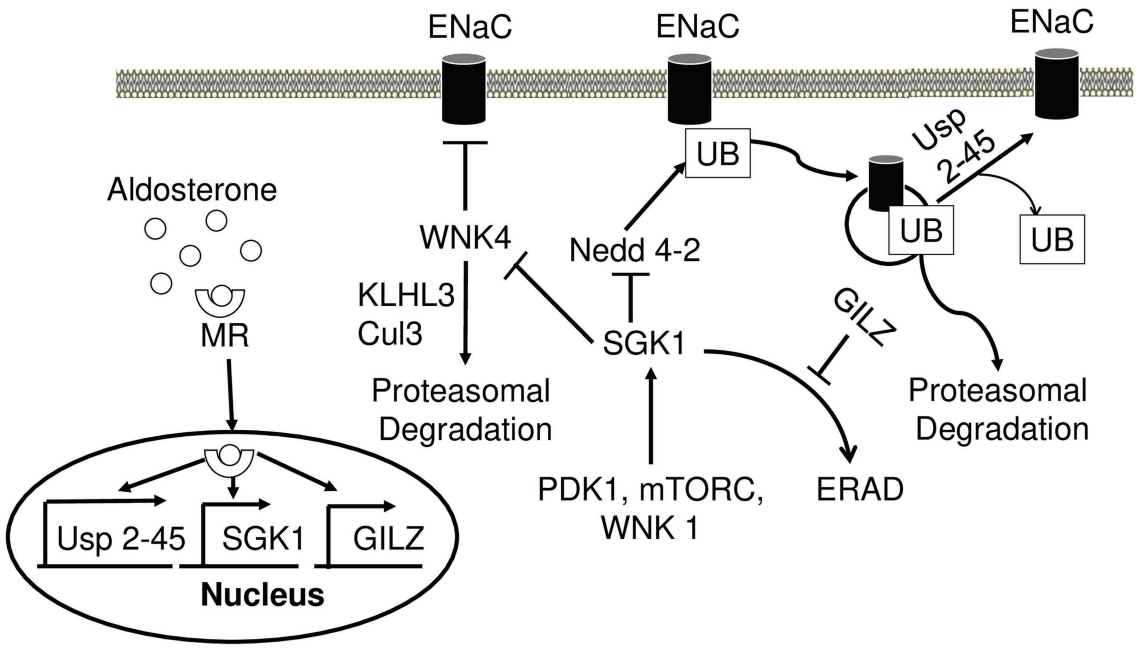

FIGURE 4 | Aldosterone regulates epithelial sodium channel (ENaC) activity and degradation. Aldosterone-bound MR translocates to the nucleus and induces transcription of USP 2-45, SGK1, and GILZ. SGK1 phosphorylates WNK4 and dampens its inhibitory action on ENaC activity. Nedd4-2 ubiquitinates ENaC and signals it for proteasomal degradation. Wnk4 is targeted to proteasomal degradation by KLHL3-Cul3 ubiquitin ligase. SGK1 inhibits this process by phosphorylating Nedd4-2 reducing its affinity to ENaC. USP2-45 removes UB from ENaC preventing its degradation. SGK1 requires phosphorylation events in order to achieve full activity, which is accomplished by PDK1, Wnk1, and mTORC. In the absence of aldosterone, SGK1 is subject to ERAD. However, in the presence of aldosterone GILZ inhibits this process increasing the stability of SGK1. MR, mineralocorticoid receptor; SGK1, serum glucocorticoid-induced kinase 1; GILZ, glucocorticoid-induced leucine zipper 1; Nedd4-2, Neural precursor cell expressed developmentally downregulated gene 4; ENaC, epithelial sodium channel; UB, ubiquitin; PDK1, pyruvate dehydrogenase kinase; ERAD, endoplasmic reticulum-associated degradation.

a crucial role in regulating ENaC (**Figure 4**). As mentioned above, the main mechanism by which the cell regulates Na^+ transport is by controlling the number of channels in the PM. In the absence of aldosterone, Nedd4-2 decreases this number by ubiquitinylating the PY motif of all three ENaC subunits and signaling the complex for degradation (Zhou et al., 2007). This mechanism is thought to be responsible for the development of Liddle syndrome, as the mutations of the PY motif prevent ubiquitination and lead to an increased number of ENaC in the PM (Rotin, 2008). In the presence of aldosterone, SGK1 phosphorylates Nedd4-2, impairing Nedd4-2 binding to ENaC, and instead increasing its affinity for 14–3–3 (Debonneville et al., 2001; Bhalla et al., 2005). Alongside SGK1, a deubiquitylating enzyme Usp2-45 also seems to be an important regulator of ENaC. Usp2-45 is upregulated upon aldosterone induction and de-ubiquitinates ENaC leading to higher cell surface expression of the channel (Fakitsas et al., 2007; Verrey et al., 2008).

WNK4 is a serine/threonine kinase, mutations of which have been identified as a potential cause for PHA II (Wilson et al., 2001; Lopez-Cayuqueo et al., 2018). The underlying mechanism behind this disease may be explained by a negative regulation of ENaC through WNK4 (**Figure 4**). Both *in vivo* and *in vitro* studies have shown a significant reduction of ENaC surface expression upon interacting with WNK4 (Ring et al., 2007a). ENaC-WNK4 interaction requires an intact COOH terminus of β and ϒ subunits but not the PY motif, differing from ENaC-Nedd4-2 interaction requiring the PY motif. In the presence of aldosterone, SGK1 phosphorylates WNK4 and abrogates its negative regulation of ENaC (Ring et al., 2007a,b; Yu et al., 2013). The clinical relevance of ENaC-WNK4 interaction is illustrated by PHA II-associated R1185C mutation of WNK4, which decreases WNK4's inhibitory effect on ENaC by enhancing SGK1-mediated phosphorylation of WNK4 at S1217 (Na et al., 2013). Aldosterone also increases the expression of kidney-specific WNK1 (kinase-deficient variant), which consequently increases transepithelial Na^+ transport in cortical collecting duct cells potentially through regulation of ENaC (Naray-Fejes-Toth et al., 2004). WNK1 appears to increase ENaC surface expression by activating SGK1 through a non-catalytic mechanism (Xu et al., 2005a,b). This appears to be dependent on phosphatidylinositol 3-kinase, as its inhibition abrogates this effect (Xu et al., 2005b). Both WNK4 and WNK1 are implicated in PHA II (Wilson et al., 2001). Two other genes, *KLHL3* and *CUL3,* encoding kelch-like 3 (Kelch) and cullin 3 (cul3) proteins, respectively, may explain the mechanism by which WNK4 and WNK1 cause PHA II. Cul3 is an integral member of cul3-RING ubiquitin ligase, an E3 ubiquitin ligase. It forms a scaffold for the RING finger protein and ubiquitin conjugating enzyme E2 (Genschik et al., 2013). Kelch is an adaptor protein that connects cul3-RING ubiquitin ligase to its targets (Ji and Prive, 2013).

Mutations in *KLHL3* and *CUL3* have been implicated in PHA II and appear to cause hypertension and electrolyte disbalance (Boyden et al., 2012; Louis-Dit-Picard et al., 2012). One mechanism by which these mutations cause PHA II is through Wnk1 and Wnk4, as both of these proteins are targets of Cul3-RING ubiquitin ligase (Ohta et al., 2013; Shibata et al., 2013b). PHA II causing mutations in KLHL3 decreases Wnk4 binding to Cul3-RING ubiquitin ligase, decreasing WNK4 degradation and increasing its levels resulting in hypertension (Mori et al., 2013; Wakabayashi et al., 2013; Wu and Peng, 2013; Susa et al., 2014).

SGK1 is expressed in many tissues, but it has a short half-life under basal conditions (Brickley et al., 2002). Upon aldosterone stimulation, A6 cells dramatically increased SGK1 expression (Chen et al., 1999). SGK1 contains a short hydrophobic motif that targets the protein to the ER where it is degraded by ER-associated degradation (ERAD). The deletion of this motif redistributes the protein into the cytoplasm and increases its half-life (Brickley et al., 2002; Arteaga et al., 2006; Belova et al., 2006; Bogusz et al., 2006). In the presence of aldosterone, this negative regulation of SGK1 is abrogated due to the action of glucocorticoid-induced leucine zipper 1 (GILZ1), the levels of which rise in the presence of the steroid hormone (Soundararajan et al., 2005). GILZ1 reduces ER localization of SGK1 and recruits it to ENaC leading to significantly lower ERAD of SGK1 and higher levels of Na^+ transport (Soundararajan et al., 2010; Rashmi et al., 2017).

Dot1a

In addition to controls of proteolytic cleavage and subcellular localization, ENaC is also regulated at the transcriptional level *via* the disruptor of telomeric silencing 1 (Dot1), a histone H3 K79 methyltransferase. Dot1 can mono, di or tri- methylate H3 K79 leading to a wide range of epigenetic control of gene expression. Dot1 is implicated in complex cellular processes, such as cell cycle regulation, cell proliferation, DNA replication, apoptosis, telomeric silencing, and blood pressure control. Dot1 has at least five isoforms (a–e) created by alternative splicing, out of which Dot1a is the most prominent in mouse kidneys (Nguyen and Zhang, 2011). Deletion of *Dot1* specifically in the connecting tubules and collecting ducts facilitated development of kidney fibrosis and reduced kidney function under three experimental settings (streptozotocin-induced diabetes, during normal aging, and after unilateral ureteral obstruction) in mice (Zhang et al., 2020).

Dot1a interacts with Af9, a putative transcription factor. Under basal conditions, Dot1a-Af9 complex binds to the specific regions of *αENaC*, where it promotes H3 K79 methylation associated with promoter and represses *αENaC* transcription (Zhang et al., 2007). Aldosterone downregulates Dot1a and Af9 expression and impairs Dot1a-Af9 interaction by SGK1-mediated Af9 phosphorylation. Consequently, the abundance of Dot1a-Af9 complex at the *αENaC* is reduced, leading to histone H3 K79 hypomethylation and derepression of *αENaC* (Zhang et al., 2007). Dot1a-Af9 complex is also negatively regulated under the basal condition through Af17, another Dot1a binding partner. Af17 competes with Af9 for binding Dot1a and facilitates Dot1a nuclear export into the cytoplasm for possible degradation, resulting in relief of Dot1a-Af9-mediated repression and an increase in *αENaC* expression (**Figure 5**; Reisenauer et al., 2009; Wu et al., 2011). Analyses of $Af17^{-/-}$ mice illustrated the significance of Dot1a-Af9-Af17 complexes in Na^+ and blood pressure handing (Chen et al., 2011). $Af17^{-/-}$ vs. WT mice had elevated histone H3 K79 methylation at the *αENaC* promoter and reduced ENaC function. The impaired ENaC function stemmed from reduced ENaC expression at both mRNA and protein levels, fewer active channels, lower open probability, and decreased effective activity. As a result, $Af17^{-/-}$ vs. WT mice displayed lower blood pressure, higher urine volume, and more sodium excretion in spite of mildly increased plasma concentrations of aldosterone. Af17 deficiency with respect to sodium handling and blood pressure, however, was completely compensated by high levels of plasma aldosterone induced by multiple methods (Chen et al., 2011). Hence, Af17 is considered as a potential locus for the maintenance of sodium and BP homeostasis and H3K79 methylation is directly linked to these processes. The potential genetic–epigenetic interplay of DOT1-AF9-AF17 in human blood pressure control was well-reviewed (Zhang et al., 2013).

DISCUSSION

Aldosterone is a vital steroid hormone produced by the adrenal glands that regulates blood pressure by affecting electrolyte and fluid balance. Aldosterone is synthesized from cholesterol in the mitochondria and SER of GC upon decreased blood pressure, although some reports suggest that heart tissue is also capable of aldosterone secretion. Lowered blood pressure results in activation of ANG II. ANG II binds its receptor on GC, resulting in the production of IP3 and DAG. IP3 and DAG raise intracellular Ca^{2+} concentration and activate PKC and p42/p44 MAPK pathway, respectively. Ca^{2+} activates CaMK, which stimulates the expression of ADS. PKC and p42/p44 are involved in the activation of STAR and CEH increasing the rate of aldosterone production. High extracellular K^+ concentration also stimulates aldosterone synthesis. At physiological serum K^+ levels, K^+ moves out of the GC through TASK 1 and three maintaining negative membrane potential. However, in the presence of ANG II or high extracellular K^+ concentration, TASK 1 and 3 are inhibited which causes depolarization of the cell leading to the entry of extracellular Ca^{2+}. These initiate similar signaling pathways as ANG II leading to aldosterone synthesis. ACTH has both acute and chronic effects on aldosterone synthesis. It activates PKA, which phosphorylates STAR and activates it. ACTH transiently stimulates aldosterone production by increasing intracellular Ca^{2+} levels. ACTH is thought to mediate ADS expression by affecting the activity of SF1; however, the mechanism is not fully understood. Aldosterone secretion is regulated by other, nontraditional factors, such as KL, leptin, natriuretic peptides, and circadian clock. KL is a protein that is associated with aging as its levels decrease with age and inversely correlates with age-related disorders. Studies in mice show that deficiency

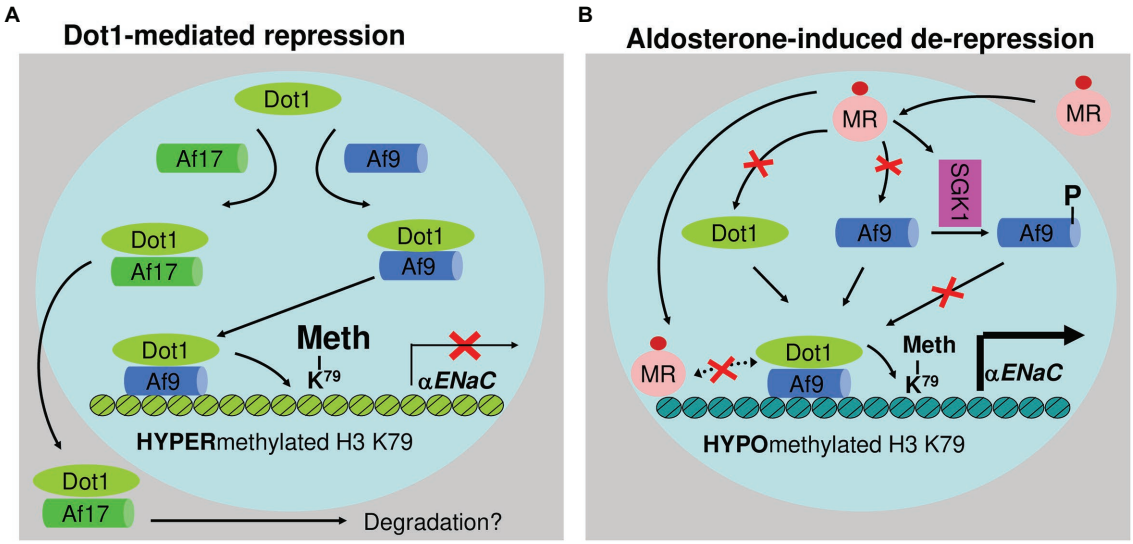

FIGURE 5 | Epigenetic control of αENaC transcription. Under basal conditions **(A)**, Af9 recruits Dot1a to form a nuclear complex, which indirectly or directly through Af9 DNA-binding activity binds specific sites of the αENaC promoter, leading to hypermethylation of histone H3 K79 and repression of αENaC transcription. Af17 relieves the repression by competing with Af9 for binding Dot1a and promoting Dot1a redistribution from the nucleus to cytoplasm. In the presence of aldosterone **(B)**, αENaC transcription is induced by a variety of mechanisms. Through the classical action, aldosterone binds and activates the mineralocorticoid receptor to bind the glucocorticoid response element in the αENaC promoter and transactivate αENaC. In parallel, aldosterone releases Dot1a–Af9-mediated repression by reducing the formation of the complex through three mechanisms: downregulating Dot1a and Af9 expression presumably via nuclear receptor-dependent or -independent (not shown) mechanisms, decreasing the Dot1a–Af9 interaction via SGK1-mediated phosphorylation of Af9 at Ser435, and counterbalancing Dot1a–Af9 complex by activating MR to compete for binding Af9. These actions collectively result in histone H3 K79 hypomethylation at specific subregions of the αENaC promoter. In all cases, Af9-free Dot1a binds DNA nonspecifically and catalyzes histone H3 K79 methylation throughout the genome under basal conditions (not shown). Revised from Chen et al. (2015). Dot1a: disruptor of telomeric silencing 1a. Meth: methylation. αENaC: α epithelial sodium channel. NR: nuclear hormone receptor. SGK1: serum glucocorticoid-induced kinase 1.

in KL stimulates aldosterone production by the adrenal gland in an ANG II-independent manner. Clinical studies in CKD patients confirm the negative correlation between KL and ANG II serum levels. Leptin is a hormone produced by adipocytes and its plasma leptin levels are high in obese patients. Leptin binds to the leptin receptor on GC and stimulates the secretion of aldosterone by activating CaMK pathway. Hypertension in obese individuals is often independent of ANG II, K^+, and ACTH concentrations. Since leptin increases aldosterone production despite inhibition of ANG II and ACTH receptors, it can explain the phenomenon seen in obese individuals. Natriuretic peptides are thought to be endogenous antagonists to RAS as their administration decreases aldosterone production despite ANG II or ACTH stimulation. Aldosterone levels tend to rise in the morning and fall in the evening, suggesting the role of PACR. One of core circadian clock proteins, Per-1 has been shown to regulate not only Na^+ transport in ASDN, but also plasma aldosterone levels.

Aldosterone stimulates Na^+ transport by regulating the expression and activity of ENaC. Aldosterone stimulates the expression and stability of SGK1, which directly and indirectly increases the expression and activity of ENaC. SGK1 phosphorylates Nedd4-2, a ubiquitin ligase that ubiquitinates a PY motif of ENaC and targets it for degradation. Upon phosphorylation by SGK1, Nedd4-2 loses its affinity to ENaC thereby increasing the number of channels in the PM. SGK1 also phosphorylates WNK4, a negative regulator of ENaC activity. Upon phosphorylation by SGK1, WNK4 weakens its interaction with ENaC. SGK1 itself is expressed in many tissues but is immediately targeted for degradation by ERAD. Aldosterone prevents its degradation by increasing the expression of GILZ, which reduces ER localization of SGK1 and directs it to ENaC. Dot1a-Af9-Af17-mediated epigenetic control of ENaC and Na^+ handling is regulated in aldosterone-dependent and -independent manners. The former involves reduction of Dot1a-Af9 complex formation through aldosterone-induced downregulation of Dot1a and Af9 and SGK1-mediated Af9 phosphorylation. The latter is achieved by competitive protein–protein interactions between Dot1a-Af9 and Dot1a-Af17.

AUTHOR CONTRIBUTIONS

AT and WZ: writing. CG, AT, and WZ: review and editing. WZ: supervision. All authors contributed to the article and approved the submitted version.

FUNDING

This work was supported by the following grants: National Institutes of Health Grants DK080236 (to WZ).

REFERENCES

Agarwal, R. (2010). Regulation of circadian blood pressure: from mice to astronauts. *Curr. Opin. Nephrol. Hypertens.* 19, 51–58. doi: 10.1097/MNH.0b013e3283336ddb

Anantharam, A., and Palmer, L. G. (2007). Determination of epithelial Na^+ channel subunit stoichiometry from single-channel conductances. *J. Gen. Physiol.* 130, 55–70. doi: 10.1085/jgp.200609716

Anderson, J. V., Struthers, A. D., Payne, N. N., Slater, J. D., and Bloom, S. R. (1986). Atrial natriuretic peptide inhibits the aldosterone response to angiotensin II in man. *Clin. Sci.* 70, 507–512.

Arima, S., Kohagura, K., Xu, H. L., Sugawara, A., Abe, T., Satoh, F., et al. (2003). Nongenomic vascular action of aldosterone in the glomerular microcirculation. *J. Am. Soc. Nephrol.* 14, 2255–2263. doi: 10.1097/01.ASN.0000083982.74108.54

Arriza, J. L., Weinberger, C., Cerelli, G., Glaser, T. M., Handelin, B. L., Housman, D. E., et al. (1987). Cloning of human mineralocorticoid receptor complementary DNA: structural and functional kinship with the glucocorticoid receptor. *Science* 237, 268–275.

Arteaga, M. F., Wang, L., Ravid, T., Hochstrasser, M., and Canessa, C. M. (2006). An amphipathic helix targets serum and glucocorticoid-induced kinase 1 to the endoplasmic reticulum-associated ubiquitin-conjugation machinery. *Proc. Natl. Acad. Sci. U. S. A.* 103, 11178–11183. doi: 10.1073/pnas.0604816103

Artemenko, I. P., Zhao, D., Hales, D. B., Hales, K. H., and Jefcoate, C. R. (2001). Mitochondrial processing of newly synthesized steroidogenic acute regulatory protein (StAR), but not total StAR, mediates cholesterol transfer to cytochrome P450 side chain cleavage enzyme in adrenal cells. *J. Biol. Chem.* 276, 46583–46596. doi: 10.1074/jbc.M107815200

Atarashi, K., Mulrow, P. J., and Franco-Saenz, R. (1985). Effect of atrial peptides on aldosterone production. *J. Clin. Invest.* 76, 1807–1811.

Atarashi, K., Mulrow, P. J., Franco-Saenz, R., Snajdar, R., and Rapp, J. (1984). Inhibition of aldosterone production by an atrial extract. *Science* 224, 992–994.

Azizan, E. A., Poulsen, H., Tuluc, P., Zhou, J., Clausen, M. V., Lieb, A., et al. (2013). Somatic mutations in ATP1A1 and CACNA1D underlie a common subtype of adrenal hypertension. *Nat. Genet.* 45, 1055–1060. doi: 10.1038/ng.2716

Bachmann, S., Bostanjoglo, M., Schmitt, R., and Ellison, D. H. (1999). Sodium transport-related proteins in the mammalian distal nephron – distribution, ontogeny and functional aspects. *Anat. Embryol.* 200, 447–468.

Bandulik, S., Penton, D., Barhanin, J., and Warth, R. (2010). TASK1 and TASK3 potassium channels: determinants of aldosterone secretion and adrenocortical zonation. *Horm. Metab. Res.* 42, 450–457. doi: 10.1055/s-0029-1243601

Bassett, M. H., Zhang, Y., Clyne, C., White, P. C., and Rainey, W. E. (2002). Differential regulation of aldosterone synthase and 11beta-hydroxylase transcription by steroidogenic factor-1. *J. Mol. Endocrinol.* 28, 125–135. doi: 10.1677/jme.0.0280125

Bassett, M. H., Zhang, Y., White, P. C., and Rainey, W. E. (2000). Regulation of human CYP11B2 and CYP11B1: comparing the role of the common CRE/Ad1 element. *Endocr. Res.* 26, 941–951. doi: 10.3109/07435800009048620

Belin de Chantemele, E. J., Mintz, J. D., Rainey, W. E., and Stepp, D. W. (2011). Impact of leptin-mediated sympatho-activation on cardiovascular function in obese mice. *Hypertension* 58, 271–279. doi: 10.1161/HYPERTENSIONAHA.110.168427

Belova, L., Sharma, S., Brickley, D. R., Nicolarsen, J. R., Patterson, C., and Conzen, S. D. (2006). Ubiquitin-proteasome degradation of serum- and glucocorticoid-regulated kinase-1 (SGK-1) is mediated by the chaperone-dependent E3 ligase CHIP. *Biochem. J.* 400, 235–244. doi: 10.1042/BJ20060905

Bey, P., Gorostizaga, A. B., Maloberti, P. M., Lozano, R. C., Poderoso, C., Cornejo Maciel, F., et al. (2003). Adrenocorticotropin induces mitogen-activated protein kinase phosphatase 1 in Y1 mouse adrenocortical tumor cells. *Endocrinology* 144, 1399–1406. doi: 10.1210/en.2002-220987

Bhalla, V., Daidie, D., Li, H., Pao, A. C., LaGrange, L. P., Wang, J., et al. (2005). Serum- and glucocorticoid-regulated kinase 1 regulates ubiquitin ligase neural precursor cell-expressed, developmentally down-regulated protein 4-2 by inducing interaction with 14-3-3. *Mol. Endocrinol.* 19, 3073–3084. doi: 10.1210/me.2005-0193

Bhargava, A., Fullerton, M. J., Myles, K., Purdy, T. M., Fundero, J. W., Pearce, D., et al. (2001). The serum- and glucocorticoid-induced kinase is a physiological mediator of aldosterone action. *Endocrinology* 142, 1587–1594. doi: 10.1210/endo.142.4.8095

Bogusz, A. M., Brickley, D. R., Pew, T., and Conzen, S. D. (2006). A novel N-terminal hydrophobic motif mediates constitutive degradation of serum- and glucocorticoid-induced kinase-1 by the ubiquitin-proteasome pathway. *FEBS J.* 273, 2913–2928. doi: 10.1111/j.1742-4658.2006.05304.x

Bollinger, T., Bollinger, A., Oster, H., and Solbach, W. (2010). Sleep, immunity, and circadian clocks: a mechanistic model. *Gerontology* 56, 574–580. doi: 10.1159/000281827

Bose, H. S., Sato, S., Aisenberg, J., Shalev, S. A., Matsuo, N., and Miller, W. L. (2000). Mutations in the steroidogenic acute regulatory protein (StAR) in six patients with congenital lipoid adrenal hyperplasia. *J. Clin. Endocrinol. Metab.* 85, 3636–3639. doi: 10.1210/jc.85.10.3636

Bose, H. S., Whittal, R. M., Marshall, B., Rajapaksha, M., Wang, N. P., Bose, M., et al. (2021). A novel mitochondrial complex of aldosterone synthase, steroidogenic acute regulatory protein, and Tom22 synthesizes aldosterone in the rat heart. *J. Pharmacol. Exp. Ther.* 377, 108–120. doi: 10.1124/jpet.120.000365

Boyden, L. M., Choi, M., Choate, K. A., Nelson-Williams, C. J., Farhi, A., Toka, H. R., et al. (2012). Mutations in kelch-like 3 and cullin 3 cause hypertension and electrolyte abnormalities. *Nature* 482, 98–102. doi: 10.1038/nature10814

Bravo, E. L. (1977). Regulation of aldosterone secretion: current concepts and newer aspects. *Adv. Nephrol. Necker Hosp.* 7, 105–120.

Brickley, D. R., Mikosz, C. A., Hagan, C. R., and Conzen, S. D. (2002). Ubiquitin modification of serum and glucocorticoid-induced protein kinase-1 (SGK-1). *J. Biol. Chem.* 277, 43064–43070. doi: 10.1074/jbc.M207604200

Bugaj, V., Pochynyuk, O., Mironova, E., Vandewalle, A., Medina, J. L., and Stockand, J. D. (2008). Regulation of the epithelial Na^+ channel by endothelin-1 in rat collecting duct. *Am. J. Physiol. Renal Physiol.* 295, F1063–F1070. doi: 10.1152/ajprenal.90321.2008

Burnett, J. C. Jr., Granger, J. P., and Opgenorth, T. J. (1984). Effects of synthetic atrial natriuretic factor on renal function and renin release. *Am. J. Phys.* 247, F863–F866.

Butterworth, M. B., Zhang, L., Heidrich, E. M., Myerburg, M. M., and Thibodeau, P. H. (2012). Activation of the epithelial sodium channel (ENaC) by the alkaline protease from *Pseudomonas aeruginosa*. *J. Biol. Chem.* 287, 32556–32565. doi: 10.1074/jbc.M112.369520

Canessa, C. M., Schild, L., Buell, G., Thorens, B., Gautschi, I., Horisberger, J. D., et al. (1994). Amiloride-sensitive epithelial Na+ channel is made of three homologous subunits. *Nature* 367, 463–467.

Castillo, A. F., Orlando, U., Helfenberger, K. E., Poderoso, C., and Podesta, E. J. (2015). The role of mitochondrial fusion and StAR phosphorylation in the regulation of StAR activity and steroidogenesis. *Mol. Cell. Endocrinol.* 408, 73–79. doi: 10.1016/j.mce.2014.12.011

Chang, S. S., Grunder, S., Hanukoglu, A., Rosler, A., Mathew, P. M., Hanukoglu, I., et al. (1996). Mutations in subunits of the epithelial sodium channel cause salt wasting with hyperkalaemic acidosis, pseudohypoaldosteronism type 1. *Nat. Genet.* 12, 248–253.

Chartier, L., Schiffrin, E., Thibault, G., and Garcia, R. (1984). Atrial natriuretic factor inhibits the stimulation of aldosterone secretion by angiotensin II, ACTH and potassium in vitro and angiotensin II-induced steroidogenesis in vivo. *Endocrinology* 115, 2026–2028.

Chen, S. Y., Bhargava, A., Mastroberardino, L., Meijer, O. C., Wang, J., Buse, P., et al. (1999). Epithelial sodium channel regulated by aldosterone-induced protein sgk. *Proc. Natl. Acad. Sci. U. S. A.* 96, 2514–2519.

Chen, W., Chen, Y., Xu, B. E., Juang, Y. C., Stippec, S., Zhao, Y., et al. (2009). Regulation of a third conserved phosphorylation site in SGK1. *J. Biol. Chem.* 284, 3453–3460. doi: 10.1074/jbc.M807502200

Chen, L., Wu, H., Pochynyuk, O. M., Reisenauer, M. R., Zhang, Z., Huang, L., et al. (2011). Af17 deficiency increases sodium excretion and decreases blood pressure. *J. Am. Soc. Nephrol.* 22, 1076–1086. doi: 10.1681/ASN.2010121270

Chen, L., Zhang, X., and Zhang, W. (2015). Regulation of alphaENaC transcription. *Vitam. Horm.* 98, 101–135. doi: 10.1016/bs.vh.2014.12.004

Cherradi, N., Bideau, M., Arnaudeau, S., Demaurex, N., James, R. W., Azhar, S., et al. (2001). Angiotensin II promotes selective uptake of high density lipoprotein cholesterol esters in bovine adrenal glomerulosa and human adrenocortical carcinoma cells through induction of scavenger receptor class B type I. *Endocrinology* 142, 4540–4549. doi: 10.1210/endo.142.10.8412

Cherradi, N., Pardo, B., Greenberg, A. S., Kraemer, F. B., and Capponi, A. M. (2003). Angiotensin II activates cholesterol ester hydrolase in bovine adrenal glomerulosa cells through phosphorylation mediated by p42/p44 mitogen-activated protein kinase. *Endocrinology* 144, 4905–4915. doi: 10.1210/en.2003-0325

Choi, M., Scholl, U. I., Yue, P., Bjorklund, P., Zhao, B., Nelson-Williams, C., et al. (2011). K+ channel mutations in adrenal aldosterone-producing adenomas and hereditary hypertension. *Science* 331, 768–772. doi: 10.1126/science.1198785

Chraibi, A., Vallet, V., Firsov, D., Hess, S. K., and Horisberger, J. D. (1998). Protease modulation of the activity of the epithelial sodium channel expressed in *Xenopus oocytes*. *J. Gen. Physiol.* 111, 127–138.

Clyne, C. D., Nguyen, A., and Rainey, W. E. (1995). The effects of KN62, a Ca^{2+}/calmodulin-dependent protein kinase II inhibitor, on adrenocortical cell aldosterone production. *Endocr. Res.* 21, 259–265. doi: 10.3109/07435809509030441

Condon, J. C., Pezzi, V., Drummond, B. M., Yin, S., and Rainey, W. E. (2002). Calmodulin-dependent kinase I regulates adrenal cell expression of aldosterone synthase. *Endocrinology* 143, 3651–3657. doi: 10.1210/en.2001-211359

Crisan, D., and Carr, J. (2000). Angiotensin I-converting enzyme: genotype and disease associations. *J. Mol. Diagn.* 2, 105–115. doi: 10.1016/S1525-1578(10)60624-1

Crivello, J. F., and Gill, G. N. (1983). Induction of cultured bovine adrenocortical zona glomerulosa cell 17-hydroxylase activity by ACTH. *Mol. Cell. Endocrinol.* 30, 97–107.

Cugini, P., Scavo, D., Cornelissen, G., Lee, J. Y., Meucci, T., and Halberg, F. (1981). Circadian rhythms of plasma renin, aldosterone and cortisol on habitual and low dietary sodium intake. *Horm. Res.* 15, 7–27.

Cuneo, R. C., Espiner, E. A., Nicholls, M. G., Yandle, T. G., and Livesey, J. H. (1987). Effect of physiological levels of atrial natriuretic peptide on hormone secretion: inhibition of angiotensin-induced aldosterone secretion and renin release in normal man. *J. Clin. Endocrinol. Metab.* 65, 765–772.

Davies, L. A., Hu, C., Guagliardo, N. A., Sen, N., Chen, X., Talley, E. M., et al. (2008). TASK channel deletion in mice causes primary hyperaldosteronism. *Proc. Natl. Acad. Sci. U. S. A.* 105, 2203–2208. doi: 10.1073/pnas.0712000105

Debonneville, C., Flores, S. Y., Kamynina, E., Plant, P. J., Tauxe, C., Thomas, M. A., et al. (2001). Phosphorylation of Nedd4-2 by Sgk1 regulates epithelial Na(+) channel cell surface expression. *EMBO J.* 20, 7052–7059. doi: 10.1093/emboj/20.24.7052

DeFronzo, R. A. (1980). Hyperkalemia and hyporeninemic hypoaldosteronism. *Kidney Int.* 17, 118–134.

Dibner, C., Schibler, U., and Albrecht, U. (2010). The mammalian circadian timing system: organization and coordination of central and peripheral clocks. *Annu. Rev. Physiol.* 72, 517–549. doi: 10.1146/annurev-physiol-021909-135821

Dijkink, L., Hartog, A., van Os, C. H., and Bindels, R. J. (2002). The epithelial sodium channel (ENaC) is intracellularly located as a tetramer. *Pflugers Arch.* 444, 549–555. doi: 10.1007/s00424-002-0855-4

Douma, L. G., Crislip, G. R., Cheng, K. Y., Barral, D., Masten, S., Holzworth, M., et al. (2020). Knockout of the circadian clock protein PER1 results in sex-dependent alterations of ET-1 production in mice in response to a high-salt diet plus mineralocorticoid treatment. *Can. J. Physiol. Pharmacol.* 98, 579–586. doi: 10.1139/cjpp-2019-0688

Douma, L. G., Solocinski, K., Holzworth, M. R., Crislip, G. R., Masten, S. H., Miller, A. H., et al. (2019). Female C57BL/6J mice lacking the circadian clock protein PER1 are protected from nondipping hypertension. *Am. J. Physiol. Regul. Integr. Comp. Physiol.* 316, R50–R58. doi: 10.1152/ajpregu.00381.2017

Eckel-Mahan, K., and Sassone-Corsi, P. (2009). Metabolism control by the circadian clock and vice versa. *Nat. Struct. Mol. Biol.* 16, 462–467. doi: 10.1038/nsmb.1595

Ehrhart-Bornstein, M., Lamounier-Zepter, V., Schraven, A., Langenbach, J., Willenberg, H. S., Barthel, A., et al. (2003). Human adipocytes secrete mineralocorticoid-releasing factors. *Proc. Natl. Acad. Sci. U. S. A.* 100, 14211–14216. doi: 10.1073/pnas.2336140100

Fakitsas, P., Adam, G., Daidie, D., van Bemmelen, M. X., Fouladkou, F., Patrignani, A., et al. (2007). Early aldosterone-induced gene product regulates the epithelial sodium channel by deubiquitylation. *J. Am. Soc. Nephrol.* 18, 1084–1092. doi: 10.1681/ASN.2006080902

Farkash, Y., Timberg, R., and Orly, J. (1986). Preparation of antiserum to rat cytochrome P-450 cholesterol side chain cleavage, and its use for ultrastructural localization of the immunoreactive enzyme by protein A-gold technique. *Endocrinology* 118, 1353–1365.

Felizola, S. J., Maekawa, T., Nakamura, Y., Satoh, F., Ono, Y., Kikuchi, K., et al. (2014). Voltage-gated calcium channels in the human adrenal and primary aldosteronism. *J. Steroid Biochem. Mol. Biol.* 144, 410–416. doi: 10.1016/j.jsbmb.2014.08.012

Fern, R. J., Hahm, M. S., Lu, H. K., Liu, L. P., Gorelick, F. S., and Barrett, P. Q. (1995). Ca^{2+}/calmodulin-dependent protein kinase II activation and regulation of adrenal glomerulosa Ca^{2+} signaling. *Am. J. Phys.* 269, F751–F760.

Firsov, D., Gautschi, I., Merillat, A. M., Rossier, B. C., and Schild, L. (1998). The heterotetrameric architecture of the epithelial sodium channel (ENaC). *EMBO J.* 17, 344–352.

Firsov, D., Schild, L., Gautschi, I., Merillat, A. M., Schneeberger, E., and Rossier, B. C. (1996). Cell surface expression of the epithelial Na channel and a mutant causing Liddle syndrome: a quantitative approach. *Proc. Natl. Acad. Sci. U. S. A.* 93, 15370–15375.

Fischer, S. S., Kempe, D. S., Leibrock, C. B., Rexhepaj, R., Siraskar, B., Boini, K. M., et al. (2010). Hyperaldosteronism in klotho-deficient mice. *Am. J. Physiol. Renal Physiol.* 299, F1171–F1177. doi: 10.1152/ajprenal.00233.2010

Fleury, A., Mathieu, A. P., Ducharme, L., Hales, D. B., and LeHoux, J. G. (2004). Phosphorylation and function of the hamster adrenal steroidogenic acute regulatory protein (StAR). *J. Steroid Biochem. Mol. Biol.* 91, 259–271. doi: 10.1016/j.jsbmb.2004.04.010

Fridmanis, D., Roga, A., and Klovins, J. (2017). ACTH receptor (MC2R) specificity: what do we know about underlying molecular mechanisms? *Front. Endocrinol.* 8:13. doi: 10.3389/fendo.2017.00013

Friis, U. G., Madsen, K., Stubbe, J., Hansen, P. B., Svenningsen, P., Bie, P., et al. (2013). Regulation of renin secretion by renal juxtaglomerular cells. *Pflugers Arch.* 465, 25–37. doi: 10.1007/s00424-012-1126-7

Fuchs-Hammoser, R., Schweiger, M., and Oelkers, W. (1980). The effect of chronic low-dose infusion of ACTH (1-24) on renin, renin-substrate, aldosterone and other corticosteroids in sodium replete and deplete man. *Acta Endocrinol.* 95, 198–206.

Funder, J. W. (2005). The nongenomic actions of aldosterone. *Endocr. Rev.* 26, 313–321. doi: 10.1210/er.2005-0004

Funder, J. W. (2006). Minireview: aldosterone and the cardiovascular system: genomic and nongenomic effects. *Endocrinology* 147, 5564–5567. doi: 10.1210/en.2006-0826

Funder, J. W., Pearce, P. T., Smith, R., and Smith, A. I. (1988). Mineralocorticoid action: target tissue specificity is enzyme, not receptor, mediated. *Science* 242, 583–585.

Funder, J. W., and Reincke, M. (2010). Aldosterone: a cardiovascular risk factor? *Biochim. Biophys. Acta* 1802, 1188–1192. doi: 10.1016/j.bbadis.2010.08.005

Garty, H., and Palmer, L. G. (1997). Epithelial sodium channels: function, structure, and regulation. *Physiol. Rev.* 77, 359–396.

Genschik, P., Sumara, I., and Lechner, E. (2013). The emerging family of CULLIN3-RING ubiquitin ligases (CRL3s): cellular functions and disease implications. *EMBO J.* 32, 2307–2320. doi: 10.1038/emboj.2013.173

Goodfriend, T. L., Ball, D. L., Egan, B. M., Campbell, W. B., and Nithipatikom, K. (2004). Epoxy-keto derivative of linoleic acid stimulates aldosterone secretion. *Hypertension* 43, 358–363. doi: 10.1161/01.HYP.0000113294.06704.64

Goodfriend, T. L., Egan, B. M., and Kelley, D. E. (1998). Aldosterone in obesity. *Endocr. Res.* 24, 789–796. doi: 10.3109/07435809809032689

Greenlee, M. M., Lynch, I. J., Gumz, M. L., Cain, B. D., and Wingo, C. S. (2011). Mineralocorticoids stimulate the activity and expression of renal H^+, K^+-ATPases. *J. Am. Soc. Nephrol.* 22, 49–58. doi: 10.1681/ASN.2010030311

Guagliardo, N. A., Yao, J., Hu, C., Schertz, E. M., Tyson, D. A., Carey, R. M., et al. (2012). TASK-3 channel deletion in mice recapitulates low-renin essential hypertension. *Hypertension* 59, 999–1005. doi: 10.1161/HYPERTENSIONAHA.111.189662

Gumz, M. L., Cheng, K. Y., Lynch, I. J., Stow, L. R., Greenlee, M. M., Cain, B. D., et al. (2010a). Regulation of alphaENaC expression by the circadian clock protein period 1 in mpkCCD(c14) cells. *Biochim. Biophys. Acta* 1799, 622–629. doi: 10.1016/j.bbagrm.2010.09.003

Gumz, M. L., Lynch, I. J., Greenlee, M. M., Cain, B. D., and Wingo, C. S. (2010b). The renal H+-K+-ATPases: physiology, regulation, and structure. *Am. J. Physiol. Renal Physiol.* 298, F12–F21. doi: 10.1152/ajprenal.90723.2008

Gumz, M. L., Rabinowitz, L., and Wingo, C. S. (2015). An integrated view of potassium homeostasis. *N. Engl. J. Med.* 373, 1787–1788. doi: 10.1056/NEJMc1509656

Gumz, M. L., Stow, L. R., Lynch, I. J., Greenlee, M. M., Rudin, A., Cain, B. D., et al. (2009). The circadian clock protein period 1 regulates expression of the renal epithelial sodium channel in mice. *J. Clin. Invest.* 119, 2423–2434. doi: 10.1172/JCI36908

Gyles, S. L., Burns, C. J., Whitehouse, B. J., Sugden, D., Marsh, P. J., Persaud, S. J., et al. (2001). ERKs regulate cyclic AMP-induced steroid synthesis through transcription of the steroidogenic acute regulatory (StAR) gene. *J. Biol. Chem.* 276, 34888–34895. doi: 10.1074/jbc.M102063200

Haerteis, S., Krappitz, M., Bertog, M., Krappitz, A., Baraznenok, V., Henderson, I., et al. (2012). Proteolytic activation of the epithelial sodium channel (ENaC) by the cysteine protease cathepsin-S. *Pflugers Arch.* 464, 353–365. doi: 10.1007/s00424-012-1138-3

Hammer, G. D., Krylova, I., Zhang, Y., Darimont, B. D., Simpson, K., Weigel, N. L., et al. (1999). Phosphorylation of the nuclear receptor SF-1 modulates cofactor recruitment: integration of hormone signaling in reproduction and stress. *Mol. Cell* 3, 521–526.

Hasegawa, T., Zhao, L., Caron, K. M., Majdic, G., Suzuki, T., Shizawa, S., et al. (2000). Developmental roles of the steroidogenic acute regulatory protein (StAR) as revealed by StAR knockout mice. *Mol. Endocrinol.* 14, 1462–1471. doi: 10.1210/mend.14.9.0515

He, B. J., and Anderson, M. E. (2013). Aldosterone and cardiovascular disease: the heart of the matter. *Trends Endocrinol. Metab.* 24, 21–30. doi: 10.1016/j.tem.2012.09.004

Heitzmann, D., Derand, R., Jungbauer, S., Bandulik, S., Sterner, C., Schweda, F., et al. (2008). Invalidation of TASK1 potassium channels disrupts adrenal gland zonation and mineralocorticoid homeostasis. *EMBO J.* 27, 179–187. doi: 10.1038/sj.emboj.7601934

Hilfenhaus, M. (1976). Circadian rhythm of the renin-angiotensin-aldosterone system in the rat. *Arch. Toxicol.* 36, 305–316.

Hirohama, D., Ayuzawa, N., Ueda, K., Nishimoto, M., Kawarazaki, W., Watanabe, A., et al. (2018). Aldosterone is essential for angiotensin II-induced upregulation of pendrin. *J. Am. Soc. Nephrol.* 29, 57–68. doi: 10.1681/ASN.2017030243

Hodges, R. R., Horikawa, Y., Rios, J. D., Shatos, M. A., and Dartt, D. A. (2007). Effect of protein kinase C and ca(2+) on p42/p44 MAPK, Pyk2, and Src activation in rat conjunctival goblet cells. *Exp. Eye Res.* 85, 836–844. doi: 10.1016/j.exer.2007.08.019

Holland, O. B., and Carr, B. (1993). Modulation of aldosterone synthase messenger ribonucleic acid levels by dietary sodium and potassium and by adrenocorticotropin. *Endocrinology* 132, 2666–2673.

Horvath, A., Szabadkai, G., Varnai, P., Aranyi, T., Wollheim, C. B., Spat, A., et al. (1998). Voltage dependent calcium channels in adrenal glomerulosa cells and in insulin producing cells. *Cell Calcium* 23, 33–42.

Huby, A. C., Antonova, G., Groenendyk, J., Gomez-Sanchez, C. E., Bollag, W. B., Filosa, J. A., et al. (2015). Adipocyte-derived hormone leptin is a direct regulator of aldosterone secretion, which promotes endothelial dysfunction and cardiac fibrosis. *Circulation* 132, 2134–2145. doi: 10.1161/CIRCULATIONAHA.115.018226

Huby, A. C., Otvos, L. Jr., and Belin de Chantemele, E. J. (2016). Leptin induces hypertension and endothelial dysfunction via aldosterone-dependent mechanisms in obese female mice. *Hypertension* 67, 1020–1028. doi: 10.1161/HYPERTENSIONAHA.115.06642

Hughey, R. P., Bruns, J. B., Kinlough, C. L., Harkleroad, K. L., Tong, Q., Carattino, M. D., et al. (2004). Epithelial sodium channels are activated by furin-dependent proteolysis. *J. Biol. Chem.* 279, 18111–18114. doi: 10.1074/jbc.C400080200

Hume, R., Kelly, R. W., Taylor, P. L., and Boyd, G. S. (1984). The catalytic cycle of cytochrome P-450scc and intermediates in the conversion of cholesterol to pregnenolone. *Eur. J. Biochem.* 140, 583–591.

Ishihara, K., Yamamoto, T., and Kubo, Y. (2009). Heteromeric assembly of inward rectifier channel subunit Kir2.1 with Kir3.1 and with Kir3.4. *Biochem. Biophys. Res. Commun.* 380, 832–837. doi: 10.1016/j.bbrc.2009.01.179

Ishimura, K., and Fujita, H. (1997). Light and electron microscopic immunohistochemistry of the localization of adrenal steroidogenic enzymes. *Microsc. Res. Tech.* 36, 445–453.

Itoh, S., Abe, K., Nushiro, N., Omata, K., Yasujima, M., and Yoshinaga, K. (1987). Effect of atrial natriuretic factor on renin release in isolated afferent arterioles. *Kidney Int.* 32, 493–497.

Ji, A. X., and Prive, G. G. (2013). Crystal structure of KLHL3 in complex with Cullin3. *PLoS One* 8:e60445. doi: 10.1371/journal.pone.0060445

Jo, Y., King, S. R., Khan, S. A., and Stocco, D. M. (2005). Involvement of protein kinase C and cyclic adenosine 3',5'-monophosphate-dependent kinase in steroidogenic acute regulatory protein expression and steroid biosynthesis in Leydig cells. *Biol. Reprod.* 73, 244–255. doi: 10.1095/biolreprod.104.037721

Kanazirska, M. V., Vassilev, P. M., Quinn, S. J., Tillotson, D. L., and Williams, G. H. (1992). Single K+ channels in adrenal zona glomerulosa cells. II. Inhibition by angiotensin II. *Am. J. Phys.* 263, E760–E765.

Kapas, S., Purbrick, A., and Hinson, J. P. (1995). Role of tyrosine kinase and protein kinase C in the steroidogenic actions of angiotensin II, alpha-melanocyte-stimulating hormone and corticotropin in the rat adrenal cortex. *Biochem. J.* 305(Pt 2), 433–438.

Kashlan, O. B., and Kleyman, T. R. (2011). ENaC structure and function in the wake of a resolved structure of a family member. *Am. J. Physiol. Renal Physiol.* 301, F684–F696. doi: 10.1152/ajprenal.00259.2011

Kayes-Wandover, K. M., and White, P. C. (2000). Steroidogenic enzyme gene expression in the human heart. *J. Clin. Endocrinol. Metab.* 85, 2519–2525. doi: 10.1210/jc.85.7.2519

Kem, D. C., Weinberger, M. H., Gomez-Sanchez, C., Kramer, N. J., Lerman, R., Furuyama, S., et al. (1973). Circadian rhythm of plasma aldosterone concentration in patients with primary aldosteronism. *J. Clin. Invest.* 52, 2272–2277.

Kleyman, T. R., and Eaton, D. C. (2020). Regulating ENaC's gate. *Am. J. Physiol. Cell Physiol.* 318, C150–C162. doi: 10.1152/ajpcell.00418.2019

Kurukulasuriya, L. R., Stas, S., Lastra, G., Manrique, C., and Sowers, J. R. (2011). Hypertension in obesity. *Med. Clin. North Am.* 95, 903–917. doi: 10.1016/j.mcna.2011.06.004

Kyossev, Z., Walker, P. D., and Reeves, W. B. (1996). Immunolocalization of NAD-dependent 11 beta-hydroxysteroid dehydrogenase in human kidney and colon. *Kidney Int.* 49, 271–281.

Lamarre-Cliche, M., de Champlain, J., Lacourciere, Y., Poirier, L., Karas, M., and Larochelle, P. (2005). Effects of circadian rhythms, posture, and medication on renin-aldosterone interrelations in essential hypertensives. *Am. J. Hypertens.* 18, 56–64. doi: 10.1016/j.amjhyper.2004.08.025

Le, T., and Schimmer, B. P. (2001). The regulation of MAPKs in Y1 mouse adrenocortical tumor cells. *Endocrinology* 142, 4282–4287. doi: 10.1210/endo.142.10.8441

Li, H., Yu, X., Cicala, M. V., Mantero, F., Benbrook, A., Veitla, V., et al. (2015). Prevalence of angiotensin II type 1 receptor (AT1R)-activating autoantibodies in primary aldosteronism. *J. Am. Soc. Hypertens.* 9, 15–20. doi: 10.1016/j.jash.2014.10.009

Loffing, J., and Kaissling, B. (2003). Sodium and calcium transport pathways along the mammalian distal nephron: from rabbit to human. *Am. J. Physiol. Renal Physiol.* 284, F628–F643. doi: 10.1152/ajprenal.00217.2002

Lopez-Cayuqueo, K. I., Chavez-Canales, M., Pillot, A., Houillier, P., Jayat, M., Baraka-Vidot, J., et al. (2018). A mouse model of pseudohypoaldosteronism type II reveals a novel mechanism of renal tubular acidosis. *Kidney Int.* 94, 514–523. doi: 10.1016/j.kint.2018.05.001

Louis-Dit-Picard, H., Barc, J., Trujillano, D., Miserey-Lenkei, S., Bouatia-Naji, N., Pylypenko, O., et al. (2012). KLHL3 mutations cause familial hyperkalemic hypertension by impairing ion transport in the distal nephron. *Nat. Genet.* 44, 456–460, S1–3. doi: 10.1038/ng.2218

Lu, M., Wang, J., Jones, K. T., Ives, H. E., Feldman, M. E., Yao, L. J., et al. (2010). mTOR complex-2 activates ENaC by phosphorylating SGK1. *J. Am. Soc. Nephrol.* 21, 811–818. doi: 10.1681/ASN.2009111168

Lubarski, I., Pihakaski-Maunsbach, K., Karlish, S. J., Maunsbach, A. B., and Garty, H. (2005). Interaction with the Na, K-ATPase and tissue distribution of FXYD5 (related to ion channel). *J. Biol. Chem.* 280, 37717–37724. doi: 10.1074/jbc.M506397200

Lymangrover, J. R., Matthews, E. K., and Saffran, M. (1982). Membrane potential changes of mouse adrenal zona fasciculata cells in response to adrenocorticotropin and adenosine 3′,5′-monophosphate. *Endocrinology* 110, 462–468.

Maack, T., Marion, D. N., Camargo, M. J., Kleinert, H. D., Laragh, J. H., Vaughan, E. D. Jr., et al. (1984). Effects of auriculin (atrial natriuretic factor) on blood pressure, renal function, and the renin-aldosterone system in dogs. *Am. J. Med.* 77, 1069–1075.

Manna, P. R., Huhtaniemi, I. T., and Stocco, D. M. (2009). Mechanisms of protein kinase C signaling in the modulation of 3′,5′-cyclic adenosine monophosphate-mediated steroidogenesis in mouse gonadal cells. *Endocrinology* 150, 3308–3317. doi: 10.1210/en.2008-1668

Martinez-Rumayor, A., Richards, A. M., Burnett, J. C., and Januzzi, J. L. Jr. (2008). Biology of the natriuretic peptides. *Am. J. Cardiol.* 101, 3–8. doi: 10.1016/j.amjcard.2007.11.012

Mitani, F., Miyamoto, H., Mukai, K., and Ishimura, Y. (1996). Effects of long term stimulation of ACTH and angiotensin II-secretions on the rat adrenal cortex. *Endocr. Res.* 22, 421–431.

Monticone, S., Hattangady, N. G., Nishimoto, K., Mantero, F., Rubin, B., Cicala, M. V., et al. (2012). Effect of KCNJ5 mutations on gene expression in aldosterone-producing adenomas and adrenocortical cells. *J. Clin. Endocrinol. Metab.* 97, E1567–E1572. doi: 10.1210/jc.2011-3132

Mori, Y., Wakabayashi, M., Mori, T., Araki, Y., Sohara, E., Rai, T., et al. (2013). Decrease of WNK4 ubiquitination by disease-causing mutations of KLHL3 through different molecular mechanisms. *Biochem. Biophys. Res. Commun.* 439, 30–34. doi: 10.1016/j.bbrc.2013.08.035

Mulatero, P., Tauber, P., Zennaro, M. C., Monticone, S., Lang, K., Beuschlein, F., et al. (2012). KCNJ5 mutations in European families with nonglucocorticoid remediable familial hyperaldosteronism. *Hypertension* 59, 235–240. doi: 10.1161/HYPERTENSIONAHA.111.183996

Na, T., Wu, G., Zhang, W., Dong, W. J., and Peng, J. B. (2013). Disease-causing R1185C mutation of WNK4 disrupts a regulatory mechanism involving calmodulin binding and SGK1 phosphorylation sites. *Am. J. Physiol. Renal Physiol.* 304, F8–F18. doi: 10.1152/ajprenal.00284.2012

Nagase, M., Yoshida, S., Shibata, S., Nagase, T., Gotoda, T., Ando, K., et al. (2006). Enhanced aldosterone signaling in the early nephropathy of rats with metabolic syndrome: possible contribution of fat-derived factors. *J. Am. Soc. Nephrol.* 17, 3438–3446. doi: 10.1681/ASN.2006080944

Nanba, K., Blinder, A. R., Rege, J., Hattangady, N. G., Else, T., Liu, C. J., et al. (2020). Somatic CACNA1H mutation as a cause of aldosterone-producing adenoma. *Hypertension* 75, 645–649. doi: 10.1161/HYPERTENSIONAHA.119.14349

Nanba, K., Chen, A., Nishimoto, K., and Rainey, W. E. (2015). Role of ca(2+)/calmodulin-dependent protein kinase kinase in adrenal aldosterone production. *Endocrinology* 156, 1750–1756. doi: 10.1210/en.2014-1782

Naray-Fejes-Toth, A., Rusvai, E., and Fejes-Toth, G. (1994). Minealocorticoid receptors and 11 beta-steroid dehydrogenase activity in renal principal and intercalated cells. *Am. J. Phys.* 266, F76–F80.

Naray-Fejes-Toth, A., Snyder, P. M., and Fejes-Toth, G. (2004). The kidney-specific WNK1 isoform is induced by aldosterone and stimulates epithelial sodium channel-mediated Na+ transport. *Proc. Natl. Acad. Sci. U. S. A.* 101, 17434–17439. doi: 10.1073/pnas.0408146101

Natarajan, R., Dunn, W. D., Stern, N., and Nadler, J. (1990). Key role of diacylglycerol-mediated 12-lipoxygenase product formation in angiotensin II-induced aldosterone synthesis. *Mol. Cell. Endocrinol.* 72, 73–80.

Natarajan, R., Stern, N., Hsueh, W., Do, Y., and Nadler, J. (1988a). Role of the lipoxygenase pathway in angiotensin II-mediated aldosterone biosynthesis in human adrenal glomerulosa cells. *J. Clin. Endocrinol. Metab.* 67, 584–591.

Natarajan, R., Stern, N., and Nadler, J. (1988b). Diacylglycerol provides arachidonic acid for lipoxygenase products that mediate angiotensin II-induced aldosterone synthesis. *Biochem. Biophys. Res. Commun.* 156, 717–724.

Nguyen, A. T., and Zhang, Y. (2011). The diverse functions of Dot1 and H3K79 methylation. *Genes Dev.* 25, 1345–1358. doi: 10.1101/gad.2057811

Nogueira, E. F., and Rainey, W. E. (2010). Regulation of aldosterone synthase by activator transcription factor/cAMP response element-binding protein family members. *Endocrinology* 151, 1060–1070. doi: 10.1210/en.2009-0977

Noreng, S., Bharadwaj, A., Posert, R., Yoshioka, C., and Baconguis, I. (2018). Structure of the human epithelial sodium channel by cryo-electron microscopy. *elife* 7:e39340. doi: 10.7554/eLife.39340

Ohnishi, T., Wada, A., Lauber, M., Yamano, T., and Okamoto, M. (1988). Aldosterone biosynthesis in mitochondria of isolated zones of adrenal cortex. *J. Steroid Biochem.* 31, 73–81.

Ohta, A., Schumacher, F. R., Mehellou, Y., Johnson, C., Knebel, A., Macartney, T. J., et al. (2013). The CUL3-KLHL3 E3 ligase complex mutated in Gordon's hypertension syndrome interacts with and ubiquitylates WNK isoforms: disease-causing mutations in KLHL3 and WNK4 disrupt interaction. *Biochem. J.* 451, 111–122. doi: 10.1042/BJ20121903

Oki, K., Plonczynski, M. W., Lam, M. L., Gomez-Sanchez, E. P., and Gomez-Sanchez, C. E. (2012a). The potassium channel, Kir3.4 participates in angiotensin II-stimulated aldosterone production by a human adrenocortical cell line. *Endocrinology* 153, 4328–4335. doi: 10.1210/en.2012-1241

Oki, K., Plonczynski, M. W., Luis Lam, M., Gomez-Sanchez, E. P., and Gomez-Sanchez, C. E. (2012b). Potassium channel mutant KCNJ5 T158A expression in HAC-15 cells increases aldosterone synthesis. *Endocrinology* 153, 1774–1782. doi: 10.1210/en.2011-1733

Okubo, S., Niimura, F., Nishimura, H., Takemoto, F., Fogo, A., Matsusaka, T., et al. (1997). Angiotensin-independent mechanism for aldosterone synthesis during chronic extracellular fluid volume depletion. *J. Clin. Invest.* 99, 855–860.

Olala, L. O., Choudhary, V., Johnson, M. H., and Bollag, W. B. (2014). Angiotensin II-induced protein kinase D activates the ATF/CREB family of transcription factors and promotes StAR mRNA expression. *Endocrinology* 155, 2524–2533. doi: 10.1210/en.2013-1485

Olejnik, A., Franczak, A., Krzywonos-Zawadzka, A., Kaluzna-Oleksy, M., and Bil-Lula, I. (2018). The biological role of klotho protein in the development of cardiovascular diseases. *Biomed. Res. Int.* 2018:5171945. doi: 10.1155/2018/5171945

Ouyang, J., Hu, D., Wang, B., Shi, T., Ma, X., Li, H., et al. (2011). Differential effects of down-regulated steroidogenic factor-1 on basal and angiotensin II-induced aldosterone secretion. *J. Endocrinol. Investig.* 34, 671–675. doi: 10.3275/7413

Pan, Y. J., and Young, D. B. (1982). Experimental aldosterone hypertension in the dog. *Hypertension* 4, 279–287.

Papadopoulou-Marketou, N., Vaidya, A., Dluhy, R., and Chrousos, G. P. (2000). "Hyperaldosteronism," in *Endotext* (South Dartmouth, MA: Endotext).

Park, J., Leong, M. L., Buse, P., Maiyar, A. C., Firestone, G. L., and Hemmings, B. A. (1999). Serum and glucocorticoid-inducible kinase (SGK) is a target of the PI 3-kinase-stimulated signaling pathway. *EMBO J.* 18, 3024–3033.

Peti-Peterdi, J., and Harris, R. C. (2010). Macula densa sensing and signaling mechanisms of renin release. *J. Am. Soc. Nephrol.* 21, 1093–1096. doi: 10.1681/ASN.2009070759

Piazza, M., Seccia, T. M., Caroccia, B., Rossitto, G., Scarpa, R., Persichitti, P., et al. (2019). AT1AA (angiotensin II Type-1 receptor autoantibodies): cause or consequence of human primary aldosteronism? *Hypertension* 74, 793–799. doi: 10.1161/HYPERTENSIONAHA.119.13388

Pilon, A., Martin, G., Bultel-Brienne, S., Junquero, D., Delhon, A., Fruchart, J. C., et al. (2003). Regulation of the scavenger receptor BI and the LDL receptor by activators of aldosterone production, angiotensin II and PMA, in the human NCI-H295R adrenocortical cell line. *Biochim. Biophys. Acta* 1631, 218–228. doi: 10.1016/S1388-1981(03)00020-9

Qian, J., Zhong, J., Yan, M., Cheng, P., Shi, H., Hao, C., et al. (2018). Circulating alpha-klotho is related to plasma aldosterone and its follow-up change predicts CKD progression. *Kidney Blood Press. Res.* 43, 836–846. doi: 10.1159/000490138

Quinn, S. J., Cornwall, M. C., and Williams, G. H. (1987). Electrical properties of isolated rat adrenal glomerulosa and fasciculata cells. *Endocrinology* 120, 903–914.

Rashmi, P., Colussi, G., Ng, M., Wu, X., Kidwai, A., and Pearce, D. (2017). Glucocorticoid-induced leucine zipper protein regulates sodium and potassium balance in the distal nephron. *Kidney Int.* 91, 1159–1177. doi: 10.1016/j.kint.2016.10.038

Reilly, R. F., and Ellison, D. H. (2000). Mammalian distal tubule: physiology, pathophysiology, and molecular anatomy. *Physiol. Rev.* 80, 277–313. doi: 10.1152/physrev.2000.80.1.277

Reimer, E. N., Walenda, G., Seidel, E., and Scholl, U. I. (2016). CACNA1H(M1549V) mutant calcium channel causes autonomous aldosterone production in HAC15 cells and is inhibited by Mibefradil. *Endocrinology* 157, 3016–3022. doi: 10.1210/en.2016-1170

Reisenauer, M. R., Anderson, M., Huang, L., Zhang, Z., Zhou, Q., Kone, B. C., et al. (2009). AF17 competes with AF9 for binding to Dot1a to up-regulate transcription of epithelial Na+ channel alpha. *J. Biol. Chem.* 284, 35659–35669. doi: 10.1074/jbc.M109.038448

Richards, J., Jeffers, L. A., All, S. C., Cheng, K. Y., and Gumz, M. L. (2013). Role of Per1 and the mineralocorticoid receptor in the coordinate regulation of alphaENaC in renal cortical collecting duct cells. *Front. Physiol.* 4:253. doi: 10.3389/fphys.2013.00253

Ring, A. M., Cheng, S. X., Leng, Q., Kahle, K. T., Rinehart, J., Lalioti, M. D., et al. (2007a). WNK4 regulates activity of the epithelial Na+ channel in vitro and in vivo. *Proc. Natl. Acad. Sci. U. S. A.* 104, 4020–4024. doi: 10.1073/pnas.0611727104

Ring, A. M., Leng, Q., Rinehart, J., Wilson, F. H., Kahle, K. T., Hebert, S. C., et al. (2007b). An SGK1 site in WNK4 regulates Na+ channel and K+ channel activity and has implications for aldosterone signaling and K+ homeostasis. *Proc. Natl. Acad. Sci. U. S. A.* 104, 4025–4029. doi: 10.1073/pnas.0611728104

Rocha, R., and Funder, J. W. (2002). The pathophysiology of aldosterone in the cardiovascular system. *Ann. N. Y. Acad. Sci.* 970, 89–100. doi: 10.1111/j.1749-6632.2002.tb04415.x

Ronti, T., Lupattelli, G., and Mannarino, E. (2006). The endocrine function of adipose tissue: an update. *Clin. Endocrinol.* 64, 355–365. doi: 10.1111/j.1365-2265.2006.02474.x

Rossier, M. F., Ertel, E. A., Vallotton, M. B., and Capponi, A. M. (1998). Inhibitory action of mibefradil on calcium signaling and aldosterone synthesis in bovine adrenal glomerulosa cells. *J. Pharmacol. Exp. Ther.* 287, 824–831.

Rossier, B. C., and Stutts, M. J. (2009). Activation of the epithelial sodium channel (ENaC) by serine proteases. *Annu. Rev. Physiol.* 71, 361–379. doi: 10.1146/annurev.physiol.010908.163108

Rossitto, G., Regolisti, G., Rossi, E., Negro, A., Nicoli, D., Casali, B., et al. (2013). Elevation of angiotensin-II type-1-receptor autoantibodies titer in primary aldosteronism as a result of aldosterone-producing adenoma. *Hypertension* 61, 526–533. doi: 10.1161/HYPERTENSIONAHA.112.202945

Rotin, D. (2008). Role of the UPS in Liddle syndrome. *BMC Biochem.* 9(Suppl 1):S5. doi: 10.1186/1471-2091-9-S1-S5

Roy, A., Al-bataineh, M. M., and Pastor-Soler, N. M. (2015). Collecting duct intercalated cell function and regulation. *Clin. J. Am. Soc. Nephrol.* 10, 305–324. doi: 10.2215/CJN.08880914

Sackmann, S., Lichtenauer, U., Shapiro, I., Reincke, M., and Beuschlein, F. (2011). Aldosterone producing adrenal adenomas are characterized by activation of calcium/calmodulin-dependent protein kinase (CaMK) dependent pathways. *Horm. Metab. Res.* 43, 106–111. doi: 10.1055/s-0030-1269899

Sadovsky, Y., Crawford, P. A., Woodson, K. G., Polish, J. A., Clements, M. A., Tourtellotte, L. M., et al. (1995). Mice deficient in the orphan receptor steroidogenic factor 1 lack adrenal glands and gonads but express P450 side-chain-cleavage enzyme in the placenta and have normal embryonic serum levels of corticosteroids. *Proc. Natl. Acad. Sci. U. S. A.* 92, 10939–10943.

Scholl, U. I., Goh, G., Stolting, G., de Oliveira, R. C., Choi, M., Overton, J. D., et al. (2013). Somatic and germline CACNA1D calcium channel mutations in aldosterone-producing adenomas and primary aldosteronism. *Nat. Genet.* 45, 1050–1054. doi: 10.1038/ng.2695

Scholl, U. I., Nelson-Williams, C., Yue, P., Grekin, R., Wyatt, R. J., Dillon, M. J., et al. (2012). Hypertension with or without adrenal hyperplasia due to different inherited mutations in the potassium channel KCNJ5. *Proc. Natl. Acad. Sci. U. S. A.* 109, 2533–2538. doi: 10.1073/pnas.1121407109

Scholl, U. I., Stolting, G., Nelson-Williams, C., Vichot, A. A., Choi, M., Loring, E., et al. (2015). Recurrent gain of function mutation in calcium channel CACNA1H causes early-onset hypertension with primary aldosteronism. *elife* 4:e06315. doi: 10.7554/eLife.06315

Sculptoreanu, A., Scheuer, T., and Catterall, W. A. (1993). Voltage-dependent potentiation of L-type Ca^{2+} channels due to phosphorylation by cAMP-dependent protein kinase. *Nature* 364, 240–243.

Seely, E. W., Conlin, P. R., Brent, G. A., and Dluhy, R. G. (1989). Adrenocorticotropin stimulation of aldosterone: prolonged continuous versus pulsatile infusion. *J. Clin. Endocrinol. Metab.* 69, 1028–1032.

Sewer, M. B., and Li, D. (2008). Regulation of steroid hormone biosynthesis by the cytoskeleton. *Lipids* 43, 1109–1115. doi: 10.1007/s11745-008-3221-2

Sewer, M. B., and Waterman, M. R. (2003). CAMP-dependent protein kinase enhances CYP17 transcription via MKP-1 activation in H295R human adrenocortical cells. *J. Biol. Chem.* 278, 8106–8111. doi: 10.1074/jbc.M210264200

Shibata, S., and Fujita, T. (2011). The kidneys and aldosterone/mineralocorticoid receptor system in salt-sensitive hypertension. *Curr. Hypertens. Rep.* 13, 109–115. doi: 10.1007/s11906-010-0175-6

Shibata, S., Rinehart, J., Zhang, J., Moeckel, G., Castaneda-Bueno, M., Stiegler, A. L., et al. (2013a). Mineralocorticoid receptor phosphorylation regulates ligand binding and renal response to volume depletion and hyperkalemia. *Cell Metab.* 18, 660–671. doi: 10.1016/j.cmet.2013.10.005

Shibata, S., Zhang, J., Puthumana, J., Stone, K. L., and Lifton, R. P. (2013b). Kelch-like 3 and Cullin 3 regulate electrolyte homeostasis via ubiquitination and degradation of WNK4. *Proc. Natl. Acad. Sci. U. S. A.* 110, 7838–7843. doi: 10.1073/pnas.1304592110

Shimkets, R. A., Warnock, D. G., Bositis, C. M., Nelson-Williams, C., Hansson, J. H., Schambelan, M., et al. (1994). Liddle's syndrome: heritable human hypertension caused by mutations in the beta subunit of the epithelial sodium channel. *Cell* 79, 407–414.

Simpson, S. A., Tait, J. F., Wettstein, A., Neher, R., Von Euw, J., Schindler, O., et al. (1954). Constitution of aldosterone, a new mineralocorticoid. *Experientia* 10, 132–133. doi: 10.1007/BF02158515

Solocinski, K., Holzworth, M., Wen, X., Cheng, K. Y., Lynch, I. J., Cain, B. D., et al. (2017). Desoxycorticosterone pivalate-salt treatment leads to non-dipping hypertension in Per1 knockout mice. *Acta Physiol.* 220, 72–82. doi: 10.1111/apha.12804

Sonoyama, T., Sone, M., Tamura, N., Honda, K., Taura, D., Kojima, K., et al. (2014). Role of endogenous ACTH on circadian aldosterone rhythm in patients with primary aldosteronism. *Endocr. Connect.* 3, 173–179. doi: 10.1530/EC-14-0086

Soundararajan, R., Wang, J., Melters, D., and Pearce, D. (2010). Glucocorticoid-induced leucine zipper 1 stimulates the epithelial sodium channel by regulating serum- and glucocorticoid-induced kinase 1 stability and subcellular localization. *J. Biol. Chem.* 285, 39905–39913. doi: 10.1074/jbc.M110.161133

Soundararajan, R., Zhang, T. T., Wang, J., Vandewalle, A., and Pearce, D. (2005). A novel role for glucocorticoid-induced leucine zipper protein in epithelial sodium channel-mediated sodium transport. *J. Biol. Chem.* 280, 39970–39981. doi: 10.1074/jbc.M508658200

Spat, A., Enyedi, P., Hajnoczky, G., and Hunyady, L. (1991). Generation and role of calcium signal in adrenal glomerulosa cells. *Exp. Physiol.* 76, 859–885.

Staruschenko, A., Adams, E., Booth, R. E., and Stockand, J. D. (2005). Epithelial Na+ channel subunit stoichiometry. *Biophys. J.* 88, 3966–3975. doi: 10.1529/biophysj.104.056804

Staub, O., Dho, S., Henry, P., Correa, J., Ishikawa, T., McGlade, J., et al. (1996). WW domains of Nedd4 bind to the proline-rich PY motifs in the epithelial Na+ channel deleted in Liddle's syndrome. *EMBO J.* 15, 2371–2380.

Steckelings, U. M., Rompe, F., Kaschina, E., Namsolleck, P., Grzesiak, A., Funke-Kaiser, H., et al. (2010). The past, present and future of angiotensin II type 2 receptor stimulation. *J. Renin-Angiotensin-Aldosterone Syst.* 11, 67–73. doi: 10.1177/1470320309347791

Stern, N., Sowers, J. R., McGinty, D., Beahm, E., Littner, M., Catania, R., et al. (1986). Circadian rhythm of plasma renin activity in older normal and essential hypertensive men: relation with inactive renin, aldosterone, cortisol and REM sleep. *J. Hypertens.* 4, 543–550.

Susa, K., Sohara, E., Rai, T., Zeniya, M., Mori, Y., Mori, T., et al. (2014). Impaired degradation of WNK1 and WNK4 kinases causes PHAII in mutant KLHL3 knock-in mice. *Hum. Mol. Genet.* 23, 5052–5060. doi: 10.1093/hmg/ddu217

Takagi, M., Takagi, M., Franco-Saenz, R., and Mulrow, P. J. (1988). Effect of atrial natriuretic peptide on renin release in a superfusion system of kidney slices and dispersed juxtaglomerular cells. *Endocrinology* 122, 1437–1442.

Takeda, R., Miyamori, I., Ikeda, M., Koshida, H., Takeda, Y., Yasuhara, S., et al. (1984). Circadian rhythm of plasma aldosterone and time dependent alterations of aldosterone regulators. *J. Steroid Biochem.* 20, 321–323.

Takeda, Y., Yoneda, T., Demura, M., Miyamori, I., and Mabuchi, H. (2000). Cardiac aldosterone production in genetically hypertensive rats. *Hypertension* 36, 495–500. doi: 10.1161/01.HYP.36.4.495

Takemoto-Kimura, S., Suzuki, K., Horigane, S. I., Kamijo, S., Inoue, M., Sakamoto, M., et al. (2017). Calmodulin kinases: essential regulators in health and disease. *J. Neurochem.* 141, 808–818. doi: 10.1111/jnc.14020

Taylor, C. W., and Thorn, P. (2001). Calcium signalling: IP3 rises again…and again. *Curr. Biol.* 11, R352–R355. doi: 10.1016/S0960-9822(01)00192-0

Teng-umnuay, P., Verlander, J. W., Yuan, W., Tisher, C. C., and Madsen, K. M. (1996). Identification of distinct subpopulations of intercalated cells in the mouse collecting duct. *J. Am. Soc. Nephrol.* 7, 260–274.

Thosar, S. S., Rueda, J. F., Berman, A. M., Lasarev, M. R., Herzig, M. X., Clemons, N. A., et al. (2019). Separate and interacting effects of the endogenous circadian system and behaviors on plasma aldosterone in humans. *Am. J. Physiol. Regul. Integr. Comp. Physiol.* 316, R157–R164. doi: 10.1152/ajpregu.00314.2018

Tokumitsu, H., Enslen, H., and Soderling, T. R. (1995). Characterization of a Ca^{2+}/calmodulin-dependent protein kinase cascade. Molecular cloning and expression of calcium/calmodulin-dependent protein kinase kinase. *J. Biol. Chem.* 270, 19320–19324.

Tremblay, A., and LeHoux, J. G. (1993). Transcriptional activation of adrenocortical steroidogenic genes by high potassium or low sodium intake. *FEBS Lett.* 317, 211–215.

Tsuruoka, S., and Schwartz, G. J. (1999). Mechanisms of HCO(−)(3) secretion in the rabbit connecting segment. *Am. J. Phys.* 277, F567–F574.

Uebele, V. N., Nuss, C. E., Renger, J. J., and Connolly, T. M. (2004). Role of voltage-gated calcium channels in potassium-stimulated aldosterone secretion from rat adrenal zona glomerulosa cells. *J. Steroid Biochem. Mol. Biol.* 92, 209–218. doi: 10.1016/j.jsbmb.2004.04.012

Varnai, P., Osipenko, O. N., Vizi, E. S., and Spat, A. (1995). Activation of calcium current in voltage-clamped rat glomerulosa cells by potassium ions. *J. Physiol.* 483(Pt 1), 67–78.

Varnai, P., Petheo, G. L., Makara, J. K., and Spat, A. (1998). Electrophysiological study on the high K+ sensitivity of rat glomerulosa cells. *Pflugers Arch.* 435, 429–431.

Verlander, J. W., Madsen, K. M., Cannon, J. K., and Tisher, C. C. (1994). Activation of acid-secreting intercalated cells in rabbit collecting duct with ammonium chloride loading. *Am. J. Phys.* 266, F633–F645.

Verrey, F., Fakitsas, P., Adam, G., and Staub, O. (2008). Early transcriptional control of ENaC (de)ubiquitylation by aldosterone. *Kidney Int.* 73, 691–696. doi: 10.1038/sj.ki.5002737

Vinson, G. P. (2016). Functional zonation of the adult mammalian adrenal cortex. *Front. Neurosci.* 10:238. doi: 10.3389/fnins.2016.00238

Wakabayashi, M., Mori, T., Isobe, K., Sohara, E., Susa, K., Araki, Y., et al. (2013). Impaired KLHL3-mediated ubiquitination of WNK4 causes human hypertension. *Cell Rep.* 3, 858–868. doi: 10.1016/j.celrep.2013.02.024

Wang, Q. J. (2006). PKD at the crossroads of DAG and PKC signaling. *Trends Pharmacol. Sci.* 27, 317–323. doi: 10.1016/j.tips.2006.04.003

Wang, J. J., Peng, K. Y., Wu, V. C., Tseng, F. Y., and Wu, K. D. (2017). CTNNB1 mutation in aldosterone producing adenoma. *Endocrinol. Metab.* 32, 332–338. doi: 10.3803/EnM.2017.32.3.332

Weidmann, P., Hellmueller, B., Uehlinger, D. E., Lang, R. E., Gnaedinger, M. P., Hasler, L., et al. (1986). Plasma levels and cardiovascular, endocrine, and excretory effects of atrial natriuretic peptide during different sodium intakes in man. *J. Clin. Endocrinol. Metab.* 62, 1027–1036.

Williams, T. A., Monticone, S., and Mulatero, P. (2015). KCNJ5 mutations are the most frequent genetic alteration in primary aldosteronism. *Hypertension* 65, 507–509. doi: 10.1161/HYPERTENSIONAHA.114.04636

Wilson, F. H., Disse-Nicodeme, S., Choate, K. A., Ishikawa, K., Nelson-Williams, C., Desitter, I., et al. (2001). Human hypertension caused by mutations in WNK kinases. *Science* 293, 1107–1112. doi: 10.1126/science.1062844

Winnay, J. N., and Hammer, G. D. (2006). Adrenocorticotropic hormone-mediated signaling cascades coordinate a cyclic pattern of steroidogenic factor 1-dependent transcriptional activation. *Mol. Endocrinol.* 20, 147–166. doi: 10.1210/me.2005-0215

Wu, H., Chen, L., Zhou, Q., and Zhang, W. (2011). AF17 facilitates Dot1a nuclear export and upregulates ENaC-mediated Na+ transport in renal collecting duct cells. *PLoS One* 6:e27429. doi: 10.1371/journal.pone.0027429

Wu, G., and Peng, J. B. (2013). Disease-causing mutations in KLHL3 impair its effect on WNK4 degradation. *FEBS Lett.* 587, 1717–1722. doi: 10.1016/j.febslet.2013.04.032

Xu, B. E., Stippec, S., Chu, P. Y., Lazrak, A., Li, X. J., Lee, B. H., et al. (2005a). WNK1 activates SGK1 to regulate the epithelial sodium channel. *Proc. Natl. Acad. Sci. U. S. A.* 102, 10315–10320. doi: 10.1073/pnas.0504422102

Xu, B. E., Stippec, S., Lazrak, A., Huang, C. L., and Cobb, M. H. (2005b). WNK1 activates SGK1 by a phosphatidylinositol 3-kinase-dependent and non-catalytic mechanism. *J. Biol. Chem.* 280, 34218–34223. doi: 10.1074/jbc.M505735200

Yao, J., Davies, L. A., Howard, J. D., Adney, S. K., Welsby, P. J., Howell, N., et al. (2006). Molecular basis for the modulation of native T-type Ca^{2+} channels in vivo by Ca^{2+}/calmodulin-dependent protein kinase II. *J. Clin. Invest.* 116, 2403–2412. doi: 10.1172/JCI27918

Yoshimoto, T., and Hirata, Y. (2007). Aldosterone as a cardiovascular risk hormone. *Endocr. J.* 54, 359–370. doi: 10.1507/endocrj.KR-80

Young, M. J., Clyne, C. D., Cole, T. J., and Funder, J. W. (2001). Cardiac steroidogenesis in the normal and failing heart. *J. Clin. Endocrinol. Metab.* 86, 5121–5126. doi: 10.1210/jcem.86.11.7925

Yu, L., Cai, H., Yue, Q., Alli, A. A., Wang, D., Al-Khalili, O., et al. (2013). WNK4 inhibition of ENaC is independent of Nedd4-2-mediated ENaC ubiquitination. *Am. J. Physiol. Renal Physiol.* 305, F31–F41. doi: 10.1152/ajprenal.00652.2012

Zachar, R. M., Skjødt, K., Marcussen, N., Walter, S., Toft, A., Nielsen, M. R., et al. (2015). The epithelial sodium channel γ-subunit is processed proteolytically in human kidney. *J. Am. Soc. Nephrol.* 26, 95–106. doi: 10.1681/ASN.2013111173

Zhang, L., Chen, L., Gao, C., Chen, E., Lightle, A. R., Foulke, L., et al. (2020). Loss of histone H3 K79 methyltransferase Dot1l facilitates kidney fibrosis by upregulating endothelin 1 through histone deacetylase 2. *J. Am. Soc. Nephrol.* 31, 337–349. doi: 10.1681/ASN.2019070739

Zhang, W., Xia, X., Reisenauer, M. R., Rieg, T., Lang, F., Kuhl, D., et al. (2007). Aldosterone-induced Sgk1 relieves Dot1a-Af9-mediated transcriptional repression of epithelial Na+ channel alpha. *J. Clin. Invest.* 117, 773–783 (Comment in the same issue of *J. Clin. Invest.* 592–595, Selection by Faculty of 1000). doi: 10.1172/JCI29850

Zhang, W., Yu, Z., Wu, H., Chen, L., Kong, Q., and Kone, B. C. (2013). An Af9 cis-element directly targets Dot1a to mediate transcriptional repression of the alphaENaC gene. *Am. J. Physiol. Renal Physiol.* 304, F367–F375. doi: 10.1152/ajprenal.00537.2011

Zhou, J., Azizan, E. A. B., Cabrera, C. P., Fernandes-Rosa, F. L., Boulkroun, S., Argentesi, G., et al. (2021). Somatic mutations of GNA11 and GNAQ in CTNNB1-mutant aldosterone-producing adenomas presenting in puberty, pregnancy or menopause. *Nat. Genet.* 53, 1360–1372. doi: 10.1038/s41588-021-00906-y

Zhou, X., Chen, K., Wang, Y., Schuman, M., Lei, H., and Sun, Z. (2016). Antiaging gene klotho regulates adrenal CYP11B2 expression and aldosterone synthesis. *J. Am. Soc. Nephrol.* 27, 1765–1776. doi: 10.1681/ASN.2015010093

Zhou, R., Patel, S. V., and Snyder, P. M. (2007). Nedd4-2 catalyzes ubiquitination and degradation of cell surface ENaC. *J. Biol. Chem.* 282, 20207–20212. doi: 10.1074/jbc.M611329200

Conflict of Interest: The authors declare that the research was conducted in the absence of any commercial or financial relationships that could be construed as a potential conflict of interest.

Publisher's Note: All claims expressed in this article are solely those of the authors and do not necessarily represent those of their affiliated organizations, or those of the publisher, the editors and the reviewers. Any product that may be evaluated in this article, or claim that may be made by its manufacturer, is not guaranteed or endorsed by the publisher.

frontiers in Physiology

ORIGINAL RESEARCH
published: 11 February 2022
doi: 10.3389/fphys.2022.784521

(Pro)renin Receptor Regulates Phosphate Homeostasis in Rats *via* Releasing Fibroblast Growth Factor-23

*Aihua Lu[1], Min Pu[1], Shiqi Mo[1], Jiahui Su[1], Jiajia Hu[1], Chunling Li[1], Weidong Wang[1] and Tianxin Yang[2]**

[1] Institute of Hypertension, Zhongshan School of Medicine, Sun Yat-sen University, Guangzhou, China, [2] Department of Internal Medicine, University of Utah and Veterans Affairs Medical Center, Salt Lake City, UT, United States

Phosphate (Pi) is one of the basic necessities required for sustenance of life and its metabolism largely relies on excretory function of the kidney, a process chiefly under the endocrine control of bone-derived fibroblast growth factor 23 (FGF23). However, knowledge gap exists in understanding the regulatory loop responsible for eliciting phophaturic response to Pi treatment. Here, we reported a novel role of (pro)renin receptor (PRR) in mediating phosphaturic response to Pi treatment *via* upregulation of FGF23 production. Male Sprague-Dawley rats were pretreated for 5 days *via* osmotic pump-driven infusion of a PRR antagonist PRO20 or vehicle, and then treated with high Pi (HP) solution as drinking fluid for the last 24 h. PRO20 reduced HP-induced Pi excretion by 42%, accompanied by blunted upregulation of circulating FGF23 and parathyroid hormone (PTH) and downregulation of renal Na/Pi-IIa expression. In cultured osteoblast cells, exposure to HP induced a 1.56-fold increase in FGF23 expression, which was blunted by PRO20 or siRNA against PRR. Together, these results suggest that activation of PRR promotes phosphaturic response through stimulation of FGF23 production and subsequent downregulation of renal Na/Pi-IIa expression.

Keywords: (pro)renin receptor, fibroblast growth factor 23, phosphate homeostasis, Na^+-dependent Pi transporter, parathyroid hormone

OPEN ACCESS

Edited by:
Hui Cai,
Emory University, United States

Reviewed by:
Eleanor DeLand Lederer,
University of Texas Southwestern Medical Center, United States
Aihua Zhang,
Nanjing Children's Hospital, China

****Correspondence:***
Tianxin Yang
Tianxin.Yang@hsc.utah.edu

Specialty section:
This article was submitted to Renal and Epithelial Physiology, a section of the journal Frontiers in Physiology

Received: *28 September 2021*
Accepted: *14 January 2022*
Published: *11 February 2022*

Citation:
Lu A, Pu M, Mo S, Su J, Hu J, Li C, Wang W and Yang T (2022) (Pro)renin Receptor Regulates Phosphate Homeostasis in Rats via Releasing Fibroblast Growth Factor-23. Front. Physiol. 13:784521. doi: 10.3389/fphys.2022.784521

INTRODUCTION

Phosphate (Pi) is an essential nutrient and component of the human body. Adequate phosphate balance is essential for the maintenance of fundamental cellular functions of the mammalian system, ranging from energy metabolism to mineral ion metabolism (Gaasbeek and Meinders, 2005). The kidney plays a pivotal role in maintenance of Pi homeostasis by adjustment of reabsorption and excretion (Shimada et al., 2004a; Urakawa et al., 2006). In the kidney, most of the filtered Pi is reabsorbed across the proximal tubule cells (Katai et al., 1999 Giral et al., 2009). Evidence from physiological studies suggests that Na^+-dependent Pi transporters in the brush-border membrane (BBM) of proximal tubular cells mediate the rate-limiting step in the overall Pi-reabsorptive process (Murer et al., 2000, 2003). An alteration of proximal tubular reabsorption

of Pi in kidney was thought to depend on the abundance of NaPi-lla (Npt2a) or NaPi-llc (Npt2c) proteins residing in the BBM (Biber and Murer, 1994; Busch et al., 1994; Shirazi-Beechey et al., 1996). Na^+- Pi cotransporter knock out mouse demonstrated that NaPi-lla was responsible for approximately 70% of BBM Na/Pi cotransport activity (Beck et al., 1998; Murer et al., 2004).

Renal handling of Pi is tightly regulated by endocrine hormones, particularly fibroblast growth factor 23 (FGF23), vitamin D_3, and PTH (Pfister et al., 1998; Shimada et al., 2004a; Liu et al., 2006; Farrow et al., 2009; Gattineni et al., 2009; Guo et al., 2013). Among these, FGF23 is a bone-derived hormone secreted by osteoblasts and osteocytes in response to increased Pi concentration as well as vitamin D (Saito et al., 2005; Antoniucci et al., 2006; Perwad et al., 2007). FGF23 acts on the distal convoluted tubule that may trigger a cascade that reduces proximal tubular Pi reabsorption (Farrow et al., 2009). Studies in animal models have shown that increased serum concentrations of FGF23 lead to renal Pi wasting through downregulation of Npt2a and Npt2c in the proximal tubule (PT) apical membrane (Larsson et al., 2004; Shimada et al., 2004b).

(Pro)renin receptor (PRR) is a member of the renin-angiotensin system (RAS) (Nguyen et al., 2002) and generally thought to serve as a specific receptor for both prorenin and renin. PRR is composed of a large N-terminal extracellular domain, a single transmembrane domain, and a short cytoplasmic domain (Burckle and Bader, 2006). The full length PRR (fPRR) is cleaved by site-1 protease (S1P) to generate N-terminal soluble PRR (sPRR) and the C-terminal membrane-bound M8-9 fragment (Nakagawa et al., 2017). Increasing evidence has demonstrated that PRR-mediated activation of the intrarenal RAS plays an essential role in renal handling of Na^+ and water balance (Gonzalez and Prieto, 2015; Lu et al., 2016a,b; Quadri and Siragy, 2016; Peng et al., 2017; Prieto et al., 2017). Activation PRR triggers multiple signaling transduction pathways such as β-catenin signaling and thus can act in a RAS-independent manner (Kouchi et al., 2017; Li et al., 2017; Gao et al., 2020). So far, there is no prior research to address a potential role of PRR in regulation of Pi homeostasis. The overall goal of the present study was to test the role of PRR in phosphaturic response to HP treatment and further to address the underlying mechanism.

MATERIALS AND METHODS

Animals

Male Sprague-Dawley rats (220–270 g) were purchased from the Medical Experimental Animal Center at Sun Yat-sen University. All animal protocols were conformed to the Experimental Animal Management Regulations of Sun Yat-sen University. Rats were acclimated in metabolic cages for 3 days prior to the start of the study. Rats were randomly divided into three experimental groups ($N = 5$ per group): (1) control group, (2) HP group, or (3) HP + PRO20 group. Animals in HP and HP + PRO20 groups drank high phosphate fluid (5 × phosphate buffered saline, pH 7.4, [Pi] = 50 mM) for 24 h (Ide et al., 2016) and the control group drank tap water. Five days prior to HP treatment, osmotic minipump (2001, Alzet, United States) was implanted to deliver vehicle or PRO20 at 700 μg/kg/d as previously described (Wang et al., 2016, 2020). Twenty four-hour urine was collected using metabolic cages.

Plasma and Urine Parameters

Plasma and urine creatinine was determined by the QuantiChrom™ Creatinine Assay Kit (DICT-500, BioAssay Syatems, United States). Plasma and urine sodium, potassium and chlorine levels were determined by the Sodium, Potassium and Chlorine Assay Kit, respectively (Nanjing Jiancheng Bioengineering Institute, China). Plasma and urine phosphorus and calcium levels were determined by the Micro Blood Phosphorus and Calcium Concentration Assay Kit, respectively (Solarbio life sciences, China). Plasma and urine soluble PRR (sPRR) levels were determined by the ELISA kit (27782, IBL, Japan). Plasma FGF23, PTH and $1,25(OH)_2D_3$ concentrations were assayed using the ELISA kits (Cloud-Clone Corp., China). All of these ELISA assays were performed according to the manufacturer's protocols.

Isolation of Renal Brush-Border Membranes

Renal BBMs were isolated by double magnesium chloride ($MgCl_2$) precipitation as previously described (Gattineni et al., 2009) with minor modifications. After removal of the renal capsule, the renal cortex was isolated and homogenized in 2 ml of cold 2 × homogenization buffer (12 mM Tris pH 7.4, 300 mM mannitol, 5 mM EGTA). $MgCl_2$ was added to a final concentration of 12 mM and samples were incubated on ice for 15 min with occasional mixing. Then the aggregated membranes were removed by 15-min centrifugation at 3,000 *g* and 4°C, and the supernatant was then centrifuged for 30 min at 40,000 *g* and 4°C. The pellet was resuspended in 1 ml of 1 × cold homogenization buffer supplemented with 12 mM $MgCl_2$. After a second incubation and 15-min centrifugation at 3,000 *g* and 4°C and the supernatant was recovered and centrifuged at 40,000 *g*, 4°C, for 30 min. The BBM pellets were resuspended in RIPA buffer. All solutions were supplemented with protease inhibitors (1 mM PMSF).

Immunoblotting

Protein samples were fractionated on SDS-PAGE (30 μg/well) and transferred to a nitrocellulose membrane (Millipore). Immunoblots were incubated overnight at 4°C with primary antibodies including anti-ACE (1:1,000, GTX100923, GeneTex, United States), anti-AGT (1:1,000, GTX103824, GeneTex, United States), anti-renin (1:1,000, sc-133145, Santa, United States), anti-PRR (1:1,000, HPA003156, Sigma, United States), anti-Npt2a (1:1,000, A6742, Abclonal, China), anti-Npt2c (1:1,000, ab155986, Abcam, United Kingdom) or anti-β-actin (1:10,000, A1978, Sigma, United States) antibody in 1.5% (w/v) bovine serum albumin (BSA, Sigma, United States) in a TBS-T buffer [150 mM NaCl, 10 mM Tris (pH 7.4/HCl), 0.2% (v/v) Tween-20]. After washing, membranes were incubated with horseradish peroxidase-conjugated secondary antibodies

(1:3,000, Thermo Fisher Scientific™ Pierce™). Specific signal was visualized by ECL kit (Thermo Fisher Scientific™ Pierce™). The protein bands were detected using Amersham Imager 600 and quantified by Image Pro Plus version 6.0 software (Molecular Dynamics).

Quantitative Reverse Transcriptase PCR

Total RNA was extracted using Trizol (TRIzol, Invitrogen) following manufacturer's instructions. RNA concentrations were quantified at 260 nm, and purity and integrity were determined using NanoDrop 2000. Reverse transcription was performed using iScript™ cDNA Synthesis Kit (Bio-Rad, United States). The mRNA expression was measured by quantitative RT-PCR using SYBR® *Premix Ex Taq*™ II (Tli RNaseH Plus, TaKaRa, China). The following primers were used: ACE: 5′-GAGCCATCCTTCCC–TTTTTC-3′ (forward) and 5′-CCACATGTTCCCTAGCAG-GT-3′ (reverse), AGT: 5′-AGCATCCTCCTTGAACTCCA-3′ (forward) and 5′-TGATTTTTGCCCAGGAT- -AGC-3′ (reverse), renin: 5′-GATCACCATGAAGGGG-GTCTCTGT-3′ (forward) and 5′-GTTCCTGAAGGGATTCTTTTGCAC-3′ (reverse), PRR: 5′-CTGGTGGCG--GGTGCTTTAG-3′ (forward) and 5′-GCTACGTCTGGGAT-TCGATCT-3′ (reverse), Npt2a: 5′-GCCAGCATGACGTTTGTTGT-3′ (forward) and 5′-ATCACACCCAGG–CCAATGAG-3′ (reverse), Npt2c:5′-TGACTGTCCAAGCGT-CTGTC-3′ (forward) and 5′-TTCATCCCGATCCCCTGACT-3′ (reverse). GAPDH served as an internal control and its primer sequences were: 5′-GTCTTCACTACCA-TGGAGAAGG-3′ (forward) and 5′-TCATGGATGACCTT-GGCCAG-3′ (reverse).

Immunohistochemistry

Under anesthesia, kidneys were harvested and fixed with 10% paraformaldehyde. Paraffin embedded kidney sections were processed for IHC as previously described (Wang et al., 2015). Primary antibody for PRR (1:200, ab40790, Abcam, United Kingdom) was incubated overnight at 4°C. Sections were washed three times with 0.01 M PBS buffer and secondary antibody horseradish peroxidase (HRP)-conjugated goat anti-rabbit (1:300, Thermo Fisher Scientific) was incubated at room temperature for an hour. The staining procedure was performed using DAB Horseradish Peroxidase Color Development Kit (P0202, Beyotime Biotechnology, China) according to the manufacturer's protocols. Immunohistochemical staining was detected with an Olympus BX 63 microscope (20 × and 40 × objective).

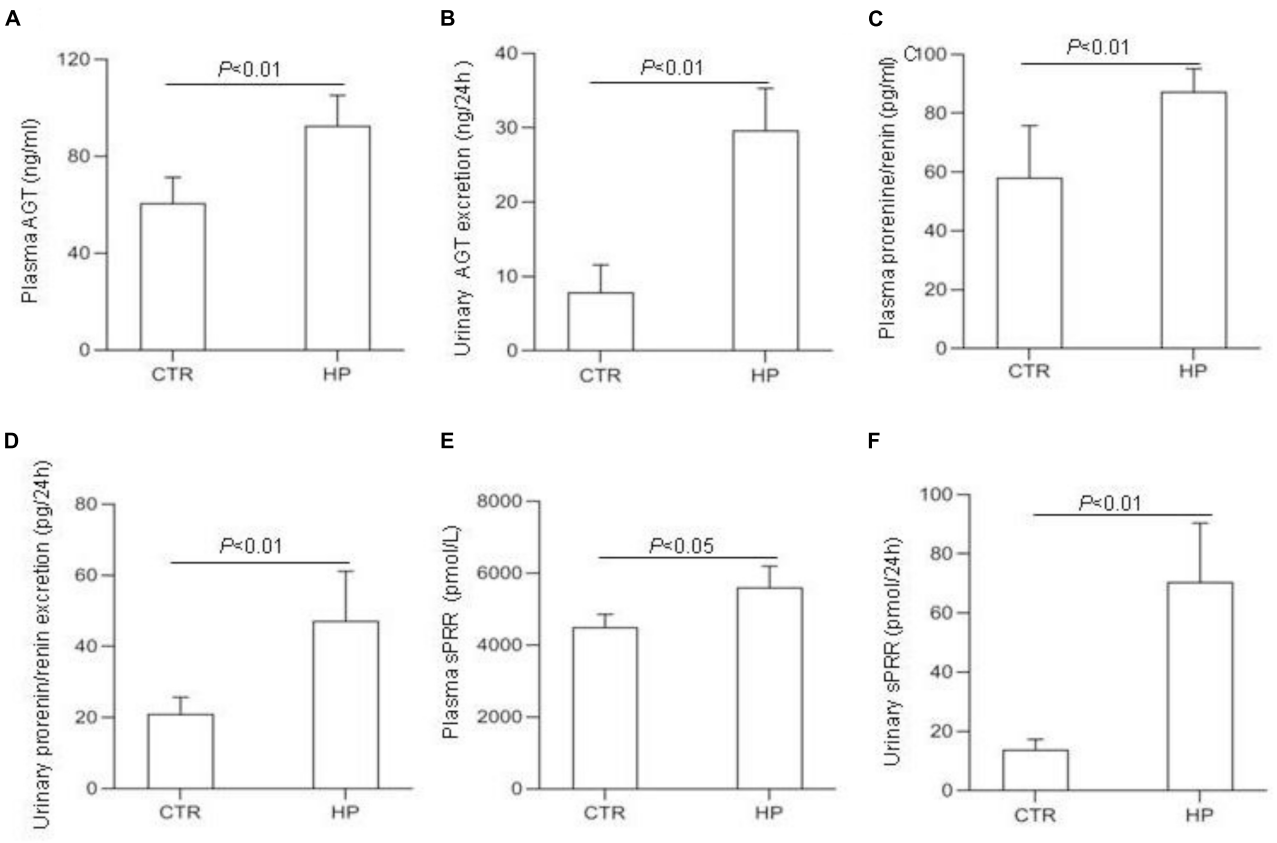

FIGURE 1 | Analysis of the RAS components in rat plasma and urine following HP intake. **(A)** Plasma angiotensin (AGT) concentration. **(B)** Urinary AGT excretion. **(C)** Plasma renin concentration. **(D)** Urinary renin excretion. **(E)** Plasma soluble (pro)renin receptor (sPRR) concentration. **(F)** Urinary sPRR excretion. CTR, control; HP, high Pi intake *N* = 5 per group. Data are Mean ± SEM.

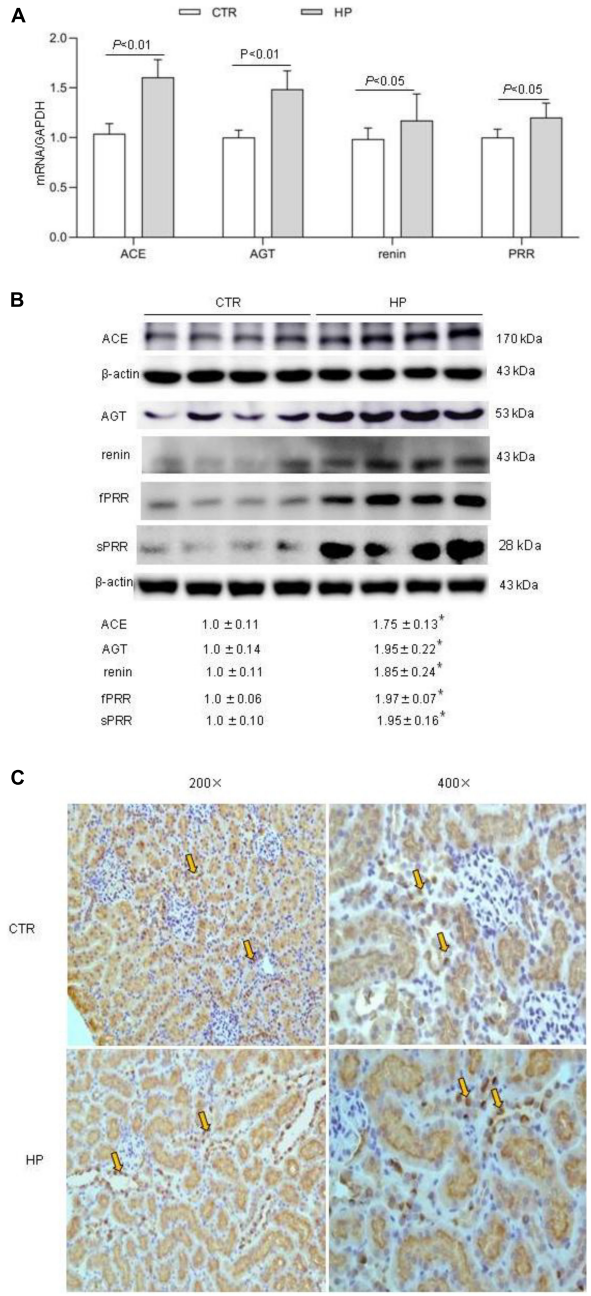

FIGURE 2 | Analysis of the RAS components in rat kidneys following HP intake. **(A)** qRT-PCR detection of renal transcripts of ACE, AGT, renin, and PRR. GAPDH was used as internal reference. **(B)** Immunoblotting analysis of renal expression of ACE, AGT, renin, fPRR and sPRR. The values indicate the corresponding densitometry analysis. β-actin was used as an internal reference. **(C)** Representative images of PRR immunostaining. Arrows indicate positive staining (200×, 400×). *N* = 5 per group. Data are Mean ± SEM. *$p < 0.05$ vs. CTR.

Cell Culture

The MC3T3-E1 cells were obtained from as a gift from Dr. Zhi Tan (Sun Yat-sen University). Cells were cultured in MEM-αalpha (Thermo Fisher Scientific) supplemented with 10% fetal bovine serum, and 1% penicillin-streptomycin. Cells were seeded on 6 well plates. After 24 h, the cells were starved in media containing 0.5% FBS for 24 h. Then the cells were treated with 10 mM Pi for another 24 h. To evaluate the effects of PRR on the levels of FGF23, PRO20 was given at 10 nM. To further verify the involvement of PRR, PRR was silenced by transfecting the cells with siRNA against PRR. Scrambled siRNA served as a control. SiRNA for mouse PRR and control siRNA were purchased from Ruibo Biotech (Guangzhou, China). After the treatment, the medium was collected and assayed for sPRR or FGF23 assays (EK5626, SAB, United States).

TABLE 1 | General physiological data in rats.

	CTR	HP	HP + PRO20
Fluid intake (ml/24 h)	25.42 ± 0.63	12.61 ± 0.38**	12.21 ± 0.58**
Urine volumes (ml/24 h)	10.41 ± 1.20	14.21 ± 0.48*	14.01 ± 0.31*
Plasma creatinine (mg/dl)	0.58 ± 0.01	0.58 ± 0.01	0.57 ± 0.02
Plasma-Na^+ (mmol/l)	126.5 ± 1.38	126.12 ± 1.73	125.47 ± 2.31
Plasma-K^+ (mmol/l)	3.68 ± 0.06	3.65 ± 0.07	3.67 ± 0.14
Plasma-Cl^- (mmol/l)	113.74 ± 1.97	115.04 ± 0.84	111.84 ± 1.55
Urinary creatinine (mg/24 h)	7.18 ± 0.43	8.07 ± 0.15	7.80 ± 0.19
Urinary Na^+ (mmol/24 h)	1.03 ± 0.03	4.58 ± 0.18**	4.41 ± 0.27**
Urinary K^+ (mmol/24 h)	3.43 ± 0.18	3.50 ± 0.09	3.46 ± 0.12
Urinary Cl^- (mmol/24 h)	1.72 ± 0.10	3.31 ± 0.05**	3.27 ± 0.08**
Plasma osmolarity (mosn/kg·H_2O)	312 ± 2.06	313 ± 0.94	312 ± 1.27
Urine osmolarity (mosn/kg·H_2O)	1,340.4 ± 34.60	1,407.00 ± 45.52	1,379.50 ± 49.75

*Data represent the means ± SEM. *p < 0.05, **p < 0.01 vs. CTR. CTR, control.*

Statistical Analysis

Data is expressed as mean ± standard error (SEM). All data points were included for analyses. Samples sizes were determined based on similar previous studies. Statistical analysis for animal and cell cultures experiments was performed by means of one-way analysis of variance (ANOVA) for multiple-group comparison or Student's *t*-test for two-group comparison. A *p*-value below 0.05 was considered statistically significant.

RESULTS

Activation of (Pro)renin Receptor and Other Renin-Angiotensin System Components by High Pi Intake

To test whether HP activated the RAS, we determined the levels of RAS components in urine and plasma from rats on normal Pi (NP) or HP intake using ELISA. The results showed that the levels angiotensinogen (AGT), renin, sPRR in urine and plasma from the HP group were significantly increased as compared with NP controls (**Figure 1**). By qRT-PCR, renal cortical mRNA expression of angiotensin-converting enzyme (ACE), AGT, renin, PRR were all increased in the HP group as compared with NP controls (**Figure 2A**). These results have been validated by Western blotting analysis. Of note, this analysis detected

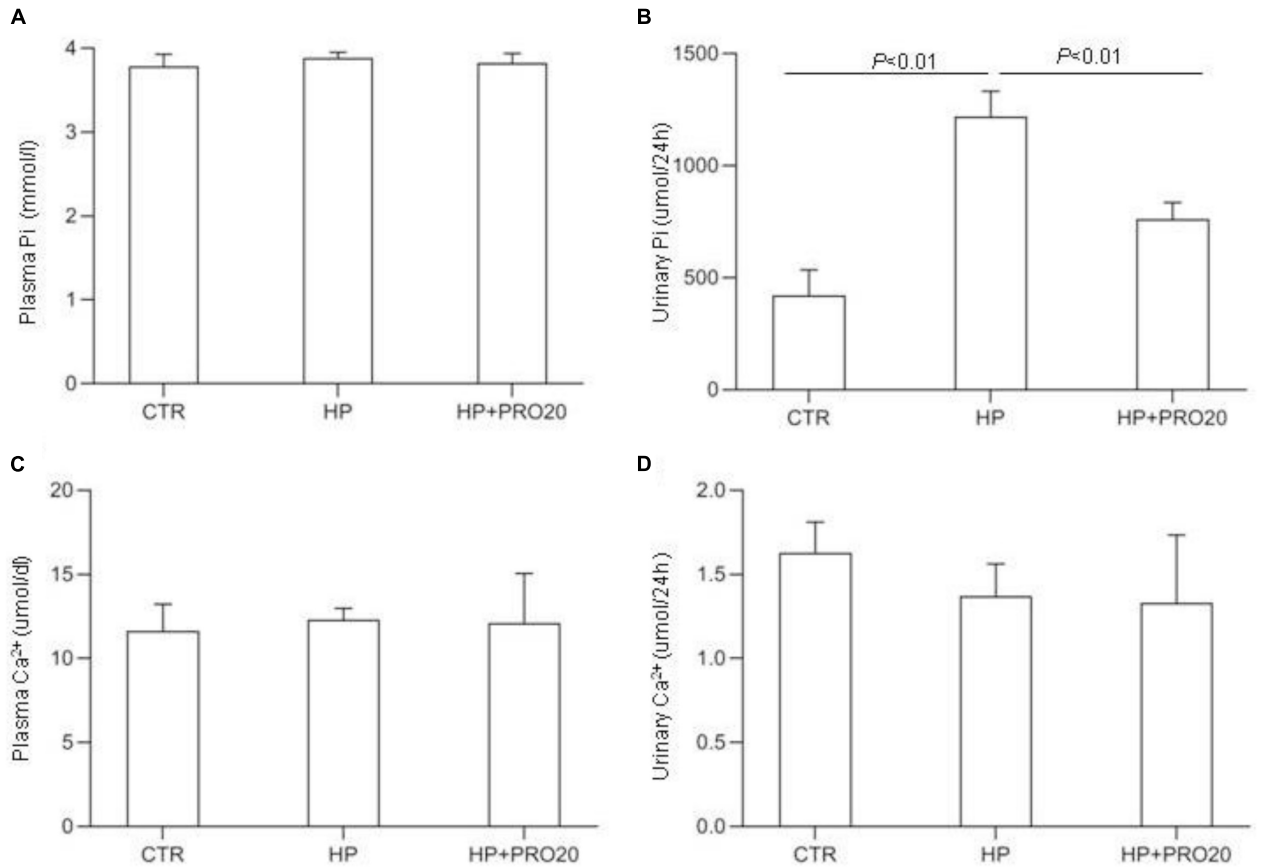

FIGURE 3 | Serum and urine biochemical parameters in NP, HP and HP + PRO20 rats. **(A)** Plasma Pi concentration; **(B)** 24-h urinary Pi excretion; **(C)** plasma Ca^{2+} concentration; **(D)** 24-h urinary Ca^{2+} excretion. *N* = 5 per group. Data are Mean ± SEM.

increases in the protein abundances of both PRR and sPRR in the kidney of HP rats (**Figure 2B**). By immunohistochemistry, PRR protein expression was elevated in the collecting duct by HP treatment (**Figure 2C**), a pattern consistent with intercalated cell labeling as reported previously (Wang et al., 2016).

Effect of PRO20 on Phosphaturic Response to High Pi Intake

SD rats drank tap water, HP fluid alone or in combination with PRO20 treatment. Basic physiological data is shown in **Table 1**. Fluid intake was less but urine output was higher in HP rats as compared with vehicle control. This was paralleled with increased 24-h urinary excretion of Na^+, K^+, and Cl^- induced by HP treatment. However, plasma creatinine and osmolality remained unchanged. None of these parameters were affected by PRO20.

To address the functional role of PRR in Pi homeostasis, we examined the effect of PRO20 on phosphaturic response to HP intake. HP intake induced a significant increase in urinary Pi excretion within 24 h and this increase was blunted by PRO20 treatment (**Figure 3B**). In parallel, HP intake elevated circulating FGF23 and PTH, both of which were nearly normalized by PRO20 treatment (**Figures 4A,B**). Despite reduced urinary Pi excretion, PRO20 treatment in HP rats did not affect plasma Pi concentration (**Figure 3A**). In a sharp contrast, plasma Ca^{2+} concentration (**Figure 3C**), urinary Ca^{2+} excretion (**Figure 3D**), or plasma $1,25(OH)_2D_3$ (**Figure 4C**) were unaffected by HP intake or PRO20 treatment.

In a separate experiment, we examined the effect of PRO20 on several key parameters of Pi homeostasis in 7-wk-old male SD rats under basal condition (n = 5 per group). The data showed that PRO20 had no effect on urinary Pi excretion (PRO20 429.2 ± 16.8 vs. CTR 432.4 ± 17.8 μmol/24 h, $p > 0.05$), plasma Pi concentration (PRO20 2.89 ± 0.06 vs. CTR 2.90 ± 0.08, mmol/L, $p > 0.05$), plasma FGF-23 (PRO20 374.3 ± 15.4 vs. CTR 381.3 ± 10.2 pg/ml, $p > 0.05$), or urine volume (PRO20 9.75 ± 0.42 vs. CTR, 10.45 ± 0.85 ml, $p > 0.05$).

Downregulation of renal expression of sodium-phosphate cotransporters is a key determinant of phosphaturic response during HP intake (Murer et al., 1999; Hernando et al., 2001; Giral et al., 2009; Bourgeois et al., 2013; Forster et al., 2013; Zhuo et al., 2020). Therefore, we determined renal expression of Npt2a and Npt2c by both qRT-PCR and Western blotting analysis. In response to HP intake, renal cortical mRNA expression of Npt2a was significantly decreased, which was blunted by PRO20 treatment (**Figure 5A**). In contrast, the mRNA expression of Npt2c showed no significant changes in the three

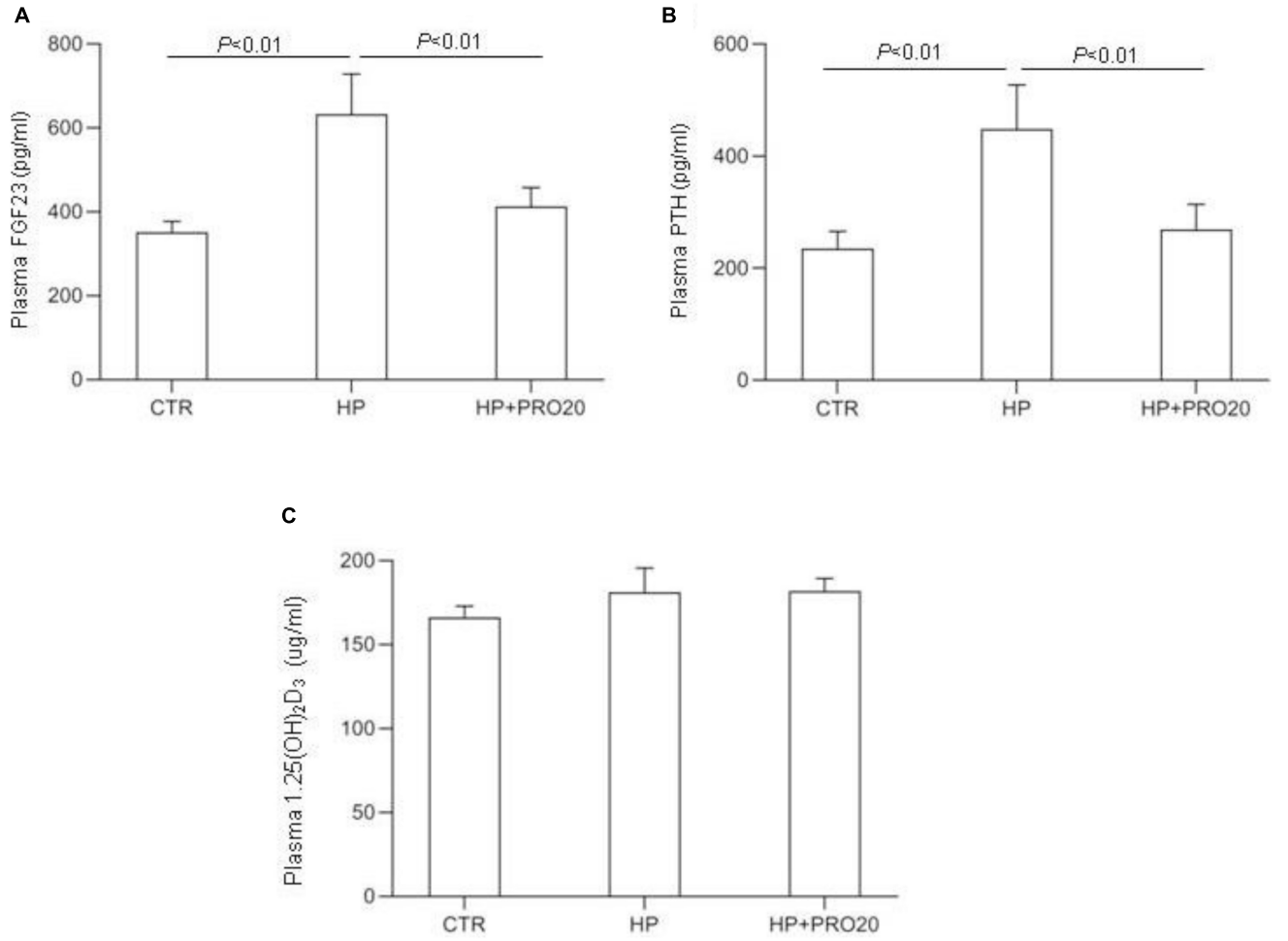

FIGURE 4 | Levels of plasma FGF23 **(A)**, plasma PTH **(B)**, and plasma $1,25(OH)_2D_3$ **(C)** were measured in CTR, HP, and HP + PRO20 rats. FGF23, fibroblast growth factor 23; PTH, parathyroid hormone; *N* = 5 per group. Data are Mean ± SEM.

groups (**Figure 5A**). Meanwhile, we examined the abundance of sodium-phosphate cotransporters in the kidney BBM by Western blotting analysis. The protein abundance of Npt2a in BBM was downregulated by HP intake as compared with the NP control and this downregulation was prevented by PRO20 (**Figure 5B**). In contrast, no change was observed in protein abundance of Npt2c in BBM (**Figure 5B**).

Effect of (Pro)renin Receptor on FGF23 Production in Cultured MC3T3-E1 Cells

The observation of suppressed circulating FGF23 concentration by PRO20 treatment during HP intake prompted us to speculate that the bone might be a potential site of PRR regulation of FGF23 release. To address this possibility, we conducted *in vitro* experiments using MC3T3-E1 cells, a mouse osteoblast cell line. The cells were exposed to normal or high Pi (10 mM Pi) for 24 h followed by examination of expression of FGF23 as well as PRR. qRT-PCR results showed that the expression of PRR and FGF23 mRNA was both significantly increased by HP treatment (**Figure 6A**). Consistent with this result, Western blotting analysis demonstrated significant elevations of protein abundance of full-length PRR (fPRR) and sPRR (**Figure 6B**). ELISA results showed that the concentrations of sPRR and FGF23 in the medium were significantly increased by HP treatment (**Figures 6C,D**).

Next, we examined the functional role of PRR in regulation of the production of FGF23 in the MC3T3-E1 cells by using PRO20. The cells were pretreated for 1 h with 10 μM PRO20 and then treated with 10 mM Pi for 24 h. By qRT-PCR, HP treatment increased the expression of FGF23 mRNA, and this increase was blunted by PRO20 (**Figure 7A**). This result was subsequently validated at protein level by ELISA (**Figure 7B**).

To further verify the above-mentioned results obtained with the pharmacological approach, we conducted independent experiments using siRNA approach to knockdown PRR. The efficacy of the gene knockdown was confirmed by qRT-PCR and Western blotting analysis (**Figures 8A,B**). PRR knockdown significantly blocked HP-induced FGF23 expression as assessed by qRT-PCR (**Figure 8C**) and ELISA (**Figure 8D**).

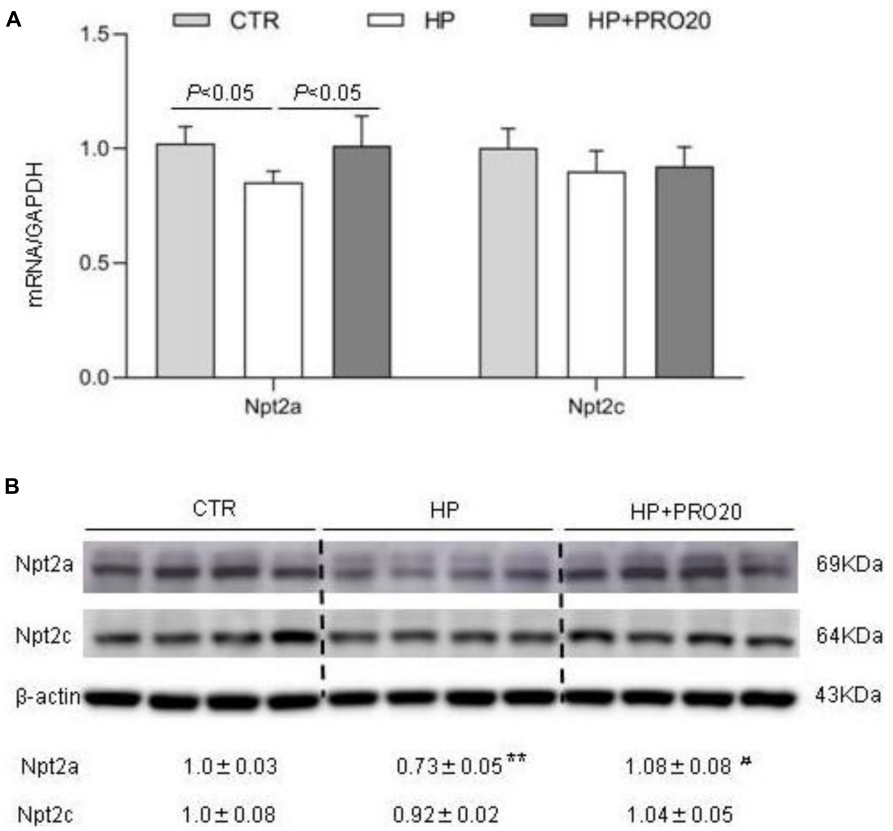

FIGURE 5 | Analysis of renal expression of Pi transporters in NP, HP and HP + PRO20 rats. **(A)** qRT-PCR analysis of renal mRNA expression of Npt2a and Npt2c. GAPDH was used as internal reference. **(B)** Immunoblotting analysis of Npt2a, and Npt2c protein expression. Brush border membrane was isolated from the kidney of all groups. The values indicate the corresponding densitometry analysis. β-actin was used as an internal reference. $N = 5$ per group. Data are Mean ± SEM. $^{**}p < 0.01$ vs. CTR, $^{\#}p < 0.05$ vs. HP.

DISCUSSION

PPR is a multi-functional protein critically involved in renal handling of Na^+, K^+ and water through RAS-dependent or -independent mechanisms (Lu et al., 2016a,b; Quadri and Siragy, 2016; Peng et al., 2017; Prieto et al., 2017; Xu et al., 2017; Ramkumar et al., 2018; Fu et al., 2019). The present study explored phosphaturic role of PRR during 24-h Pi loading. Following HP intake, the levels of circulating sPRR along with renal expression of PRR and other components of the RAS were all elevated in parallel with increased plasma FGF23 and PTH. PRR antagonism with PRO20 effectively suppressed HP-induced FGF23 and PTH levels and urinary Pi excretion albeit with unchanged plasma Pi concentration. Cell culture experiments offered a cellular mechanism of PRR regulation of FGF23 expression in an osteoblast cell line.

In response to HP intake, the levels of PRR/sPRR were elevated as evidenced by increased circulating sPRR, the cleavage product of PRR, and renal expression of PRR. The source of sPRR under HP intake remains obscure. Immunostaining mapped HP-induced PRR expression in the collecting duct (CD) with a pattern of labeling in intercalated cells (ICs) as previously reported (Wang et al., 2016). It is intriguing that the CD may serve as a potential site for the generation of sPRR during HP intake although other organs such as bone or parathyroid gland may also be involved. ICs were initially thought to primarily regulate acid-base metabolism. However, emerging evidence suggests novel sensing function of ICs during urinary tract infection and acute kidney injury (Miao and Abraham, 2014; Azroyan et al., 2015; Battistone et al., 2020). More recent evidence suggests a paracrine mechanism whereby mediators such as sPRR or prostaglandins are produced by ICs and act in the neighboring principal cells of the CD to regulate Na^+ and water reabsorption in the distal nephron (Lu et al., 2016a,b; Xu et al., 2020). Our results indicate a possibility that IC PRR may be involved in regulation of Pi homeostasis by releasing sPRR that may target other organs to control production of phosphaturic hormones such as FGF23. The involvement of IC-derived sPRR in renal handling of Pi should be tested by future investigation.

Although PRR was initially identified as a specific receptor for prorenin and renin, its relationship with RAS has been debated (Binger and Muller, 2013). Recently, abundant evidence from our group strongly supports PRR as an important regulator of intrarenal RAS during water deprivation (Wang et al., 2016), angiotensin II-induced hypertension (Wang et al., 2014, 2017) and chronic kidney injury (Fang et al., 2018), favoring

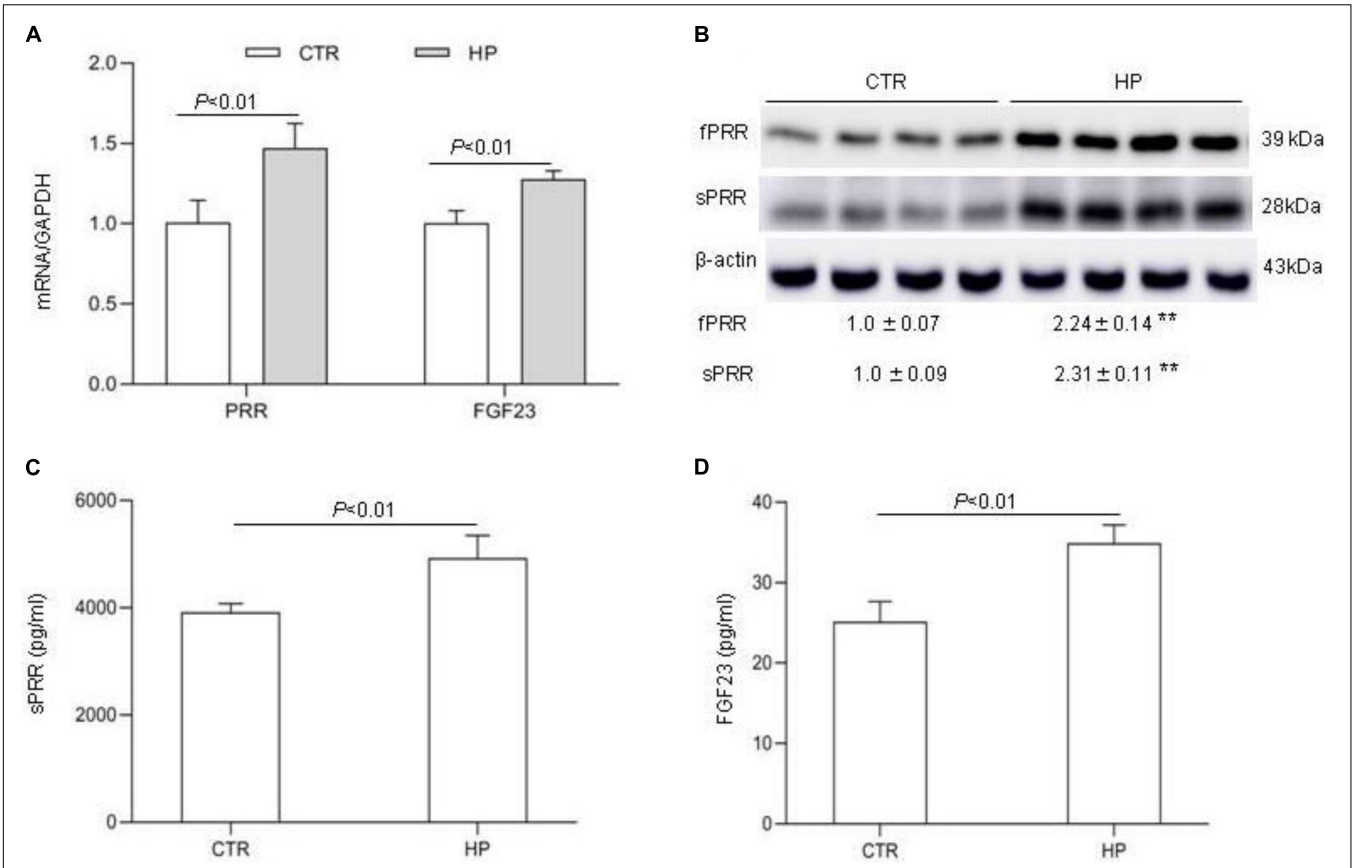

FIGURE 6 | PRR mediation of FGF23 production in cultured osteoblast cells in response to Pi treatment. MC3T3-E1 cells were exposed to vehicle or 10 mM Pi for 24 h, followed by analysis of the levels of FGF23 and PRR/sPRR. **(A)** qRT-PCR analysis of mRNA expression of PRR and FGF23. GAPDH was used as internal reference. **(B)** Immunoblotting analysis of protein abundances of fPRR and sPRR. The values indicate the corresponding densitometry analysis. β-actin was used as an internal reference. **(C)** ELISA detection of medium sPRR. **(D)** ELISA detection of medium FGF23. $N = 4$, Data are Mean ± SEM. $^{**}p < 0.01$ vs. CTR.

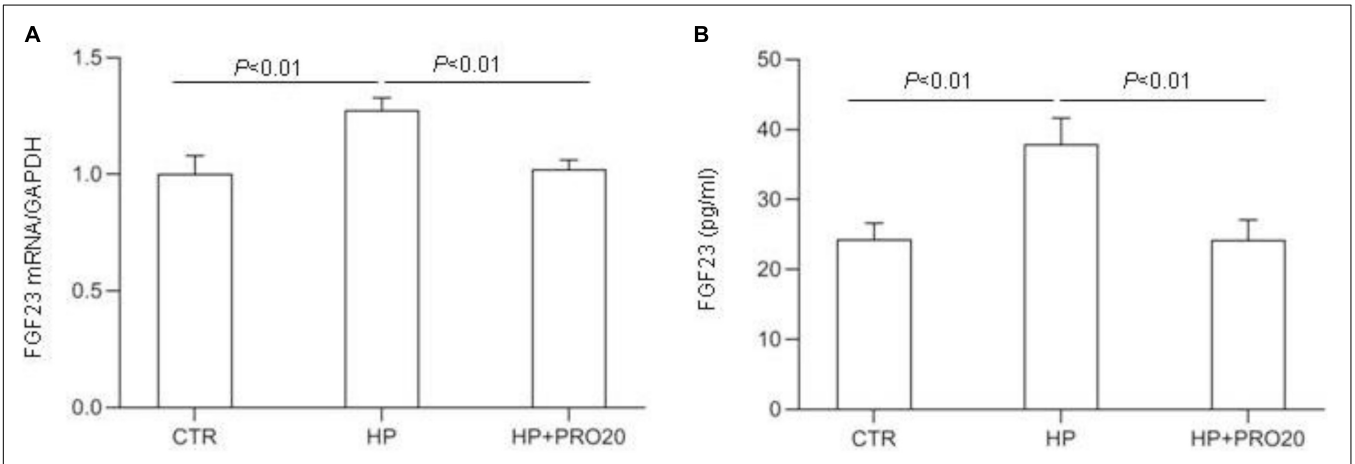

FIGURE 7 | Effects of PRO20 on the expression of FGF23 in MC3T3-E1 cells. The MC3T3-E1 cells were pretreated with PRO20 (10 μM) for 1 h, then treated with Pi (10 mM) for 24 h. **(A)** qRT-PCR analysis of mRNA expression of FGF23. GAPDH was used as internal reference. **(B)** ELISA detection of medium FGF23. $N = 4$, Data are Mean ± SEM.

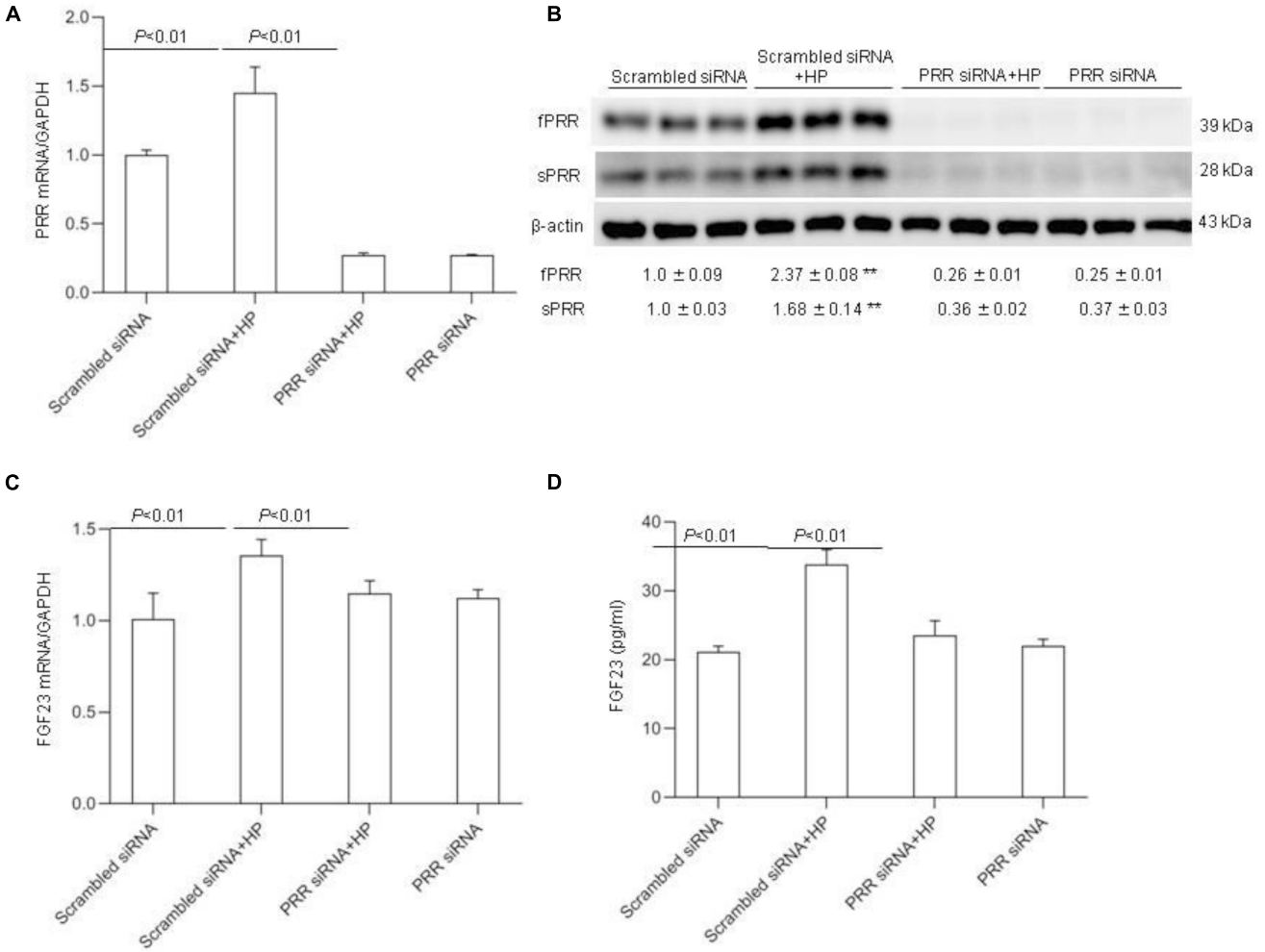

FIGURE 8 | Effects PRR siRNA on HP induced FGF23 levels in MC3T3-E1 cells. The cells were transfected with scrambled or siRNA against PRR, and then treated with vehicle or 10 mM Pi for 24 h. **(A)** qRT-PCR detection of PRR mRNA expression normalized by GAPDH. **(B)** Immunoblotting analysis of protein abundances of fPRR and sPRR were detected by Western blotting. The values indicate the corresponding densitometry analysis. β-actin was used as an internal reference. **(C)** qRT-PCR analysis of mRNA expression of FGF23 normalized by GAPDH. **(D)** ELISA analysis of medium FGF23. $N = 4$, Data are Mean ± SEM, $^{**}p < 0.01$ vs. CTR.

PRR as integrative member of the RAS. Along this line, the present study offered new evidence of activation of the RAS during HP intake. In this regard, HP treatment induced plasma and urinary excretion and renal expression of AGT and renin in parallel with elevated levels of PRR/sPRR. Future studies are needed to determine dependence of the canonical RAS components on PRR and its functional contribution to Pi homeostasis.

We employed a pharmacological approach to provide functional evidence for a novel role of PRR in mediating phosphaturic response to HP intake in rats. PRO20 has been extensively characterized as a highly specific and effective inhibitor of PRR owing to its peptide decoy activity (Danser, 2015; Li et al., 2015). Administration of PRO20 was highly effective in attenuating HP-induced urinary Pi excretion and phosphaturic hormones such as FGF23 and PTH. These hormones primarily target the kidney to downregulate abundance of Npt2a in the brush border of proximal tubules. Indeed, HP-induced downregulation of Npt2a was prevented by PRO20 treatment. The result support phosphaturic role of PRR during Pi treatment. Of note, despite impaired phosphaturic response, PRO20 didn't elevate plasma Pi concentration during HP treatment. This might be due to the relatively short duration of HP treatment. Under this condition, effective compensatory mechanism might be activated and able to maintain normal level of plasma Pi concentration.

Osteoblast cells are a known source of FGF23 production during HP intake (Liu et al., 2003; Ferrari et al., 2005; Perwad et al., 2005; Lindberg et al., 2015; Goltzman et al., 2018). Considering the observation that PRO20 effectively suppressed HP-induced circulating level of FGF23, we hypothesized that

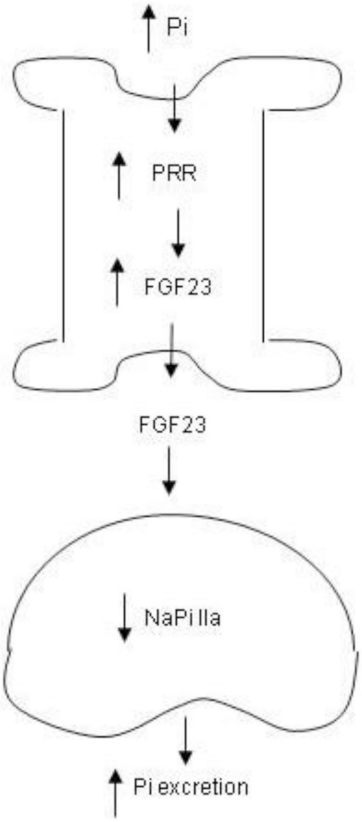

FIGURE 9 | Schematic illustration of the PRR-mediated phosphaturic response. In response to high Pi, PRR expression is elevated in the bone, leading to elevation of FGF23 production. Then FGF23 is released to the circulation and acts in the kidney to suppress NaPi IIa expression, resulting in increased Pi excretion.

FGF23 production might be under the direct control of PRR in cultured osteoblast cells. Using a cell culture model of osteoblast cells, we obtained compelling evidence that HP-induced FGF23 mRNA expression and release were blunted by PRO20 and siRNA against PRR. We provided further evidence that PRR expression was stimulated by HP treatment. An issue may arise that the relative importance of PRR in osteoblast cells vs. the kidney for the control of FGF23 production remains unclear and should warrant future investigation.

Besides FGF23, PTH is another important regulator of Pi metabolism (Graciolli et al., 2009; Lombardi et al., 2020). In the present study, we were able to show an inhibitory effect of PRO20 on HP-induced plasma PTH level, indicating a potential role of PRR in regulation of the release of PTH, presumably from parathyroid gland. There is no information about expression and function of PRR in this organ in the context of PTH regulation. We would like to acknowledge this major limitation of the present study.

We would also like to acknowledge the limitation of the HP protocol used in the present study although this protocol has been validated by a previous study (Ide et al., 2016). The HP fluid contains high NaCl which may confoundingly influence Pi transport in the kidney through modulation of status of NaPi transporter. This possibility is suggested by the previous observation that subcellular distribution of NaPi-2 was altered following high salt diet (Yang et al., 2008), but with unchanged total abundance of this transporter. In contrast, as shown by the present study, the total abundance of NaPi-2 was downregulated by 24-h HP intake. This result seems to support a primary role of NaPi-2 in regulating homeostasis of Pi, probably not Na^+. Indeed, besides NaPi-2, Na^+ transport occurs *via* numerous other Na^+ transporters and channels in various nephron segments. Additionally, it seems hard to explain why HP intake reduced fluid intake that was contradictorily associated with increased urine output and urinary Na^+ excretion. Fortunately, we found no sign of severe dehydration as evidenced by unchanged plasma osmolality. This might be due to the short duration of the experiment and fluid balance can be maintained by activation of compensatory mechanisms.

In conclusion, we for the first time identified PRR as a novel mediator of phosphaturic response to HP intake. The phosphaturic action of PRR seemed to be mediated by stimulation of production of FGF23 as well as PTH (**Figure 9**). *In vitro* evidence from cultured osteoblast cells demonstrated that PRR directly mediated HP-induced FGF23 release. Overall, the present study has uncovered a previously undescribed PRR/FGF23 axis in regulation of Pi homeostasis.

DATA AVAILABILITY STATEMENT

The raw data supporting the conclusions of this article will be made available by the authors, without undue reservation.

ETHICS STATEMENT

The animal study was reviewed and approved by the Institutional Animal Care and Use Committee, Sun Yat-sen University.

AUTHOR CONTRIBUTIONS

TY and AL designed the research and wrote the manuscript. AL, JS, SM, MP, and JH performed the experiments. AL analyzed the data. AL, CL, WW, and TY edited and revised manuscript. TY approved final version of manuscript. All authors approved the final version of the manuscript.

FUNDING

This work was supported by the National Natural Science Foundation of China (Grant No. 81630013). TY was Senior Research Career Scientist in Department of Veterans Affairs.

REFERENCES

Antoniucci, D. M., Yamashita, T., and Portale, A. A. (2006). Dietary phosphorus regulates serum fibroblast growth factor-23 concentrations in healthy men. *J. Clin. Endocrinol. Metab.* 8, 3144–3149. doi: 10.1210/jc.2006-0021

Azroyan, A., Cortez-Retamozo, V., Bouley, R., Liberman, R., Ruan, Y. C., Kiselev, E., et al. (2015). Renal intercalated cells sense and mediate inflammation via the P2Y14 receptor. *PLoS One* 3:e0121419. doi: 10.1371/journal.pone.0121419

Battistone, M. A., Mendelsohn, A. C., Spallanzani, R. G., Allegretti, A. S., Liberman, R. N., Sesma, J., et al. (2020). Proinflammatory P2Y14 receptor inhibition protects against ischemic acute kidney injury in mice. *J. Clin. Invest.* 7, 3734–3749. doi: 10.1172/JCI134791

Beck, L., Karaplis, A. C., Amizuka, N., Hewson, A. S., Ozawa, H., and Tenenhouse, H. S. (1998). Targeted inactivation of Npt2 in mice leads to severe renal phosphate wasting, hypercalciuria, and skeletal abnormalities. *Proc. Natl. Acad. Sci. U.S.A.* 9, 5372–5377. doi: 10.1073/pnas.95.9.5372

Biber, J., and Murer, H. (1994). A molecular view of renal Na-dependent phosphate transport. *Ren. Physiol. Biochem.* 3-4, 212–215. doi: 10.1159/000173822

Binger, K. J., and Muller, D. N. (2013). Autophagy and the (Pro)renin receptor. *Front. Endocrinol.* 4:155. doi: 10.3389/fendo.2013.00155

Bourgeois, S., Capuano, P., Stange, G., Muhlemann, R., Murer, H., Biber, J., et al. (2013). The phosphate transporter NaPi-IIa determines the rapid renal adaptation to dietary phosphate intake in mouse irrespective of persistently high FGF23 levels. *Pflugers Arch.* 11, 1557–1572. doi: 10.1007/s00424-013-1298-9

Burckle, C., and Bader, M. (2006). Prorenin and its ancient receptor. *Hypertension* 4, 549–551. doi: 10.1161/01.HYP.0000241132.48495.df

Busch, A., Waldegger, S., Herzer, T., Biber, J., Markovich, D., Hayes, G., et al. (1994). Electrophysiological analysis of Na+/Pi cotransport mediated by a transporter cloned from rat kidney and expressed in Xenopus oocytes. *Proc. Natl. Acad. Sci. U.S.A.* 17, 8205–8208. doi: 10.1073/pnas.91.17.8205

Danser, A. H. (2015). The Role of the (Pro)renin receptor in hypertensive disease. *Am. J. Hypertens.* 10, 1187–1196. doi: 10.1093/ajh/hpv045

Fang, H., Deng, M., Zhang, L., Lu, A., Su, J., Xu, C., et al. (2018). Role of (pro)renin receptor in albumin overload-induced nephropathy in rats. *Am. J. Physiol. Renal. Physiol.* 6, F1759–F1768. doi: 10.1152/ajprenal.00071.2018

Farrow, E. G., Davis, S. I., Summers, L. J., and White, K. E. (2009). Initial FGF23-mediated signaling occurs in the distal convoluted tubule. *J. Am. Soc. Nephrol.* 5, 955–960. doi: 10.1681/ASN.2008070783

Ferrari, S. L., Bonjour, J. P., and Rizzoli, R. (2005). Fibroblast growth factor-23 relationship to dietary phosphate and renal phosphate handling in healthy young men. *J. Clin. Endocrinol. Metab.* 3, 1519–1524. doi: 10.1210/jc.2004-1039

Forster, I. C., Hernando, N., Biber, J., and Murer, H. (2013). Phosphate transporters of the SLC20 and SLC34 families. *Mol. Aspects Med.* 2-3, 386–395. doi: 10.1016/j.mam.2012.07.007

Fu, Z., Hu, J., Zhou, L., Chen, Y., Deng, M., Liu, X., et al. (2019). (Pro)renin receptor contributes to pregnancy-induced sodium-water retention in rats via activation of intrarenal RAAS and alpha-ENaC. *Am. J. Physiol. Renal Physiol.* 3, F530–F538. doi: 10.1152/ajprenal.00411.2018

Gaasbeek, A., and Meinders, A. E. (2005). Hypophosphatemia: an update on its etiology and treatment. *Am. J. Med.* 10, 1094–1101. doi: 10.1016/j.amjmed.2005.02.014

Gao, X., Zhang, S., Wang, D., Cheng, Y., Jiang, Y., and Liu, Y. (2020). (Pro)renin receptor contributes to hypoxia/reoxygenation-induced apoptosis and autophagy in myocardial cells via the beta-catenin signaling pathway. *Physiol. Res.* 3, 427–438. doi: 10.33549/physiolres.934210

Gattineni, J., Bates, C., Twombley, K., Dwarakanath, V., Robinson, M. L., Goetz, R., et al. (2009). FGF23 decreases renal NaPi-2a and NaPi-2c expression and induces hypophosphatemia in vivo predominantly via FGF receptor 1. *Am. J. Physiol. Renal Physiol.* 2, F282–F291. doi: 10.1152/ajprenal.90742.2008

Giral, H., Caldas, Y., Sutherland, E., Wilson, P., Breusegem, S., Barry, N., et al. (2009). Regulation of rat intestinal Na-dependent phosphate transporters by dietary phosphate. *Am. J. Physiol. Renal Physiol.* 5, F1466–F1475. doi: 10.1152/ajprenal.00279.2009

Goltzman, D., Mannstadt, M., and Marcocci, C. (2018). Physiology of the calcium-parathyroid hormone-Vitamin D axis. *Front. Horm. Res.* 50, 1–13. doi: 10.1159/000486060

Gonzalez, A. A., and Prieto, M. C. (2015). Roles of collecting duct renin and (pro)renin receptor in hypertension: mini review. *Ther. Adv. Cardiovasc. Dis.* 4, 191–200. doi: 10.1177/1753944715574817

Graciolli, F. G., Neves, K. R., dos Reis, L. M., Graciolli, R. G., Noronha, I. L., Moyses, R. M., et al. (2009). Phosphorus overload and PTH induce aortic expression of Runx2 in experimental uraemia. *Nephrol. Dial. Transplant.* 5, 1416–1421. doi: 10.1093/ndt/gfn686

Guo, J., Song, L., Liu, M., Segawa, H., Miyamoto, K., Bringhurst, F. R., et al. (2013). Activation of a non-cAMP/PKA signaling pathway downstream of the PTH/PTHrP receptor is essential for a sustained hypophosphatemic response to PTH infusion in male mice. *Endocrinology* 5, 1680–1689. doi: 10.1210/en.2012-2240

Hernando, N., Karim-Jimenez, Z., Biber, J., and Murer, H. (2001). Molecular determinants for apical expression and regulatory membrane retrieval of the type IIa Na/Pi cotransporter. *Kidney Int.* 2, 431–435. doi: 10.1046/j.1523-1755.2001.060002431.x

Ide, N., Olauson, H., Sato, T., Densmore, M. J., Wang, H., Hanai, J. I., et al. (2016). In vivo evidence for a limited role of proximal tubular Klotho in renal phosphate handling. *Kidney Int.* 2, 348–362. doi: 10.1016/j.kint.2016.04.009

Katai, K., Miyamoto, K., Kishida, S., Segawa, H., Nii, T., Tanaka, H., et al. (1999). Regulation of intestinal Na+-dependent phosphate co-transporters by a low-phosphate diet and 1,25-dihydroxyvitamin D3. *Biochem. J.* 343, 705–712. doi: 10.1042/bj3430705

Kouchi, M., Shibayama, Y., Ogawa, D., Miyake, K., Nishiyama, A., and Tamiya, T. (2017). (Pro)renin receptor is crucial for glioma development via the Wnt/beta-catenin signaling pathway. *J. Neurosurg.* 4, 819–828. doi: 10.3171/2016.9.JNS16431

Larsson, T., Marsell, R., Schipani, E., Ohlsson, C., Ljunggren, O., Tenenhouse, H. S., et al. (2004). Transgenic mice expressing fibroblast growth factor 23 under the control of the alpha1(I) collagen promoter exhibit growth retardation, osteomalacia, and disturbed phosphate homeostasis. *Endocrinology* 7, 3087–3094. doi: 10.1210/en.2003-1768

Li, W., Sullivan, M. N., Zhang, S., Worker, C. J., Xiong, Z., Speth, R. C., et al. (2015). Intracerebroventricular infusion of the (Pro)renin receptor antagonist PRO20 attenuates deoxycorticosterone acetate-salt-induced hypertension. *Hypertension* 2, 352–361. doi: 10.1161/HYPERTENSIONAHA.114.04458

Li, Z., Zhou, L., Wang, Y., Miao, J., Hong, X., Hou, F. F., et al. (2017). (Pro)renin receptor is an amplifier of Wnt/beta-catenin signaling in kidney injury and fibrosis. *J. Am. Soc. Nephrol.* 8, 2393–2408. doi: 10.1681/ASN.2016070811

Lindberg, I., Pang, H. W., Stains, J. P., Clark, D., Yang, A. J., Bonewald, L., et al. (2015). FGF23 is endogenously phosphorylated in bone cells. *J. Bone. Miner. Res.* 3, 449–454. doi: 10.1002/jbmr.2354

Liu, S., Guo, R., Simpson, L. G., Xiao, Z. S., Burnham, C. E., and Quarles, L. D. (2003). Regulation of fibroblastic growth factor 23 expression but not degradation by PHEX. *J. Biol. Chem.* 39, 37419–37426. doi: 10.1074/jbc.M304544200

Liu, S., Zhou, J., Tang, W., Jiang, X., Rowe, D. W., and Quarles, L. D. (2006). Pathogenic role of Fgf23 in Hyp mice. *Am. J. Physiol. Endocrinol. Metab.* 1, E38–E49. doi: 10.1152/ajpendo.00008.2006

Lombardi, G., Ziemann, E., Banfi, G., and Corbetta, S. (2020). Physical activity-dependent regulation of parathyroid hormone and calcium-phosphorous metabolism. *Int. J. Mol. Sci.* 15:5388. doi: 10.3390/ijms21155388

Lu, X., Wang, F., Liu, M., Yang, K. T., Nau, A., Kohan, D. E., et al. (2016a). Activation of ENaC in collecting duct cells by prorenin and its receptor PRR: involvement of Nox4-derived hydrogen peroxide. *Am. J. Physiol. Renal Physiol.* 11, F1243–F1250. doi: 10.1152/ajprenal.00492.2015

Lu, X., Wang, F., Xu, C., Soodvilai, S., Peng, K., Su, J., et al. (2016b). Soluble (pro)renin receptor via beta-catenin enhances urine concentration capability as a target of liver X receptor. *Proc. Natl. Acad. Sci. U.S.A.* 13, E1898–E1906. doi: 10.1073/pnas.1602397113

Miao, Y., and Abraham, S. N. (2014). Kidney alpha-intercalated cells and lipocalin 2: defending the urinary tract. *J. Clin. Invest.* 7, 2844–2846. doi: 10.1172/JCI76630

Murer, H., Forster, I., and Biber, J. (2004). The sodium phosphate cotransporter family SLC34. *Pflugers Arch.* 5, 763–767. doi: 10.1007/s00424-003-1072-5

Murer, H., Forster, I., Hernando, N., Lambert, G., Traebert, M., and Biber, J. (1999). Posttranscriptional regulation of the proximal tubule NaPi-II transporter in

response to PTH and dietary P(i). *Am. J. Physiol.* 5, F676–F684. doi: 10.1152/ajprenal.1999.277.5.F676

Murer, H., Hernando, N., Forster, I., and Biber, J. (2000). Proximal tubular phosphate reabsorption: molecular mechanisms. *Physiol. Rev.* 4, 1373–1409. doi: 10.1152/physrev.2000.80.4.1373

Murer, H., Hernando, N., Forster, I., and Biber, J. (2003). Regulation of Na/Pi transporter in the proximal tubule. *Annu. Rev. Physiol.* 65, 531–542. doi: 10.1146/annurev.physiol.65.042902.092424

Nakagawa, T., Suzuki-Nakagawa, C., Watanabe, A., Asami, E., Matsumoto, M., Nakano, M., et al. (2017). Site-1 protease is required for the generation of soluble (pro)renin receptor. *J. Biochem.* 4, 369–379. doi: 10.1093/jb/mvw080

Nguyen, G., Delarue, F., Burckle, C., Bouzhir, L., Giller, T., and Sraer, J. D. (2002). Pivotal role of the renin/prorenin receptor in angiotensin II production and cellular responses to renin. *J. Clin. Invest.* 11, 1417–1427. doi: 10.1172/JCI0214276

Peng, K., Lu, X., Wang, F., Nau, A., Chen, R., Zhou, S. F., et al. (2017). Collecting duct (pro)renin receptor targets ENaC to mediate angiotensin II-induced hypertension. *Am. J. Physiol. Renal Physiol.* 2, F245–F253. doi: 10.1152/ajprenal.00178.2016

Perwad, F., Azam, N., Zhang, M. Y., Yamashita, T., Tenenhouse, H. S., and Portale, A. A. (2005). Dietary and serum phosphorus regulate fibroblast growth factor 23 expression and 1,25-dihydroxyvitamin D metabolism in mice. *Endocrinology* 12, 5358–5364. doi: 10.1210/en.2005-0777

Perwad, F., Zhang, M. Y., Tenenhouse, H. S., and Portale, A. A. (2007). Fibroblast growth factor 23 impairs phosphorus and vitamin D metabolism in vivo and suppresses 25-hydroxyvitamin D-1alpha-hydroxylase expression in vitro. *Am. J. Physiol. Renal Physiol.* 5, F1577–F1583. doi: 10.1152/ajprenal.00463.2006

Pfister, M. F., Ruf, I., Stange, G., Ziegler, U., Lederer, E., Biber, J., et al. (1998). Parathyroid hormone leads to the lysosomal degradation of the renal type II Na/Pi cotransporter. *Proc. Natl. Acad. Sci. U.S.A.* 4, 1909–1914. doi: 10.1073/pnas.95.4.1909

Prieto, M. C., Reverte, V., Mamenko, M., Kuczeriszka, M., Veiras, L. C., Rosales, C. B., et al. (2017). Collecting duct prorenin receptor knockout reduces renal function, increases sodium excretion, and mitigates renal responses in ANG II-induced hypertensive mice. *Am. J. Physiol. Renal Physiol.* 6, F1243–F1253. doi: 10.1152/ajprenal.00152.2017

Quadri, S., and Siragy, H. M. (2016). (Pro)renin receptor contributes to regulation of renal epithelial sodium channel. *J. Hypertens.* 3, 486–494. doi: 10.1097/HJH.0000000000000825

Ramkumar, N., Stuart, D., Mironova, E., Abraham, N., Gao, Y., Wang, S., et al. (2018). Collecting duct principal, but not intercalated, cell prorenin receptor regulates renal sodium and water excretion. *Am. J. Physiol. Renal Physiol.* 3, F607–F617. doi: 10.1152/ajprenal.00122.2018

Saito, H., Maeda, A., Ohtomo, S., Hirata, M., Kusano, K., Kato, S., et al. (2005). Circulating FGF-23 is regulated by 1alpha,25-dihydroxyvitamin D3 and phosphorus in vivo. *J. Biol. Chem.* 4, 2543–2549. doi: 10.1074/jbc.M408903200

Shimada, T., Hasegawa, H., Yamazaki, Y., Muto, T., Hino, R., Takeuchi, Y., et al. (2004a). FGF-23 is a potent regulator of vitamin D metabolism and phosphate homeostasis. *J. Bone Miner. Res.* 3, 429–435. doi: 10.1359/JBMR.0301264

Shimada, T., Urakawa, I., Yamazaki, Y., Hasegawa, H., Hino, R., Yoneya, T., et al. (2004b). FGF-23 transgenic mice demonstrate hypophosphatemic rickets with reduced expression of sodium phosphate cotransporter type IIa. *Biochem. Biophys. Res. Commun.* 2, 409–414. doi: 10.1016/j.bbrc.2003.12.102

Shirazi-Beechey, S. P., Penny, J. I., Dyer, J., Wood, I. S., Tarpey, P. S., Scott, D., et al. (1996). Epithelial phosphate transport in ruminants, mechanisms and regulation. *Kidney Int.* 4, 992–996. doi: 10.1038/ki.1996.142

Urakawa, I., Yamazaki, Y., Shimada, T., Iijima, K., Hasegawa, H., Okawa, K., et al. (2006). Klotho converts canonical FGF receptor into a specific receptor for FGF23. *Nature* 7120, 770–774. doi: 10.1038/nature05315

Wang, F., Lu, X., Liu, M., Feng, Y., Zhou, S. F., and Yang, T. (2015). Renal medullary (pro)renin receptor contributes to angiotensin II-induced hypertension in rats via activation of the local renin-angiotensin system. *BMC Med.* 13:278. doi: 10.1186/s12916-015-0514-1

Wang, F., Lu, X., Peng, K., Du, Y., Zhou, S. F., Zhang, A., et al. (2014). Prostaglandin E-prostanoid4 receptor mediates angiotensin II-induced (pro)renin receptor expression in the rat renal medulla. *Hypertension* 2, 369–377. doi: 10.1161/HYPERTENSIONAHA.114.03654

Wang, F., Lu, X., Peng, K., Fang, H., Zhou, L., Su, J., et al. (2016). Antidiuretic action of collecting duct (Pro)renin receptor downstream of vasopressin and PGE2 Receptor EP4. *J. Am. Soc. Nephrol.* 10, 3022–3034. doi: 10.1681/ASN.2015050592

Wang, F., Sun, Y., Luo, R., Lu, X., Yang, B., and Yang, T. (2020). COX-2-independent activation of renal (pro)renin receptor contributes to DOCA-salt hypertension in rats. *Am. J. Physiol. Renal Physiol.* 4, F647–F653. doi: 10.1152/ajprenal.00112.2020

Wang, L., Zhu, Q., Lu, A., Liu, X., Zhang, L., Xu, C., et al. (2017). Sodium butyrate suppresses angiotensin II-induced hypertension by inhibition of renal (pro)renin receptor and intrarenal renin-angiotensin system. *J. Hypertens.* 9, 1899–1908. doi: 10.1097/HJH.0000000000001378

Xu, C., Lu, A., Wang, H., Fang, H., Zhou, L., Sun, P., et al. (2017). (Pro)Renin receptor regulates potassium homeostasis through a local mechanism. *Am. J. Physiol. Renal Physiol.* 3, F641–F656. doi: 10.1152/ajprenal.00043.2016

Xu, C., Wang, F., Chen, Y., Xie, S., Sng, D., Reversade, B., et al. (2020). ELABELA antagonizes intrarenal renin-angiotensin system to lower blood pressure and protects against renal injury. *Am. J. Physiol. Renal Physiol.* 5, F1122–F1135. doi: 10.1152/ajprenal.00606.2019

Yang, L. E., Sandberg, M. B., Can, A. D., Pihakaski-Maunsbach, K., and McDonough, A. A. (2008). Effects of dietary salt on renal Na+ transporter subcellular distribution, abundance, and phosphorylation status. *Am. J. Physiol. Renal Physiol.* 4, F1003–F1016. doi: 10.1152/ajprenal.90235.2008

Zhuo, M. Q., Lv, W. H., Xu, Y. H., and Luo, Z. (2020). Isolation and characterization of three sodium-phosphate cotransporter genes and their transcriptional regulation in the grass carp *Ctenopharyngodon idella*. *Int. J. Mol. Sci.* 21:8228. doi: 10.3390/ijms21218228

Conflict of Interest: The authors declare that the research was conducted in the absence of any commercial or financial relationships that could be construed as a potential conflict of interest.

Publisher's Note: All claims expressed in this article are solely those of the authors and do not necessarily represent those of their affiliated organizations, or those of the publisher, the editors and the reviewers. Any product that may be evaluated in this article, or claim that may be made by its manufacturer, is not guaranteed or endorsed by the publisher.

frontiers | Frontiers in Physiology

ORIGINAL RESEARCH
published: 26 April 2022
doi: 10.3389/fphys.2022.800055

Dissecting the Effects of Aldosterone and Hypokalemia on the Epithelial Na^+ Channel and the NaCl Cotransporter

*Mathias Kristensen, Robert A. Fenton and Søren B. Poulsen**

Department of Biomedicine, Aarhus University, Aarhus, Denmark

Primary hyperaldosteronism (PA) is characterized by aldosterone excess and hypertension. This may be linked to increased renal Na^+ reabsorption *via* the epithelial Na^+ channel (ENaC) and the NaCl cotransporter (NCC). The majority of PA patients have normal plasma K^+ levels, but a subset of cases are associated with hypokalemia. High NCC levels observed in long-term studies with aldosterone-infused rodents have been attributed to direct effects of aldosterone. Aldosterone can also increase active phosphorylated NCC (pT58-NCC) acutely. However, direct effects of aldosterone on NCC have been contested by recent studies indicating that it is rather an indirect effect of hypokalemia. We therefore set out to determine isolated long-term aldosterone and K^+ effects on ENaC and NCC using various *in vivo* and *ex vivo* approaches. In mice, aldosterone-induced hypokalemia was prevented by simultaneous amiloride infusion, coupled to increased cleavage of α- and γENaC but no effect on NCC. Regression analyses of *in vivo* data showed a positive correlation between aldosterone/K^+ and αENaC but a negative correlation with NCC and pT58-NCC. *Ex vivo*, exposure of kidney tubules for 21 h to aldosterone increased cleavage of αENaC and γENaC, but no effects were observed on NCC or pT58-NCC. Exposure of tubules to low K^+ media reduced αENaC but increased NCC and pT58-NCC. As hypokalemia can enhance cell proliferation markers in the distal convoluted tubule (DCT), we hypothesized that aldosterone infusion would increase proliferating cell nuclear antigen (PCNA) expression. Infusion of aldosterone in mice for 6 days greatly increased PCNA expression in the DCT. Collectively, *in vivo* and *ex vivo* data suggest that both aldosterone and K^+ can increase ENaC directly. In contrast, the observed increase in abundance and phosphorylation of NCC in aldosterone-infused mice is likely an indirect effect of enhanced ENaC-mediated K^+ secretion and subsequent hypokalemia. Thus, it is possible that NCC may only be increased in PA when the condition is associated with hypokalemia.

Keywords: amiloride, conns syndrome, eplerenone, mineralocorticoid receptor, thiazide-sensitive cotransporter

OPEN ACCESS

Edited by:
Weidong Wang,
Sun Yat-sen University, China

Reviewed by:
Gilles Crambert,
ERL8228 Métabolisme et Physiologie Rénales, France
Daria Ilatovskaya,
Augusta University, United States

****Correspondence:***
Søren B. Poulsen
sbpo@biomed.au.dk

Specialty section:
This article was submitted to Renal and Epithelial Physiology, a section of the journal Frontiers in Physiology

Received: *22 October 2021*
Accepted: *31 March 2022*
Published: *26 April 2022*

Citation:
Kristensen M, Fenton RA and Poulsen SB (2022) Dissecting the Effects of Aldosterone and Hypokalemia on the Epithelial Na^+ Channel and the NaCl Cotransporter. Front. Physiol. 13:800055. doi: 10.3389/fphys.2022.800055

INTRODUCTION

Primary hyperaldosteronism (PA), also known as Conns syndrome (Conn, 1955), is the underlying cause of high blood pressure in approximately 10% of subjects diagnosed with hypertension (Schirpenbach and Reincke, 2007; Rossi, 2010; Kayser et al., 2016; Monticone et al., 2017). It is primarily caused by bilateral idiopathic hyperplasia or aldosterone producing adenomas and is

characterized by autonomous excess of circulatory aldosterone and suppression of renin (Schirpenbach and Reincke, 2007; Moraitis and Stratakis, 2011). PA may be associated with hypokalemia, and this parameter was initially used for diagnosing the disease (Kaplan, 1967; Ganguly, 1998; Buffolo et al., 2017). Later it became clear that the majority of patients with PA are normokalemic (Fagugli and Taglioni, 2011; Moraitis and Stratakis, 2011). Although the two subgroups are well-described, limited knowledge exists on how hyperaldosteronism affects renal Na^+ reabsorption during normokalemia compared to hypokalemia.

PA is prevalently mimicked in rodents by infusing aldosterone *via* mini-pumps (Kim et al., 1998; Nielsen et al., 2007; Poulsen and Christensen, 2017; Poulsen et al., 2018). Commonly observed is that aldosterone infusion induces hypokalemia and increases kidney protein abundances of the epithelial Na^+ channel (ENaC) and NaCl cotransporter (NCC) in the distal tubule (Kim et al., 1998; Nielsen et al., 2007; Poulsen and Christensen, 2017; Poulsen et al., 2018). ENaC and NCC are important for fine-tuning Na^+ reabsorption, K^+ secretion and regulating blood pressure as documented by various animal models and diseases such as Liddle's syndrome and Pseudohypoaldosteronism Type II (increased ENaC and NCC activity may contribute to the observed hypertension) and in Pseudohypoaldosteronism Type I and Gitelman syndrome (reduced ENaC and NCC activity may cause hypotension) (Pradervand et al., 1999; Kleta and Bockenhauer, 2006; Christensen et al., 2010; Furgeson and Linas, 2010).

It was previously accepted that aldosterone stimulates ENaC and NCC *via* direct effects on the tubule segments in which they are expressed (Arroyo et al., 2011a; Arroyo et al., 2011b). However, while direct effects of aldosterone on ENaC are well-established, (Loffing et al., 2001; Gaeggeler et al., 2005; Poulsen et al., 2018), it is still debated whether long-term aldosterone excess has a direct stimulatory effect on NCC. For example, aldosterone infusion did not stimulate NCC when hypokalemia was corrected by a high K^+ diet (Terker et al., 2016). Furthermore, NCC abundance and phosphorylation (active form) are essentially the same in mineralocorticoid receptor (MR)-negative versus MR-containing distal convoluted tubule (DCT) cells (Czogalla et al., 2016). On the other hand, acute aldosterone exposure can strongly increase cAMP independently of the MR (Haseroth et al., 1999), and because NCC is a target of cAMP, NCC may potentially be a target of aldosterone *via* an MR-independent pathway. This is supported by our recent study showing that 30 min aldosterone exposure increases cAMP in mpkDCT cells and increases NCC phosphorylation in kidney tubules *ex vivo* (Cheng et al., 2019). Similar findings are reported in studies on mDCT15 cells showing that aldosterone increases NCC phosphorylation after 12–36 h exposure (Ko et al., 2013).

Hence, the major aim of the current study was to dissect the isolated effects of aldosterone and hypokalemia on ENaC and NCC using a variety of *in vivo* and *ex vivo* approaches (see **Supplementary Figure S1** for experimental design). As ENaC is critical for the kidney's ability to reabsorb Na^+ and secrete K^+ (Christensen et al., 2010; Poulsen et al., 2016), we hypothesized that a combined infusion of aldosterone and the ENaC blocker amiloride in mice would prevent the aldosterone-induced drop in plasma K^+, allowing us to investigate aldosterone effects independently of hypokalemia. Second, we studied isolated long-term effects (21 h) of aldosterone and K^+ on ENaC and NCC *ex vivo* in kidney tubules. Third, as hypokalemia can induce cell proliferation in the DCT that may contribute to increased NCC abundance (Saritas et al., 2018), we investigated the effect of aldosterone on cell proliferation in the DCT.

MATERIALS AND METHODS

Animal Protocols

All procedures were performed in agreement with a license issued by the Animal Experiments Inspectorate, Ministry of Food, Agriculture and Fisheries, Danish Veterinary and Food Administration.

All animal experiments were performed at Department of Biomedicine, Aarhus University, Denmark. C57BL/6JBomTac male mice (Taconic, Laven, Denmark) were housed at 27°C in metabolic cages (Tecniplast, Buguggiate, Italy) in which they had free access to water and powdered rodent chow. Three experimental protocols were applied.

Protocol 1. A protocol was established for infusing aldosterone. Mice were administered aldosterone [A9477; Sigma-Aldrich/Merck, St. Louis, MO, United States; 100 μg/kg per 24 h dissolved in polyethylene glycol 300 (PEG 300)] or control vehicle (PEG300) for 6 days *via* osmotic minipumps (Alzet model 1007D, Alza Corporation, Palo Alto, CA, United States). Mice were fed a powdered standard mouse chow diet [1324 (0.22% Na^+, 0.92% K^+), Altromin Spezialfutter GmbH & Co. KG, Large, Germany]. Aldosterone increased plasma aldosterone and reduced plasma K^+, and increased protein abundances of αENaC and NCC (**Supplementary Figure S2**). The results are in line with previous studies addressing chronic effects of raised plasma aldosterone in rodents (van der Lubbe et al., 2011; Nguyen et al., 2013; Poulsen and Christensen, 2017; Poulsen et al., 2018).

Protocol 2. A protocol was established for infusing amiloride. Mice were administered amiloride (A7410; Sigma-Aldrich/Merck; 2.6 mg/kg per 24 h in PEG 300) or control vehicle (PEG 300) for 6 days *via* osmotic minipumps (Alzet model 1007D, Alza Corporation). Mice were fed a powdered standard mouse chow diet [1324 (0.22% Na^+, 0.92% K^+) Altromin Spezialfutter GmbH & Co. KG]. Amiloride increased plasma aldosterone, plasma angiotensin II (ANGII) and αENaC in the kidney (**Supplementary Figure S3**), suggesting that this dose sufficiently blocked ENaC and in response activated the renin-angiotensin-aldosterone system.

Protocol 3. Mice were administered vehicle (PEG300) on a control diet (0.22% Na^+, 0.98% K^+), amiloride + aldosterone (2.6 and 100 μg/kg/24 h, respectively, in PEG 300) on a control diet, or vehicle (PGE300) on a low K^+ diet (0.22% Na^+, 0.01% K^+). Diets were prepared from a Na^+, Cl^- and K^+ deficient diet (C1054, Altromin Spezialfutter GmbH & Co. KG) and appropriate amounts of NaCl and K^+ citrate were added.

Collection and Analysis of Blood

In *protocol 1 and 3*, blood was drawn under terminal isoflurane anesthesia from the retro orbital sinus using an ammonium heparin-coated end-to-end pipette (Vitrex, Herlev, Denmark). Blood was collected in a 1.5 ml Eppendorf Tubes and immediately centrifuged at 5,000 *g* for 2 min. In *protocol 2*, blood was drawn under terminal isoflurane anesthesia *via* the portal vein using a 0.6 × 25 mm needle containing 5 µL Li^+ heparin solution. Blood was then transferred to a 1.5 ml Eppendorf Tube and immediately centrifuged at 5,000 *g* for 2 min. Plasma aldosterone and ANGII concentrations were determined using enzyme immunoassay kits (aldosterone: EIA-5298; DRG International Inc., Springfield, NJ, United States; angiotensin II: EKE-002-12, Phoenix Pharmaceuticals, Inc., Burlingame, CA, United States). Plasma K^+ and Na^+ concentrations were measured using a clinical flame photometer (Model 420, Sherwood Scientific, Cambridge, United Kingdom).

Ex vivo Studies on Kidney Tubule Suspensions

Male C57BL/6JBomTac mice (Taconic) were isoflurane-anesthetized and kidneys were perfused *via* the left heart ventricle with 37°C warm enzyme solution containing 1.5 mg/ml collagenase type B (Roche, Basel, Switzerland) in buffer A (125 mM NaCl, 30 mM glucose, 0.4 mM KH_2PO_4 1.6 mM K_2HPO_4, 1 mM $MgSO_4$, 10 mM Na-acetate, 1 mM α-ketoglutarate, 1.3 mM Ca-gluconate, 5 mM glycine, 48 µg/ml trypsin inhibitor, and 50 µg/ml DNase, pH 7.4). Each kidney was removed and transferred to a 2-ml Eppendorf Tube containing 37°C enzyme solution. Kidneys were cut in ~1 mm pieces with scissors and mixed continuously at 850 rpm in a thermomixer (at 37°C, Eppendorf, Hamburg, Germany) for 5 min to facilitate detachment of tubules from one another. During the 5 min, tissue was pipetted up and down 3 × 10 times. Kidney pieces were then allowed to sediment and the supernatant containing detached tubules were transferred to a separate tube. Fresh enzyme solution was then transferred to the remaining kidney pieces and incubated at 850 rpm for 3 min and pipetted 2 × 10 times. Subsequently, detached tubules were washed 3 times in commercial cell media DMEM/F12 (L0092, biowest, Riverside, MO, United States; for aldosterone experiments) or custom-made DMEM/F12 (Terker et al., 2015) for K^+ experiments. Finally, tubules were dissolved in 50 ml of the desired cell media and 2 ml tubules per well was transferred to 6-well plates. Tubules were then allowed to sediment whereafter media was removed and replaced by 3 ml media with the desired aldosterone and K^+ concentrations. Tubules were then incubated at 37°C and 5% CO_2 for 21 h. Preincubation of tubules for 21 h and subsequent exposure to 10 µM salbutamol for 2 h (Selleckchem, Houston, TX) increased pT58-NCC [**Supplementary Figure S4** (Poulsen et al., 2021),], thus documenting the viability of the tubules.

Semi-Quantitative Immunoblotting

Whole-kidney samples were prepared as described previously (Poulsen and Christensen, 2017). Kidney tubule samples were prepared by removing the cell media and adding 300 µL Laemmli sample buffer (containing 0.1 M SDS) to each well. Samples were then transferred to 1.5 ml Eppendorf Tubes, sonicated 3x5 pulses on ice, and heated to 65°C for 15 min. Semi-quantitative immunoblotting was performed as previously described (Poulsen and Christensen, 2017). In brief, membranes were incubated overnight at 4°C with the primary rabbit antibodies αENaC (Sorensen et al., 2013), γENaC [5163 (Masilamani et al., 1999; Nielsen et al., 2002)], NCC [SPC-402D, StressMarq Biosciences Inc. Victoria, BC, Canada; employed in Poulsen and Christensen (2017)] or pT58-NCC [1251 (Pedersen et al., 2010),]. Subsequently, membranes were labeled with secondary Goat Anti-Rabbit antibody (P0448, Dako, Santa Clara, CA, United States) for 1 h at room temperature. Labeling was visualized using the Enhanced Chemiluminescence system (GE Healthcare, Chicago, IL, United States) or SuperSignal West Femto Chemiluminescent Substrate (Thermo Scientific, Rockford, IL, United States). Immunoreactivity was visualized using an ImageQuant LAS 4000 imager (GE Healthcare). Densiometric analyses were performed in Image Studio Lite Ver. 5.2 (Qiagen, Hilden, Germany). Coomassie-stained gels were used to correct quantification for deviations in protein loading. The maximal deviations in total protein concentrations between samples on individual blots were ±10%. All uncropped blots and coomassies are shown in **Supplementary Material**.

Immunohistochemical Labeling and Cell Counting

Paraffin-embedded kidneys from a former study were used (Poulsen and Christensen, 2017) and labeled as previously described (Poulsen and Christensen, 2017). Two-µm sections were labelled for light microscopy (NCC; SPC-402D, StressMarq Biosciences Inc.; secondary antibody: goat-anti-rabbit P0448, Dako, Glostrup, Denmark) or double-immunolabeled for confocal laser scanning microscopy (NCC; SPC-402D; StressMarq Biosciences Inc. and PCNA; P8825; Sigma-Aldrich). Imaging was performed using a Leica light microscope equipped with a digital camera (Leica, Wetzlar, Germany) and a Leica TCS SL laser scanning confocal microscope and Leica confocal software (Leica). Brightness was digitally enhanced on presented images. Percent PCNA-positive cells in DCT were assessed directly in the microscope by counting the total number of cells and PCNA-positive cells in 10 NCC-positive tubules per mouse [6 days aldosterone infusion; on average 125 nuclei per mouse (range 84–155 nuclei); tissue was obtained from Poulsen and Christensen (2017)] or 20 NCC-positive tubules per mouse [*Protocol 3*; on average 196 nuclei per mouse (range 156–251 nuclei)]. The number of NCC-positive cells per mm^2 cortex was counted on images of a single kidney slice from each mouse. The cortical area was measured in ImageJ (Schneider et al., 2012) and was defined as the area containing glomeruli and NCC-positive tubules. On average, 485 tubules and 2,560 cells were counted per mouse.

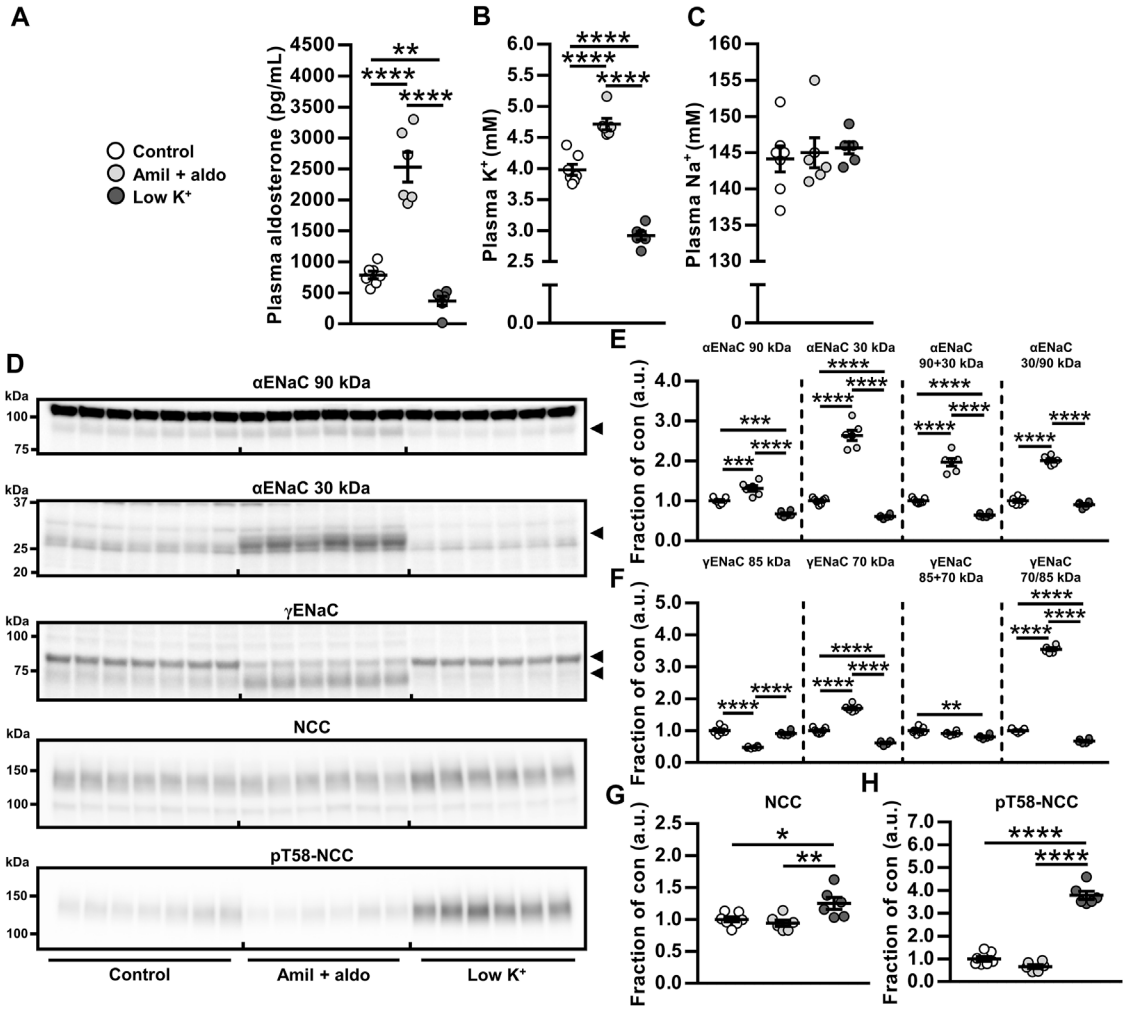

FIGURE 1 | Aldosterone did not increase NCC when hypokalemia was prevented by amiloride infusion. **(A–C)** Amiloride + aldosterone (amil + aldo) infusion for 6 days increased levels of plasma aldosterone and K^+ while a 6 days low K^+ diet reduced plasma levels of aldosterone and K^+. **(E,F)** Cleavages of αENaC and γENaC were increased by amiloride + aldosterone infusion but reduced by the low K^+ diet. **(G,H)** NCC and pT58-NCC were not significantly changed in response to amiloride + aldosterone infusion but they were increased by a low K^+ diet. Arrows in panel **(D)** indicate cleaved and non-cleaved forms of αENaC (90 and 30 kDa) and γENaC (85 and 70 kDa). Data are presented as dot plots and mean ± SEM. $n = 7$ (Control) or $n = 6$ per group (amiloride + aldosterone and low K^+ diet). Statistical comparisons were performed using a one-way ANOVA followed by post-hoc testing with FDR-correction **(A–C** and **E–H).** $^*p < 0.05$, $^{**}p < 0.01$, $^{****}p < 0.0001$, $^{****}p < 0.0001$.

Statistical Analyses

Pairwise comparisons of data meeting the statistical assumptions of normality and variance homogeneity were performed using Students two-sided *t*-test, while data only meeting assumptions of normality were analyzed using Satterthwaite's two-sided unequal variance *t*-test. If not meeting the assumptions of normality, data were ln- or square-root transformed in accordance with Sokal and Rohlf (Sokal and Rohlf, 1995) or analyzed with a Mann-Whitney *U*-test. Proportion data were logit-transformed (Sokal and Rohlf, 1995). Pairwise comparisons of more than two groups were performed using a one-way ANOVA. If not meeting the assumptions of normality and variance homogeneity, data were either ln- or square-root transformed (Sokal and Rohlf, 1995), or analyzed with a Kruskal–Wallis ANOVA on Ranks. For comparisons of more than two groups, *p*-values were adjusted for multiple comparisons using Benjamini-Yekutieli FDR correction (Narum, 2006). Line and curve fittings were performed as using linear or non-linear regression (one phase decay model). Analyses were carried out using Stata 12.0 (StataCorp, College Station, TX, United States) for Windows, SigmaPlot 12.0 (Systat Software, Inc., Chicago, Il, United States) for Windows or GraphPad Prism 7.02 (GraphPad Software, San Diego, CA, United States) for Windows. All values are presented as individual data points and mean ± SEM. All data in this paper are available on request.

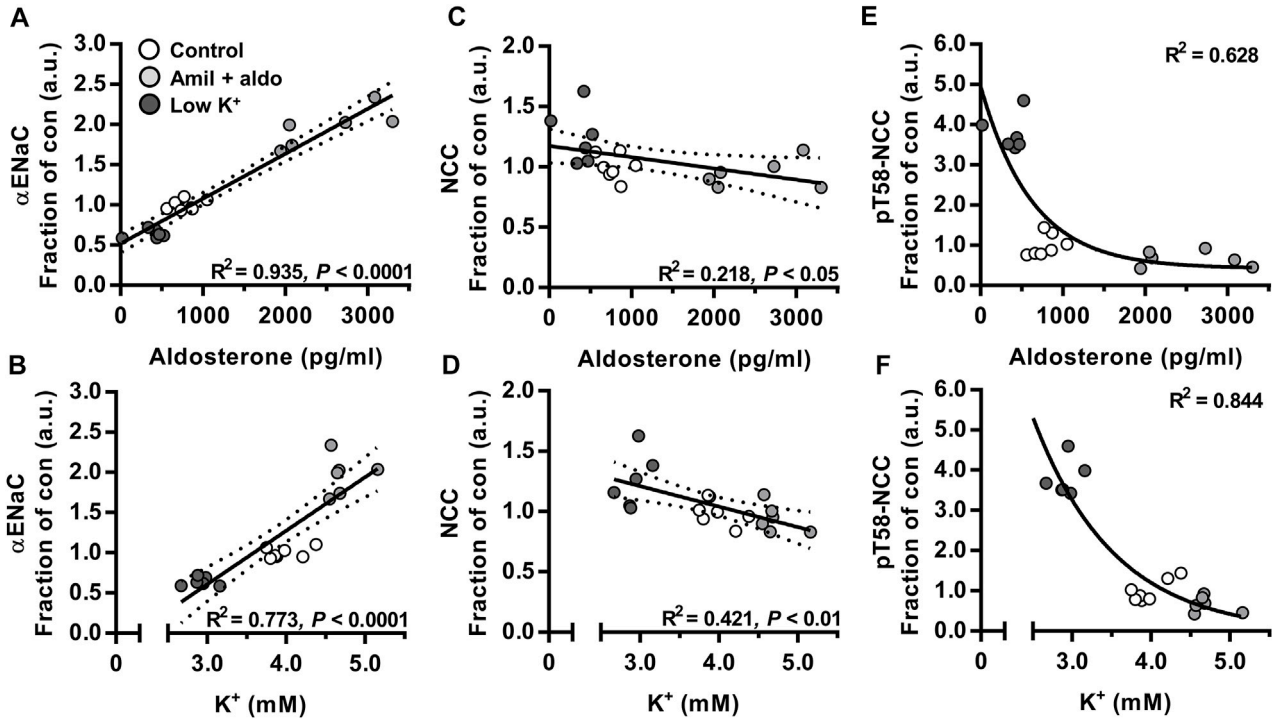

FIGURE 2 | Plasma aldosterone and K^+ correlated positively with cleaved αENaC but negatively with NCC and pT58-NCC. Data on mice that were infused with amiloride + aldosterone (amil + aldo) or fed a low K^+ for 6 days (**Figure 1**) were further analyzed using regression modeling. $n = 7$ per group (Control) or $n = 6$ per group (amil + aldo and low K^+ diet). Data were analyzed using linear **(A–D)** or non-linear regression analysis [one-phase decay model **(E,F)**].

RESULTS

Aldosterone did Not Increase NCC When Hypokalemia was Prevented by Amiloride Infusion

We first tested the hypothesis that the aldosterone-induced increase in NCC protein would not occur in the absence of hypokalemia. Co-administration of aldosterone and the ENaC blocker amiloride increased plasma levels of aldosterone and K^+ whereas a low K^+ diet reduced aldosterone and K^+ plasma levels (protocol 3, **Figures 1A,B**). Thus, amiloride prevented the aldosterone-induced hypokalemia but preserved the hyperaldosteronism. Amiloride + aldosterone increased full-length αENaC (90 kDa), cleaved αENaC (30 kDa), total αENaC (90 + 30 kDa) and the ratio between cleaved and full-length αENaC (30/90 kDa) (**Figures 1D,E**). A low K^+ diet in contrast reduced full-length αENaC (90 kDa), cleaved αENaC (90 kDa) and total αENaC (90 + 30 kDa) (**Figures 1D,E**). Amiloride + aldosterone reduced full-length γENaC (85 kDa), and increased cleaved γENaC (70 kDa) and the ratio between cleaved and full-length γENaC (70/85 kDa) (**Figures 1D,F**). Furthermore, the low K^+ diet reduced cleaved γENaC (70 kDa) and the ratio between cleaved and full-length γENaC (70/85 kDa) (**Figures 1D,F**). NCC and phosphorylated NCC (pT58-NCC) were not significantly affected by the amiloride + aldosterone infusion when analyzing data with a one-way anova (**Figures 1D,G,H**). In terms of pT58-NCC, the less conservative Student's 2-tailed *t*-test showed a significant decrease in pT58-NCC ($p = 0.029$). However, the low K^+ diet increased both NCC and pT58-NCC (**Figures 1D,G,H**).

Plasma Aldosterone and K^+ Correlated Positively With Cleaved αENaC but Negatively With NCC and pT58-NCC

To correlate cleaved αENaC, NCC and pT58-NCC *in vivo* over a range of aldosterone and K^+ plasma concentrations, data presented in **Figure 1** were analyzed using regression analyses. We found a positive correlation between total αENaC (30 + 90 kDa) and plasma levels of aldosterone and K^+ (**Figures 2A,B**). On the contrary, for both NCC and pT58-NCC, a negative correlation was found with plasma aldosterone and K^+ (**Figures 2C–F**).

Aldosterone Increased ENaC but did Not Affect Abundance or Phosphorylation of NCC *Ex Vivo*

To examine direct and independent effects of aldosterone or K^+ on ENaC, NCC and pT58-NCC, we established an *ex vivo* tubule suspension protocol allowing us to study isolated compound effects over a 21 h period. We first performed a

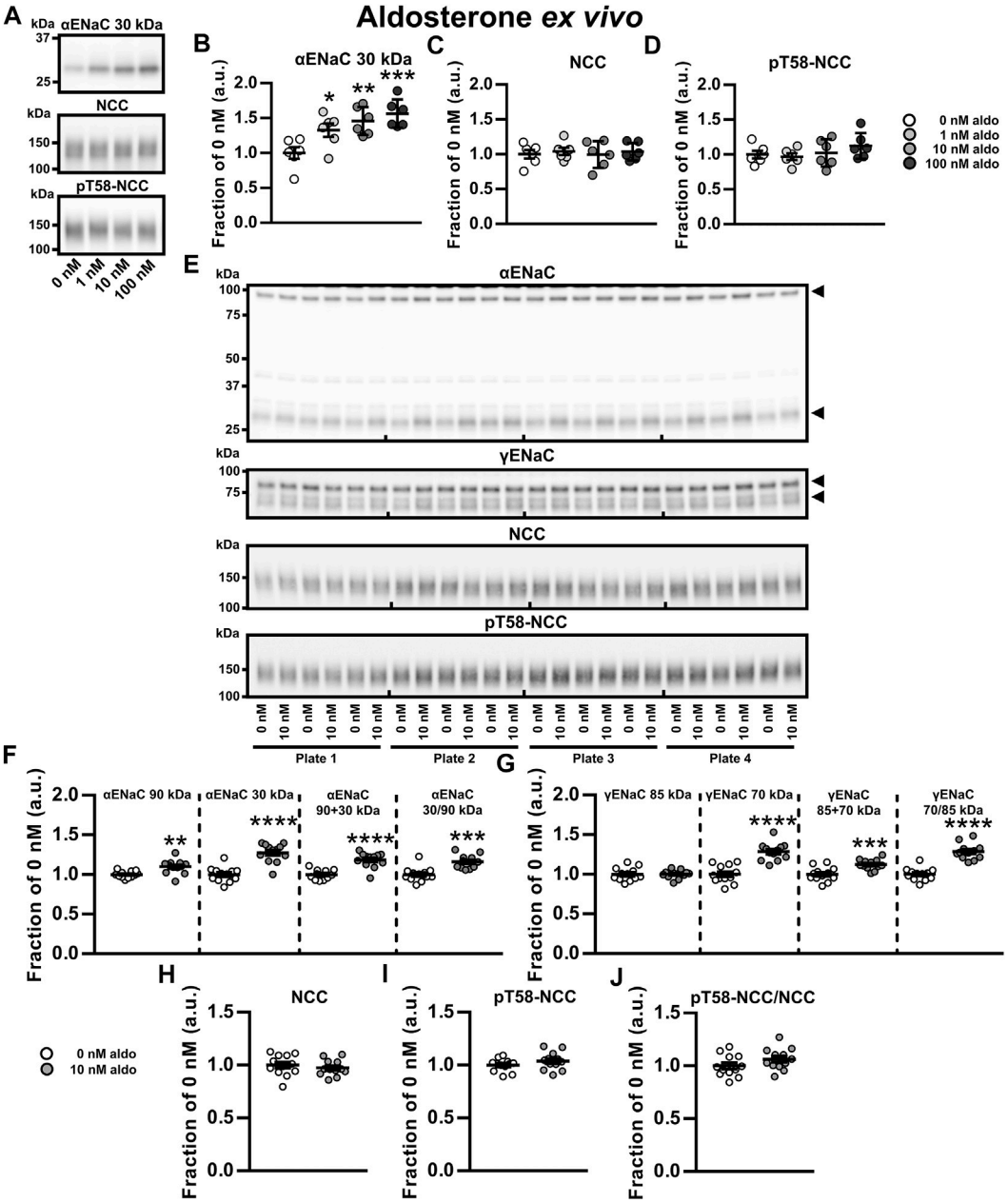

FIGURE 3 | Aldosterone increased ENaC but did not affect abundance or phosphorylation of NCC *ex vivo*. **(A–D)** A dose-response *ex vivo* experiment on kidney tubule suspensions showed that exposure to physiologically relevant aldosterone (aldo) concentrations (1, 10 and 100 nM) for 21 h increased cleaved αENaC (30 kDa) whereas no significant effect was found on NCC and pT58-NCC. **(E,F)** Exposure to 10 nM aldosterone increased non-cleaved αENaC (90 kDa), cleaved αENaC (30 kDa), total αENaC (90 + 30 kDa) and the ratio between non-cleaved and cleaved αENaC (30/90 kDa). **(E,G)** Furthermore, 10 nM aldosterone increased cleaved γENaC (70 kDa), total γENaC (85 + 70 kDa) and the ratio between non-cleaved and cleaved γENaC (70/85 kDa). **(E, H–J)** No significant effect was found on NCC, pT58-NCC or the pT58-NCC/NCC ratio. Arrows in panel **E** indicate cleaved and non-cleaved forms of αENaC (90 and 30 kDa) and γENaC (85 and 70 kDa). Data are presented as dot plots and mean ± SEM. Experiments were perform in 6-well plates and quantified values were normalized to 0 nM aldosterone within individual plates. $n = 6$ per group **(A–D)** or $n = 12$ per group **(E–J).** Statistical comparisons were performed using a one-way ANOVA followed by post-hoc testing with FDR-correction **(A–D),** Satterthwaite's 2-tailed unequal variance *t*-test [panel **(F)**, αENaC 90 kDa] or Student's 2-tailed *t*-tests [all other comparison tests in panel **(F–J)**]. $^{*}p < 0.05$, $^{**}p < 0.01$, $^{***}p < 0.001$, $^{****}p < 0.0001$.

dose-response experiment with physiologically relevant aldosterone concentrations (0, 1, 10 and 100 nM, corresponding to 360, 3,600 and 36,000 pg/ml, respectively). All tested concentrations increased cleaved αENaC (30 kDa, **Figures 3A,B**). However, none of the concentrations changed NCC or pT58-NCC significantly (**Figures 3A,C,D**).

We further assessed the effect of 10 nM aldosterone on full-length and cleaved αENaC and γENaC. Full-length αENaC

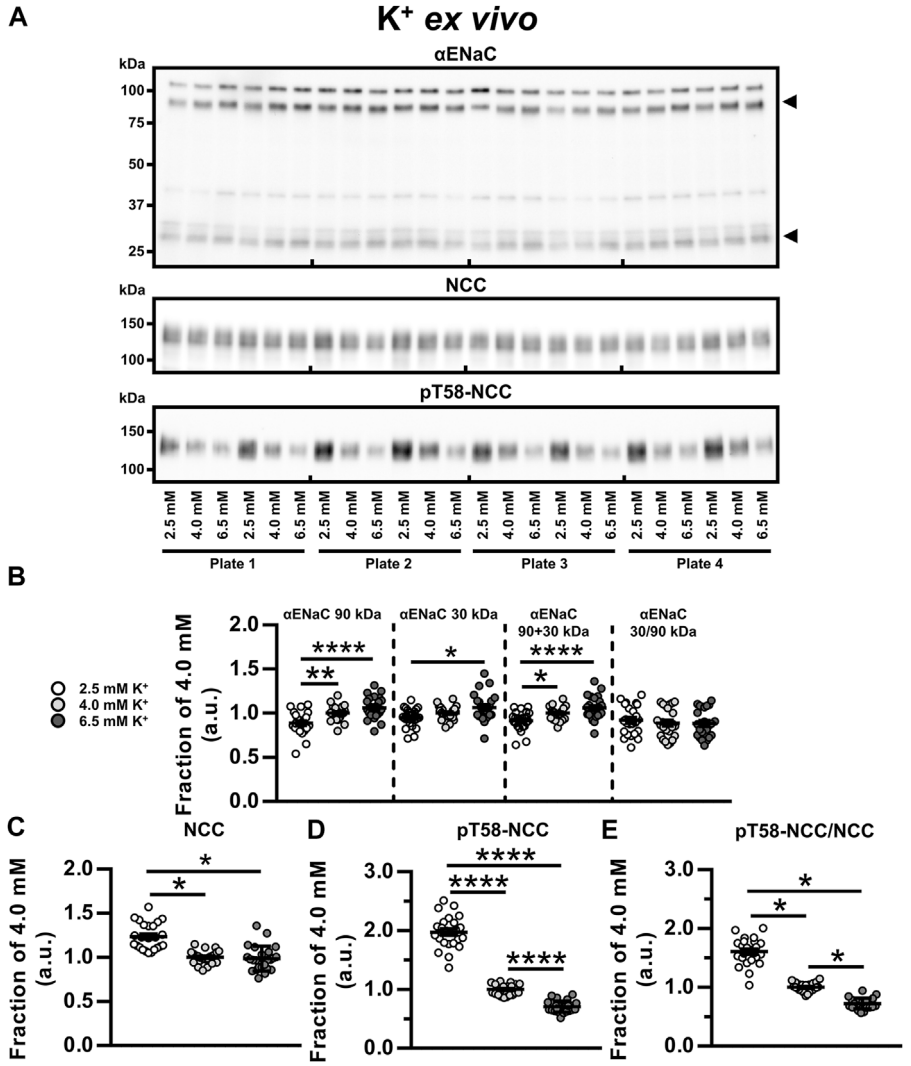

FIGURE 4 | Low K^+ reduced αENaC but increased NCC and pT58-NCC *ex vivo*. **(A, B)** Semiquantitative immunoblotting showed that *ex vivo* exposure of kidney tubule suspensions for 21 h to 2.5 mM K^+, as compared to 6.5 mM K^+, significantly reduced non-cleaved αENaC (90 kDa), cleaved αENaC (30 kDa) and total αENaC (90 + 30 kDa). **(A,C)** Exposure to 2.5 mM K^+ increased NCC compared to 4.0 and 6.5 mM K^+. **(A,D,E)** Exposure to 2.5 mM K^+ increased pT58-NCC and the pT58-NCC/NCC ratio compared to 4.0 and 6.5 mM K^+. Moreover, 6.5 mM K^+ reduced pT58-NCC and the pT58-NCC/NCC ratio compared to 4.0 mM K^+. Experiments were perform in 6-well plates and quantified values were normalized to 4.0 mM K^+ within individual plates. Data from three individual experiments were pooled. Data are presented as dot plots and mean ± SEM. $n = 24$ per group. Statistical comparisons were performed using a one-way ANOVA followed by post-hoc testing with FDR-correction (αENaC 90 kDa, αENaC 90 + 30 kDa, αENaC 30/90 kDa and pT58-NCC) or Kruskal–Wallis ANOVA on Ranks (αENaC 30 kDa, NCC and pT58-NCC/NCC). $^*p < 0.05$, $^{**}p < 0.01$**, $^{****}p < 0.0001$.

(90 kDa), cleaved αENaC (30 kDa), total αENaC (90 + 30 kDa) and the ratio between cleaved and full-length αENaC were all increased by aldosterone (**Figures 3E,F**). No effect was observed on full-length γENaC (85 kDa) (**Figures 3E,G**), but cleaved γENaC (70 kDa), total γENaC (85 + 70 kDa) and the ratio between cleaved and full-length γENaC (70/85 kDa) were increased by aldosterone (**Figures 3E,G**). Once again, 10 nM aldosterone did not significantly affect abundances of NCC and pT58-NCC (**Figures 3E,H–J**). Similar findings on αENaC and NCC were observed in an additional experiment with a higher sample size ($N = 30$ per group) (**Supplementary Figure S5**). Together, this data indicate that *ex vivo* exposure of kidney tubules to aldosterone increases the abundance and the cleavage of α- and γENaC but has no effect on NCC.

Low K^+ Reduced αENaC but Increased NCC and pT58-NCC *Ex Vivo*

To examine the isolated effects of K^+, kidney tubules were exposed to 2.5, 4.0 and 6.5 mM K^+ *ex vivo* for 21 h. Compared to 4.0 and 6.5 mM K^+, exposure to 2.5 mM K^+ reduced full-length αENaC (90 kDa) and total αENaC (90 + 30 kDa)

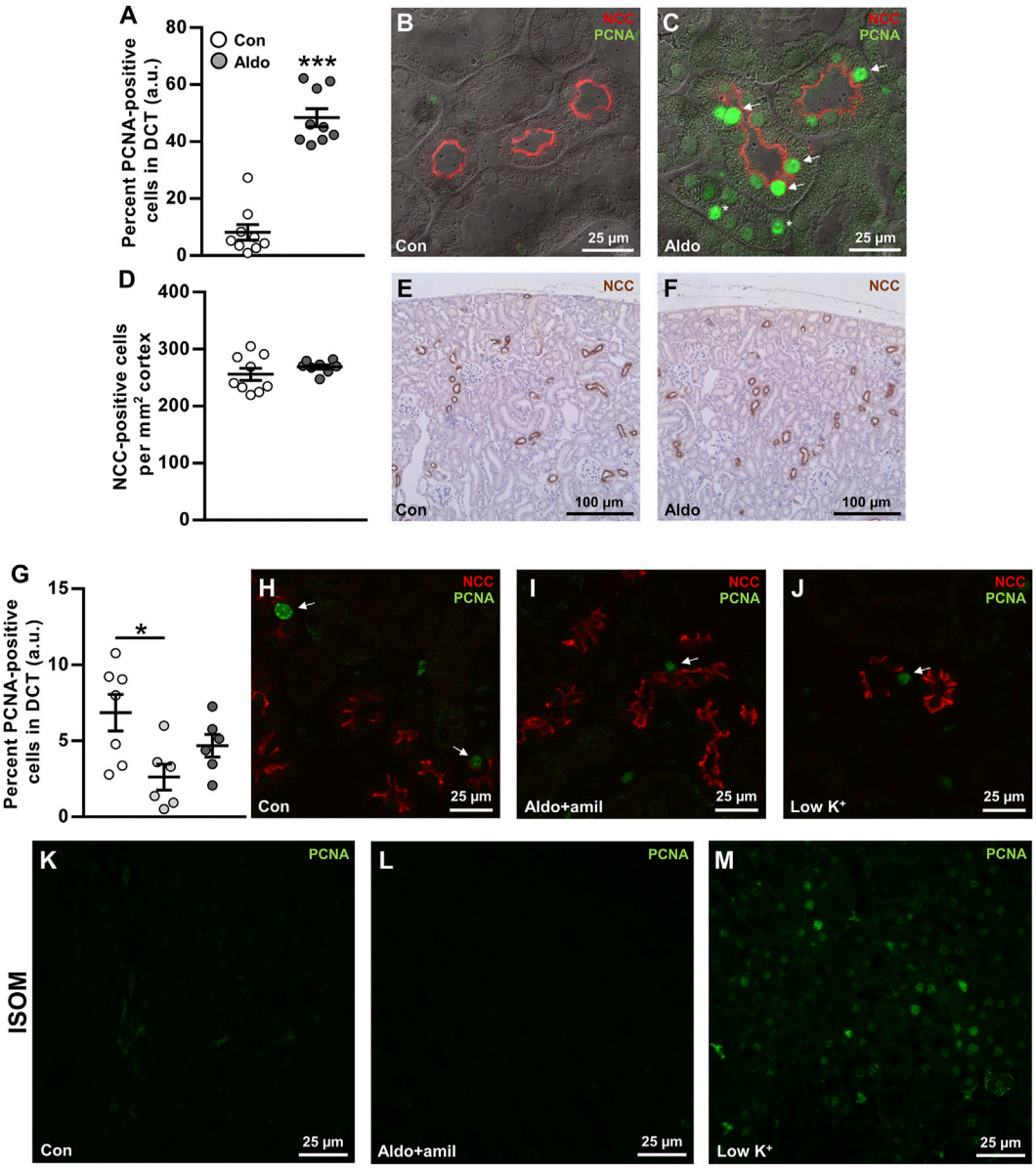

FIGURE 5 | Aldosterone infusion for 6 days increased the proliferation marker PCNA in renal DCT. **(A–C)** The percent PCNA-positive cells in the DCT was markedly increased by 6 days aldosterone infusion. Arrows indicate PCNA in DCT cells. Asterisks indicate PCNA in non-DCT cells. **(D–F)** The numbers of DCT cells/mm^2 cortex were not changed significantly by 6 days aldosterone infusion. **(G–J)** Amiloride + aldosterone infusion for 6 days reduced the number of PCNA-positive DCT cells, whereas no significant effect was found in mice fed a low K^+ diet for 6 days. Arrows indicate PCNA in DCT cells. **(K–M)** In the inner stripe of the outer medulla (ISOM), qualitative assessment showed greater PCNA labeling in mice fed a low K^+ diet whereas no clear effect was observed in the mice infused with amiloride + aldosterone. Kidney tissue in panel **(A–F)** originated from a previously published study (Poulsen and Christensen, 2017). Data are presented as dot plots and mean ± SEM. $n = 9$ [control and aldosterone **(A–F)**], $n = 7$ [control **(G–M)**] or $n = 6$ [amiloride + aldosterone and low K^+ **(G–M)**]. Statistical comparisons were performed using Satterthwaite's 2-tailed unequal variance *t*-test **(A,D)** or a one-way ANOVA followed by post-hoc testing with FDR-correction **(G)**. $^*p < 0.05$, $^{***}p < 0.001$.

(**Figures 4A,B**). Furthermore, cleaved αENaC (30 kDa) was reduced by 2.5 mM compared to 6.5 mM K^+ (**Figures 4A,B**). NCC and pT58-NCC were significantly increased by 2.5 mM K^+ compared to 4.0 mM K^+ (**Figures 4A,C–E**). In the 21 h timeframe, 6.5 mM K^+ did not significantly alter NCC compared to 4.0 mM K^+, whereas it significantly reduced pT58-NCC (**Figures 4A,C–E**).

Aldosterone Infusion for 6 days Increased the Proliferation Marker PCNA in Renal DCT

Hypokalemia has previously been associated with increased cell proliferation in the DCT after 3 days (Saritas et al., 2018) and increased DCT length after 4 weeks (Su et al., 2020). We hypothesized that similar effects would occur after infusion with aldosterone. Sections from a previous study (Poulsen and

Christensen, 2017), in which mice had developed frank hypokalemia in response to 6 days aldosterone infusion, were fluorescence-labeled with NCC (DCT cell marker) and the proliferation marker, PCNA. DCT cells positive for PCNA were markedly increased in aldosterone-infused mice (**Figures 5A–C**), but there was no significant effect on the number of DCT cells per mm^2 cortex (**Figures 5D–F**).

To study the effects of aldosterone on PCNA expression in the DCT in a condition without hypokalemia, we labeled sections from mice that had been infused with amiloride + aldosterone or fed a low K^+ diet for 6 days (*Protocol 3*). The amiloride + aldosterone infusion reduced the number of PCNA-labeled DCT cells, but no significant effect was observed in mice fed the low K^+ diet (**Figures 5G–J**). However, when assessing the inner stripe of the outer medulla (ISOM), PCNA expression was clearly increased by the low K^+ diet.

DISCUSSION

Various studies have reported contrasting data on whether aldosterone has a direct effect on the DCT to increase NCC (Ko et al., 2013; Czogalla et al., 2016; Terker et al., 2016; Cheng et al., 2019). To investigate this further, we used *in vivo* and *ex vivo* approaches to study K^+-independent/isolated long-term effects of aldosterone on NCC. Our data showed that blocking ENaC during aldosterone excess prevented the development of hypokalemia and the observed increase in NCC when aldosterone was administered alone. Testing the isolated effect of aldosterone *ex vivo* supported that aldosterone had no long-term effect on NCC and that low K^+, independently of aldosterone, could increase the abundance and phosphorylation of NCC. This effect may be mediated *via* basolateral K^+ channels because the stimulatory effect of low K^+ on NCC is absent in Kir4.1 and Kir5.1 KO mice (Malik et al., 2018; Wang et al., 2018). Normally, high levels of glucocorticoids are thought to occupy the MR and prevent aldosterone from exerting a regulatory effect in the DCT1, which lacks the glucocorticoid inactivating enzyme, 11β-hydroxysteroid dehydrogenase 2. However, even in our *ex vivo* setting, without potential occupancy of the MR by glucocorticoids, no effects of aldosterone on NCC were observed within a 21 h period. In contrast, both α- and γENaC were clearly regulated by aldosterone *ex vivo*. Collectively, our data support that the stimulatory effect of long-term aldosterone excess on NCC is due to secondary effects of reduced plasma K^+ (**Figure 6**).

A question is why *ex vivo* aldosterone exposure of kidney tubules increases NCC phosphorylation acutely (Cheng et al., 2019) but not long-term. Similarly to aldosterone, we have recently shown in kidney tubules that the β2-adrenergic receptor agonist salbutamol increases NCC phosphorylation acutely (Poulsen et al., 2021). However, exposing tubules to salbutamol for 24 h did not affect NCC abundance or phosphorylation (**Supplementary Figure S6**), but yet, after keeping tubules in control media for 21 h they still responded to salbutamol by increasing NCC phosphorylation (**Supplementary Figure S4**). Why is there this deviation between acute and chronic stimulation of receptors mediating NCC phosphorylation? One possible explanation is that the effects of hormones may wane rapidly despite continues exposure. For example, the β2-adrenergic receptor can be desensitized due to uncoupling of the receptor from the G protein resulting in reduced stimulation of cAMP production (Hausdorff et al., 1990), potentially explaining why the salbutamol effect on NCC phosphorylation was transient. Since aldosterone can increase cAMP independently of the MR (Haseroth et al., 1999), a similar mechanism may exist for aldosterone, which could explain the diverging effect of acute and long-term exposure on NCC phosphorylation. Thus, it is possible that the role of aldosterone in the DCT mainly is to adjust NaCl reabsorption acutely. It should be highlighted that *in vitro* exposure of mDCT15 cells to aldosterone for 12–36 h increased NCC phosphorylation (Ko et al., 2013), but why there are discrepancies between aldosterone effects *ex vivo* and *in vitro* is unclear.

Our *ex vivo* tubule studies also extend the current knowledge on how ENaC is regulated. Previous studies addressing how aldosterone regulates abundance and proteolytic activation/cleavage of ENaC are limited to *in vivo* and cell system studies (Rossier and Stutts, 2009). As mentioned, *in vivo* infusion of aldosterone in mice changes a number of physiological parameters including plasma K^+ and Na^+ levels (Poulsen and Christensen, 2017). Here, we show that both the abundances and cleavage of α- and γENaC are increased directly by aldosterone in native kidney tubules *ex vivo*. Furthermore, we show that K^+ in itself can increase the abundance of αENaC, building on the recent observations that ENaC is directly regulated by K^+ independently of aldosterone. This includes studies on Kir4.1 KO mice, which have increased expression of ENaC subunits (Su et al., 2016), and on cell studies showing that the stimulatory effect of K^+ on ENaC currents may depend on Kir4.1/5.1 (Sorensen et al., 2019). The K^+-induced increase in αENaC found in the present study may occur *via* a similar mechanism.

Six days aldosterone infusion markedly increased the expression of the cell proliferation marker, PCNA, in the DCT. Similarly, Saritas et al. (2018) showed an increase in the proliferation marker Ki-67, in the DCT of mice fed a low K^+ diet for 3 days. To test if the increase in PCNA expression by aldosterone could be secondary to hypokalemia, we further assessed kidneys from mice that were infused with amiloride + aldosterone (had mild hyperkalemia) and mice that were fed a low K^+ diet for 6 days (were hypokalemic). PCNA expression in the DCT was significantly reduced by amiloride + aldosterone infusion. A possible explanation for this could be that K^+ channels are involved in controlling cell-cycle progression and that this was influenced by the high plasma K^+ levels (Urrego et al., 2014). In the low K^+ group, PCNA expression was clearly increased in the ISOM, but in contrast to Saritas et al. (2018), we did not observe any significant effect on cell proliferation in the DCT. While this finding was unexpected, it is possible that the effects of a low K^+ diet on cell proliferation are different at 3 days relative to 6 days. This is supported by that PCNA expression is markedly greater in mice fed a high K^+ diet for 3 days compared

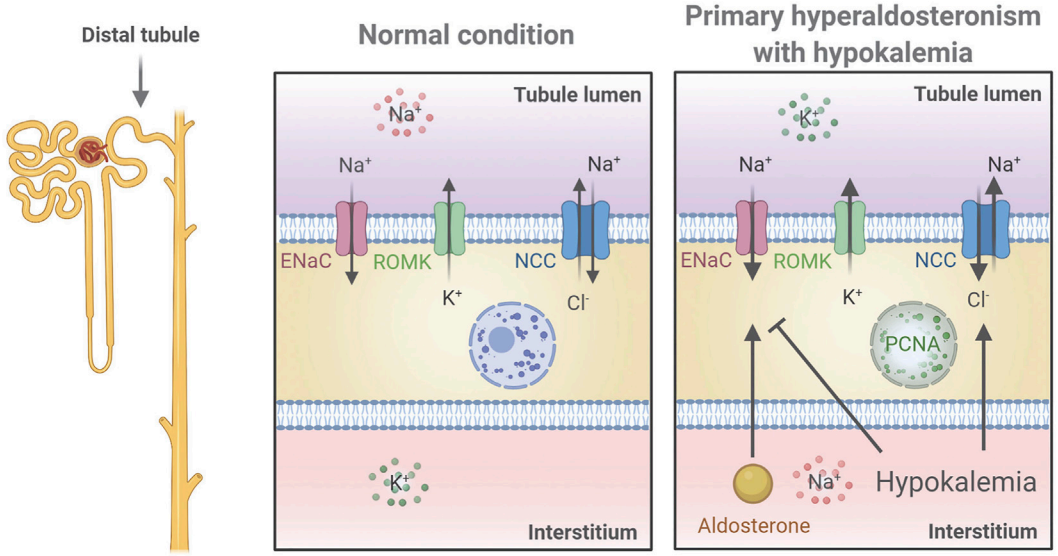

FIGURE 6 | Proposed mechanistic regulation of NCC and ENaC in the renal distal tubule in a mouse model of primary hyperaldosteronism associated with hypokalemia. Aldosterone stimulates ENaC to increase Na^+ reabsorption thus promoting K^+ secretion *via* ROMK leading to hypokalemia. Hypokalemia stimulates NCC and furthermore works as negative feedback to aldosterone by inhibiting ENaC. Finally, increased plasma aldosterone increases PCNA in the nucleus indicating cell proliferation, but whether this occurs directly or indirectly *via* stimulation of DCT cells was not determined. The figure was created with BioRender.com.

to 14 days (Cheval et al., 2004). Thus, cell proliferation may be most pronounced during the initial face after shifting animals to a low K^+ diet. How does that correlate with the greater PCNA expression observed after 6 days of aldosterone infusion in our study? Perhaps aldosterone infusion, in contrast to a low K^+ diet, does not affect plasma K^+ levels for the first couple of days. Thus, the 6 days aldosterone infusion might be more comparable to a 3-days low K^+ diet. A final possibility is that, by using the proliferation marker PCNA that is maximal expressed during the S phase (Nemoto et al., 1993), we do not detect cells in the G1, G2, or M-phase that would be detected using Ki-67 (Saritas et al., 2018).

Saritas et al. (2018) did not quantify the length of the DCT in response to a low K^+ diet. In a more recent study it was however reported that a low K^+ diet increased the DCT length by 13% after 4 weeks of low K^+ diet (Su et al., 2020). We did not observe a significant increase in the number of DCT cells per mm^2 cortex after 6 days aldosterone infusion, but it is possible that a longer infusion time was required in order to have an effect. However, increased PCNA labeling was not limited to the DCT but was also observed in other cortical tubules. Thus, it cannot be excluded that the whole cortical region proliferated and therefore masked a potential increase in the DCT length. In a clinical context, it has not been investigated if renal cell proliferation is changed in patients with PA and whether this could contribute to the etiology of the disease.

Our study indicates that high NCC levels in rodent models with high aldosterone are most likely a response to hypokalemia occurring as a result of aldosterone enhanced ENaC activity. This is in line with what is reported in other studies (Terker et al., 2016). How can this knowledge contribute clinically? We speculate that renal NCC protein abundance is only increased by aldosterone excess if it is associated with hypokalemia. An obvious strategy to lower BP during aldosterone excess could be to reduce Na^+ reabsorption using thiazide treatment. However, reducing NCC activity with thiazide may increase Na^+ delivery to ENaC-expressing segments and enhance K^+ secretion (McDonough and Youn, 2017), lowering plasma K^+ even more. Therefore, ENaC inhibitors, such as benzamil and amiloride, could be better options for lowering BP under this condition as they could reduce Na^+ reabsorption *via* ENaC, normalize plasma K^+ and ultimately normalize NCC. This basic experimental proposal needs to be tested further. However, it is in line with current clinical therapy strategies using ENaC inhibitors for reducing renal Na^+ retention and treating hypertension in PA (Cobb and Aeddula, 2021).

DATA AVAILABILITY STATEMENT

The original contributions presented in the study are included in the article/**Supplementary Material**, further inquiries can be directed to the corresponding author.

ETHICS STATEMENT

The animal study was reviewed, approved and issued by the Animal Experiments Inspectorate, Ministry of Food, Agriculture and Fisheries, Danish Veterinary and Food Administration.

AUTHOR CONTRIBUTIONS

SP made the conception of the work. MK and SP performed experiments. MK, RF and SP analyzed and interpreted data. SP and RF drafted the manuscript. All authors approved the final manuscript and agree to be accountable for all aspects of the work.

FUNDING

This work is supported by a grant from the Leducq Foundation for Cardiovascular Research (Potassium in Hypertension Network), the Novo Nordisk Foundation, the Lundbeck Foundation, and the Danish Medical Research Council.

ACKNOWLEDGMENTS

We thank I. M. S. Paulsen for technical assistance on immunohistochemical labeling. The αENaC antibody was kindly provided by J. Loffing (Institute of Anatomy, University of Zurich, Zurich, Switzerland). **Figure 6** was created with BioRender.com.

SUPPLEMENTARY MATERIAL

The Supplementary Material for this article can be found online at: https://www.frontiersin.org/articles/10.3389/fphys.2022.800055/full#supplementary-material

REFERENCES

Arroyo, J. P., Lagnaz, D., Ronzaud, C., Vázquez, N., Ko, B. S., Moddes, L., et al. (2011a). Nedd4-2 Modulates Renal Na^+-Cl^- Cotransporter via the Aldosterone-SGK1-Nedd4-2 Pathway. *Jasn* 22, 1707–1719. doi:10.1681/asn.2011020132

Arroyo, J. P., Ronzaud, C., Lagnaz, D., Staub, O., and Gamba, G. (2011b). Aldosterone Paradox: Differential Regulation of Ion Transport in Distal Nephron. *Physiology* 26, 115–123. doi:10.1152/physiol.00049.2010

Buffolo, F., Monticone, S., Burrello, J., Tetti, M., Veglio, F., Williams, T., et al. (2017). Is Primary Aldosteronism Still Largely Unrecognized? *Horm. Metab. Res.* 49, 908–914. doi:10.1055/s-0043-119755

Cheng, L., Poulsen, S. B., Wu, Q., Esteva-Font, C., Olesen, E. T. B., Peng, L., et al. (2019). Rapid Aldosterone-Mediated Signaling in the DCT Increases Activity of the Thiazide-Sensitive NaCl Cotransporter. *Jasn* 30, 1454–1470. doi:10.1681/asn.2018101025

Cheval, L., Duong Van Huyen, J. P., Bruneval, P., Verbavatz, J.-M., Elalouf, J.-M., and Doucet, A. (2004). Plasticity of Mouse Renal Collecting Duct in Response to Potassium Depletion. *Physiol. Genomics* 19, 61–73. doi:10.1152/physiolgenomics.00055.2004

Christensen, B. M., Perrier, R., Wang, Q., Zuber, A. M., Maillard, M., Mordasini, D., et al. (2010). Sodium and Potassium Balance Depends on αENaC Expression in Connecting Tubule. *Jasn* 21, 1942–1951. doi:10.1681/asn.2009101077

Cobb, A., and Aeddula, N. R. (2021). *Primary Hyperaldosteronism*. Treasure Island (FL): StatPearls.

Conn, J. W. (1955). Presidential Address. I. Painting Background. II. Primary Aldosteronism, a New Clinical Syndrome. *J. Lab. Clin. Med.* 45, 3–17.

Czogalla, J., Vohra, T., Penton, D., Kirschmann, M., Craigie, E., and Loffing, J. (2016). The Mineralocorticoid Receptor (MR) Regulates ENaC but Not NCC in Mice with Random MR Deletion. *Pflugers Arch-European J. Physiol.* 468, 849–858. doi:10.1007/s00424-016-1798-5

Fagugli, R. M., and Taglioni, C. (2011). Changes in the Perceived Epidemiology of Primary Hyperaldosteronism. *Int. J. Hypertens.* 2011, 162804. doi:10.4061/2011/162804

Furgeson, S. B., and Linas, S. (2010). Mechanisms of Type I and Type II Pseudohypoaldosteronism. *Jasn* 21, 1842–1845. doi:10.1681/asn.2010050457

Gaeggeler, H.-P., Gonzalez-Rodriguez, E., Jaeger, N. F., Loffing-Cueni, D., Norregaard, R., Loffing, J., et al. (2005). Mineralocorticoid versus Glucocorticoid Receptor Occupancy Mediating Aldosterone-Stimulated Sodium Transport in a Novel Renal Cell Line. *Jasn* 16, 878–891. doi:10.1681/asn.2004121110

Ganguly, A. (1998). Primary Aldosteronism. *N. Engl. J. Med.* 339, 1828–1834. doi:10.1056/nejm199812173392507

Haseroth, K., Gerdes, D., Berger, S., Feuring, M., Gunther, A., Herbst, C., et al. (1999). Rapid Nongenomic Effects of Aldosterone in Mineralocorticoid-Receptor-Knockout Mice. *Biochem. Biophysical Res. Commun.* 266, 257. doi:10.1006/bbrc.1999.1771

Hausdorff, W. P., Caron, M. G., and Lefkowitz, R. J. (1990). Turning off the Signal: Desensitization of Beta-Adrenergic Receptor Function. *FASEB j.* 4, 2881–2889. doi:10.1096/fasebj.4.11.2165947

Kaplan, N. M. (1967). Hypokalemia in the Hypertensive Patient. *Ann. Intern. Med.* 66, 1079–1090. doi:10.7326/0003-4819-66-6-1079

Käyser, S. C., Dekkers, T., Groenewoud, H. J., van der Wilt, G. J., Carel Bakx, J., van der Wel, M. C., et al. (2016). Study Heterogeneity and Estimation of Prevalence of Primary Aldosteronism: A Systematic Review and Meta-Regression Analysis. *J. Clin. Endocrinol. Metab.* 101, 2826–2835. doi:10.1210/jc.2016-1472

Kim, G.-H., Masilamani, S., Turner, R., Mitchell, C., Wade, J. B., and Knepper, M. A. (1998). The Thiazide-Sensitive Na-Cl Cotransporter Is an Aldosterone-Induced Protein. *Proc. Natl. Acad. Sci. U.S.A.* 95, 14552–14557. doi:10.1073/pnas.95.24.14552

Kleta, R., and Bockenhauer, D. (2006). Bartter Syndromes and Other Salt-Losing Tubulopathies. *Nephron Physiol.* 104, p73–80. doi:10.1159/000094001

Ko, B., Mistry, A. C., Hanson, L., Mallick, R., Wynne, B. M., Thai, T. L., et al. (2013). Aldosterone Acutely Stimulates NCC Activity via a SPAK-Mediated Pathway. *Am. J. Physiology-Renal Physiol.* 305, F645–F652. doi:10.1152/ajprenal.00053.2013

Loffing, J., Zecevic, M., Féraille, E., Kaissling, B., Asher, C., Rossier, B. C., et al. (2001). Aldosterone Induces Rapid Apical Translocation of ENaC in Early Portion of Renal Collecting System: Possible Role of SGK. *Am. J. Physiology-Renal Physiol.* 280, F675–F682. doi:10.1152/ajprenal.2001.280.4.f675

Malik, S., Lambert, E., Zhang, J., Wang, T., Clark, H. L., Cypress, M., et al. (2018). Potassium Conservation Is Impaired in Mice with Reduced Renal Expression of Kir4.1. *Am. J. Physiol. Ren. Physiol.* 315, F1271–F1282. doi:10.1096/fasebj.2020.34.s1.05912

Masilamani, S., Kim, G.-H., Mitchell, C., Wade, J. B., and Knepper, M. A. (1999). Aldosterone-mediated Regulation of ENaC α, β, and γ Subunit Proteins in Rat Kidney. *J. Clin. Invest.* 104, R19–R23. doi:10.1172/jci7840

McDonough, A. A., and Youn, J. H. (2017). Potassium Homeostasis: the Knowns, the Unknowns, and the Health Benefits. *Physiology* 32, 100–111. doi:10.1152/physiol.00022.2016

Monticone, S., Burrello, J., Tizzani, D., Bertello, C., Viola, A., Buffolo, F., et al. (2017). Prevalence and Clinical Manifestations of Primary Aldosteronism Encountered in Primary Care Practice. *J. Am. Coll. Cardiol.* 69, 1811–1820. doi:10.1016/j.jacc.2017.01.052

Moraitis, A., and Stratakis, C. (2011). Adrenocortical Causes of Hypertension. *Int. J. Hypertens.* 2011, 624691. doi:10.4061/2011/624691

Narum, S. R. (2006). Beyond Bonferroni: Less Conservative Analyses for Conservation Genetics. *Conserv Genet.* 7, 783–787. doi:10.1007/s10592-005-9056-y

Nemoto, R., Kawamura, H., Miyakawa, I., Uchida, K., Hattori, K., Koiso, K., et al. (1993). Immunohistochemical Detection of Proliferating Cell Nuclear Antigen (PCNA)/cyclin in Human Prostate Adenocarcinoma. *J. Urol.* 149, 165–169. doi:10.1016/s0022-5347(17)36031-7

Nguyen, M. T. X., Lee, D. H., Delpire, E., and McDonough, A. A. (2013). Differential Regulation of Na^+ transporters along Nephron during ANG II-dependent Hypertension: Distal Stimulation Counteracted by Proximal Inhibition. *Am. J. Physiology-Renal Physiol.* 305, F510–F519. doi:10.1152/ajprenal.00183.2013

Nielsen, J., Kwon, T.-H., Frøkiær, J., Knepper, M. A., and Nielsen, S. (2007). Maintained ENaC Trafficking in Aldosterone-Infused Rats during Mineralocorticoid and Glucocorticoid Receptor Blockade. *Am. J. Physiology-Renal Physiol.* 292, F382–F394. doi:10.1152/ajprenal.00212.2005

Nielsen, J., Kwon, T.-H., Masilamani, S., Beutler, K., Hager, H., Nielsen, S., et al. (2002). Sodium Transporter Abundance Profiling in Kidney: Effect of Spironolactone. *Am. J. Physiology-Renal Physiol.* 283, F923–F933. doi:10.1152/ajprenal.00015.2002

Pedersen, N. B., Hofmeister, M. V., Rosenbaek, L. L., Nielsen, J., and Fenton, R. A. (2010). Vasopressin Induces Phosphorylation of the Thiazide-Sensitive Sodium Chloride Cotransporter in the Distal Convoluted Tubule. *Kidney Int.* 78, 160–169. doi:10.1038/ki.2010.130

Poulsen, S. B., Cheng, L., Penton, D., Kortenoeven, M. L. A., Matchkov, V. V., Loffing, J., et al. (2021). Activation of the Kidney Sodium Chloride Cotransporter by the β2-adrenergic Receptor Agonist Salbutamol Increases Blood Pressure. *Kidney Int.* 100, 321–335. doi:10.1016/j.kint.2021.04.021

Poulsen, S. B., and Christensen, B. M. (2017). Long-term Aldosterone Administration Increases Renal Na^+-Cl^- Cotransporter Abundance in Late Distal Convoluted Tubule. *Am. J. Physiology-Renal Physiol.* 313, F756–F766. doi:10.1152/ajprenal.00352.2016

Poulsen, S. B., Limbutara, K., Fenton, R. A., Pisitkun, T., and Christensen, B. M. (2018). RNA Sequencing of Kidney Distal Tubule Cells Reveals Multiple Mediators of Chronic Aldosterone Action. *Physiol. Genomics* 50, 343–354. doi:10.1152/physiolgenomics.00084.2017

Poulsen, S. B., Praetorius, J., Damkier, H. H., Miller, L., Nelson, R. D., Hummler, E., et al. (2016). Reducing αENaC Expression in the Kidney Connecting Tubule Induces Pseudohypoaldosteronism Type 1 Symptoms during K^+ Loading. *Am. J. Physiology-Renal Physiol.* 310, F300–F310. doi:10.1152/ajprenal.00258.2015

Pradervand, S., Wang, Q., Burnier, M., Beermann, F., Horisberger, J. D., Hummler, E., et al. (1999). A Mouse Model for Liddle's Syndrome. *Jasn* 10, 2527–2533. doi:10.1681/asn.v10122527

Rossi, G. P. (2010). Prevalence and Diagnosis of Primary Aldosteronism. *Curr. Hypertens. Rep.* 12, 342–348. doi:10.1007/s11906-010-0134-2

Rossier, B. C., and Stutts, M. J. (2009). Activation of the Epithelial Sodium Channel (ENaC) by Serine Proteases. *Annu. Rev. Physiol.* 71, 361–379. doi:10.1146/annurev.physiol.010908.163108

Saritas, T., Puelles, V. G., Su, X.-T., McCormick, J. A., Welling, P. A., and Ellison, D. H. (2018). Optical Clearing in the Kidney Reveals Potassium-Mediated Tubule Remodeling. *Cel Rep.* 25, 2668–2675. doi:10.1016/j.celrep.2018.11.021

Schirpenbach, C., and Reincke, M. (2007). Primary Aldosteronism: Current Knowledge and Controversies in Conn's Syndrome. *Nat. Rev. Endocrinol.* 3, 220–227. doi:10.1038/ncpendmet0430

Schneider, C. A., Rasband, W. S., and Eliceiri, K. W. (2012). NIH Image to ImageJ: 25 Years of Image Analysis. *Nat. Methods* 9, 671–675. doi:10.1038/nmeth.2089

Sokal, R. R., and Rohlf, F. J. (1995). *Biometry: The Priniciples and Practices of Statistics in Biological Research*. 3rd ed. New York: W.H. Freeman.

Sørensen, M. V., Saha, B., Jensen, I. S., Wu, P., Ayasse, N., Gleason, C. E., et al. (2019). Potassium Acts through mTOR to Regulate its Own Secretion. *JCI Insight* 5, e126910. doi:10.1172/jci.insight.126910

Sorensen, M. V., Grossmann, S., Roesinger, M., Gresko, N., Todkar, A. P., Barmettler, G., et al. (2013). Rapid Dephosphorylation of the Renal Sodium Chloride Cotransporter in Response to Oral Potassium Intake in Mice. *Kidney Int.* 83, 811–824. doi:10.1038/ki.2013.14

Su, X.-T., Zhang, C., Wang, L., Gu, R., Lin, D.-H., and Wang, W.-H. (2016). Disruption of KCNJ10 (Kir4.1) Stimulates the Expression of ENaC in the Collecting Duct. *Am. J. Physiology-Renal Physiol.* 310, F985–F993. doi:10.1152/ajprenal.00584.2015

Su, X. T., Saritas, T., Yang, C. L., Welling, P. A., and Ellison, D. H. (2020). Four Weeks of Dietary Potassium Restriction Causes Distal Convoluted Tubule Remodeling. *FASEB J.* 34, 1. doi:10.1096/fasebj.2020.34.s1.05912

Terker, A. S., Yarbrough, B., Ferdaus, M. Z., Lazelle, R. A., Erspamer, K. J., Meermeier, N. P., et al. (2016). Direct and Indirect Mineralocorticoid Effects Determine Distal Salt Transport. *Jasn* 27, 2436–2445. doi:10.1681/asn.2015070815

Terker, A. S., Zhang, C., McCormick, J. A., Lazelle, R. A., Zhang, C., Meermeier, N. P., et al. (2015). Potassium Modulates Electrolyte Balance and Blood Pressure through Effects on Distal Cell Voltage and Chloride. *Cel Metab.* 21, 39–50. doi:10.1016/j.cmet.2014.12.006

Urrego, D., Tomczak, A. P., Zahed, F., Stühmer, W., and Pardo, L. A. (2014). Potassium Channels in Cell Cycle and Cell Proliferation. *Phil. Trans. R. Soc. B* 369, 20130094. doi:10.1098/rstb.2013.0094

van der Lubbe, N., Lim, C. H., Fenton, R. A., Meima, M. E., Jan Danser, A. H., Zietse, R., et al. (2011). Angiotensin II Induces Phosphorylation of the Thiazide-Sensitive Sodium Chloride Cotransporter Independent of Aldosterone. *Kidney Int.* 79, 66–76. doi:10.1038/ki.2010.290

Wang, M.-X., Cuevas, C. A., Su, X.-T., Wu, P., Gao, Z.-X., Lin, D.-H., et al. (2018). Potassium Intake Modulates the Thiazide-Sensitive Sodium-Chloride Cotransporter (NCC) Activity via the Kir4.1 Potassium Channel. *Kidney Int.* 93, 893–902. doi:10.1016/j.kint.2017.10.023

Conflict of Interest: The authors declare that the research was conducted in the absence of any commercial or financial relationships that could be construed as a potential conflict of interest.

Publisher's Note: All claims expressed in this article are solely those of the authors and do not necessarily represent those of their affiliated organizations, or those of the publisher, the editors and the reviewers. Any product that may be evaluated in this article, or claim that may be made by its manufacturer, is not guaranteed or endorsed by the publisher.

Advantages of publishing in Frontiers

OPEN ACCESS
Articles are free to read for greatest visibility and readership

FAST PUBLICATION
Around 90 days from submission to decision

HIGH QUALITY PEER-REVIEW
Rigorous, collaborative, and constructive peer-review

TRANSPARENT PEER-REVIEW
Editors and reviewers acknowledged by name on published articles

Frontiers
Avenue du Tribunal-Fédéral 34
1005 Lausanne | Switzerland

Visit us: www.frontiersin.org
Contact us: frontiersin.org/about/contact

REPRODUCIBILITY OF RESEARCH
Support open data and methods to enhance research reproducibility

DIGITAL PUBLISHING
Articles designed for optimal readership across devices

FOLLOW US
@frontiersin

IMPACT METRICS
Advanced article metrics track visibility across digital media

EXTENSIVE PROMOTION
Marketing and promotion of impactful research

LOOP RESEARCH NETWORK
Our network increases your article's readership